RC
1042
.N87
1985
v.2

U.S. Department
of Transportation
**National Highway
Traffic Safety
Administration**

DOT HS 807 430

December 1985

Final Technical Report

Experimental Data for Development of Finite Element Models: Head/Thoraco-Abdomen/Pelvis Volume II: THORACO-ABDOMEN

DEPARTMENT OF
TRANSPORTATION
AUG 4
LIBRARY

This document is available to the public from the National Technical Information Service, Springfield, Virginia 22161.

The United States Government does not endorse products or manufacturers. Trade or manufacturers' names appear only because they are considered essential to the object of this report.

RC
1042
.N87
1985
v.2

Technical Report Documentation Page

1. Report No.	2. Government Accession No.	3. Recipient's Catalog No.
DOT HS 807 430		

4. Title and Subtitle	5. Report Date
Experimental Data for Development of Finite Element Models, Head/Thoraco-Abdomen/Pelvis Vol.II: Thoraco-Abdomen	December 31, 1985
	6. Performing Organization Code
7. Author(s) Guy S. Nusholtz and Patricia S. Kaiker	8. Performing Organization Report No. UMTRI-85-55-2
9. Performing Organization Name and Address Biosciences Division, Transportation Research Institute, The University of Michigan, 2901 Baxter Road, Ann Arbor, MI 48109	10. Work Unit No.
	11. Contract or Grant No. DOT-HS-7-01636
12. Sponsoring Agency Name and Address National Highway Traffic Safety Administration Department of Transportation, Seventh and E Streets, S.W., Washington, DC 20590	13. Type of Report and Period Covered July 1977-Dec. 1983
	14. Sponsoring Agency Code

15. Supplementary Notes

Experimental data.

16. Abstract

Validation of biomechanical computer models of impact biodynamics cannot be accomplished without descriptive experimental data. The research program, therefore, involved data gathering on the kinematics and damage response of three human cadaver subsystems: the head, the thoraco-abdomen, and the pelvis. 14 unembalmed human cadavers were utilized in 68 dynamic impact tests. The research program entailed 14 head impacts (6 subjects), 41 thoraco-abdominal impacts (11 subjects), and 13 pelvis impacts (10 subjects). In addition, the thoraco-abdominal tests were supplemented with static three-point bending tests conducted on rib specimens from 5 of the dynamically tested cadavers.

DEPARTMENT OF TRANSPORTATION
AUG 4
LIBRARY

17. Key Words	18. Distribution Statement
Impact Biomechanics, Head, Thoraco-Abdomen, Pelvis, Experimental Data	Document is available to the public from the National Technical Information Service, Springfield, VA 22161

19. Security Classif. (of this report)	20. Security Classif. (of this page)	21. No. of Pages	22. Price
		388	

TABLE OF CONTENTS - THORACO-ABDOMINAL SERIES

Page

TECHNICAL REPORT DOCUMENTATION PAGE.....i

TABLE OF CONTENTS.....iii

LIST OF FIGURES..... v

LIST OF TABLES.....vii

1.0 INTRODUCTION.....111

2.0 ANATOMICAL CONSIDERATIONS.....116

3.0 GOAL OF THORACO-ABDOMINAL SERIES IMPACT TESTING...121

4.0 METHODOLOGY.....127
4.1 Methods and Procedures of Impact Testing.....127
4.11 Subjects.....127
4.12 Pre-Test Preparation.....127
Morgue.....127
Anatomy Lab.....129
Radiology Lab.....129
Dark Room.....129
Physiology Lab.....129
Impact Lab.....130
Impact Lab and Instrumentation Room Electronics.....130
4.13 Instrumentation Surgery.....131
Nine-Accelerometer Head Plate.....131
Sternal Mounts.....131
Rib Mounts.....131
Thoracic Vertebral Mounts.....131
Vascular Repressurization.....133
Pulmonary Repressurization.....135
Trachea Tube.....135
4.14 Trial Test.....135
Timing.....137
Equipment.....138
Linear Pendulum Impact Device.....138
Load Plate.....139
UMTRI Pneumatic Ballistic Impact Device.....139
Data Handling.....142
Pressure Measurement.....142
Photokinemetrics System.....142
4.15 Impact Testing.....144
4.16 Post-Test Autopsy.....144
4.2 Data Analysis and Final Report.....145
4.21 Photokinemetrics.....145
4.22 Frame Fields.....146
Frenet-Serret Frame.....146

Principal Direction.....147
4.23 Transfer Function Analysis.....148
4.24 Statistical Measures.....149
Auto-Correlation Function.....149
Cross-Correlation Function.....150
Coherence Function.....151
4.25 Pressure Time Duration Determination.....151
4.26 Force Time-History Determination....152
4.27 Force Deflection Measurement.....153

5.0 RESULTS.....154

6.0 DISCUSSION.....166
6.1 First Series Force Time-History.....166
6.2 First Series Acceleration Time-History.....167
6.3 First Series Impact Response.....173
6.4 First Series Secondary Direction of Acceleration.....181
6.5 First Series Transfer Functions.....182
6.6 First Series Damage Response.....187
6.7 Third Series Response.....189
6.8 Third Series Force Time-History.....190
6.9 Third Series Acceleration Time-History.....193
6.10 Third Series Impact Response.....200
6.11 Transfer Functions.....203

7.0 CONCLUSIONS.....204

8.0 REFERENCES.....209

9.0 APPENDIX B: TEST PROTOCOL.....B1

10.0 APPENDIX D: ANTHROPOMETRY.....D1

11.0 APPENDIX E: THORACO-ABDOMINAL SERIES DATA.....E1

LIST OF FIGURES - THORACO-ABDOMINAL SERIES

Figures

1 The Thoraco-Abdomen.....117

2 First Series Initial Conditions.....123

3 Second Series Initial Conditions.....125

4 Third Series Initial Conditions.....126

5 Accelerometer Mounting Platforms.....132

6 Abdominal Vascular Repressurization.....134

7 Pulmonary Repressurization.....136

8 Linear Pendulum Impact Device.....140

9 Load Plate.....141

10A UMTRI Pneumatic Ballistic Pendulum Impact Device.....143

10B Steering Wheel Angle.....143

11 Comparison of First-Series Force-Time Waveform...168

12 First Series Acceleration Time-History R4L - Test 82E006.....170

13 First Series Farside Lag between Peak Force and Peak Acceleration.....172

14 First Series Frontal Thoracic Tap Principal Direction Triads.....174

15 First Series 45° Thoracic Tap Principal Direction Triads.....175

16 First Series Lateral Thoracic Tap (Arms Down) Principal Direction Triads.....176

17 First Series Lateral Thoracic Tap (Arms Up) Principal Direction Triads.....177

18 First Series Impedance Angle for Nearside Impacts 82E043, 82E045, and 82E046.....179

19 First Series Impedance Angle for Farside Impacts.180

20 First Series Secondary Direction of Acceleration Impedance Characteristics..183

21 First Series Farside/Nearside Impact Transfer Functions.....185

22 First Series Mechanical Impedance for 8.5 m/s Velocity Impact Principal Direction Triad.....186

23 First Series Transfer Function for R4R/R4L Triax.188

24 Reconstruction of Digitization of High-Speed Film for Third Series Test 82E131B.....191

LIST OF TABLES - THORACO-ABDOMINAL SERIES

Tables

1 THORACO-ABDOMINAL SERIES BIOMETRY.....128

2A FIRST SERIES INITIAL CONDITIONS.....155

2B SECOND SERIES INITIAL CONDITIONS.....156

2C THIRD SERIES INITIAL CONDITIONS.....156

3 FIRST SERIES LOW-VELOCITY THORACIC TAPS - ACCELEROMETER RESPONCE PEAKS (G's).....157

4 FIRST SERIES HIGH-VELOCITY THORACIC IMPACTS - ACCELEROMETER RESPONSE PEAKS (G's).....159

5 FIRST SERIES PEAK FORCES.....160

6 FIRST SERIES HEAD RESPONSE SUMMARY.....160

7 PEAK PRESSURES.....161

8 SECOND SERIES THORAX DROP ONTO LOAD PLATE ACCELEROMETER PRESONSE PEAKS (G's).....162

9 THIRD SERIES KINEMATIC TEST SUMMARY.....163

10 RESEARCH PROGRAM AUTOPSY SUMMARY.....164

CHAPTER 2

EXPERIMENTAL DATA FOR DEVELOPMENT OF FINITE ELEMENT MODELS - THORACO- ABDOMEN

Contract No. DOT-NHTSA-C-HS-7-01636 UM Acct. No. 015651

1.0 INTRODUCTION

The research program, Experimental Data for Development of Finite Element Models, involved data gathering on the kinematic response of three human cadaver subsystems: 1) the thorax, 2) the head, and 3) the pelvis. Information on injury response as well as the relationship between impact parameters and the resulting injury are presented. Each impact target investigation subsystem is presented as a self-contained chapter in this final report. This chapter presents the thorax series, Chapter 1 presents the head series, and Chapter 3 presents the pelvis series.

The research program utilized 14 cadavers in 68 dynamic impact tests. For the thorax subsystem experiments, 11 subjects received a total of 41 impacts; for the head series, 6 subjects received a total of 14 impacts; and for the pelvis series, 10 subjects received a total of 13 impacts. The thorax experiments were supplemented with static three-point bending tests on rib specimens from 5 of the same dynamically-tested cadavers.

Injuries to the thorax and upper abdominal regions follow head injuries as the second most frequent cause of death [43][1]. Of these, injuries to the heart and its superior vessels, notably to the aorta, and injuries to the spleen or liver and their vessels are especially significant. Clinical and experimental evidence have shown that major sites of aortic injury were at points of aortic tethering and commonly

---

[1]Numbers in parentheses denote references at end of paper.

involve lacerations with a transverse orientation [118]. Although there have been several theories about the mechanisms of aortic injury,[2] one suggested that increased blood pressure, secondary to chest compression or to the hydrodynamic effect of acceleration, stresses aortic tissue until explosive rupture [53,118]. However, modelling stresses in a cylindrical model inflated by pressure implied the resultant injury would be a longitudinal rather than a transverse laceration [40]. A transverse laceration, in such a model, would not be expected because materials testing of aortic tissue had shown that the transverse strength was only 20% greater [68-70,118]. However, if increased blood pressure produced a local ballooning of the aorta into a spherical shape in which transverse strength would be less than longitudinal strength, a transverse laceration would be expected [70]. It has been suggested that increased blood pressure during thoraco-abdominal impact cannot be the only mechanism of aortic injury. Impact testing has shown that while high blood over-pressures resulted in injury, lower pressures resulted in greater injury depending upon differing thoraco-abdominal impact sites [77,118]. Additional mechanisms of aortic injury probably involve displacement which increases strain at tethering points [96,125,131] and compression [11,96,107], which also increases tissue strain, as well as stresses induced by changing hydrodynamic pressures [77,116]. Disease processes also seem to make the aorta more vulnerable to injury during thoraco-abdominal impact conditions [15,20,67]. The response of the heart and

---

[2] See especially references 2,4,11,13,15-18,20,22,28,36,38,41,44,53, 60,67-70,77,89.

aorta during impact were affected by direct contact with the diaphragm, the thoraco-abdominal wall and the lung tissue [101].

One of the most common physiological responses to blunt abdominal impact is hypovolemic shock due to the laceration of blood vessels, and subsequent intraperitoneal bleeding [83]. A wide range of hepatic injuries have been clinically observed and defined. At one extreme are complex rupture injuries of the hepatic parenchyma and laceration of the hepatic and portal veins. These injuries are almost invariably associated with shock at the time of initial presentation and are generally fatal [62]. In contrast, some AIS 2-3 hepatic lacerations will have stopped bleeding by the time of operation [1,83].

The extensive literature on abdominal trauma addresses many of the mechanical and physiological processes that take place during blunt impact to the thoraco-abdomen, yet still leaves many questions unanswered.[3] Living human response to blunt abdominal impact has been modelled with both cadaver and animal surrogates [62,110].

In one study of hepatic injury in which cadaver livers were injected with barium to reproduce their vertura turgor and then dropped from varying heights, the results showed that 0.3 N-M of energy produced capsular tears and 2.8-3.4 N-M were needed to produce bursting injuries [62]. Apparently, turgidity in ex-vivo livers significantly influences injury [62]. Isolated, perfused ex-vivo non-human primate livers have been subjected to controlled blunt impact and the results compared to those produced by blunt upper and lower abdominal impact to cadaver animals [114]. 3.3 N-M of energy was needed to produce and AIS 3 liver injury in an intact animal, while only 1.4 N-M of energy was needed to

---

[3]See references 29,30,62,90,95,127.

produce a similar injury in the directly exposed liver [114]. As might be expected, when impact was directed to the lower abdomen, much higher forces were necessary to create a liver injury similar in severity to that produced by upper abdominal impact [101]. Longitudinal lacerations of the liver were associated with liver displacement in both the right-left and inferior-superior directions [83] without severe thoracic compression. During impacts of 12 ms or less, the hepatic system was observed to act as a deformable structure with little response attributable to rigid body motion, and AIS-rated degree of injury was lower in unrepressurized postmortem subjects than in live, anesthetized animal subjects [83].

Using animals and human cadavers as surrogates, several biomechanical studies of blunt thoracic impact have been carried out in an attempt to determine the kinematic and the injury response associated with thoracic trauma. The information obtained from these experiments has been used to correlate impact parameters to injury patterns and has also been the basis of mathematical and physical models known as anthropomorphic test devices. Through these efforts a better understanding of the mechanisms of thoracic injury may be achieved. Several studies have used this approach to determine the mechanisms of thoracic injury [2,13-14,30,33,49,56-57,65-67,73,78,83, 89,91,98,103,105,116,118,122,130,143,146].

Nahum, Kroell, et al. [64-67, 89-91] gathered kinematic and injury response data on cadavers subjected to blunt anterior-posterior sternal impact and correlated the computed response parameters. Maximum acceleration and the severity index for the sternum and spine had an inverse correlation for a given type of impact; chest deflection,

conversely, was found to correlate directly with the degree of injury (AIS). Robbins, et al. [116] used sled impacts to generate blunt thoracic impact data from both cadavers and non-human primates. Thoracic accelerometer data were found to provide a good basis for generating analytical functions for the prediction of injury. These and other thoracic impact data were used by Eppinger, et al. [28-30] to formulate a methodology for injury prediction based solely on acceleration response data. In addition, a study by Nusholtz, et al. [98] investigated the response of cadavers as well as live and postmortem non-human primates to blunt lateral thoraco-abdominal impact, resulting in additional kinematic and injury response data.

Eppinger and Chan [29] utilized an approximate finite impulsive response (AFIR) characterization of the human thorax to model thoracic acceleration response in lateral impacts. The left and right upper rib acceleration response was modeled from both rigid wall and pendulum impacts and compared with good agreement to actual impact data. It was suggested that the simulated digital impulsive response signature could be used in conjunction with lateral impact injury criteria to identify impact conditions which would minimize the severity of trauma and lead to improved passenger protection in automobiles.

Kallieris, et al. [56] compared acceleration response to damage response for ten cadavers in lateral impact tests against rigid and cushioned barriers. The reproducibility of the kinematic response observed by these authors prompted the suggestion that a single anthropomorphic test device might be representative of the kinematic response of a large section of the population with respect to lateral

impacts, but other independent physical factors would be necessary to ascertain the concomitant injuries.

2.0 ANATOMICAL CONSIDERATIONS - The torso, between the base of the neck and the hip joint area, includes the thorax above and the abdominal-pelvic region below. The abdomen and the pelvic cavities, although frequently described separately, are continuous from one to another, with bony landmarks used as reference points to separate the two (Figure 1).

The human thorax is bounded laterally by the rib cage, in back by the twelve thoracic vertebrae, and in front by the sternum. The first rib is covered by the medial end of the clavicle so that the inlet to the thorax is relatively narrow, being approximately 5 by 8 cm. The outlet of the thorax is closed by the respiratory diaphragm which has openings through it for the passage of the aorta, esophagus, and the inferior vena cava.

The thorax is divisible into three units: the right and left plural cavities and the central group of structures called the "mediastinum." The mediastinum is bounded by the vertebrae posteriorly, and the deep surface of the sternum anteriorly. Laterally, the reflections of the plura from the posterior body wall attach anteriorly to the sternum and costal cartilages. Structures pass to and from the lungs through the plura. Above and below the mediastinum laterally are the passageways for the great vessels to and from the heart. Running through the center of the mediastinum are the trachea and esophagus.

The heart is in the pericardial sac, a tough fibrous membrane that completely encloses it. The pericardial sac attaches to the roots of the great vessels superiorly. The base of the pericardium is fused to

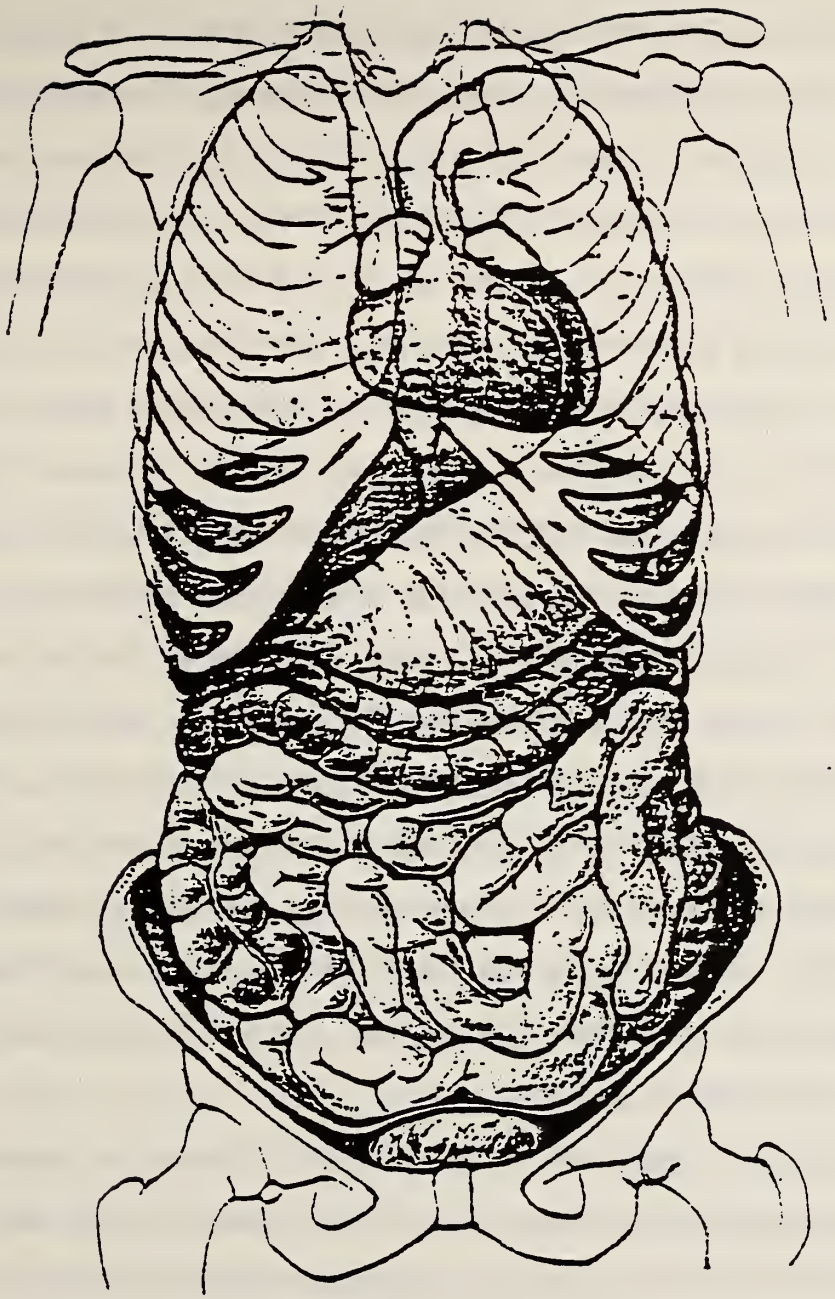

Figure 1

The Thoraco-Abdomen

the central tendinous area of the respiratory diaphragm so that the heart and pericardial sac are not noticeably displaced during forced respiration. The heart is fairly well-tethered in position by its pericardial attachments. Above the aorta and the superior vena cava, are tributaries or branches. All of these structures and the other structures of the mediastinum are surrounded by and packed with connective tissue and a modicum of fat. Because the connective tissue surrounds and attaches one structure to another, there is a relatively stable tether mechanism in the superior mediastinum above the heart. Posteriorly, the pulmonary vessels also secure the heart within the pericardial sac. The arch of the aorta passes vertically upward and, at approximately the costal cartilage area, arches posteriorly to the left, so that the descending thoracic aorta is found on the left side of the bodies of the thoracic vertebrae. Throughout its entire course, the descending aorta is firmly attached beside the vertebrae. This tie-down mechanism consists of the intercostal arteries that arise from the descending aorta and pass through all the intercostal spaces, the dense connective tissue adjacent to the descending aorta, plus the aorta's overlaying parietal plura that passes from the ribs posteriorly to form the lateral mediastinal wall.

Since the descending aorta is rigidly attached in place by the structures mentioned above, under impact conditions the aorta and heart are unable to move as a unit. The most frequent site of a tear of the aorta is at the junction of the arch in the descending portion where there is a ligament that ties the aorta to the pulmonary artery--the ligamentum arteriosum. It is usually just distal to this attachment

point, the undersurface of the aortic arch, where most aortic tears are found.

The abdomen is separated from the thoracic cavity by the thin muscular respiratory diaphragm. The diaphragm is a double-cupula structure when seen in the anterior-posterior view. In sagittal view, it is a domed structure. All of the abdominal structures are found beneath the diaphragm, in front of the posterior body wall, extending to the urogenital diaphragm at the base of the pelvis. The abdominal cavity is enclosed by muscles that surround it, and posteriorly by the lumbosacral vertebral column. The anterior abdominal wall is a simple plane consisting chiefly of a laminated muscular wall--muscles that are sheet-like, with heavy aponeuroses. Anteriorly, there are three flat muscles--the external and internal abdominal oblique muscles, and the transverse abdominus muscle. These form the anterior, lateral, and partially, the posterior body wall. Anteriorly, just off the midline, are two vertical, fairly heavy muscles, the rectus abdominus muscles.

The inner aspect of the abdominal wall is lined by the peritoneal sac. Within the abdomen there are solid and hollow organs. The hollow organs are the components of the gastrointestinal tract--the stomach, duodenum, ileum, jejunum, colon, rectum, and the anal canal. Also, the urinary bladder and uterus are considered hollow organs. The solid organs are the pancreas and kidneys, the ovaries in the pelvic cavity, the spleen and liver, and the suprarenal glands.

The stomach is the enlargement of the very short abdominal portion of the esophagus. It is found in the upper half of the abdomen with the spleen behind and to its left, and the liver to its right. The gastrointestinal tract, when empty, is a fairly tight muscular tube;

however, when filled with food, feces or gas, it is an extremely thin-walled structure and perhaps vulnerable to trauma. The blood vessels to most of the gastrointestinal tract pass from the abdominal aorta, located against the anterior vertebral bodies, and through the mesentery, a thin sheet-like membrane, which when significantly displaced, can easily be torn, rupturing the enclosed blood vessels.

Extending between the stomach and the liver is a very thin filamentous peritoneal layer, the gastro-heptic ligament. At its lower free end, this peritoneal sheet surrounds the blood vessels that pass to and from the liver, the associated autonomic nerves, and the common bile duct. This portion of the gastro-hepatic ligament actually attaches to the upper portion of the duodenum and is most properly termed the "hepato-duodenal" ligament. It extends from the hilum, the entranceway of the liver, to the posterior body wall at the right side of the vertebral column near where the duodenum is affixed.

The liver, a solid blood-filled organ, is approximately 1/40th of the total body weight. It is located in the upper-right quadrant of the abdomen and is firmly attached to the underside of the diaphragm by very short reflections of the peritoneum covering the liver--the liver capsule. These thin peritoneal attachments are less than a centimeter long, adhering directly to the undersurface of the liver. With the rise and fall of the right dome of the diaphragm during respiration, the liver moves in synchrony with breathing. Anteriorly, laterally, and posteriorly, the lower ribs cover the major portion of the liver.

The spleen is a very small blood-filled organ, about the size of a fist, which lies against the posterior body wall, on the diaphragm at the 9th, 10th and 11th rib level. It is basically free to move, since

it possesses an encapsulation of a peritoneum, the splenic capsule, and all of its blood vessels enter and leave the spleen through the hilum, which is attached to the posterior body wall.

Both the liver and spleen are anatomically abdominal organs. However, from an anterior view, the liver is almost completely housed and protected by the lower ribs, as is the spleen on the opposite side of the body. Thus, functionally, in an impact event, the liver and the spleen react as thoracic soft-tissue organs protected by the rib cage rather than as abdominal organs. Not infrequently, impacts to the lower rib cage will cause the underlying liver to rupture. Similarly, impacts to the left side, especially to the left posterior rib area, will rupture the spleen. A further detailed description of thoracic and abdominal anatomy and common injuries can be found elsewhere [1,51-52].

3.0 GOAL OF THORACO-ABDOMINAL SERIES IMPACT TESTING

The thorax impact experiments consisted of three test series which used the unembalmed cadaver as human surrogate. All test series were guided by a detailed test protocol[4] [1-152]. Gross kinematic motion was documented on high-speed film and injury/damage was assessed by gross autopsy examination.

In the first test series, 5 male unembalmed, represurrized cadavers were subjected to a series of three to five low-energy impacts in three initial positions (frontal, 45°, and lateral) to obtain basic kinematic information, plus a single high-energy lateral thorax impact to gain additional kinematic and damage response data. These subjects were

---

[4]The protocol for the use of cadavers in this study was approved by the University of Michigan Medical Center and followed guidelines established by the U.S. Public Health Service and those recommended by the National Academy of Sciences, National Research Council.

instrumented with an array of 18 thoracic accelerometers to measure the impact response of the thorax, and with 9 accelerometers mounted on a single plate on the head to determine three-dimensional motion. Triaxial accelerometer clusters were rigidly attached to the right and left fourth ribs, upper sternum, and T1 and T12 thoracic vertebrae. Single accelerometers were affixed to the right and left eighth ribs and lower sternum. The subject was placed in a restraint harness which was suspended from an overhead pulley system (Figure 2). The head was suspended in a natural position by a rope tied to a head harness, threaded through an electronic ropecutter, and tied to the overhead pulley. Prior to impact, the electronic ropecutter was activated so that the subject was unrestrained at impact. The vascular and pulmonary systems of the thoraco-abdomen were repressurized prior to impact. The impacting device was a 25 kg linear or pneumatic ballistic pendulum. The subject was struck with a free-traveling mass (25 kg) which was fitted with a 15 cm round rigid metal surface. For different impact tests, various materials were affixed to this surface to produce different force-time and load distribution.

In the second test series, one male unembalmed cadaver was dropped onto a load plate five times, and two others, once. The cadavers were instrumented with nine accelerometers mounted on a single plate on the head, plus three triaxes on the thorax (thoracic vertebrae T1, T6 and T12). Each subject was suspended by two primary harness systems, connected to ceiling hoists by individual ropes threaded through ropecutters (Figure 3). The ceiling power hoists were perpendicular to the long axis of the subject, permitting positioning of the hoists anywhere within the horizontal plane, thus facilitating arrangement of

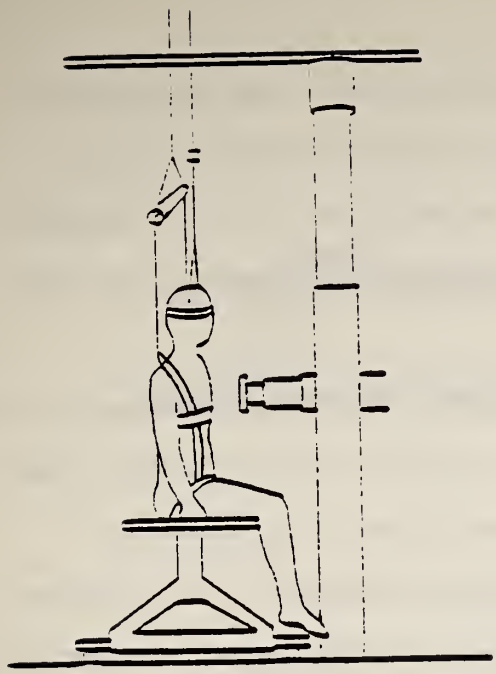

Frontal

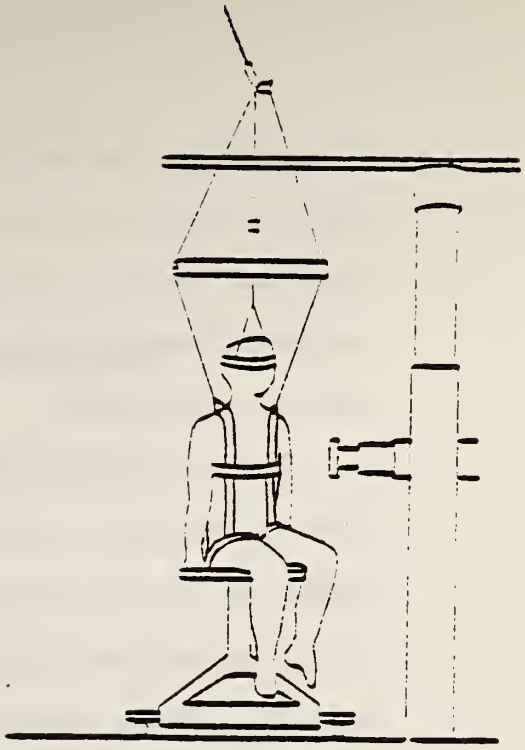

45° degree

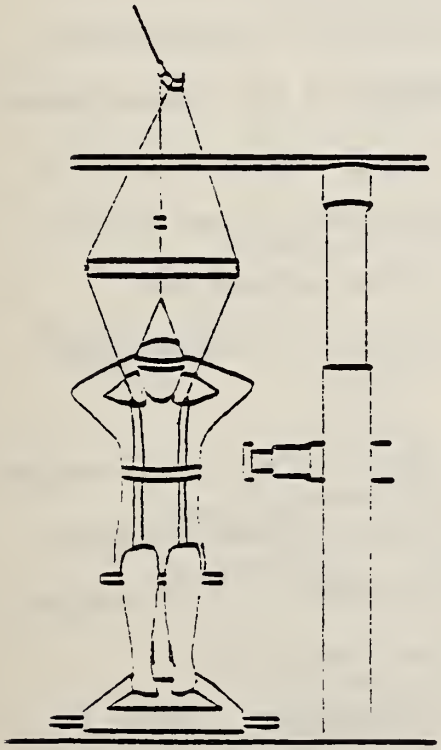

Lateral (arms up)

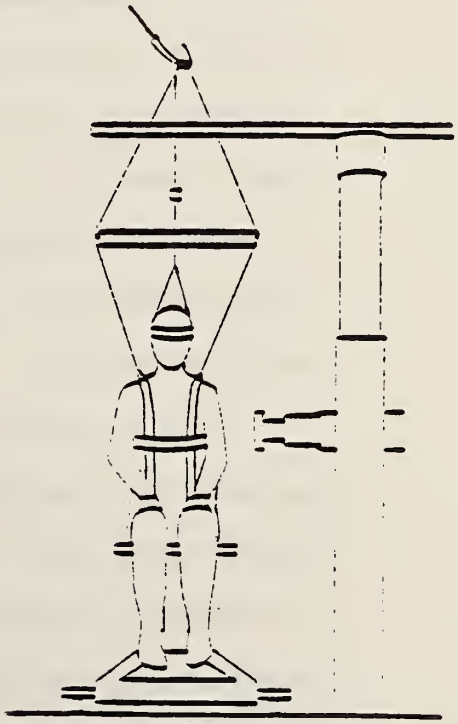

Lateral (arms down)

Figure 2

First Series Initial Conditions

the subject in variable pre-impact configurations. The timing control system fired the ropecutters, permitting a long-duration horizontal free-fall onto the load plate. Impact velocity was 1.2 m/s. Kinematic parameters measured included force, nine head accelerations, and nine spinal accelerations.

In the third test series, 2 unembalmed repressurized cadavers, one male and one female, were subjected to a total of three steering wheel impacts to the thoraco-abdomen, delivered by the 25 kg pneumatic ballistic pendulum impactor. A load cell was affixed to the steering column to measure the axial steering wheel assembly force. The subject was positioned seated on friction reducing clear plastic covering balsa wood blocks (Figure 4). The stationary test subject was struck at velocities up to 12 m/s. Nine accelerometers affixed to the skull measured three-dimensional motion of the head and 18 accelerometers mounted on the thorax documented impact response of the thoraco-abdomen (triaxes on T1 and T12 thoracic vertebrae, R8L and R8R ribs, and the lower sternum plus uniaxes on the upper sternum and R4L and R4R ribs). The vascular and pulmonary systems of the thoraco-abdomen were repressurized prior to impact. Vascular pressure in the descending aorta was measured.

For all three test series, the impact motion of the thoraco-abdomen was analyzed using anatomical, Frenet-Serret and Principal Direction Triad frame fields. Results are presented in terms of time-histories of the kinematic variables (accelerations, forces, velocities, displacements, pressures, auto- and cross-correlations). Impact transfer functions are presented for mechanical impedance and paired kinematic parameters.

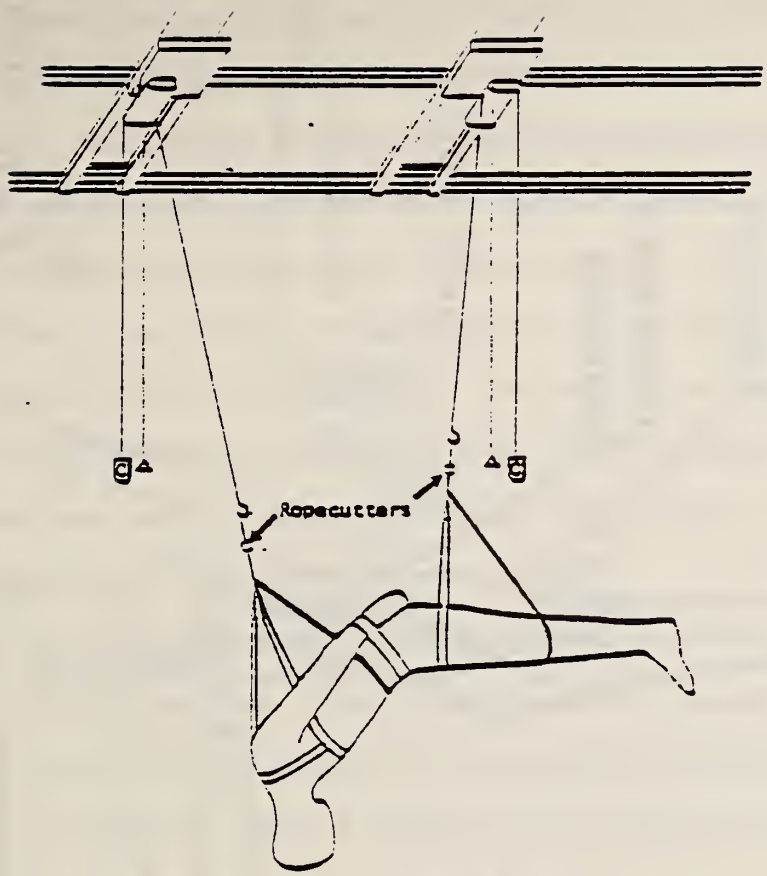

Figure 3

Second Series Initial Conditions

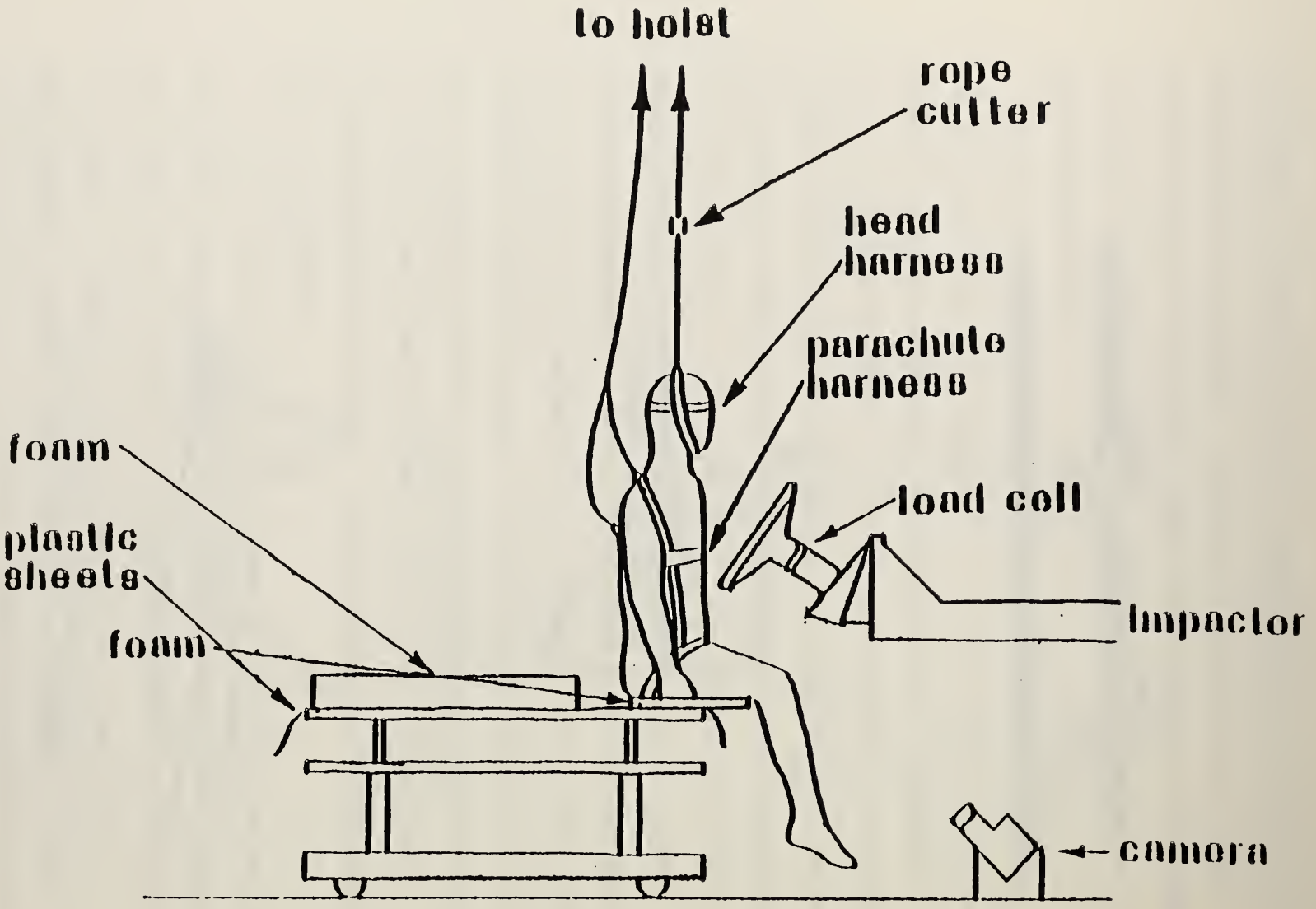

Figure 4

Third Series Initial Conditions

4.0 METHODOLOGY:

4.1 Methods and Procedures of Impact Testing:

The execution and coordination of the testing sequence is guided by the use of a detailed protocol which is included in Appendix B [1-152]. The testing sequence is outlined below and additional information about application of specific techniques to analogous biomechanics problems can be found elsewhere [2, 95-101]. Six groups of procedures are associated with the impact testing-data gathering-analysis activities. They are: 1) pre-test preparation, 2) instrumentation surgery, 3) trial test, 4) impact testing, 5) post-test autopsy and injury coding in DOT format, and 6) analysis and reporting to the sponsor.

4.11 Subjects - The eleven unembalmed cadavers, 10 male (Caucasina) and 1 female (Negro) used in these three thorax series were obtained from the University of Michigan Department of Anatomy. Table 1 summarizes the biometric data.

4.12 Pre-test Preparation - The arrival of a test subject cannot be predicted more than a half a day in advance. Generally, preparation for a test sequence begins the day a subject is received. The subject requires a day and a half of preparation, which is sufficient time to set up the impact lab and run equipment checks which include a trial test. The areas requiring special preparation are outlined below.

Morgue - Following transfer to UMTRI, cadaver subjects are stored at 4°C in coolers until subsequent use.

Table 1
Thorax Series Biometry

Cadaver Number	Age	Sex	Height cm	Weight kg	Shoulder Breadth cm	Chest Breadth cm	Waist Breadth cm	Hip Breadth cm	Chest Circum-ference cm	Chest Depth cm
000	60	M	184.0	52	31.8	27.5	29.2	25.0	80.0	17.7
020	67	M	179.8	77	33.2	32.9	24.0	36.0	101.0	25.0
040	65	M	169.0	87	35.4	33.5	32.0	33.5	101.0	25.0
060	60	M	169.8	67	34.7	29.6	23.0	28.6	88.5	23.0
079	62	M	175.8	76	34.7	34.0		31.5		
089	51	M	169.0	83	30.4	34.2		31.0		
080	44	M	171.0	72	32.5	33.8	25.0	31.4	101.0	23.6
090	51	M	180.0	68	33.3	31.9		30.0		50.1
100	60	M	182.0	77	31.4	32.0	31.3	33.9	92.3	23.0
120	20	F	162.6	46	31.0	23.6	21.9	27.2	69.7	18.5
130	57	M	175.2	73	33.5	32.4	31.9	33.9	96.5	24.7

Anatomy Lab - Sanitary preparation, anthropometry, and surgical instrumentation of the test subject is done in the Anatomy Lab. All tools, materials, and instrumentation equipment necessary to prepare the subject are constructed or laid out in advance. Included in the setup are surgical instruments, measuring equipment, gauze and toweling, accelerometer mounting hardware, modified French Foley catheters and other pressurization hardware, and clothing for the cadaver subjects.

Radiology Lab - The table and X-Ray head are positioned and a sufficient supply of film is loaded into the X-Ray cassettes. Adequate film is loaded so that the test sequence can be completed without interruption. A subject may be X-rayed here on three occasions: when it is received to check for structural integrity and surgical implants, after instrumentation to check that equipment is positioned properly and pressurization fluid can flow correctly, and when the impact testing is over, orthogonal X-Rays of the head are taken.

Dark Room - Chemicals are mixed for X-Ray developing. Labels for X-Rays are prepared. Courier forms and packaging for the 16 mm high-speed films are readied.

Physiology Lab - 16 mm high-speed films are chemically hypersensitized in an oven at 30-35°C with forming gas for 24 hours in order to obtain better image clarity. The saline-dye pressurization fluid is prepared here. Dental acrylic to be used as an instrumentation mounting medium is mixed here under a hood.

Impact Lab - Test facilities, recording equipment, accelerometers and transducers must be assembled, wired, and trial-tested. In addition, a portable cart containing surgical equipment for wiring the subject with accelerometers and transducers is prepared. Impact padding (Styrofoam and Ensolite) and support materials for the subject (balsa wood, foam, rope) are assembled near the impact pendulum or load plate. The high-speed cameras are tested and loaded with film. All electrical equipment is connected to a power source.

Impact Lab and Instrumentation Room Electronics - The input/output voltage characteristics of all analog tape channels are checked by calibration at predetermined voltage levels. The tape channel calibrations are determined when the test pulses are played back off tape through a computer routine.

All accelerometers and pressure transducers are labeled and wired through a patch panel into the Instrumentation Room. From there, the signals are passed through amplifiers if necessary and connected to their designated channels as input to the analog tape recorders. Amplifiers are adjusted for the proper gain. The accelerometer and pressure transducers must have their excitation voltages set on the amplifiers, while their piezoresistive nature requires balancing to be performed on the amplifiers. Instrumentation Room wiring cannot be completed until the timer box and the devices it operates, such as lights, high-speed cameras, and ropcutters are wired and set for the proper control, delay and run times. Final wiring is

completed in the Instrumentation Room and the system is prepared for a trial test.

4.13 Instrumentation Surgery - In the Anatomy Lab the test subject is surgically instrumented with the required test hardware. The hardware includes accelerometer mounts, vascular and cerebrospinal catheters, and a trachea tube.

Nine-Accelerometer Head Plate - The nine-accelerometer plate is installed in the following manner. A two-by-two inch section of scalp is removed from the right occipital-parietal area. Four small screws are then placed in a trapezoidal pattern in the skull within the dimensions of the accelerometer plate mount. Quick setting dental acrylic is molded around the screws to form a securing medium. The plate mount is then placed in the acrylic base. See Figure 5 for the orientation of the plate mount.

Sternal Mounts - Skin incisions expose the attachment points on the upper and lower sternum. Small nails placed in the exposed sternum form a mooring for the dental acrylic which is used as a mounting medium for the accelerometer mounts (Figure 5).

Rib Mounts - For rib mounts, incisions are made over the fourth and eighth ribs on each lateral side so that the flat part of the rib is exposed. To ensure rigidity, the mounts are fitted with pins and tied with wire to the flat surface of each exposed rib (Figure 5).

Thoracic Vertebral Mounts - Incisions are made over the T1 and T12 thoracic vertebrae. Supports for the accelerometer mounts

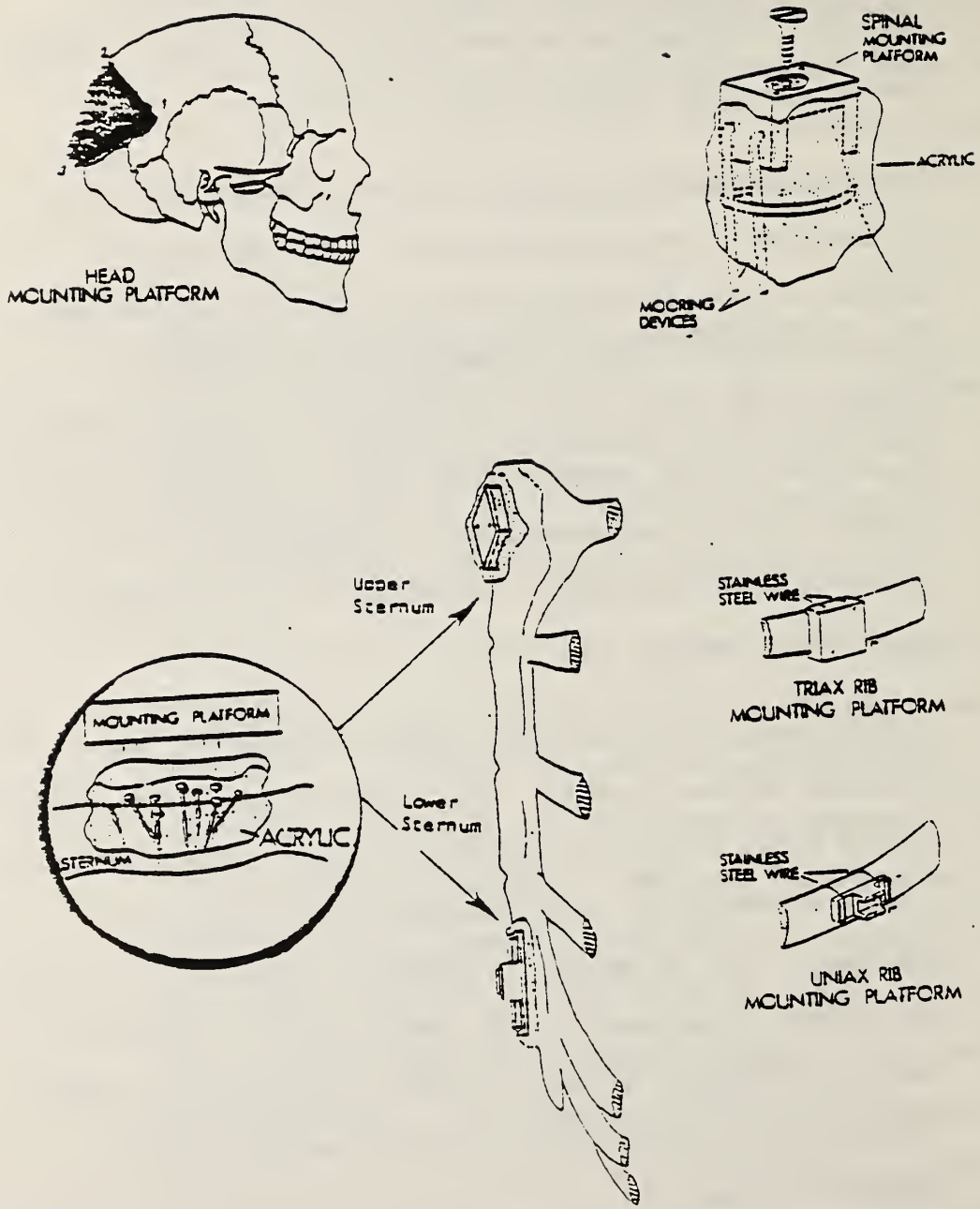

Figure 5

Accelerometer Mounting Platforms

are anchored on the lamina for each bilaterally, such that they flank the spinous process. The accelerometer mount itself is fitted over these supports and screwed directly into the spinous process. Acrylic is applied under and around the mounts to insure structural rigidity (See Figure 5).

Vascular Repressurization - The subject's abdominal vascular system is repressurized just prior to impact. A Kulite pressure transducer guided through the carotid artery, and positioned in the descending aorta just below the diaphragm, monitors both the degree of initial pressurization and the change in vascular system pressure during impact. The pressurizing fluid is introduced via the catheters through a channel in the center of the two occluding balloons. Both balloons are positioned in the aorta, one above the diaphragm, the other above the aortic termination (Figure 6).

Surgical insertion of the modified catheters follows three patterns depending on whether access through the femoral arteries is possible. Through an incision in the femoral artery, a catheter is guided up the arterial system, where the balloon occludes the aortic termination. Another catheter is guided through an incision in the common carotid artery into the descending aorta, occluding it slightly above the diaphragm. When the femoral arteries cannot be used, due to plaque accumulation, either a double balloon catheter is used to occlude the aorta below the diaphragm and at the common iliac arteries, or two catheters, one in each common carotid artery are used to occlude these same locations. Critical to

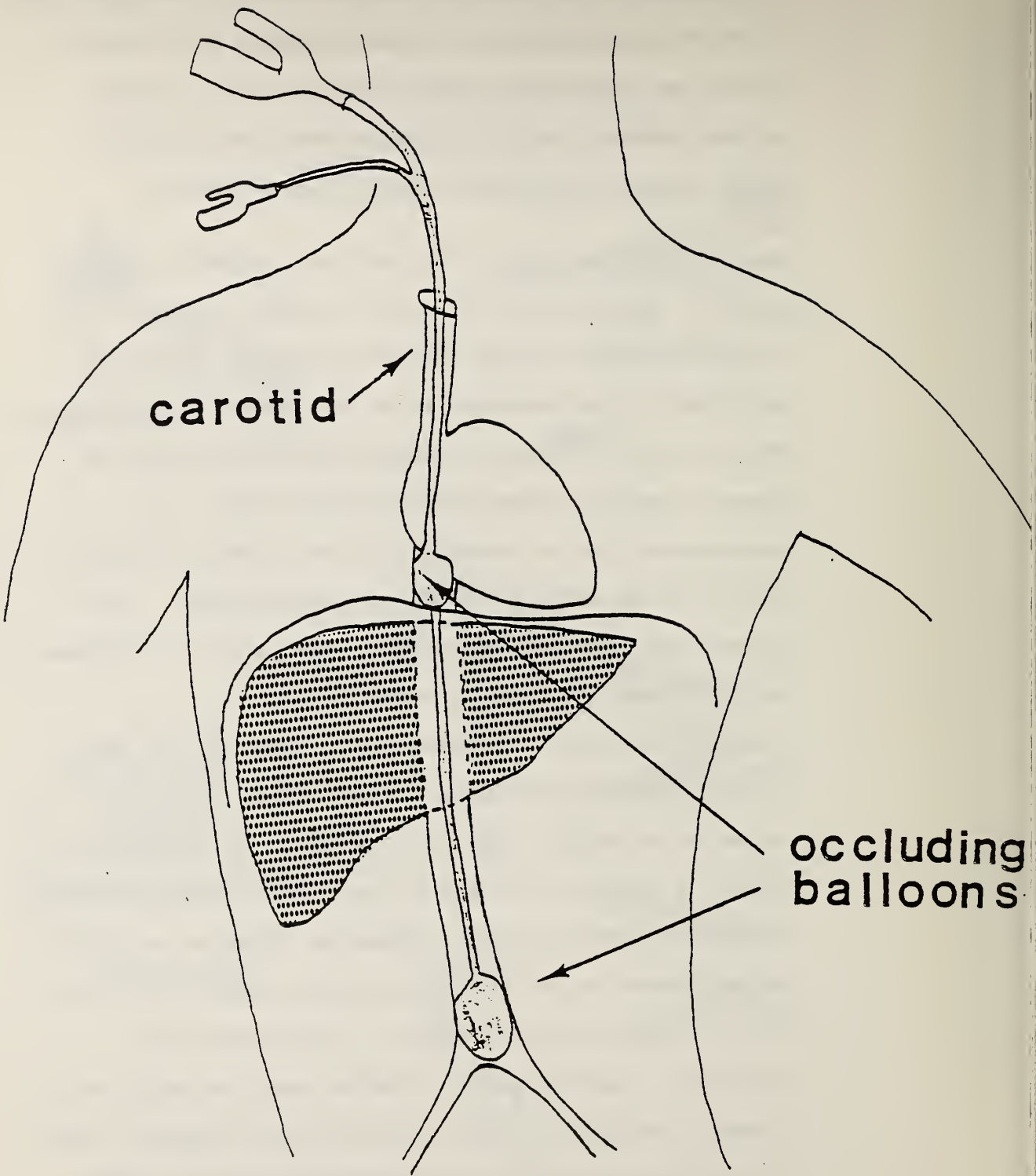

Figure 6

Abdominal Vascular Repressurization

the study is that the liver be fluid-filled before impact [72]. This is done by pressurizing the area between the two occluding balloons above normal physiological pressure. One to two minutes before impact the pressure was pulsed between 100-200 mm Hg. Immediately prior to impact the pressure was dropped to 70 mm Hg.

Pulmonary Repressurization - A tracheotomy is performed to place a tube in the trachea, which is connected to a compressed air reservoir so that the pulmonary system can be pressurized to 15 mm Hg. An Endevco pressure transducer is inserted into the tracheal tube to measure the dynamic pulmonary pressure at initial pressurization and during the change in pressure throughout the impact (Figure 7).

Trachea Tube - The trachea is cut lengthwise below the laryngeal prominence and two tie wraps are looped around the trachea. Next a polyethylene tube is inserted into the trachea and it is tied off.

4.14 Trial Test - To insure that all mechanical and electronic equipment is functioning and wired appropriately for the test design, trial tests of the equipment are performed on the day before the test, allowing sufficient time to locate and correct system defects.

Accelerometers, amplifiers, umbilical cables, and recorders are tested by suspending a rubber cylinder weighing approximately 20 pounds in front of the pendulum impactor with all of the accelerometers taped to it. A preliminary check of the accelerometers and amplifiers is made to insure proper

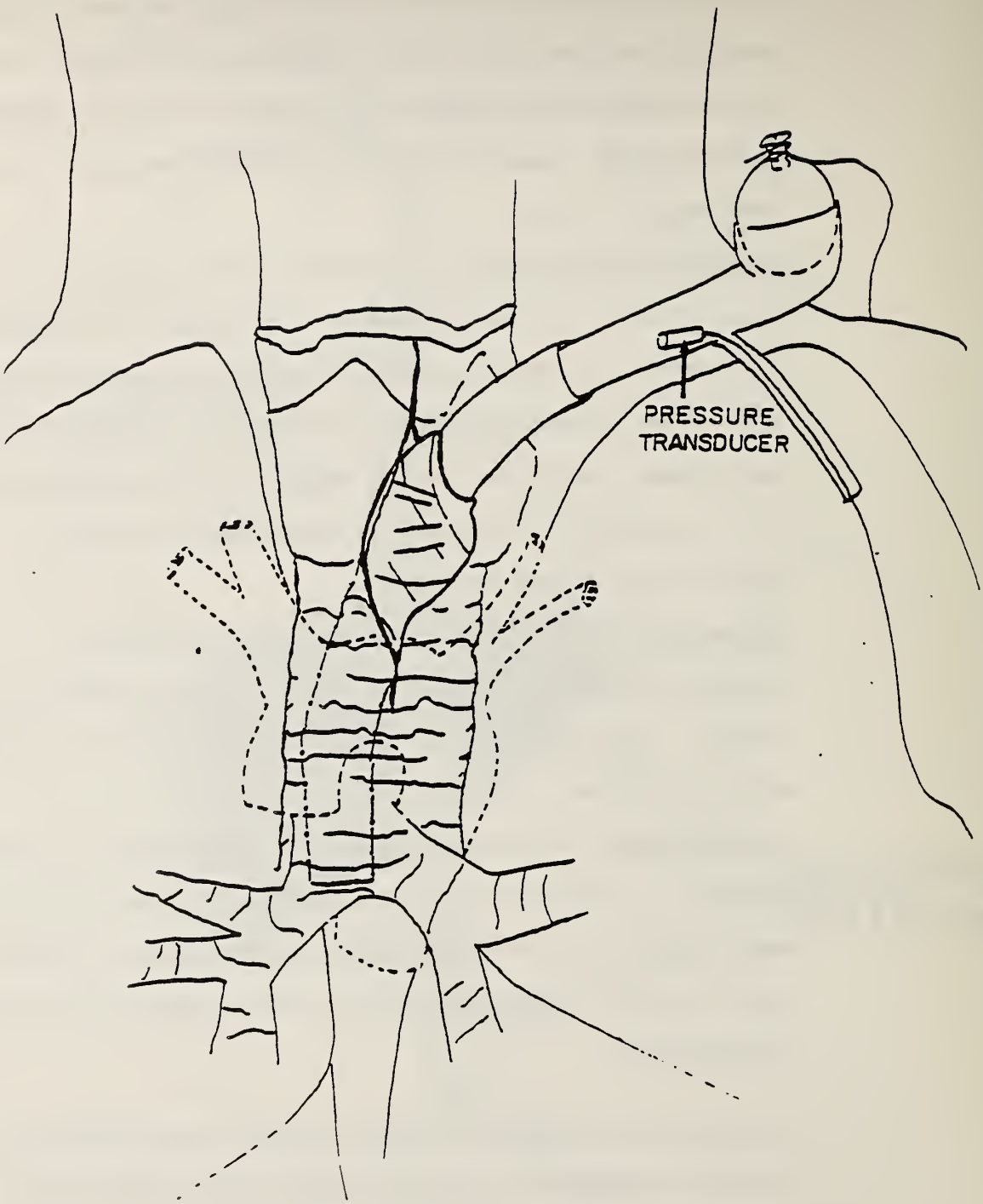

Figure 7

Pulmonary Repressurization

balancing and noise levels. The pendulum is then manually released via the impactor piston and the rubber cylinder is impacted. The signals from all accelerometers are recorded on the analog tape recorders. All channels are played back immediately on the brush chart for inspection purposes. The pendulum accelerometer is also tested in this procedure. Pressure transducers are tested individually by sending a signal directly to the brush chart recorder. The timer box, cameras, lights, ropecutter, and velocity probe are tested individually. Triaxial clusters, uniax accelerometers and pressure transducers are then labeled for their specific point of attachment to the subject and placed in protective sleeves.

Three classes of operations take place before and during impact that are necessary for the documentation of the impact event: events associated with recording of electromechanical accelerometer and transducer output, events associated with photometrics documentation, and events associated with the pendulum impactor.

Timing - The impact test event sequence is initiated by an operator-controlled manual switch and is thereafter controlled by signals generated by a specially constructed timer box. The timing requirements of the events associated with these signals are such that the lights, HyCam and Photosonics 1B cameras are synchronized so that both cameras are running at the correct speed and the test subject is fully illuminated at the time of impact. In addition, the cameras are sequenced to be

operational for the minimum amount of time. This economizes the amount of effort associated with photokinemetric documentation (changing film, etc.) and allows for a smoother running test sequence.

The recording equipment must be at operational speed before the pendulum is released. Additional events which must occur just prior to impact are the release of the subject from the restrained position and the activation of the sequencing gate. During the impact event for the first and third test series, the output of the piston accelerometer must be fit into a "corridor" or window so that the pre-impact acceleration from rest and the post-impact acceleration from end-of-stroke are not recorded. The pendulum must be released so that impact will occur within the assigned time corridor. A sychronizing contact strobe, which places simultaneous electrical and photographic signals on the analog tape and high-speed film, must occur near the beginning of impact.

Equipment - The basic test equipment included the timer box control, a signal conditioning unit for the force signal, the accelerometer-transducer patch panels, the impacting device, the high-voltage power supplies, the cameras, the photographic lights, and the restraints (hoists, ropecutter). Each piece that played a significant role in the data acquisition was described below.

Linear Pendulum Impact Device - The UMTRI linear pendulum impact device, using a free-falling pendulum as an energy

source, struck a 25 kg impact piston. The piston was guided by a set of Thomson linear ball bushings. Axial loads were calculated from data recorded using a Setra Model 111 accelerometer (Figure 8).

Impact conditions between tests were controlled by varying impact velocity and the type and depth of padding on the impactor surface. Piston velocity was measured by timing the pulses from a magnetic probe which sensed the motion of the targets on the piston.

Load Plate - Thorax drop impacts utilized the UMTRI load plate. The load plate used to measure axial and shear forces in these impact tests consisted of a metal platform which rested on four piezoelectric force transducers, one at each corner (Figure 9). At the base of each transducer was a ball bearing, which could rotate but was constrained from movement in the horizontal plane by a plexiglass template. The output signals from the transducers underwent a series of processing steps prior to being recorded on analog tape.

UMTRI Pneumatic Ballistic Pendulum Impact Device - The impact device consisted of a 25 kg ballistic pendulum mechanically coupled to the UMTRI pneumatic impact device (cannon) which was used as the energy source. The cannon consisted of an air reservoir and a ground and honed cylinder with a carefully fitted metal-alloy piston. The piston was connected to the ballistic pendulum with a nylon cable. The piston (Figure 10A) was propelled by compressed air through the cylinder from the air reservoir chamber, accelerating the ballistic pendulum to

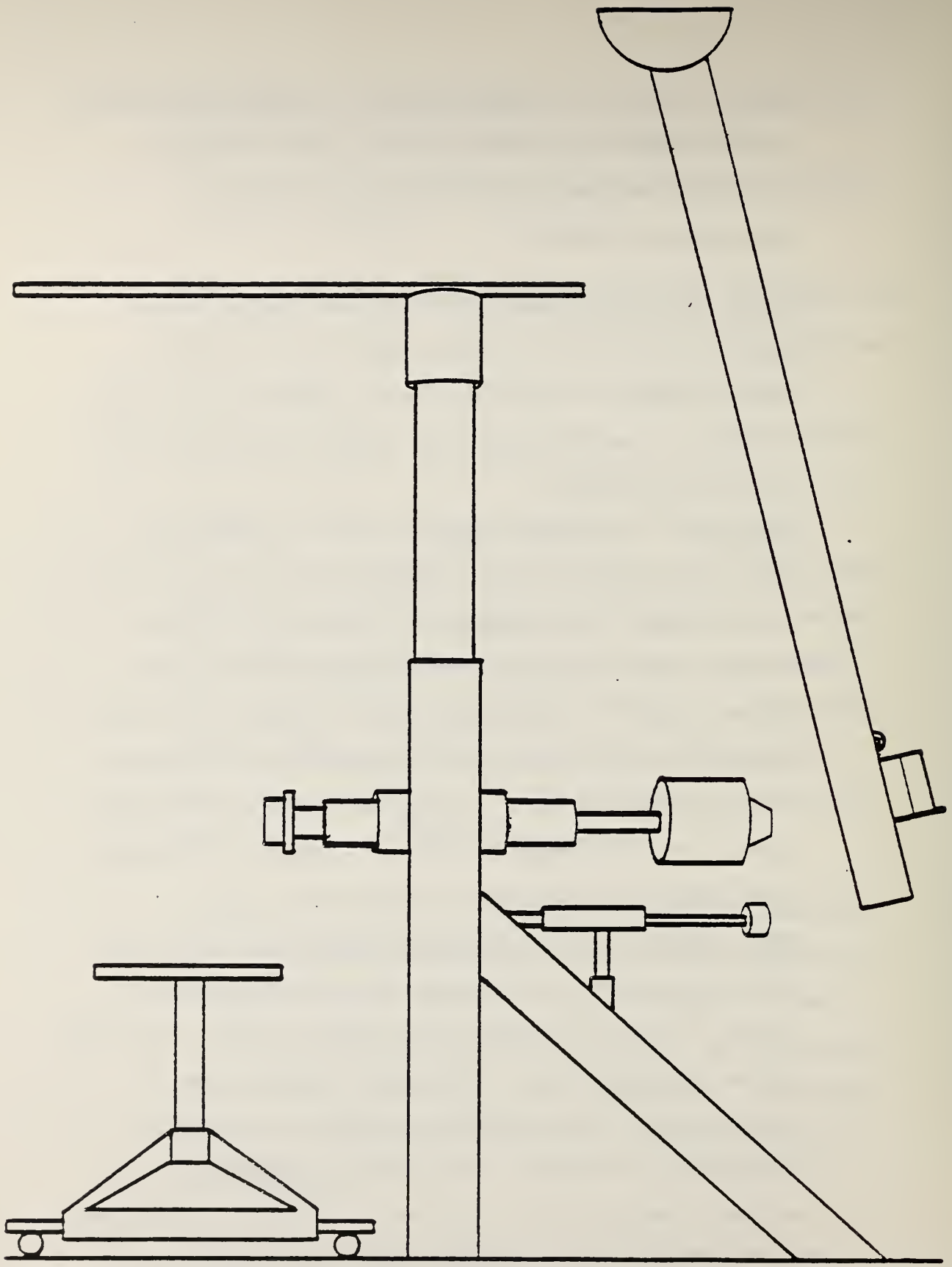

Figure 8

Linear Pendulum Impact Device

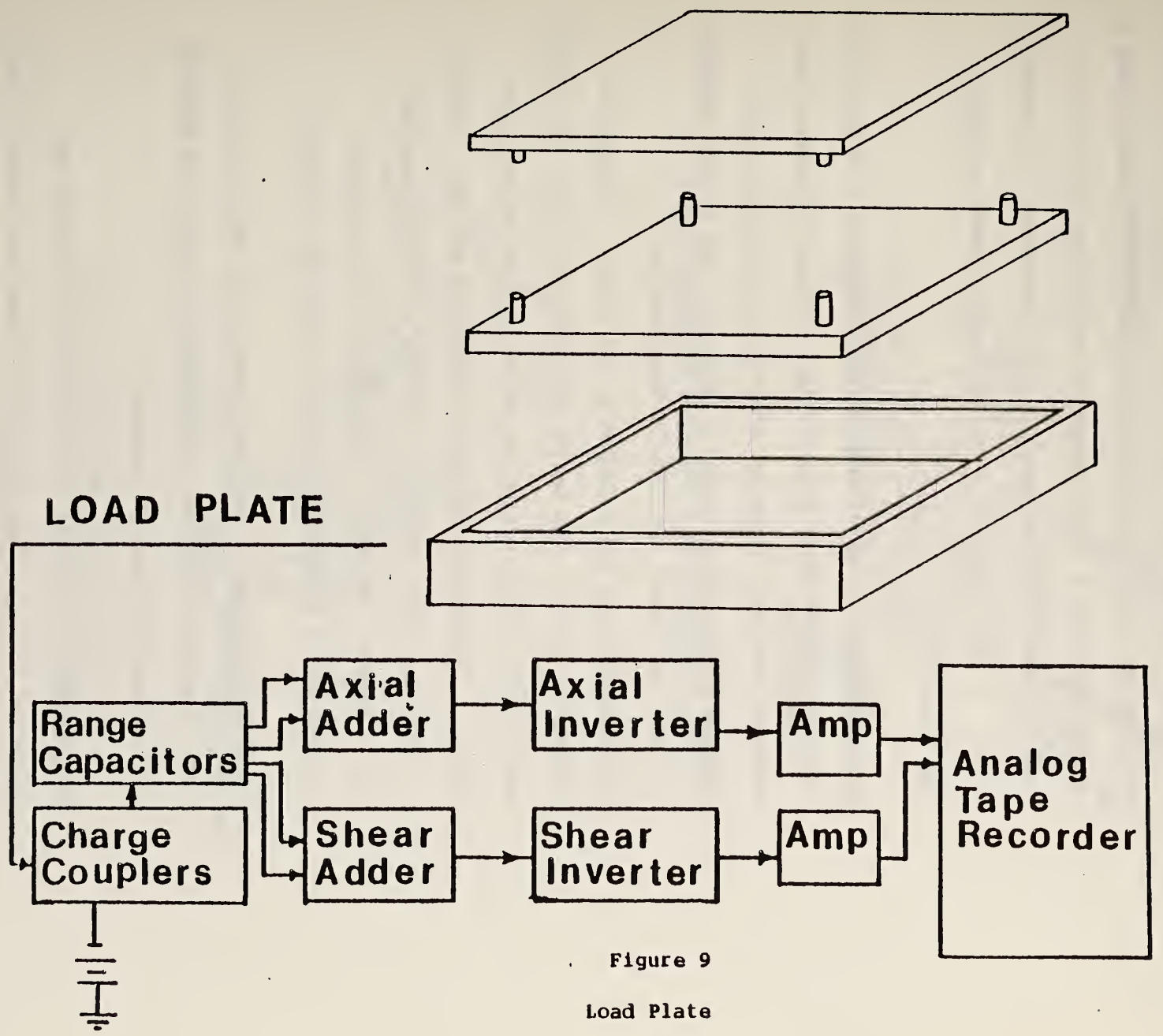

Figure 9

Load Plate

become a free-traveling impactor. The ballistic pendulum was fitted with an inertia-compensated load cell which was rigidly mounted to a steering wheel.

The steering wheel angle (defined as the angle formed between a vertical line and a line tangent to the top and bottom of the steering wheel) could be changed in 5° increments in a range of 0°-45°. A 1981 Chevrolet Citation steering wheel was used. (See Figure 10.)

Data Handling - All accelerometer and transducer time histories (pendulum force, impact acceleration, vascular pressures, nine head-accelerations, eighteen thoracic accelerations) were recorded unfiltered on either a Honeywell 7600 FM Tape Recorder or a Bell and Howell CEC 3300/FM Tape Recorder. A synchronizing gate was recorded on all tapes. All data was recorded at 30 ips. The analog data on the FM tapes was played back for digitizing through the proper anti-aliasing analog filters. The analog-to-digital process for all data, results in a digital signal sampled at 6400 Hz equivalent sampling rate. The raw transducer time histories were digitally filtered with a Butterworth filter at 1000 Hz, 6th order.

Pressure Measurement - Vascular pressure was measured with a Kulite pressure transducer and pulmonary pressure was measured with an Endevco pressure transducer.

Photokinemetrics System - The motion of the subject was determined from the high-speed (1000 frames per second) film by following the motion of single-point phototargets on the thorax

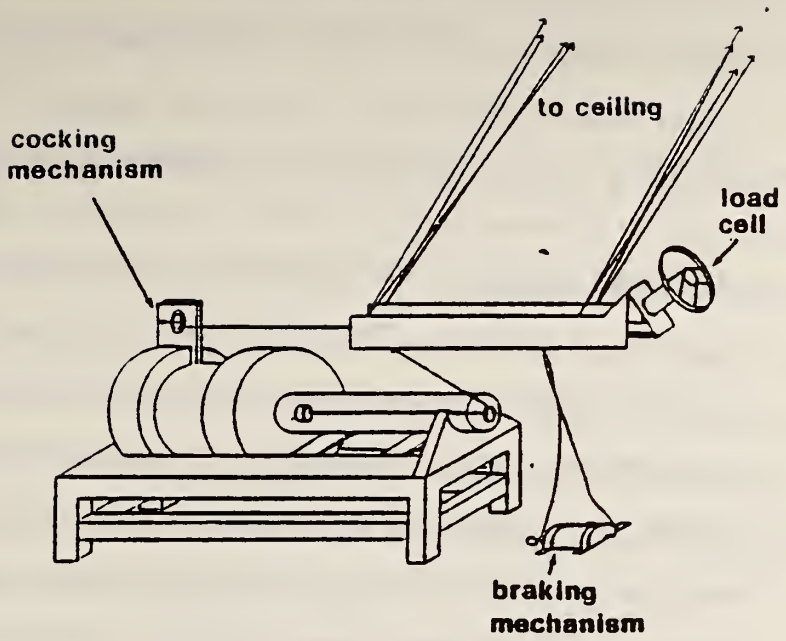

A. UMTRI Pneumatic Ballistic Pendulum Impact Device

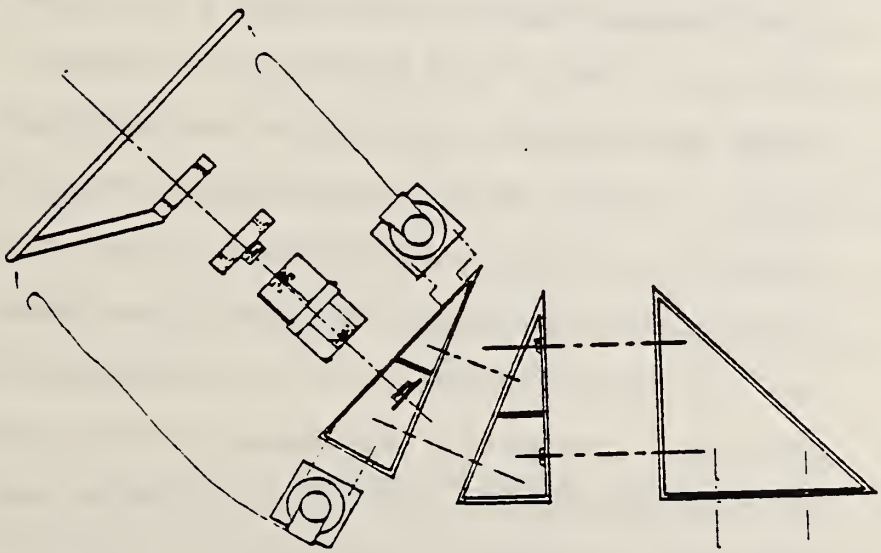

Steering Wheel Mounting System
Wedges of different sizes can be inserted to vary steering wheel angle in 5 degree increments.

B. Steering Wheel Angle

Figure 10

and on the impactor piston. For selected impacts, a Hycam camera operating at 3000 frames per second provided a close-up lateral view of the thorax. For these impacts, the Photosonics provided a overall lateral view at 1000 frames per second.

4.15 Impact Testing - The unembalmed cadavers were stored at 4°C prior to testing. The cadaver was X-Rayed as part of the structural damage evaluation and anthropomorphic measurements were recorded. Next, the cadaver was instrumented, sanitarily dressed and transported to the testing room where the accelerometers and pressure transducers were attached. The subject was positioned. Next, pretest X-rays and photographs were taken. Pressurization was checked. Then the subject was impacted. See Table 1 for a summary of initial conditions.

4.16 Post-Test Autopsy - After impact testing, the test subject was brought to the Anatomy Lab for autopsy. A gross autopsy was performed. All injuries were recorded in the test protocol on charts and brief descriptions were also written in the protocol. 35 mm still photographs in color and in black and white were taken of all significant tissue damages. These were later coded according to the AIS-80 scheme and reported in DOT format. Occasionally, knowledgeable medical professionals were consulted when more descriptive information might better characterize the observed tissue damages than the AIS-80 coding permits. All of this information was used in the analysis and reconstruction of mechanisms of injury and was included in the written reports to the sponsor.

4.2 Data Analysis and Final Report - The techniques used to analyze the results are outlined below. Additional information can be found in [73-74,95-101].

4.21 Photokinemetrics - Analytical photogrammetry is used in these experiments to describe the geometry of anatomical structures and their motion in the laboratory reference frame. The objective space coordinates of points of interest were obtained once the coordinates of well-defined points in an image space and the calibration translation and rotations were specified. The points in an image space were obtained with a camera and preserved on film.

Motion of an anatomical structure in space was obtained by measuring the time-history of the position of a photographic target which had a well-defined position and orientation, relative to a predefined anatomical landmark. Defined descriptors of translations and rotations (position, velocity, acceleration) were associated with rigid body motion in object space. Once these descriptors were obtained and digitized, they were used to characterize the dynamic response of the subject under study and to assist in understanding injury mechanism(s).

In these tests the descriptors chosen were based upon anatomical structures in a two-dimensional image space produced by a camera. The descriptors were two-dimensional and did not take into account rotations and translations which moved objects in and out of a plane of gross whole body motion.

4.22 Frame Fields - As the thorax moves through space, any point on the thorax generates a path in space. In thorax injury research we are interested in the description of the path of instrumented points on the thorax and events which occur as these points move. A very effective tool for analyzing the motion of each point, as it moves along a curved path in space, is the concept of a moving frame. The path generated as the point travels through space is a function of time and velocity. A vector field is a function which assigns a uniquely defined vector to each point along a path. Thus, any collection of three mutually orthogonal unit vectors defined on a path is a frame field. Therefore, any vector defined on the path (for example, acceleration) may be resolved into three orthogonal components of any well-defined frame field, such as the laboratory or anatomical reference frames.

In biomechanics research, frame fields are defined based on anatomical reference frames. Other frame fields such as the Frenet-Serret frame or the Principal Direction Triad, which contain information about the motion embedded in the frame field, have also been used to describe motion resulting from impact.

The Frenet-Serret Frame [508-509] consists of three mutually orthogonal vectors T, N, B. At any point in time a unit vector can be constructed that is co-directional with the velocity vector. This normalized velocity vector defines the tangent direction T. A second unit vector N is constructed by

forming a unit vector co-directional with the time derivative of the tangent vector T (The derivative of a unit vector is normal to the vector.). To complete the orthogonal frame, a third unit vector B (the unit binormal) can be defined as the cross product T x N. This procedure defines a frame at each point along the path of the anatomical center. Within the frame field, the linear acceleration is resolved into two distinct types. The tangent acceleration [Tan(T)] is always the rate of change of speed (absolute velocity) and the normal acceleration [Nor(N)] gives information about the change in direction of the velocity vector. The binormal direction contains no acceleration information.

Principal Direction - One method of determining the principal direction of motion and constructing the Principal Direction Triad was to determine the direction of the acceleration vector in the moving frame of the triaxial accelerometer cluster and then describe the transformation necessary to obtain a new moving frame that would have one of its axes in the principal direction. A single point in time at which the acceleration was a maximum was chosen to define the directional cosines for transforming from the triax frame to a new frame in such a way that the resultant acceleration vector (AR) and the "principal" unit vector (A1) were co-directional. This then was used to construct a new frame rigidly fixed to the triax, but differing from the original one by an initial rotation. After completing the necessary transformation, a

comparison between the magnitude of the principal direction and the resultant acceleration was performed.

4.23 Transfer Function Analysis - The relationship between an accelerometer/transducer time-history at a given point and the accelerometer/transducer time-history of another given point of a human surrogate biomechanical system can be expressed in the frequency domain through the use of a frequency-response transfer function. This input-output function is a complex-valued function in the frequency domain and can be expressed by a magnitude and a phase at a given frequency. Transfer functions can be determined from the Fourier transforms of the input-output response time-histories or from the spectral densities of the input and output response signals. In the case of a force and a pressure, such as impact force and vascular pressure, a transformation of the form:

$$(X)(iw) = (F)[F(t)]/(F)[P(t)]$$

can be calculated from the transformed quantities, where w is the given frequency, and F[F(t)] and F[P(t)] are the Fourier transforms of the impact force time-history and the vascular pressure time-history, respectively.

A transformation of simultaneously monitored accelerometer/transducer time-histories can be used to obtain the frequency-response functions of impact force and accelerations of remote points. Once the frequency-response functions are obtained, a transfer function of the form:

$$(Z)(iw) = (w) \quad (F)[F(t)]/(F)[A(t)]$$

can be calculated from the transformed quantities. w is the given frequency and F[F(t)] and F[A(t)] are the Fourier transforms of the impact forces and accelerations of the point of interest at the given frequency.

This particular transfer function is the mechanical transfer impedance which can be defined as the ratio between simple harmonic driving force and corresponding velocity of the point of interest.

4.24 Statistical Measures - To describe some of the fundamental properties of a time-history, such as acceleration or force, three types of statistical measures are used. They are the Auto-correlation Function, the Cross-Correlation Function, and the Coherence Function.

The Auto-correlation Function is the correlation between two points on a time-history, and is a measure of the dependence of the amplitude at time t_1, on the amplitude at time t_2 where t_1 and t_2 are two points on a time-history separated by a given lag (t_1-t_2). The auto-correlation function is formally defined as the average over the ensemble of the product of two amplitudes:

$$Rx(t_1,t_2) = x_1,x_2,p(x_1,x_2,t_1,t_2)dx_1,dx_2$$

where x_1,x_2 are the amplitudes of the time-history and $p(x_1,x_2,t_1,t_2)$ is the joint probability density. Through the use of a Fourier transform, a discrete time-history of a finite

duration is transformed into an auto-correlation function which illustrates the continuous function. For example, the Power Spectral Density Function is a quantity that describes the frequency or spectral properties of a single time-history. It is the Fourier transform of an auto-correlation function and is sometimes called the "Auto Spectral Density" function. Since it is devoid of phase information, only transfer function magnitude can be obtained from the Power Spectral Density Function.

The Cross-Correlation Function is a measure of how predictable, on the average, a time-history at any particular moment in time is from another time-history at any other particular moment in time. The cross-correlation of the time-histories of two signals begins by taking the Fourier transform of both time-histories (Y_1,Y_2). The cross-spectral density describes the joint spectral properties of two time-histories. Phase information is retained in cross-spectral density so that both the magnitude and phase of the transfer function are obtained. The cross-spectral density is the complex-valued function ($Y_1 \bullet Y_2^*$). The cross-correlation is then the Fourier transform of the cross-spectral density.

Cross-correlation between acceleration measurements at two different points of a material body may be determined to study the propagation of differential motion through the material body. Cross-correlation functions are also not restricted to correlation of parameters with the same physical units; for

example, the cross-correlation between the applied force and the acceleration response to that force can be determined.

The Coherence Function $cxy^2(w)$, is a measure of the quality of a given transfer function at a given frequency:

$$cxy^2(w) = \frac{|Gxy(w)|^2}{Gxx(w)Gyy(w)}$$

where Gxx(w) and Gyy(w) are the power spectral densities of the two signals, respectively. (Power Spectral Density is a Fourier transform of each signal's auto-correlation.) $|Gxy(w)|^2$ is the Cross-Spectral Density function squared. (Cross-Spectral Density is the Fourier transform of the cross-correlation of the two signals at w, the given frequency.) In general, $0 \leq cxy^2(w) \leq 1$. Values of $cxy^2(w)$ near 1 indicate that the two signals can be considered causally connected at that frequency. Values significantly below 1 at a given frequency indicate that the transfer function at that frequency cannot accurately be determined. In the case of an input-output relationship, values of $cxy^2(w)$ less than 1 indicate that the output is not attributable to the input and is perhaps due to extraneous noise. The coherence function in the frequency domain is analogous to the correlation coefficient in the time domain. For more information on this measure see [501].

4.25 Pressure Time Duration Determination - Two different types of pressure-time histories were observed, unimodal and bimodal. The unimodal waveform was characterized by one maximum and the bimodal waveform by two local maxima. In order to define the pressure duration, a standard procedure was adopted which

determined the beginning and end of a pulse. This procedure began by determining the peak, or the first peak in the case of a bimodal waveform. Next, the left half of the pulse, defined from the point where the pulse started to rise until the time of peak, was least-squares fitted with a straight line. This rise line intersected the time axis at a point which was taken as the formal beginning of the pulse. A similar procedure was followed for the right half of this pulse, i.e., a least-squares straight line was fitted to the fall section of the pulse, which was defined from the peak to the point where the pulse minimum occurred. The point where this line intersected the time axis was the formal end of the pulse in the unimodal case, and the formal end of the first peak in the bimodal case. The pressure duration for a unimodal waveform was defined by these points. For a bimodal waveform, these two points were used to determine the first pressure duration. Another least-squares straight line was fitted to the fall section of the second pulse. The point at which this line intersected the time axis was the formal end of the waveform, and the total pressure duration was then defined from this point and the beginning point.

4.26 Force Time-History Determination - In general the force-time histories were unimodal with a single maximum, smoothly rising, peaking and then falling. Various padding configurations on the striker surface effected different force time-history durations. Force duration was determined using the same techniques for determining pressure duration, that is

similar boundary defining and least-squares straight-line fitting techniques were employed.

4.27 Force Deflection Measurement - A string pot transducer was used to measure pendulum displacement. The impactor force transducer assembly consisted of a piezoelectric load washer with a piezoelectric accelerometer mounted internally for inertial compensation. The uniaxial load cell was located on a rigid column directly behind the steering wheel hub. Deflection was obtained by the displacement signal obtained from the stringpot transducer, as well as from observed high-speed photokinematics. In the third test series, the position of the steering wheel with respect to the test subject had the lower rim positioned just below the liver. This was accomplished through the use of pre-test in-place X-rays.

5.0 RESULTS

The data are presented in abbreviated form to show those trends which are felt to be representative of important factors in thoraco-abdominal impact response. Table 2A summarizes initial conditions for the first series, 2B for the second series and 2C for the third series. Table 3 lists the accelerometer response peaks for the first series low-velocity thoracic taps, and Table 4 lists this information for the high-velocity thoracic impacts. Table 5 lists peak forces for the first series. Table 6 summarizes head response for the first series. Table 7 lists the peak aortic and tracheal pressures for the first series. Table 8 summarizes the accelerometer response peaks for the second series, thorax drop onto load plate impacts. Table 9 summarizes the kinematic response of the third series. Table 10 summarizes the autopsy observations for the entire research program. Examples of raw accelerometer/transducer time-histories, auto-and cross-correlations, mechanical impedance, transfer functions and power spectra are included in Appendix E. Although detailed analysis of the response of the thorax to blunt impact from all directions and energy levels was beyond the scope of the research program, in the first test series, the response associated with low-energy impact from three different directions, as well as that associated with lateral impact at 8.5 m/s was investigated. In addition, in the second test series free-fall impact at 1.2 m/s was studied. Also, in the third test series steering wheel assembly impact up to 11 m/s was investigated.

TABLE 2A. FIRST SERIES INITIAL CONDITIONS

Test Number	Impact Configuration	Velocity (m/sec)	Padding
Cadaver 000			
82E004	Sternum Tap	2.1	None
82E005	45° Left Thorax Tap	2.0	None
82E006	Left Side Thorax Tap	1.9	None
82E007	Left Side Thorax Impact	8.4	10cm Ensolite
Cadaver 020			
82E023	Sternum Tap	2.0	0.5cm Ensolite
82E024	45° Left Thorax Tap	2.0	0.5cm Ensolite
82E025	Left Thorax Tap Arms Up	2.0	0.5cm Ensolite
82E026	Left Thorax Tap Arms Down	2.0	0.5cm Ensolite
82E027	Left Thorax Impact	8.5	0.5cm Ensolite
Cadaver 040			
82E043	Sternum Tap	2.0	0.5cm Ensolite
82E044	45° Left Thorax Tap	2.0	0.5cm Ensolite
82E045	Lateral Tap	2.0	0.5cm Ensolite
82E046	Lateral Tap Arms Up	2.0	0.5cm Ensolite
82E047	Lateral Tap	2.0	10.0cm Ensolite
82E048	Left Side Thorax Impact	8.5	10.0cm Ensolite
Cadaver 060			
82E063	Sternum Tap	2.0	0.5cm Ensolite
82E064	45° Left Thorax Tap	2.0	0.5cm Ensolite
82E065	Left Thorax Tap Arms Down	2.0	0.5cm Ensolite
82E066	Left Thorax Impact	8.5	0.5cm Ensolite
Cadaver 080			
83E083	Sternum Tap	2.1	0.5 cm Ensolite
83E084	45° Lateral Tap	2.0	0.5 cm Ensolite
83E085	Lateral Tap	1.9	0.5 cm Ensolite
83E086	Left Side Thorax Impact	8.4	10.0 cm Ensolite
Cadaver 100			
83E104	Sternum Tap	2.2	0.5cm Ensolite
83E105	45° Lateral Tap	2.2	0.5cm Ensolite
83E106	Lateral Tap	2.2	0.5cm Ensolite
83E107	Left Side Thorax Impact	8.5	10.0cm Ensolite

TABLE 2B. SECOND SERIES INITIAL CONDITIONS

Test Number	Impact Configuration	Velocity m/s	Padding
Cadaver 079			
83E071	Drop to Load Plate	1.2	None
83E072	Drop to Load Plate	1.2	None
83E073	Drop to Load Plate	1.2	None
83E074	Drop to Load Plate	1.2	None
83E075	Drop to Load Plate	1.2	None
Cadaver 089			
83E076	Drop to Load Plate	1.2	None
Cadaver 090			
83E092	Drop to Load Plate	1.2	None

TABLE 2C. THIRD SERIES INITIAL CONDITIONS

Test Number	Steering Wheel Impact Configuration	Velocity m/s	Padding
Cadaver 120			
83E121A	Frontal Thorax Impact	2.7	None
83E121B	Frontal Thorax Impact	5.0	None
83E121C	Frontal Thorax Impact	9.5	None
Cadaver 130			
83E131A	Frontal Thorax Impact	2.7	None
83E131B	Frontal Thorax Impact	5.0	None
83E131C	Frontal Thorax Impact	12.0	None

TABLE 3. FIRST SERIES LOW VELOCITY THORACIC TAPS - ACCELEROMETER RESPONSE PEAKS (G's)

Test Number	P-A	T1 R-L	I-S	P-A	T12 R-L	I-S	P-A	U.S. R-L	I-S	P-A	R4R R-L	I-S	P-A	R4L R-L	I-S	R8R	R8L	LS
Cadaver 000																		
82E004	7.2	4.5	2.4	4.3	2.3	NA	28	10	NA	4.8	10	75	5.7	7.7	4.9	11	10	20
82E005	2.7	3.8	2.4	1.3	1.0	2.5	3.8	35	NA	2.4	3.2	2.4	6.6	9.8	1.5	4.2	14	9.2
82E006	1.1	0.4	5.2	2.6	0.7	4.4	2.8	6.2	NA	NA	6.0	3.4	4.9	5.1	3.0	5.4	4.0	3.4
Cadaver 020																		
82E023	4.0	0.6	2.9	2.4	0.6	1.3	8.8	1.8	4.2	2.5	2.8	3.4	2.2	2.7	2.6	4.0	2.7	10
82E024	3.0	1.3	1.7	2.2	1.8	1.0	7.4	3.4	2.6	2.7	2.8	3.0	6.3	2.6	1.4	1.7	2.8	10
82E025	2.3	2.3	1.1	2.6	2.4	1.2	3.7	4.9	2.6	2.1	5.6	1.6	9	8	2.1	3.4	2.8	10
82E026	1.4	2.9	1.0	1.8	1.8	0.8	1.9	6.2	2.2	1.1	4.2	2.1	4.8	14	3.6	3.2	11	5.0
Cadaver 040																		
82E043	2.7	0.7	2.8	1.9	0.4	0.8	11	5.4	8.8	2.6	2.8	3.4	2.9	1.5	1.0	2.5	1.9	12
82E044	1.5	1.6	1.9	1.7	1.2	0.8	6.2	4.3	5.7	2.4	2.8	3.4	4.5	3.4	3.4	2.1	4.5	4.
82E045	0.7	2.6	1.8	2.6	3.5	1.0	6.2	9.3	11	1.7	3.8	2.2	11	5.4	3.2	11	20	6
82E046	0.6	2.8	1.5	1.5	1.2	0.7	0.2	5.1	3.5	1.5	3.2	1.2	3.3	7.2	4.9	2.3	7.2	2.

TABLE 3. FIRST SERIES LOW VELOCITY THORACIC TAPS - ACCELEROMETER RESPONSE PEAKS (G's) CONTINUED

Test Number	T1 P-A	T1 R-L	T1 I-S	T12 P-A	T12 R-L	T12 I-S	U.S. P-A	U.S. R-L	U.S. I-S	R4R P-A	R4R R-L	R4R I-S	R4L P-A	R4L R-L	R4L I-S	R8R	R8L	LS
82E047	0.5	1.7	1.1	0.6	0.9	0.6	1.2	NA	1.3	0.7	2.1	0.7	2.1	5.0	2.5	5.4	7.2	2.1
Cadaver 060 82E063	4.8	1.5	2.8	2.4	0.5	1.7	8.9	3.0	7.5	5.1	7.0	4.7	7.0	4.8	3.7	8.3	6.8	18
82E064	4.4	4.2	2.6	2.0	5.6	2.9	7.0	4.4	3.7	4.9	3.2	5.8	9.1	6.3	0.1	4.7	18	8.7
82E065	1.2	0.8	8.1	2.7	1.5	3.3	2.5	3.9	3.3	4.1	4.2	2.8	10	4.1	8.5	5.5	16	6.3
Cadaver 100 83E104	4.2	1.1	1.0	3.0	2.3	0.1	11	2.2	3.1	3.0	2.0	3.5	4.6	4.7	5.2	2.0	2.8	17
83E105	6.6	5.1	1.7	3.0	5.0	0.1	12	2.8	2.0	6.9	3.4	4.7	8.6	11	7.7	4.0	9.4	15
83E106	4.1	7.7	1.2	2.6	5.3	0.1	2.9	9.0	3.7	3.9	4.8	3.9	7.1	12	10	5.8	13	9.2

TABLE 4. FIRST SERIES HIGH VELOCITY THORACIC IMPACTS - ACCELEROMETER RESPONSE PEAKS (G'S)

Test Number	T1			T12			U.S.			R4R			R4L				
	P-A	R-L	I-S	P-A	R-L	I-S	P-A	R-L	I-S	P-A	R-L	I-S	P-A	R-L	I-S	R8R	R8L	LS
82E007	21	21	31	24	18	27	36	24	NA	30	104	44	37	77	26	36	92	19
82E027	42	49	40	51	22	29	84	110	90	38	52	30	14	170	68	31	150	113
82E048	5.7	17	12	18	11	7.2	16	21	43	21	19	12	9.9	56	18	17	41	26
82E066	13	11	55	34	21	32	38	59	15	28	67	37	160	32	215	43	54	70
83E107	9.6	25	12	5.6	32	1.4	11	23	17	11	10	4.7	28	45	24	11	46	26

TABLE 5. FIRST SERIES PEAK FORCES

Test Number	Peak Force (N)	Duration (ms)
82E004	980	NA
82E005	560	95
82E006	770	85
82E007	NA	NA
82E023	440	75
82E024	390	80
82E025	490	80
82E026	450	80
82E027	9800	60
82E043	430	80
82E044	430	80
82E045	570	80
82E046	400	90
82E047	400	100
82E048	7000	45
82E063	410	80
82E064	380	80
82E065	520	70
82E066	NA	
83E104	660	65
83E105	1200	70
83E106	1200	65
83E107	NA	

TABLE 6. FIRST SERIES HEAD RESPONSE SUMMARY

Test No.	Ang Acc Res (rd/s/s)	Ang Vel Res (rd/s)	Lin Acc Res (m/s/s)	Lin Vel Res (m/s)	HIC
82E007	1400	20	14	5	18
82E027	1750	30	38	6	113
82E048	1750	20	30	5	102
82E066	1000	20	12	6	50
83E107	2500	30	16	5	20

TABLE 7. PEAK PRESSURES (psi)

Test No.	Aorta Pressure	Trachea Pressure
82E004	NA	NA
82E005	NA	NA
82E006	NA	NA
82E007	NA	NA
82E023	0.9	0.2
82E024	0.6	0.5
82E025	0.3	0.6
82E026	0.4	0.2
82E027	7.68	NA
82E043	0.8	0.1
82E044	0.4	0.4
82E045	0.1	0.4
82E046	0.2	0.5
82E047	0.3	0.6
82E048	1.8	0.9
82E063	0.6	0.1
82E064	1.0	0.1
82E065	0.6	0.1
82E066	14.1	2.3
83E104	0.1	0.0
83E105	0.1	0.0
83E106	0.1	0.0
83E107	4.1	1.3

TABLE 8. SECOND SERIES
THORAX DROP ONTO LOAD PLATE
ACCELEROMETER RESPONSE PEAKS (G's)

Test No	Force lb	T1 P-A	T1 R-L	T1 I-S	T6 P-A	T6 R-L	T6 I-S	T12 P-A	T12 R-L	T12 I-S	A1 T1	A2 T1	A3 T1	AR T1	A1 T6	A2 T6	A3 T6	AR T6	A1 T12	A2:T12	A3:T12	AR:T12
83E071	-296.4	-14.0	15.1	-17.5	-5.9	-5.5	-7.5	-6.4	-4.8	4.8	23.2	16.4	-10.2	23.2	7.5	7.3	3.4	7.5	7.3	5.7	2.3	7.3
83E072	-387.7	16.0	-20.3	-23.8	26.6	34.0	-54.9	7.8	-17.6	-17.3	32.2	17.4	14.4	32.2	57.1	34.1	23.9	57.1	19.6	18.1	-7.7	19.6
83E073	-306.1	-9.3	-7.4	7.4	-12.7	-4.8	-5.1	-10.0	-5.3	-5.5	10.8	7.4	-7.2	10.8	13.4	6.7	5.3	13.4	10.3	6.1	-5.1	10.3
83E074	-428.6	-13.9	-10.9	9.2	-12.6	-5.8	-8.7	-10.1	-6.7	-7.5	17	11.9	-10.5	17	14.3	8.2	-6.6	14.3	10.2	10.1	48.8	10.2
83E075	-375.4	-7.6	-6.9	15.0	-11.3	-28.3	24.7	-24	-9.2	13.8	17.4	6.3	5.4	17.4	37.6	16.4	8.0	37.6	25.1	12.3	-7.8	25.1
83E076	-446.2	-17.6	-5.7	10.7	-5.1	6.1	9.5	-3.9	8.1	17.3	18.1	10.1	-7.1	18.1	9.6	8.1	-3.3	9.6	17.4	8.8	1.1	17.4
83E092	LOSS OF DATA TAPE MALFUNC-TION																					

TABLE 9. THIRD SERIES KINEMATIC TEST SUMMARY

Test No.	Force [N] (Time [ms])	Trachea Pressure [kpa] (Time [ms])	Aorta [kpa] (Time [ms])	A1:T1 [G] (Time [ms])	A1:T12 [G] (Time [ms])	A1:Ls [G] (Time [ms])	A1:R8R [G] (Time [ms])	A1:R8L [G] (Time [ms])	R4R [G] (Time [ms])	R4L [G] (Time [ms])
83E121-A	2000 (30)	2.1 (38)	N-N (-)	24 (35)	19 (32)	11 (35	16 (38)	9 (34)	3 66	N-N (-)
83E121-B	3000 (65)	4.1 (79)	N-N (-)	29 (65)	- (-)	69 (60)	42 (46)	17 (49)	23 (53)	N-N (-)
83E121-C	10400 (41)	11 (37)	N-N (-)	N-N (-)	N-N (-)	110 (26)	N-N (-)	N-N (-)	N-N (-)	N-N (-)
83E131-A	870 (87)	3.5 (75)	N-N (-)	3 (81)	10 (109)	7 (22)	5 (57)	6 (49)	N-N (-)	1 (44)
83E131-B	2700 (65)	6.2 (48)	N-N (-)	14 (56)	9 (49)	27 (33)	22 (39)	47 (55	8 (52)	7 (48)
83E131-C	4400 (51)	6.2 (48)	N-N (-)	38 (59)	13 (74)	100 (43)	71 (40)	100 (45)	15 (56)	35 (50)

TABLE 10. RESEARCH PROGRAM AUTOPSY SUMMARY

82E007

Thorax Impact
- Incomplete fractures to ribs on left side at R3, R5, R7.
- Petechial hemorrhage on pericardium near ascending aorta.

82E027

Thorax Impact
- Incomplete fractures to ribs on left side: 4 on R2, 1 on R3, 2 on R4, 2 on R5, and 1 on R6.
- Complete separation of acromion and clavicle.

82E048

Thorax Impact
- Incomplete fractures to ribs on left side at R3, R7, and R8.

82E066

Thorax Impact
- Left clavicle was fractured at the acromion juncture.
- Left ribs R2 through R6 fractured in two places.

83E108

Thorax Impact
- Left ribs R2 through R5 fractured with R3 and R4 fractured in two places.

83E075

Thorax Drop Impact onto Load Plate
- No injuries observed.

83E076

Thorax Drop Impact onto Load Plate
- No injuries observed.

83E092

Thorax Drop Impact onto Load Plate
- No injuries observed

TABLE 10. RESEARCH PROGRAM AUTOPSY SUMMARY -Continued

83E121C

- Hemorrhage in diaphgragm
- Contused spleen
- Hepatic vein torn
- 8 cm laceration at junction of major-minor lobes of liver
- 5 cm tear in medial liver
- Liver severed from its tethers

83E131C

- Closed fractures of ribs R3L, R7L, R8L, R9L
- Hemorrhage left inferior pericardium
- Contusion in heart on right lateral side
- Contusion in tissue connecting esophagus-stomach
- Contused stomach
- Contused transverse colon
- 90% tear of disk between cervical vertebrae C6-C7
- 40% tear of disk between cervical vertebrae C5-C6
- 30% tear of disk between cervical vertebrae C4-C5
- Partial tear of anterior longitudinal ligament at C5

6.0 DISCUSSION

In the first test series, the response of the thorax to blunt impact was observed from (1) the contact force-time history of the impact piston; (2) the accelerations obtained from the triaxial accelerometer clusters and uniaxial accelerometers fitted to the thoracic skeletal structure; and (3) the analysis of the high-speed photokinemetrics. The various accelerations were subsequently expressed as vectors and described in the appropriate reference frames. While general trends were observed in a majority of the impact tests, the specific response was found to depend on several experimental parameters of the impacting device, such as the velocity of the impactor, the padding of the impact surface, and the direction of impact with respect to the test subject.

6.1 First Series Force-Time History - A total of nineteen tests were conducted with a 2 m/s impactor velocity. Tests 82E004-006, 82E023-026, 82E043-47, 82E063-65, 83E104-106, and 83E108 comprise this group of tests in which five different cadavers were impacted with a 26 kg piston padded with 0.5 cm Ensolite. The tests were divided into four groups depending on the impact direction and the position of the arms: frontal sternum tap, 45° thoracic rib cage tap, lateral tap to the arms, and lateral tap to the thoracic rib cage with the arms positioned up. The force-time histories were derived from either the acceleration of the linear pendulum piston or from the compensated force of the pneumatic impact device. For these nineteen tap tests, the peak force varied from 0.4 to 1.2 kN and was approximately 60 to 120 milliseconds in duration. The impact force typically reached its peak value in the initial third of the force trace and then decreased in magnitude, although exceptions

were noted: some tests resulted in a multimodal response with one or more local maxima. In general, the characteristics of the force-time waveforms seem to be as closely associated to a given test subject as to the direction of impact or to the position of the test subjects. An example is shown in Figure 11 in which tests 82E023-82E026 and 82E043-82E046 are compared. This observation is surprising in light of certain test configurations in which the impactor did not act directly upon the thorax but through the shoulder and arm.

6.2 First Series Acceleration Time-History - A rigorous comparison of the acceleration response between different points on the thorax was not possible in the first test series due to the complex nature of the thoracic skeletal response. Differences in the waveform of the acceleration time-history at the various instrumented points of the thorax, as well as in the particulars of the impact conditions, limited the analysis to certain characteristics of the response found to be independent of the direction of impact.

The gross overall motion of the thorax during impact was in the general direction of impact, although some rotations were observed about the R-L axis for frontal impacts and, for side impacts, about the I-S and P-A axes. The overall motion was determined from the high-speed films and transducer time-histories. A comparison of the integrated time-history for the principal direction of the nearside accelerometer cluster for the 2 m/s impacts--sternum for frontal and R4L (Rib 4, left side) for side and 45° impacts--and the velocity of the phototargets indicate that they were in reasonable agreement near the end of impact; however, it must be noted that errors introduced in the integration of the

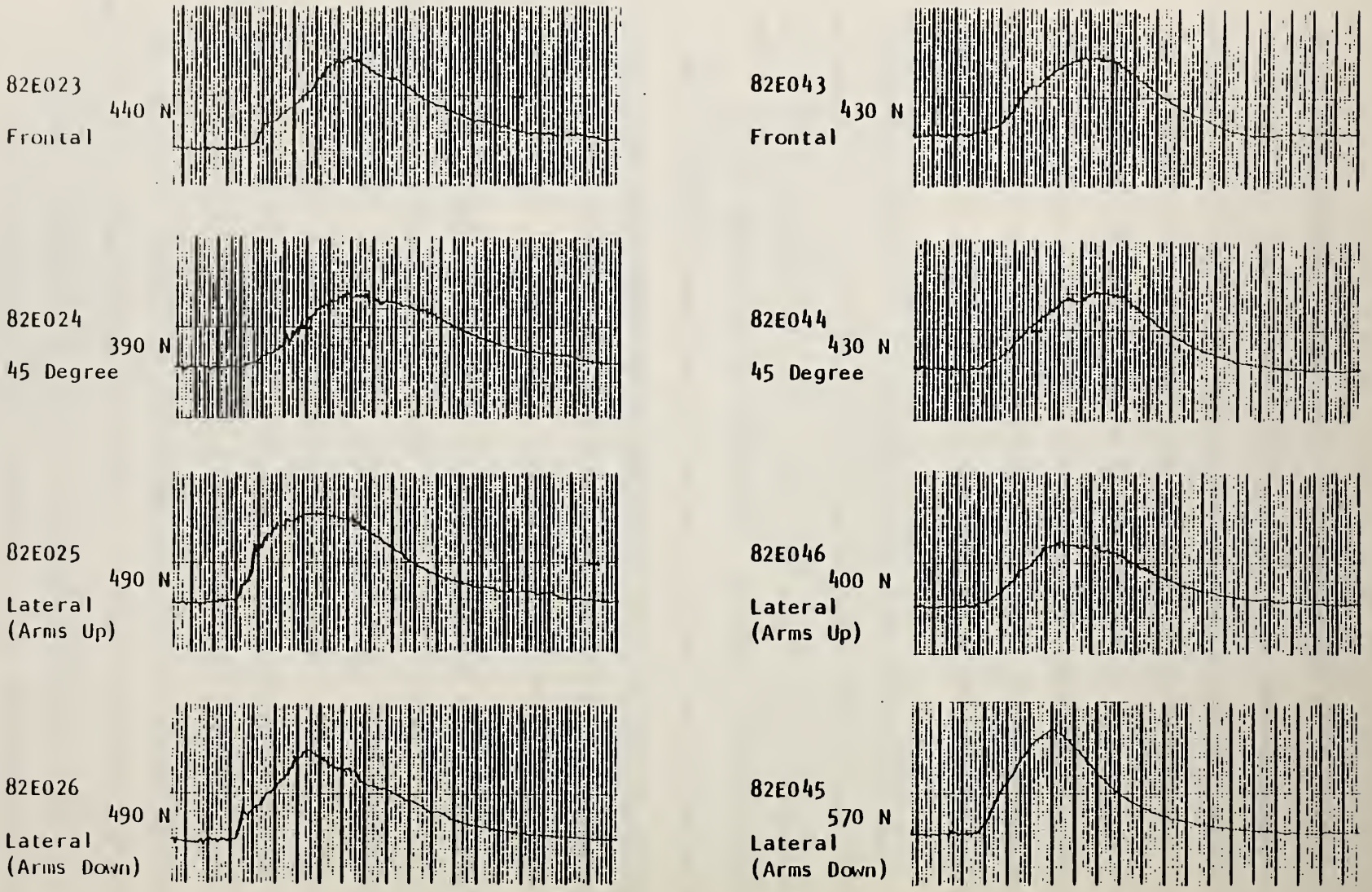

Figure 11

Comparison of First-Series Force-Time Waveform

acceleration-time-history, as well as errors associated with obtaining the differentiated motion of the phototargets from a two-dimensional image, limited the comparison. Peak velocities obtained from the principle direction acceleration for the nearside triaxes were typically 1-1.5 m/s for the 2 m/s impacts.

Although the gross motion of the thorax could be described in a general sense from the acceleration-time history of the principal direction, a one-dimensional response was not sufficient to describe the acceleration-time history of several of the instrumented points on the thorax in the first test series. However, a secondary direction was found such that no significant acceleration could be found in the third direction for these points. This implies that, in general, a description of the acceleration response of certain points on the thoracic skeletal structure requires an "acceleration plane." Figure 12 shows the accelerometer time-histories of the R4L for Test 82E006 for the principal (A1), secondary (A2), and resultant (AR) accelerations, as well as the integration of the principal (V1) and secondary (V2) directions. Significant accelerations in at least two directions for several points were observed in a majority of the tests, regardless of the direction of impact.

In the first test series, the magnitude of peak acceleration and the time at which the maxima occurred were found to be dependent on the accelerometer location relative to the point of impact. The peak acceleration of a point nearest to impact was typically three to four times greater in magnitude than the point furthest from impact. In addition, the relative phasing of the peak acceleration between the

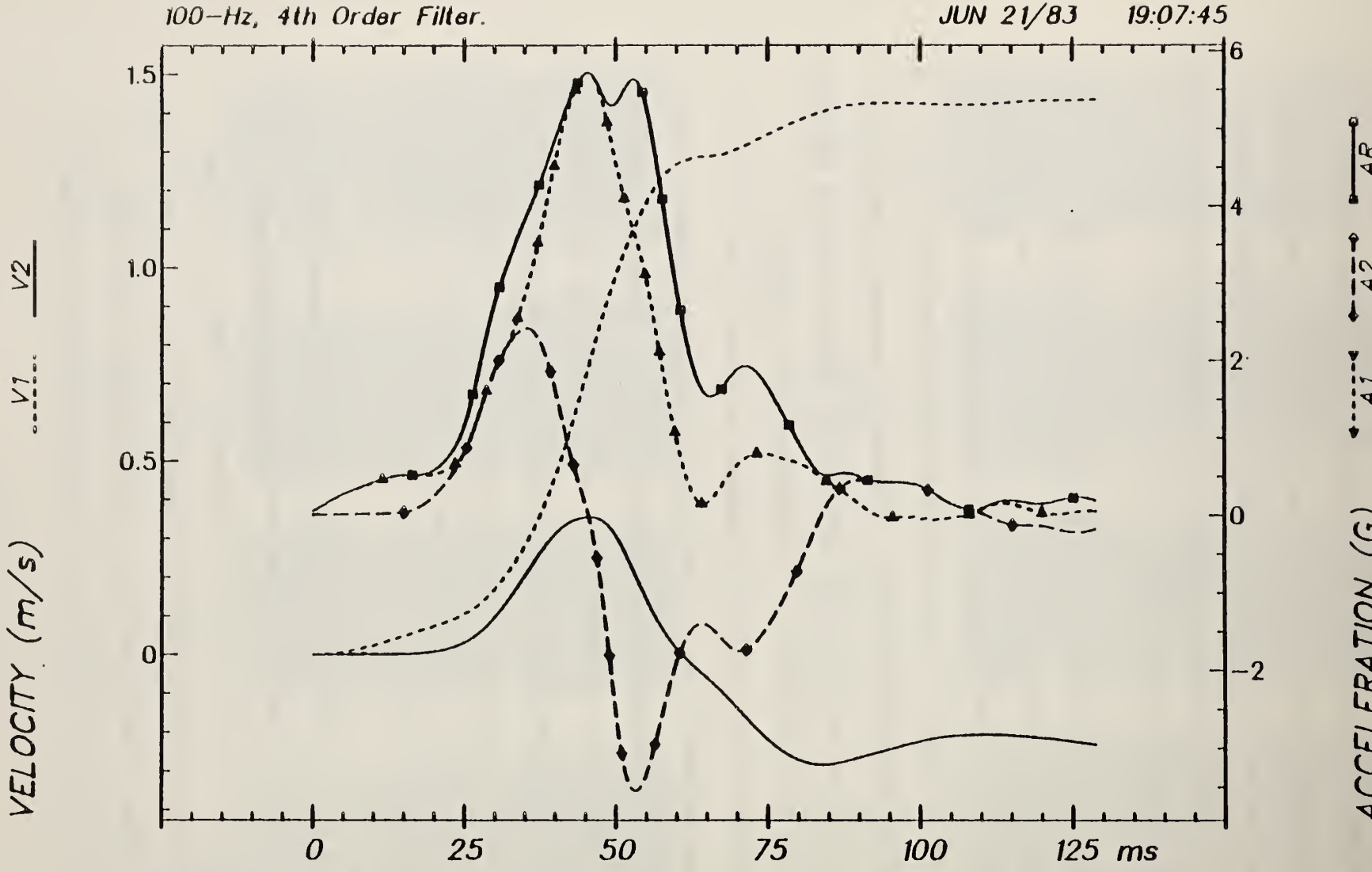

Figure 12

First Series Acceleration Time-History
R4L, Test 82E006

nearside and farside of impact was sequential with the occurrence of the peak force. In general, the peak and resultant accelerations of the nearside--upper and lower sternum for frontal impacts and R4L and R8L (Rib 8, left side) for lateral impacts--occurred prior to the peak force. The peak and resultant accelerations for those points further from impact generally occurred after the peak force: R4R (Rib 4, right side)/R8R (Rib 8, right side) and R4L/R8L for frontal impacts, the upper and lower sternum and T1 and T12 for lateral impacts. The side impacts displayed the largest lag in peak accelerations, followed by the sternum impacts; the 45° impacts resulted in the most coherent response between the sternum and the R4L and R8L ribs. The observed lag between peak force and peak acceleration was as much as 10 milliseconds for the farside of impact (Figure 13).

The waveforms of the principle acceleration time-history for frontal and side impacts seem to be relatively similar for the nearside (upper sternum for frontal impacts and R4L and R8L for lateral impacts) for a given impact velocity, although there were exceptions (Test 82E063). The acceleration waveform of the nearside, in general, was characterized by a smooth rise up to peak acceleration, proceeding to a negative acceleration near peak force, and subsequently either became positive and returned to negative or remained negative. On the other hand, the farside acceleration response was more complex before peak acceleration. Either a multimodal waveform with several local maxima or a delay between the initiation of impact and the most significant part of the acceleration response was observed. In addition, a lower peak acceleration lagged behind the nearside peak acceleration.

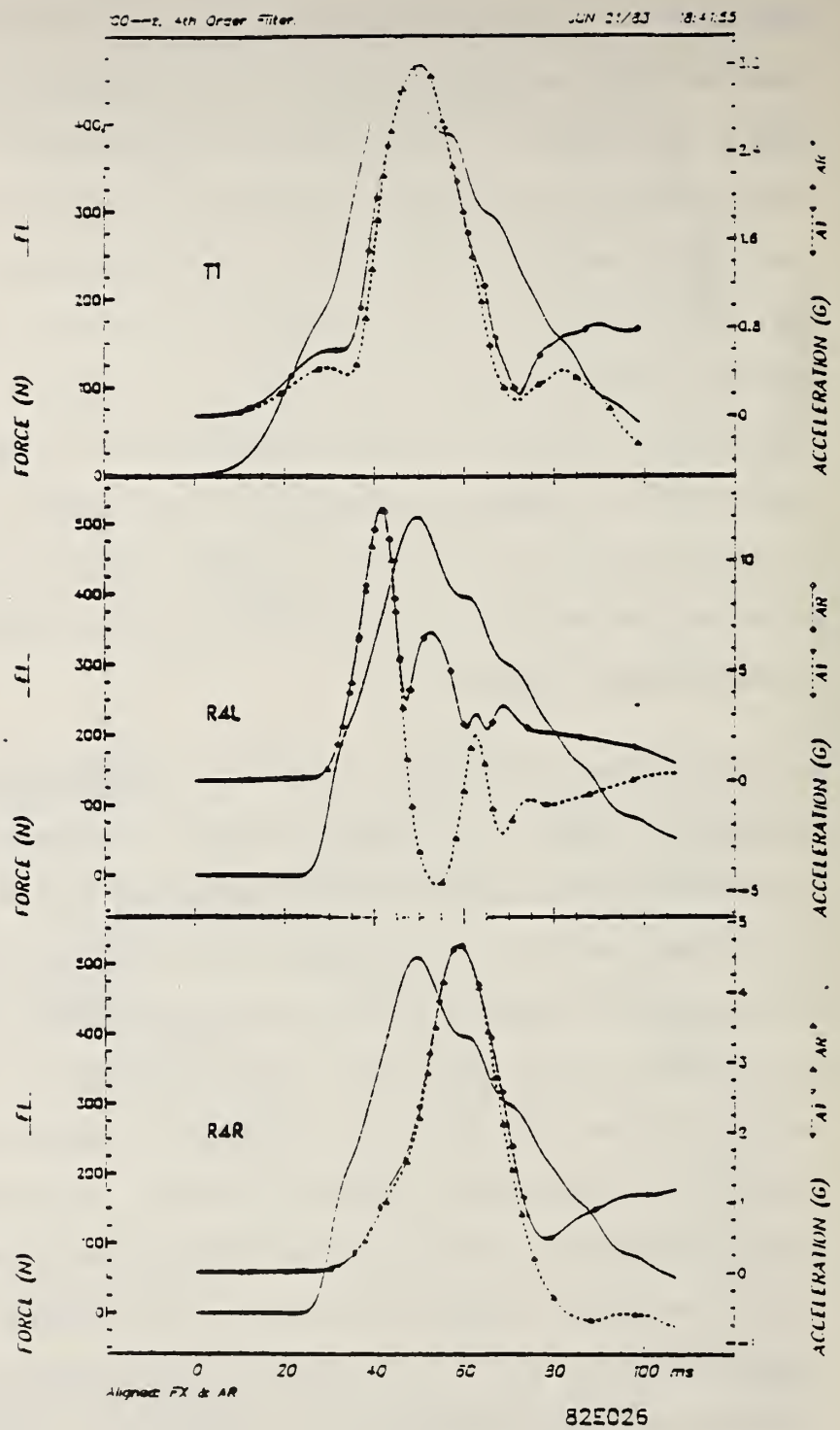

Figure 13

First Series Far Side Lag between Peak Force and Peak Acceleration

Physically, these observations imply that the response of the thorax to blunt impact could be interpreted as the response of one deformable body (the thorax) in contact with other material bodies (e.g., arm, neck, impactor). The waveform which was associated with the acceleration response of each point on the thorax was, therefore, influenced by the force input (obtained through the use of an impactor in this case) and the physical characteristics of the thorax. For those points near the point of impact, the acceleration response was influenced by the external driving force. For those points distal to the point of impact, the response was more related to a system response. This may in part explain why other researchers [56,116] see a relative similarity of response of test subjects for the nearside accelerometers and the greater variation for the farside response.

6.3 First Series Impact Response - Figures 14-17 represent the mechanical impedance magnitude transfer function for subject 040. The results shown in these figures were generated from the principal direction triad and contain four data traces, one each for R4L, R4R, the upper sternum, and T1. The impact surface was padded with .5cm of Ensolite (AL) and the results of the following multiple impacts are shown: front sternum tap, 45° tap, arms up lateral tap, and arms down lateral tap. The results presented here are considered representative of general trends observed in a majority of the first series tests.

The first series impact response of the thorax as observed in the mechanical impedance results have the following characteristics: 1) local minima in impedance were observed in all significant accelerations in the anatomical reference frames or the principal direction triad and

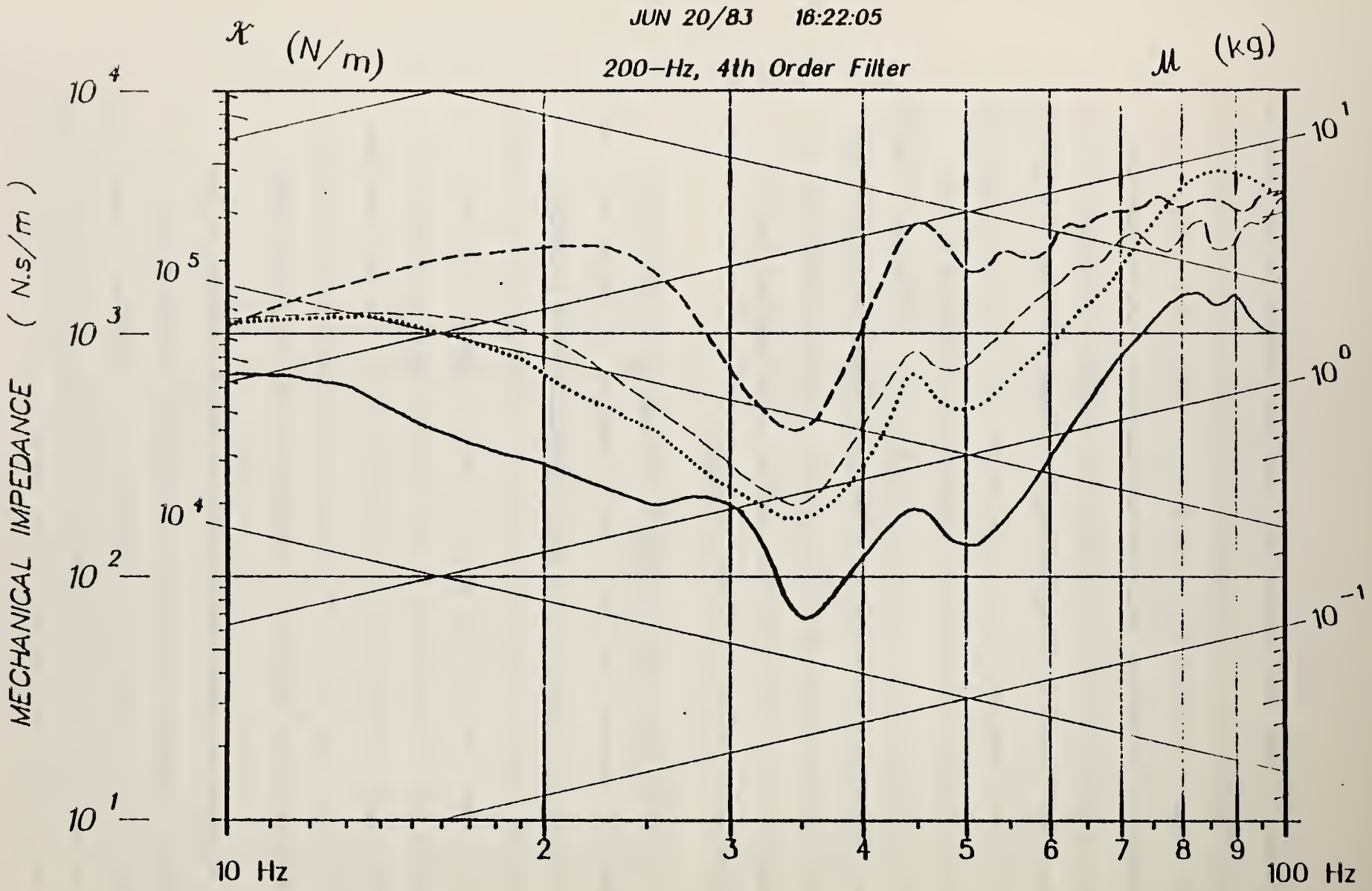

Figure 14

First Series
Frontal Thoracic Tap
Principal Direction Triads

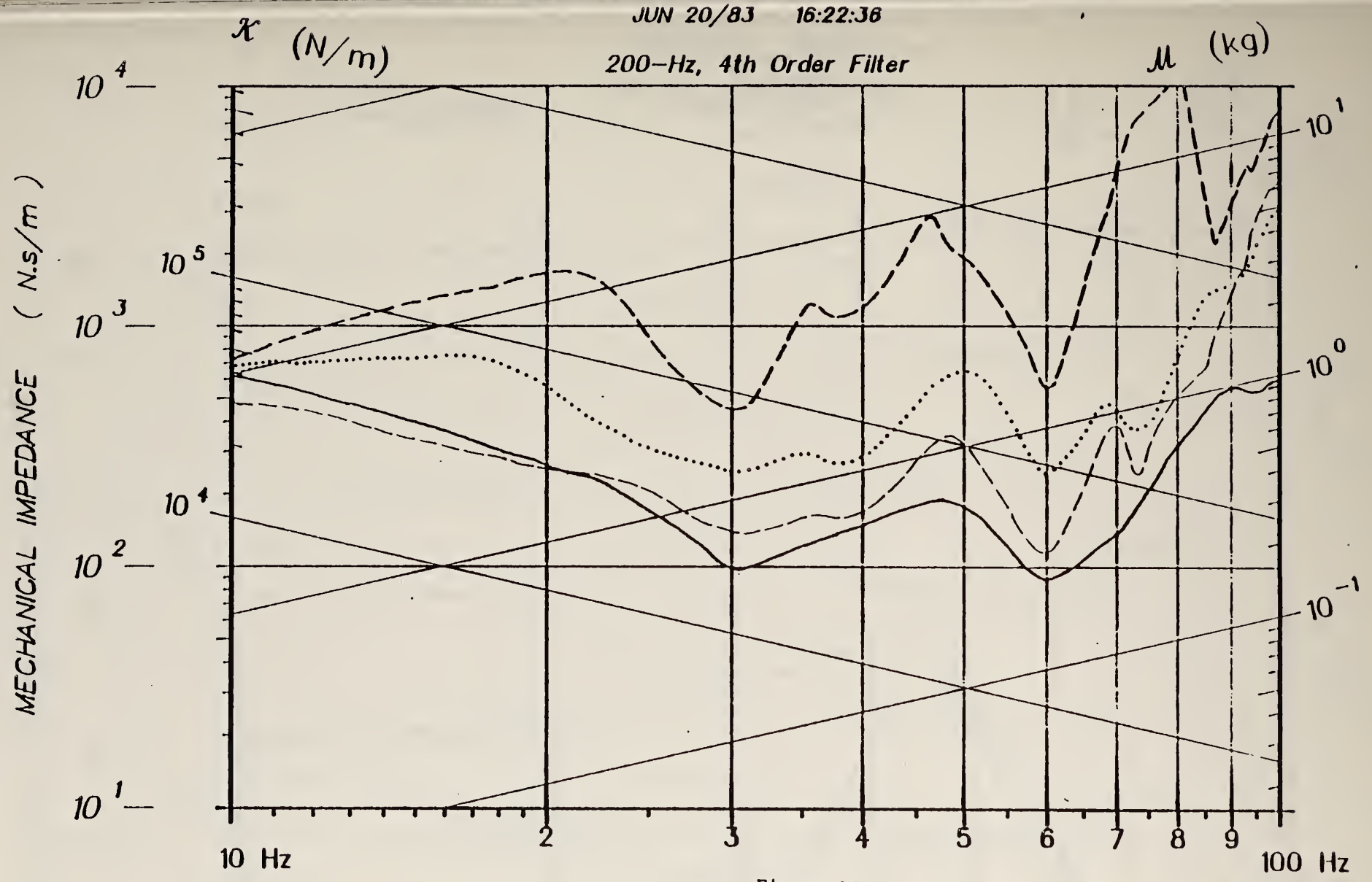

Figure 15

Z=F1/V1 for **82E044**

First Series
45° Thoracic Tap
Principal Direction Triads

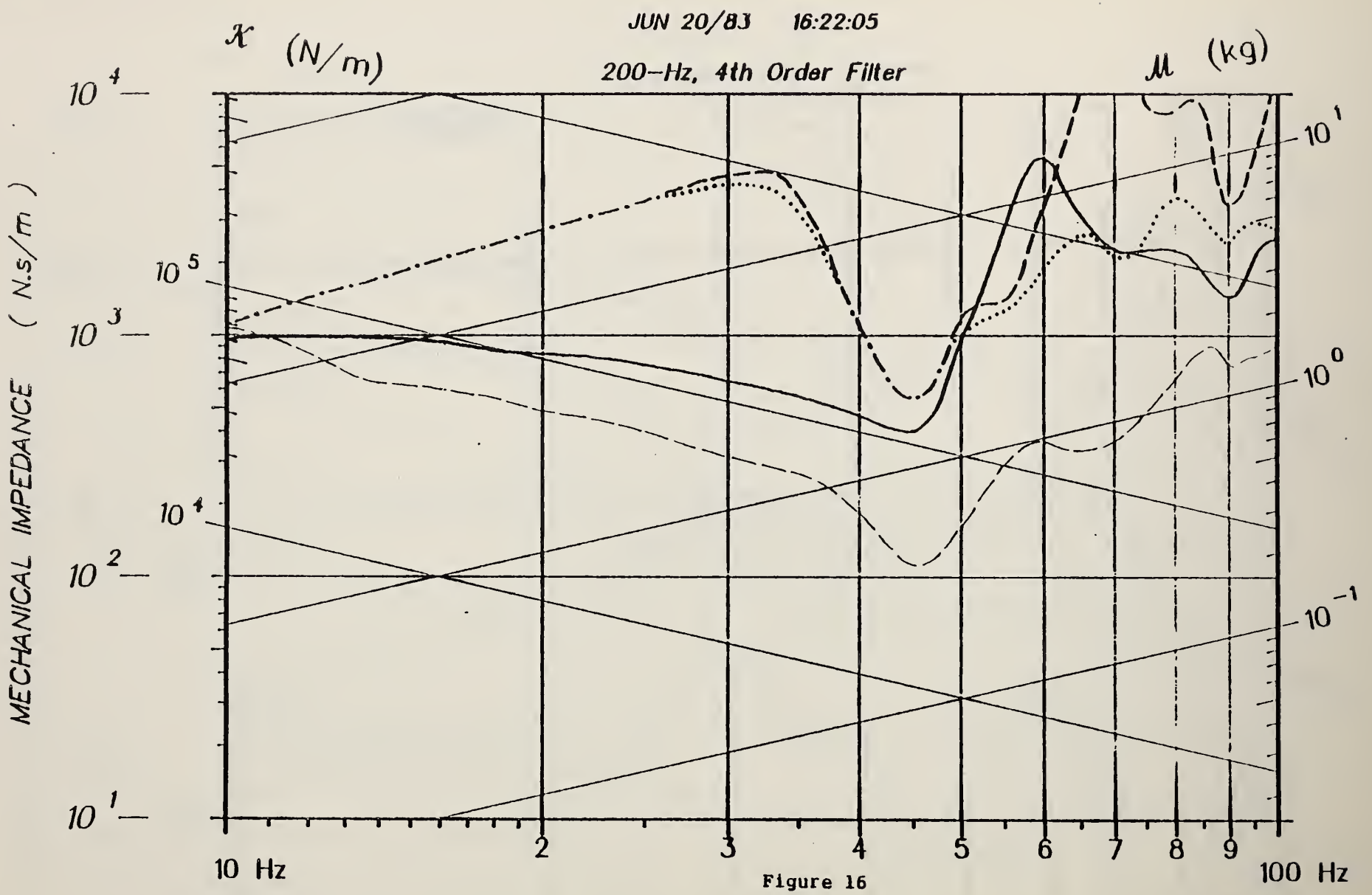

Figure 16

Z=F1/V1 for **82E045**

First Series
Lateral Thoracic Tap
(Arms Down)
Principal Direction Triads

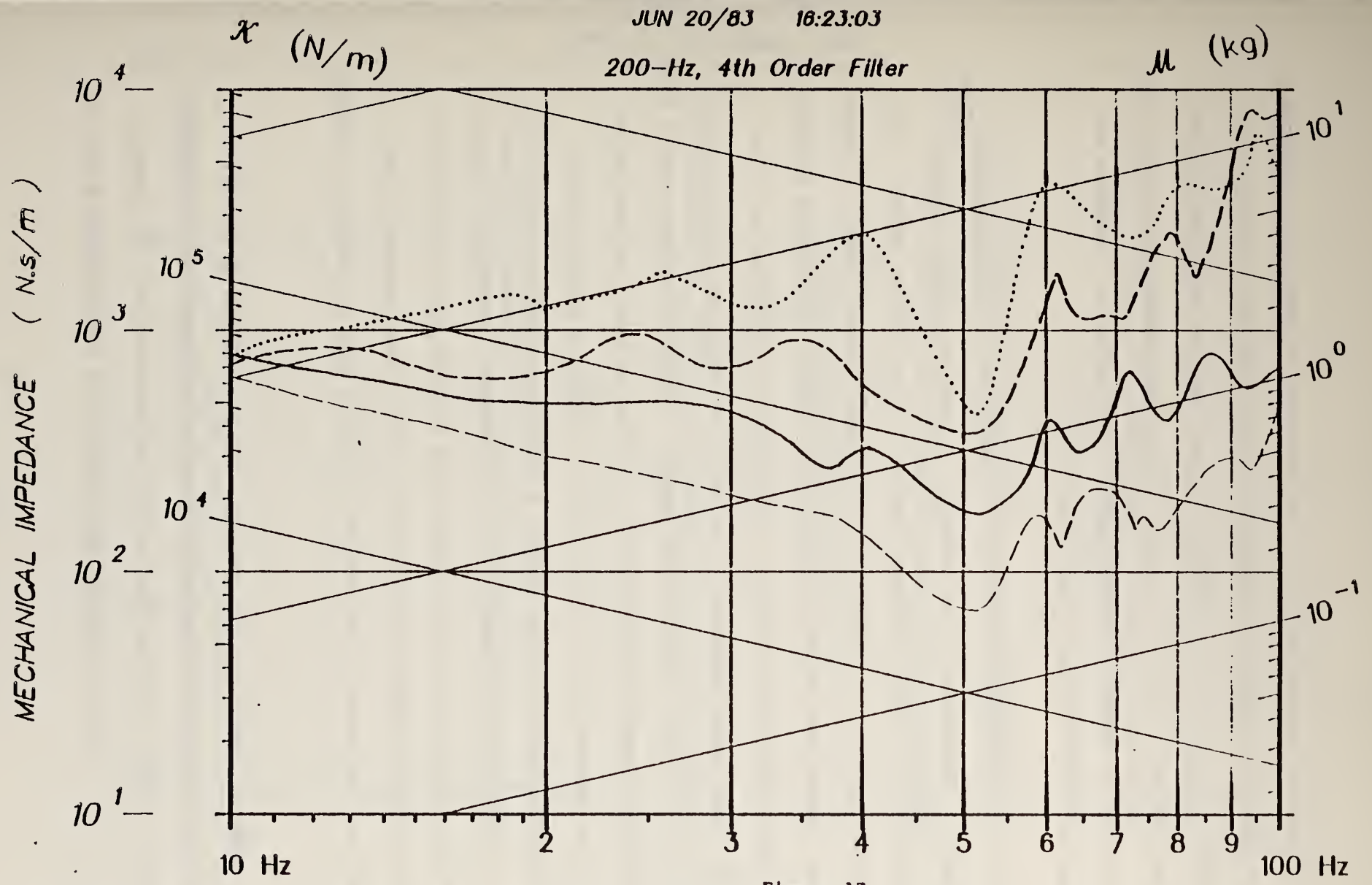

Figure 17

Z=F1/V1 for **82E046**

First Series
Lateral Thoracic Tap
(Arms Up)
Principal Direction Triads

the uniaxial accelerometers; 2) the magnitude of mechanical impedance of the nearside to impact decreased up to the first local minima; 3) a second local minima was observed for most tests at approximately twice the frequency of the first minima; and 4) for those points further from the point of impact, a greater value of the mechanical impedance was observed from 10 Hz up to the first local minima.

Only one local minima, however, was observed in the arms-up lateral impacts. The minima of the mechanical impedance response tended to appear within certain frequency ranges. In the frontal impacts, the minima range from 32-38 and 65-80 Hz; lateral impacts result in minima from 42-48 Hz and 80-100 Hz; and for 45° impacts, minima were observed between 27-32 Hz and 57-66 Hz. The decrease in impedance up to the first local minima exhibited a "spring-like" characteristic for many of the first series' front and side impacts. Although the magnitude of the mechanical impedance indicates that a spring constant for the thorax could be between $3x10^4$ to $8x10^4$ N/m^2, the phase of these transfer functions, however, do not exhibit a spring-like behavior (Figure 18). In certain tests, the magnitude of the mechanical impedance for the farside acceleration rose as a mass line of 15-25 kg up to the first local minima. However, similar to the spring-like behavior of the nearside, the phase of the transfer functions were not mass-like (Figure 19).

In terms of free vibrations, the local minima observed in all first series tests was not necessarily related to resonances of the thoracic system. During the occurrence of the peak acceleration, the impactor was still in contact with the test subject. In addition, the amount of

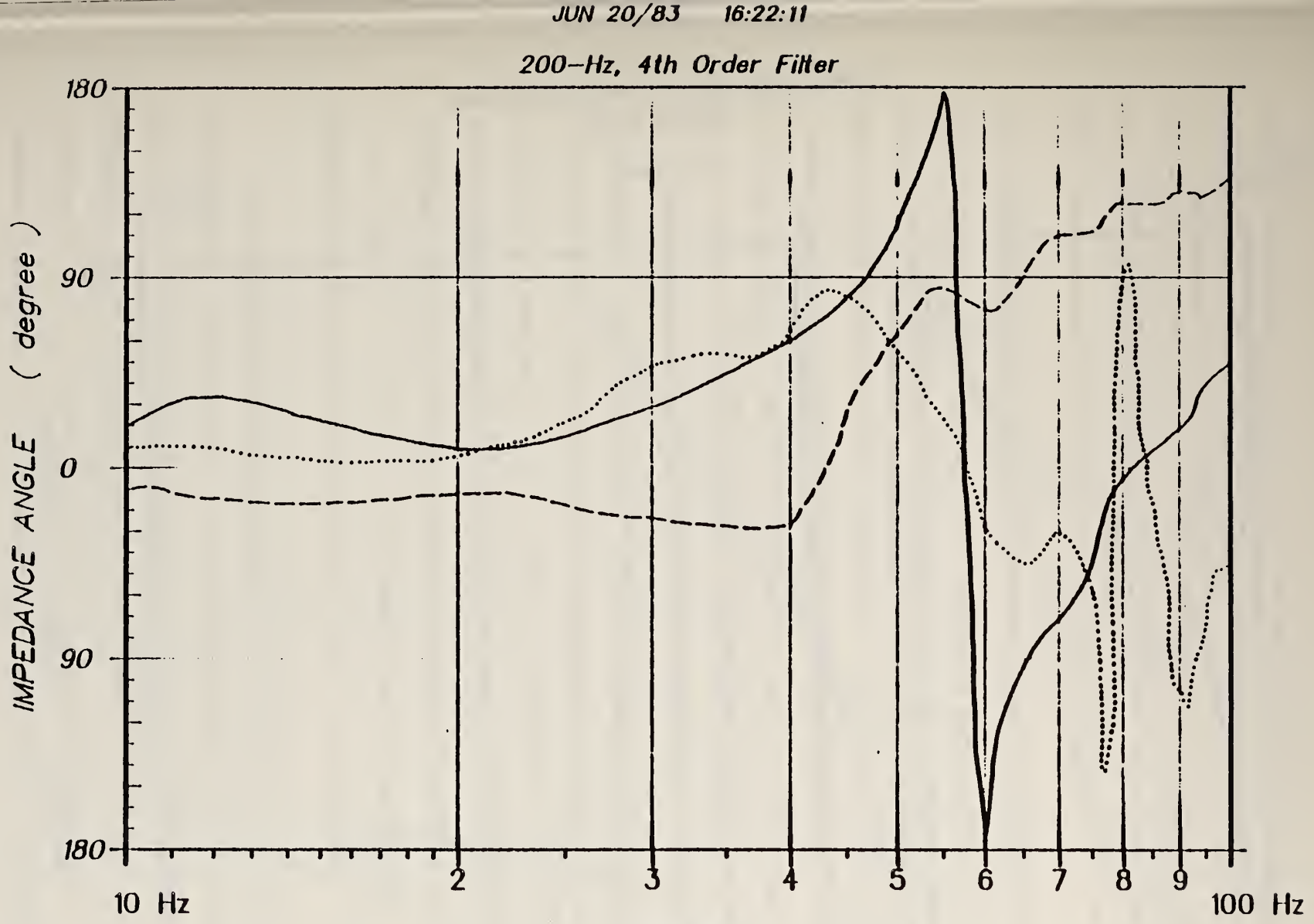

Figure 18

First Series

Impedance Angle for Nearside Impacts
82E043, 82E045, and 82E046

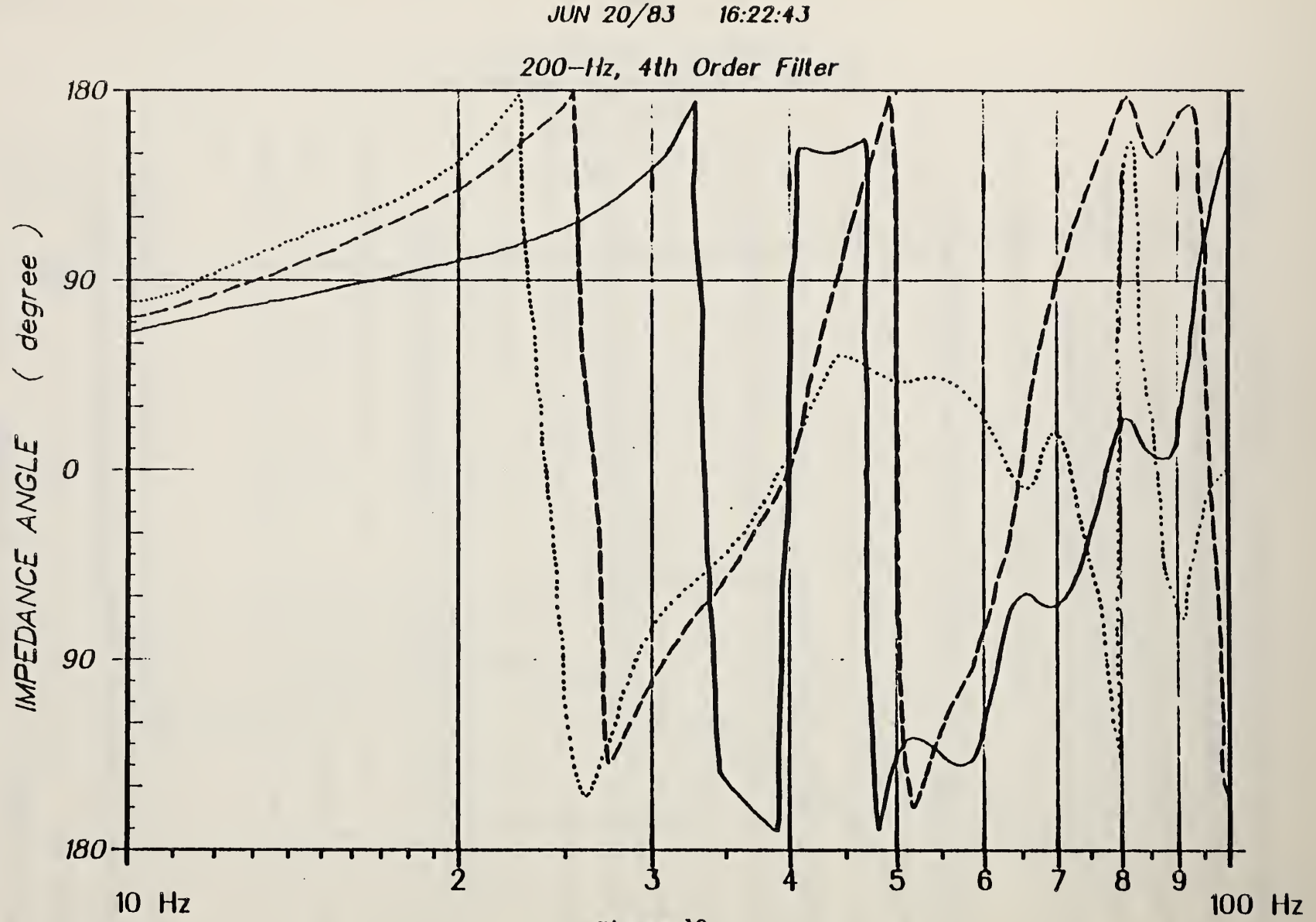

Figure 19

First Series
Impedance Angle for Far Side Impacts

area of the impactor in contact with the test subject varied for different directions of impact. This may, in part, have caused the differences in local minima of mechanical impedance for different impact directions as well as different initial conditions (e.g., arms-up, arms-down).

The the first series' response of the thorax can be further generalized by the nearside and farside mechanical impedance results of the low-energy (2 m/s) impacts. In the frequency range at 10-35 Hz, the magnitudes of impedance of the nearside were consistently lower than the farside impedance magnitudes. Physically, the lower impedance values of the nearside indicate that there was less resistance to the external driving force at the point of impact. A decreasing impedance up to the first minima was previously ascribed to an "elastic-like" response for the nearside, versus a "mass-like" farside response related to gross whole body motion. These results were consistent with the observed acceleration response and serve to qualify the observed differences in acceleration waveforms of the nearside and farside. At low-velocity, therefore, the thorax seemed to absorb the energy of impact by deforming to the action of the piston in a non-damaging way and subsequently rebounding with gross whole body motion as well as differential motion.

6.4 First Series Secondary Direction of Acceleration - An example of the impedance characteristics of the secondary direction acceleration are shown in Figure 20 for Test 82E026. In general, the magnitudes of impedance of the secondary direction were higher in the low frequency range below the first local minima, than the principal direction impedance magnitudes. At the local minima, the principal and secondary

direction impedance values were similar. At higher frequencies, the secondary direction impedance magnitudes tended to be greater than the principle direction, but not to the same level as observed prior to the first minima.

6.5 First Series Transfer Functions - One of the goals of the first test series study was to quantitatively characterize the response of the thoracic skeletal structure in terms of a transfer function between any two points on the thorax which possessed a significant component of acceleration. In this regard, transfer functions were generated between an acceleration package and any other accelerometer package, resulting in a number of transfer functions for each point which generated the corresponding response of every other point. An example of an application of this approach is the use of the nearside principal direction response to predict the farside principal direction response, as shown in Figure 21, where the transfer functions for the farside and nearside were generated for a sternum impact (Test 82E043), and three lateral impacts (Tests 82E045, 82E046, and 82E047). When a transfer function was generated between any two points such that the denominator was obtained from the accelerometer package nearest to impact, the transfer function had the characteristics of a low-pass filter. Transfer functions which were generated further from the point of impact displayed an increasingly greater attenuation. In the case of lateral impacts, the transfer functions which were generated from the nearside principal direction acceleration and the upper sternum principal direction acceleration had less attenuation than the corresponding transfer function of T1 or lower sternum for the P-A direction. This seems to indicate that there was a load path through the arm and

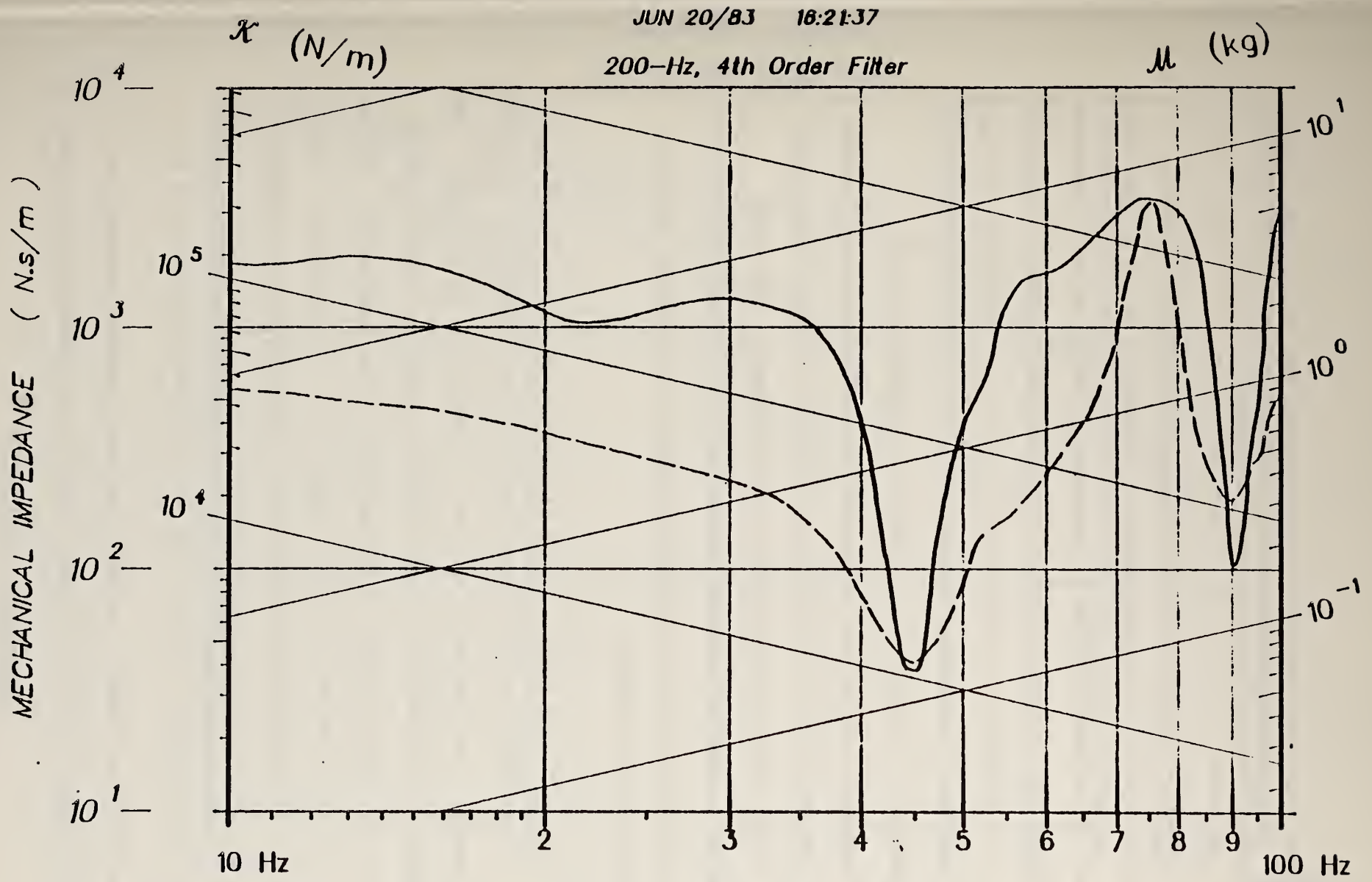

Figure 20

Z=F1/V1 for **82E026**

First Series

Secondary Direction of Acceleration

Impedance Characteristics

shoulder (via the clavicle) to the thorax and that the sternum, in particular, was influenced by such a load path.

In general, the transfer functions which were generated from the significant acceleration components of the various points of the thorax result in responses typified as decreasing in magnitude with increasing frequency and varying in phase at each different frequency. Therefore, if it is reasonable to assume that the thorax is a deformable structure, the response of the thorax is dependent on the load path and the energy management of the system (gross motion, differential motion, or dissipation). In the first series tests, a sufficient area of contact had been maintained to eliminate such effects as loading on a single rib. The transfer functions which were obtained in this study, therefore, should be regarded as characteristic of blunt impact involving large areas of the thorax and may not be general to other types of thoracic loading.

In Tests 82E027 and 82E048, the 26 kg impactor had a velocity of 8.5 m/s. In Test 82E027, a rigid impact, the shoulder structure was destroyed by damage to the clavicle as well as 11 fractures to the rib cage. The impedance of the farside of impact showed a mass-like response similar to the low-velocity impact of the nearside for the same subject, but the first local minima was at 120 Hz (Figure 22). In Test 82E048, 10 cm of padding was placed on the impactor surface and only four rib fractures were observed. The mechanical impedance response was similar to the mid-velocity impacts with the first local minima occurring at 52 Hz.

In general, the transfer functions that were generated between the nearside and farside R4 principal directions and associated with the

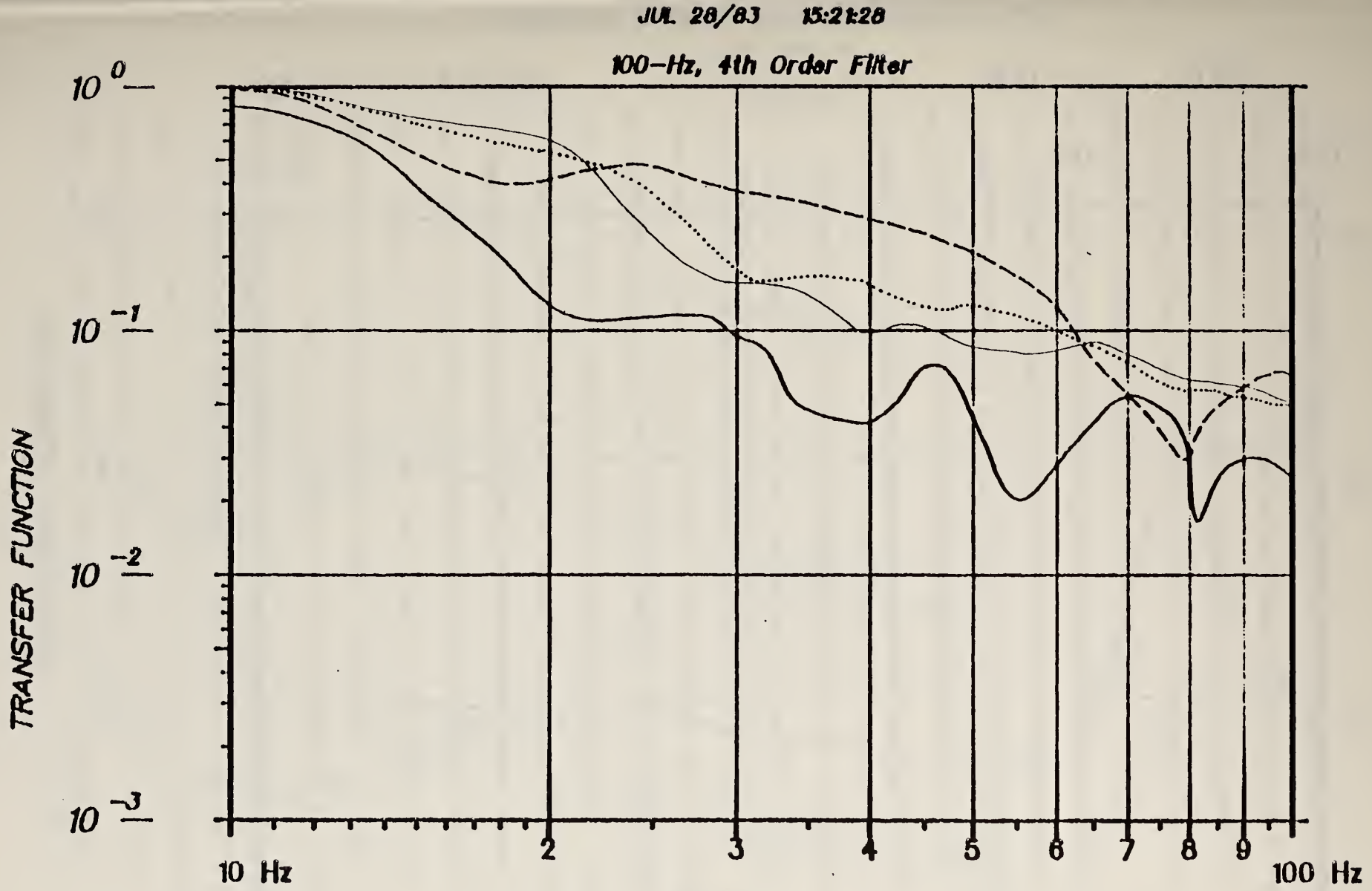

Figure 21

First Series

Farside/Nearside Impact Transfer Functions

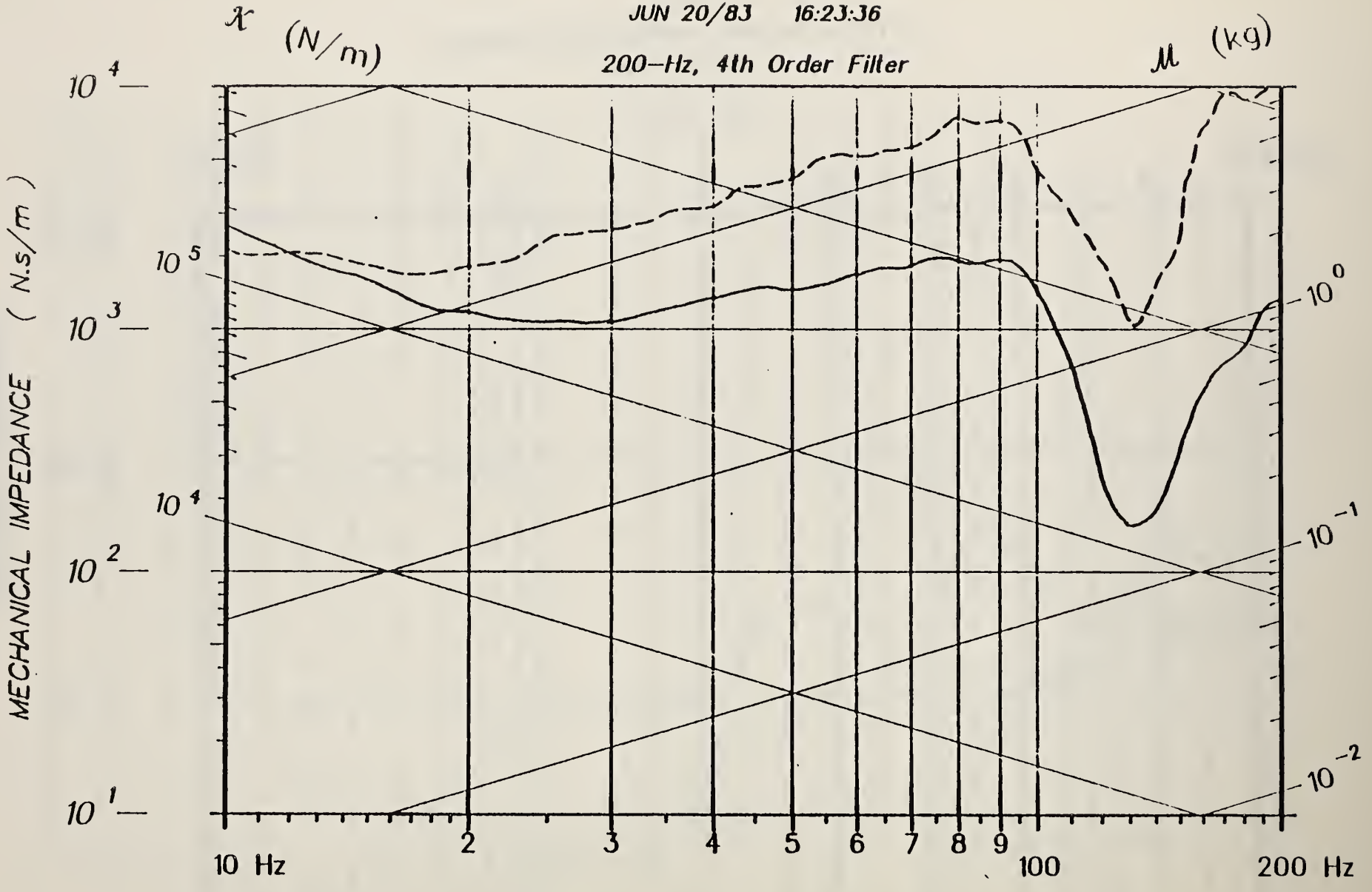

Figure 22

First Series

Mechanical Impedance for 8.5 m/s Velocity Impact
Principal Direction Triads

rigid impacts for Tests 82E027 and 82E066 had less attenuation than were observed in the low velocity impacts and padded impacts at the 8.5 m/s velocity (Figure 23). Physically, this implies that the thorax structure could have been effectively stiffer for the tests at higher velocities. A similar observation had been made previously [53,65] when it was suggested that the thorax stiffens under higher impact velocity. It should be noted, however, that the velocity of the linear piston constantly changes during the impact event and that energy management of the thoracic structure for a given impact mass may actually be the intrinsic factor relating the thorax response to the impact velocity.

In the first series low-velocity (non-damaging) impacts, the response of the subjects seemed to have certain characteristics in both the time-histories and frequency domain that were similar for all impact directions, although the specifics of a given response may be influenced by the impact direction as well as the biometrics of the population at large. For lateral impacts at different impact energy levels, resulting in differing degrees of damage to the skeletal structure, the response changed in both the time-histories and the frequency domain (e.g., the local minima in the mechanical impedance transfer function occurring at higher frequency). This implies that a single linear model may be inadequate to characterize thoracic impact response for all impact energy levels. However, the changes in response seemed to be consistent and analytically describable.

6.6 First Series Damage Response - Tests 82E06.1 27 and 82E06.1 66, rigid lateral impacts at 8.5 m/s with the 26 kg piston, produced damage to the clavicle and thoracic rib cage in both test subjects. The addition of 10 cm of padding to the impact surface resulted in no

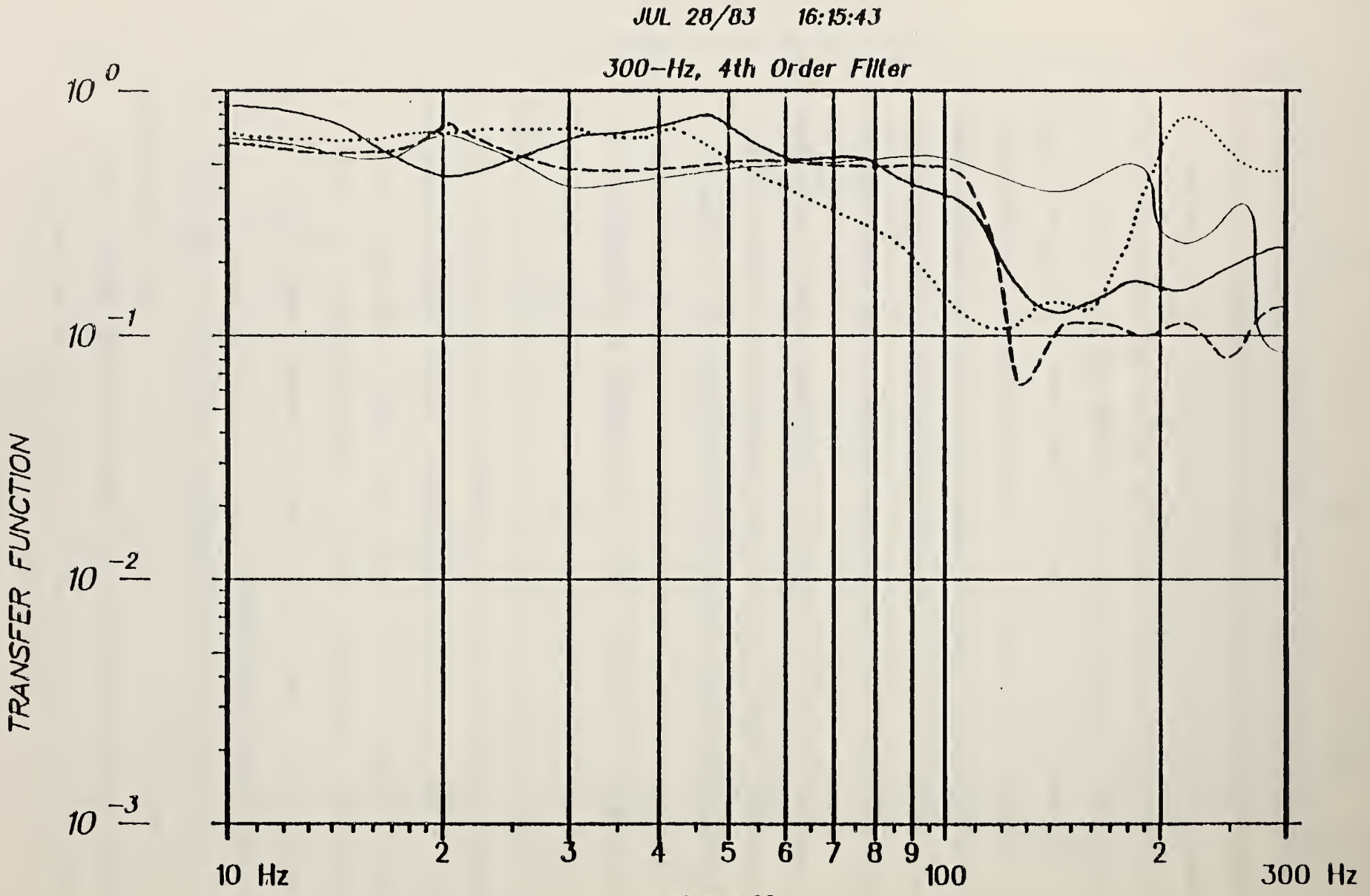

Figure 23

First Series

Transfer Function for R4R/R4L Triax

injuries sustained to the shoulder-arm-clavicle complex with fewer rib fractures in four subsequent tests at 8.5 m/s with the 26 kg piston (Tests 82E007, 82E048, 82E107). If the shoulder structure remained intact, it could have been an effective means by which the load to the thorax was better distributed. The approximate velocity at which a rigid impact to the shoulder should begin to produce damages to the thoracic skeletal structure seemed to be 4.6 m/s. No injuries were observed in the neck of any of the test subjects for the first test series.

Table 8 summarizes the kinematic response of the second series thorax drop impact onto a load plate. Impact velocity was 1.2 m/s and no damage was observed in the gross autopsy.

6.7 Third Series Response - The response of the cadaver to direct loading from a steering wheel system was observed from: 1) the force obtained from a load cell placed directly behind the steering wheel hub, 2) the accelerations obtained from the triaxial and uniaxal accelerometers fitted to the thoracic skeletal structure, 3) the pressure transducers placed in the descending aorta and trachea, and 4) the analysis of the high-speed photokinemetrics. The various accelerations were subsequently expressed as vectors and described in appropriate reference frames. While general trends were observed in the third series tests, the specific response was found to be dependent on: the impactor velocity, the impactor mass, the contact profile of the steering wheel with the thorax, as well as on the biovariablity of the subjects. In addition, the response of the thorax had certain characteristics in both the time and frequency domain that were simliar to blunt impacts to the sternum using a flat impactor.

With the use of triaxial and uniaxal accelerometers attached to the thoracic skeletal structure, the response of the thorax was defined as a continuum of "events" characterized by the motion of the thorax as estimated by the accelerometers and the relationship of this motion to the steering wheel hub force. Examples of events which were used to characterize impact response for the third series force time-history were: the initiation of impact response, denoted by Q_1 on the accompanying graphs; the positive maximum, denoted by Q_2; and the estimated end of impact, denoted by Q_3. In general, during an anterior-to-posterior direction steering wheel impact, the lower rim of the steering wheel contacted the abdomen at the Q_1 event. During the Q_1-Q_2 interval the steering wheel spokes interacted with the thoracic cage as the subject rotated forward. Finally, the hub of the steering wheel contacted the sternum close to the the Q_2 event, and the subject rotated far enough forward so that the chin protruded above the upper rim of the steering wheel, or the face contacted the rim. In general, the test subject stayed in this position for the remainder of the test. See Figure 24 for illustration of this motion.

6.8 Third Series Force Time-History - The force time-histories were derived from the compensated force of the load cell positioned behind the steering wheel hub. The third test series consisted of three impacts, respectively, of low-, medium-, and high velocity to unembalmed, repressurized cadavers. The low- and mid-velocity impacts were at non-injurious levels. The force time-histories were smooth, typically unimodal (only one significant local maximum) curves with occasional multimodal abberations (See examples given in Appendix E).

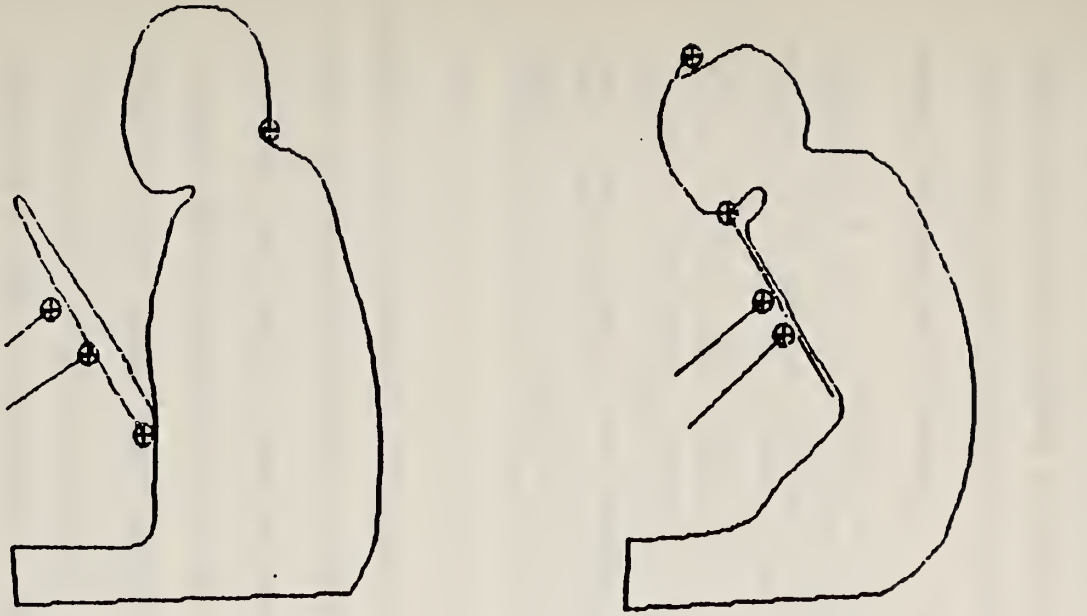

Figure 24

Reconstruction of Digitization of

High-Speed Film for Third Series Test 83E131B

For the third series low-velocity impacts, the magnitude of the steering wheel hub force varied between 800 N and 2500 N, with an average value of 1600 N. The Q_1 to Q_2 as well as the Q_2-Q_3 interval were significantly different from later tests in which a 65 kg pendulum was used [96]. This was consistent with observations based on the high-speed photokinemetrics. The velocity of the pendulum during the Q_1-Q_3 interval decreased to a much greater degree than that of later 65 kg pendulum tests [96]. This phenomenon is believed to be a result of the interaction of the test subject with the pendulum in such a way that a significant percentage of the pendulum's energy was transferred to the test subject. Including the later tests showed that in general, the Q_1-Q_2 interval was longer than the Q_2-Q_3 interval, indicating a greater rate of fall than rise. The Q_1-Q_2 interval was typically about 70 ms, with the Q@-Q_3 interval about 50 ms when the later tests were included in the sample [96].

For the third series mid-velocity impacts, the magnitude of the steering wheel hub force varied between 2500 N and 4500 N, with an average value of 3500 N. Similar to the low-velocity impacts, these lower mass tests did not display a waveform similar to that of the later higher mass pendulum tests [96]. Including the later tests showed that, in general, the Q_1-Q_2 interval was the same as the Q_2-Q_3 interval, indicating a symmetric curve. The Q_1-Q_2 and Q_2-Q_3 intervals were about 50 ms each [96].

For the third series high-velocity impacts, the magnitude of the steering wheel hub force varied between 4,500 N and 10,000 N, with an average value of 6200 N. Similar to the low- and mid-velocity impacts,

these lower mass tests displayed a different waveform than that of the later higher mass pendulum impacts [96]. The high-velocity steering wheel impact waveforms were most similar to the first test series pendulum impacts using a moving mass impactor with a flat surface [101]. Including the later tests showed that, in general, the Q_1-Q_2 interval was shorter than the Q_2-Q_3 interval, indicating a greater rate of rise than decline [96]. The Q_1-Q_2 interval was about 30 ms, with the Q_2-Q_3 interval approximately 70 ms.

Observations from the high-speed photokinemetrics, in conjunction with observations from the steering wheel hub force, indicated that for impactors using a moving pendulum, a difference between the first test series flat surface impacts and the third test series steering wheel impacts was that in the steering wheel impacts the subject rotated forward (head toward the knees) in such a way that all the mass of the body trunk rested on the steering wheel (Figure 24). While in the first test series flat surface impacts, the impactor contacted the sternum and the subject rotated backwards (head and torso away from the knees) with a smaller portion of the body mass interacting with the pendulum. The increased effective mass of the test subject in a steering wheel impact as compared to a flat surface impact may indicate a necessity for using a heavier mass pendulum for steering wheel impacts than that used for flat surface impact to the sternum [101].

6.9 Third Series Acceleration Time-History - A comparison of the acceleration response of the thorax between the third test series steering wheel impacts and the first test series flat surface impacts [101] showed that steering wheel loading produced a more complex

response from the thoracic skeletal structure. Differences in the waveform of the acceleration time-history, as well as the particulars of the impact conditions, limited the analysis to certain general characteristics of the response.

The gross overall motion of the thorax during steering wheel impact was, in general, three-dimensional. As the lower rim of the steering wheel penetrated the abdomen, the test subject started to rotate around the the right-left axis. The thoracic cage was first deformed by the steering wheel rim near the lower ribs. Next, the thorax was deformed by the steering wheel spokes. Finally, the steering wheel hub contacted the sternum, compressing the midsection of the thorax. If the steering wheel deformed asymmetrically, the gross motion of the test subject moved out of the plane of the impact. Three-dimensional gross motion out of the plane impact was generally seen only in the high-velocity impacts.

Although the gross motion of the thorax in steering wheel impacts could be described, in a general sense, for short time durations (less than 50 ms) using the principal direction acceleration triad, a one-dimensional acceleration description was not sufficient for description of the acceleration time-histories of several points on the thorax. This conclusion stems from comparison of the doubly integrated difference of the lower sternum acceleration and T12 acceleration compared to the deflection obtained from film and stringpots. After 50 ms, the acceleration time-history no longer was able to reliably predict the deflection. In addition, for triaxial accelerometers, in most cases, a secondary direction could not be found, so that no significant

acceleration could be observed in the third direction. This implied that, in general, the response of the thorax in steering wheel impacts requires a three-dimensional description the thoracic cage be used. In the accelerometer time-histories in Appendix E, the principal direction acceleration is labeled A1, the secondary, A2, and the tertiary, A3.

The results for the first series blunt frontal thoracic impacts using a flat impactor [101] showed that: the magnitude of peak acceleration and the time at which the maxima occured were found to be dependent upon the accelerometer location relative to the point of impact. The peak acceleration of a point nearest to the center of impact was typically three to four times greater in magnitude than a point furthest from impact. In addition, the relative phasing of the peak acceleration between the "sternum" and "spine" was sequential with the occurrence of the peak force. In general, the peak of the principal direction accelerations of the upper and lower sternum occurred prior to the peak force. The peak of the principal direction acceleration for those points further away from the center of impact generally occurred after the peak force: ribs R4R/R8R and T1/T12. The acceleration waveform of the sternum, in general, was characterized by a smooth rise up to peak acceleration, proceeded to a negative acceleration near peak force, and subsequently either became positive and returned to negative, or remained negative. On the other hand, the spinal acceleration response was more complex before peak acceleration. Either a multimodal waveform with several local maxima, or a delay between the initiation of impact and the most significant part of the acceleration response was observed. In addition, the spinal acceleration lagged behind the peak force.

Unlike the first test series flat surface sternal impact response [101], the third test series steering wheel impact response shows that: the relationship and the time at which it occurs for all triaxial accelerometer packages in terms of peak acceleration and the Q_2 event of the force time-history was impact-velocity dependent. For low-velocity steering wheel impacts (2.5-3 m/s), all acceleration maxima, in general, occurred before the Q_2 event of the force. In most cases, for mid-velocity steering wheel impacts the maximum accelerations occurred before the Q_2 force event; however, occassionally, the maximum spine or sternal accelerations occurred after the Q_2 force event. In general, for high-velocity steering wheel impacts, the sternal accelerations occurred before the Q_2 force event, with the spinal acceleration maxima occurring after the Q_2 force event.

Unlike the first test series flat surface impacts [101], the magnitude of the principal direction accelerations for triaxial accelerometers in the third test series low- and mid-velocity steering wheel impacts did not display the same relationships to each other. The principal direction magnitudes of sternal accelerations were 20-50 percent higher than those of the spinal accelerations in the steering wheel impacts. In contrast, the principal direction magnitudes of the high-velocity steering wheel impacts were 4-5 times as high as the spinal accelerations (similar to those flat surface impacts to the sternum [101]). The waveforms were significantly more complex for steering wheel impacts than for flat surface frontal impacts to the sternum [101], in terms of the number and magnitude of local maxima. This may have been the result of the complex interaction of the body trunk (both

of the thoracic cage and of the abdominal area) with the steering wheel. Unlike the first test series flat surface frontal impacts to the sternum [101], different components of the steering wheel contacted the thoracic cage at different points in time. In addition, both symmetric and asymmetric deformation of the steering wheel caused input loading of the thoracic cage that was not observed in the first test series impacts to the sternum using a flat surface impactor [101].

Because of the complex nature of the third test series steering wheel impact acceleration time-histories of various instrumented points on the thoracic cage, comparisons between signals were made using auto- and cross-correlations. Because of the inherent three-dimensional motion in steering wheel impacts, comparisons were not made past 50 ms lags. Peaks in the cross-correlation function correspond to the transmission lag between the two variables that were being correlated. For the steering wheel hub force and the principal direction acceleration variables, the physical path of energy transmission was not well determined. Therefore, the cross-correlation function gave an estimate of the average input transmission lag from the force time-history to the given accelerometer cluster.

The third test series relative phasing of the maximum value of the cross-correlation function between the steering wheel hub force and the principal direction acceleration for the lower sternum, ribs R8R, R8L and thoracic vertebra T12 indicated that the force lagged all of the principal direction acceleration. The lags, in general, for the low velocity impacts were: for lower sternum, 20-25 ms; for ribs R8R and R8L, 20-25 ms; for thoracic vertebra T12, 15-25 ms; and for thoracic

vertebra T1, 0-15 ms. The lags for mid-velocity impacts were: for lower sternum, 15-25 ms; for ribs R8R and R8L, 15-25 ms; for thoracic vertebra T12, 15-25 ms; and for thoracic vertebra T1, 0-15 ms. The lags for the high-velocity impacts were: for lower sternum, 5-15 ms; for ribs R8R and R8L, 5-15 ms; for thoracic vertebra T12, 0-10 ms; and for thoracic vertebra T1, 0-10 ms. In some of the tests, at all three velocity ranges, the greatest lags were observed for the lower sternum, with intermediate lags for the ribs R8R and R8L, and the least lags for the spinal accelerations. However, this trend was not general enough to indicate a clear load path from the sternum to the spine. This observation is consistent with the concept that there was not one but several load paths occurring. Unlike the first test series, blunt frontal sternum impacts with a flat surface impactor [101], in which the sternum was loaded first and then the rib and spine accelerations were a result of the sternum motion; in the steering wheel impacts, the spine was initially loaded by the contact of the ribs with the spokes and lower rim of the steering wheel. In the steering wheel impacts, the loading of the sternum, then, came after the initial load path had been established.

The third test series magnitude of the principal direction acceleration for the triaxial accelerometer clusters, in terms of the maximum value of the auto-correlation (zero lag), was consistent with the results obtained by using the maximum value of the acceleration when the raw accelerometer time- history was filtered at 150 Hz, 4th order. The maximum for the auto-correlation function for the sternal acceleration for low- and mid-velocity impacts was 4-6 times higher than that of the maximum auto-correlation for the spine at thoracic vertebra T12. For

high velocity impacts, the maximum of the auto-correlation function was 15-20 times the maximum of the spinal accelerometers.

Observations of the third test series auto- and cross-correlation functions indicated that: 1) the most rapidly varying signal was the lower sternum, with ribs R8R and R8L being intermediate, and the least varying signal being the spinal accelerations; 2) although ribs R8R and R8L showed the best correlations for low- and mid-velocity impacts, the high- velocity impacts did not indicate a similar response for both sides of the thorax at that level; 3) for all-velocity impacts, the best correlations between principal direction acceleration and the force signal were spinal acceleration; 4) the high-velocity impacts were, to a greater degree, different from the low- and mid-velocity impacts than the low- and mid-velocity impacts were from each other; and 5) the varying load paths were most significant for the rib R8R and R8L triaxial accelerometer clusters.

Physically, these observations imply that the response of the thorax to steering wheel impact can be interpreted as the response of one deformable body (the thorax) in contact with another deformable body (the steering wheel). The waveform which was associated with the acceleration response of each point on the thorax was influenced by a number of load paths (originating from the steering wheel hub, the spokes, and the lower rim). The point in time at which each of these load paths become significant for a given steering wheel configuration depends on the impact velocity, the number of loads paths, and the biovariability of the population.

6.10 Third Series Impact Response - Figures 25,26 and 27 represent the mechanical impedance transfer function for the third test series Impact 83E131C. The results shown in these figures were generated from the principal direction triad and steering wheel hub force and contain three traces per graph, one each for low-, mid-, and high- velocity impacts. The transfer function includes the response of the steering wheel. The results presented here are considered representative of the general trends observed in a majority of the third test series impacts.

In the third test series, the impact response of the thoraco-abdomen observed in the mechanical impedance data has the following characteristics which are similar to those of frontal thoracic impacts made with a flat surface impactor in the first test series [101]: 1) local minima in impedance were observed in all significant accelerations in the anatomical reference frames or the principal direction triad, and the uniaxial accelerometers; 2) the magnitude of the lower sternum decreased from 15 Hz to the first local minimum; 3) a second local minimum was observed for some tests; 4) for those instrumented points further from the center of the impactor contact, a greater value of mechanical impedance was observed from 15 Hz up to the first local minimum, with ribs R8R and R8L having the most similar impedance values; 5) the impedance values for all significant accelerations increased as velocity increased, and 6) the first local minimum increased in frequency as impact velocity increased.

The impact response of the steering wheel observable in the mechanical impedance data has the following characteristics which were different from those of the first test series frontal thoracic impacts [101]: 1)

the mechanical impedance values were higher in the steering wheel impacts in the low frequency (below 15 Hz); 2) the low frequency components in the steering wheel data (those below 15 Hz) for a given velocity impact were characteristically the same for all principal directions; 3) for the third test series sternum impacts, the second local minimum generally occurred at 3 times the first local minimum, while for the first series frontal impacts with a flat impactor [101], the second local minimum occurred at 2 times the first local minimum, 4) in general, the ribs R8R and R8L transfer function for the principal direction acceleration for steering wheel impacts differed from each other to a greater degree than those of the flat surface impacts to the sternum [101], and 5) the first local minimum was clearly observed in all mechanical impedance transfer functions for any significant acceleration for the sternum impacts with a flat impactor [101]. This was not always the case for steering wheel impacts. The first local minimum of the mechanical impedance occurred in the 32-38 Hz range in the first test series flat surface impacts for the sternum [101], while in the third test series steering wheel impacts of similar impact velocity for the sternum, it occurred in the 20-25 Hz range.

The local minima observed in all of the third series tests were not necessarily related to resonances of the thoracic system in terms of free vibrations. During the force time-history, the steering wheel had a constantly changing load surface as well as a constantly changing load direction. In addition, the direction of the loading with respect to the test subject changed as the test subject rotated onto the steering wheel. This may, in part, have caused the differences observed in the first local minima for the mechanical impedance for the different impact

velocities. The complex loading conditions may have resulted in the differences which were observed between the flat surface impacts and the steering wheel impacts in terms of mechanical impedance.

In the third test series, the local minima (resonances) for the sternum were: for low-velocity impacts, 20-25 Hz; for mid-velocity impacts, 25-35 Hz; and for high-velocity impacts 30-45 Hz. Similar to the flat surface impacts of the first test series [101], the decrease in the magnitude of the mechanical impedance up to the first local minimum for the lower sternum, indicated that a spring value for low-velocity impacts was $3x10^4$; $6x10^4$ for mid- velocity impacts; and $9x10^4$ for high-velocity impacts. Similar to the blunt frontal impacts made with the flat surface impactor in the first test series [101], the magnitude of the mechanical impedance displayed spring-like characteristics, while the phase did not.

In many of the first test series flat surface impaccts [101], the magnitude of the mechanical impedance for the spine principal direction exhibited a mass-like behavior between 15-25 kg. In the third test series steering wheel impacts, the magnitude of the mechanical impedance for the spine was closer to a damper of $1.5x10^3$ n.s/m up to the first local minimum. However, similar to the spring-like behavior of the sternum, the phase of the transfer function was not damper-like. In addition, the complexity (larger number of maximum and minimum) of the mechanical impedance transfer function was greater for the third test series steering wheel impacts than for the first test series blunt sternum impacts [101].

The similarity between the sternum response of the third test series steering wheel impacts and the first test series flat surface impacts [101], in terms of mechanical impedance magnitude, is believed to be a result of the observation that the major loading of the steering wheel on the sternum was from the steering wheel hub. The differences in the traces associated with the ribs (R8R and R8L) and the spine between the steering wheel impacts and the blunt frontal flat surface impacts [101], was a result of a number of different load paths to those anatomical structures.

6.11 Transfer Functions - One of the goals of the third test series was to quantitatively characterize the response of the thoracic skeletal structure in terms of a transfer function between any two points on the thorax which possessed a significant component of acceleration. In this regard, transfer functions were generated between any given accelerometer package and any other given accelerometer package, resulting in a number of transfer functions for each point generating the corresponding response of every other point. When a transfer function was generated between two points such that the denominator was obtained from the accelerometer package of the sternum, the transfer function had the characteristics of a low-pass filter. Transfer functions which were generated further from the point of impact (R8R and R8L, T1 and T12) displayed an increasingly greater attenuation. In general, the transfer functions which were generated from the significant acceleration components of the various points of the thorax resulted in responses typified as a general decrease in magnitude with increasing frequency and varying in phase at each different frequency. Although there was a general decrease in the magnitude of this transfer

function, the magnitude did not decrease to the same degree as similar transfer functions generated for the first test series in which a flat surface impactor was used [101]. Therefore, if it is reasonable to assume that the thorax is a deformable structure, the response of the thorax is dependent upon the load path and upon the energy management of the system (gross motion, differential motion, or dissipation).
In the third test series impacts, a complicated load path was obtained through the use of a steering wheel, and such effects as loading of a single rib may have occurred for short time durations. The increased complexity, as well as the larger variation in transfer functions generated in the third test series impacts compared to others [98,101], indicated a much more complex loading path. Although there were clear similarities between the first test series flat surface impacts [101] and the third test series steering wheel impacts, the difference was significant enough so as to caution against using one to predict the other.

In general, the transfer functions that were generated for the first test series between the lower sternum and the thoracic vertebra T12, associated with the low- and mid-velocity impacts, showed less attenuation than were observed in the third test series low-velocity steering wheel impacts. Physically, this implies that the thoracic structure could have been effectively stiffer as the impact velocity increased. Similar observations have been made previously which suggest that the thorax stiffens under higher-impact velocity [53,65].

7.0 CONCLUSIONS

The first test series was a limited, preliminary study, using unembalmed cadavers, of some important kinematic factors and damage modes of the

thoracic skeletal structure associated with blunt impact of the thorax. Because of the complex nature of the thorax during an impact event, more work is necessary before these kinematic factors can be generalized to describe thoracic skeletal response. However the following conclusions are drawn from the first test series:

1) For lateral impacts a single linear model seems inadequate to characterize thoracic impact response for all impact velocities. In terms of mechanical impedance (generated between various points on the thoracic skeletal structure and the impact force) as well as transfer functions (generated between points on the thoracic cage), there seems to be a significant difference between low velocity (non-damaging) and high velocity (damaging) impact responses.

2) In low-energy, non-damaging impacts (2 m/s with a 26 kg impactor) the response of the subjects seems to have certain characteristics in both the time and frequency domain that are similar for all impact directions. In general the thorax acts as a deformable body during blunt impact with the transmitted energy partitioned as both differential and gross whole body motion. In particular, the nearside and farside response differ with greater deformation occurring at the nearside locales. Similarities are seen between the impact responses of the different nearside locales (left side for lateral impacts and sternum for frontal impacts) and between the different farside locales (right side for lateral impacts and spine for frontal).

3) The description of three-dimensional acceleration of select points on the skeletal structure is invaluable to the understanding of thoracic

impact response. The results obtained from a single dimensinal descriptor (such as right-to-left acceleration velocity or displacement for lateral impacts) seems inadequate to characterize thoracic impact response.

4) For the second test series, the low frequency components of a mechanical impedance transfer function indicate an effective mass was near half of the whole body mass.

5) For the third test series, steering wheel impacts using a 25 kg pendulum produced significantly different results, in terms of steering wheel hub force and thoracic cage acceleration from that of a 65 kg pendulum [96]. In a steering wheel impact using a low mass pendulum (25 kg), the amount of energy transferred to the test subject can significantly affect the velocity of the impactor during impact. Potentially, this would lead to greater variability in the impact response, as the test subject mass would, to a greater degree than that of a heavier pendulum (65 kg), affect the impact response [96].

6) The heart-aorta, the liver, and the spleen are soft-tissue organs which are protected by the thoracic cage. The responses of the bony structures of the thoracic cage are critical factors in the mechanism of injuries for these organs. Therefore, in terms of dynamic and injury responses, the liver and spleen should be considered thoracic organs.

7) For frontal impacts using a steering wheel assembly, a single linear model seems inadequate to characterize thoracic impact response for

all impact velocities. In terms of mechanical impedance (generated between various points on the thoracic cage and steering wheel hub force) as well as transfer functions between two points on the thoracic cage, there seems to be a significant difference between low-velocity (non-damaging) and high-velocity (damaging) impact response.

8) The complex interaction of the steering wheel with the thoracic cage requires a three-dimensional description of impact response in terms of: 1) gross whole body motion, and 2) differential motion as determined by the acceleration response of selected points on the skeletal structure. The results obtained from accelerometers fixed to the thoracic cage imply a complex thoracic response as well as multiple paths of energy transmission. When the body trunk is impacted by the steering wheel, load paths originate from the rim, the spokes, and the hub. The degree and point in time at which these load paths dominate the thoracic response is dependent upon the initial configuration of the steering wheel in regard to the test subject, as well as upon the biovariability of the population.

9) Severe injuries which involve the major arteries or veins in the organs protected by the thoracic cage seem to be impact-position dependent. Thoraco-abdominal impact tolerance levels based on deflection or velocity may be inadequate to the situations which occur in steering wheel impacts. Although velocity and deflection seem to be important parameters in determining thoraco-abdominal impact tolerance levels, severe injuries involving the major arteries or veins were observed to be impact position and initial test

configuration dependent in the response programs reported here. Location of the heart and liver with respect to the impact structure is an important criteria that needs to be addressed in thoraco-abdominal impact.

10) Changes in the material properties of soft tissues after death may have significant effect on the damage pattern in the postmortem subject when compared to live humans. In particular, postmortem change of the mediastinal tissue can have significant effects on the injury pattern of the heart-aorta system of a canine model produced as a result of blunt impact to the sternum.

ACKNOWLEDGEMENTS

The three test series in the Experimental Data for Development of Finite Element Models: Head/Thoraco-Abdomen/Pelvis research program were funded by the United States Department of Transportation, National Highway Traffic Safety Administration, Contract No. DOT-HS-7-01636. The authors wish to acknowledge the technical assistance of Donald F. Huelke, Nabih Alem, John Melvin, Bryan Suggitt, Gail Muscott, Paula Lux, Marvin Dunlap, Don Erb, and Jean Brindamour. The authors also acknowledge the contributions of Jeff Pinsky, Allen C. Bosio, Zheng Lou, Valerie Moses, Wendy Gould, Steven Richter, Peter Schuetz, Shawn Cowper, Tim Jordan, Patrice Muscott, and Reza Salehi. A special thank you goes to Jeff Marcus.

8.0 REFERENCES

1. The Abbreviated Injury Scale (AIS), 1980 revision, American Association for Automotive Medicine, Morton Grove, IL.

2. Alem, N.M., et al. 1978. Whole-Body Human Surrogate Response to Three-Point Harness Restraint. In: 22nd Stapp Car Crash Conference Proceedings, pp. 359-399.

3. Beckman, D.L. and Friedman, B.A. 1972. Mechanics of Cardiothoracic Injury in Primates. Journal of Trauma 12(7):620-629. July.

4. Beckman, D.L. and Palmer, M.F. 1969. Response of the Primate Thorax to Experimental Impact. In: 13th Stapp Car Crash Conference Proceedings, pp. 270-281.

5. Beckman, D.L., Palmer, M.F. and Roberts, V.L. 1971. Mechanisms of Cardio-thoracic Injury. In: International Assoc. for Accident and Traffic Medicine Conference Proceedings, pp. 300-304.

6. Beckman, D.L., Palmer, M.F. and Roberts, V.L. 1970. Thoracic Force-Deflection Studies in Living and Embalmed Primates. HSRI ASME 70-BHF-8.

7. Brinn, J. and Staffeld, S.E. 1972. The Effective Displacement Index--An Analysis Technique for Crash Impacts of Anthropometric Dummies. In: 15th Stapp Car Crash Conference Proceedings, pp. 817-824.

8. Brinn, J. and Staffeld, S.E. 1970. Evaluation of Impact Test Accelerations: A Damage Index for the Head and Torso. In: 14th Stapp Car Crash Conference Proceedings, pp. 188-202.

9. Burdi, A.R. 1970. Thoracic and Abdominal Anatomy. In: Huelke, D.F., ed., Human Anatomy, Impact Injuries, and Human Tolerances, SAE 700195, pp. 52-68.

10. Burow, K.H. 1972. Injuries of the Thorax and of the Lower Extremities to Forces Applied by Blunt Object. In: 15th Conference Proceedings American Assoc. for Automotive Medicine, pp. 122-150.

11. Burow, K. and Kramer, M. 1973. Experimental Investigations on the Type and Severity of Fractures in the Chest Cavity. [in German] International Conference on the Biokinetics of Impacts Proceedings, pp. 387-397.

12. Cammack, K., et al. 1959. Deceleration Injuries of the Thoracic Aorta. Arch. Surg. 79.

13. Cesari, D., and Ramet, M. 1979. Evaluation of Human Tolerance in Frontal Impacts. In: 23rd Stapp Car Crash Conference Proceedings, pp. 873-914.

14. Cesari, D., Ramet, M. and Bloch, J. 1981. Influence of Arm Position on Thoracic Injuries in Side Impact. In: 25th Stapp Car Crash Conference Proceedings, pp. 271-297.

15. Chapon, A. 1984. Evaluation of the Research Results of the Biomechanics Programme (Phases I, II and III). In: Benjamin, T.E.A., ed., Biomechanics of Impacts in Road Accidents, Luxembourg: Commission of the European Communities, pp. 541-554.

16. Charles, K.P., et al., 1977. Traumatic Rupture of the Ascending Aorta and Aortic Valve Following Blunt Chest Trauma. Journal of Thoracic and Cardiovascular Surgery 73(2):208-211. Feb.

17. Cheng, R., et al. 1982. Injuries to the Cervical Spine Caused by a Distributed Frontal Load to the Chest. 26th Stapp Car Crash Conference Proceedings, pp. 1-40.

18. Clowes, A.M. and Clowes, M.M. 1980. Influence of Chronic Hypertension on Injured and Uninjured Arteries in Spontaneously Hypertensive Rats. Laboratory Investigations 43(6).

19. Cooper, G.J., et al. 1982. The Biomechanical Response of the Thorax to Nonpenetrating Impact with Particular Reference to Cardiac Injuries. Journal of Trauma 22(12):994-1008.

20. Cooper, G.J., et al., 1981. Prediction of Chest Wall Displacement and Heart Injury from Impact Characteristics of a Non-penetrating Projectile. Proceedings 6th International IRCOBI Conference on the Biomechanics of Impacts, pp. 297-312.

21. Cooper, G.J., et al., 1981. Visualization of Heart Movement Following Non-penetrating Impact Using Cine and Flash X-Ray. Proceedings 6th International IRCOBI Conference on the Biomechanics of Impacts, pp. 313-320.

22. Cotte, J.P. 1977. Semi-static Loading of Baboon Torsos. 3rd International Conference on Impact Trauma Proceedings, pp. 165-179.

23. Crancer, A. and O'Neall, P. 1970. A Record Analysis of Washington Drivers with License Restrictions for Heart Disease. Northwest Medicine 69(June):409-416.

24. Culver, R.H., et al., 1978. Evaluation of Intrathoracic Response Using High-speed Cineradiography. 6th New England Bioengineering Conference Proceedings, pp. 365-369.

25. Culver, R.H., et al. 1977. Feasibility of Investigating the Mechanisms of Aortic Trauma Using High-speed Cineradiography. UM-HSRI-77-53.

26. Digges, K.H. 1983. Dynamic Response of the Human Thorax When Subjected to Frontal Impact. O.U.E.L. 1453/83. Oxford University (England), Dept. of Engineering Science.

27. Digges, K.H. 1983. Mathematical Model of the Human Thorax When Subjected to Frontal Impact During an Automobile Crash. O.U.E.L. 1454/83. Oxford University (England), Dept. of Engineering Science.

28. Eppinger, R.H. 1978. Prediction of Thoracic Injury Using Measurable Experimental Parameters. 6th International Technical Conference on Experimental Safety Vehicles, NHTSA, pp. 770-780.

29. Eppinger, R.H. and Chan, H.S. 1981. Thoracic Injury Prediction via Digital Convolution Theory. 25th Stapp Car Crash Conference Proceedings, pp. 369-393.

30. Eppinger, R.H., Augustyn, K., and Robbins, D.H. 1978. Development of a Promising Universal Thoracic Trauma Prediction Methodology. In: 22nd Stapp Car Crash Conference Proceedings, pp. 209-268.

31. Fanyon, A., et al. 1978. Methods for Backing-up the Conclusions of Accident Reconstructions Carried Out with Instrumented Cadavers. Proceedings 3rd International Meeting on the Simulation and Reconstruction of Impacts in Collisions, pp. 220-233.

32. Fine, P.R., Kuhlemeier, K.V. and DeVivo, M.J. 1979. Residual Cardiovascular Damage Resulting from Nonpenetrating Steering Wheel Impact. Proceedings 23rd Conference American Assoc. for Automotive Medicine, pp. 28-42.

33. Foret-Brund, J.Y., et al. 1978. Correlation Between Thoracic Lesions and Force Values Measured at the Shoulder of 92 Belted Occupants Involved in Real Accidents. In: 22nd Stapp Car Crash Conference Proceedings, pp. 28-42.

34. Frey, C.F., et al. 1973. A Fifteen-Year Experience with Automotive Hepatic Trauma. Journal of Trauma 13(11):1039-1049.

35. Frey, C.F. 1970. Injuries to the Thorax and Abdomen. In: Human Anatomy, Impact Injuries and Human Tolerances. SAE Paper No. 700195.

36. Gauthier, R.K. 1984. Thoracic Trauma. Emergency Medical Services 13(3):28, 30-35. May/June.

37. Gloyns, P.F., et al. 1979. Analysis of Additional Accident Data Relating to the Performance of Steering Systems Developed to Comply with Current Safety Regulations. Birmingham University (England), Dept. of Transportation and Environmental Planning.

38. Gloyns, P.F., et al. 1973. Field Investigations of the Injury Protection Offered by Some "Energy Absorbing" Steering Systems. International Conference on the Biokinetics of Impacts Proceedings, pp. 399-410.

39. Gloyns, P.F., Hayes, H.R.M. and Rattenbury, S.J. 1980. Protection of the Car Driver from Steering System Induced Injuries. In: Towards Safer Passenger Cars, London: Mechanical Engineering Publications, Ltd., pp. 23-30.

40. Got, C., et al. 1975. Morphological, Chemical and Physical Characteristics of the Ribs and Their Relationship to Induced Deflection of the Thorax. [in French] In: Cotte, J.P. and Presle, M.M., eds., Biomechanics of Serious Trauma, Bron: IRCOBI, pp. 220-228.

41. Gotze, L., Flory, P.J. and Otte, D. 1980. Biomechanics of Aortic Rupture at Classical Location in Traffic Accidents. Thoracic and Cardiovascular Surgery (West Germany).

42. Granik, G. and Stein, I. 1973. Human Ribs: Static Testing as a Promising Medical Application. Journal of Biomechanics 6(3):237-240.

43. Greendyke, R.M. 1966. Traumatic Rupture of Aorta: Special Reference to Automobile Accidents. Journal of the American Medical Association 195(7), February.

44. Gurdjian, E.S., et al. 1979. Impact Injury and Crash Protection, Springfield, IL: Charles C. Thomas.

45. Haut, R.C., et al. 1978. Cardiovascular Response of an Atherosclerotic Animal Model to Thoracic Impact. Proceedings of the First Mid-Atlantic Conference on Bio-Fluid Mechanics, Blacksburg, VA, August.

46. Hennig, K. and Franke, D. 1979. Rupture of the Heart After Blunt Thoracic Trauma. [in German] Unfallheilkunde 82(7):297-305.

47. Hess, R.L., Weber, K. and Melvin, J.W. 1982. Review of Research on Thoracic Impact Tolerance and Injury Criteria Related to Occupant Protection. In: Occupant Crash Interaction with the Steering System, SAE 820474, pp. 93-119.

48. Hess, R.L., Weber, K. and Melvin, J.W. 1981. Review of Literature and Regulation Relating to Thoracic Impact Tolerance and Injury Criteria. UM-HSRI-81-38. Highway Safety Research Institute, Ann Arbor, MI.

49. Horsh, J.D., et al. 1979. Response of Belt Restrained Subjects in Simulated Lateral Impact. In: 23rd Stapp Car Crash Conference Proceedings, pp. 69-103.

50. Hossack, D.W. 1980. Rupture of the Aorta in Road Crash Victims. Australian and New Zealand Journal of Accident Surgery 50(2).

51. Huelke, D.F. 1982. Steering Assembly Performance and Driver Injury Severity in Frontal Crashes. In: Occupant Crash Interaction with the Steering System, SAE 820474, pp. 1-30.

52. Huelke, D.F. 1976. The Anatomy of the Human Chest. In: The Human Thorax-Anatomy, Injury and Biomechanics, SAE P-67, pp. 1-9.

53. Jonsson, A., et al. 1979. Dynamic Factors Influencing the Production of Lung Injury in Rabbits Subjected to Blunt Chest Wall Impact. Aviation, Space and Environmental Medicine 50(4):325-337.

54. Kaleps, I. 1975. Thoracic Dynamics During Blunt Impact. In: Saczalski, K., et al., eds., Aircraft Crashworthiness, Charlottesville: University Press of Virginia, pp. 235-252.

55. Kallieris, D., et al. 1979. Thorax Acceleration Measures at the 6th Thoracic Vertebra in Connection to Thorax and Spinal Column Injury Degree. Proceedings 4th International IRCOBI Conference on the Biomechanics of Trauma, pp. 184-197.

56. Kallieris, D., Mattern, H., and Schmidt, G. 1981. Quantification of Side Impact Responses and Injuries. In: 25th Stapp Car Crash Conference Proceedings, pp. 329-366.

57. Kallieris, D., et al. 1982. Comparison Between Frontal Impact Tests With Cadavers and Dummies in a Simulated True Car Restraint Environment. In: 26th Stapp Car Crash Conference Proceedings, pp. 353-367.

58. Kalny, J. and Sezak, Z. 19?? Transport Fractures of the Sternum. [in Chechoslovakian] Acta Chirurgiae Orthopaedicae et Traumatologiae Chechoslovaca 42(5):459-466. Oct.

59. Kazarian, L.E., Hahn, J.W. and von Gierke, H.E. 1970. Biomechanics of the Vertebral Column and Internal Organ Response to Seated Spinal Impact in the Rhesus Monkey (Macaca mulatta). 14th Stapp Car Crash Conference Proceedings, pp. 121-143.

60. King, A.I. and Khalil, T.B. 1982. Crash Injury Studies. GMR-3904. Wayne State University, Detroit, MI.

61. Klotz, O. and Simpson, W. 1932. Spontaneous Rupture of the Aorta. American Journal Medical Science 184:455.

62. Kramer, M. 1976. Injury Index in Accident--Simulated Trauma of Chest and Lower Leg. [in German] Unfallheilkunde 79(2): 61-69. Feb.

63. Kramer, M. and Heger, A. 1975. Severity Indices for Chest and Lower Leg Injuries. [in German] In: Cotte, J.P. and Presle, M.M., eds., Biomechanics of Serious Trauma, Bron: IRCOBI, pp. 229-239.

64. Kroell, C.K. 1976. Thoracic Response to Blunt Frontal Loading. In: The Human Thorax--Anatomy, Injury and Biomechanics, SAE P-67, pp. 49-77.

65. Kroell, C.K., et al. 1981. Interrelationship of Velocity and Chest Compression in Blunt Thoracic Impact to Swine. 25th Stapp Car Crash Conference Proceedings, pp. 549-579.

66. Kroell, C.K., Schneider, D.C., and Nahum, A.M. 1974. Impact Tolerance and Response of the Human Thorax II. In: 18th Stapp Car Crash Conference Proceedings, pp. 383-457.

67. Kroell, C.K., Schneider, D.C., and Nahum, A.M. 1972. Impact Tolerance and Response of the Human Thorax. In: 15th Stapp Car Crash Conference Proceedings, pp. 84-134.

68. Liu, Y.K. 1968. The Human Body Under Time-Dependent Boundary Conditions. University of Michigan, Ann Arbor, Dept. of Engineering Mechanics. March.

69. Liu, Y.K. and Wickstrom, J.K. 1973. Estimation of the Inertial Property Distribution of the Human Torso from Segmented Cadaveric Data. In: Kenedi, R.M., ed., Perspectives in Biomedical Engineering, London: Macmillan Press, Ltd., pp. 203-213.

70. Lundevall, J. 1964. The Mechanism of Traumatic Rupture of the Aorta. Acta Path. Microbiol. 62:34.

71. Martin, J.D., Jr., ed. 1969. Trauma to the Thorax and Abdomen. Emory University School of Medicine, Dept. of Surgery, Atlanta, GA.

72. Mays, E.T. 1966. Bursting Injuries of the Liver. Archives of Surgery 93(92)103.

73. Melvin, J.W. 1976. Biomechanics of Lateral Thoracic Injury. In: The Human Thorax -- Anatomy, Injury and Biomechanics, Warrendale, PA: SAE, pp. 79-84.

74. Melvin, J.W., et al. 1973. Impact Injury Mechanisms in Abdominal Organs. 17th Stapp Car Crash Conference Proceedings, pp. 115-126.

75. Melvin, J.W., Robbins, D.H.; Stalnaker, R.L. and Eppinger, R.H. 1977. Prediction of Multidirectional Thoracic Impact Injuries. 3rd International Conference on Impact Trauma Proceedings, pp. 281-285A.

76. Melvin, J.W. and Wineman, A.S. 1975. Thoracic Model Improvements (Experimental Tissue Properties). HSRI UM-HSRI-BI-74-2-1/DOT/HS 801 557, UM-HSRI-BI-74-2-2/DOT/HS 801 558, and UM-HSRI-BI-74-2-3 DOT/HS 801 559.

77. Mertz, H.J. 1984. A Procedure for Normalizing Impact Response Data, SAE 840884.

78. Mertz, H.J. and Gadd, C.W. 1972. Thoracic Response of the Whole-Body Acceleration. In: 15th Stapp Car Crash Conference Proceedings, pp. 135-157.

79. Modell, H.I. and Baumgardner, F.W. 1984. Influence of the Chest Wall on Regional Intrapleural Pressure During Acceleration (+Gz) Stress. Aviation, Space, and Environmental Medicine 55(10):896-902. Oct.

80. Mohan, D. 1976. Passive Mechanical Properties of Human Aortic Tissue. PhD Dissertation, Bioengineering, The University of Michigan.

81. Mohan, D. and Melvin, J. 1983. Failure Properties of Passive Human Aortic Tissue II - Biaxial Tension Tests. Journal of Biomechanics 16(1).

82. Mohan, D. and Melvin, J. 1982. Failure Properties of Passive Human Aortic Tissue I - Uniaxial Tension Tests. Journal of Biomechanics 15(11).

83. Morgan, R.M., Marcus, J.H., and Eppinger, R.H. 1981. Correlation of Side Impact Dummy/Cadaver Tests. Journal of Bone and Joint Surgery 43-A(3): 327-351. April.

84. Morris, J.M., Lucas, D.B. and Bresler, B. 1961. Role of the Trunk in Stability of the Spine. Journal of Bone and Joint Surgery 43-A(3):327-351. April.

85. Mulder, D.S. 1980. Chest Trauma - Current Concepts. Canadian Journal of Surgery 23(4).

86. Mulligan, G.W., et al. 1976. An Introduction to the Understanding of Blunt Chest Trauma. In: The Human Thorax - Anatomy, Injury, and Biomechanics. P-67, Warrendale, PA: Society of Automotive Engineers, October.

87. Nahum, A.M. 1973. Chest Trauma. In: Biomechanics and Its Application to Automotive Design, SAE, NY.

88. Nahum, A.M., et al. 1971. The Biomechanical Basis for Chest Impact Protection: I. Force-Deflection Characteristics of the Thorax. Journal of Trauma 11(10):874-882. Oct.

89. Nahum, A.M., et al. 1970. Deflection of the Human Thorax Under Sternal Impact. In: 1970 International Automobile Safety Conference Compendium, SAE, pp. 797-807.

90. Nahum, A.M., Kroell, C.K. and Schneider, D.C. 1973. The Biomechanical Basis of Chest Impact Protection. II. Effects of Cardiovascular Pressurization. Journal of Trauma 13(5):443-459. May.

91. Nahum, A.M., Schneider, D.C. and Kroell, C.K. 1975. Cadaver Skeletal Response to Blunt Thoracic Impact. 19th Stapp Car Crash Conference Proceedings, pp. 259-293.

92. Neathery, R.F. and Lobdell, T.E. 1973. Mechanical Simulation of Human Thorax Under Impact. 17th Stapp Car Crash Conference Proceedings, pp. 451-466.

93. Newman, R.J. and Jones, I.S. 1984. A Prospective Study of 413 Consecutive Car Occupants with Chest Injuries. Journal of Trauma 24(2):129-135. Feb.

94. Nickerson, J.L. 1962. International Body Movements Resulting from Externally Applied Sinusoidal Forces. Chicago Medical School, IL. AMRL-TDR-62-81. July.

95. Nusholtz, G. 1977. Vascular and Respiratory Pressurization of the Thorax. 5th Annual Committee Reports and Technical Discussions International Workshop on Human Subjects for Biomechanical Research, pp. 81-95.

96. Nusholtz, G.S., et al. 1985. Thoraco-Abdominal Response to Steering Wheel Impacts. In: 29th Stapp Car Crash Conference Proceedings.

97. Nusholtz, G.S., et al. 1981. Response of the Cervical Spine to Superior-Inferior Head Impact. In: 25th Stapp Car Crash Conference Proceedings, pp. 197-237.

98. Nusholtz, G.S., et al. 1980. Thoraco-abdominal Response and Injury. 24th Stapp Car Crash Conference Proceedings, pp. 187-228.

99. Nusholtz, G.S., Lux, P., and Janicki, M.A. 1982. Experimental Data for Use with Biomechanical Models. Interim Report. Volume 2, Ann Arbor, MI: The University of Michigan Transportation Research Institute.

100. Nusholtz, G.S., Melvin, J.W. and Alem, N. 1979. Head Impact Response Comparisons of Human Surrogates. In: 23rd Stapp Car Crash Conference Proceedings, pp. 497-541.

101. Nusholtz, G.S., Melvin, J.W. and Lux, P. 1983. The Influence of Impact Energy and Direction on Thoracic Response. 27th Stapp Car Crash Conference Proceedings, pp. 69-94.

102. Park, W.H. and Okunseinde, O. 1977. The Development of a New Impact System for Canine Thorax Impact Studies. Proceedings HOPE International JSME Symposium, pp. 423-432.

103. Patrick, L.M. 1981. Impact Force-deflection of the Human Thorax. 25th Stapp Car Crash Conference Proceedings, pp. 471-496.

104. Plank, G.R. 1978. Review of Chest Deflection Measurement Techniques and Transducers. Final Report. Transportation Systems Center, Cambridge, MA.

105. Pope, M.E., et al. 1979. Postural Influences on Thoracic Impact. 23rd Stapp Car Crash Conference Proceedings, pp. 765-795.

106. Primm, R.K., Karp, R.B. and Schrank, J.P. 1979. Multiple Cardiovascular Injuries and Motor Vehicle Accidents. American Medical Assoc. Journal 241(23):2540-2541. June.

107. Raschke, K., Eckert, P. and Kohne, U. 1972. The Role of the Liver and Pancreas Injuries along with Multiple Injuries. [in German] Monatsschrift fur Unfallheilkunde, Versicherungs-, Versogungs-und Verkehrsmedizin 75(3):117-123.

108. Reddi, M.M., et al. 1975. Thoracic Impact Injury Mechanism. F-C3417/DOT/HS 801 710 and 711. Franklin Institute Research Laboratories, Philadelphia, PA.

109. Reddi, M.M. and Tsai, H.C. 1977. Computer Simulation of Human Thoracic Skeletal Response. F-C4216-1/DOT/HS 803 208, 209, 210. Franklin Institute Research Laboratories, Philadelphia, PA.

110. Rittenhouse, E.A., et al. 1969. Traumatic Rupture of the Thoracic Aorta. Ann. of Surg. 170:86.

111. Roberts, S.B. 1975. Intrusion of the Sternum into the Thoracic Cavity During Frontal Chest Impact and Injury Potential. In: Saczalski, K., et al., eds., Aircraft Crashworthiness, Charlottesville: University Press of Virginia, pp. 253-271.

112. Roberts, V.L. 1967. Experimental Studies on Thoracic and Abdominal Injuries. In: Selzer, M.L., et al., eds., The Prevention of Highway Injury, Highway Safety Research Institute, Ann Arbor, MI, pp. 211-215.

113. Roberts, V.L. and Beckman, D.L. 1970. The Mechanisms of Chest Injuries. In: Gurdjian, E.S., et al., eds., Impact Injury and Crash Protection, Charles C. Thomas Publisher, pp. 86-100.

114. Roberts, V.L., Jackson, F.R. and Berkas, E.M. 1966. Heart Motion Due to Blunt Trauma to the Thorax. 10th Stapp Car Crash Conference Proceedings, pp. 242-248.

115. Roberts, V.L., Moffat, R.C. and Berkas, E.M. 1966. Blunt Trauma to the Thorax--Mechanism of Vascular Injuries. 9th Stapp Car Crash Conference Proceedings, pp. 3-12.

116. Robbins, D.H., Melvin, J.W., and Stalnaker, R.L. 1976. In: 20th Stapp Car Crash Conference Proceedings, pp. 697-729.

117. Sacreste, J., et al. 1984. Evaluation of the Influence of Inter-Individual Differences on the Injury Level: Application to Accident Reconstructions with Cadavers. In: Benjamin, T.E.A., ed., Biomechanics of Impacts in Road Accidents, Luxembourg: Commission of the European Communities, pp. 246-269.

118. Sacreste, J., et al. 1982. Proposal for a Thorax Tolerance Level in Side Impacts Based on 62 Tests Performed With Cadavers Having Known Bone Condition. In: 26th Stapp Car Crash Conference Proceedings, pp. 155-171.

119. Sacreste, J., et al. 1979. Progress in the Interpretation of Cadaver Injuries. Proceedings 7th International Workshop on "Human Subjects for Biomechanical Research", pp. 209-211.

120. Sances, A., Jr., et al. 1984. Biodynamics of Vehicular Injuries. In: Peters, G.A. and Peters, B.J., eds., Automotive Engineering and Litigation, NY: Garland Law Publishing, pp. 449-550.

121. Schmidt, G. 1979. Rib-Cage Injuries Indicating the Direction and Strength of Impact. Forensic Science 13(2):103-110. March/April.

122. Schmidt, G., et al. 1975. Neck and Thoracic Tolerance Levels of Belt-Protected Occupants in Head-On Collisions. In: 19th Stapp Car Crash Conference Proceedings, pp. 225-257.

123. Schreck and R.M., Viano, D.C. 1973. Thoracic Impact: New Experimental Approaches Leading to Model Synthesis. 17th Stapp Car Crash Conference Proceedings, pp. 437-450.

124. Sevitt, S. 1977. The Mechanisms of Traumatic Rupture of the Thoracic Aorta. British Journal of Surgery 64(3): 166-173. March.

125. Sevitt, S. 1977. Traumatic Ruptures of the Aorta: A Clinico-Pathological Study. Injury:The British Journal of Accident Surgery 8(3):159-173.

126. Shatsky, S.A., et al. 1974. Traumatic Distortions of the Primate Head and Chest: Correlations of Biomechanical, Radiological and Pathological Data. 18th Stapp Car Crash Conference Proceedings, pp. 351-381. SAE Paper No. 741186.

127. Shatsky, S.A. 1973. Flash X-Ray Cinematography During Impact Injury. In: 17th Stapp Car Crash Conference Proceedings. SAE Paper No. 730978.

128. Society of Automotive Engineers. 1976. The Human Thorax--Anatomy, Injury, and Biomechanics, SAE P-67.

129. Stalnaker, R.L. and Mohan, D. 1974. Human Chest Impact Protection Criteria. 3rd International Conference on Occupant Protection Proceedings, pp. 384-393.

130. Stalnaker, R.L., Roberts, V.L., and McElhaney, J.H. 1973. Side Impact Tolerance to Blunt Trauma. In: 17th Stapp Car Crash Conference Proceedings, pp. 377-408.

131. Strassman, G. 1947. Traumatic Rupture of the Aorta. American Heart Journal 33:508.

132. Sutorious, D.J., Schreiber, J.T. and Helmsworth, J.A. 1973. Traumatic Disruption of the Thoracic Aorta. Journal of Trauma 13(July):583.

133. Symbas, P.N. 1977. Great Vessel Injuries. American Heart Journal 92(4).

134. Terhune, K.W., Smist, T.E. and Hendricks, D.L. 1982. Steering Column Special Study Data Analysis. 6804-Y-1/DOT/HS 806 287. Calspan Field Services, Inc., Buffalo, NY.

135. Trollope, M.L., et al. 1973. The Mechanism of Blunt Injury in Abdominal Trauma. Journal of Trauma 13:962-970.

136. Verriest, J.P., Chapon, A. and Trauchessec, R. 1981. Cinephotogrammetrical Study of Porcine Thoracic Response to Belt Applied Load in Frontal Impact--Comparison between Living and Dead Subjects. 25th Stapp Car Crash Conference Proceedings, pp. 499-545.

137. Viano, D.C. 1983. Biomechanics of Nonpenetrating Aortic Trauma: A Review. In: 27th Stapp Car Crash Conference Proceedings, pp. 109-114. SAE Paper No. 831608.

138. Viano, D.C. 1983. Cardiovascular Injury from Blunt Thoracic Impact of Epinephrine and Isoproterenol Injected Rabbits. Journal of Aviation, Space, and Environmental Medicine (August).

139. Viano, D.C. 1978. Thoracic Injury Potential. Proceedings 3rd International Meeting on the Simulation and Reconstruction of Impacts in Collisions, pp. 142-156.

140. Viano, D.C., et al. 1978. Factors Influencing Biomechanical Response and Closed Chest Trauma in Experimental Thoracic Impacts. In: Huelke, D.F., ed., 22nd Proceedings American Assoc. for Automotive Medicine, pp. 67-82.

141. Viano, D.C., et al. 1978. Sensitivity of Porcine Thoracic Responses and Injuries to Various Frontal and a Lateral Impact Site. 22nd Stapp Car Crash Conference Proceedings, pp. 167-207.

142. Viano, D.C. and Artinian, C.G. 1978. Myocardial Conducting System Dysfunctions from Thoracic Impact. Journal of Trauma 18(6):452-459.

143. Viano, D.C., Kroell, C.K. and Warner, C.Y. 1977. Comparative Thoracic Impact Response of Living and Sacrificed Porcine Siblings. 21st Stapp Car Crash Conference Proceedings, pp. 627-709.

144. Viano, D.C. and Haut, R.C. 1978. Factors Influencing Biomechanical Response and Closed Chest Trauma in Experimental Thoracic Impact. American Association for Automotive Medicine, Ann Arbor, MI, July.

145. Viano, D.C. and Lau, V.K. 1983. Role of Impact Velocity and Chest Compression in Thoracic Injury. Aviation, Space, and Environmental Medicine 54(1):16-21. Jan.

146. Viano, D.C. and Warner, C.Y. 1976. Thoracic Impact Response of Live Porcine Subjects. In: 20th Stapp Car Crash Conference Proceedings. SAE Paper No. 860823.

147. Walfishch, G., et al. 1982. Tolerance Limits and Mechanical Characteristics of the Human Thorax in Frontal and Side Impact Transposition of These Characteristics into Protection Criteria. Proceedings 7th International IRCOBI Conference on the Biomechanics of Impacts, pp. 122-139.

148. Walt, A.J. and Wilson, R.F. 1973. Blunt Abdominal Injuries: An Overview. In: Biomechanics and Its Application to Automotive Design, NY: SAE.

149. William, G., et al. 1976. An Introduction to the Understanding of Blunt Chest Trauma. In: The Human Thorax--Anatomy, Injury, and Biomechanics, SAE P-67, pp. 11-36.

150. Wilson, S.K. and Hutchins, G.M. 1982. Aortic Dissecting Aneurysms Causative Factors in 204 Subjects. Archives of Pathological Laboratory Medicine 106(4).

151. Wiott, J.F. 1975. The Radiologic Manifestations of Blunt Chest Trauma. American Medical Assoc. Journal 231(5):500-503. Feb.

152. Zehnder, M.A. 1960. Accident Mechanism and Accident Mechanics of the Aortic Rupture in the Closed Thorax Trauma. Thoraxchirurgie und Vasculaere Chirurgie 8.

9.0 APPENDIX B
TEST PROTOCOL

DEPARTMENT OF TRANSPORTATION

MULTIPLE IMPACT TESTS

_____ Through _____

as performed by

the Biomechanics Department of

the Highway Safety Research Institute

Ann Arbor, Michigan

1982-1983 E Series

This protocol for the use of cadavers in this test series was approved by the Committee to Review Grants for Clinical Research of the University of Michigan Medical Center and follows guidelines established by the U.S. Public Health Service and those recommended by the National Academy of Sciences, National Research Council.

TABLE OF CONTENTS

Head Impact 2

Head Impact 4

Front Tap 6

Left Side Tap 8

Left Side Tap - Arms Up 10

Left Side Tap - Arms Down 12

Left Side Impact 14

Pelvic Impact 16

PRE-SURGERY 24

ANTHROPOMETRY 25

Anatomical Anomalies 26

MOUNTS 27

Rib and Sternum Mounts 27

Pressurization 28

Head 9-AX Mount 31

Head Transducers 32

Pelvis Mount 34

Spinal Mounts 36

Cerebrospinal Pressurization 37

POST-SURGERY 38

X-Ray 38

Preparation 38

ELECTRONICS 39

PRETEST TRIAL RUN 39

HEAD IMPACT 1 40

Final Checklist 43

HEAD IMPACT 2 44
Timer Box Setup 45
Final Checklist 46
THORAX TAPS 47
Thorax Front Tap 47
Timer Box Setup 49
Final Checklist 50
45° Thorax Tap 51
Timer Box Setup 53
Final Checklist 54
Optional Arms-Up Thorax Tap 55
Timer Box Setup 57
Final Checklist 58
Arms-Down Thorax Tap 59
Timer Box Setup 61
Final Checklist 62
THORAX IMPACT 63
Timer Box Setup 64
Final Checklist 65
PELVIS IMPACT 66
Timer Box Setup 68
Final Checklist 69
POST TEST PROCEDURE 70
AUTOPSY 72
APPENDICES 75
Anatomy Room Setup 76
Sled Lab Setup 80

Cart Setup 81
Autopsy Setup 83
Timer Box Setup 85
Pendulum Wierdness 86

TEST DESCRIPTION

Cadaver No._____ Sex:_____ Height:_____ Weight:_____

Test No._____ (Head, Shoulder, Pelvis)

Test description: Head impact, subject in a normal seated position, neck angle approx. 10° forward, impact to forehead, angle of head determined by tangent forehead plane.

Type of Impactor: PENDULUM

Type of Bumper: WHITE VIBRATHANE

Type of Striker: 25 Kg PISTON, 15cm DIA.

Impactor Angle: 50°(5.0m/s)

Padding:_____

Pre-Impact Travel: 14cm

Post-Impact Travel: 16cm

35mm stills:

___ Black and White

___ Color

CAMERAS		POSITION
Photosonics 1:	1000	P-A, S-I
Photosonics 2:	_____	_____
HyCam:	3000	P-A, S-I

INSTRUMENTATION

ACCELEROMETERS		TARGETS		TRANSDUCERS	
Head (9 AX)	X	Head	X	Trachea	___
Up. Sternum (3-AX)	___	Acromion	X	Ascending Aorta	___
Lwr. Sternum (1)	___	Sternum (2)	___	Internal Carotid	X
Spine (2 triax)	X	Spine	___		
Pelvis (9 AX)	___	Pelvis	___	Subdural 1:	X
Lwr. Rib R8 (2)	___			2:	X
Up. Rib R4 (2 triax)	___			3:	X
				4:	?

TEST DESCRIPTION

Cadaver No._____ Sex:_____ Height:_____ Weight:_____

Test No._____ (Head, Shoulder, Pelvis)

Test description:_____
Head impact, same as previous.

Type of Impactor: PENDULUM

Type of Bumper: WHITE VIBRATHANE

Type of Striker: 25 Kg PISTON, 15cm DIA.

Impactor Angle: 50°(5.0m/s)

Padding:_____

Pre-Impact Travel: 14cm

Post-Impact Travel: 16cm

35mm stills:

___ Black and White

___ Color

CAMERAS		POSITION
Photosonics 1:	1000	P-A, S-I
Photosonics 2:		
HyCam:	3000	P-A, S-I

INSTRUMENTATION

ACCELEROMETERS		TARGETS		TRANSDUCERS	
Head (9 AX)	X	Head	X	Trachea	
Up. Sternum (3-AX)		Acromion	X	Ascending Aorta	
Lwr. Sternum (1)		Sternum (2)		Internal Carotid	X
Spine (2 triax)	X	Spine			
Pelvis (9 AX)		Pelvis		Subdural 1:	X
Lwr. Rib R8 (2)				2:	X
Up. Rib R4 (2 triax)				3:	X
				4:	?

COMMENTS:

TEST DESCRIPTION

Cadaver No._____ Sex:____ Height:____ Weight:____

Test No._____ (Head, Shoulder, Pelvis)

Test description: Front tap, mid-sternum, angle of thorax determined by sternum tangent plane, top of impact 54 cm from seat pan.

Type of Impactor: PENDULUM

Type of Bumper: WHITE VIBRATHANE

Type of Striker: 25 Kg PISTON, 21cm. sq.

Impactor Angle: 17°(2m/s)

Padding: .5cm ensolite

Pre-Impact Travel: 8cm

Post-Impact Travel: 22cm

35mm stills:

___ Black and White

___ Color

CAMERAS		POSITION
Photosonics 1:	1000	P-A, S-I
Photosonics 2:		
HyCam:	3000	P-A, S-I

INSTRUMENTATION

ACCELEROMETERS		TARGETS		TRANSDUCERS	
Head (9-AX)	X	Head	X	Trachea	X
Up. Sternum (3-AX)	X	Acromion	X	Ascending Aorta	X
Lwr. Sternum (1)	X	Sternum (2)	X	Internal Carotid	___
Spine (2 triax)	X	Spine	___		
Pelvis (9-AX)	___	Pelvis	___	Subdural 1:	___
Lwr. Rib R8 (2)	X			2:	___
Up. Rib R4 (2 triax)	X			3:	___
				4:	___

COMMENTS:

TEST DESCRIPTION

Cadaver No._____ Sex:____ Height:____ Weight:____

Test No._____ (Head, Shoulder, Pelvis)

Test description: Left side tap, 45°P-A into R-L, normal seated posture, move arm if necessary, top of impact 54 cm above seat pan.

Type of Impactor: PENDULUM

Type of Bumper: WHITE VIBRATHANE

Type of Striker: 25 Kg PISTON, 21cm. sq.

Impactor Angle: 17°(2m/s)

Padding: .5cm ensolite

Pre-Impact Travel: 8cm

Post-Impact Travel: 22cm

35mm stills:

___ Black and White

___ Color

CAMERAS		POSITION
Photosonics 1:	1000	45° P-A into R-L, S-I
Photosonics 2:	_____	_____
HyCam:	3000	45° P-A into R-L, S-I

INSTRUMENTATION

ACCELEROMETERS		TARGETS		TRANSDUCERS	
Head (9-AX)	X	Head	X	Trachea	X
Up. Sternum (3-AX)	X	Acromion	X	Ascending Aorta	X
Lwr. Sternum (1)	X	Sternum (2)	X	Internal Carotid	___
Spine (2 triax)	X	Spine	___		
Pelvis (9-AX)	___	Pelvis	___	Subdural 1:	___
Lwr. Rib R8 (2)	X			2:	___
Up. Rib R4 (2 triax)	X			3:	___
				4:	___

COMMENTS:

TEST DESCRIPTION

Cadaver No._____ Sex:_____ Height:_____ Weight:_____

Test No._____ (Head, Shoulder, Pelvis)

Test description: Left side tap arms up, position arms to minimize interference from scapula as well as centering piston in the R-L/I-S plane, normal seated posture. Top of impact 54 cm above seat pan. (This test may be dropped.)

Type of Impactor: PENDULUM

Type of Bumper: WHITE VIBRATHANE

Type of Striker: 25 Kg PISTON, 21cm sq.

Impactor Angle: 17°(2m/s)

Padding: .5cm ensolite

Pre-Impact Travel: 8cm

Post-Impact Travel: 22cm

35mm stills:

___ Black and White

___ Color

CAMERAS		POSITION
Photosonics 1:	1000	R-L, S-I
Photosonics 2:		
HyCam:	3000	R-L, S-I

INSTRUMENTATION

ACCELEROMETERS		TARGETS		TRANSDUCERS	
Head (9-AX)	X	Head	X	Trachea	X
Up. Sternum (3-AX)	X	Acromion	X	Ascending Aorta	X
Lwr. Sternum (1)	X	Sternum (2)	X	Internal Carotid	___
Spine (2 triax)	X	Spine	___		
Pelvis (9-AX)	___	Pelvis	___	Subdural 1:	___
Lwr. Rib R8 (2)	X			2:	___
Up. Rib R4 (2 triax)	X			3:	___
				4:	___

COMMENTS:

TEST DESCRIPTION

Cadaver No._____ Sex:_____ Height:_____ Weight:_____

Test No._____ (Head, Shoulder, Pelvis)

Test description: Left side tap arms down, normal seated posture, in the R-L/I-S plane, top of impact 54 cm above seat pan.

Type of Impactor: PENDULUM

Type of Bumper: WHITE VIBRATHANE

Type of Striker: 25 Kg PISTON, 21cm sq.

Impactor Angle: 17°(2m/s)

Padding: .5cm ensolite

Pre-Impact Travel: 8cm

Post-Impact Travel: 22cm

35mm stills:

___ Black and White

___ Color

CAMERAS		POSITION
Photosonics 1:	1000	R-L, S-I
Photosonics 2:		
HyCam:	3000	R-L, S-I

INSTRUMENTATION

ACCELEROMETERS		TARGETS		TRANSDUCERS	
Head (9-AX)	X	Head	X	Trachea	X
Up. Sternum (3-AX)	X	Acromion	X	Ascending Aorta	X
Lwr. Sternum (1)	X	Sternum (2)	X	Internal Carotid	___
Spine (2 triax)	X	Spine	___		
Pelvis (9-AX)	___	Pelvis	___	Subdural 1:	___
Lwr. Rib R8 (2)	X			2:	___
Up. Rib R4 (2 triax)	X			3:	___
				4:	___

COMMENTS:

TEST DESCRIPTION

Cadaver No._____ Sex:____ Height:____ Weight:____

Test No._____ (Head, Shoulder, Pelvis)

Test description: Left side impact, same as left side arms down tap.

Type of Impactor: PENDULUM

Type of Bumper: WHITE VIBRATHANE

Type of Striker: 25 Kg PISTON, 21cm sq.

Impactor Angle: 100°(8.8m/s)

Padding: 15cm APR pads

Pre-Impact Travel: 9cm

Post-Impact Travel: 21cm

35mm stills:

___ Black and White

___ Color

CAMERAS		POSITION
Photosonics 1:	1000	R-L,S-I
Photosonics 2:		
HyCam:	3000	R-L, S-I

INSTRUMENTATION

ACCELEROMETERS		TARGETS		TRANSDUCERS	
Head (9-AX)	X	Head	X	Trachea	X
Up. Sternum (3-AX)	X	Acromion	X	Ascending Aorta	X
Lwr. Sternum (1)	X	Sternum (2)	X	Internal Carotid	___
Spine (2 triax)	X	Spine	___		
Pelvis (9-AX)	___	Pelvis	___	Subdural 1:	___
Lwr. Rib R8 (2)	X			2:	___
Up. Rib R4 (2 triax)	X			3:	___
				4:	___

COMMENTS:

TEST DESCRIPTION

Cadaver No._____ Sex:_____ Height:_____ Weight:_____

Test No._____ (Head, Shoulder, Pelvis)

Test Description: Pelvic impact, right side, 8cm anterior to trochanterion, centered on femur.

Type of Impactor: PENDULUM

Type of Bumper: WHITE VIBRATHANE

Type of Striker: 25 Kg PISTON, 15cm DIA.

Impactor Angle: 100°(8.8m/s)

Padding: .5cm ensolite

Pre-Impact Travel: 12cm

Post-Impact Travel: 18cm

35mm stills:

___ Black and White

___ Color

CAMERAS		POSITION
Photosonics 1:	1000	R-L, S-I
Photosonics 2:		
HyCam:	3000	R-L, S-I

INSTRUMENTATION

ACCELEROMETERS		TARGETS		TRANSDUCERS	
Head (9-AX)	___	Head	___	Trachea	___
Up. Sternum (3-AX)	___	Acromion	___	Ascending Aorta	___
Lwr. Sternum (1)	___	Sternum (2)	___	Internal Carotid	___
Spine (2 triax)	X	Spine	X		
Pelvis (9-AX)	X	Pelvis	X	Subdural 1:	___
Lwr. Rib R8 (2)	___			2:	___
Up. Rib R4 (2 triax)	___			3:	___
				4:	___

COMMENTS:

TEST DESCRIPTION

Cadaver No._____ Sex:_____ Height:_____ Weight:_____

Test No._____ (Head, Shoulder, Pelvis)

Test description:_____

_____

_____

_____

_____

Type of Impactor:_____

Type of Bumper:_____

Type of Striker:_____

Impactor Angle:_____

Padding:_____

Pre-Impact Travel:_____

Post-Impact Travel:_____

35mm stills:

___ Black and White

___ Color

CAMERAS		POSITION
Photosonics 1:	_____	_____
Photosonics 2:	_____	_____
HyCam:	_____	_____

INSTRUMENTATION

ACCELEROMETERS		TARGETS		TRANSDUCERS	
Head (9-AX)	___	Head	___	Trachea	___
Up. Sternum (3-AX)	___	Acromion	___	Ascending Aorta	___
Lwr. Sternum (1)	___	Sternum (2)	___	Internal Carotid	___
Spine (2 triax)	___	Spine	___		
Pelvis (9-AX)	___	Pelvis	___	Subdural 1:	___
Lwr. Rib R8 (2)	___			2:	___
Up. Rib R4 (2 triax)	___			3:	___
				4:	___

COMMENTS:

TEST DESCRIPTION

Cadaver No._____ Sex:_____ Height:_____ Weight:_____

Test No._____ (Head, Shoulder, Pelvis)

Test description:_____

_____

_____

_____

_____

Type of Impactor:_____

Type of Bumper:_____

Type of Striker:_____

Impactor Angle:_____

Padding:_____

Pre-Impact Travel:_____

Post-Impact Travel:_____

35mm stills:

___ Black and White

___ Color

CAMERAS		POSITION
Photosonics 1:	_____	_____
Photosonics 2:	_____	_____
HyCam:	_____	_____

INSTRUMENTATION

ACCELEROMETERS		TARGETS		TRANSDUCERS	
Head (9-AX)	___	Head	___	Trachea	___
Up. Sternum (3-AX)	___	Acromion	___	Ascending Aorta	___
Lwr. Sternum (1)	___	Sternum (2)	___	Internal Carotid	___
Spine (2 triax)	___	Spine	___		
Pelvis (9-AX)	___	Pelvis	___	Subdural 1:	___
Lwr. Rib R8 (2)	___			2:	___
Up. Rib R4 (2 triax)	___			3:	___
				4:	___

COMMENTS:

TEST DESCRIPTION

Cadaver No._____ Sex:____ Height:____ Weight:____

Test No._____ (Head, Shoulder, Pelvis)

Test description:_____

_____

_____

_____

_____

Type of Impactor:_____

Type of Bumper:_____

Type of Striker:_____

Impactor Angle:_____

Padding:_____

Pre-Impact Travel:_____

Post-Impact Travel:_____

35mm stills:

___ Black and White

___ Color

CAMERAS		POSITION
Photosonics 1:	_____	_____
Photosonics 2:	_____	_____
HyCam:	_____	_____

INSTRUMENTATION

ACCELEROMETERS		TARGETS		TRANSDUCERS	
Head (9-AX)	___	Head	___	Trachea	___
Up. Sternum (3-AX)	___	Acromion	___	Ascending Aorta	___
Lwr. Sternum (1)	___	Sternum (2)	___	Internal Carotid	___
Spine (2 triax)	___	Spine	___		
Pelvis (9-AX)	___	Pelvis	___	Subdural 1:	___
Lwr. Rib R8 (2)	___			2:	___
Up. Rib R4 (2 triax)	___			3:	___
				4:	___

COMMENTS:

PRE-SURGERY

TASK	TIME	COMMENTS
Pick up cadaver from U of M Anatomy Dept. and transport to HSRI Biomedical lab.		
Weigh cadaver and log cadaver information.		
Store cadaver if necessary.		
Sanitary preparation.		
Pretest X-rays: (KV/MA/T) head A-P (100/10/1) ___/___/___ thorax A-P (90/10/1) ___/___/___ thorax A-P(2) (90/10/1) ___/___/___ pelvis (105/10/1) ___/___/___ femur (80/10/1) ___/___/___		
Anthropometry.		

ANTHROPOMETRY

Height:_____

Weight:_____

Sex:_____

Age:_____

Stature: left:_____ right:_____

Suprasternale height:_____

Substernale height:_____

Substernale depth:_____

Substernale breadth:_____

Substernale circumference:_____

Vertex to 12th rib:_____

Head to C7:_____

Mastoid to vertex: left:_____ right:_____

Tragon to vertex: left:_____ right:_____

Menton to vertex:_____

Bitragon diameter:_____

Acromion height: left:_____ right:_____

Acromion to tip of finger:_____

Biacromion:_____

Axillary breadth:_____

Axillary depth:_____

Axillary circumference:_____

Head breadth (R-L):_____

Head depth (A-P):_____

Head circumference:_____

Neck circumference:_____

Bitrochanteric breadth:_____

Symphysion depth:_____

Vertex to Symphysion:_____

Bispinous (ASIS) diameter:_____

Biiliocristale breadth:_____

ASIS to Symphysion:_____

Anatomical Anomalies / Clinical Observations

1. Head: a. Brain b. Skull

2. Neck:

3. Thorax: a. Ribs b. Heart c. Lungs d. Diaphragm

4. Pelvis:

5. Femur

6. Abdomen

RIB AND STERNUM MOUNTS

TASK	TIME	COMMENTS
Locate right and left R4 by palpation.		
Make incisions over ribs near flat region. Surface must be normal to the R-L vector.		
Loop two pieces of wire (1/2" apart) around each rib.		
Locate R8 by counting down from R4 and up from R12.		
Make incision over rib near flat region. Surface must be normal to the R-L vector.		
Make incisions over suprasternale and substernale.		
Secure mounts to rib by anchoring with pins and wire.		
Screw lag bolt into each acromion.		

PRESSURIZATION

TASK	TIME	COMMENTS
Locate right carotid and cut lengthwise.		
Locate right vertebral artery and ligate.		
Loop six pieces of string around carotid artery.		
Insert fabricated Foley catheter (#18 or #20) into descending aorta.		
Insert Kulite shield into ascending aorta.		
Insert Kulite shield into carotid artery.		
Insert arterial pressurization catheters into carotid artery.		
Using syringe, squirt acrylic into artery. Tie and sew.		
Locate left carotid, cut, loop strings.		
Locate left vertebral artery and ligate.		

PRESSURIZATION (CONT'D)

TASK	TIME	COMMENTS
Insert arterial pressurization catheters (#10, #12, or #14) into carotid artery.		
Acrylic, tie and sew.		
Locate trachea and cut lengthwise.		
Loop two Tie Wraps around trachea.		
Insert polyethelyne tube snugly, tie and sew.		
Calibrate lungs.		
Pulmonary pressure relief valve calibration.		
Vascular flow check.		
Sternal geometry if necessary.		

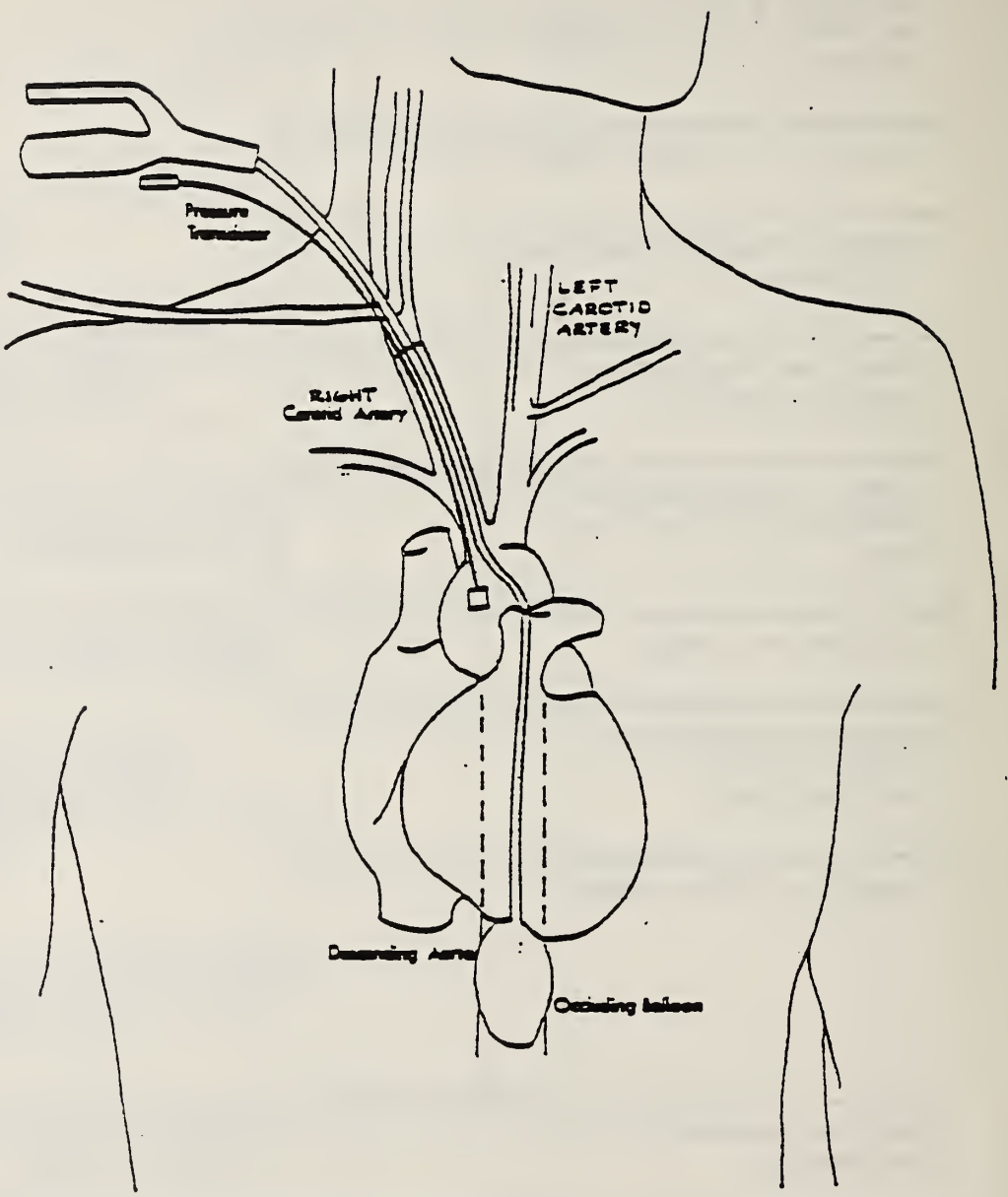
Pressure
Transducer
LEFT
CAROTID
ARTERY
RIGHT
Carotid Artery
Descending Aorta
Occluding Balloon

HEAD 9-AX MOUNT

TASK	TIME	COMMENTS
With cadaver facing down, remove a 2x2" area of scalp spanning the right parietal and occipital bones.		
Drill three holes in a triangular pattern, approximately the size of the 9-ax plate.		
Insert three screws.		
Attach four feet to the 9-ax plate such that three of the feet can be positioned near the screws on the exposed forehead.		
Place acrylic around screws.		
Place plate on top of acrylic base, making sure the acrylic goes through the center holes in the plate.		
Insert a strain relief bolt in the acrylic base of the head platform. Make sure bolt does not contact plate.		

HEAD TRANSDUCERS

TASK	TIME	COMMENTS
Holes for transducers go on frontal,parietal, and occipital bones. Make sure no Xducers will contact the impacting surface. Also, the holes should not be drilled into suture.		
To drill holes, remove a 1/4" dia. circle of scalp.		
Drill through skull with a #7 drill. Be sure not to drill through the dura.		
Perforate the dura without cutting brain.		
Tap hole with a No.7 tap.		
Pinhead screws are attached 2cm from each transducer. Acrylic is applied to each area, carefully molding around the transducers.		
Note positions of head transducers on the figure.		

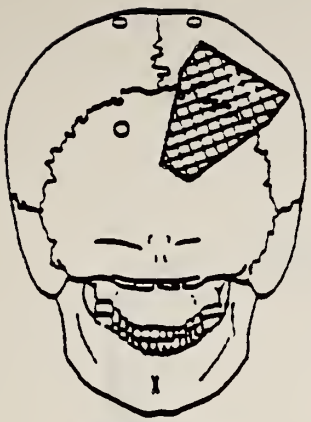

Posterior View

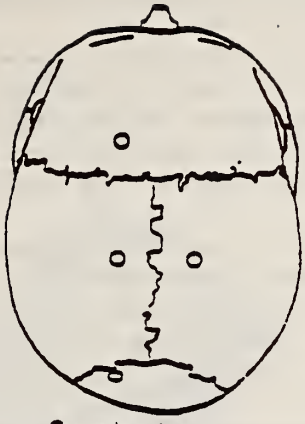

Superior View

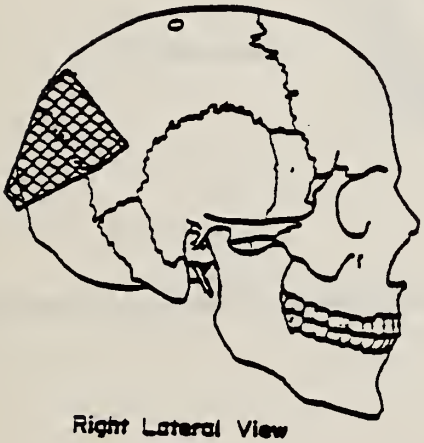

Right Lateral View

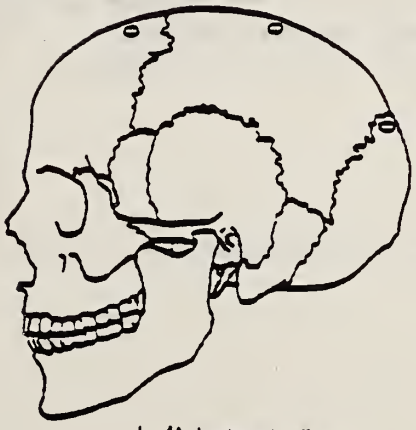

Left Lateral View

PELVIS MOUNT

TASK	TIME	COMMENTS
Locate the posterior-superior iliac spines.		
Screw two lag bolts into each spine such that the large 9-ax plate spans the bolts.		
Attach four feet to the plate such that the feet are near the lag bolts.		
Place acrylic around screws and feet.		
Imbed feet and posterior surface into acrylic.		
Test plate to see that it is secure.		

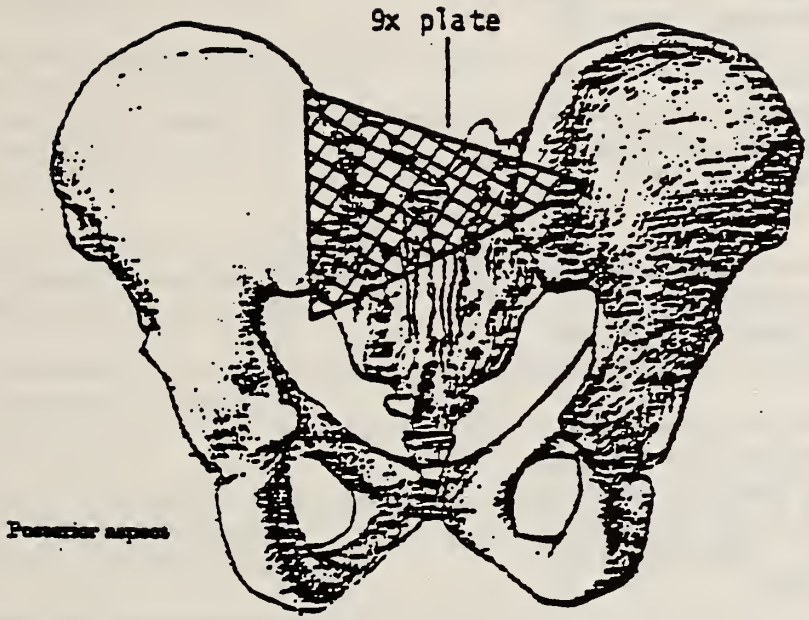
9x plate
Posterior aspect

SPINAL MOUNTS

TASK	TIME	COMMENTS
Spinal mounts go on T1 and T12.		
Make incisions over T1 and T12. Clear muscle and tissue away from process, but do not cut between processes.		
Drill a small hole 1/4" deep in each process.		
Screw mounts on with wood screws (be sure screws are in process).		
Place stabilizing and mooring probic devices on each side of the laminae. Secure with Tie Wraps.		
Mold acrylic around (and under) mounts and mooring devices and allow to dry.		
Make sure accelerom-eters are anatomically oriented.		
Spinal geometry if necessary.		

CEREBROSPINAL PRESSURIZATION

TASK	TIME	COMMENTS
Locate L2 by palpation and counting from T12.		
Core a small hole in the lamina.		
Insert Foley catheter (#14 or #16) such that balloon is in mid-thorax.		
Insert small screws in lamina and process.		
Seal off hole with acrylic.		
Check for structural integrity of vertebra.		
Cerebral-spinal flow check.		
Check pressurization.		

PREPARATION

TASK	TIME	COMMENTS
Dress cadaver.		
Place head and body harnesses on cadaver.		
Store cadaver if necessary.		
Transport cadaver to sled lab, being careful not to damage mounts.		
Place head, sternum, and rib transducers on cadaver. Stuff and sew.		
Set up pressurization equipment (pulmonary, cerebro-spinal, vascular head and vascular thorax).		

ELECTRONICS CHECK AND PRETEST TRIAL RUN

Electronics Check

___ check accelerometers (excitation and zero)
___ check wiring and cables
___ mount accelerometers in triax clusters
___ check amplifiers
___ calibrate tape with impedance-matching amp
___ recorder
___ complete wiring
___ check pendulum accelerometer
___ check velocity, strobe, gate, timer, rope cutters
___ run trial test
___ load cell mounted on pendulum day before test
___ load Photosonics and HyCam cameras with Kodak 16mm 7242-#FB-430 color film

Pretest Trial Run

1. ___ Suspend rubber tube five inches from pendulum with fiber tape.
2. ___ Tape all accelerometers to seat with paper tape.
3. ___ Attach the contact switches to the load cell and shock absorber with paper tape.
4. ___ Run trial test.
5. ___ Record all signals, gate, and strobe.
6. ___ Put a one-volt signal on a junk tape and check to see if one volt is played back. Use signal generator or impedance-matching amp with the scope to calibrate output.

HEAD IMPACT 1

Test No._____

TASK	TIME	COMMENTS
Head impact 1.		
Attach ball targets and phototargets.		
Change padding on impactor head surface.		
Set up head catch and spinal backup.		
Final positioning (see figure).		
Measure and record head and neck angles		
Setup photos.		
Final checklist.		
Start pressurization of vascular and cerebrospinal systems.		
Finish pressurizatons.		
Run test.		

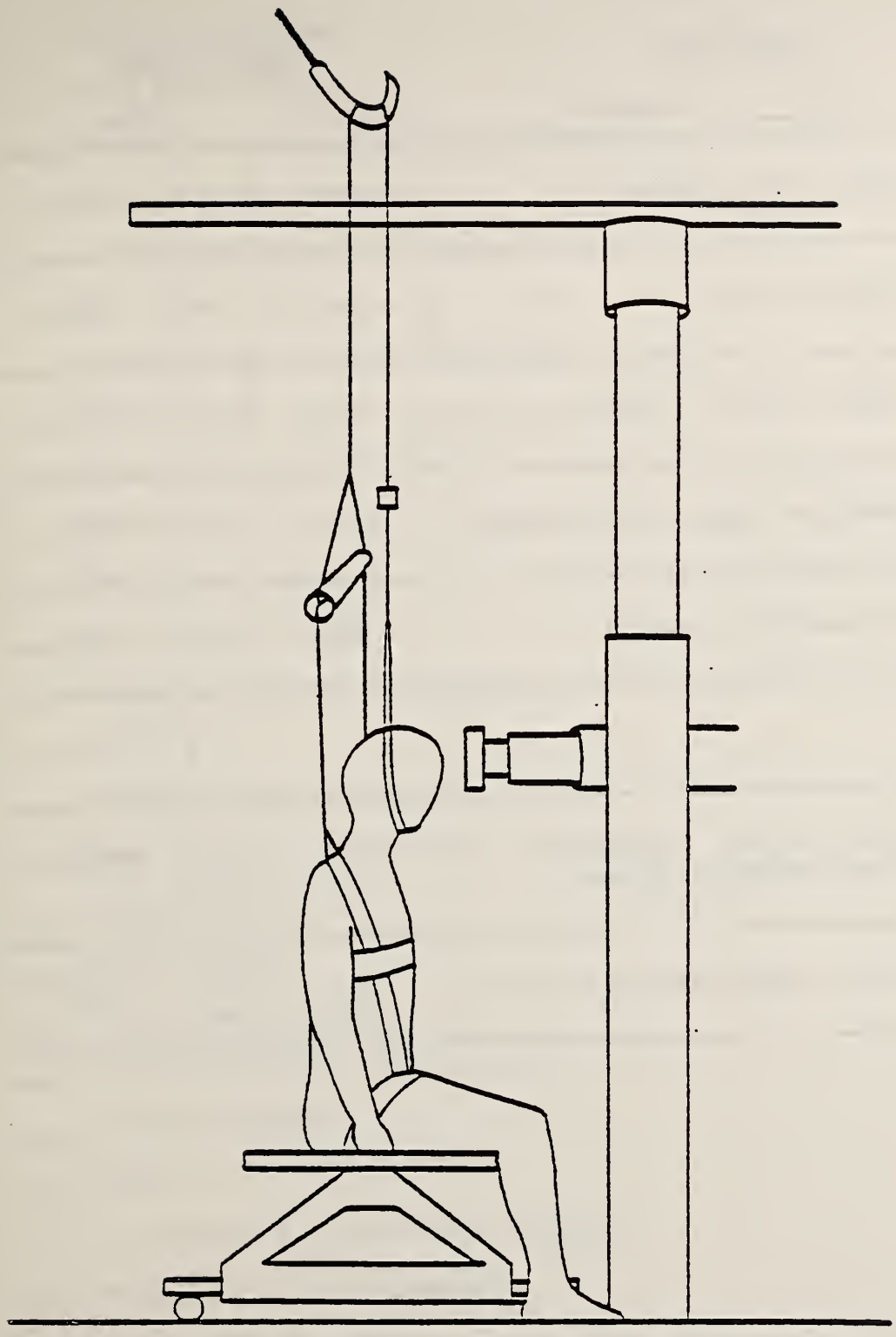

HEAD IMPACT 1

Timer Box Setup

EQUIPMENT _____ Impact	TIMER VALUES Delay		Run
Gate (from strobe 1)	0011	1	0170
Lights (start)	0001	2	2500
HyCam (start)	1200	3	1600
Pendulum rope cutter(start)	1390	4	0050
Photosonics (start)	1000	5	1600
		6	
Head, pelvis, rope cutter (from velocity probe)	0001	7	0050
Piston Acceleration Corridor	0009	8	0050

FINAL CHECKLIST

____ check transducers

____ tape positioned

____ slots for velocity probe lined up

____ both strobes charged

____ timer box values correct

____ all timer box switches to 'off'

____ rope cutter threaded and ready

____ nylon (rope cutter) string unfrayed

____ rope cutter cable free

____ cameras set

____ Newtonian reference

____ calibration target

____ targets in view of cameras

____ padding

____ correct timers charged

____ gate trigger established

____ timing lights on

____ doors locked

____ final positioning

____ correct pressure system used

____ pendulum raised

____ power on

____ all pressure connections secured

____ zero piston accelerometer

____ head and neck angles

HEAD IMPACT 2

Test No._____

TASK	TIME	COMMENTS
Reposition as for tap.		
Check spinal brace and head catch.		
Final positioning		
Measure and record head and neck angles		
Setup photos.		
Start pressurization of vascular and cerebrospinal systems.		
Final checklist..		
Finish pressurization.		
Run test.		

HEAD IMPACT 2

Timer Box Setup

EQUIPMENT _____ Impact	TIMER VALUES Delay		Run
Gate (from strobe 1)	0008	1	0170
Lights (start)	0001	2	2600
HyCam (start)	1200	3	1600
Pendulum rope cutter(start)	1290	4	0050
Photosonics (start)	1000	5	1600
		6	
Head, pelvis, rope cutter (from velocity probe)	0001	7	0050
Piston Acceleration Corridor	0009	8	0050

FINAL CHECKLIST

____ check transducers

____ tape positioned

____ slots for velocity probe lined up

____ both strobes charged

____ timer box values correct

____ all timer box switches to 'off'

____ rope cutter threaded and ready

____ nylon (rope cutter) string unfrayed

____ rope cutter cable free

____ cameras set

____ Newtonian reference

____ calibration target

____ targets in view of cameras

____ padding

____ correct timers charged

____ gate trigger established

____ timing lights on

____ doors locked

____ final positioning

____ correct pressure system used

____ pendulum raised

____ power on

____ all pressure connections secured

____ zero piston accelerometer

____ head and neck angles

THORAX FRONT TAP

Test No._____

TASK	TIME	COMMENTS
Place seat in position and square on pendulum.		
String up rope cutters.		
Position subject as per figure with body and head harnesses. Protect any mounts that may be hit with gauze and padding.		
Subject should be in normal sitting position with back inclined approx. 10° forwards.		
Attach ball targets and phototargets.		
Place one of the pressure transducers that was in the head in the trachea, and place the Kulite in the descending aorta.		
Final positioning and setup photos (see fig)		
Final checklist.		
Start pressurization of vascular and respiratory systems.		
Finish pressurization.		
Run test.		

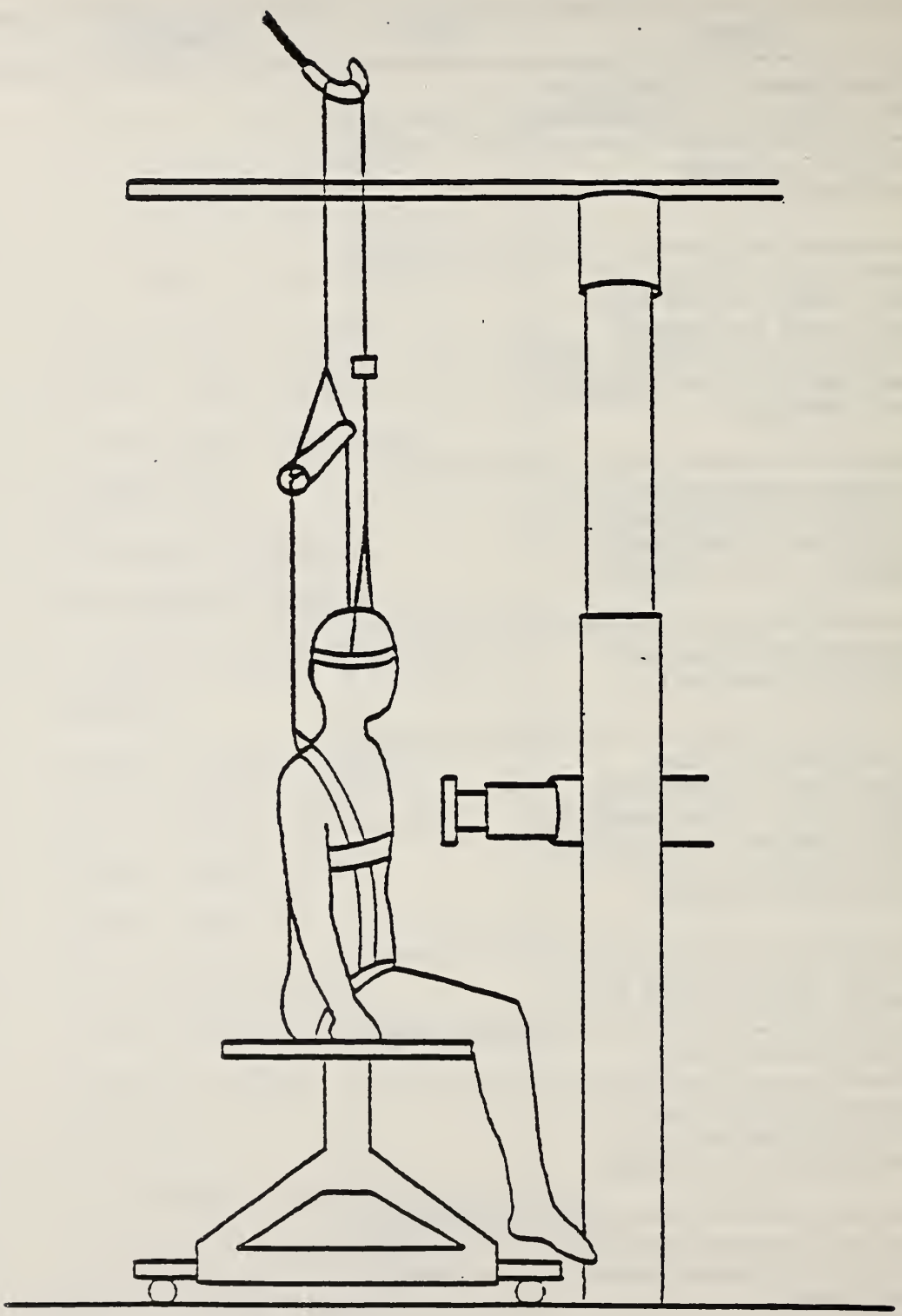

B52

THORAX FRONT TAP

Timer Box Setup

EQUIPMENT _____ Impact	TIMER VALUES Delay		Run
Gate (from strobe 1)	0021	1	0170
Lights (start)	0001	2	2600
HyCam (start)	1200	3	1600
Pendulum rope cutter(start)	1400	4	0050
Photosonics (start)	1000	5	1600
		6	
Head, pelvis, rope cutter (from velocity probe)	0001	7	0050
Piston Acceleration Corridor	0012	8	0150

FINAL CHECKLIST

____ check transducers

____ tape positioned

____ slots for velocity probe lined up

____ both strobes charged

____ timer box values correct

____ all timer box switches to 'off'

____ rope cutter threaded and ready

____ nylon (rope cutter) string unfrayed

____ rope cutter cable free

____ cameras set

____ Newtonian reference

____ calibration target

____ targets in view of cameras

____ padding

____ correct timers charged

____ gate trigger established

____ timing lights on

____ doors locked

____ final positioning

____ correct pressure system used

____ pendulum raised

____ power on

____ all pressure connections secured

____ zero piston accelerometer

____ head and neck angles

45° THORAX TAP

Test No._____

TASK	TIME	COMMENTS
Place seat in position.		
String up rope cutters.		
Position subject as per figure with body and head harnesses. Protect any mounts that may be hit with gauze and padding.		
Subject should be in normal sitting position with back inclined approx. 10° forwards.		
Attach ball targets and phototargets.		
Final positioning and setup photos (see fig)		
Final checklist.		
Start pressurization of vascular and respiratory systems.		
Finish pressurization.		
Run test.		

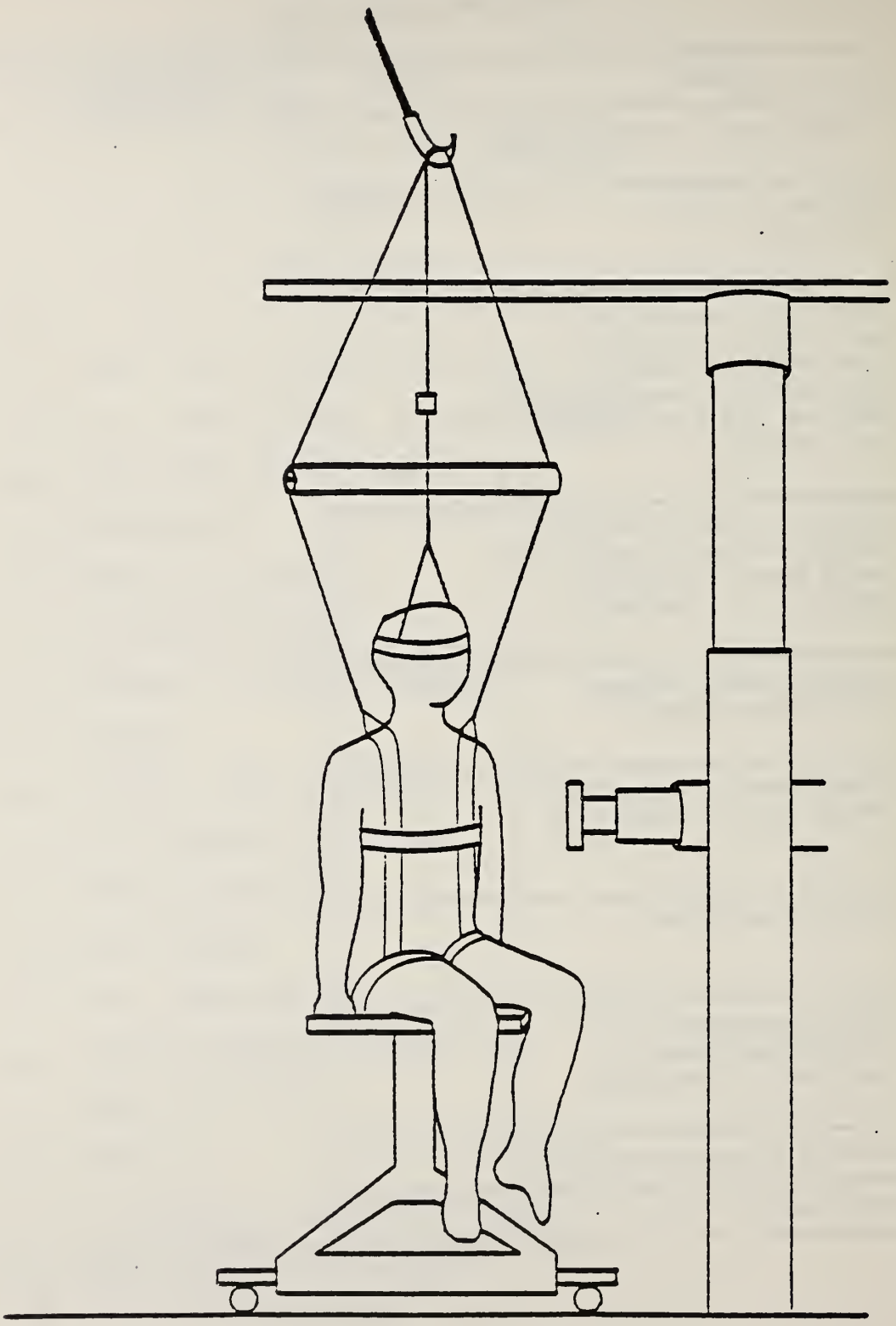

B56

45° THORAX TAP

Timer Box Setup

EQUIPMENT	TIMER VALUES		
_____ Impact	Delay		Run
Gate (from strobe 1)	0021	1	0170
Lights (start)	0001	2	2600
HyCam (start)	1200	3	1600
Pendulum rope cutter(start)	1400	4	0050
Photosonics (start)	1000	5	1600
		6	
Head, pelvis, rope cutter (from velocity probe)	0001	7	0050
Piston Acceleration Corridor	0012	8	0150

FINAL CHECKLIST

____ check transducers

____ tape positioned

____ slots for velocity probe lined up

____ both strobes charged

____ timer box values correct

____ all timer box switches to 'off'

____ rope cutter threaded and ready

____ nylon (rope cutter) string unfrayed

____ rope cutter cable free

____ cameras set

____ Newtonian reference

____ calibration target

____ targets in view of cameras

____ padding

____ correct timers charged

____ gate trigger established

____ timing lights on

____ doors locked

____ final positioning

____ correct pressure system used

____ pendulum raised

____ power on

____ all pressure connections secured

____ zero piston accelerometer

____ head and neck angles

OPTIONAL ARMS-UP THORAX TAP

Test No._____

TASK	TIME	COMMENTS
Place seat in position.		
String up rope cutters.		
Position subject as per figure with body and head harnesses. Protect any mounts that may be hit with gauze and padding.		
Subject should be in normal sitting position with back inclined approx. 10° forwards.		
Attach ball targets and phototargets.		
Final positioning and setup photos see drawings and figures by ***PAULA LUX***		
Final checklist.		
Start pressurization of vascular and respiratory systems.		
Finish pressurization.		
Run test.		

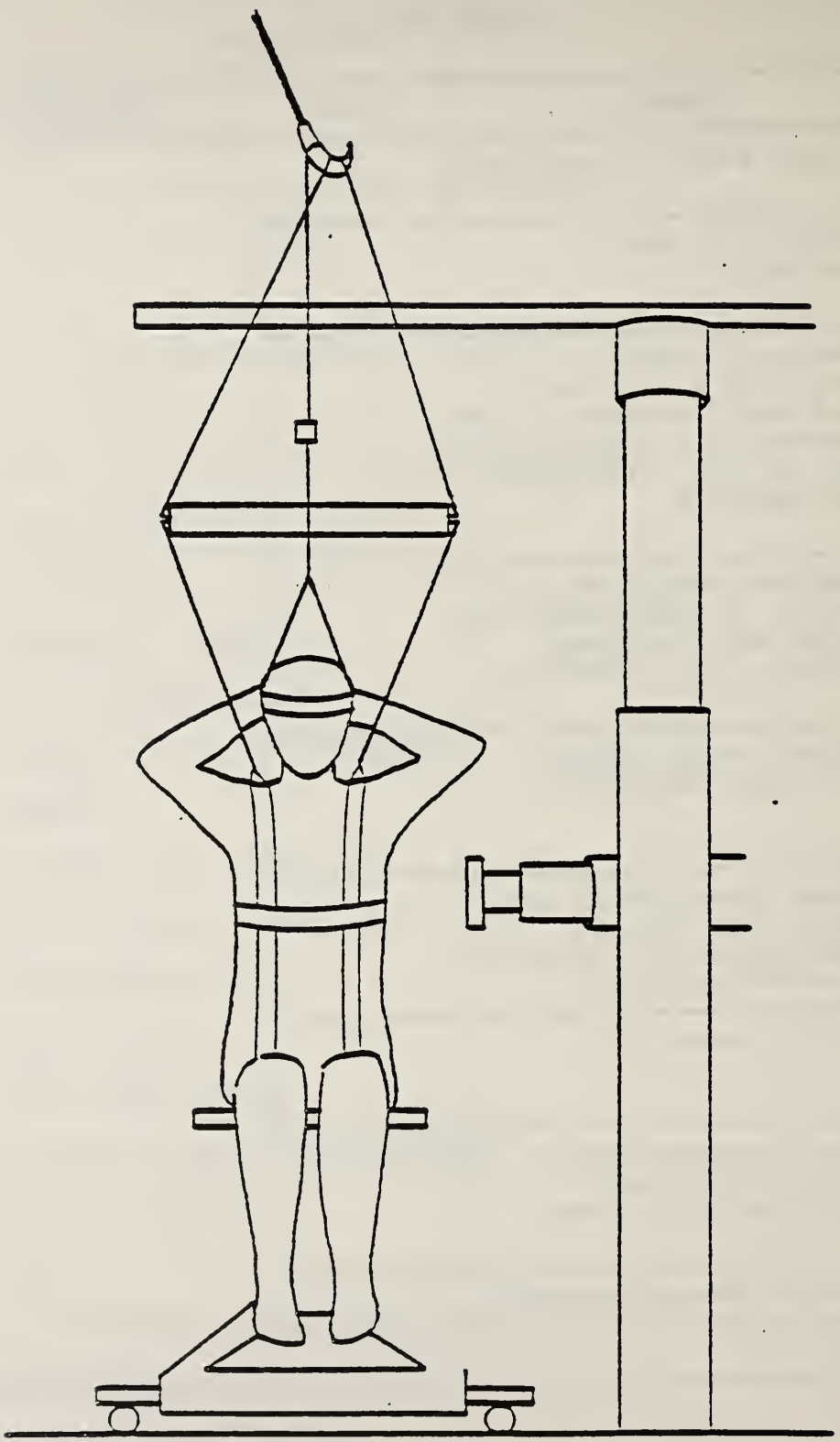

B60

Thcrax taps - 56

OPTIONAL ARMS-UP THORAX TAP

Timer Box Setup

EQUIPMENT	TIMER VALUES		
_____ Impact	Delay		Run
Gate (from strobe 1)	0021	1	0170
Lights (start)	0001	2	2600
HyCam (start)	1200	3	1600
Pendulum rope cutter(start)	1400	4	0050
Photosonics (start)	1000	5	1600
		6	
Head, pelvis, rope cutter (from velocity probe)	0001	7	0050
Piston Acceleration Corridor	0012	8	0150

FINAL CHECKLIST

____ check transducers

____ tape positioned

____ slots for velocity probe lined up

____ both strobes charged

____ timer box values correct

____ all timer box switches to 'off'

____ rope cutter threaded and ready

____ nylon (rope cutter) string unfrayed

____ rope cutter cable free

____ cameras set

____ Newtonian reference

____ calibration target

____ targets in view of cameras

____ padding

____ correct timers charged

____ gate trigger established

____ timing lights on

____ doors locked

____ final positioning

____ correct pressure system used

____ pendulum raised

____ power on

____ all pressure connections secured

____ zero piston accelerometer

____ head and neck angles

ARMS-DOWN THORAX TAP

Test No._____

TASK	TIME	COMMENTS
Place seat in position.		
String up rope cutters.		
Position subject as per figure with body and head harnesses. Protect any mounts that may be hit with gauze and padding.		
Subject should be in normal sitting position with back inclined approx. 10° forwards.		
Attach ball targets and phototargets.		
Final positioning and setup photos (see fig)		
Final checklist.		
Start pressurization of vascular and respiratory systems.		
Finish pressurization.		
Run test.		

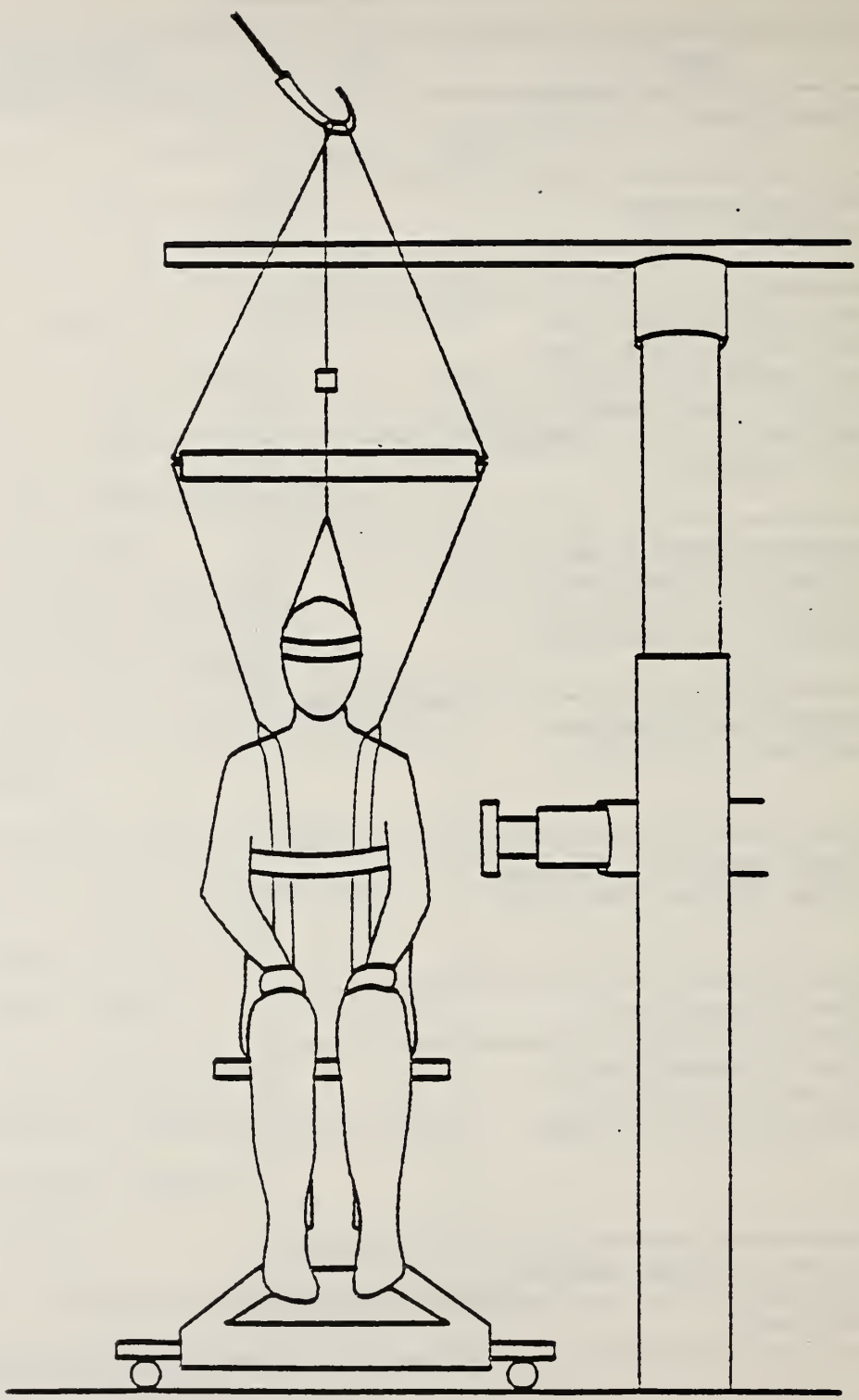

ARMS-DOWN THORAX TAP

Timer Box Setup

EQUIPMENT _____ Impact	TIMER VALUES Delay		Run
Gate (from strobe 1)	0021	1	0170
Lights (start)	0001	2	2600
HyCam (start)	1200	3	1600
Pendulum rope cutter(start)	1400	4	0050
Photosonics (start)	1000	5	1600
		6	
Head, pelvis, rope cutter (from velocity probe)	0001	7	0050
Piston Acceleration Corridor	0012	8	0150

FINAL CHECKLIST

____ check transducers

____ tape positioned

____ slots for velocity probe lined up

____ both strobes charged

____ timer box values correct

____ all timer box switches to 'off'

____ rope cutter threaded and ready

____ nylon (rope cutter) string unfrayed

____ rope cutter cable free

____ cameras set

____ Newtonian reference

____ calibration target

____ targets in view of cameras

____ padding

____ correct timers charged

____ gate trigger established

____ timing lights on

____ doors locked

____ final positioning

____ correct pressure system used

____ pendulum raised

____ power on

____ all pressure connections secured

____ zero piston accelerometer

____ head and neck angles

THORAX IMPACT

Test No._____

TASK	TIME	COMMENTS
Reposition for shoulder (arms down) impact.		
Set up catch net.		
Slacken body harness.		
Start pressurization of vascular and respiratory systems.		
Final checklist.		
Finish pressurization.		
Run test		

ARMS-DOWN THORAX IMPACT

Timer Box Setup

EQUIPMENT _____ Impact	TIMER VALUES Delay		Run
Gate (from strobe 1)	0006	1	0170
Lights (start)	0001	2	2600
HyCam (start)	1200	3	1600
Pendulum rope cutter(start)	1220	4	0050
Photosonics (start)	1000	5	1600
		6	
Head, pelvis, rope cutter (from velocity probe)	0002	7	0050
Piston Acceleration Corridor	0006	8	0050

FINAL CHECKLIST

____ check transducers

____ tape positioned

____ slots for velocity probe lined up

____ both strobes charged

____ timer box values correct

____ all timer box switches to 'off'

____ rope cutter threaded and ready

____ nylon (rope cutter) string unfrayed

____ rope cutter cable free

____ cameras set

____ Newtonian reference

____ calibration target

____ targets in view of cameras

____ padding

____ correct timers charged

____ gate trigger established

____ timing lights on

____ doors locked

____ final positioning

____ correct pressure system used

____ pendulum raised

____ power on

____ all pressure connections secured

____ zero piston accelerometer

____ head and neck angles

PELVIS IMPACT

Test No._____

TASK	TIME	COMMENTS
Install pelvic and spinal accelerometers. Stuff and sew. Pad pelvic plate.		
Attach ball targets and phototargets.		
Change padding on impact head surface.		
Final positioning, setup photos (see fig)		
Final checklist.		
Run test.		

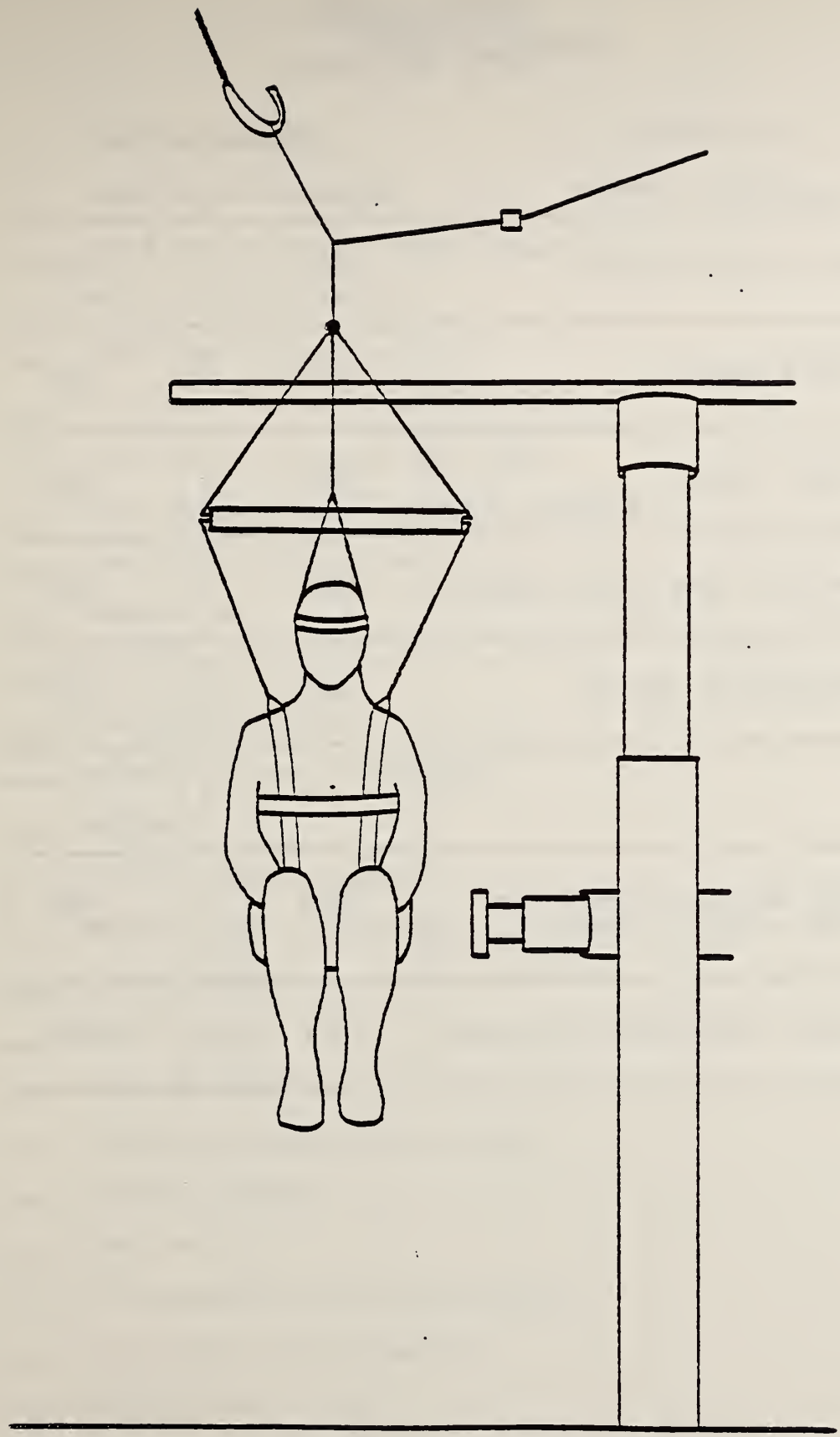

PELVIS IMPACT

Timer Box Setup

EQUIPMENT _____ Impact	TIMER VALUES Delay		 Run
Gate (from strobe 1)	0006	1	0170
Lights (start)	0001	2	2600
HyCam (start)	1200	3	1600
Pendulum rope cutter(start)	1220	4	0050
Photosonics (start)	1000	5	1600
		6	
Head, pelvis, rope cutter (from velocity probe)	0002	7	0050
Piston Acceleration Corridor	0006	8	0050

FINAL CHECKLIST

____ check transducers

____ tape positioned

____ slots for velocity probe lined up

____ both strobes charged

____ timer box values correct

____ all timer box switches to 'off'

____ rope cutter threaded and ready

____ nylon (rope cutter) string unfrayed

____ rope cutter cable free

____ cameras set

____ Newtonian reference

____ calibration target

____ targets in view of cameras

____ padding

____ correct timers charged

____ gate trigger established

____ timing lights on

____ doors locked

____ final positioning

____ correct pressure system used

____ pendulum raised

____ power on

____ all pressure connections secured

____ zero piston accelerometer

____ head and neck angles

POST TEST PROCEDURE

TASK	TIME	COMMENTS
Remove all targets and triax clusters.		
Store cadaver if necessary.		
Transport cadaver to anatomy lab.		
Remove all instrumentation, except for 9AX head plate.		
Remove head and transport it to X-Ray Room for post test radiographs.		

Z-X
(Profile)

Z-Y
(Frontal)

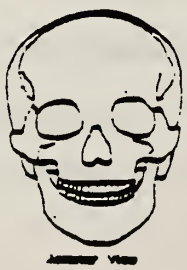

X-RAYS (X-RAY ROOM)

Reference Point	Z-X Distance from Table	Z-Y Distance from Table
R. Eye		
L. Eye		
R. Ear		
L. Ear		
Q1		
Q2		
Q3		
CG		

KVP MA SEC LABEL

Z-X _____/_____/_____/_____ (100/10/1)

Z-Y _____/_____/_____/_____ (100/10/1)

TASK	TIME	COMMENTS
After completion of radiographs, transport head to Anatomy Room for commencement of Autopsy.		
Autopsy		
SAVE RIBS RIGHT SIDE 4, 5, 6		

Observed Injuries

1. Head: a. Brain b. Kull

2. Neck:

3. Thorax: a. Ribs b. Heart c. Lungs d. Diaphragm

4. Pelvis:

5. Femur

6. Abdomen

COMMENTS:

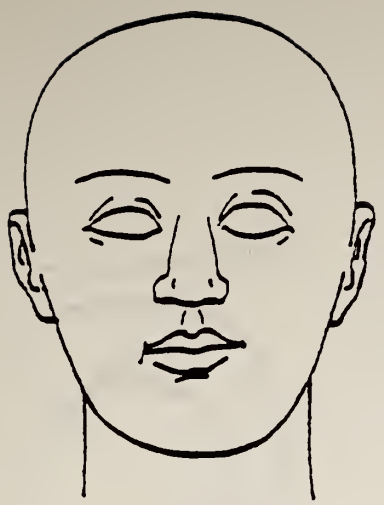

Anterior View

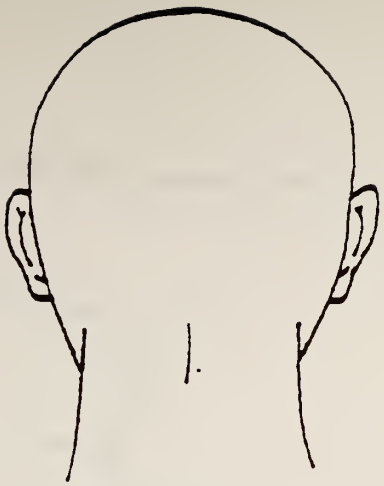

Posterior View

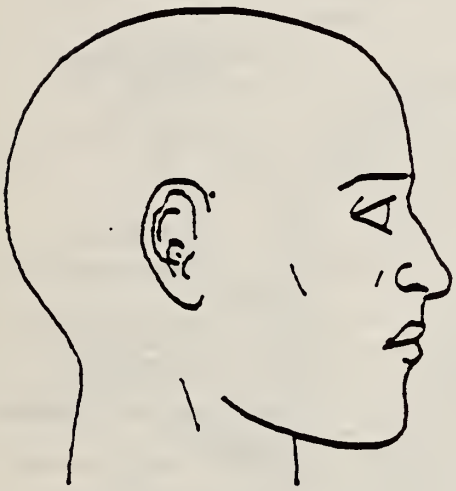

Right Lateral View

Left Lateral View

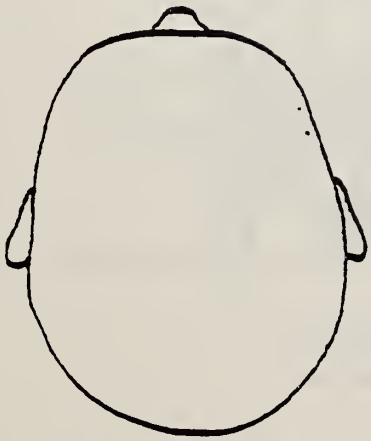

Superior View

TEST NO. _____

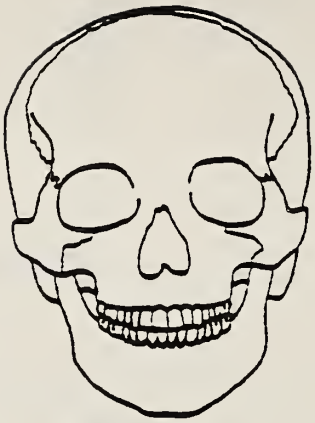

Anterior View

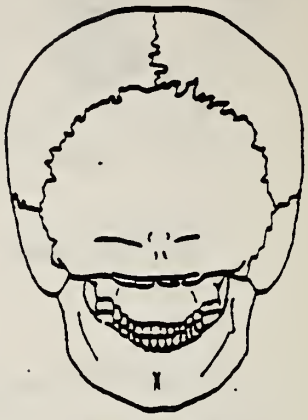

Posterior View

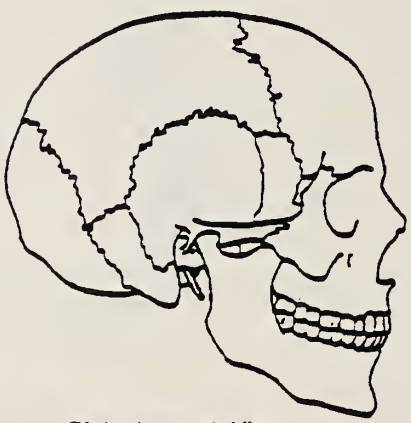

Right Lateral View

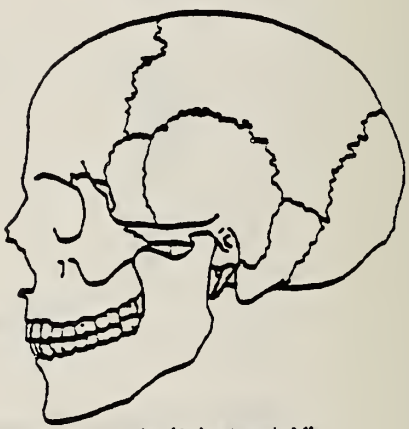

Left Lateral View

Inferior View

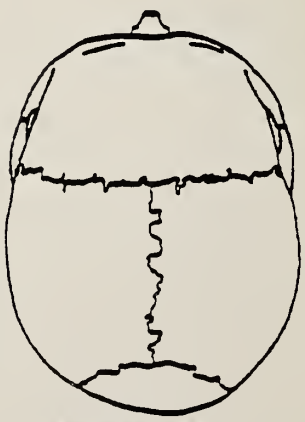

Superior View

TEST NO. _____

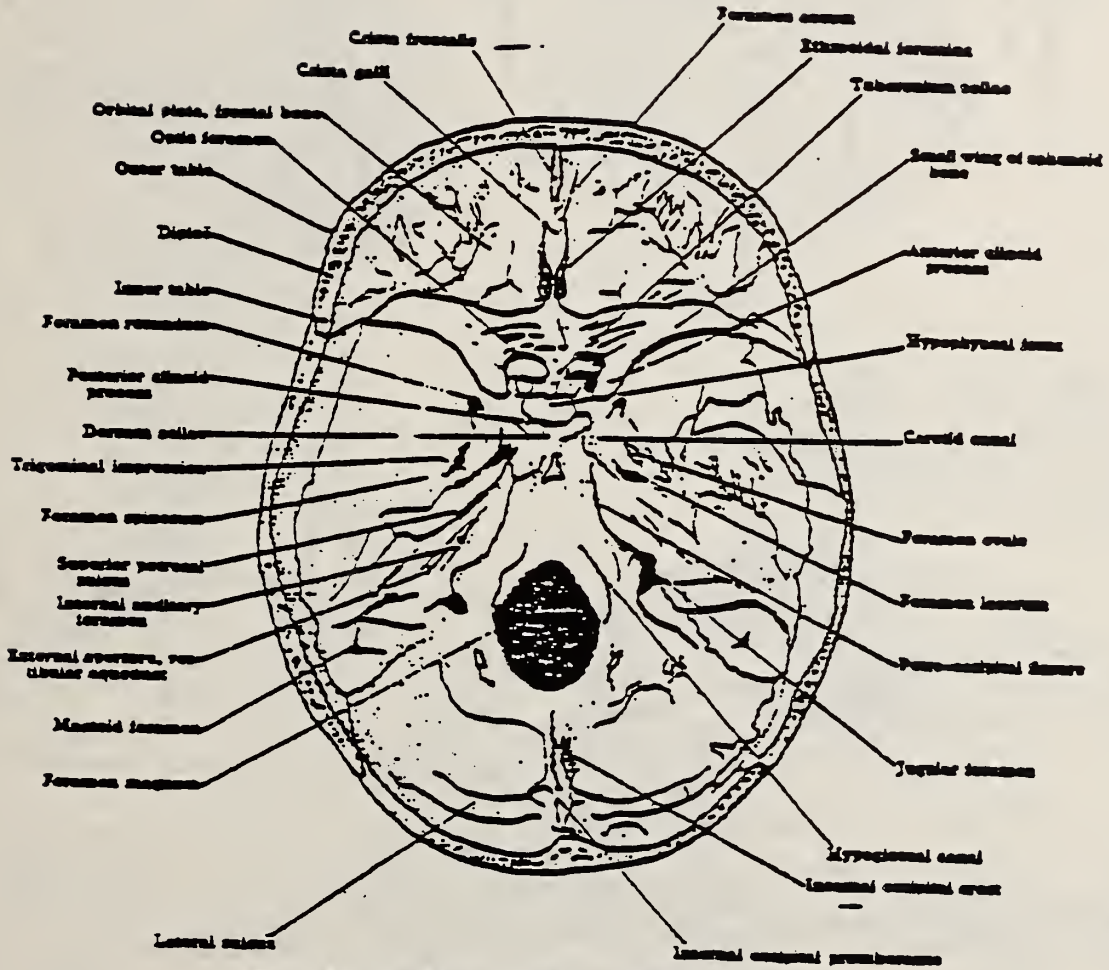

FIG. 109.—THE SKULL, INTERNAL ASPECT OF THE BASE.

TEST NO

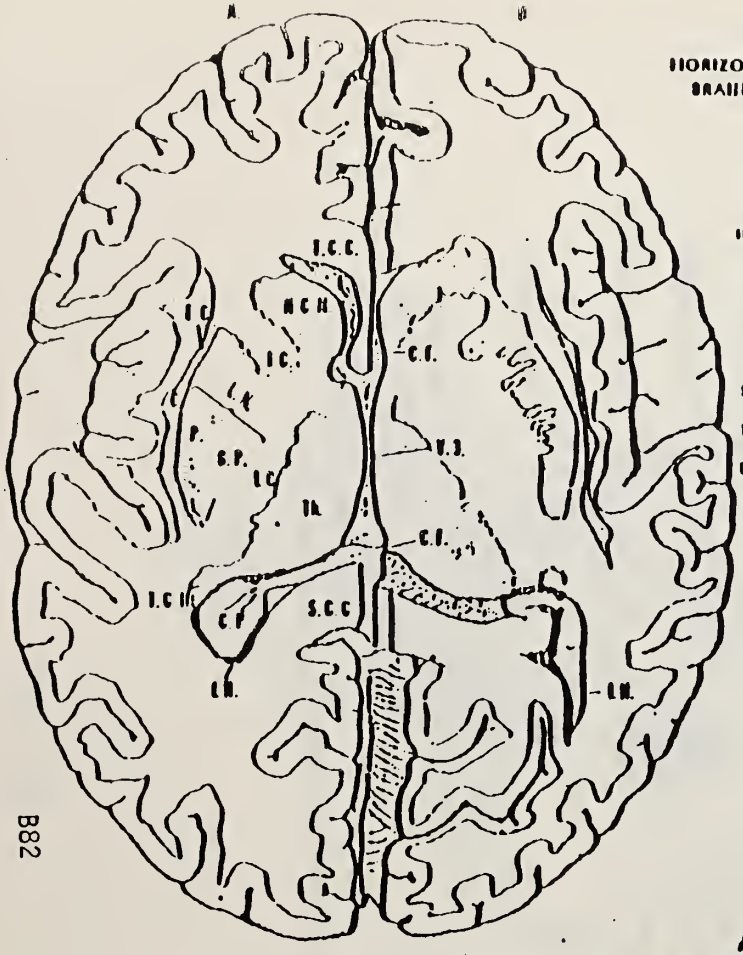

HORIZONTAL SECTIONS OF BRAIN AT TWO LEVELS

C. — Claustrum
C.F. — Crus of Fornix
C.P. — Choroid Plexus
I.C. — Internal Capsule
G.P. — Globus Pallidus
H.C.H. — Head of Caudate Nucleus
I.C. — Internal Capsule
I.H. — Inferior Horn of Lateral Ventricle
L.H. — Lenticular Nucleus
P. — Putamen
S.C.C. — Splenium of Corpus Callosum
I.C.C. — Trunk of Corpus Callosum
I.C.H. — Tail of Caudate Nucleus
Th. — Thalamus
V.D. — 3rd Ventricle

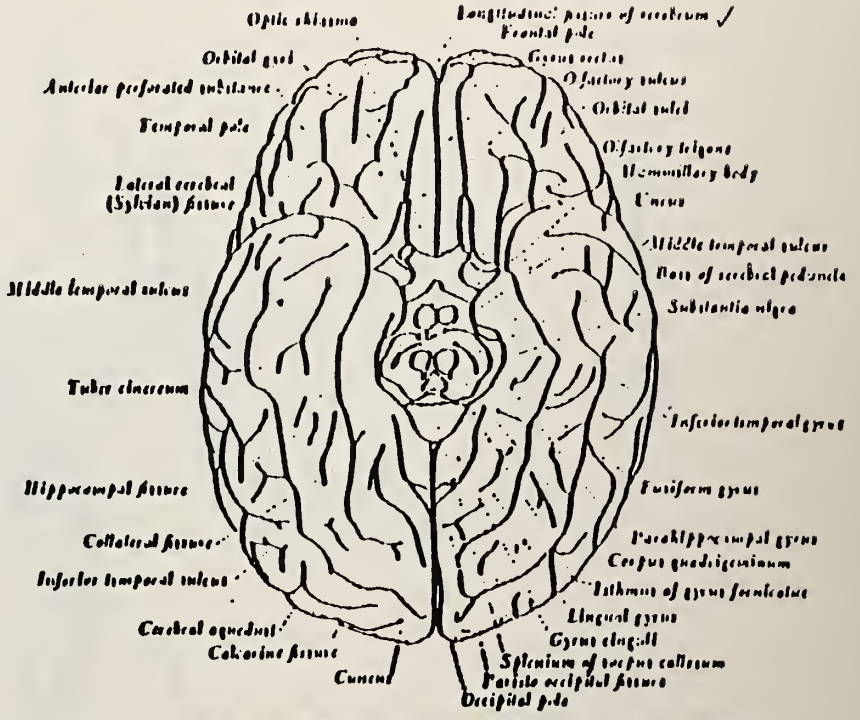

Basal aspect of the human cerebral hemisphere. (Schaeffer-McMurrich.)

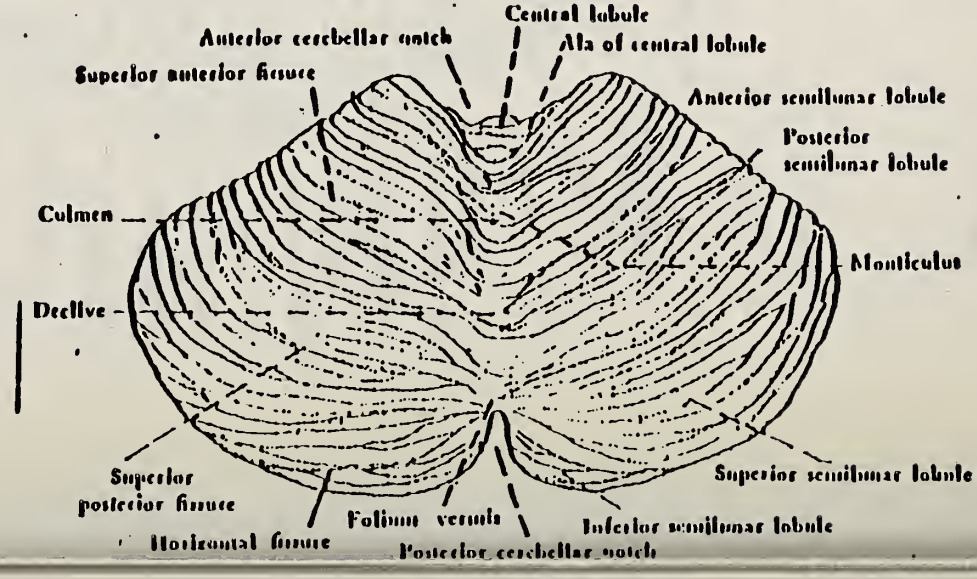

B82

TEST NO. _____

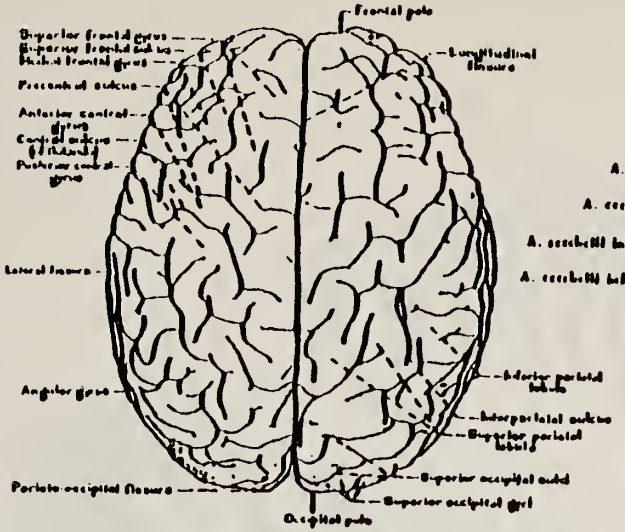

— Cerebral Hemisphere Viewed from Above.

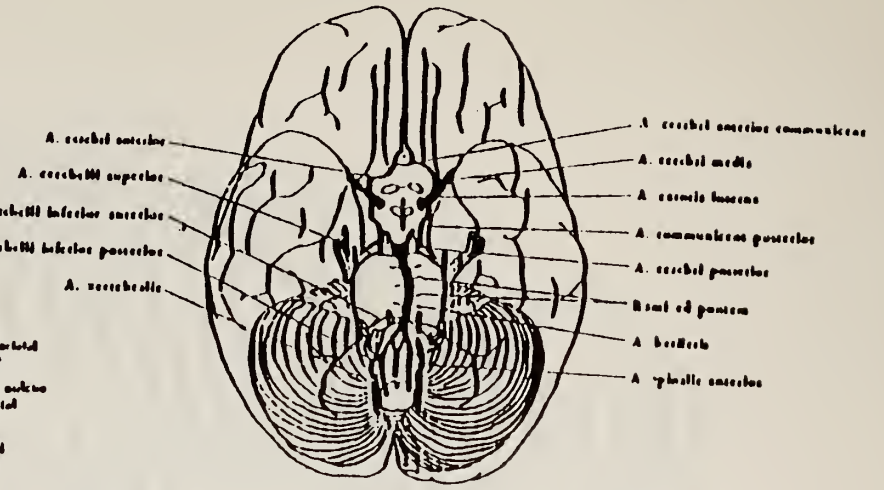

TEST NO. _____

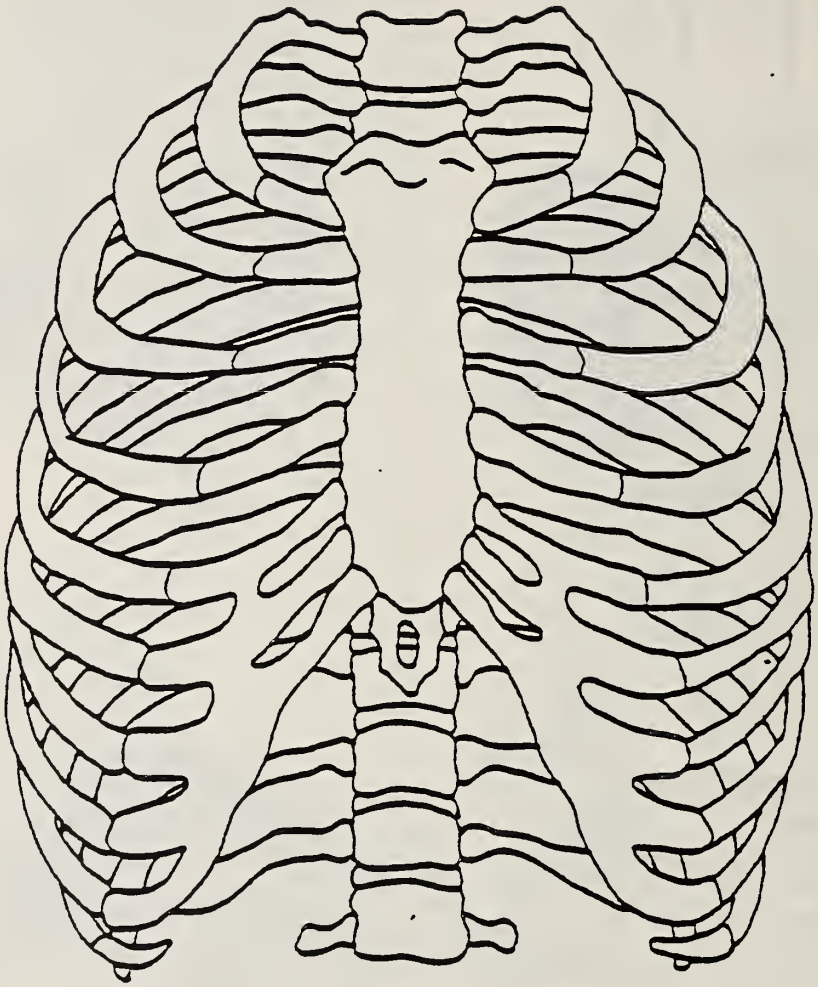

ANTERIOR THORAX

Test No._____

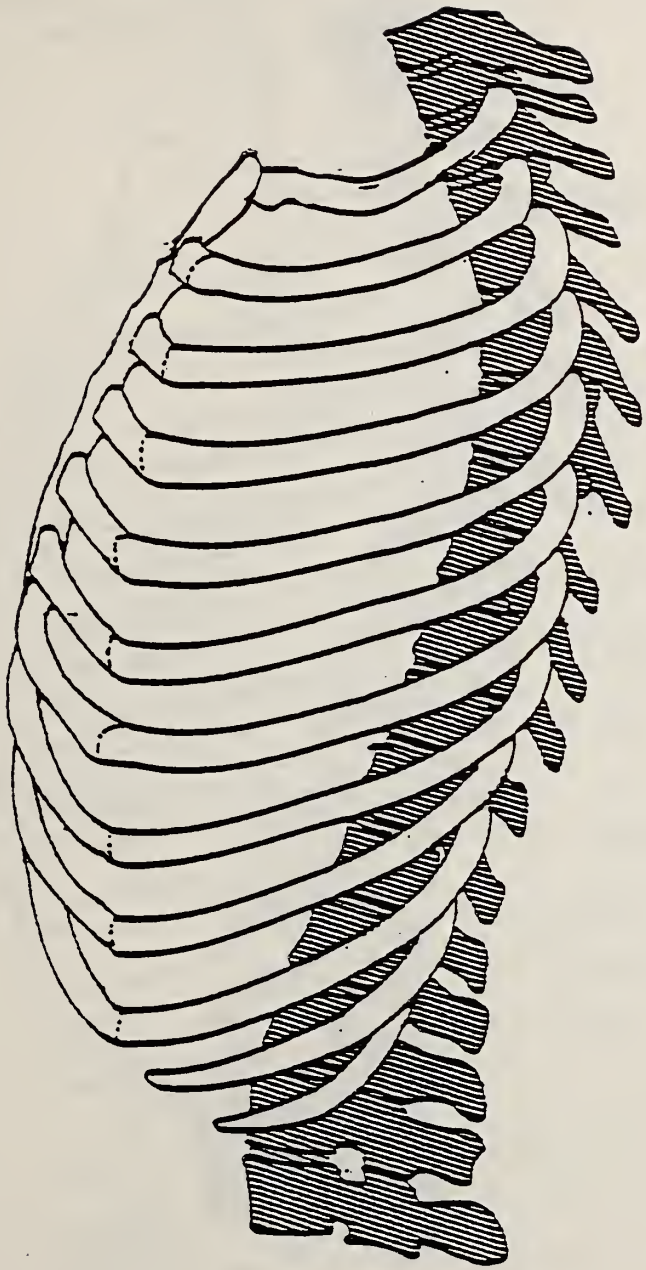

Test No. _____

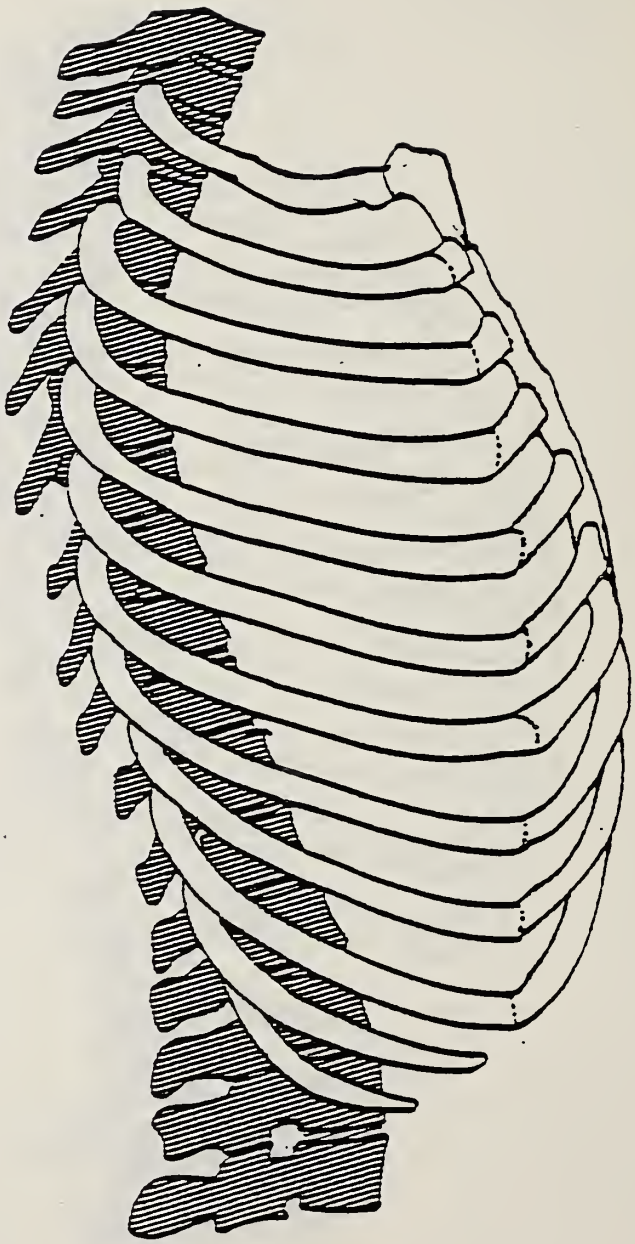

TEST NO. _____

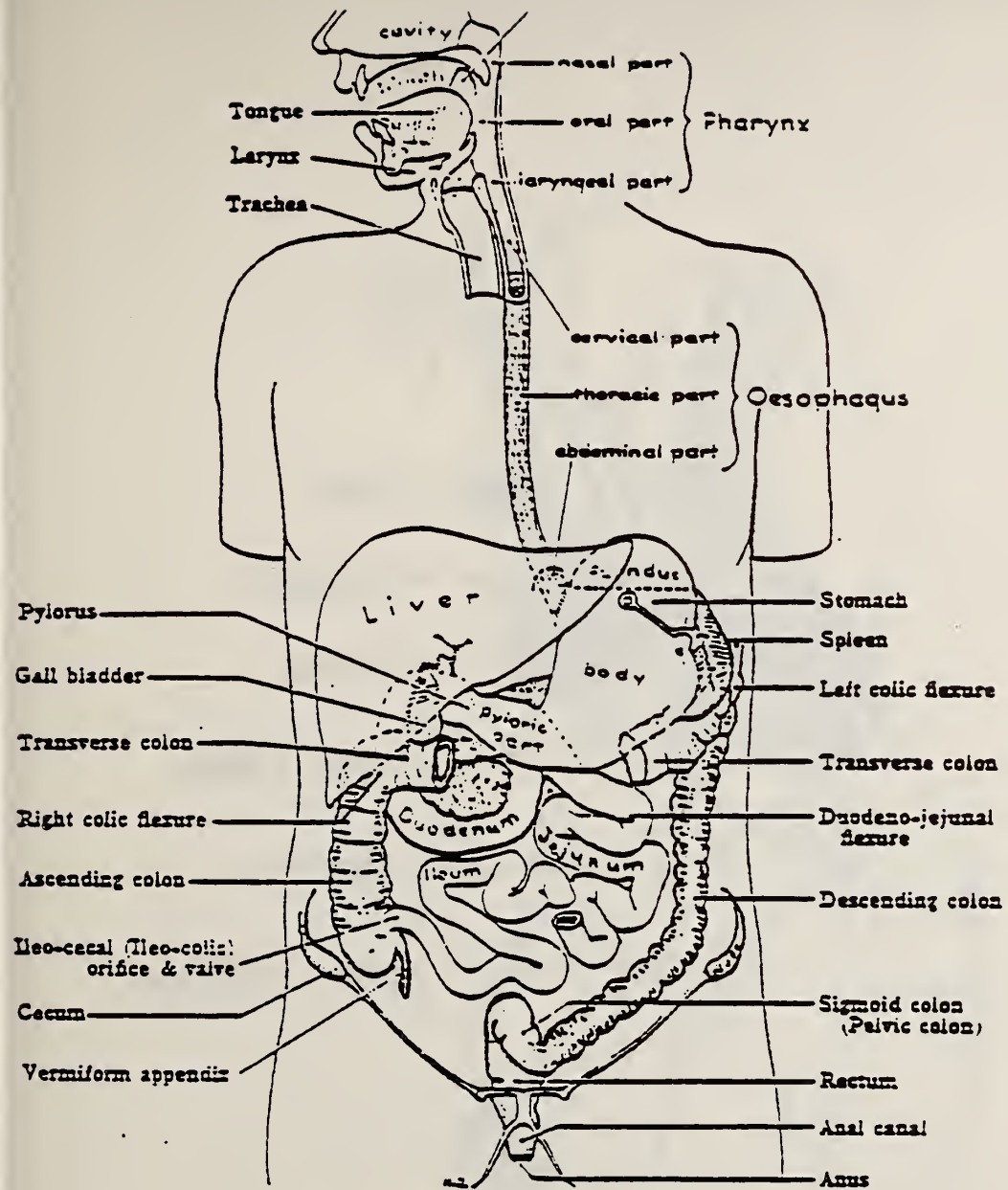
cavity
nasal part
oral part
laryngeal part
Pharynx
Tongue
Larynx
Trachea
cervical part
thoracic part
abdominal part
Oesophagus
Liver
Pylorus
Gall bladder
Transverse colon
Right colic flexure
Ascending colon
Ileo-cecal (Ileo-colic) orifice & valve
Cecum
Vermiform appendix
Stomach
Spleen
Left colic flexure
Transverse colon
Duodeno-jejunal flexure
Descending colon
Sigmoid colon (Pelvic colon)
Rectum
Anal canal
Anus

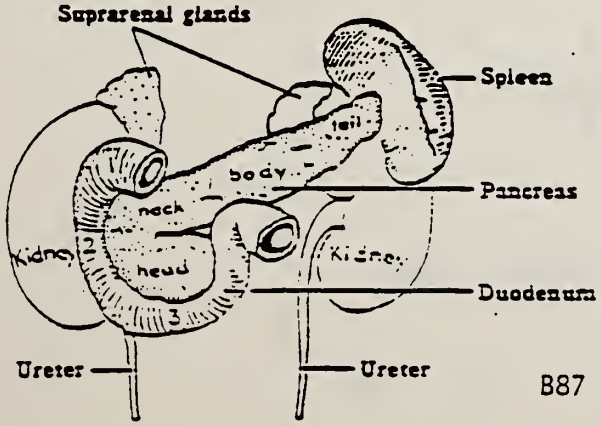
Suprarenal glands
Spleen
Pancreas
Duodenum
Ureter
Ureter

Test No._____

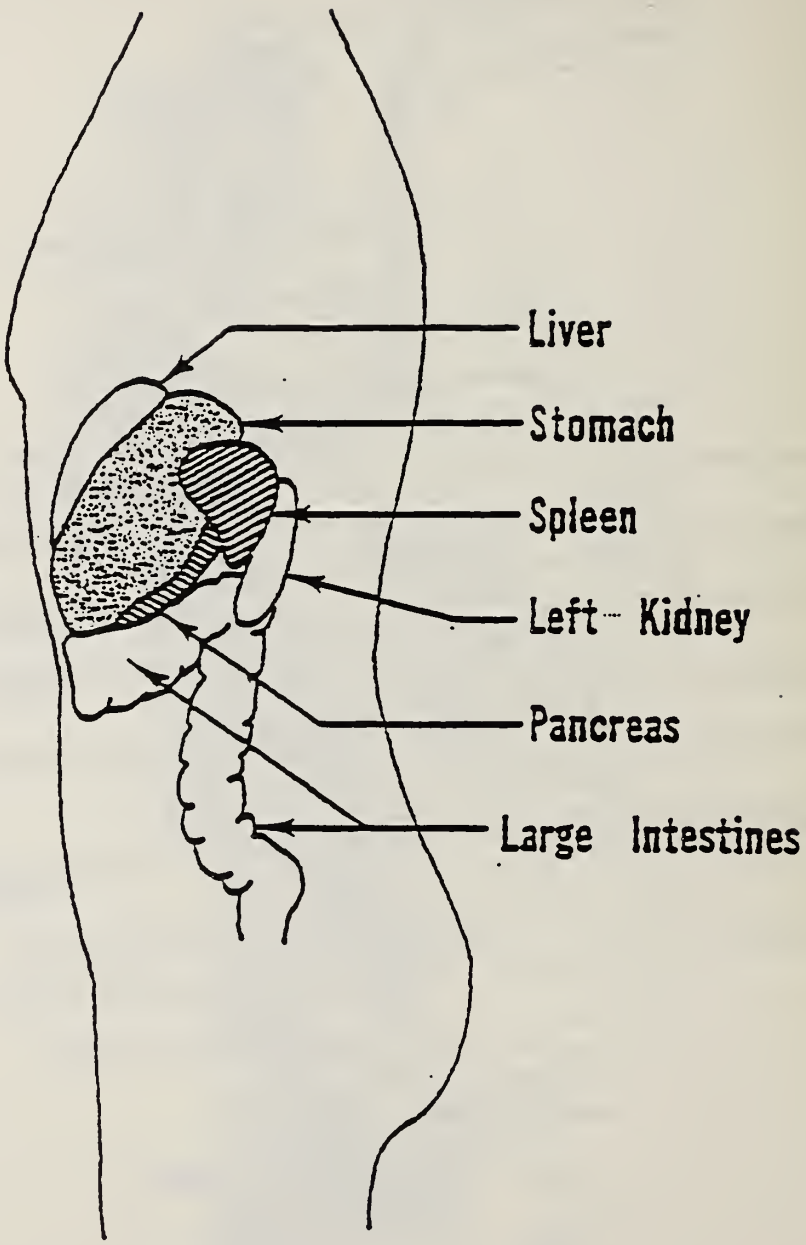

LEFT SIDE

TEST NO. _____

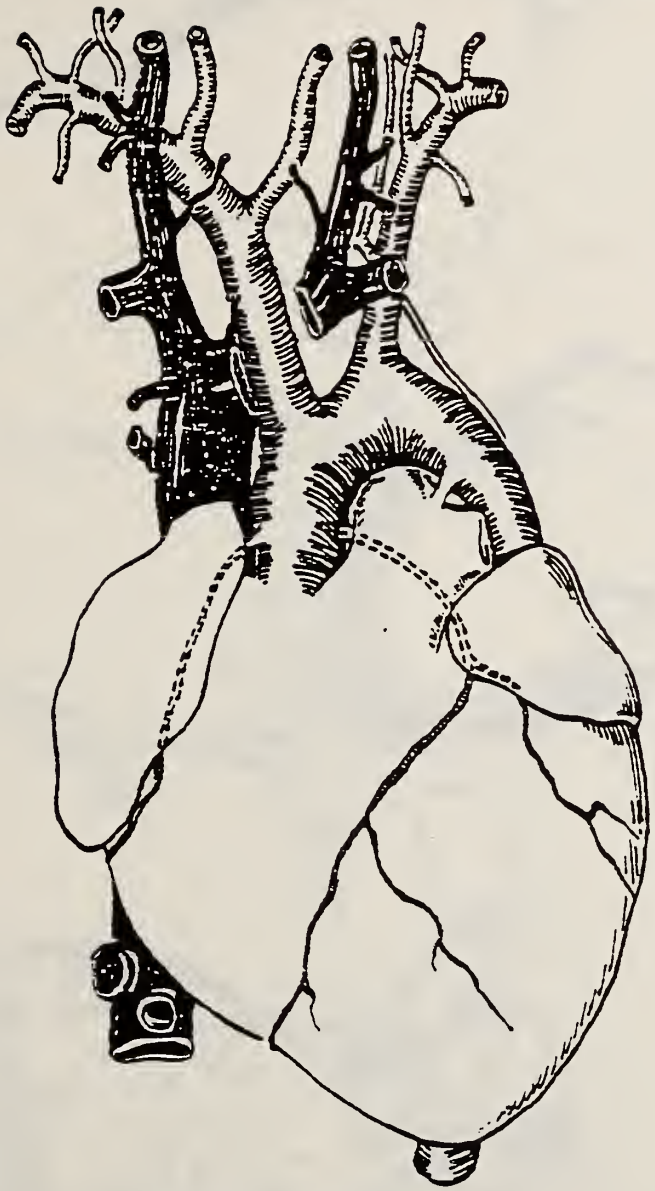

TEST NO. _____

Left Side View of Pericardium and Diaphragm

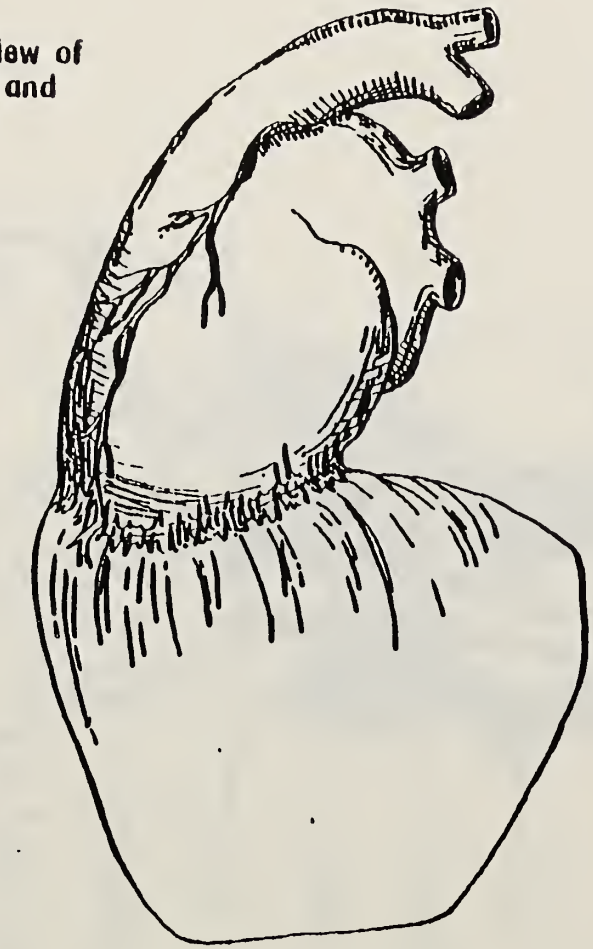

Diaphragmatic View of Heart

B90

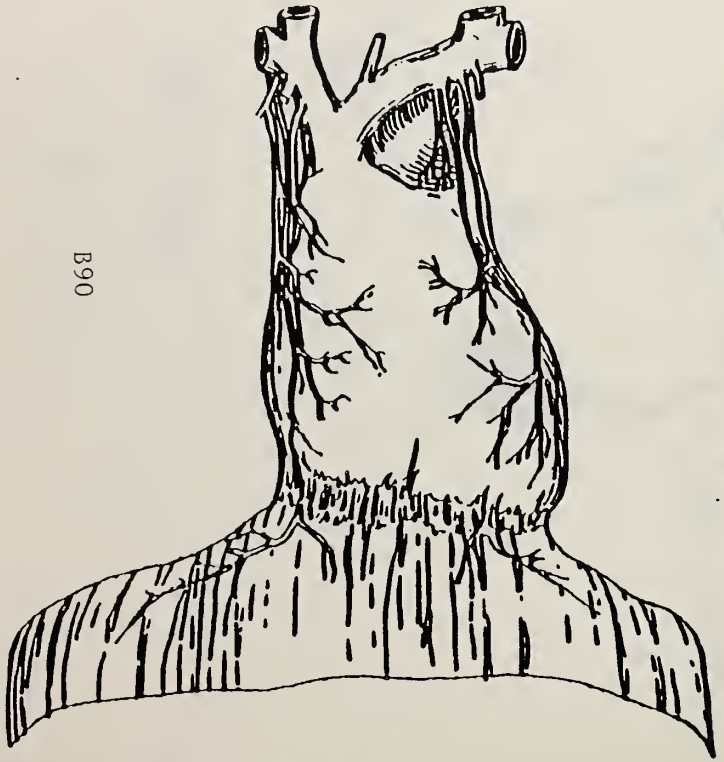

B90

Anterior View of Pericardium and Diaphragm

LIVER IMPACT AUTOPSY SUMMARY

'EST NO. _____

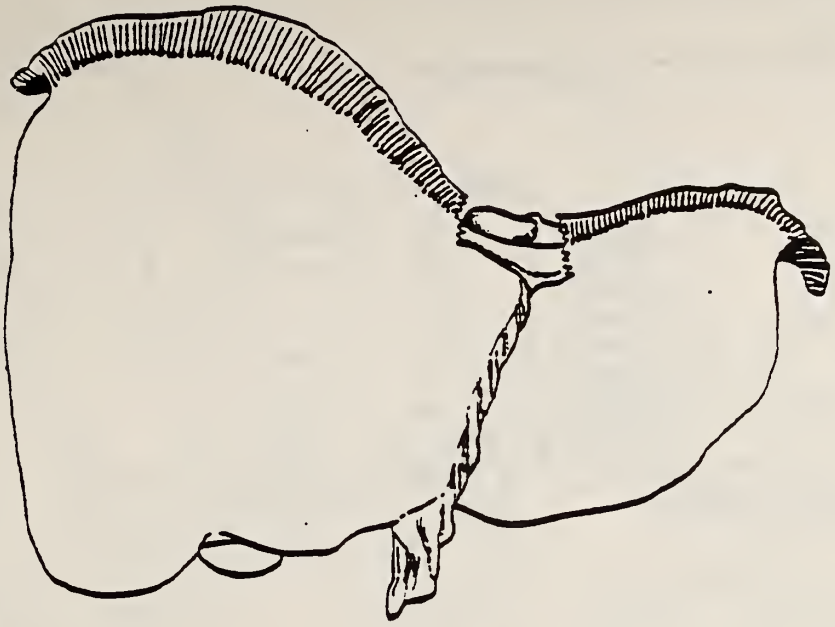

SUPERIOR SURFACE OF THE LIVER

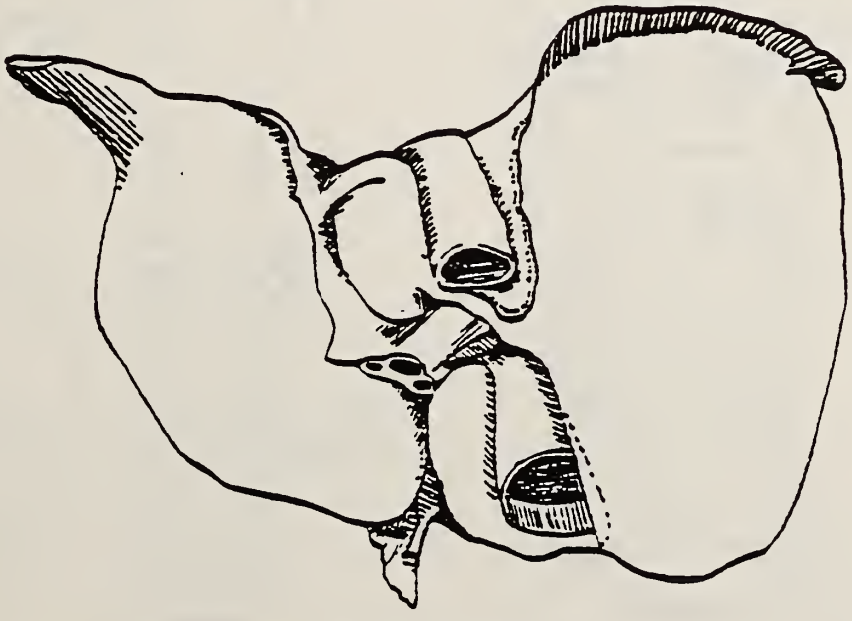

VISCERAL SURFACE OF THE LIVER

TEST NO. _____

DATE _____

PATELLA

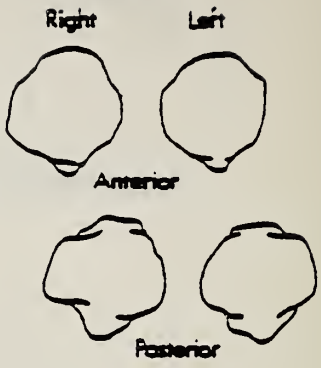

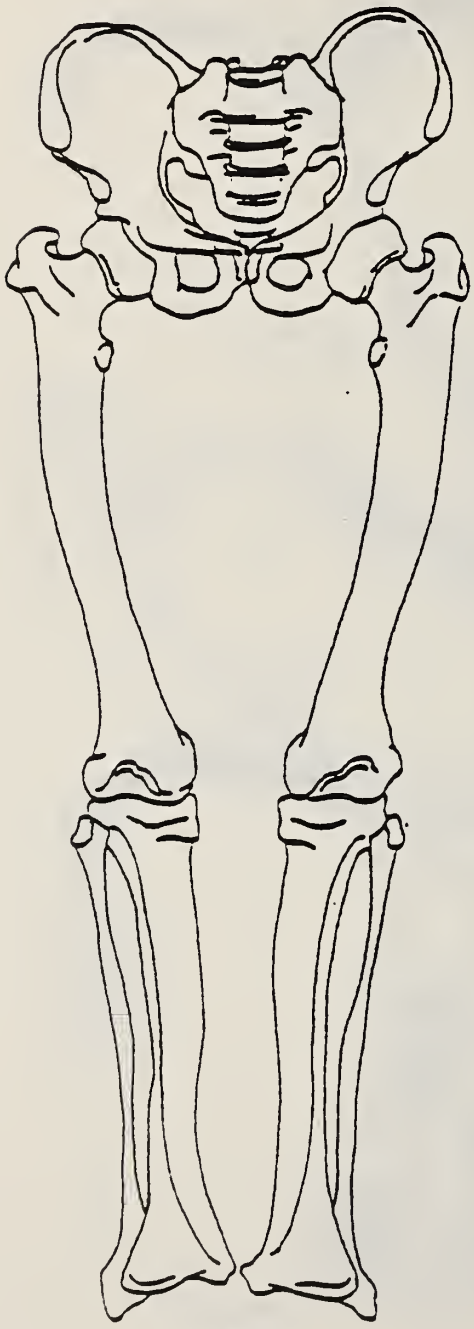

LOWER EXTREMITIES

TEST NO. _____

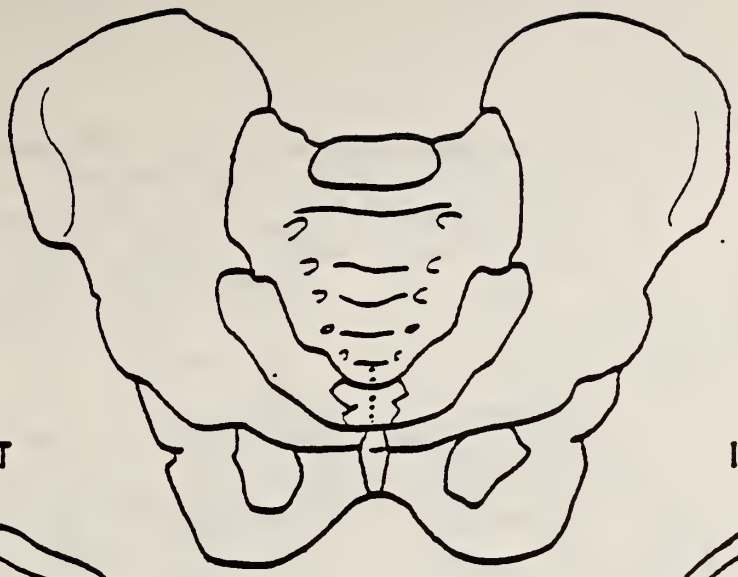

OUTER ASPECT

INNER ASPECT

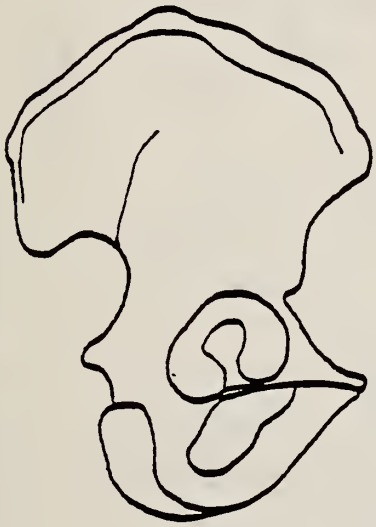

RIGHT ILIUM

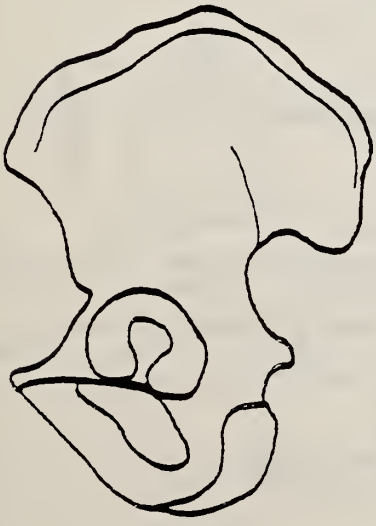

LEFT ILIUM

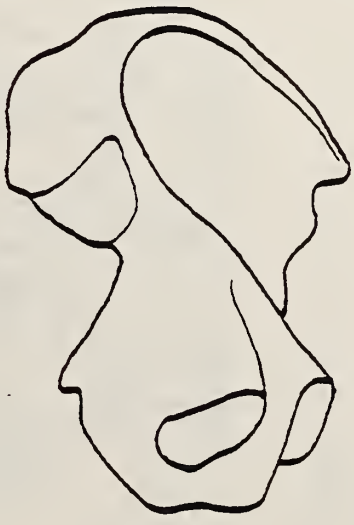

TEST NO. _____

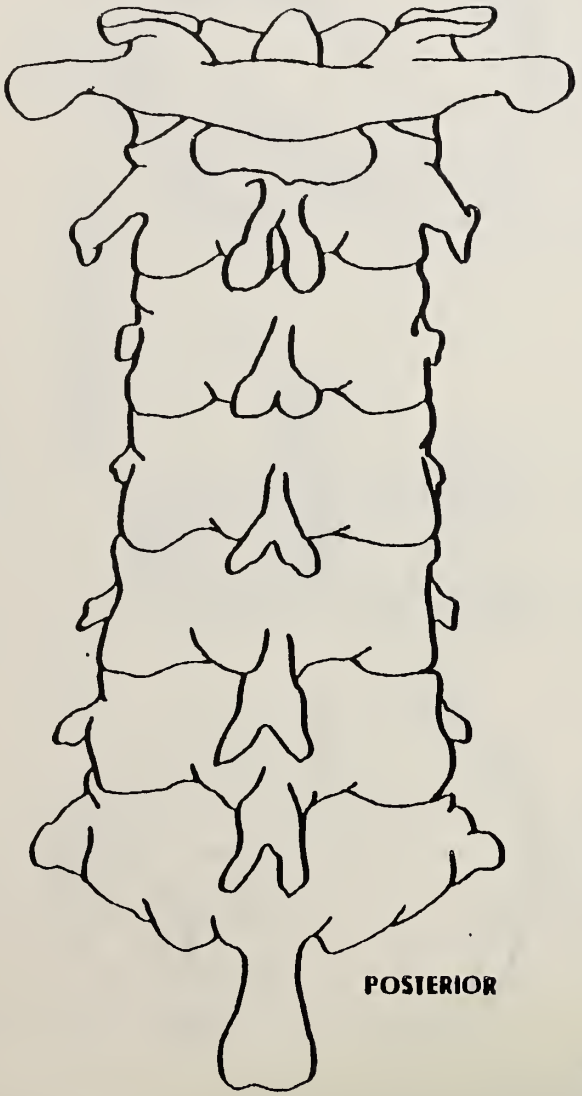

POSTERIOR

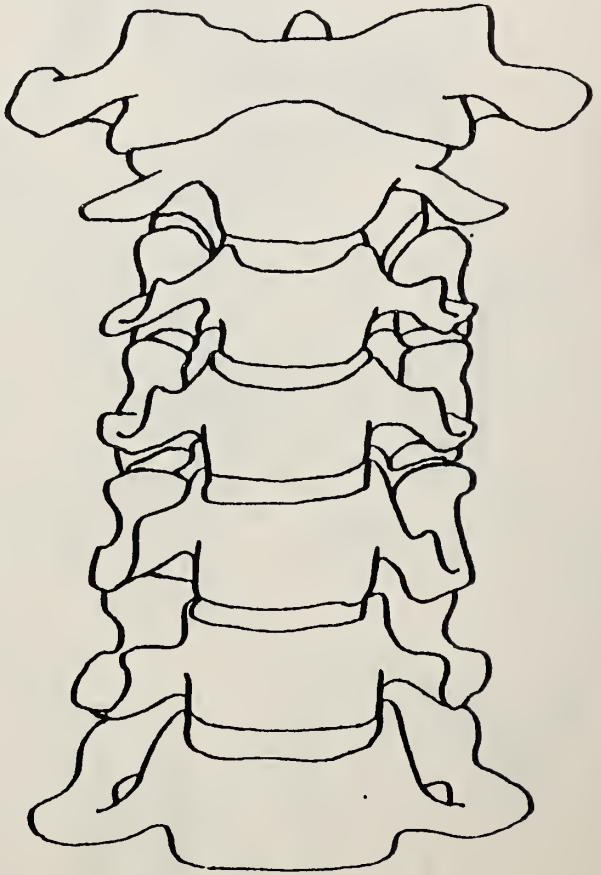

ANTERIOR

CERVICAL VERTEBRAE

B94

TEST NO. _____

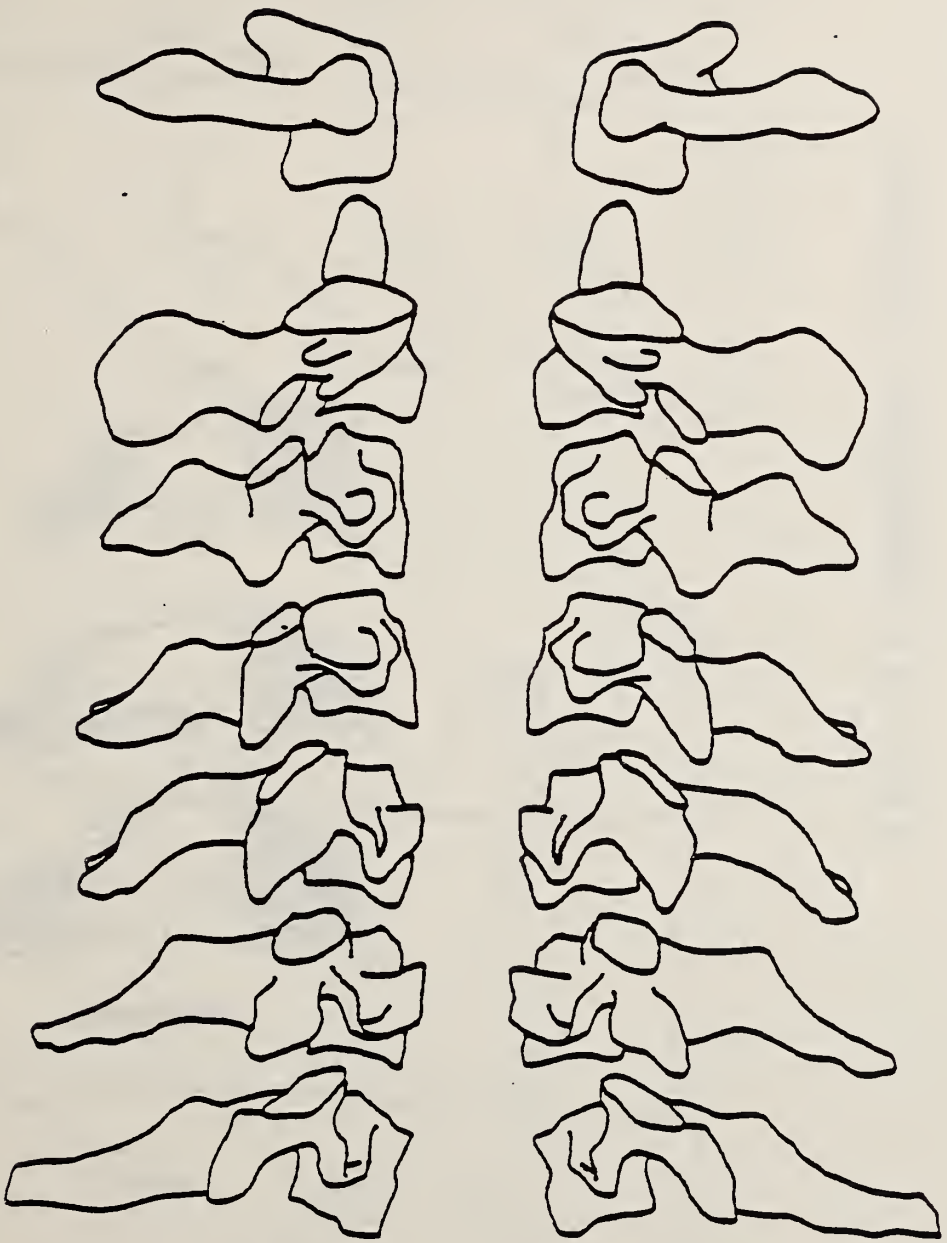

Right Profile

Left Profile

TEST NO. _____

Cross Section

TEST NO. _____

THORACIC VERTEBRAE (T1 - T4)

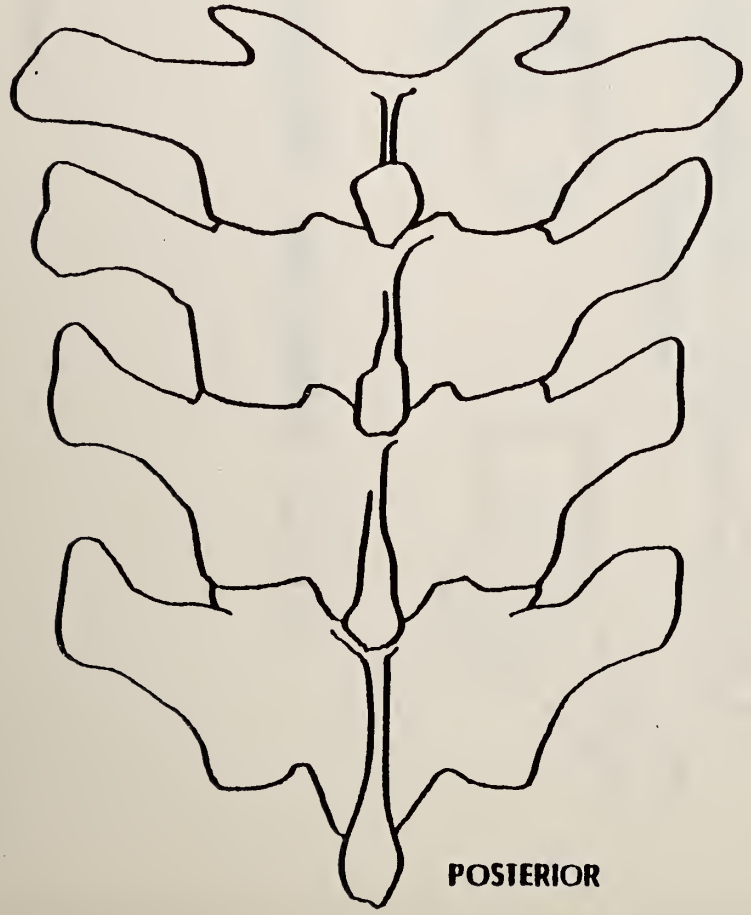

POSTERIOR

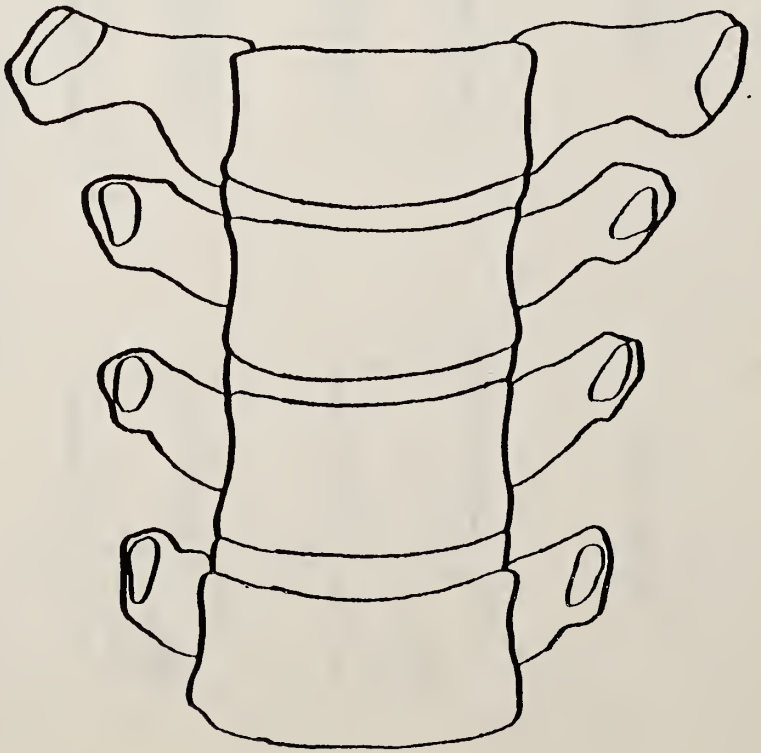

ANTERIOR

B97

TEST NO. _____

THORACIC VERTEBRAE (T1 - T4)

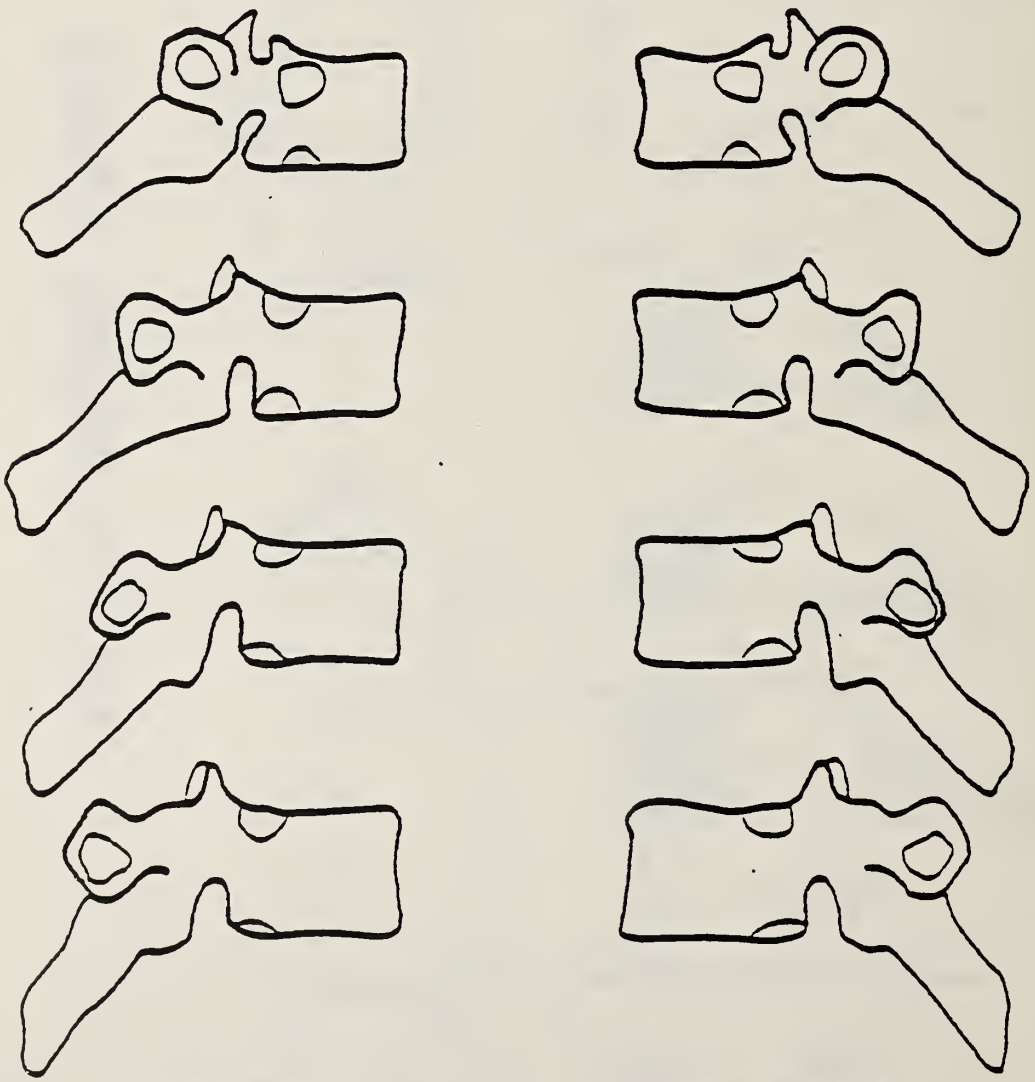

RIGHT PROFILE

LEFT PROFILE

APPENDICES

Anatomy Room Setup
Sled Lab Setup
Cart Setup
Autopsy Setup
Timer Box Setup
Pendulum Wierdness

MEASUREMENT

___ Anthropometer

___ Metric measuring tape

PAPER AND PLASTICS

___ Visqueen on autopsy table

___ Blue pads on table

___ Gauze

TAPES AND STRINGS

___ Silver tape

___ Masking tape

___ Adhesive tape

___ Fiber tape

___ Flat waxed string

SCALPELS

___ 2 large (#8) handles

___ 2 medium (#4) handles

___ 2 small (#3) handles

___ 2 #60 blades

___ 5 #22 blades

___ 5 #15 blades

___ 2 #12 blades

FORCEPS

___ 2 hooked

___ 2 large plain

___ 2 small plain

HEMOSTATS

___ needle

___ small straight

___ small curved

___ large straight

___ large curved

SCISSORS

___ 2 small

___ 2 medium

___ 2 large

SPREADERS

___ 2 large

___ 2 medium

NEEDLES

___ 2 double curved

___ 8 Trocar with stainless steel lockwire

___ 2 5cc sringes

CLOTHING

___ Tampons

___ Thermoknit longjohns and top

___ Cotton socks

___ Blue vinyl pants and top

___ Head and body harnesses

PRESSURIZATION

___ Modified Foley (#18 or #20) balloon catheters

___ Kulite shield

___ Tracheal tube

___ Right and left carotid pressurization catheters (Foley #10-14)

___ Cerebral spinal catheter (Foley #14-16)

___ Respiratory pressure tank

___ Manometer

___ Fluid pressure tank

___ 7% saline solution with India ink

BOLTS AND SCREWS

___ 6 self-tapping lag bolts

___ 3 lengths of wood screws

___ 1-72 screws

___ 10-32 tap

___ Strain relief bolt

___ Wood and metal self-tapping screw boxes

MOUNTS

___ Spine(2)

___ Rib (2, triax)

___ Rib (2, uniax, R-L)

___ Nine-accelerometer plates (large, small, and 8 feet)

___ Sternum

___ Substernale

___ Suprasternale (triax)

___ Dental acrylic

___ Bone wax

TOOLS

___ Electric hair clippers

___ Electric drill

___ Drill bits (No. 7, approx. 1/16", etc.)

___ large and small screwdrivers

___ nut driver (for lag bolts)

___ wire twisters

___ bone shears

___ Executive Slinky object space calibrated and nearly functional

MATERIALS

___ balsa wood

___ rags

___ foam (at least 2 sheets of 3x4 ft 6")

___ Ensolite

___ Styrofoam

___ Dow Ethafoam

___ Overhead support bar

ROPE CUTTERS

___ head, 1/8"

___ pendulum (with spring, 3/16")

___ nylon strings (10 24" 3/16"; 10 18" 1/8")

___ shock absorber and styrofoam bumper

WEIGHTS

___ steel blocks on pendulum

MISCELLANEOUS

___ calculator

___ bone wax

___ Pressurization equipment (pulmonary, thoracic arterial, head arterial, cerebral spinal)

___ Timer box

___ Strobes

___ Head impact back brace and foam padding

TAPES

___ adhesive

___ fiber

___ silver

___ masking

___ black

___ double stick

PAPER AND PLASTIC

___ blue pads

___ gauze

___ gloves

___ plastic garbage bags

SCALPELS

___ 1 medium (#4) handle

___ 1 small (#3) handle

___ 2 #22 blades

___ 2 #15 blades

___ 1 #12 blade

SURGICAL TOOLS

___ 2 forceps

___ 2 hemostats

___ large scissors

___ 2 double curved needles

STRING

___ flat waxed string

___ black thread

TOOLS

___ small (1-72) screwdriver

___ large screwdriver

___ nut driver

___ ball driver (6-32, 0-80)

___ 1-72 screws

___ 2-56 screws

___ 0-80 screws

___ wiretwisters

MISCELLANEOUS

___ ball targets

___ paper targets

___ bone wax

___ vaseline

___ Q-tips

___ tubing connectors

___ tie wraps

___ lockwire

___ 50cc syringe

___ pulmonary pressurization relief valves

AUTOPSY SETUP

PAPER AND PLASTICS

___ Visqueen on autopsy table

___ blue pads

___ gauze

TAPE

___ silver tape

___ masking tape

___ fiber tape

SCALPELS

___ 2 large (#8) handles

___ 2 medium (#4) handles

___ 2 small (#3) handles

___ 2 #60 blades

___ 5 #22 blades

___ 5 #15 blades

___ 2 #12 blades

FORCEPS

___ 2 hooked

___ 2 large plain

___ 2 small plain

HEMOSTATS

___ needle

___ small straight

___ small curved

___ large straight

___ large curved

SCISSORS

___ 2 small

___ 2 medium

___ 2 large

SPREADERS

___ 3 medium

___ 3 large

MISCELLANEOUS

___ Stryker saw and blade

___ bone shears

___ wedge

___ rib cutters

TIMER BOX SETUP

EQUIPMENT _____ Impact	TIMER VALUES Delay		 Run
Gate (from strobe 1)	0012-y	1	0150
Lights (start)	0001	2	2600
HyCam (start)	1200	3	1600
Pendulum rope cutter(start)	2200-x*	4	0050
Photosonics (start)	1000	5	1600
		6	
Head, pelvis, rope cutter (from velocity probe)	0001	7	0050
Piston Acceleration Corridor	1 + Z	8	0050-0150

* x obtained from elliptic integral of the first kind. For 100° .87 sec, 20 ° .70 sec. y=angle/20 Z=210/angle

PENDULUM WEIRDNESS

Average	60.84	61.00	61.26	61.56
Standard Deviation	±.28	±.37	±.05	±.23
Period	3.042	3.050	3.063	3.078
(MGL/I)÷2	2.065	2.060	2.051	2.041
t/2pi	.484	.485	.487	.489

10.0 APPENDIX D: ANTHROPOMETRY

HUMAN SUBJECT INFORMATION

CADAVER NO.: 000 DURATION OF BED CONFINEMENT Unknown

AGE: 60 SEX: M CAUSE OF DEATH: Unknown

PHYSICAL APPEARANCE: Caucasian DATE OF DEATH: 3/21/82

ANOMALY: None

ANTHROPOMETRY

0 - Weight*	52 kg	
1 - Stature**	184 cm	
2 - Shoulder (acromial) Height	159.4 cm	62.8 in
3 - Vertex to Symphysion Length	91.2 cm	35.9 in
4 - Waist Height	109.8 cm	43.2 in
5 - Shoulder Breadth (Biacromial Breadth)	31.8 cm	12.5 in
6 - Chest Breadth	27.9 cm	11 in
7 - Waist Breadth	29.2 cm	11.5 in
8 - Hip Breadth	25 cm	9.8 in
9 - Shoulder to Elbow Length (Acromion-radiale Length)	999	999
10 - Forearm-hand Length (elbow-middle finger)	999	999
11 - Tibiale Height	999	999
12 - Ankle Height (outside) (lateral malleous)	999	999
13 - Foot Breadth	999	999
14 - Foot Length	999	999

Note: * weight in kilograms

** lengths in centimeters

*** measures 16 and 17 must be made in case where the subject will be used in the seated position during the tests. In all other cases enter 9999 when under these measures.

LABORATORY UMTRI TEST NO. 82E001-3 82E004-7 82E008

15 - Top of Head to Trochanterion Length.....	88.5 cm	34.8 in
16 - Seated Height***.....	999	999
17 - Knee Height (seated)***.....	999	999
18 - Head Length.....	19.7 cm	7.8 in
19 - Head Breadth.....	15.7 cm	6.2 in
20 - Head to Chin Height (Vertex to Mentum).....	22.8 cm	9 in
21 - Biceps Circumference.....	999	999
22 - Elbow Circumference.....	999	999
23 - Forearm Circumference.....	999	999
24 - Wrist Circumference.....	999	999
25 - Thigh Circumference.....	999	999
26 - Lower Thigh Circumference.....	999	999
27 - Knee Circumference.....	999	999
28 - Calf Circumference.....	999	999
29 - Ankle Circumference.....	999	999
30 - Neck Circumference.....	32.3 cm	12.7 in
31 - Scye (armpit-shoulder) Circumference.....	999	999
32 - Chest Circumference.....	79.3 cm	31.2 in
33 - Waist Circumference.....	999	999
34 - Buttock Circumference.....	999	999
35 - Chest Depth.....	15.8 cm	6.2 in
36 - Waist Depth.....	999	999
37 - Buttock Depth.....	999	999
38 - Interscye.....	999	999

LABORATORY UMTRI TEST NO. 82E001-3 82E004-7 82E008

HUMAN SUBJECT INFORMATION

CADAVER NO.: 020 DURATION OF BED CONFINEMENT Unknown

AGE: 67 SEX: M CAUSE OF DEATH: Unknown

PHYSICAL APPEARANCE: Caucasian DATE OF DEATH: 3/23/82

ANOMALY: Excessive fat increased time required for spinal mounts

ANTHROPOMETRY

0 - Weight*	77 kg	
1 - Stature**	179.8 cm	
2 - Shoulder (acromial) Height	156 cm	61.4 in
3 - Vertex to Symphysion Length	88.5 cm	34.8 in
4 - Waist Height	107.3 cm	42.2 in
5 - Shoulder Breadth (Biacromial Breadth)	33.2 cm	13.1 in
6 - Chest Breadth	32.7 cm	12.9 in
7 - Waist Breadth	24 cm	9.4 in
8 - Hip Breadth	36 cm	14.2 in
9 - Shoulder to Elbow Length (Acromion-radiale Length)	999	999
10 - Forearm-hand Length (elbow-middle finger)	999	999
11 - Tibiale Height	999	999
12 - Ankle Height (outside) (lateral malleous)	999	999
13 - Foot Breadth	999	999
14 - Foot Length	999	999

Note: * weight in kilograms

** lengths in centimeters

*** measures 16 and 17 must be made in case where the subject will be used in the seated position during the tests. In all other cases enter 9999 when under these measures.

LABORATORY UMTRI TEST NO. 82E021-22 82E023-27 82E028

15 - Top of Head to Trochanterion Length.....	999	999
16 - Seated Height***.....	999	999
17 - Knee Height (seated)***.....	999	999
18 - Head Length.....	21 cm	8.2 in
19 - Head Breadth.....	15.8 cm	6.2 in
20 - Head to Chin Height (Vertex to Mentum).....	24.9 cm	9.8 in
21 - Biceps Circumference.....	999	999
22 - Elbow Circumference.....	999	999
23 - Forearm Circumference.....	999	999
24 - Wrist Circumference.....	999	999
25 - Thigh Circumference.....	999	999
26 - Lower Thigh Circumference.....	999	999
27 - Knee Circumference.....	999	999
28 - Calf Circumference.....	999	999
29 - Ankle Circumference.....	999	999
30 - Neck Circumference.....	42 cm	16.5 in
31 - Scye (armpit-shoulder) Circumference.....	999	999
32 - Chest Circumference.....	99 cm	39 in
33 - Waist Circumference.....	999	999
34 - Buttock Circumference.....	999	999
35 - Chest Depth.....	22.2 cm	8.7 in
36 - Waist Depth.....	999	999
37 - Buttock Depth.....	999	999
38 - Interscye.....	999	999

LABORATORY UMTRI TEST NO. 82E021-22 82E023-27 82E028

HUMAN SUBJECT INFORMATION

CADAVER NO.: 040 DURATION OF BED CONFINEMENT Unknown

AGE: 65 SEX: M CAUSE OF DEATH: Myocardial infarction

PHYSICAL APPEARANCE: Caucasian DATE OF DEATH: 3/27/82

ANOMALY: Upper ribs very close together and embedded in deep fat.

ANTHROPOMETRY

0 - Weight*	87 kg	
1 - Stature**	169.2 cm	
2 - Shoulder (acromial) Height	146.7 cm	57.8 in
3 - Vertex to Symphysion Length	81.8 cm	32.2 in
4 - Waist Height	102 cm	40.2 in
5 - Shoulder Breadth (Biacromial Breadth)	35.4 cm	13.9 in
6 - Chest Breadth	32.7 cm	12.9 in
7 - Waist Breadth	32 cm	12.6 in
8 - Hip Breadth	33.5 cm	13.2 in
9 - Shoulder to Elbow Length (Acromion-radiale Length)	999	999
10 - Forearm-hand Length (elbow-middle finger)	999	999
11 - Tibiale Height	999	999
12 - Ankle Height (outside) (lateral malleous)	999	999
13 - Foot Breadth	999	999
14 - Foot Length	999	999

Note: * weight in kilograms

** lengths in centimeters

*** measures 16 and 17 must be made in case where the subject will be used in the seated position during the tests. In all other cases enter 9999 when under these measures.

LABORATORY UMTRI TEST NO. 82E041-42 82E043-48 82E049

15 - Top of Head to Trochanterion Length.....	999	999
16 - Seated Height***.....	999	999
17 - Knee Height (seated)***.....	999	999
18 - Head Length.....	20 cm	7.9 in
19 - Head Breadth.....	16.5 cm	6.5 in
20 - Head to Chin Height (Vertex to Mentum).....	21.4 cm	8.4 in
21 - Biceps Circumference.....	999	999
22 - Elbow Circumference.....	999	999
23 - Forearm Circumference.....	999	999
24 - Wrist Circumference.....	999	999
25 - Thigh Circumference.....	999	999
26 - Lower Thigh Circumference.....	999	999
27 - Knee Circumference.....	999	999
28 - Calf Circumference.....	999	999
29 - Ankle Circumference.....	999	999
30 - Neck Circumference.....	50.4 cm	19.8 in
31 - Scye (armpit-shoulder) Circumference.....	999	999
32 - Chest Circumference.....	104.5 cm	41.1 in
33 - Waist Circumference.....	999	999
34 - Buttock Circumference.....	999	999
35 - Chest Depth.....	23.8 cm	9.4 in
36 - Waist Depth.....	999	999
37 - Buttock Depth.....	999	999
38 - Interscye.....	999	999

LABORATORY UMTRI TEST NO. 82E041-42 82E043-48 82E049

HUMAN SUBJECT INFORMATION

CADAVER NO.: 050 DURATION OF BED CONFINEMENT Unknown

AGE: 60 SEX: M CAUSE OF DEATH: Coronary thrombosis

PHYSICAL APPEARANCE: Caucasian DATE OF DEATH: 6/7/82

ANOMALY: Right and left ribs R4-R5 broken, probably from CPR.

ANTHROPOMETRY

0 - Weight*	67 kg	
1 - Stature**	180.2 cm	
2 - Shoulder (acromial) Height	155.7 cm	61.8 in
3 - Vertex to Symphysion Length	999	999
4 - Waist Height	999	999
5 - Shoulder Breadth (Biacromial Breadth)	37.5 cm	14.8 in
6 - Chest Breadth	999	999
7 - Waist Breadth	999	999
8 - Hip Breadth	999	999
9 - Shoulder to Elbow Length (Acromion-radiale Length)	999	999
10 - Forearm-hand Length (elbow-middle finger)	999	999
11 - Tibiale Height	999	999
12 - Ankle Height (outside) (lateral malleous)	999	999
13 - Foot Breadth	999	999
14 - Foot Length	999	999

Note: * weight in kilograms

** lengths in centimeters

*** measures 16 and 17 must be made in case where the subject will be used in the seated position during the tests. In all other cases enter 9999 when under these measures.

LABORATORY UMTRI TEST NO. 82E051-53

15 - Top of Head to Trochanterion Length.....	999	999
16 - Seated Height***.....	999	999
17 - Knee Height (seated)***.....	999	999
18 - Head Length.....	20 cm	7.9 in
19 - Head Breadth.....	16.2 cm	6.4 in
20 - Head to Chin Height (Vertex to Mentum).....	999	999
21 - Biceps Circumference.....	999	999
22 - Elbow Circumference.....	999	999
23 - Forearm Circumference.....	999	999
24 - Wrist Circumference.....	999	999
25 - Thigh Circumference.....	999	999
26 - Lower Thigh Circumference.....	999	999
27 - Knee Circumference.....	999	999
28 - Calf Circumference.....	999	999
29 - Ankle Circumference.....	999	999
30 - Neck Circumference.....	40.5 cm	15.9 in
31 - Scye (armpit-shoulder) Circumference.....	999	999
32 - Chest Circumference.....	999	999
33 - Waist Circumference.....	999	999
34 - Buttock Circumference.....	999	999
35 - Chest Depth.....	999	999
36 - Waist Depth.....	999	999
37 - Buttock Depth.....	999	999
38 - Interscye.....	999	999

LABORATORY UMTRI TEST NO. 82F051-53

HUMAN SUBJECT INFORMATION

CADAVER NO.: 060 DURATION OF BED CONFINEMENT Unknown

AGE: 60 SEX: M CAUSE OF DEATH: Unknown

PHYSICAL APPEARANCE: Caucasian DATE OF DEATH: 6/1/82

ANOMALY: None

ANTHROPOMETRY

0 - Weight*	67 kg	
1 - Stature**	169.8 cm	
2 - Shoulder (acromial) Height	148.4 cm	58.4 in
3 - Vertex to Symphysion Length	86.1 cm	33.9 in
4 - Waist Height	99.8 cm	39.3 in
5 - Shoulder Breadth (Biacromial Breadth)	34.7 cm	13.7 in
6 - Chest Breadth	29.1 cm	11.5 in
7 - Waist Breadth	23 cm	9.1 in
8 - Hip Breadth	28.6 cm	11.3 in
9 - Shoulder to Elbow Length (Acromion-radiale Length)	999	999
10 - Forearm-hand Length (elbow-middle finger)	999	999
11 - Tibiale Height	999	999
12 - Ankle Height (outside) (lateral malleous)	999	999
13 - Foot Breadth	999	999
14 - Foot Length	999	999

Note: * weight in kilograms

** lengths in centimeters

*** measures 16 and 17 must be made in case where the subject will be used in the seated position during the tests. In all other cases enter 9999 when under these measures.

LABORATORY UMTRI TEST NO. 82E061-62 82E063-66 82E067

15 - Top of Head to Trochanterion Length.....	999	999
16 - Seated Height***.....	999	999
17 - Knee Height (seated)***.....	999	999
18 - Head Length.....	19.2 cm	7.6 in
19 - Head Breadth.....	15.5 cm	6.1 in
20 - Head to Chin Height (Vertex to Mentum).....	22.1 cm	8.7 in
21 - Biceps Circumference.....	999	999
22 - Elbow Circumference.....	999	999
23 - Forearm Circumference.....	999	999
24 - Wrist Circumference.....	999	999
25 - Thigh Circumference.....	999	999
26 - Lower Thigh Circumference.....	999	999
27 - Knee Circumference.....	999	999
28 - Calf Circumference.....	999	999
29 - Ankle Circumference.....	999	999
30 - Neck Circumference.....	44.6 cm	17.6 in
31 - Scye (armpit-shoulder) Circumference.....	999	999
32 - Chest Circumference.....	90.2 cm	35.5 in
33 - Waist Circumference.....	999	999
34 - Buttock Circumference.....	999	999
35 - Chest Depth.....	21.6 cm	8.5 in
36 - Waist Depth.....	999	999
37 - Buttock Depth.....	999	999
38 - Interscye.....	999	999

LABORATORY UMTRI TEST NO. 82E061-62 82E063-66 82E067

HUMAN SUBJECT INFORMATION

CADAVER NO.: 070 DURATION OF BED CONFINEMENT unknown

AGE: 61 SEX: M CAUSE OF DEATH: unknown

PHYSICAL APPEARANCE: Caucasian DATE OF DEATH: 9/9/82

ANOMALY:

Ribs broken during CPR attached to sternum with wire.

ANTHROPOMETRY

0 - Weight*		55 kg
1 - Stature**	181 cm	
2 - Shoulder (acromial) Height	156 cm	61.4 in
3 - Vertex to Symphysion Length	999	999
4 - Waist Height	999	999
5 - Shoulder Breadth (Biacromial Breadth)	36.2 cm	14.3 in
6 - Chest Breadth	999	999
7 - Waist Breadth	999	999
8 - Hip Breadth	999	999
9 - Shoulder to Elbow Length (Acromion-radiale Length)	999	999
10 - Forearm-hand Length (elbow-middle finger)	999	999
11 - Tibiale Height	999	999
12 - Ankle Height (outside) (lateral malleous)	999	999
13 - Foot Breadth	999	999
14 - Foot Length	999	999

Note: * weight in kilograms

** lengths in centimeters

*** measures 16 and 17 must be made in case where the subject will be used in the seated position during the tests. In all other cases enter 9999 when under these measures.

LABORATORY UMTRI TEST NO. 82E071

15 - Top of Head to Trochanterion Length.....	999	999
16 - Seated Height***.....	999	999
17 - Knee Height (seated)***.....	999	999
18 - Head Length.....	20.6 cm	8.1 in
19 - Head Breadth.....	15.3 cm	6 in
20 - Head to Chin Height (Vertex to Mentum).....	999	999
21 - Biceps Circumference.....	999	999
22 - Elbow Circumference.....	999	999
23 - Forearm Circumference.....	999	999
24 - Wrist Circumference.....	999	999
25 - Thigh Circumference.....	999	999
26 - Lower Thigh Circumference.....	999	999
27 - Knee Circumference.....	999	999
28 - Calf Circumference.....	999	999
29 - Ankle Circumference.....	999	999
30 - Neck Circumference.....	32 cm	12.6 in
31 - Scye (armpit-shoulder) Circumference.....	999	999
32 - Chest Circumference.....	999	999
33 - Waist Circumference.....	999	999
34 - Buttock Circumference.....	999	999
35 - Chest Depth.....	999	999
36 - Waist Depth.....	999	999
37 - Buttock Depth.....	999	999
38 - Interscye.....	999	999

LABORATORY UMTRI TEST NO. 82E071

HUMAN SUBJECT INFORMATION

CADAVER NO.: 079 DURATION OF BED CONFINEMENT Unknown

AGE: 51 SEX: M CAUSE OF DEATH: Myocardial infarction

PHYSICAL APPEARANCE: Caucasian DATE OF DEATH: 2/26/83

ANOMALY: Structures weakened from CPR.

ANTHROPOMETRY

0 - Weight*	83 kg	
1 - Stature**	169 cm	
2 - Shoulder (acromial) Height	146.5 cm	57.7 in
3 - Vertex to Symphysion Length	999	999
4 - Waist Height	999	999
5 - Shoulder Breadth (Biacromial Breadth)	30.4 cm	12 in
6 - Chest Breadth	34.2 cm	13.5 in
7 - Waist Breadth	999	999
8 - Hip Breadth	31 cm	12.2 in
9 - Shoulder to Elbow Length (Acromion-radiale Length)	999	999
10 - Forearm-hand Length (elbow-middle finger)	999	999
11 - Tibiale Height	999	999
12 - Ankle Height (outside) (lateral malleous)	999	999
13 - Foot Breadth	999	999
14 - Foot Length	999	999

Note: * weight in kilograms

** lengths in centimeters

*** measures 16 and 17 must be made in case where the subject will be used in the seated position during the tests. In all other cases enter 9999 when under these measures.

LABORATORY UMTRI TEST NO. 83E076

15 - Top of Head to Trochanterion Length.....	999	999
16 - Seated Height***.....	999	999
17 - Knee Height (seated)***.....	999	999
18 - Head Length.....	20 cm	7.8 in
19 - Head Breadth.....	16 cm	6.3 in
20 - Head to Chin Height (Vertex to Mentum).....	999	999
21 - Biceps Circumference.....	999	999
22 - Elbow Circumference.....	999	999
23 - Forearm Circumference.....	999	999
24 - Wrist Circumference.....	999	999
25 - Thigh Circumference.....	999	999
26 - Lower Thigh Circumference.....	999	999
27 - Knee Circumference.....	999	999
28 - Calf Circumference.....	999	999
29 - Ankle Circumference.....	999	999
30 - Neck Circumference.....	36 cm	14.2 in
31 - Scye (armpit-shoulder) Circumference.....	999	999
32 - Chest Circumference.....	999	999
33 - Waist Circumference.....	999	999
34 - Buttock Circumference.....	999	999
35 - Chest Depth.....	999	999
36 - Waist Depth.....	999	999
37 - Buttock Depth.....	999	999
38 - Interscye.....	999	999

LABORATORY UMTRI TEST NO. 83E076

HUMAN SUBJECT INFORMATION

CADAVER NO.: 080 DURATION OF BED CONFINEMENT Unknown

AGE: 44 SEX: M CAUSE OF DEATH: Pulmonary edema

PHYSICAL APPEARANCE: Caucasian DATE OF DEATH: 3/6/83

ANOMALY: . Left rib R4 weakened. Sternum weakened.

ANTHROPOMETRY

0 - Weight*	72 kg	
1 - Stature**	171 cm	
2 - Shoulder (acromial) Height	147.4 cm	58 in
3 - Vertex to Symphysion Length	88 cm	34.6 in
4 - Waist Height	89.5 cm	35.2 in
5 - Shoulder Breadth (Biacromial Breadth)	32.5 cm	12.8 in
6 - Chest Breadth	33.8 cm	13.3 in
7 - Waist Breadth	25 cm	9.8 in
8 - Hip Breadth	31.4 cm	12.4 in
9 - Shoulder to Elbow Length (Acromion-radiale Length)	999	999
10 - Forearm-hand Length (elbow-middle finger)	999	999
11 - Tibiale Height	999	999
12 - Ankle Height (outside) (lateral malleous)	999	999
13 - Foot Breadth	999	999
14 - Foot Length	999	999

Note: * weight in kilograms

** lengths in centimeters

*** measures 16 and 17 must be made in case where the subject will be used in the seated position during the tests. In all other cases enter 9999 when under these measures.

LABORATORY UMTRI TEST NO. 83E081-82 83E083-86 83E087-88

15 - Top of Head to Trochanterion Length.....	999	999
16 - Seated Height***.....	999	999
17 - Knee Height (seated)***.....	999	999
18 - Head Length.....	19.8 cm	7.8 in
19 - Head Breadth.....	15.5 cm	6.1 in
20 - Head to Chin Height (Vertex to Mentum).....	23 cm	9.1 in
21 - Biceps Circumference.....	999	999
22 - Elbow Circumference.....	999	999
23 - Forearm Circumference.....	999	999
24 - Wrist Circumference.....	999	999
25 - Thigh Circumference.....	999	999
26 - Lower Thigh Circumference.....	999	999
27 - Knee Circumference.....	999	999
28 - Calf Circumference.....	999	999
29 - Ankle Circumference.....	999	999
30 - Neck Circumference.....	57 cm	22.4 in
31 - Scye (armpit-shoulder) Circumference.....	999	999
32 - Chest Circumference.....	100 cm	39.4 in
33 - Waist Circumference.....	999	999
34 - Buttock Circumference.....	999	999
35 - Chest Depth.....	15.3 cm	6 in
36 - Waist Depth.....	999	999
37 - Buttock Depth.....	999	999
38 - Interscye.....	999	999

LABORATORY UMTRI TEST NO. 83E081-82 83E083-86 83E087-88

HUMAN SUBJECT INFORMATION

CADAVER NO.: 089 DURATION OF BED CONFINEMENT Unknown

AGE: 62 SEX: M CAUSE OF DEATH: Myocardial infarction

PHYSICAL APPEARANCE: Caucasian DATE OF DEATH: 1/26/83

ANOMALY: None

ANTHROPOMETRY

0 - Weight*	76 kg	
1 - Stature**	175.8 cm	
2 - Shoulder (acromial) Height	152 cm	59.8 in
3 - Vertex to Symphysion Length	84.5 cm	33.3 in
4 - Waist Height	999	999
5 - Shoulder Breadth (Biacromial Breadth)	34.7 cm	13.7 in
6 - Chest Breadth	34 cm	13.4 in
7 - Waist Breadth	999	999
8 - Hip Breadth	31.5 cm	12.4 in
9 - Shoulder to Elbow Length (Acromion-radiale Length)	999	999
10 - Forearm-hand Length (elbow-middle finger)	999	999
11 - Tibiale Height	999	999
12 - Ankle Height (outside) (lateral malleous)	999	999
13 - Foot Breadth	999	999
14 - Foot Length	999	999

Note: * weight in kilograms

** lengths in centimeters

*** measures 16 and 17 must be made in case where the subject will be used in the seated position during the tests. In all other cases enter 9999 when under these measures.

LABORATORY UMTRI TEST NO. 83E071-75 83E091

15 - Top of Head to Trochanterion Length.....	999	999
16 - Seated Height***.....	999	999
17 - Knee Height (seated)***.....	999	999
18 - Head Length.....	19.0 cm	7.5 in
19 - Head Breadth.....	15.3 cm	6 in
20 - Head to Chin Height (Vertex to Mentum).....	999	999
21 - Biceps Circumference.....	999	999
22 - Elbow Circumference.....	999	999
23 - Forearm Circumference.....	999	999
24 - Wrist Circumference.....	999	999
25 - Thigh Circumference.....	999	999
26 - Lower Thigh Circumference.....	999	999
27 - Knee Circumference.....	999	999
28 - Calf Circumference.....	999	999
29 - Ankle Circumference.....	999	999
30 - Neck Circumference.....	37 cm	14.6 in
31 - Scye (armpit-shoulder) Circumference.....	999	999
32 - Chest Circumference.....	999	999
33 - Waist Circumference.....	999	999
34 - Buttock Circumference.....	999	999
35 - Chest Depth.....	999	999
36 - Waist Depth.....	999	999
37 - Buttock Depth.....	999	999
38 - Interscye.....	999	999

LABORATORY UMTRI TEST NO. 83E071-75 83E091

HUMAN SUBJECT INFORMATION

CADAVER NO.: 090 DURATION OF BED CONFINEMENT Unknown

AGE: 51 SEX: M CAUSE OF DEATH: Cerebral Contusion

PHYSICAL APPEARANCE: Caucasian DATE OF DEATH:

ANOMALY: None

ANTHROPOMETRY

0 - Weight*	68 kg	
1 - Stature**	180 cm	
2 - Shoulder (acromial) Height	155.4 cm	61.2 in
3 - Vertex to Symphysion Length	999	999
4 - Waist Height	999	999
5 - Shoulder Breadth (Biacromial Breadth)	33.3 cm	13.1 in
6 - Chest Breadth	31.9 cm	12.6 in
7 - Waist Breadth	999	999
8 - Hip Breadth	30 cm	11.8 in
9 - Shoulder to Elbow Length (Acromion-radiale Length)	999	999
10 - Forearm-hand Length (elbow-middle finger)	999	999
11 - Tibiale Height	999	999
12 - Ankle Height (outside) (lateral malleous)	999	999
13 - Foot Breadth	999	999
14 - Foot Length	999	999

Note: * weight in kilograms

** lengths in centimeters

*** measures 16 and 17 must be made in case where the subject will be used in the seated position during the tests. In all other cases enter 9999 when under these measures.

LABORATORY UMTRI TEST NO. 83E092 83E093

15 - Top of Head to Trochanterion Length.....	999	999
16 - Seated Height***.....	999	999
17 - Knee Height (seated)***.....	999	999
18 - Head Length.....	19.4 cm	7.6 in
19 - Head Breadth.....	15.5 cm	6.1 in
20 - Head to Chin Height (Vertex to Mentum).....	999	999
21 - Biceps Circumference.....	999	999
22 - Elbow Circumference.....	999	999
23 - Forearm Circumference.....	999	999
24 - Wrist Circumference.....	999	999
25 - Thigh Circumference.....	999	999
26 - Lower Thigh Circumference.....	999	999
27 - Knee Circumference.....	999	999
28 - Calf Circumference.....	999	999
29 - Ankle Circumference.....	999	999
30 - Neck Circumference.....	37 cm	14.6 in
31 - Scye (armpit-shoulder) Circumference.....	999	999
32 - Chest Circumference.....	999	999
33 - Waist Circumference.....	999	999
34 - Buttock Circumference.....	999	999
35 - Chest Depth.....	999	999
36 - Waist Depth.....	999	999
37 - Buttock Depth.....	999	999
38 - Interscye.....	999	999

LABORATORY UMTRI TEST NO. 83E092 83E093

HUMAN SUBJECT INFORMATION

CADAVER NO.: 100 DURATION OF BED CONFINEMENT Unknown

AGE: 60 SEX: M CAUSE OF DEATH: Cardiac arrest - Carcinoma of Pancreas

PHYSICAL APPEARANCE: Caucasian DATE OF DEATH: 5/20/83

ANOMALY: Right rib R7 is abnormal.

ANTHROPOMETRY

0 - Weight*	76.5 kg	
1 - Stature**	182.3 cm	
2 - Shoulder (acromial) Height	158.5 cm	62.4 in
3 - Vertex to Symphysion Length	91.7 cm	36.1 in
4 - Waist Height	108.6 cm	42.8 in
5 - Shoulder Breadth (Biacromial Breadth)	31.4 cm	12.4 in
6 - Chest Breadth	27 cm	10.6 in
7 - Waist Breadth	31.3 cm	12.3 in
8 - Hip Breadth	33.9 cm	13.3 in
9 - Shoulder to Elbow Length (Acromion-radiale Length)	999	999
10 - Forearm-hand Length (elbow-middle finger)	999	999
11 - Tibiale Height	999	999
12 - Ankle Height (outside) (lateral malleous)	999	999
13 - Foot Breadth	999	999
14 - Foot Length	999	999

Note: * weight in kilograms

** lengths in centimeters

*** measures 16 and 17 must be made in case where the subject will be used in the seated position during the tests. In all other cases enter 9999 when under these measures.

LABORATORY UMTRI TEST NO. 83E101-103 83E104-108 83E109

15 - Top of Head to Trochanterion Length.....	999	999
16 - Seated Height***.....	999	999
17 - Knee Height (seated)***.....	999	999
18 - Head Length.....	19.3 cm	7.6 in
19 - Head Breadth.....	14.6 cm	5.7 in
20 - Head to Chin Height (Vertex to Mentum).....	21.8 cm	8.6 in
21 - Biceps Circumference.....	999	999
22 - Elbow Circumference.....	999	999
23 - Forearm Circumference.....	999	999
24 - Wrist Circumference.....	999	999
25 - Thigh Circumference.....	999	999
26 - Lower Thigh Circumference.....	999	999
27 - Knee Circumference.....	999	999
28 - Calf Circumference.....	999	999
29 - Ankle Circumference.....	999	999
30 - Neck Circumference.....	38.3 cm	15.1 in
31 - Scye (armpit-shoulder) Circumference.....	999	999
32 - Chest Circumference.....	91.7 cm	36.1 in
33 - Waist Circumference.....	999	999
34 - Buttock Circumference.....	999	999
35 - Chest Depth.....	22.5 cm	8.9 in
36 - Waist Depth.....	999	999
37 - Buttock Depth.....	999	999
38 - Interscye.....	999	999

LABORATORY UMTRI TEST NO. 83E101-103 83E104-108 83E109

HUMAN SUBJECT INFORMATION

CADAVER NO.: 120 DURATION OF BED CONFINEMENT Unknown

AGE: 20 SEX: F CAUSE OF DEATH: Renal failure

PHYSICAL APPEARANCE: Negro DATE OF DEATH: 8/22/83

ANOMALY: Sores on skin probably from needle punctures.

ANTHROPOMETRY

0 - Weight*.....	46 kg	
1 - Stature**.....	162.7 cm	
2 - Shoulder (acromial) Height.....	141.6 cm	55.7 in
3 - Vertex to Symphysion Length.....	76.3 cm	30 in
4 - Waist Height.....	99.2 cm	39.1 in
5 - Shoulder Breadth (Biacromial Breadth).....	31 cm	12.2 in
6 - Chest Breadth.....	25.7 cm	10.1 in
7 - Waist Breadth.....	21.9 cm	8.6 in
8 - Hip Breadth.....	27.2 cm	10.7 in
9 - Shoulder to Elbow Length (Acromion-radiale .. Length)	999	999
10 - Forearm-hand Length (elbow-middle finger)....	999	999
11 - Tibiale Height.....	999	999
12 - Ankle Height (outside) (lateral malleous)....	999	999
13 - Foot Breadth.....	999	999
14 - Foot Length.....	999	999

Note: * weight in kilograms

** lengths in centimeters

*** measures 16 and 17 must be made in case where the subject will be used in the seated position during the tests. In all other cases enter 9999 when under these measures.

LABORATORY UMTRI TEST NO. 83E121A-C

15 - Top of Head to Trochanterion Length.....	72.9 cm	28.7 in
16 - Seated Height***.....	999	999
17 - Knee Height (seated)***.....	999	999
18 - Head Length.....	18.9 cm	7.4 in
19 - Head Breadth.....	14.4 cm	5.7 in
20 - Head to Chin Height (Vertex to Mentum).....	24.5 cm	9.6 in
21 - Biceps Circumference.....	999	999
22 - Elbow Circumference.....	999	999
23 - Forearm Circumference.....	999	999
24 - Wrist Circumference.....	999	999
25 - Thigh Circumference.....	999	999
26 - Lower Thigh Circumference.....	999	999
27 - Knee Circumference.....	999	999
28 - Calf Circumference.....	999	999
29 - Ankle Circumference.....	999	999
30 - Neck Circumference.....	32 cm	12.6 in
31 - Scye (armpit-shoulder) Circumference.....	999	999
32 - Chest Circumference.....	71.4 cm	28.1 in
33 - Waist Circumference.....	999	999
34 - Buttock Circumference.....	999	999
35 - Chest Depth.....	17.6 cm	6.9 in
36 - Waist Depth.....	999	999
37 - Buttock Depth.....	999	999
38 - Interscye.....	999	999

LABORATORY UMTRI TEST NO. 83E121A-C

HUMAN SUBJECT INFORMATION

CADAVER NO.: 130 DURATION OF BED CONFINEMENT Unknown

AGE: 57 SEX: M CAUSE OF DEATH: Acute myocardial infarction

PHYSICAL APPEARANCE: Caucasian DATE OF DEATH: 9/11/83

ANOMALY: Autopsy revealed evidence of previous thoracic surgery. Ribs weakened at cartilaginous junction.

ANTHROPOMETRY

0 - Weight*	72.5 kg	
1 - Stature**	175.3 cm	
2 - Shoulder (acromial) Height	151.4 cm	59.6 in
3 - Vertex to Symphysion Length	87.5 cm	34.4 in
4 - Waist Height	104.8 cm	41.3 in
5 - Shoulder Breadth (Biacromial Breadth)	33.5 cm	13.2 in
6 - Chest Breadth	33.2 cm	13.1 in
7 - Waist Breadth	31.9 cm	12.6 in
8 - Hip Breadth	33.9 cm	13.3 in
9 - Shoulder to Elbow Length (Acromion-radiale Length)	999	999
10 - Forearm-hand Length (elbow-middle finger)	999	999
11 - Tibiale Height	999	999
12 - Ankle Height (outside) (lateral malleous)	999	999
13 - Foot Breadth	999	999
14 - Foot Length	999	999

Note: * weight in kilograms

** lengths in centimeters

*** measures 16 and 17 must be made in case where the subject will be used in the seated position during the tests. In all other cases enter 9999 when under these measures.

LABORATORY UMTRI TEST NO. 83E131A-C

15 - Top of Head to Trochanterion Length.....	999	999
16 - Seated Height***.....	999	999
17 - Knee Height (seated)***.....	999	999
18 - Head Length.....	21.5 cm	8.5 in
19 - Head Breadth.....	15.4 cm	6.1 in
20 - Head to Chin Height (Vertex to Mentum).....	25.9 cm	10.2 in
21 - Biceps Circumference.....	999	999
22 - Elbow Circumference.....	999	999
23 - Forearm Circumference.....	999	999
24 - Wrist Circumference.....	999	999
25 - Thigh Circumference.....	999	999
26 - Lower Thigh Circumference.....	999	999
27 - Knee Circumference.....	999	999
28 - Calf Circumference.....	999	999
29 - Ankle Circumference.....	999	999
30 - Neck Circumference.....	42.2 cm	16.6 in
31 - Scye (armpit-shoulder) Circumference.....	999	999
32 - Chest Circumference.....	99.8 cm	39.3 in
33 - Waist Circumference.....	999	999
34 - Buttock Circumference.....	999	999
35 - Chest Depth.....	23.5 cm	9.3 in
36 - Waist Depth.....	999	999
37 - Buttock Depth.....	999	999
38 - Interscye.....	999	999

LABORATORY UMTRI TEST NO. 83E131A-C

APPENDIX E

11.0 THORACO-ABDOMINAL SERIES DATA

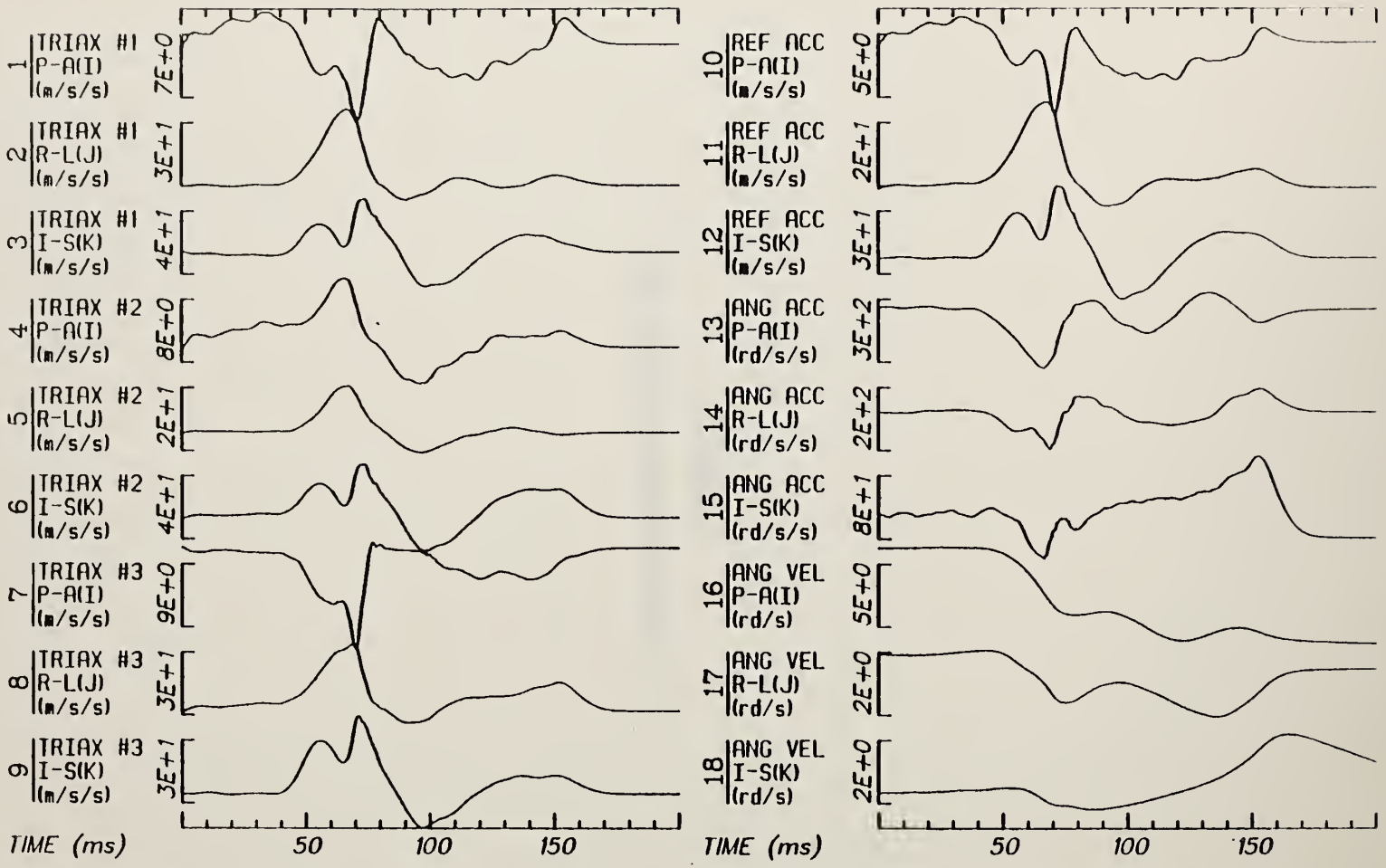

Run ID: 82E004 H7 Disk: 82E004.3 File: 1 Date: MAY 12, 1985 Sheet: 1

*Filter:1600*4C*

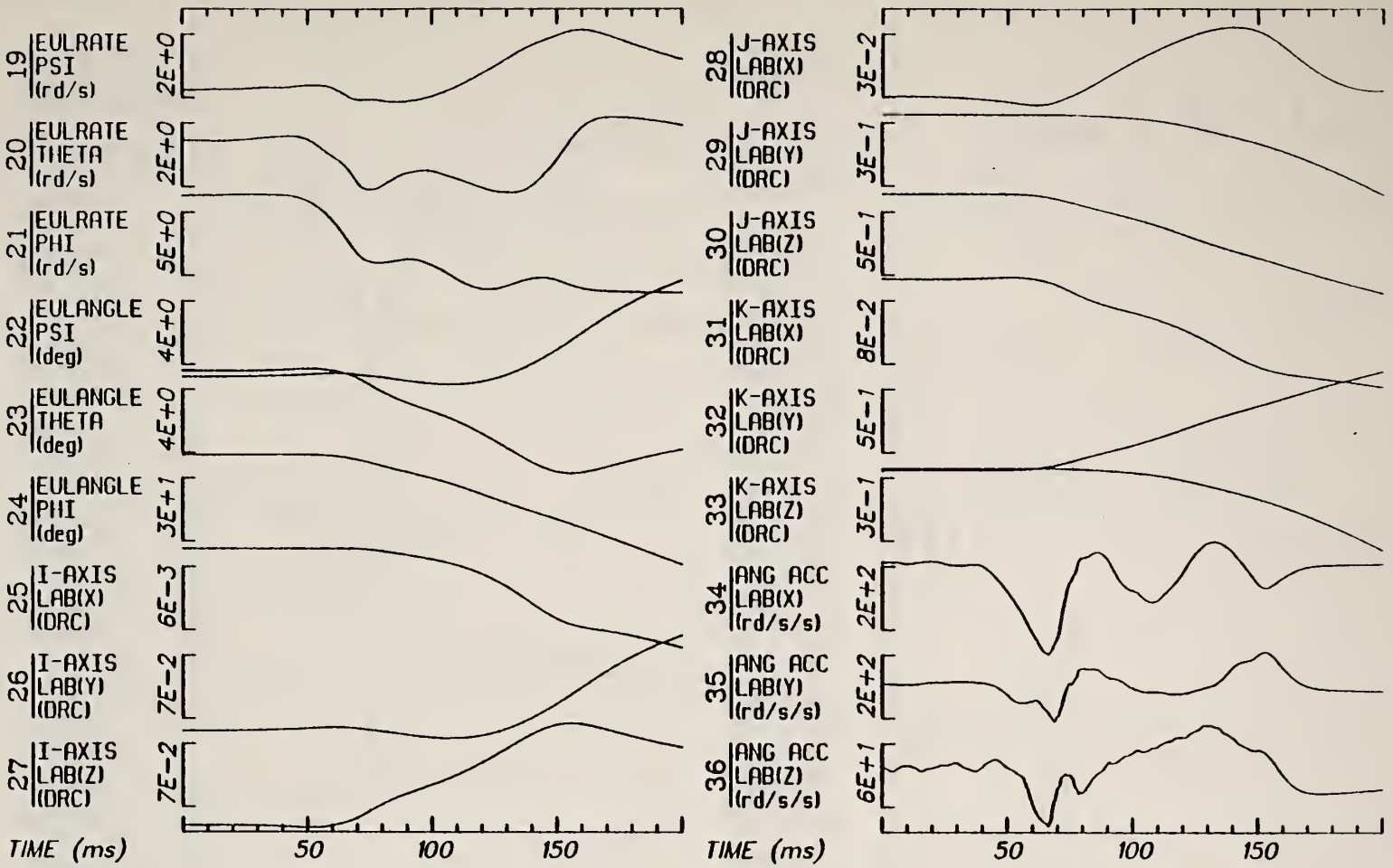

Run ID: 82E004 H7 Disk: 82E004.3 File: 1 Date: MAY 12, 1985 Sheet: 2

*Filter:1600*4C*

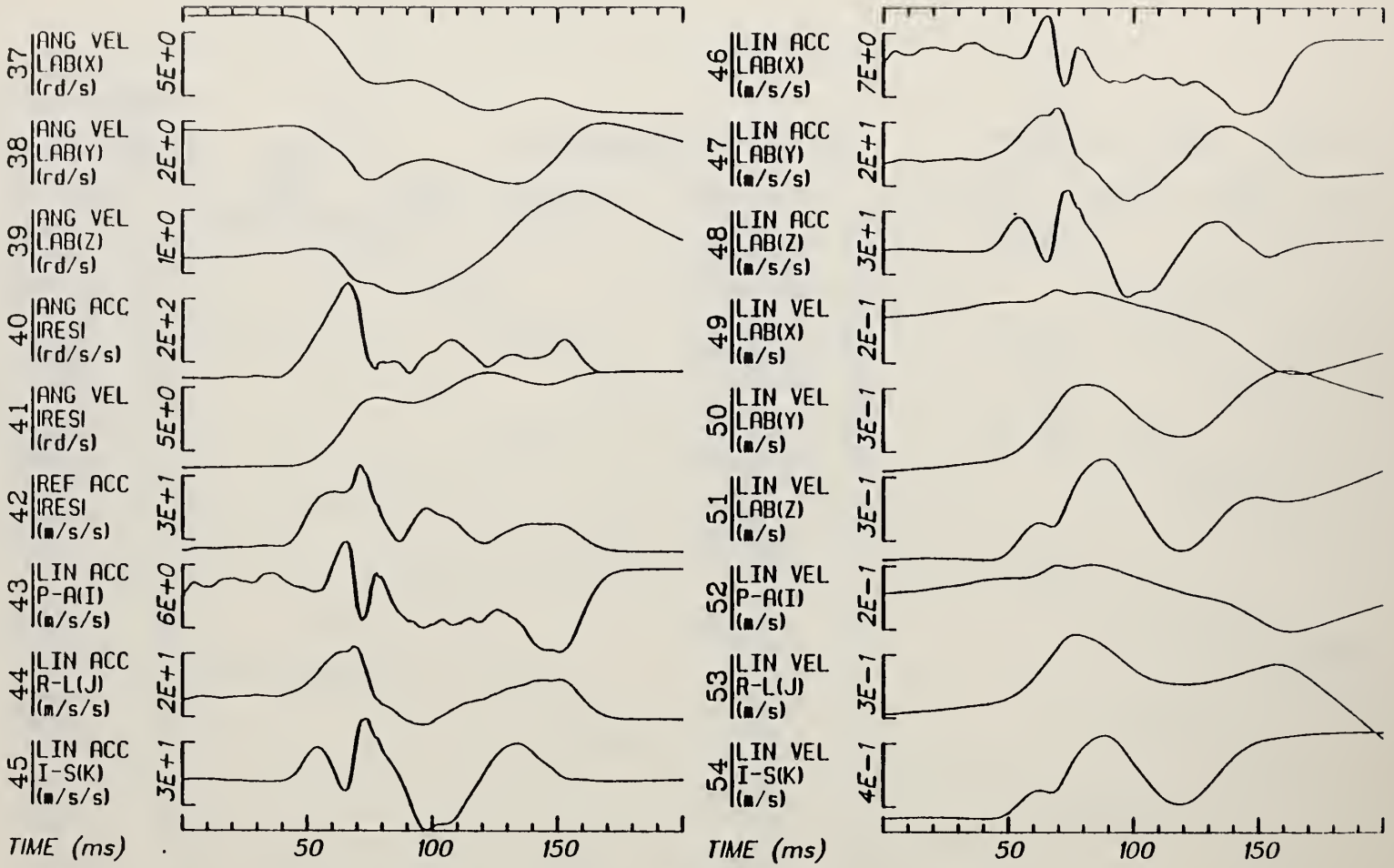

Run ID: 82E004 H7 Disk: 82E004.3 File: 1 Date: MAY 12, 1985 Sheet: 3

*Filter:1600*4C*

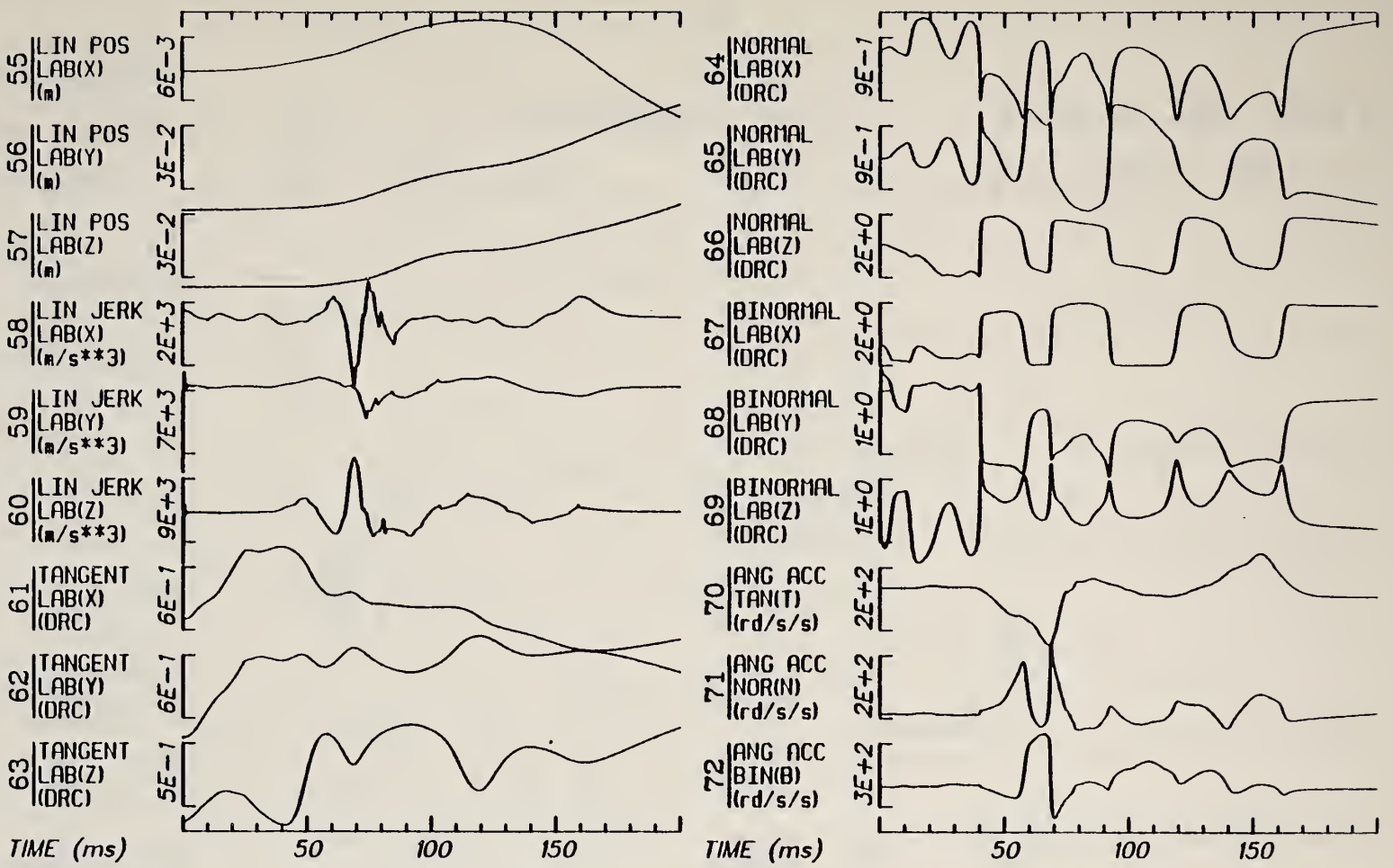

Run ID: 82E004 H7 Disk: 82E004.3 File: 1 Date: MAY 12, 1985 Sheet: 4

*Filter:1600*4C*

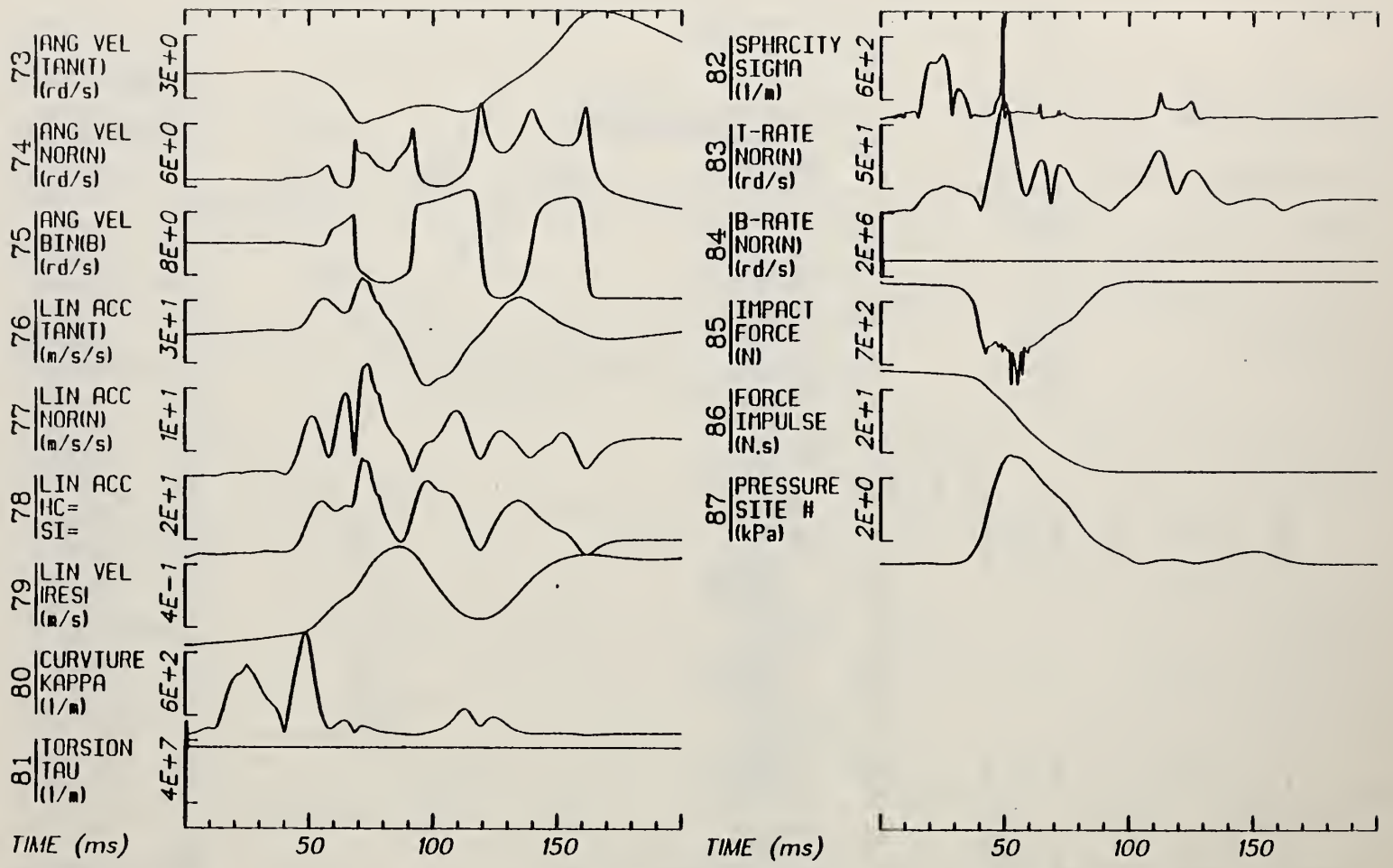

Run ID: 82E004 H7 Disk: 82E004.3 File: 1 Date: MAY 12, 1985 Sheet: 5

*Filter:1600*4C*

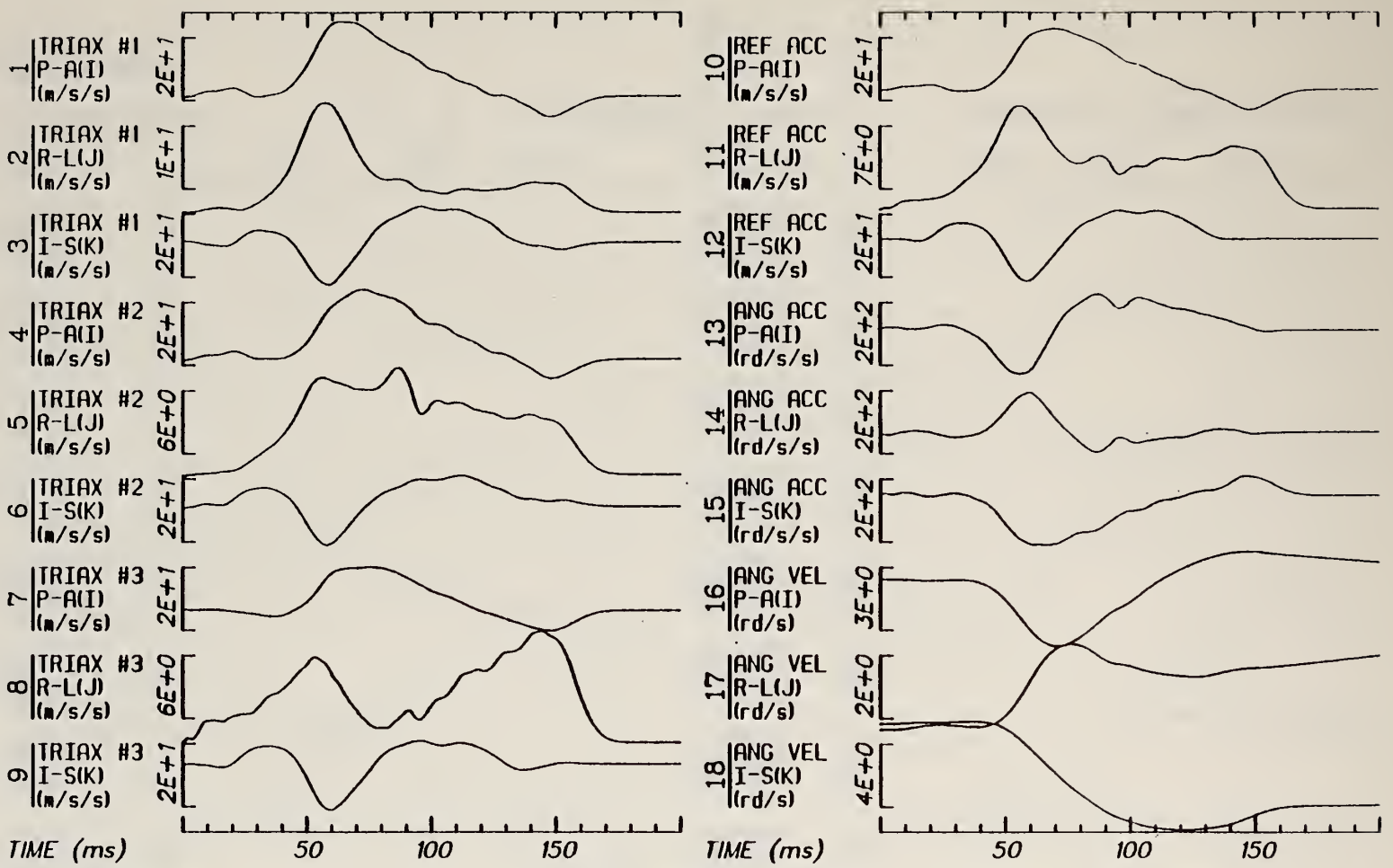

Run ID: 82E005 Disk: 82E005.3 File: 1 Date: MAY 12, 1985 Sheet: 1

*Filter:1600*4C*

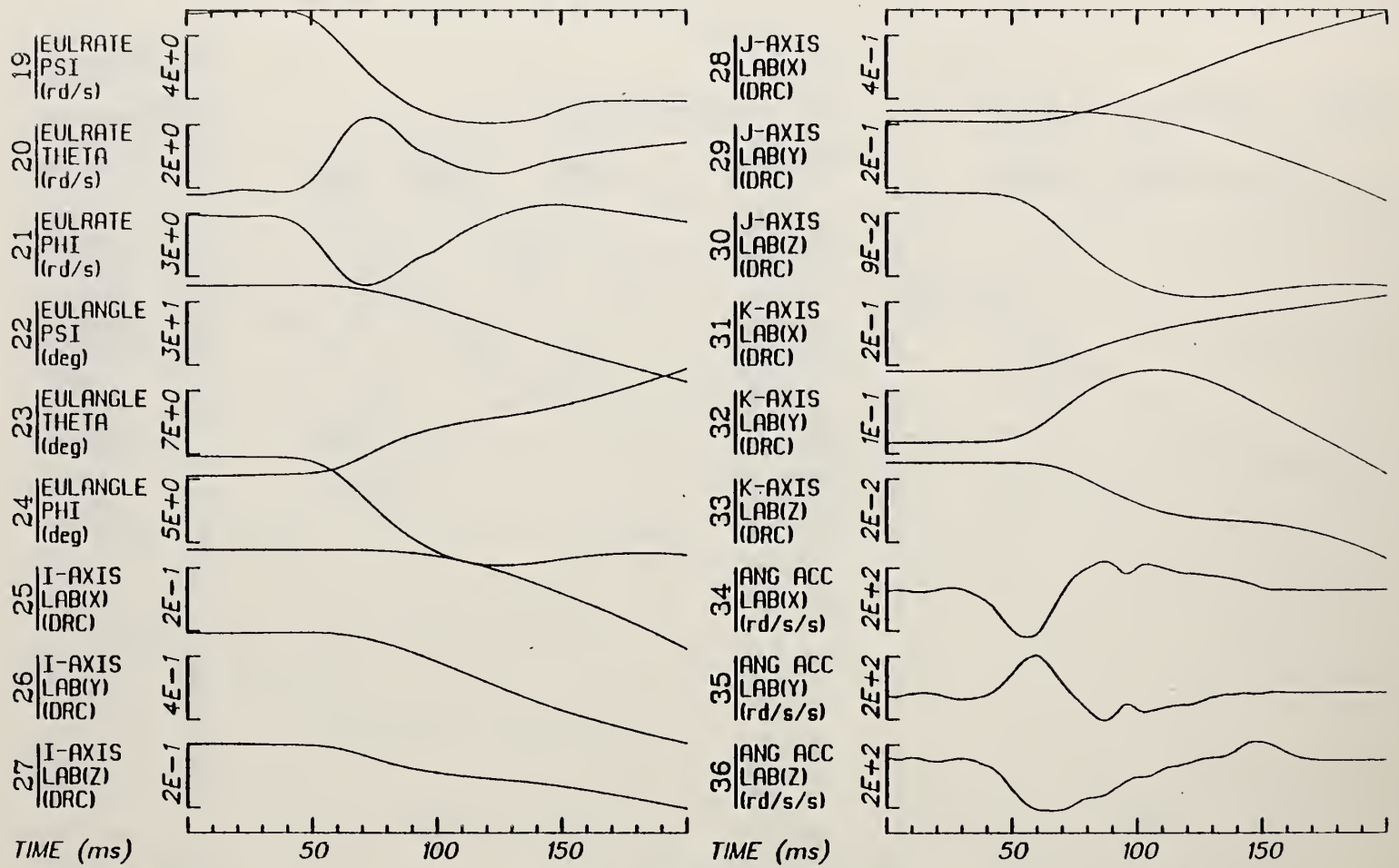

Run ID: 82E005 Disk: 82E005.3 File: 1 Date: MAY 12, 1985 Sheet: 2

*Filter:1600*4C*

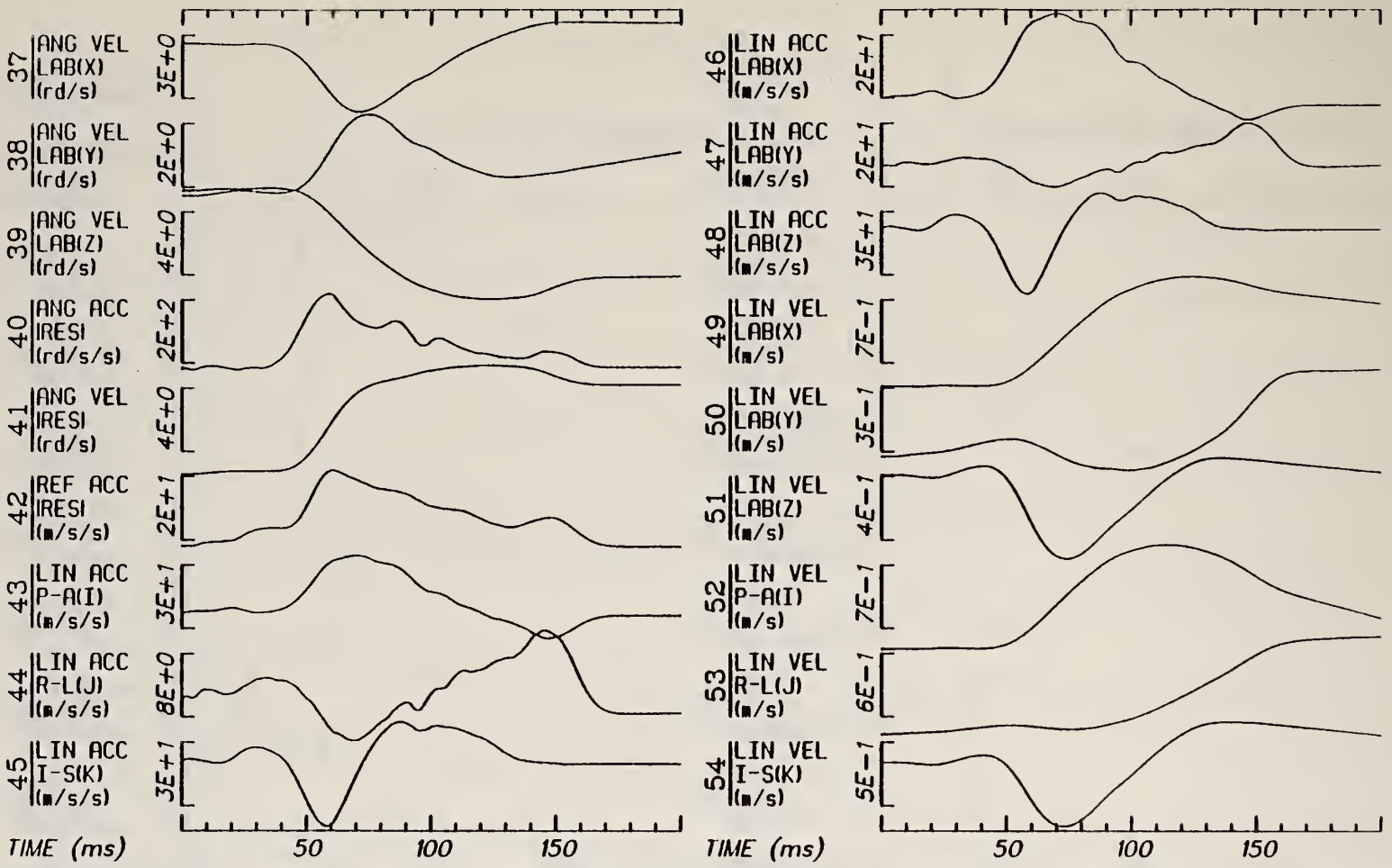

Run ID: 82E005 Disk: 82E005.3 File: 1 Date: MAY 12, 1985 Sheet: 3

*Filter:1600*4C*

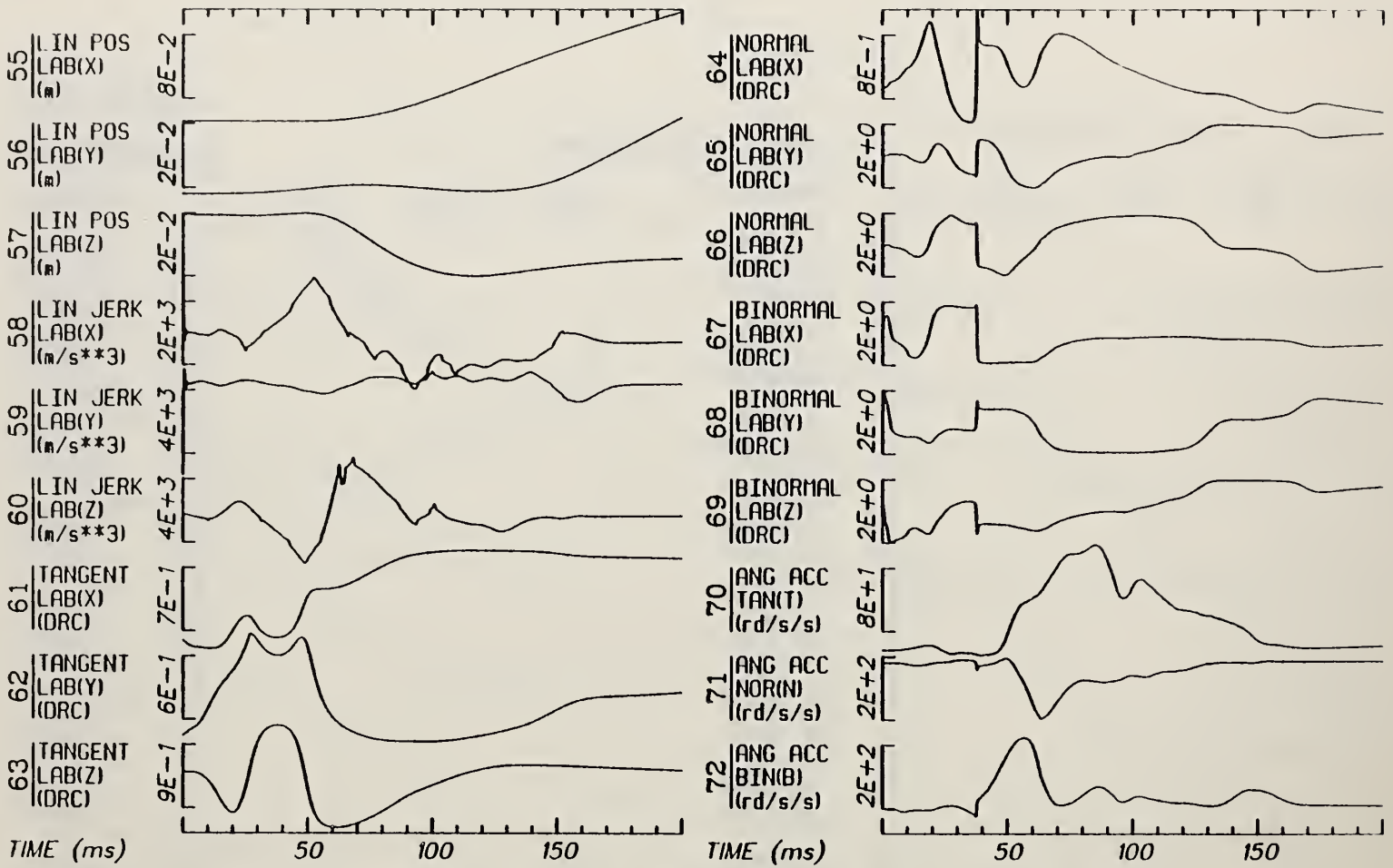

Run ID: 82E005 Disk: 82E005.3 File: 1 Date: MAY 12, 1985 Sheet: 4

*Filter:1600*4C*

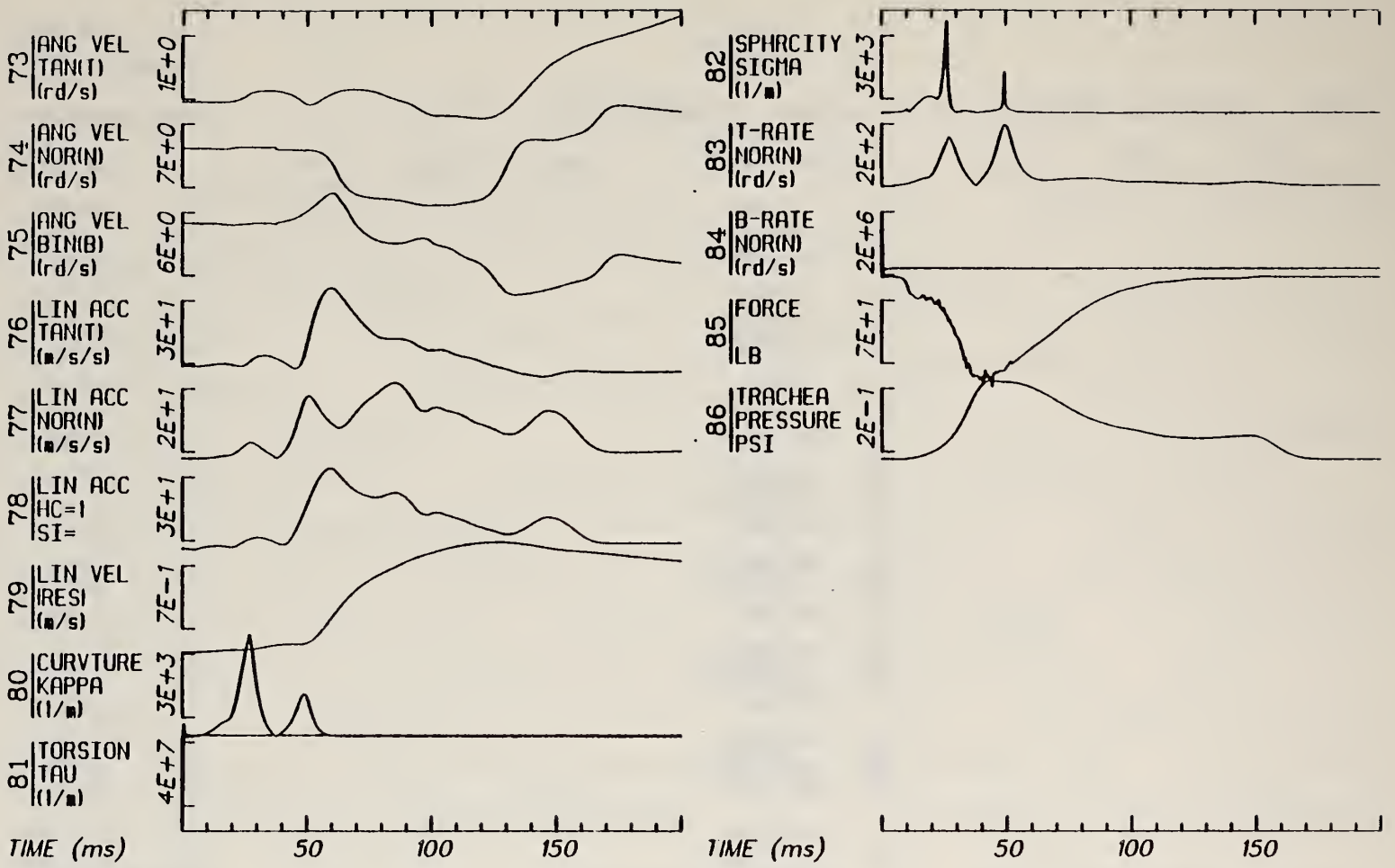

Run ID: 82E005 Disk: 82E005.3 File: 1 Date: MAY 12, 1985 Sheet: 5

*Filter:1600*4C*

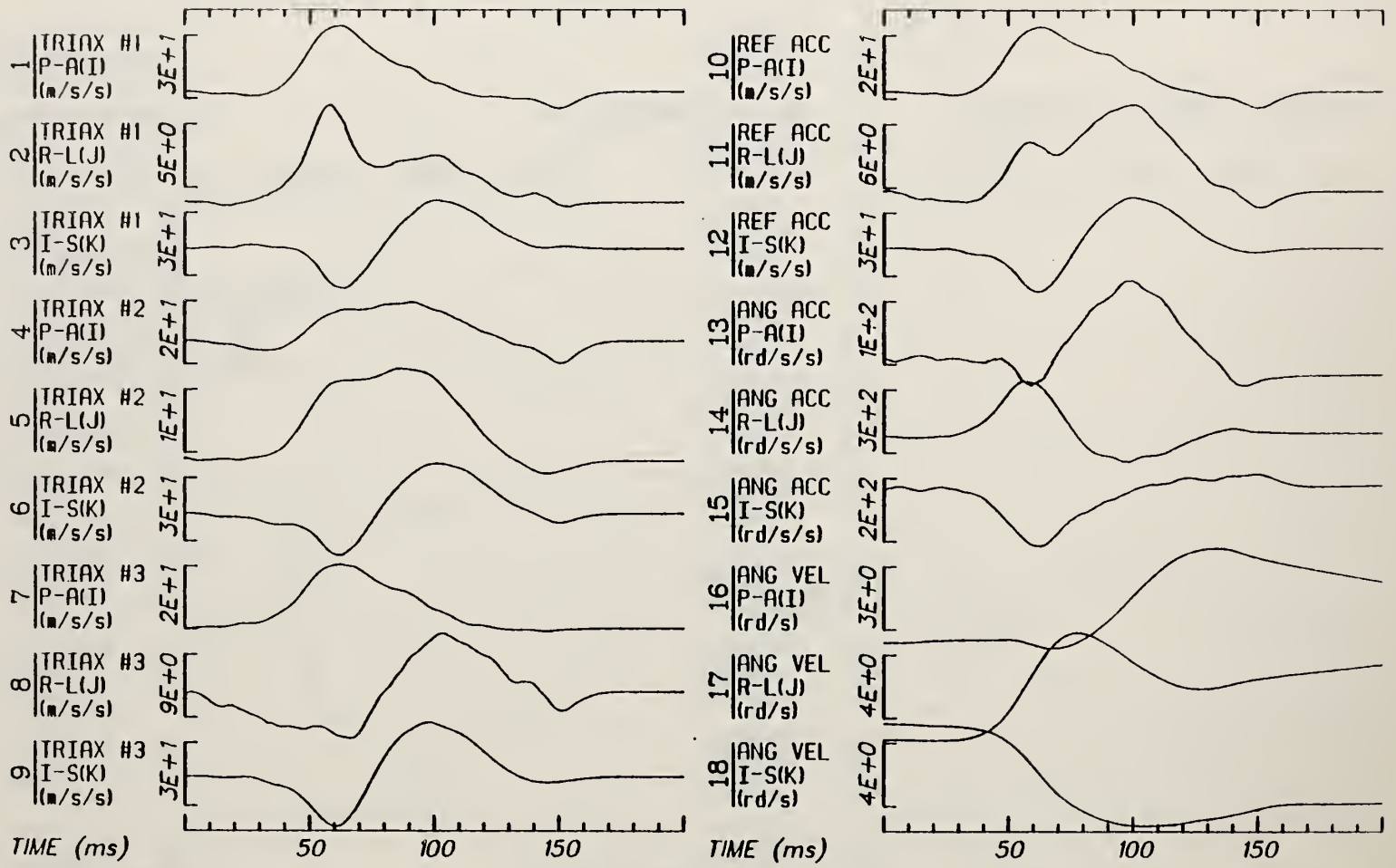

Run ID: 82E006 Disk: 82E006.3 File: 1 Date: MAY 12, 1985 Sheet: 1

*Filter:1600*4C*

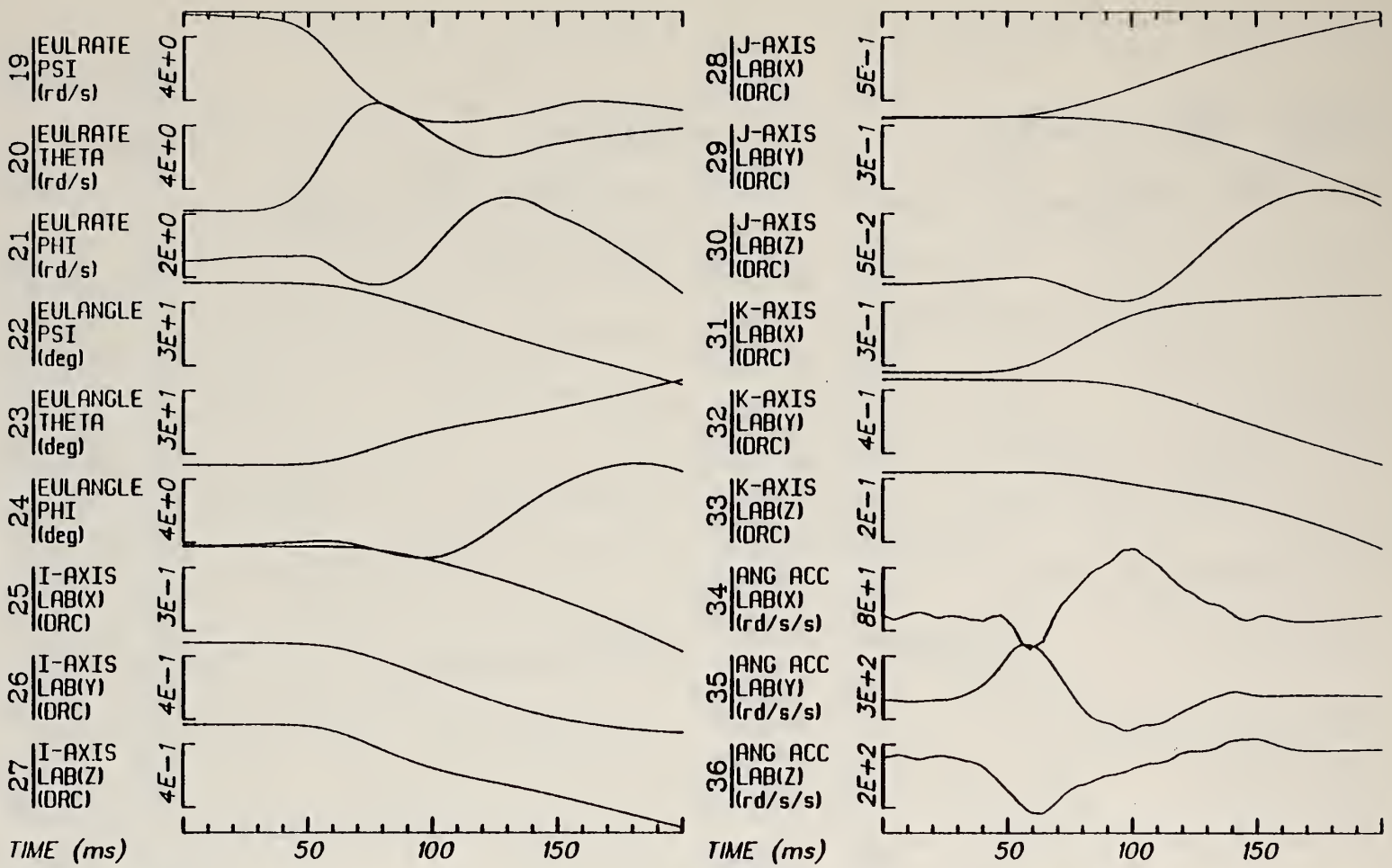

Run ID: 82E006 Disk: 82E006.3 File: 1 Date: MAY 12, 1985 Sheet: 2

*Filter:1600*4C*

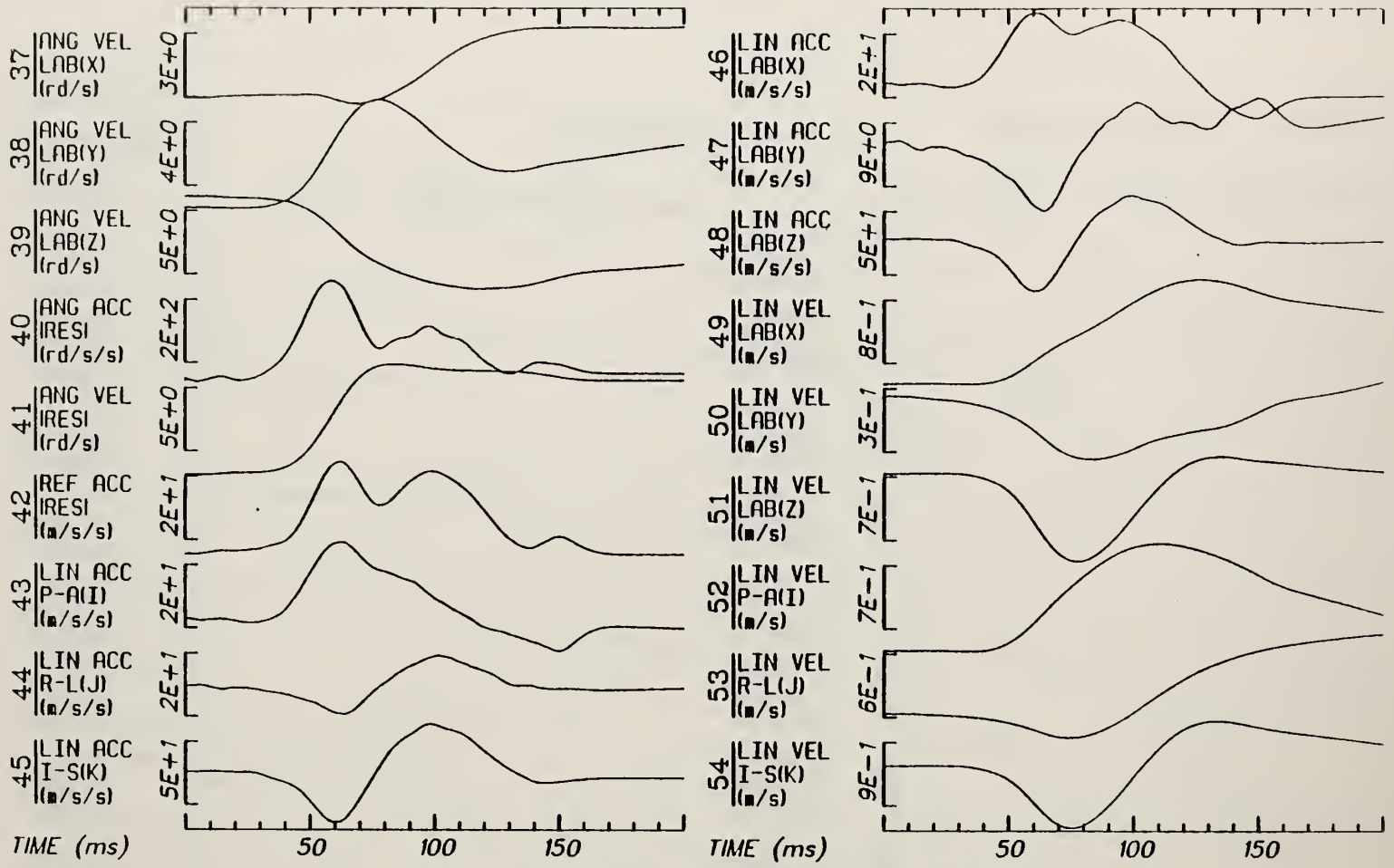

Run ID: 82E006 Disk: 82E006.3 File: 1 Date: MAY 12, 1985 Sheet: 3

*Filter:1600*4C*

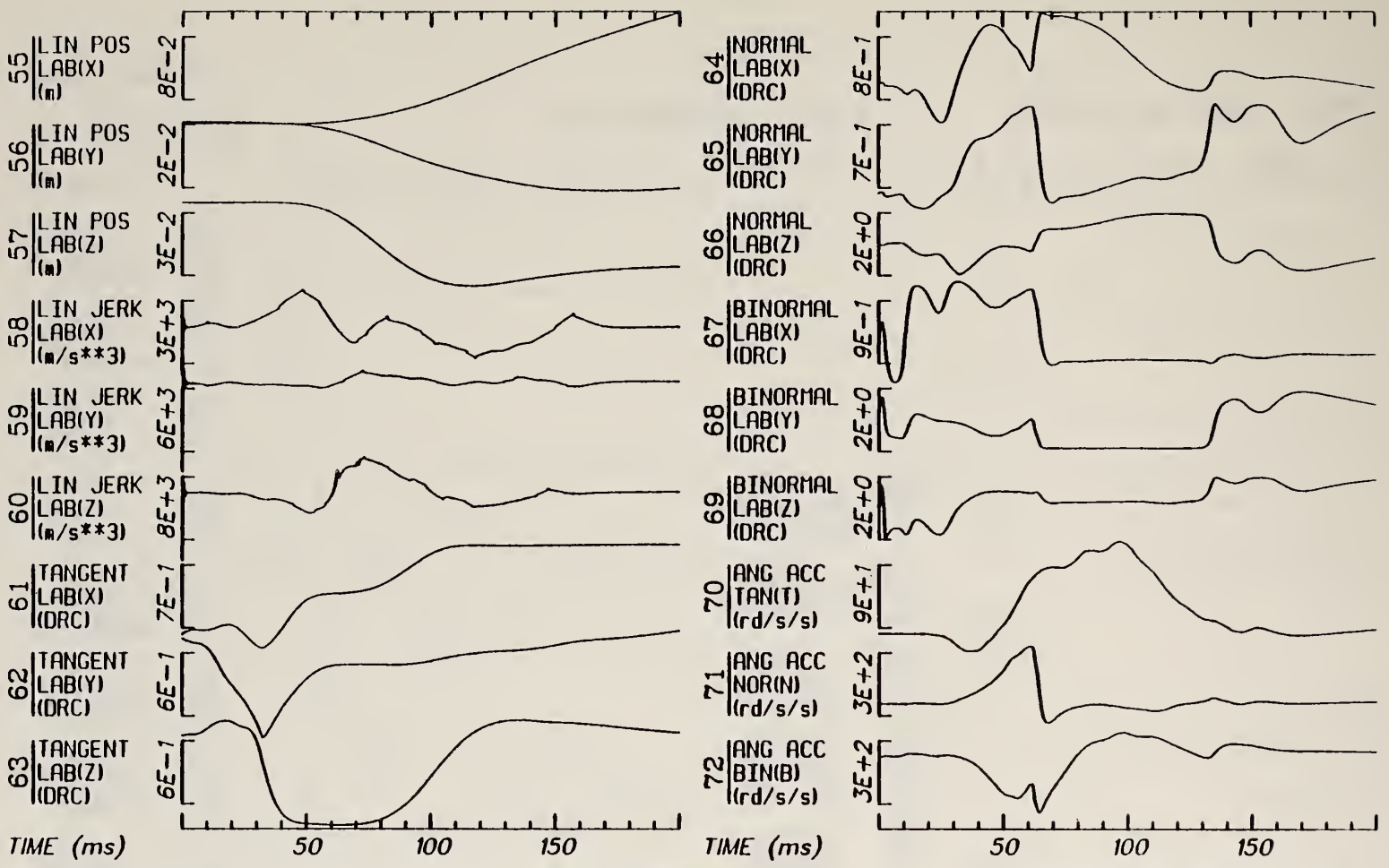

Run ID: 82E006 Disk: 82E006.3 File: 1 Date: MAY 12, 1985 Sheet: 4

*Filter:1600*4C*

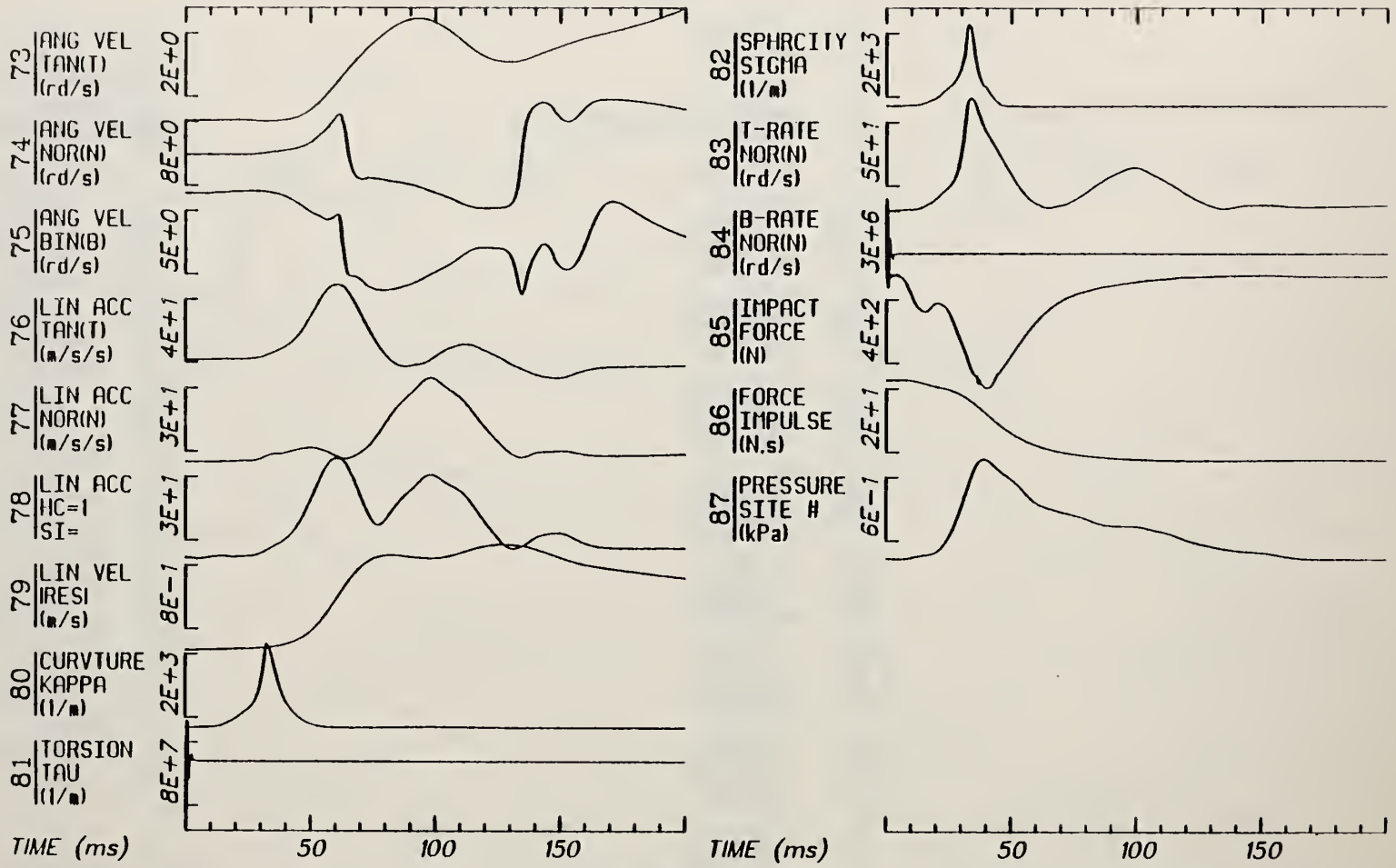

Run ID: 82E006 Disk: 82E006.3 File: 1 Date: MAY 12, 1985 Sheet: 5

*Filter:1600*4C*

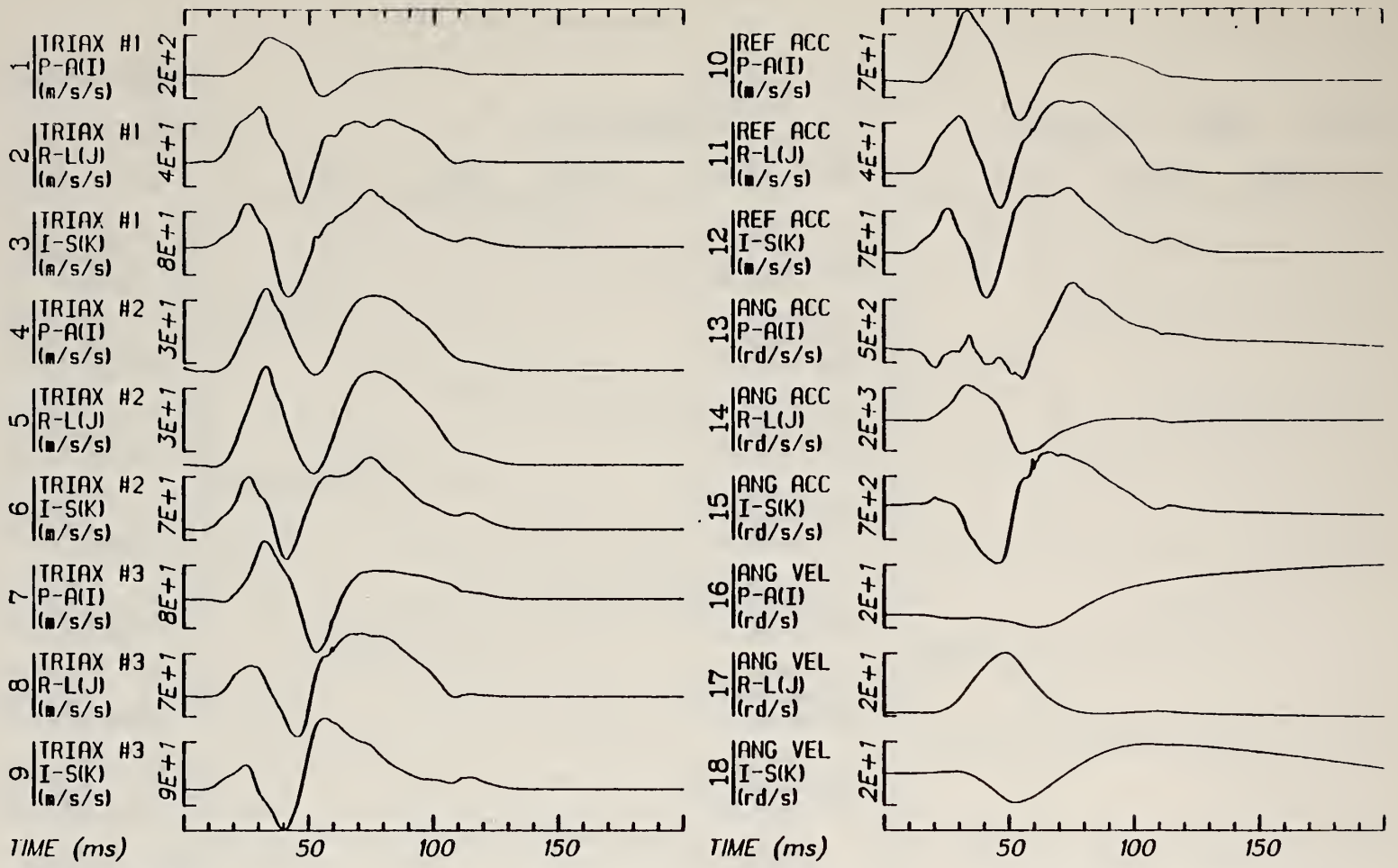

Run ID: 82E007 Disk: 82E007.3 File: 1 Date: MAY 12, 1985 Sheet: 1

*Filter:1600*4C*

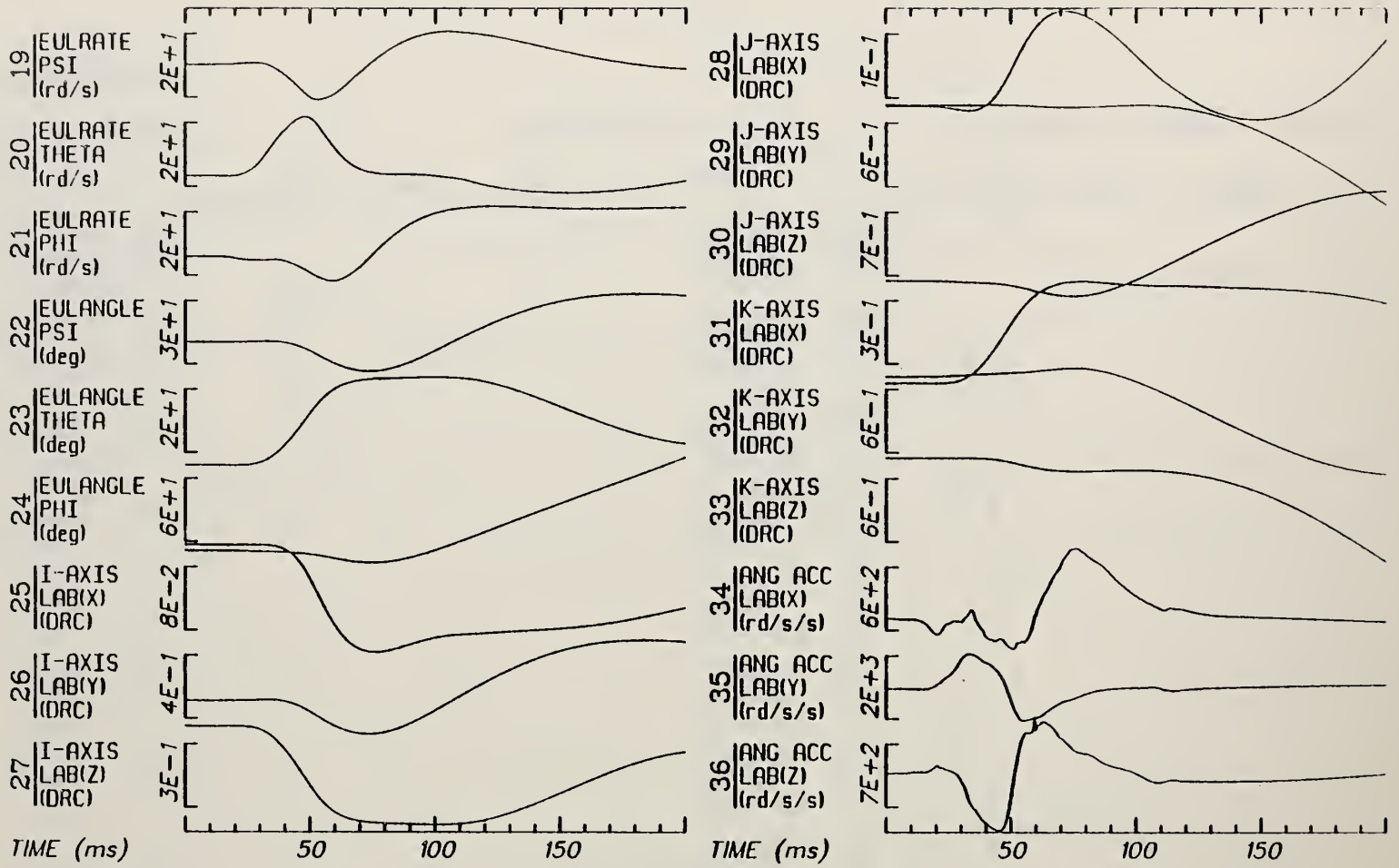

Run ID: 82E007 Disk: 82E007.3 File: 1 Date: MAY 12, 1985 Sheet: 2

*Filter:1600*4C*

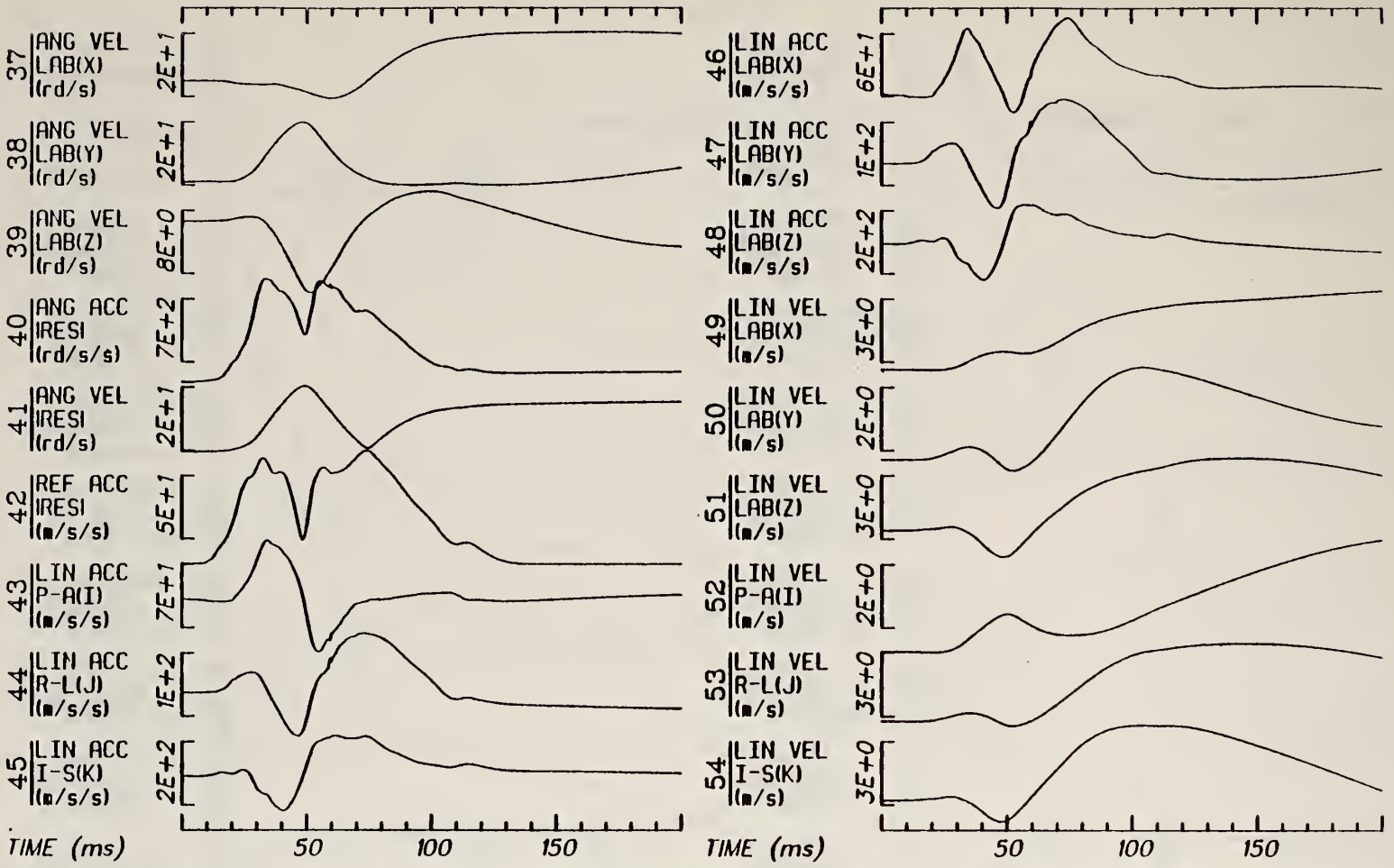

Run ID: 82E007 Disk: 82E007.3 File: 1 Date: MAY 12, 1985 Sheet: 3

*Filter:1600*4C*

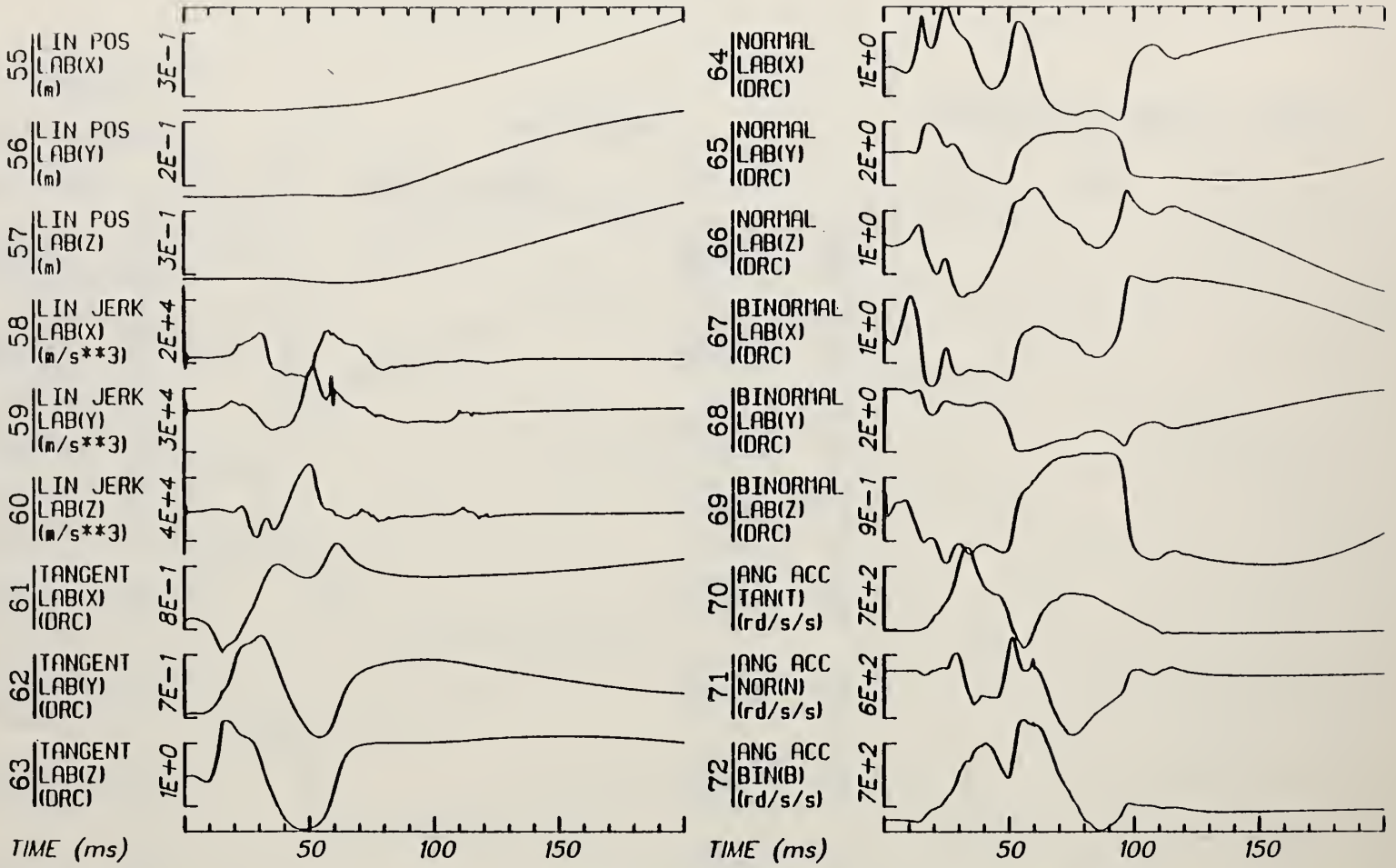

Run ID: 82E007 Disk: 82E007.3 File: 1 Date: MAY 12, 1985 Sheet: 4

*Filter:1600*4C*

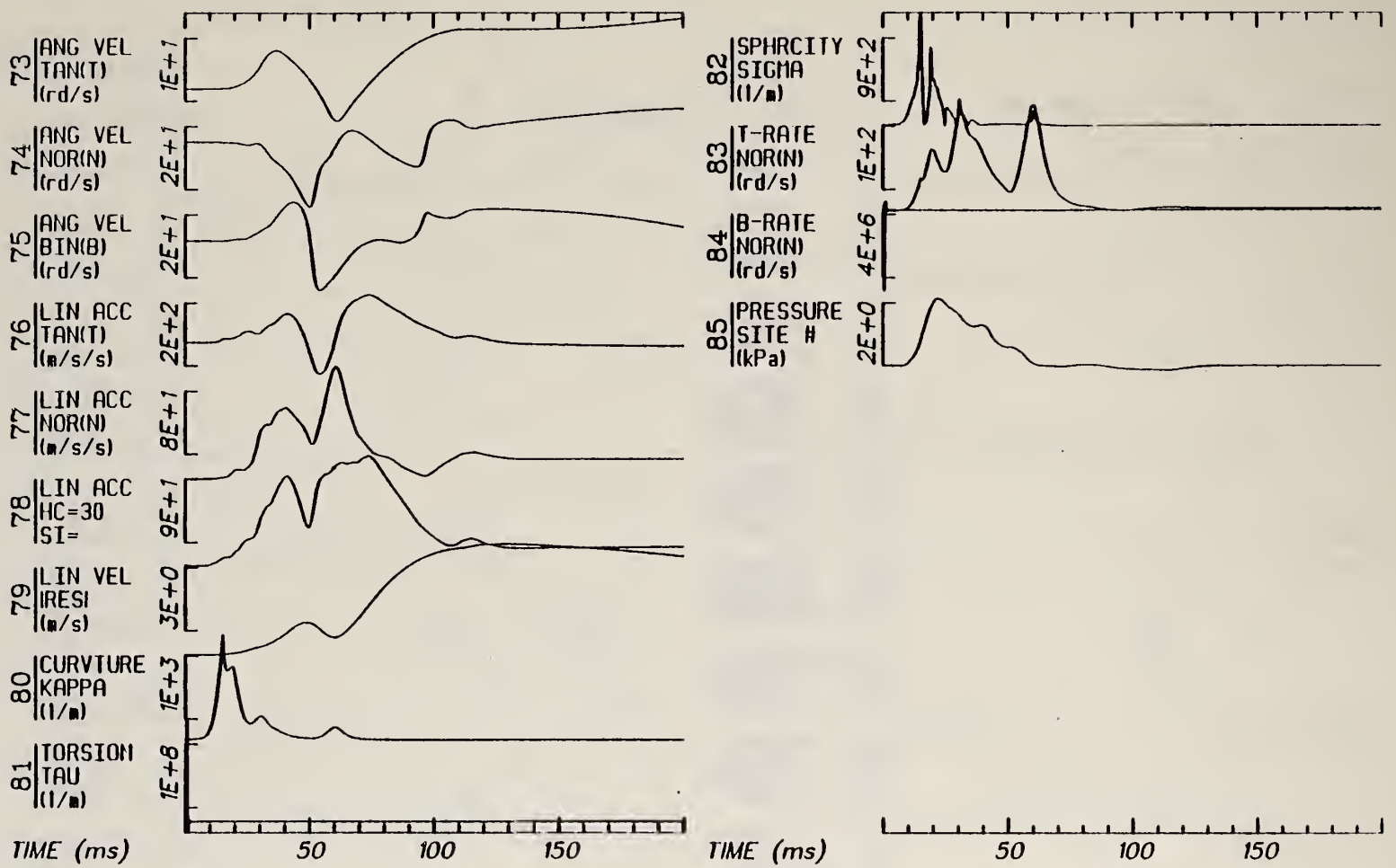

Run ID: 82E007 Disk: 82E007.3 File: 1 Date: MAY 12, 1985 Sheet: 5

*Filter:1600*4C*

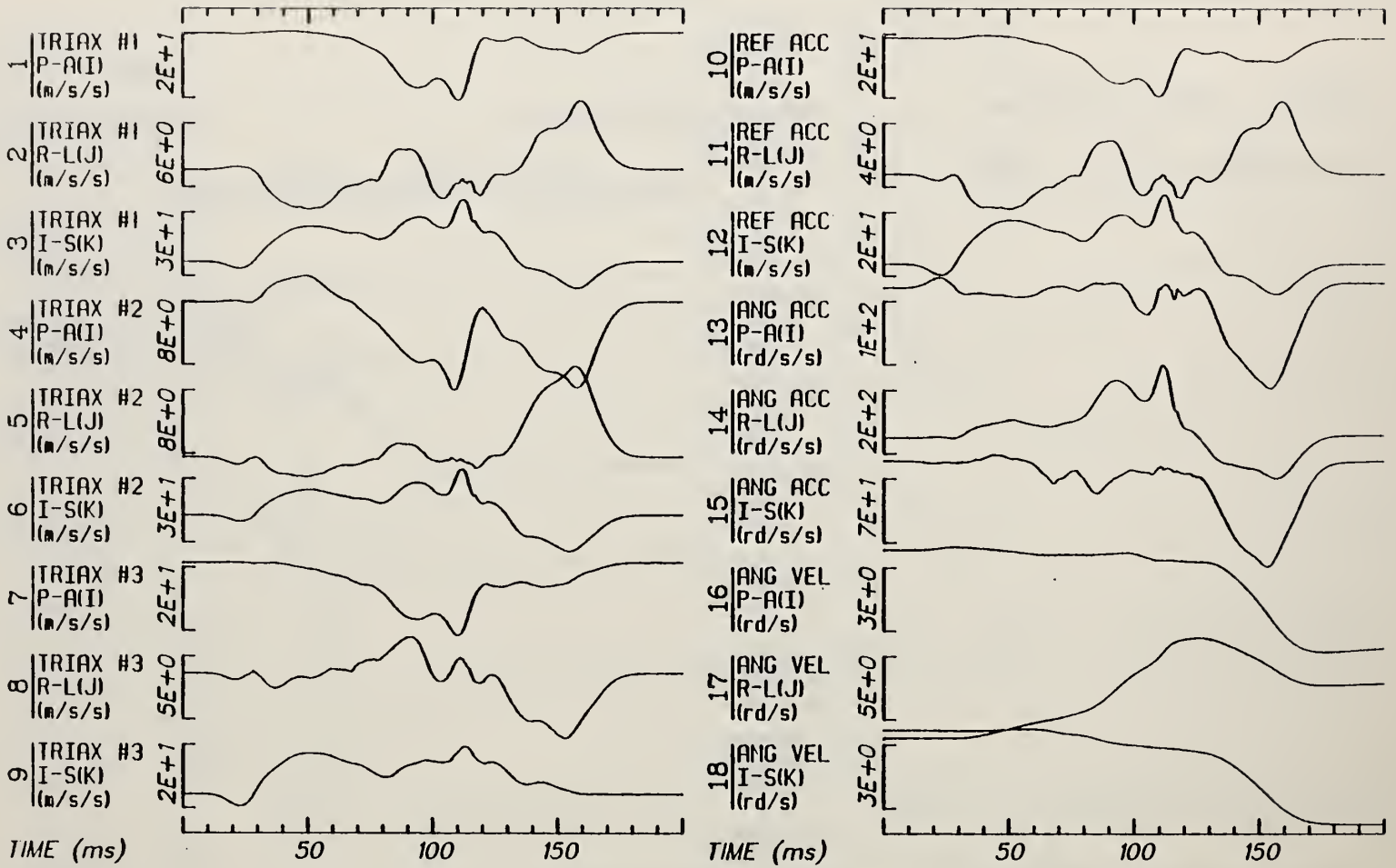

Run ID: 82E023 Disk: 82E023.3 File: 1 Date: MAY 12, 1985 Sheet: 1

*Filter:1600*4C*

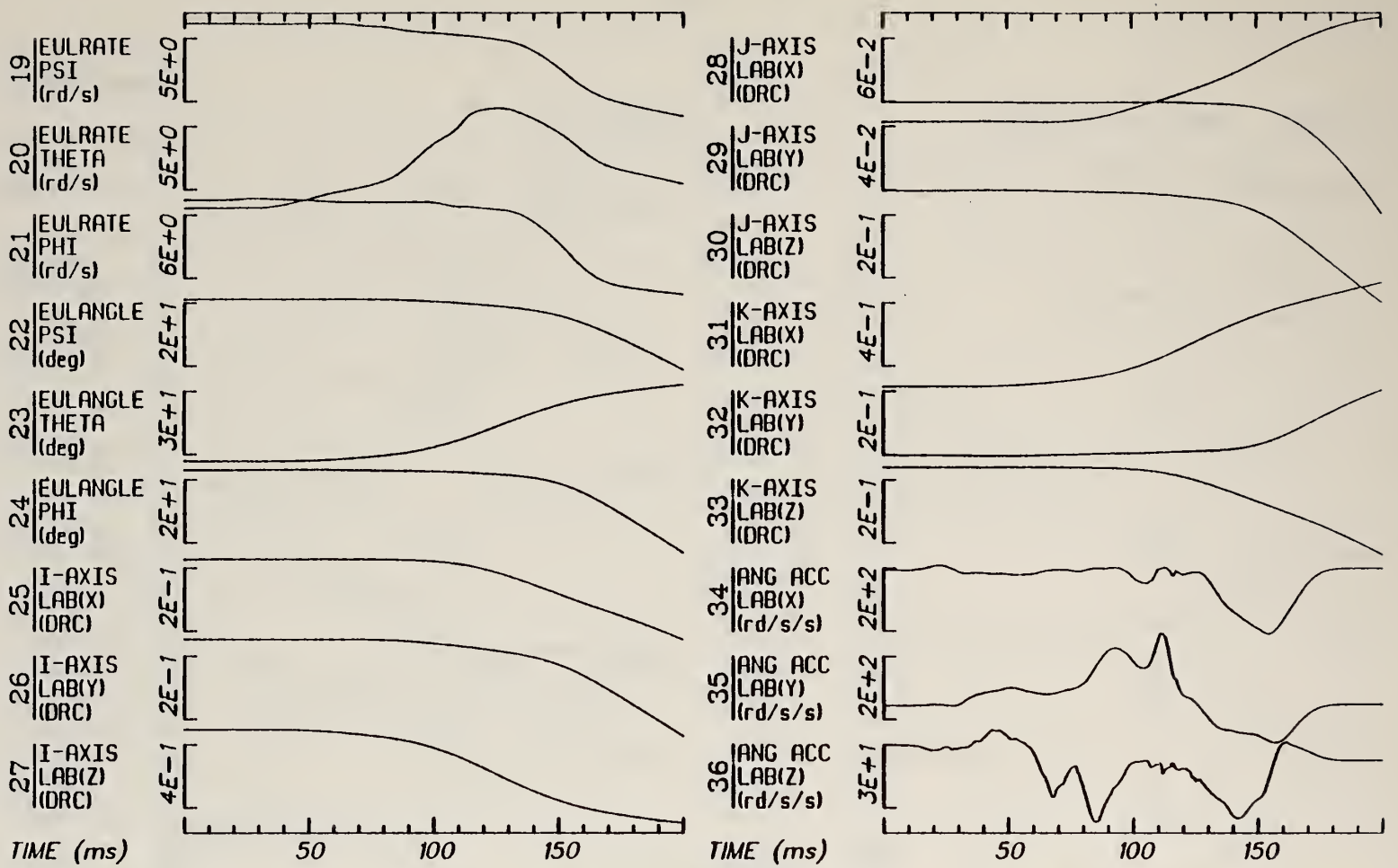

Run ID: 82E023 Disk: 82E023.3 File: 1 Date: MAY 12, 1985 Sheet: 2

*Filter:1600*4C*

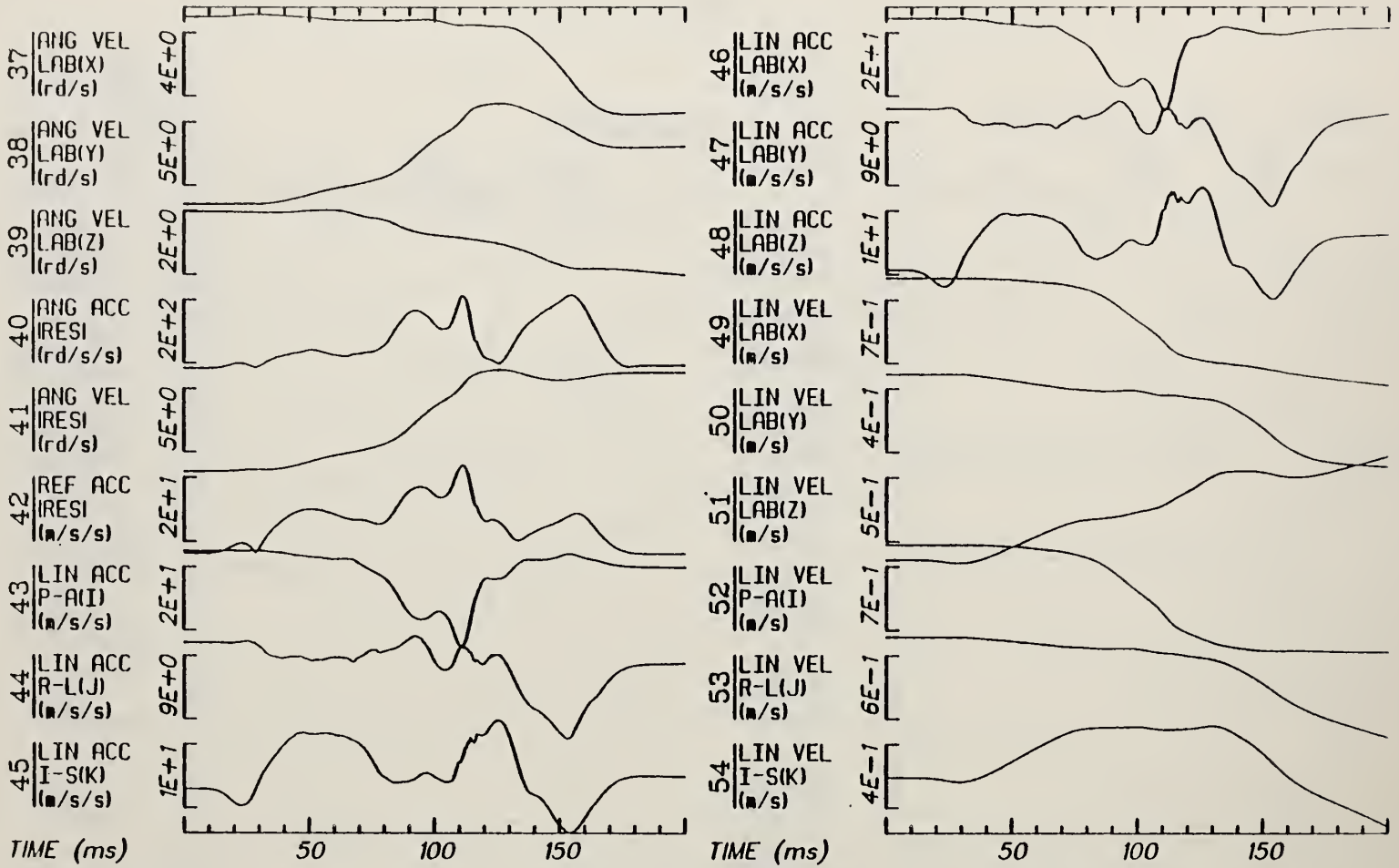

Run ID: 82E023 Disk: 82E023.3 File: 1 Date: MAY 12, 1985 Sheet: 3

*Filter:1600*4C*

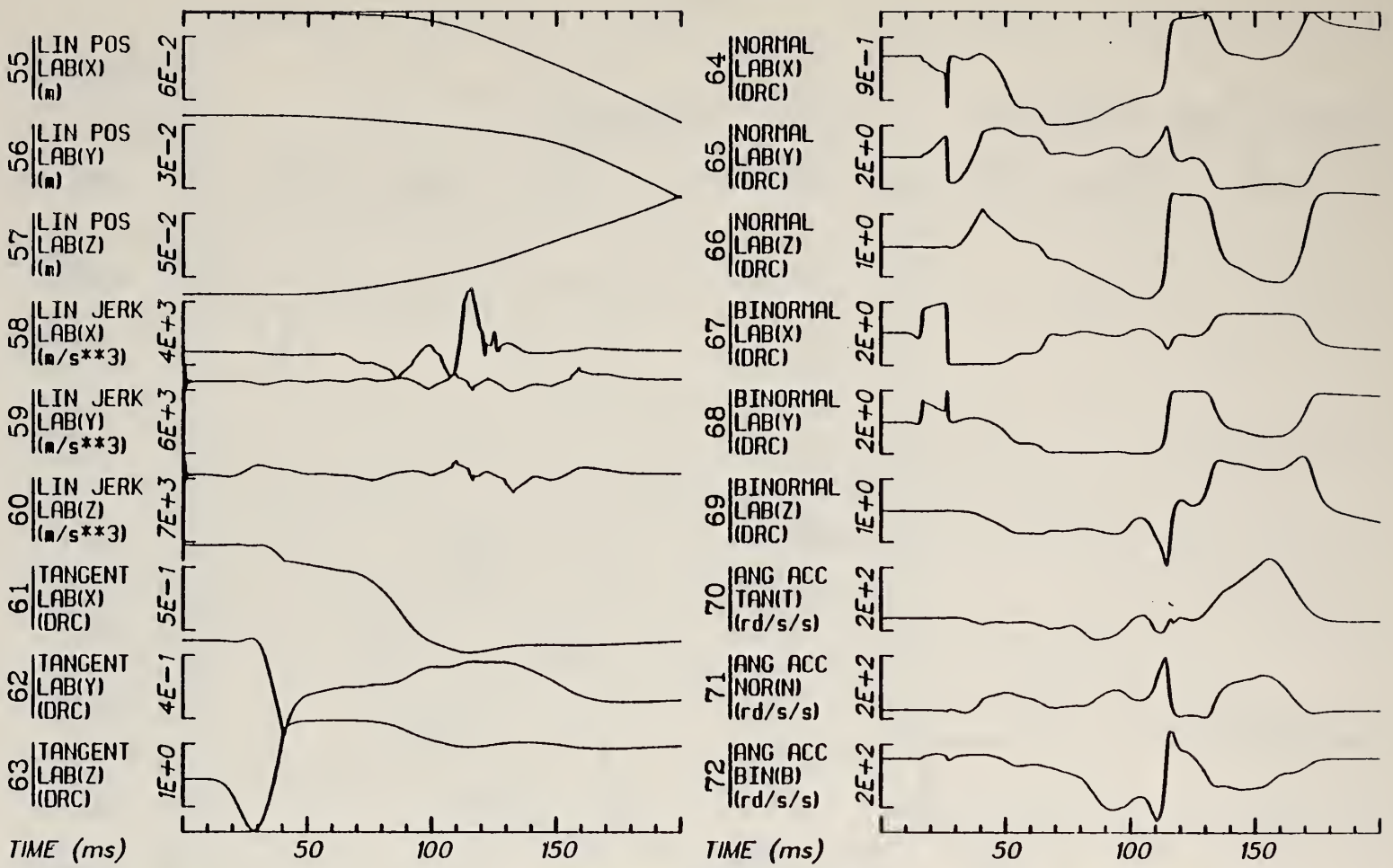

Run ID: 82E023 Disk: 82E023.3 File: 1 Date: MAY 12, 1985 Sheet: 4

*Filter:1600*4C*

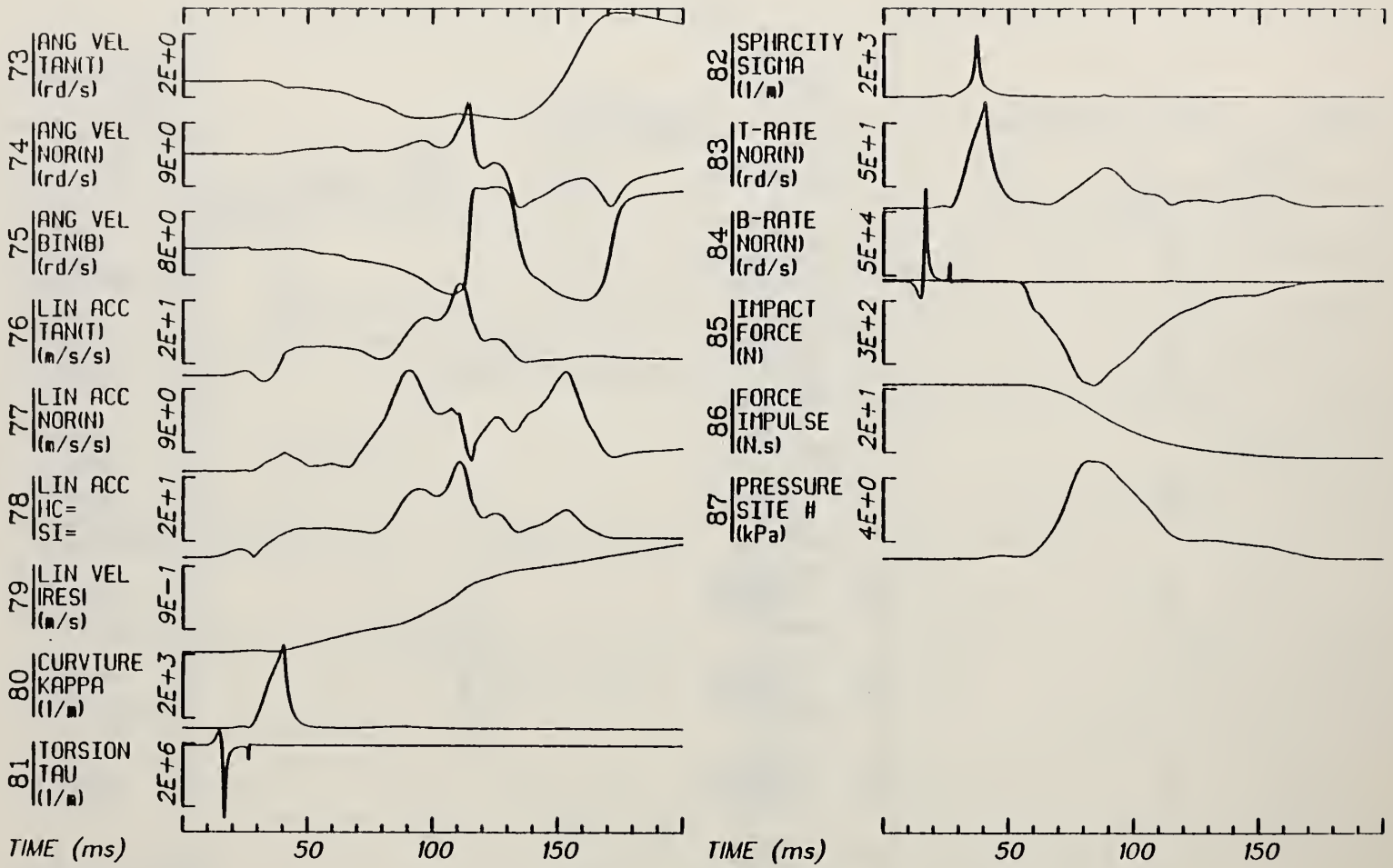

Run ID: 82E023 Disk: 82E023.3 File: 1 Date: MAY 12, 1985 Sheet: 5

*Filter:1600*4C*

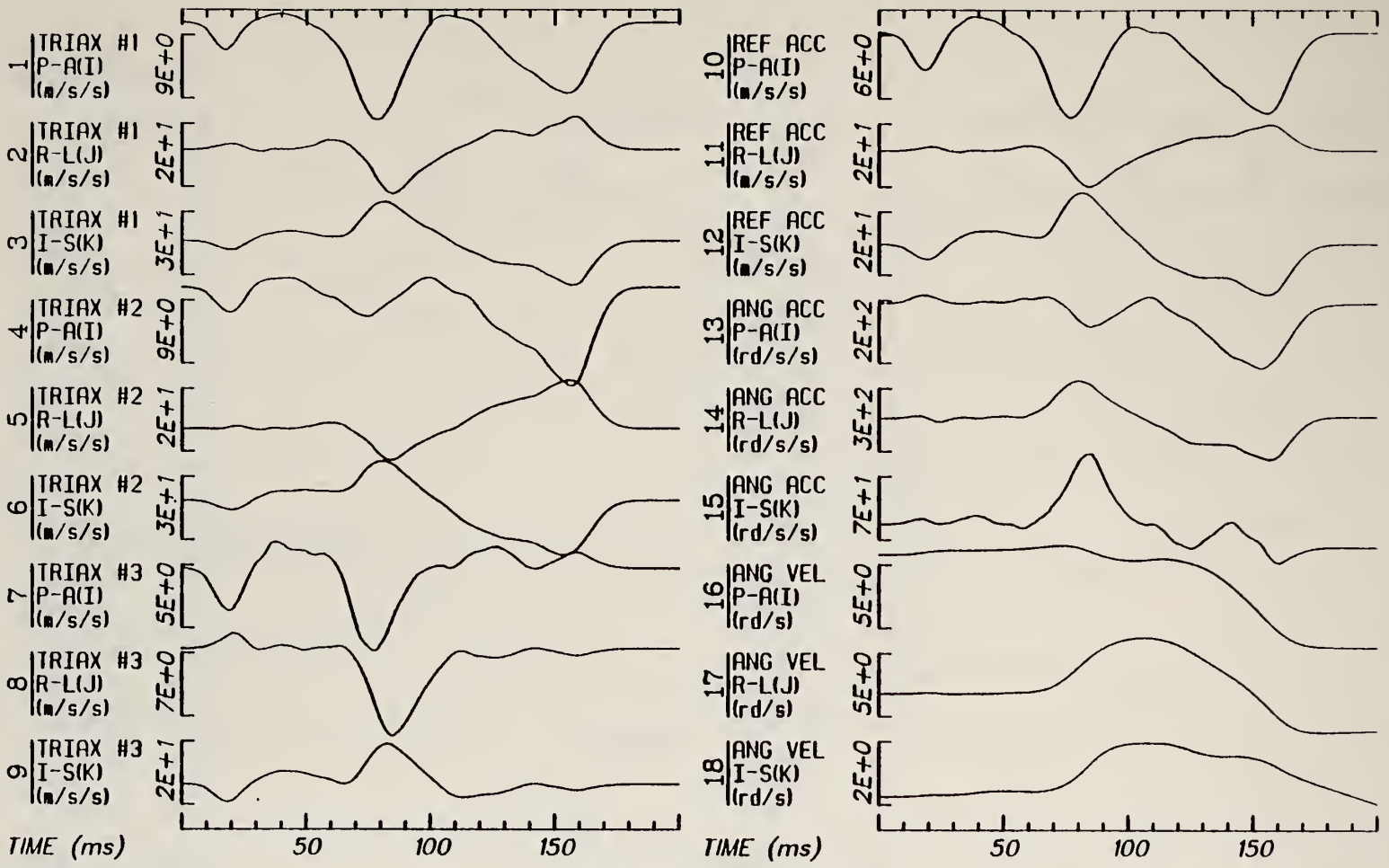

Run ID: 82E024 Disk: 82E024.3 File: 1 Date: MAY 12, 1985 Sheet: 1

*Filter:1600*4C*

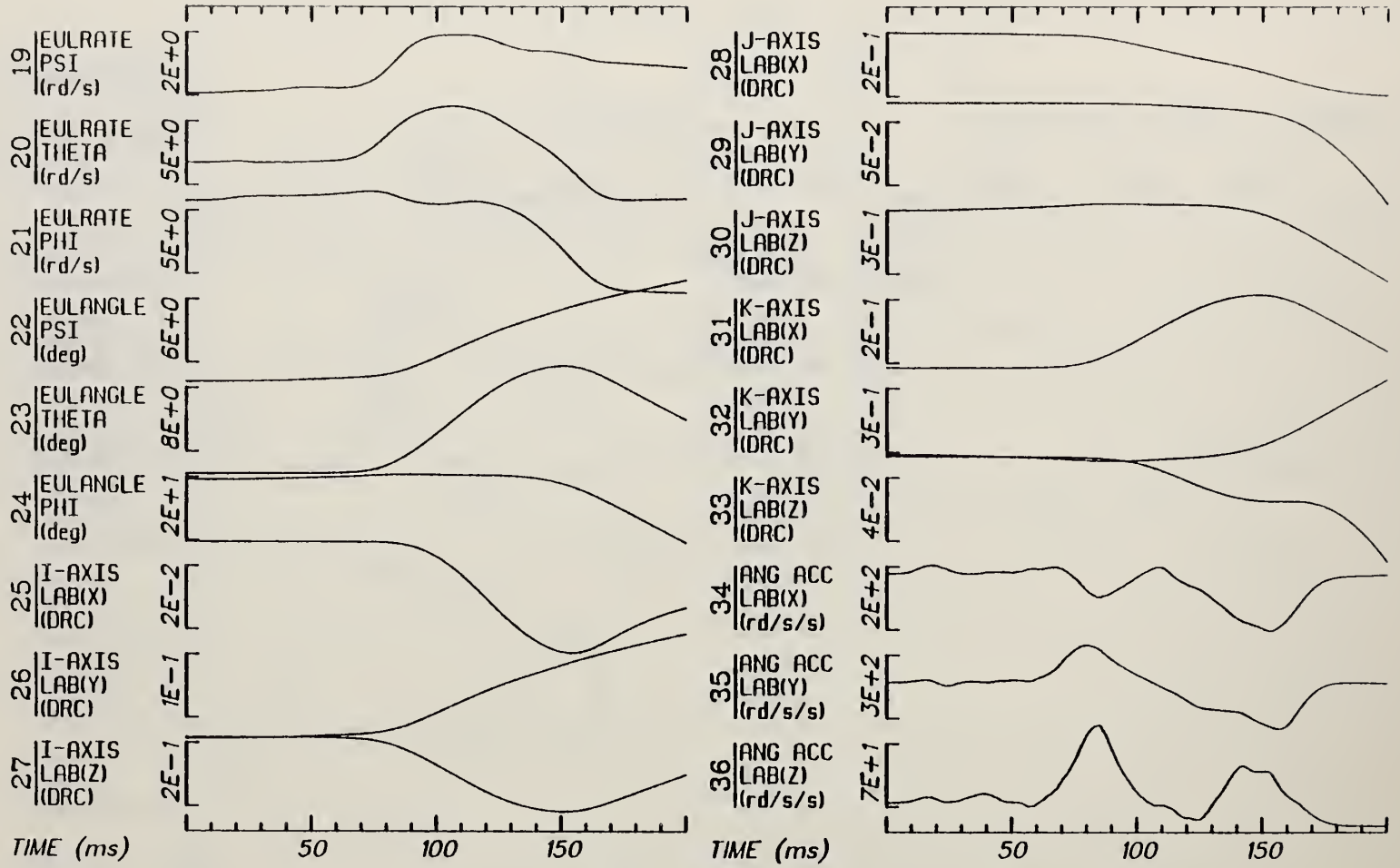

Run ID: 82E024 Disk: 82E024.3 File: 1 Date: MAY 12, 1985 Sheet: 2

*Filter:1600*4C*

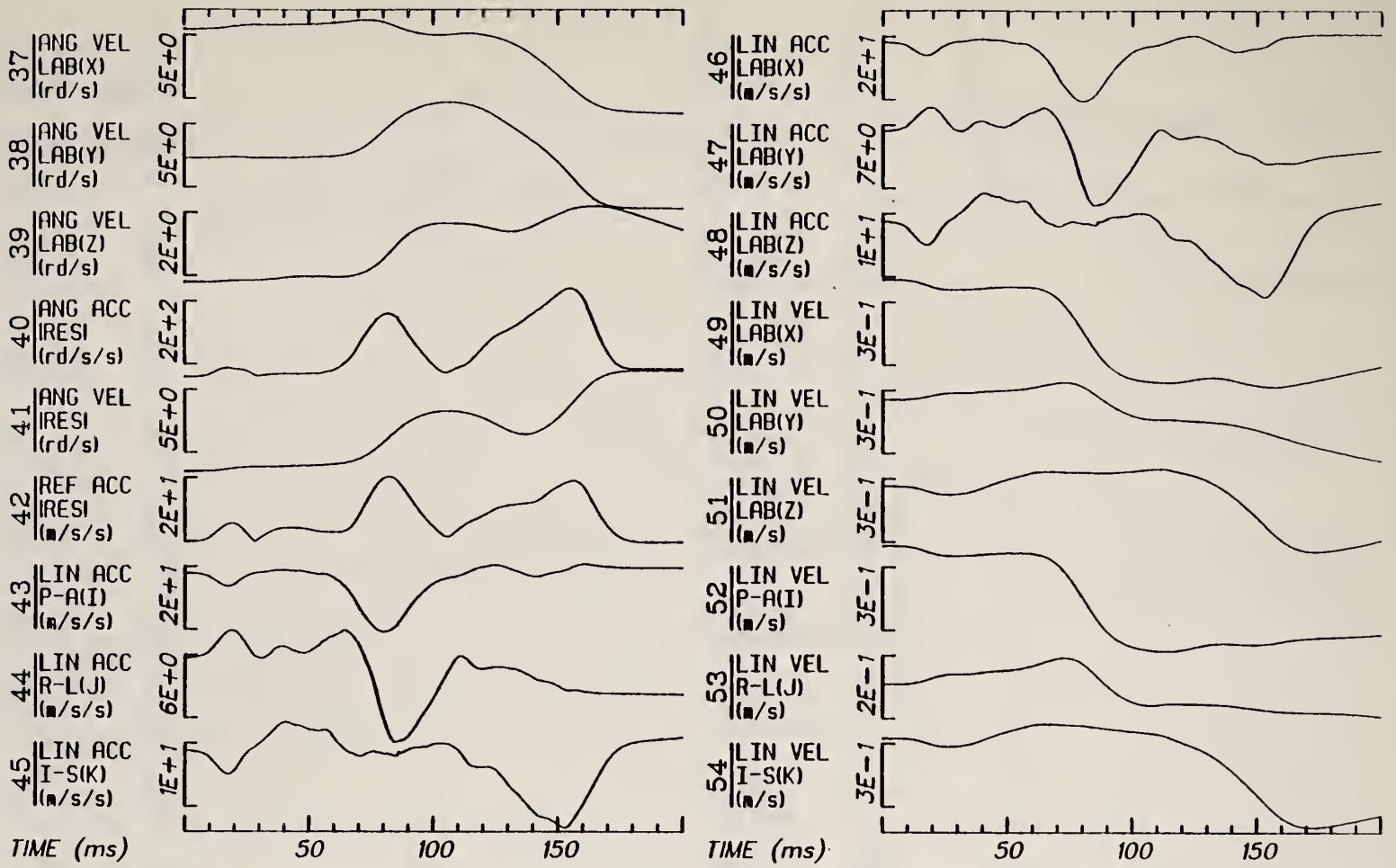

Run ID: 82E024 Disk: 82E024.3 File: 1 Date: MAY 12, 1985 Sheet: 3

*Filter:1600*4C*

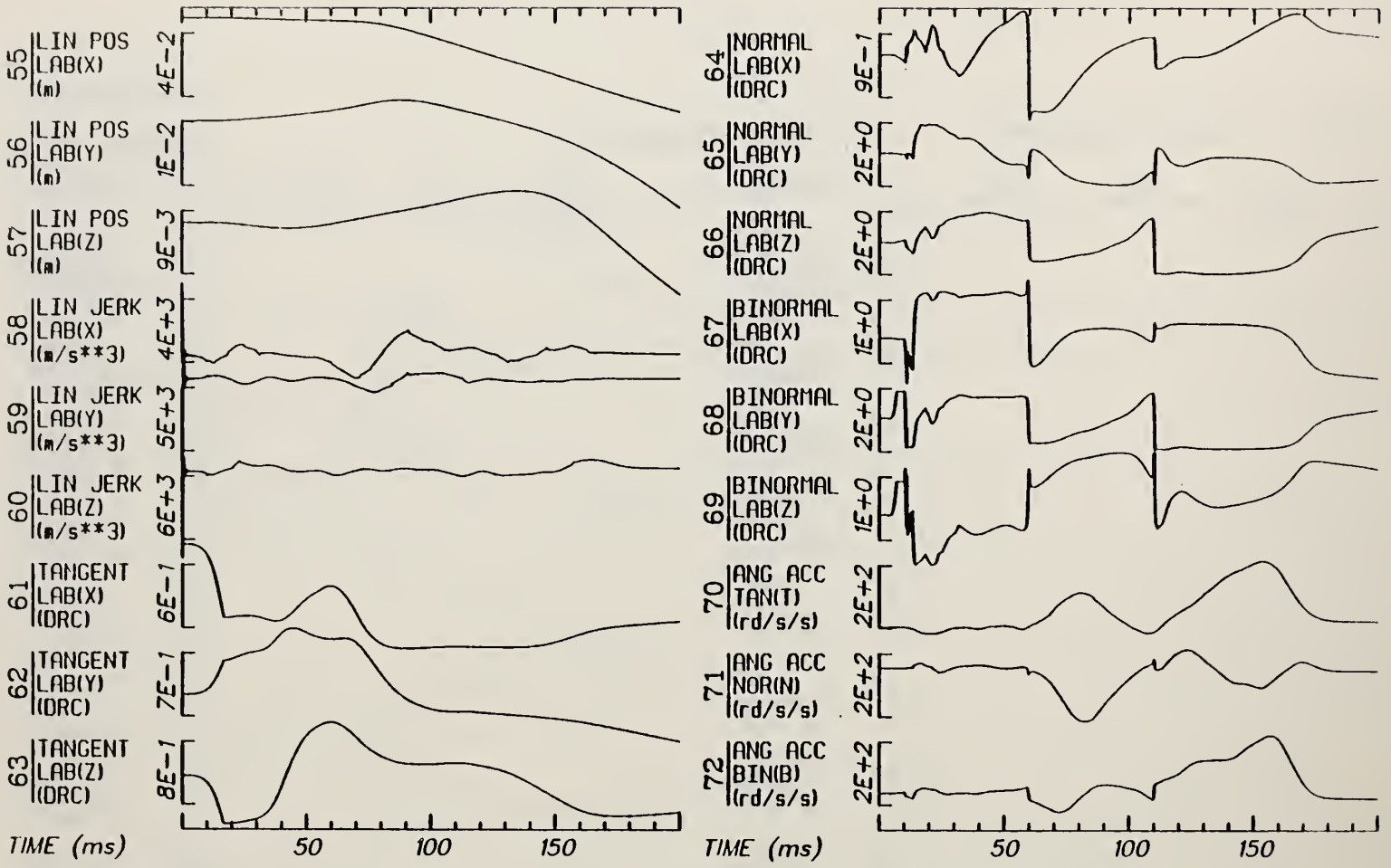

Run ID: 82E024 Disk: 82E024.3 File: 1 Date: MAY 12, 1985 Sheet: 4

*Filter:1600*4C*

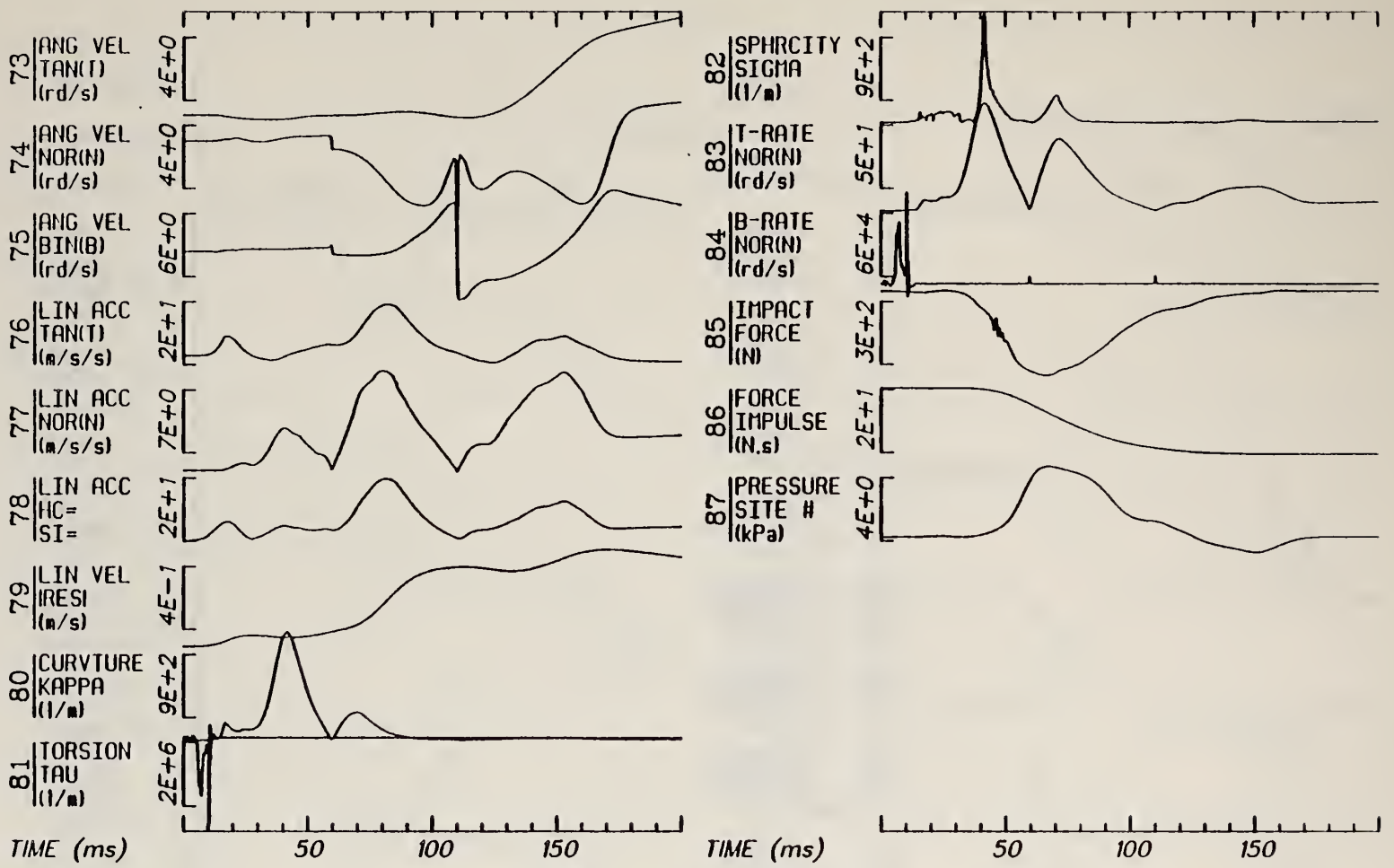

Run ID: 82E024 Disk: 82E024.3 File: 1 Date: MAY 12, 1985 Sheet: 5

*Filter:1600*4C*

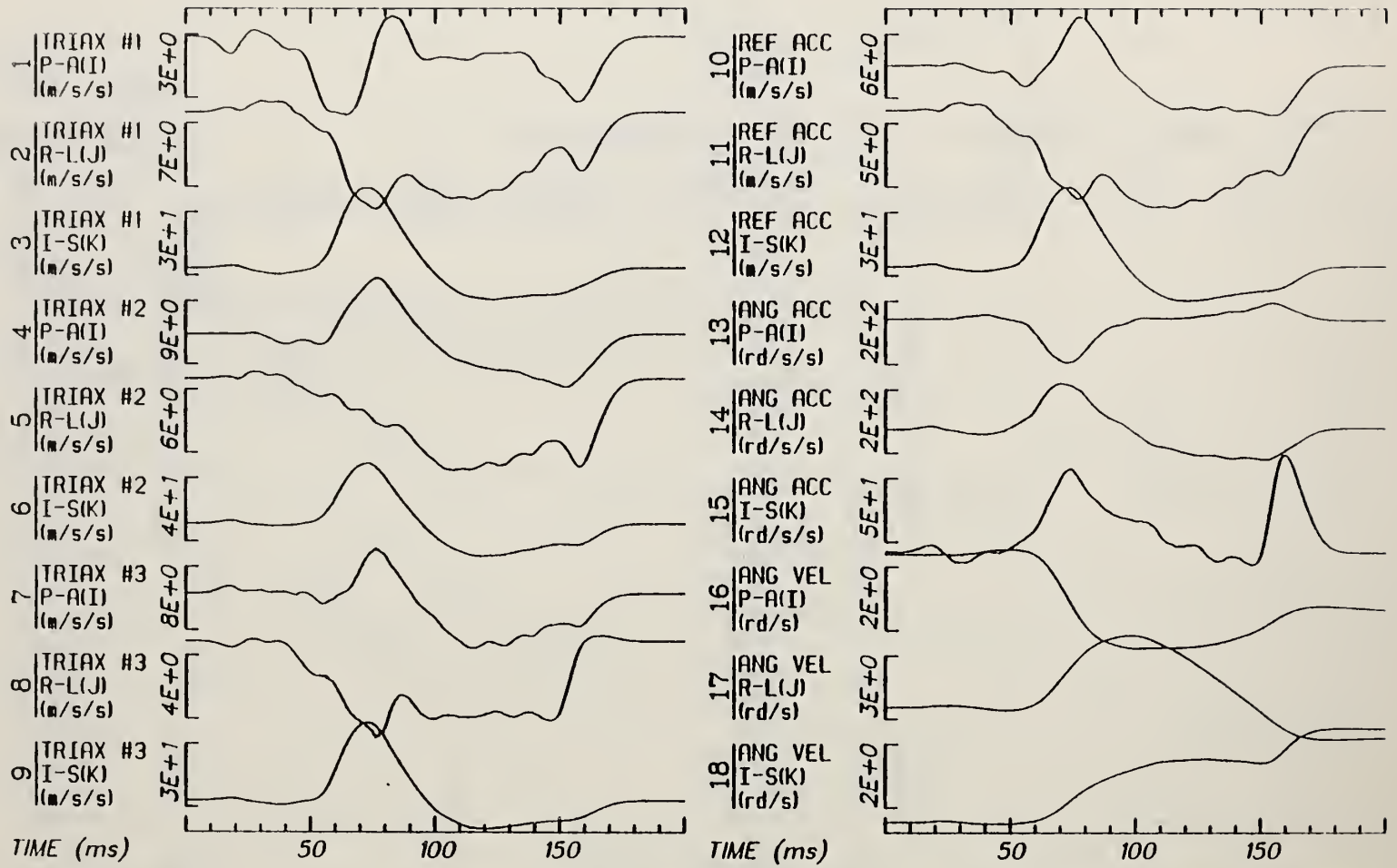

Run ID: 82E025 Disk: 82E025.3 File: 1 Date: MAY 12, 1985 Sheet: 1

*Filter:1600*4C*

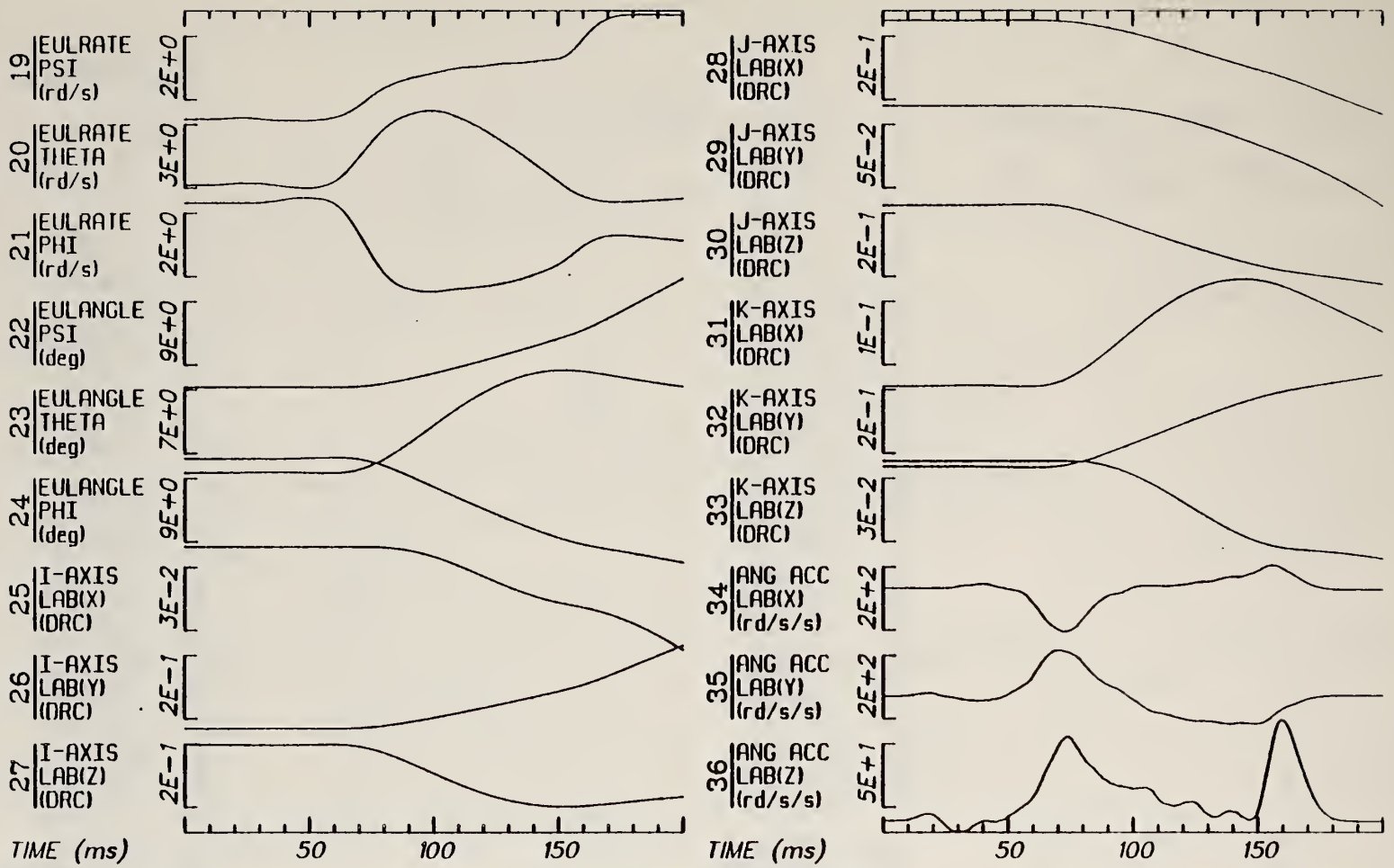

Run ID: 82E025 Disk: 82E025.3 File: 1 Date: MAY 12, 1985 Sheet: 2

*Filter:1600*4C*

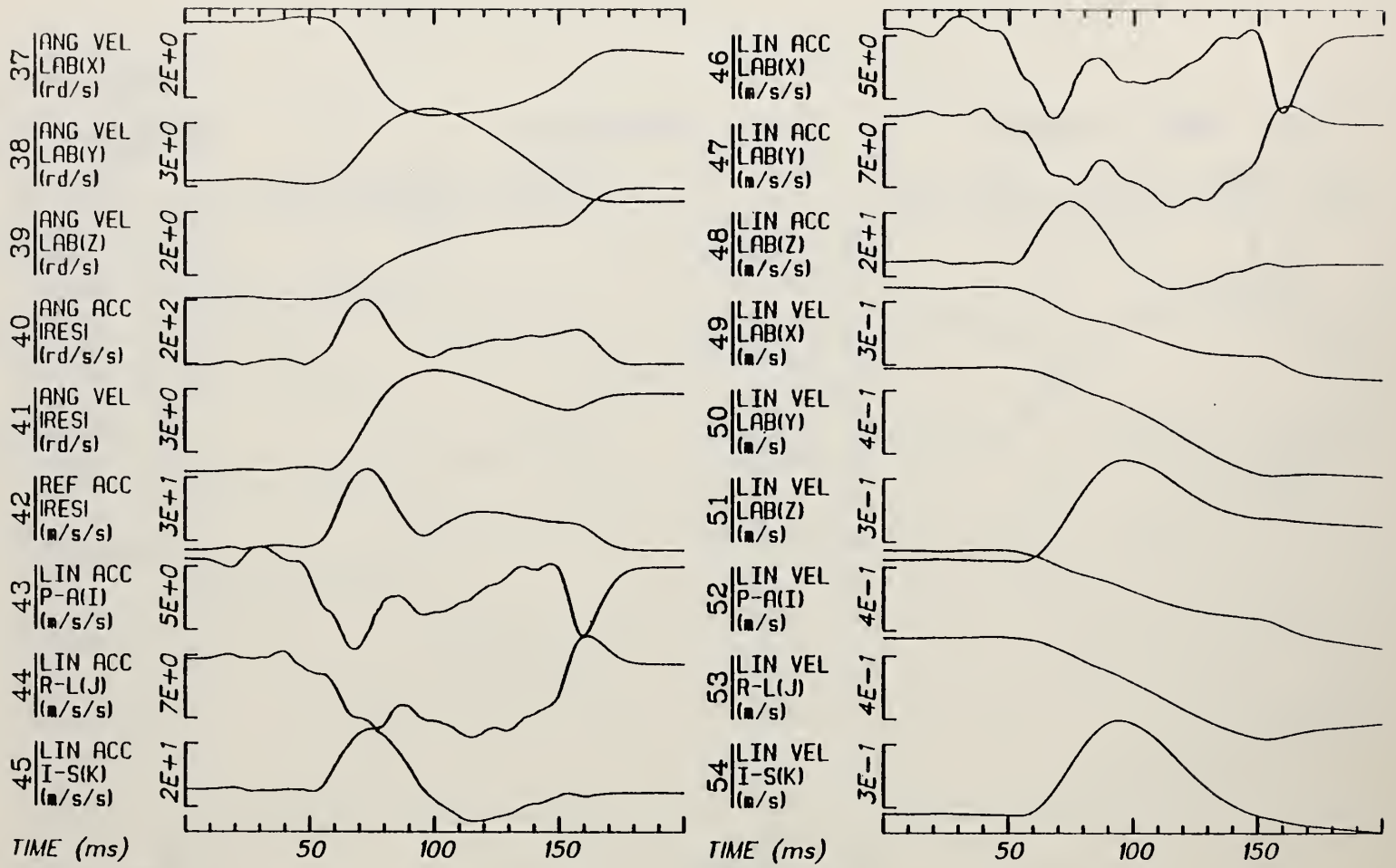

Run ID: 82E025 Disk: 82E025.3 File: 1 Date: MAY 12, 1985 Sheet: 3

*Filter:1600*4C*

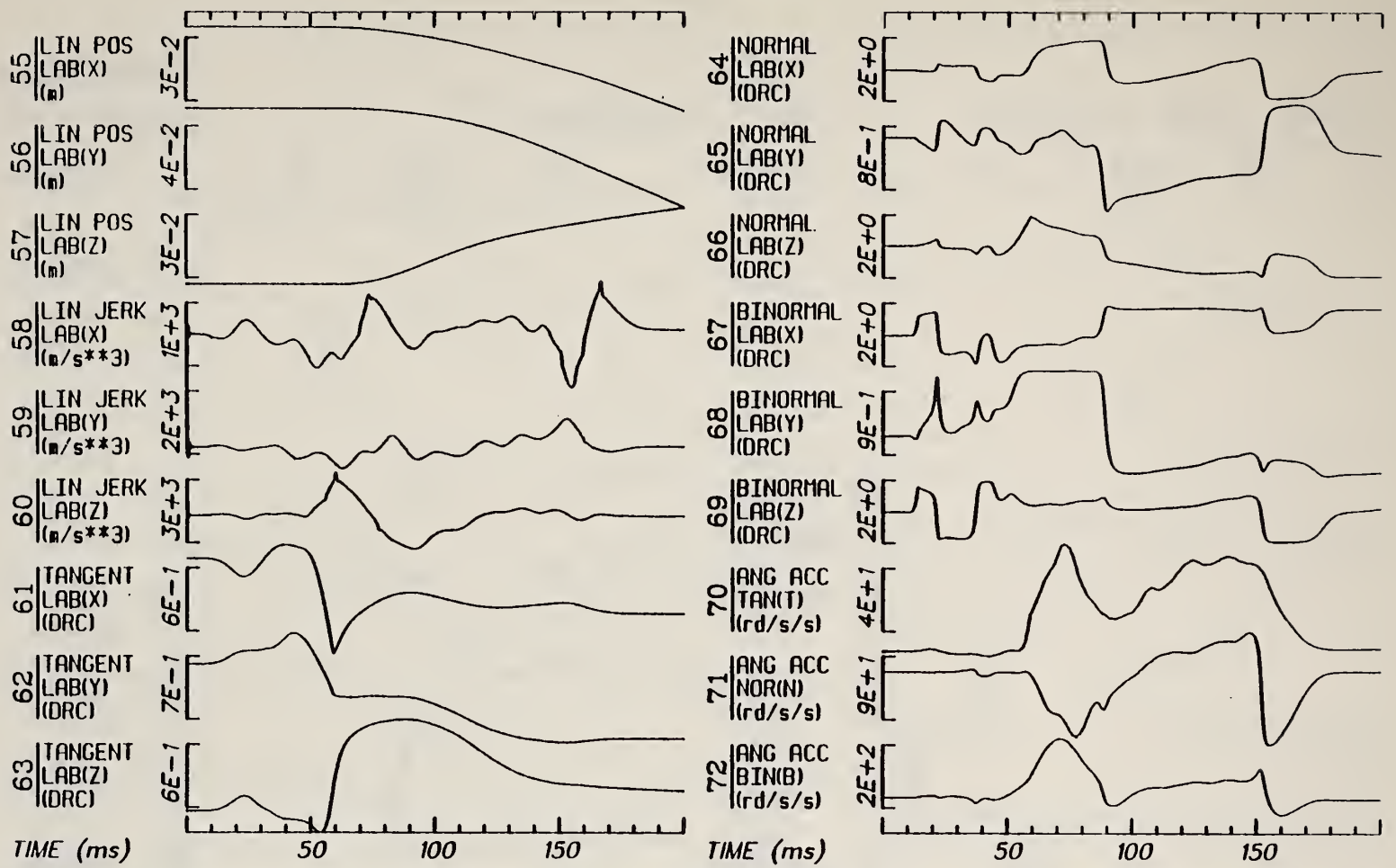

Run ID: 82E025 Disk: 82E025.3 File: 1 Date: MAY 12, 1985 Sheet: 4

*Filter:1600*4C*

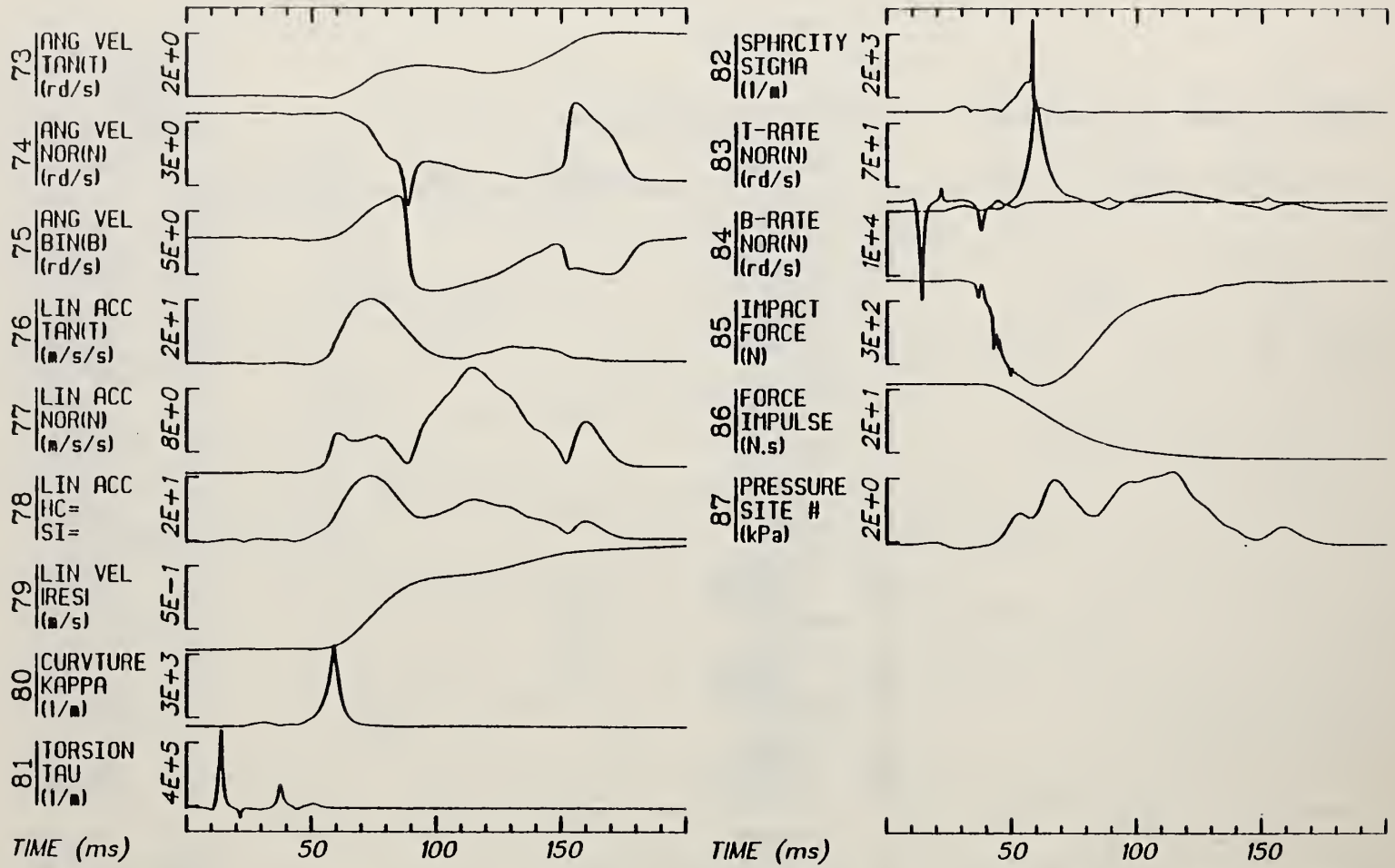

Run ID: 82E025 Disk: 82E025.3 File: 1 Date: MAY 12, 1985 Sheet: 5

*Filter:1600*4C*

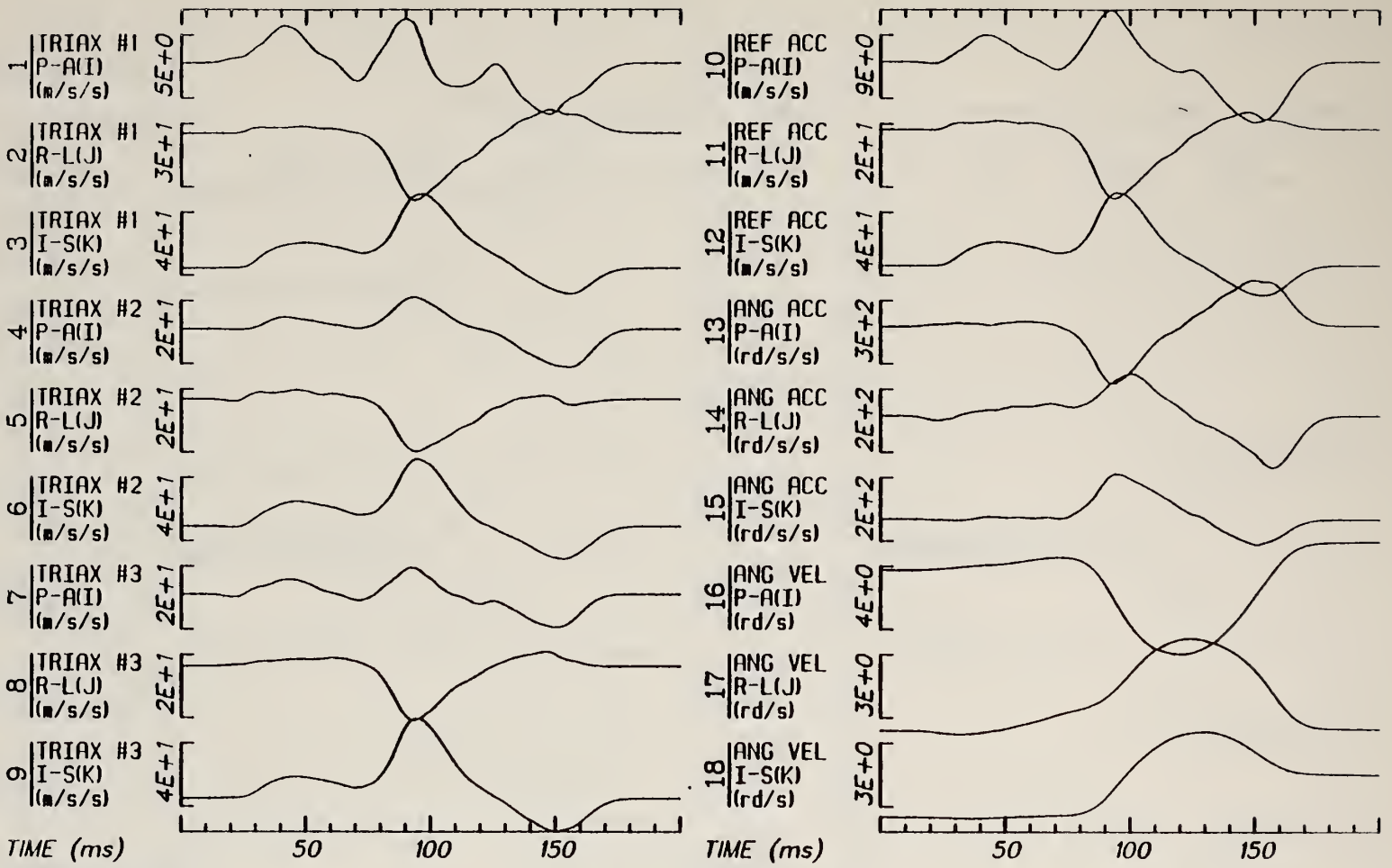

Run ID: 82E026 Disk: 82E026.3 File: 1 Date: MAY 12, 1985 Sheet: 1

*Filter:1600*4C*

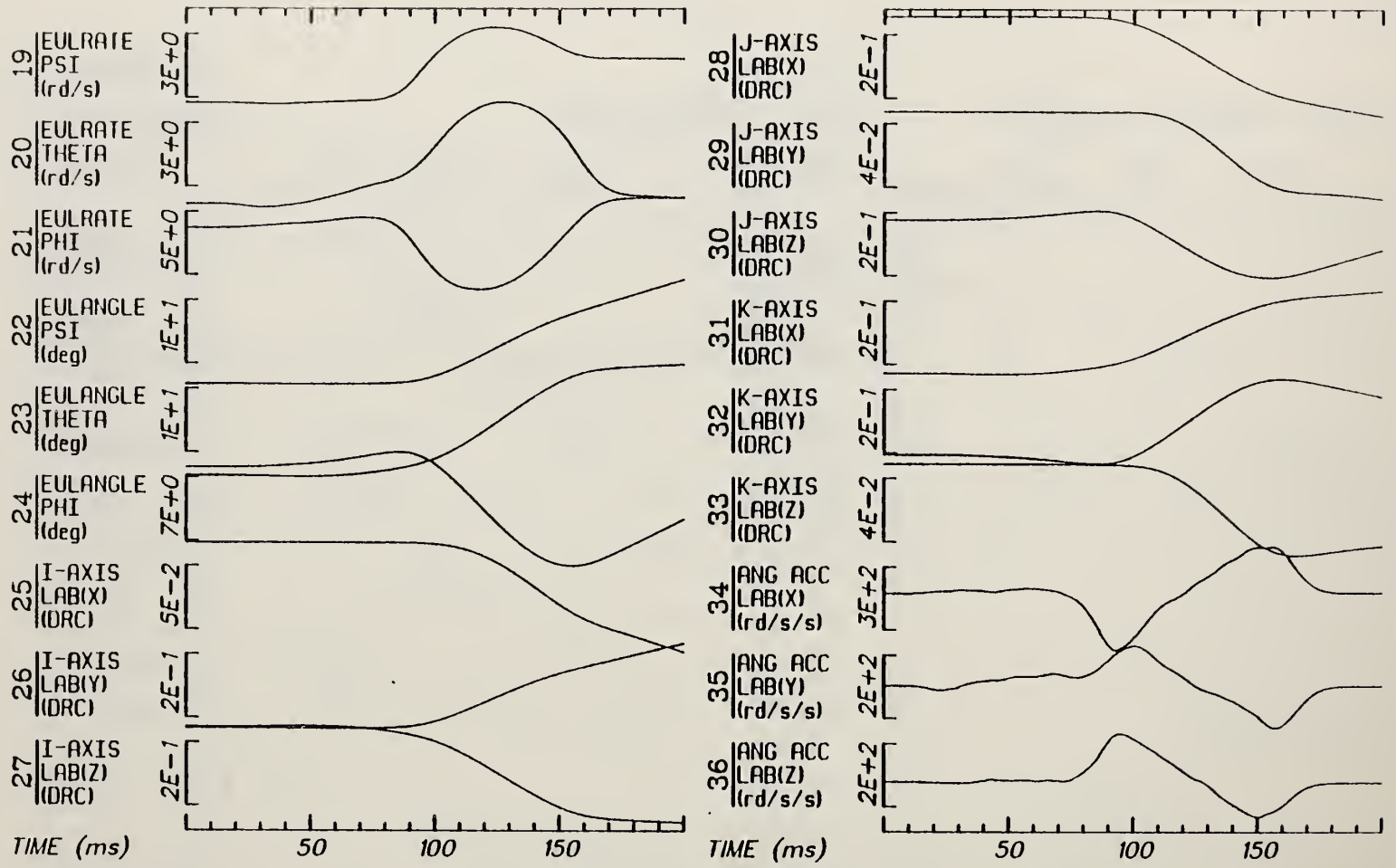

Run ID: 82E026 Disk: 82E026.3 File: 1 Date: MAY 12, 1985 Sheet: 2

*Filter:1600*4C*

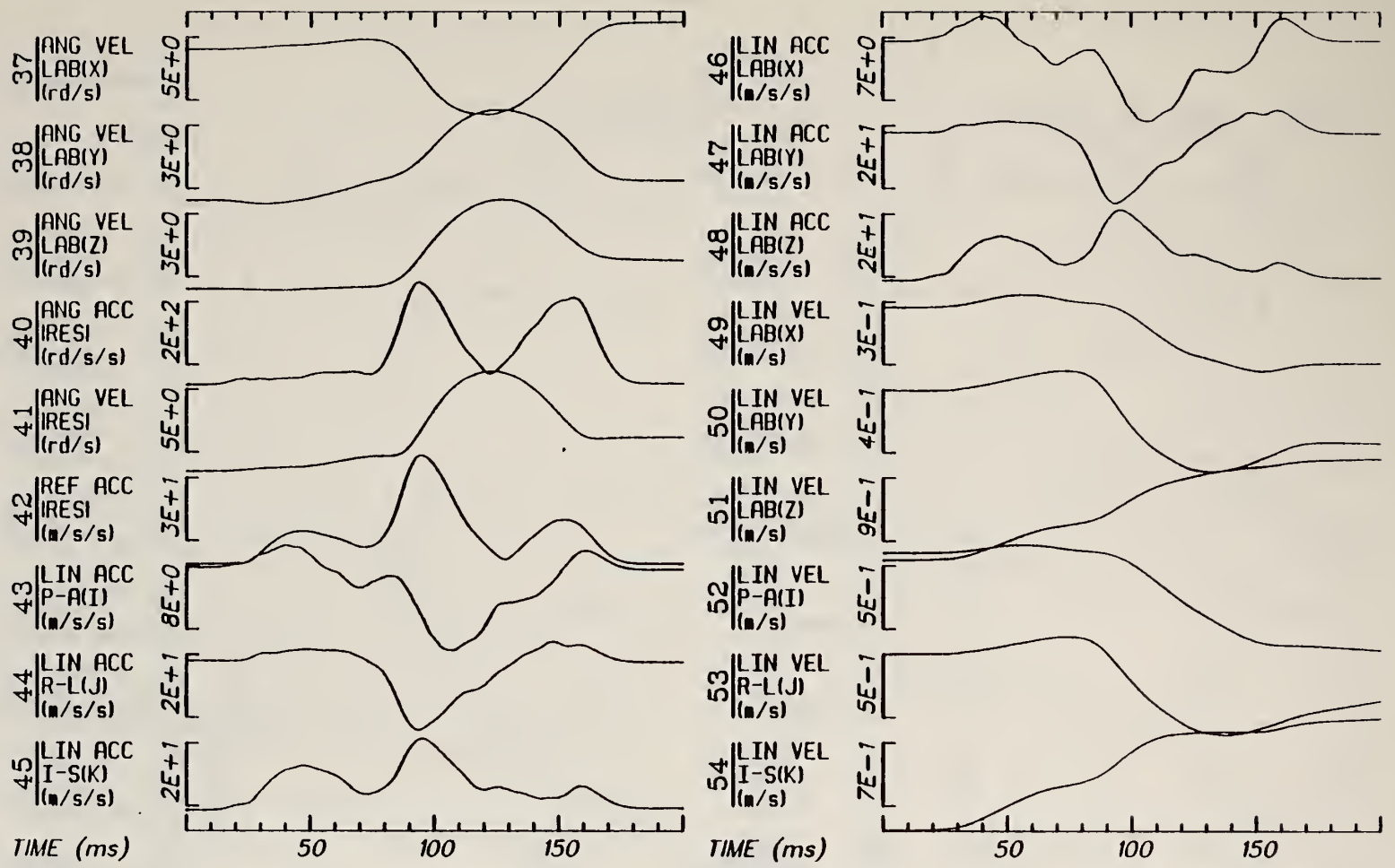

Run ID: 82E026 Disk: 82E026.3 File: 1 Date: MAY 12, 1985 Sheet: 3

*Filter:1600*4C*

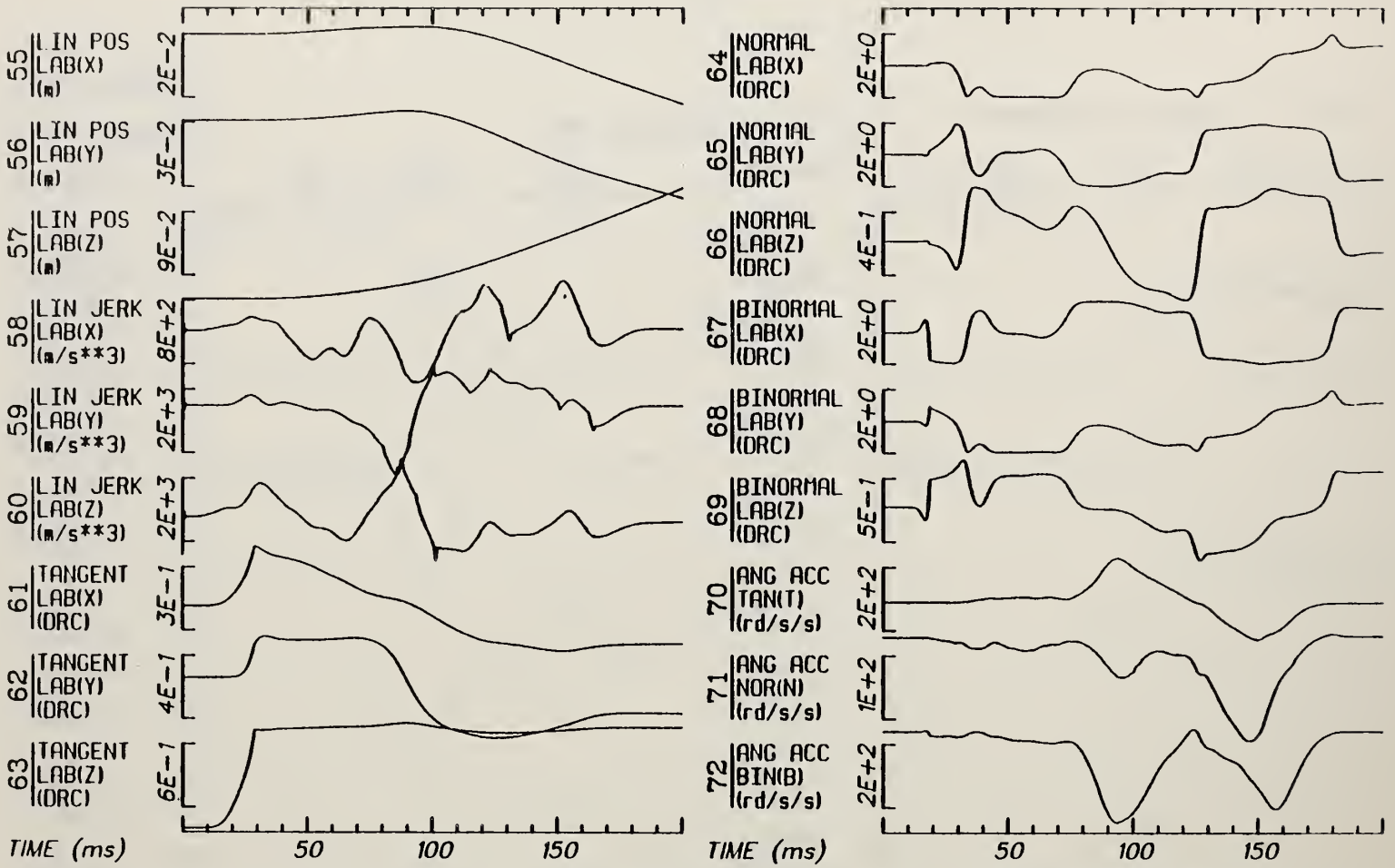

Run ID: 82E026 Disk: 82E026.3 File: 1 Date: MAY 12, 1985 Sheet: 4

*Filter:1600*4C*

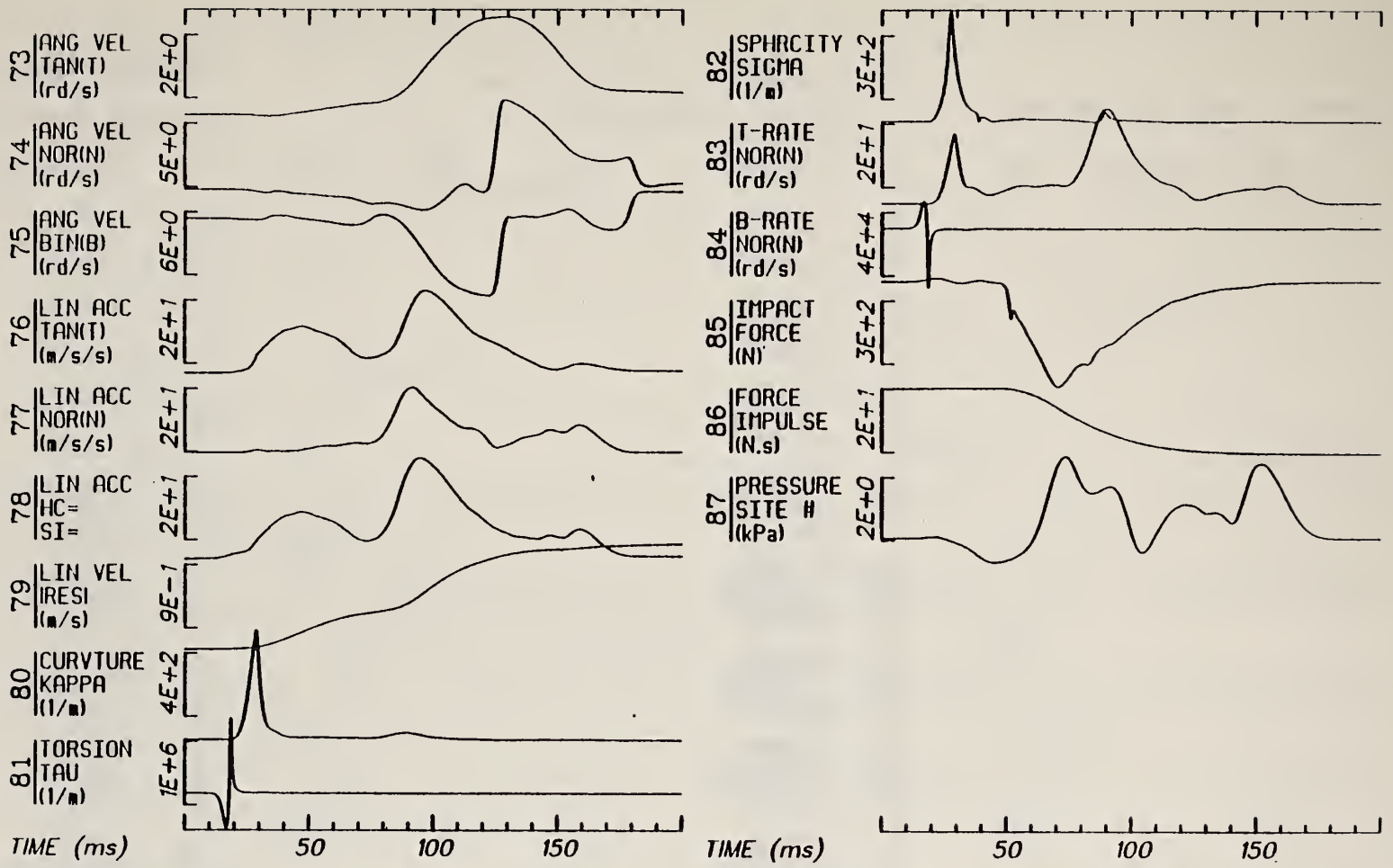

Run ID: 82E026 Disk: 82E026.3 File: 1 Date: MAY 12, 1985 Sheet: 5

*Filter:1600*4C*

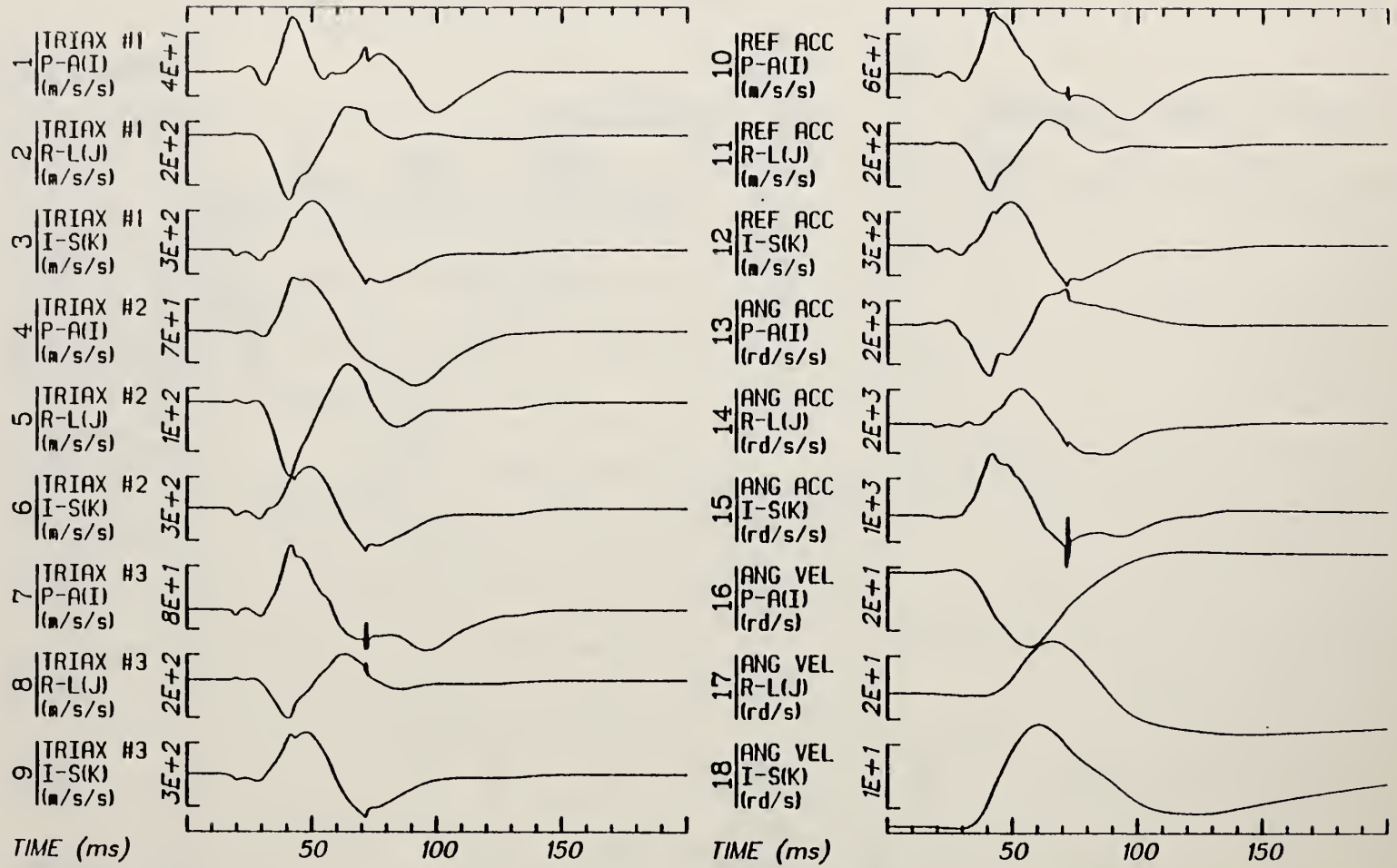

Run ID: 82E027 Disk: 82E027.3 File: 1 Date: MAY 12, 1985 Sheet: 1

*Filter:1600*4C*

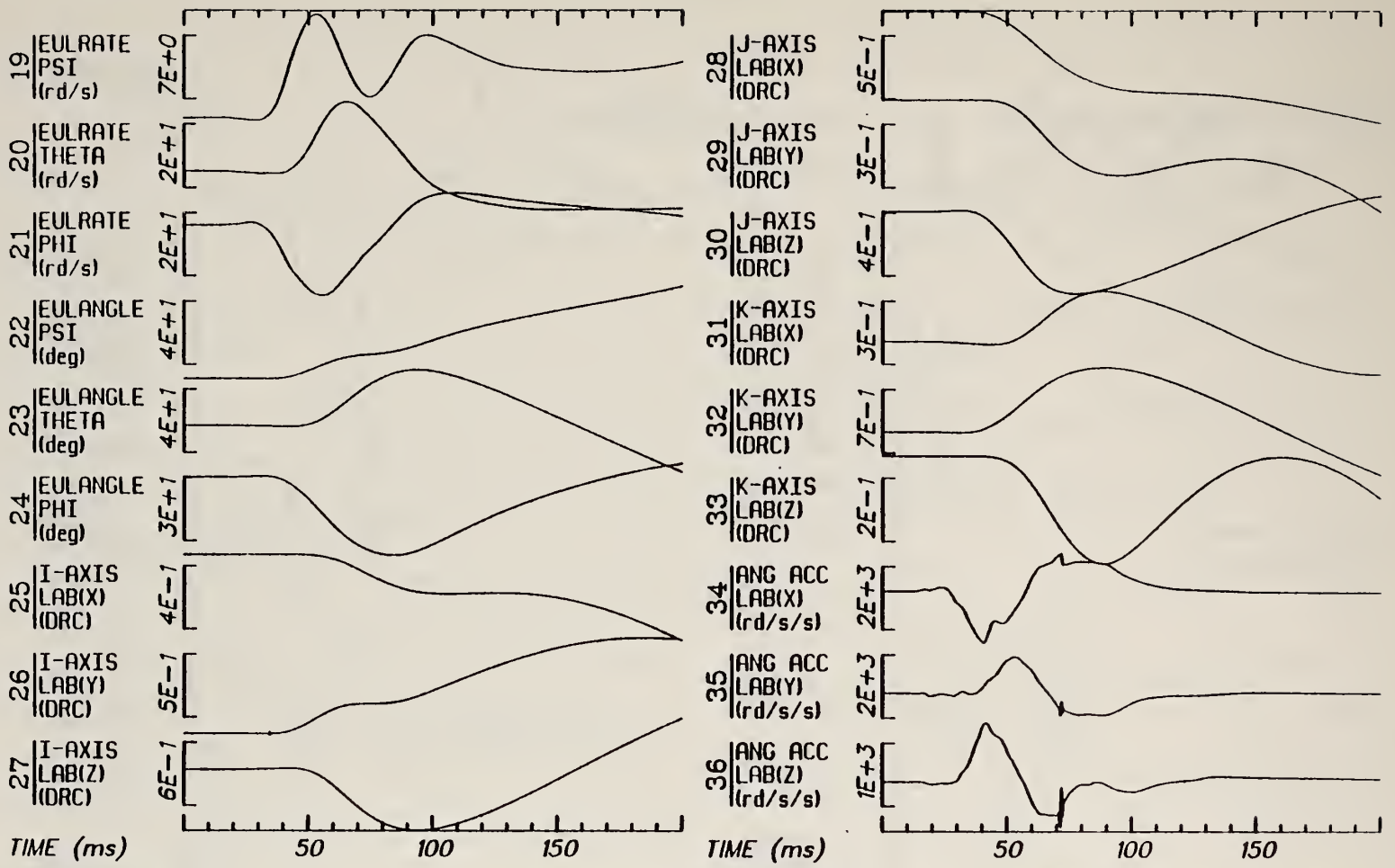

Run ID: 82E027 Disk: 82E027.3 File: 1 Date: MAY 12, 1985 Sheet: 2

*Filter:1600*4C*

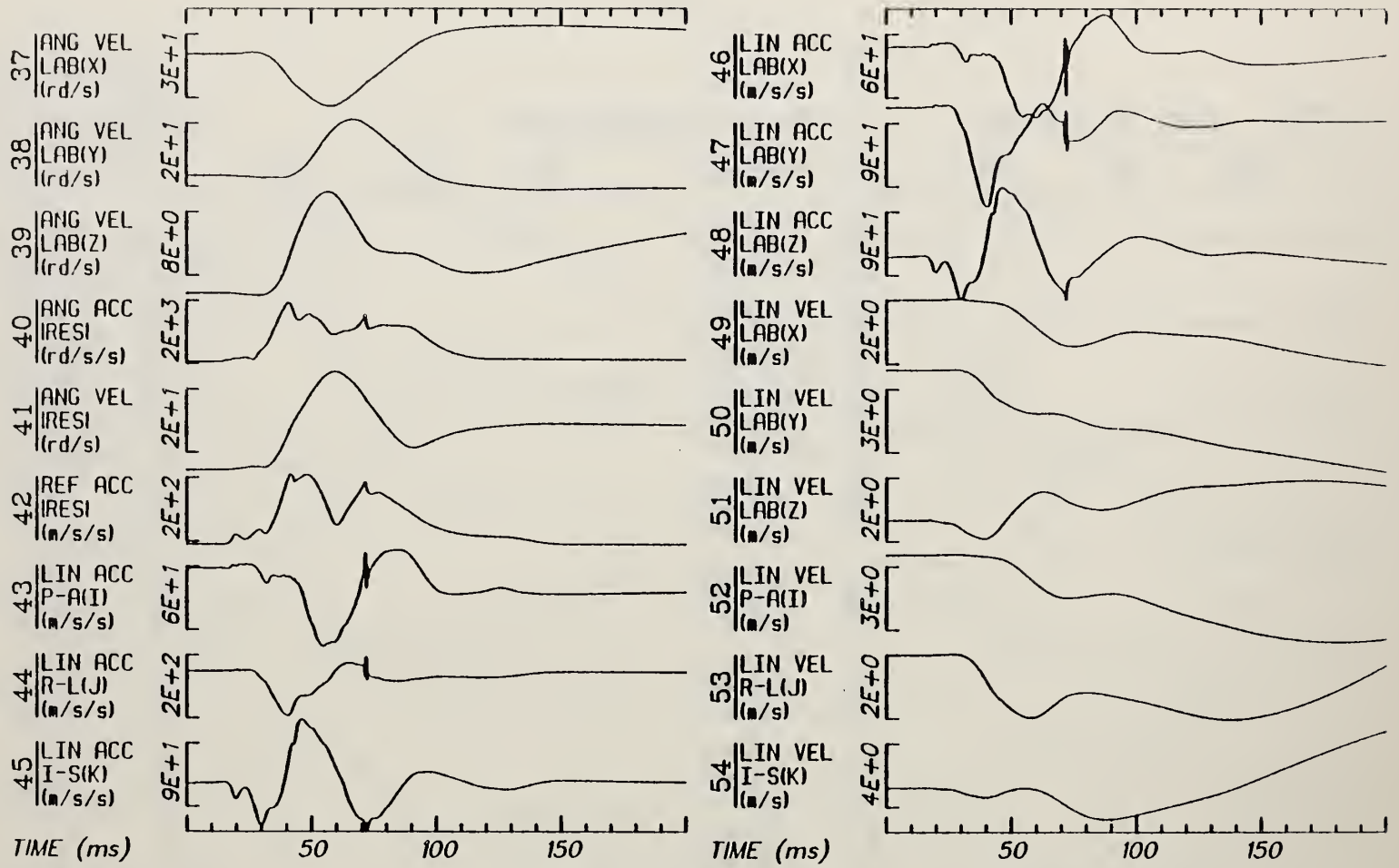

Run ID: 82E027 Disk: 82E027.3 File: 1 Date: MAY 12, 1985 Sheet: 3

*Filter:1600*4C*

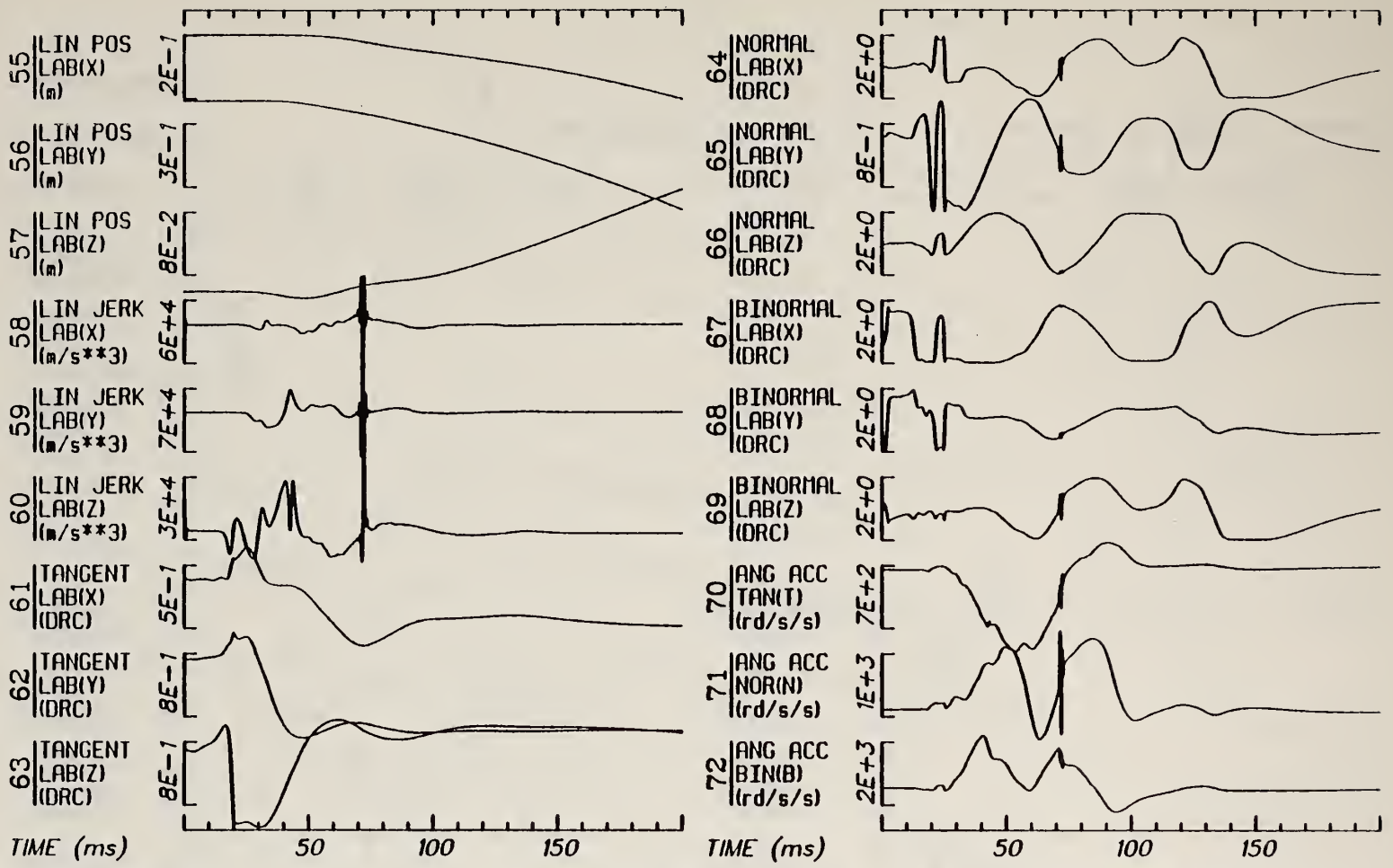

Run ID: 82E027 Disk: 82E027.3 File: 1 Date: MAY 12, 1985 Sheet: 4

*Filter:1600*4C*

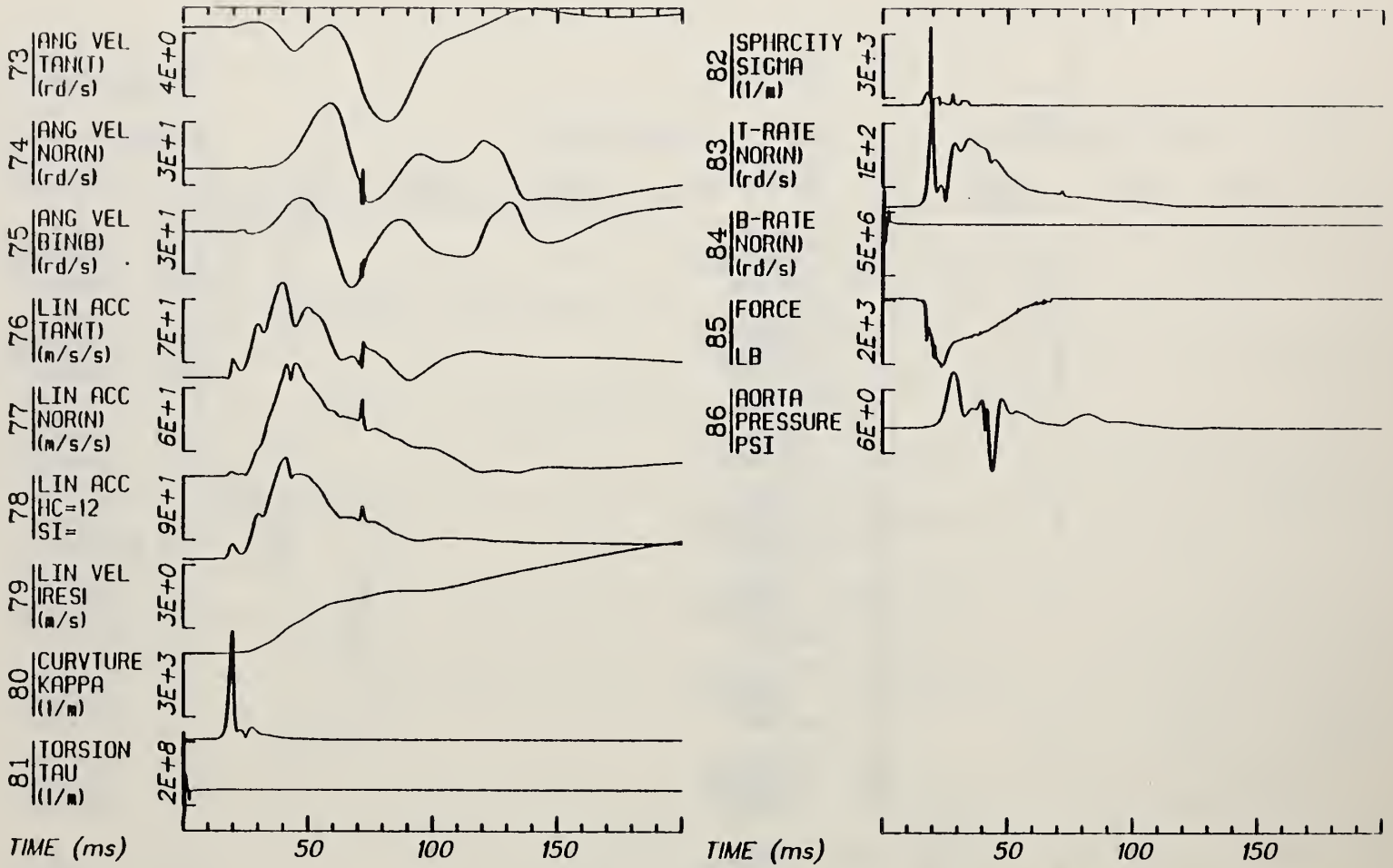

Run ID: 82E027 Disk: 82E027.3 File: 1 Date: MAY 12, 1985 Sheet: 5

*Filter:1600*4C*

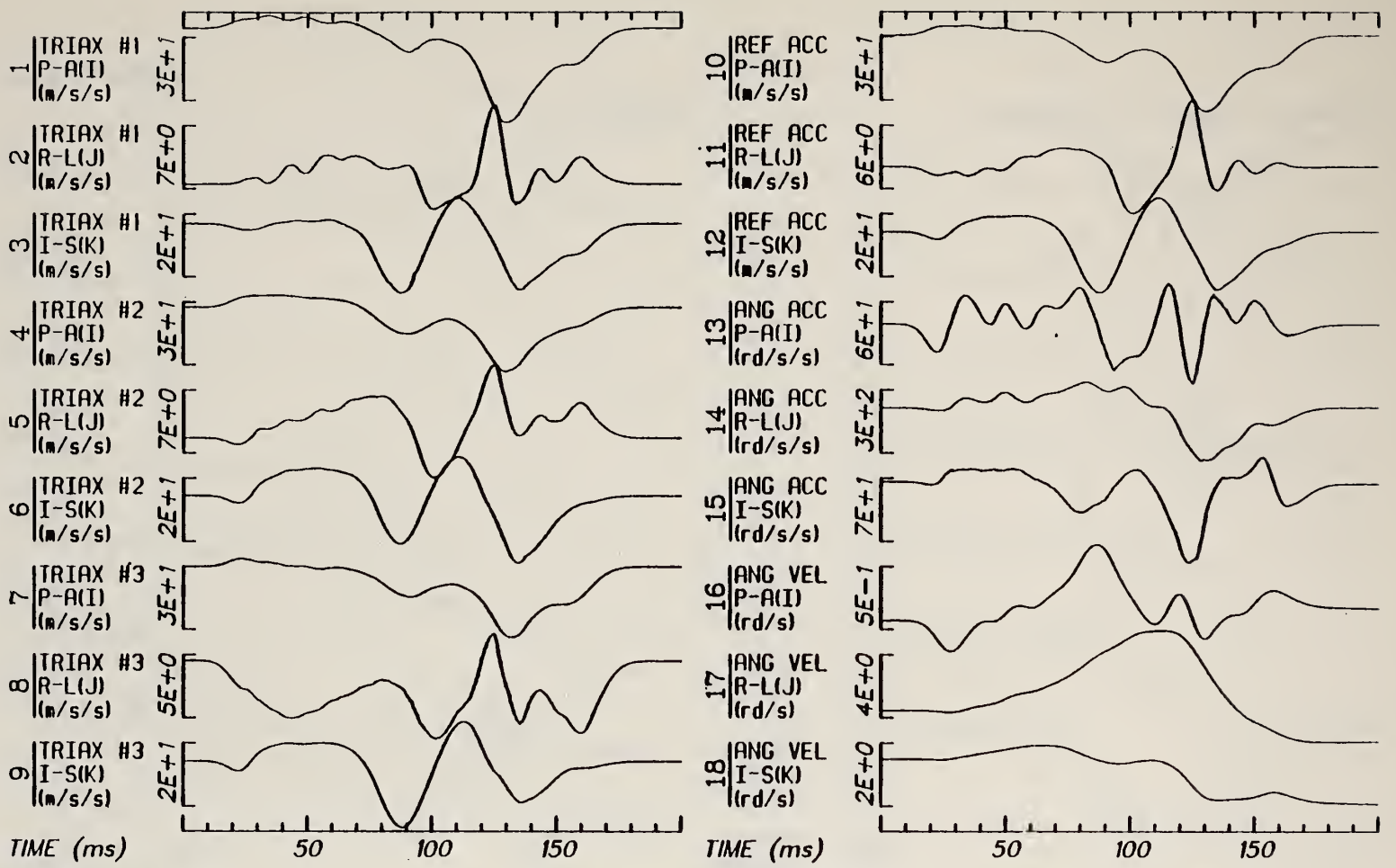

Run ID: 82E043 Disk: 82E043.3 File: 1 Date: MAY 12, 1985 Sheet: 1

*Filter:1600*4C*

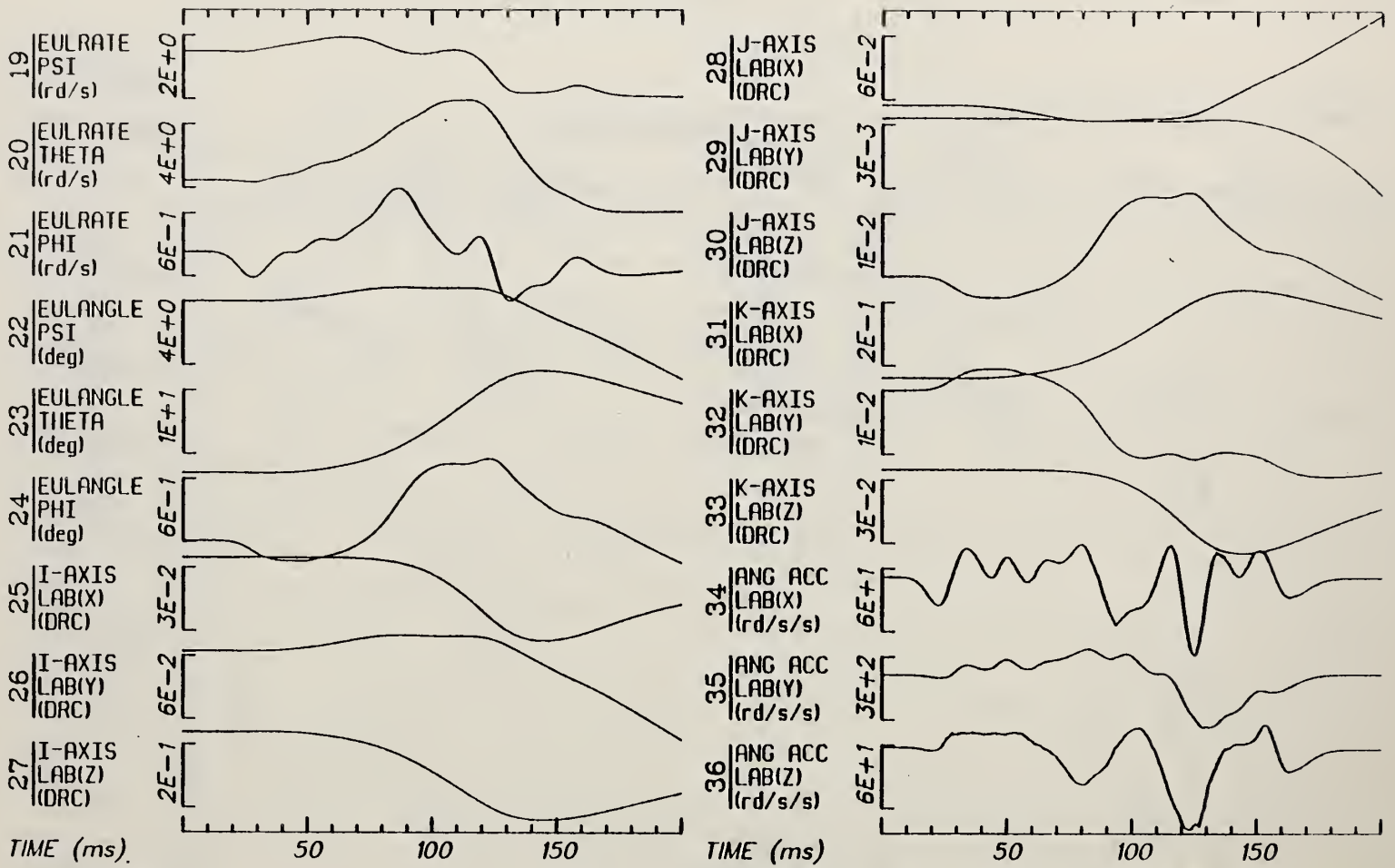

Run ID: 82E043 Disk: 82E043.3 File: 1 Date: MAY 12, 1985 Sheet: 2

*Filter:1600*4C*

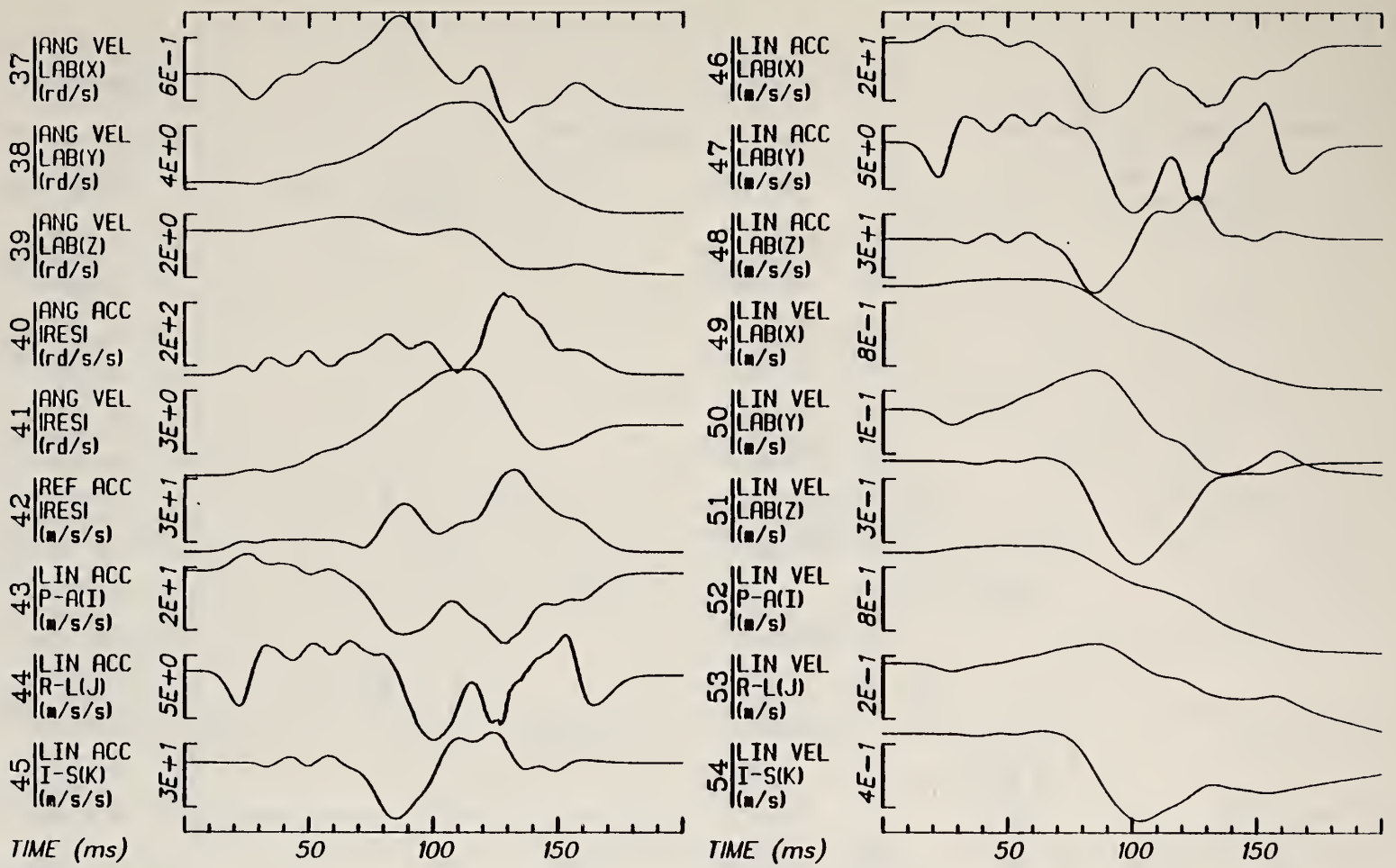

Run ID: 82E043 Disk: 82E043.3 File: 1 Date: MAY 12, 1985 Sheet: 3

*Filter:1600*4C*

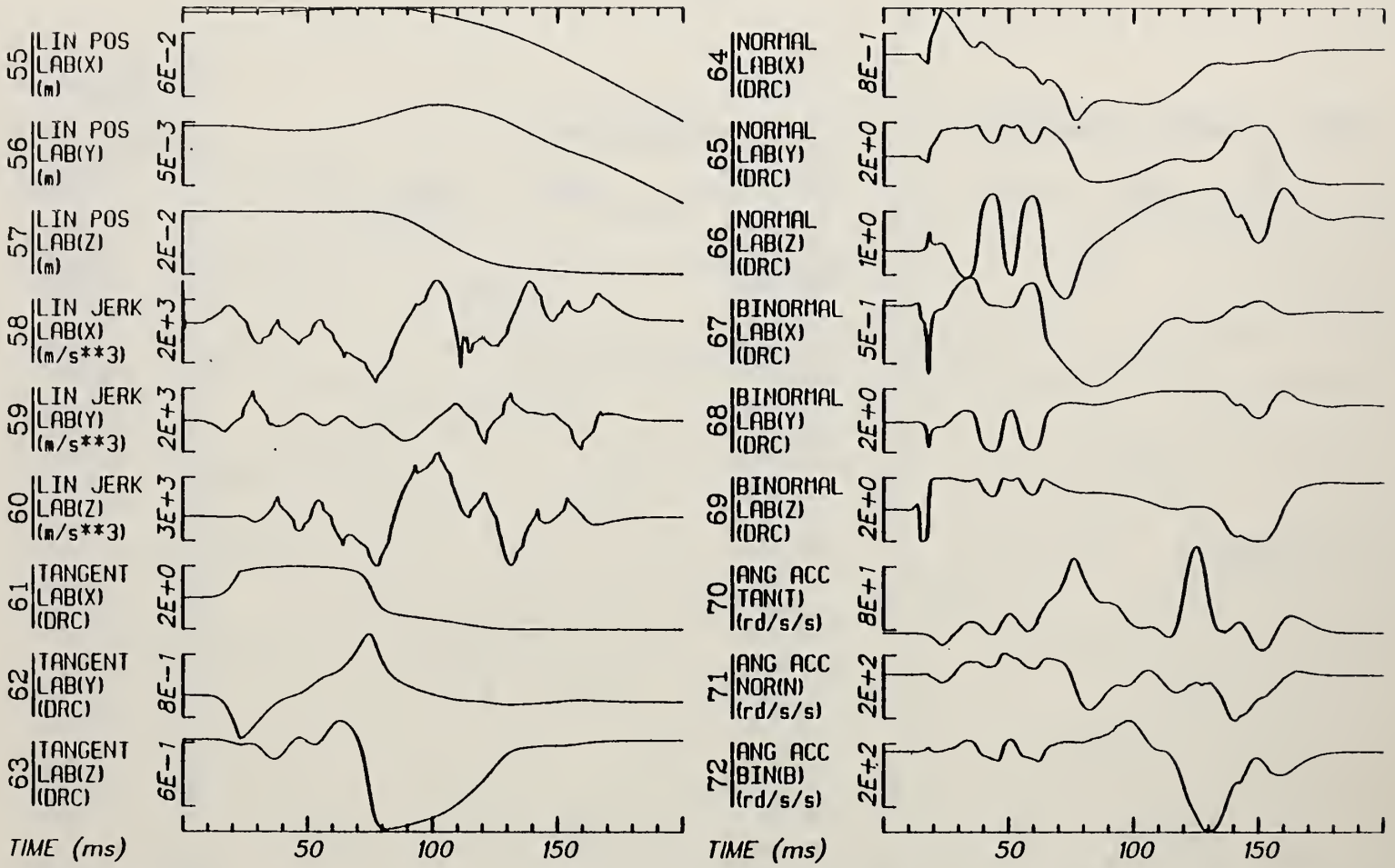

Run ID: 82E043 Disk: 82E043.3 File: 1 Date: MAY 12, 1985 Sheet: 4

*Filter:1600*4C*

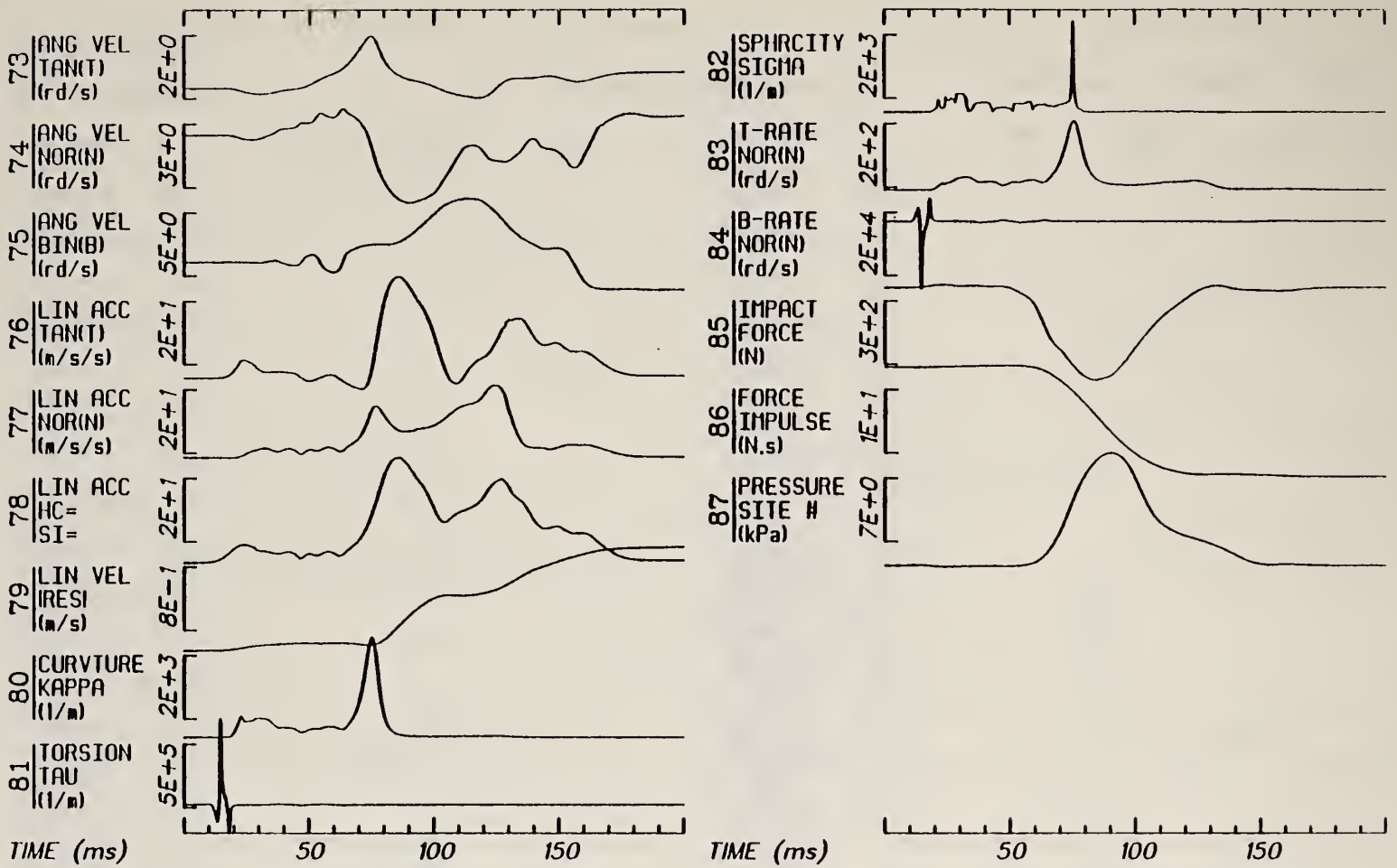

Run ID: 82E043 Disk: 82E043.3 File: 1 Date: MAY 12, 1985 Sheet: 5

*Filter:1600*4C*

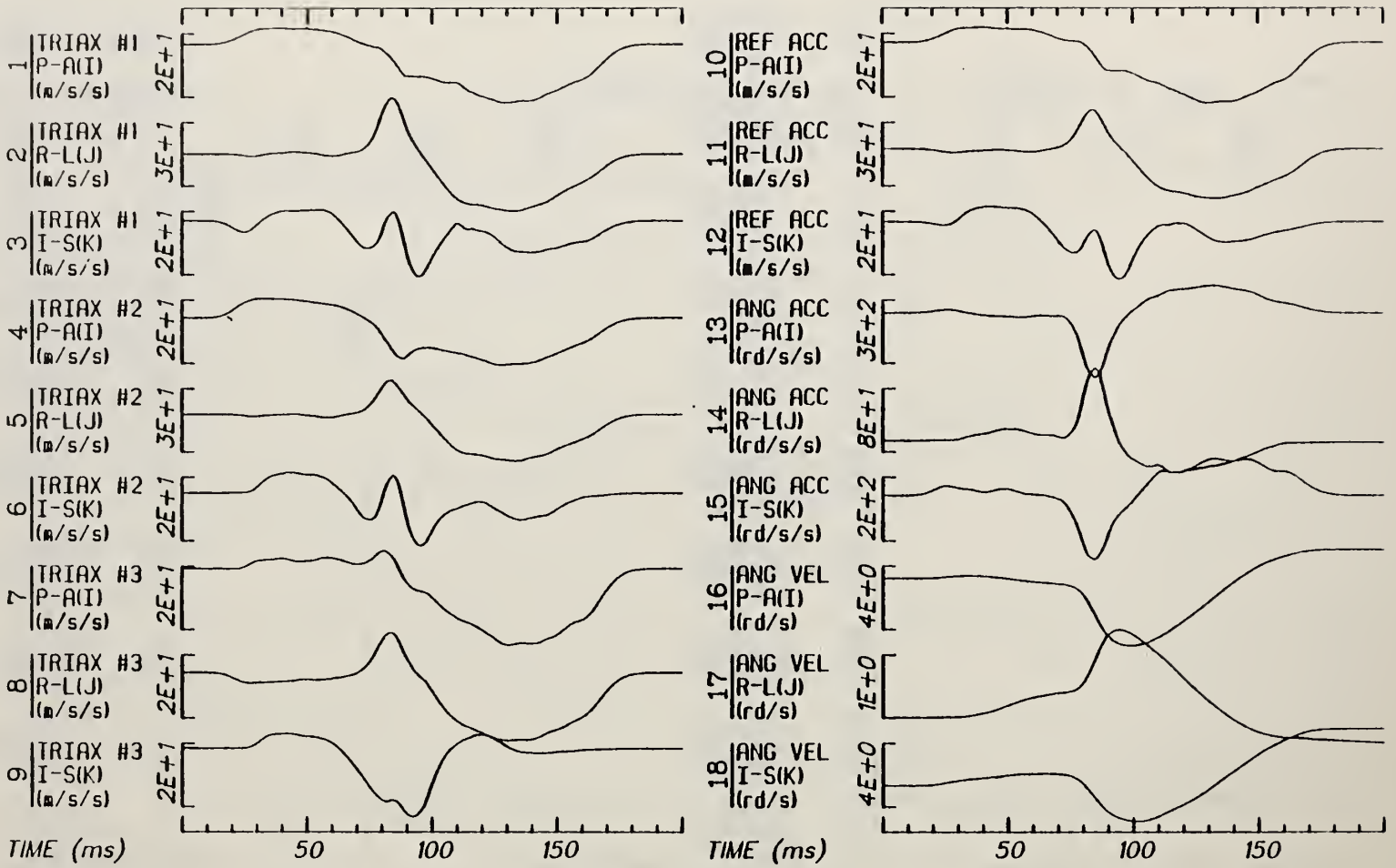

Run ID: 82E044 Disk: 82E044.3 File: 1 Date: MAY 12, 1985 Sheet: 1

*Filter:1600*4C*

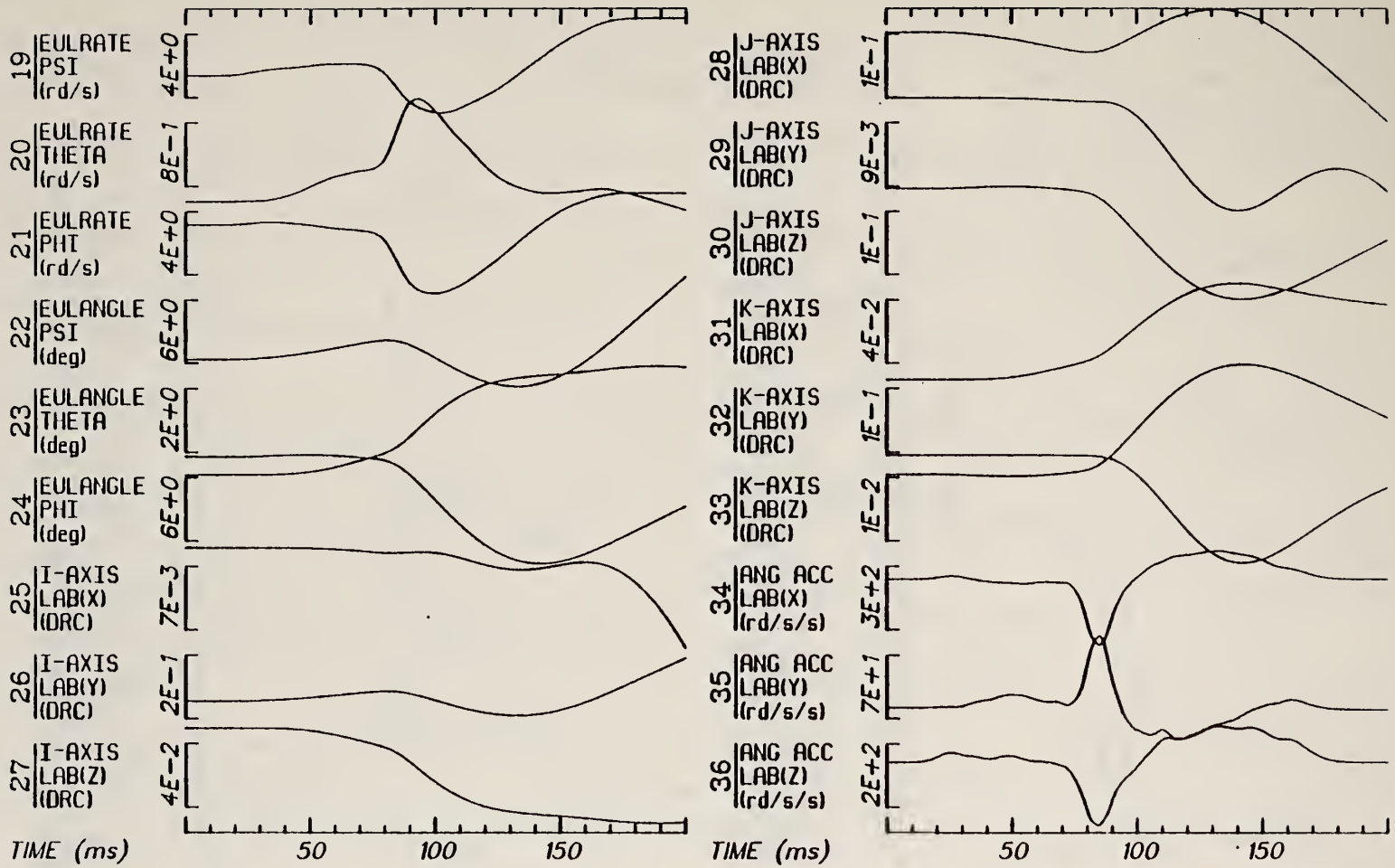

Run ID: 82E044 Disk: 82E044.3 File: 1 Date: MAY 12, 1985 Sheet: 2

*Filter:1600*4C*

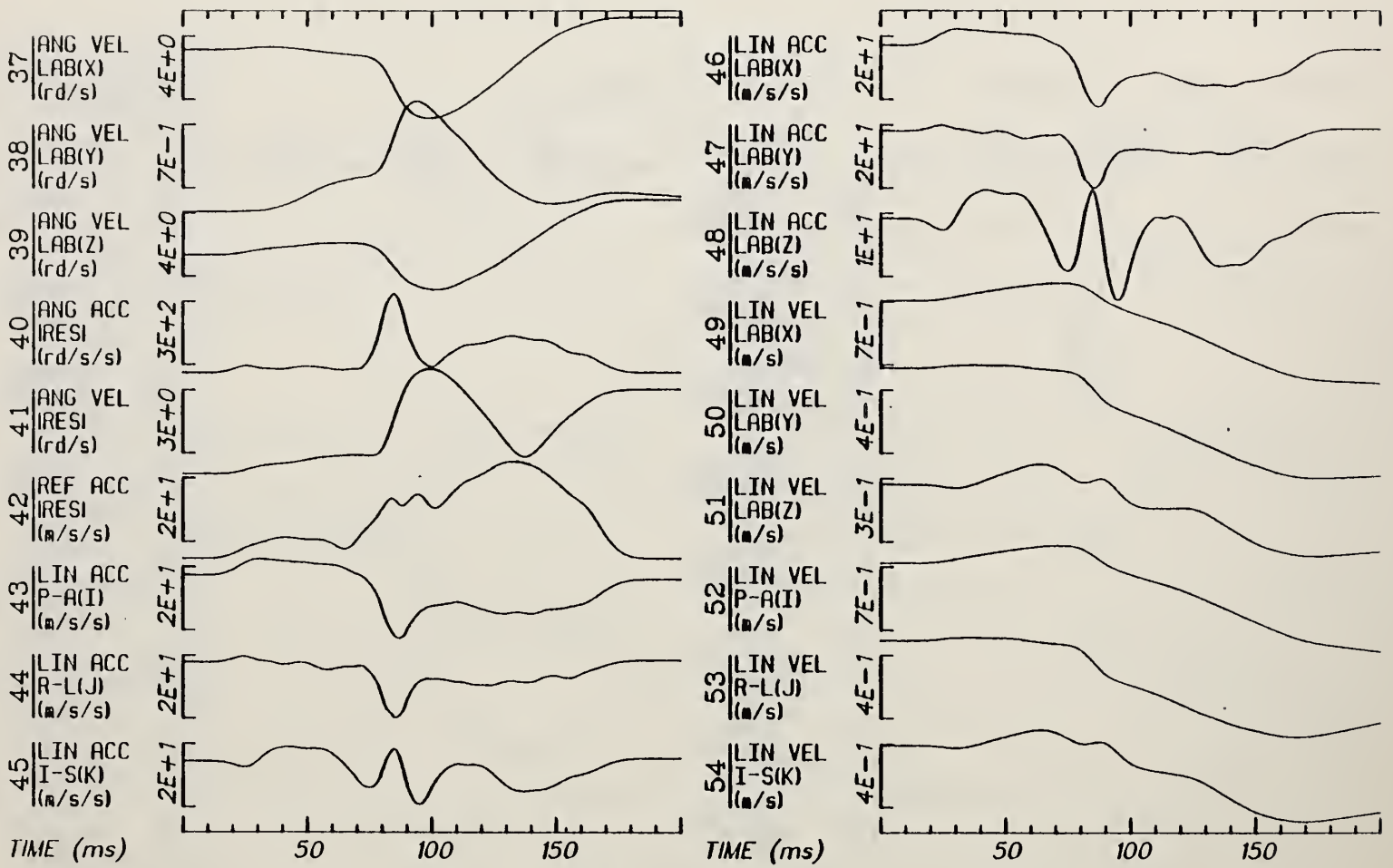

Run ID: 82E044 Disk: 82E044.3 File: 1 Date: MAY 12, 1985 Sheet: 3

*Filter:1600*4C*

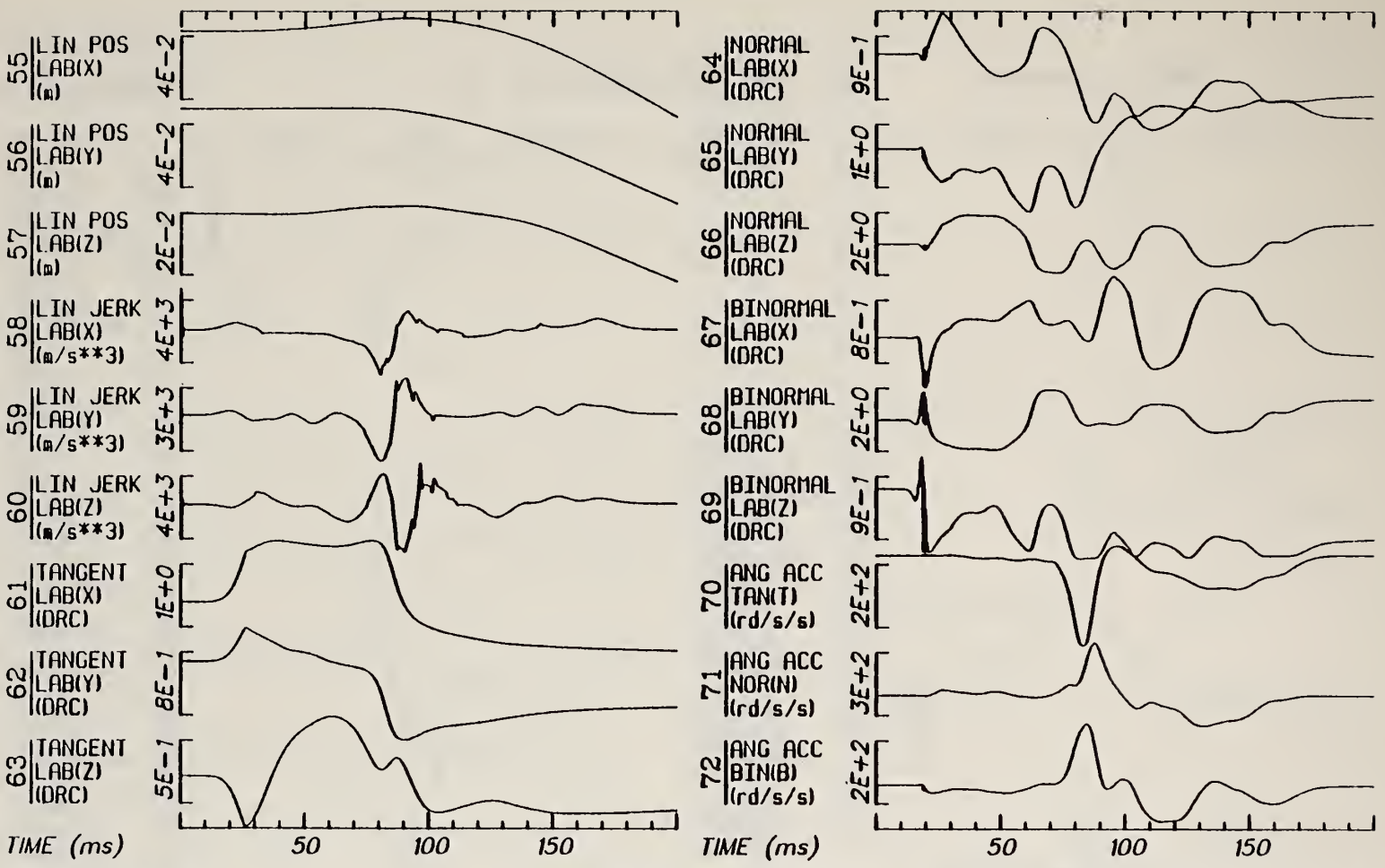

Run ID: 82E044 Disk: 82E044.3 File: 1 Date: MAY 12, 1985 Sheet: 4

*Filter:1600*4C*

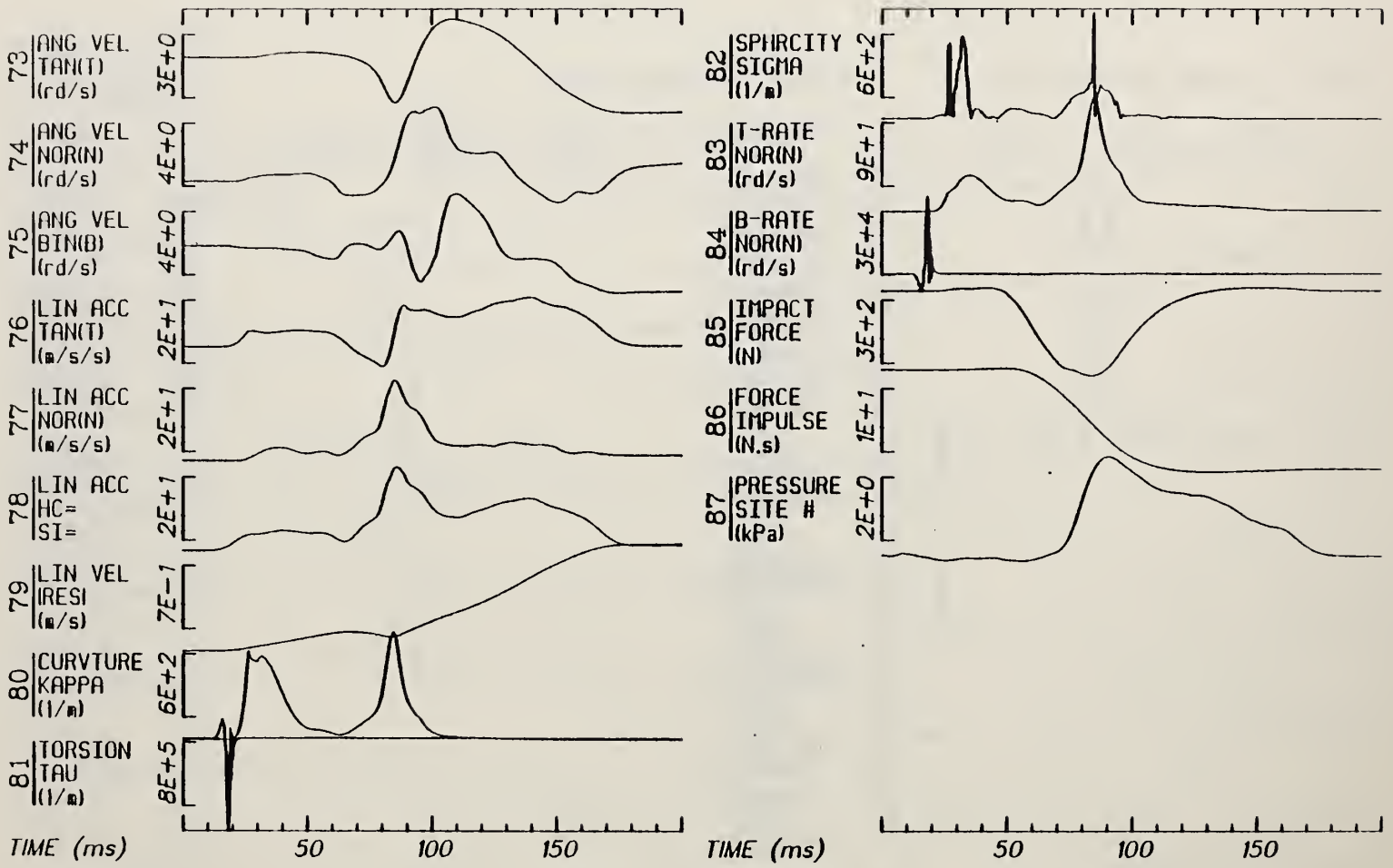

Run ID: 82E044 Disk: 82E044.3 File: 1 Date: MAY 12, 1985 Sheet: 5

*Filter:1600*4C*

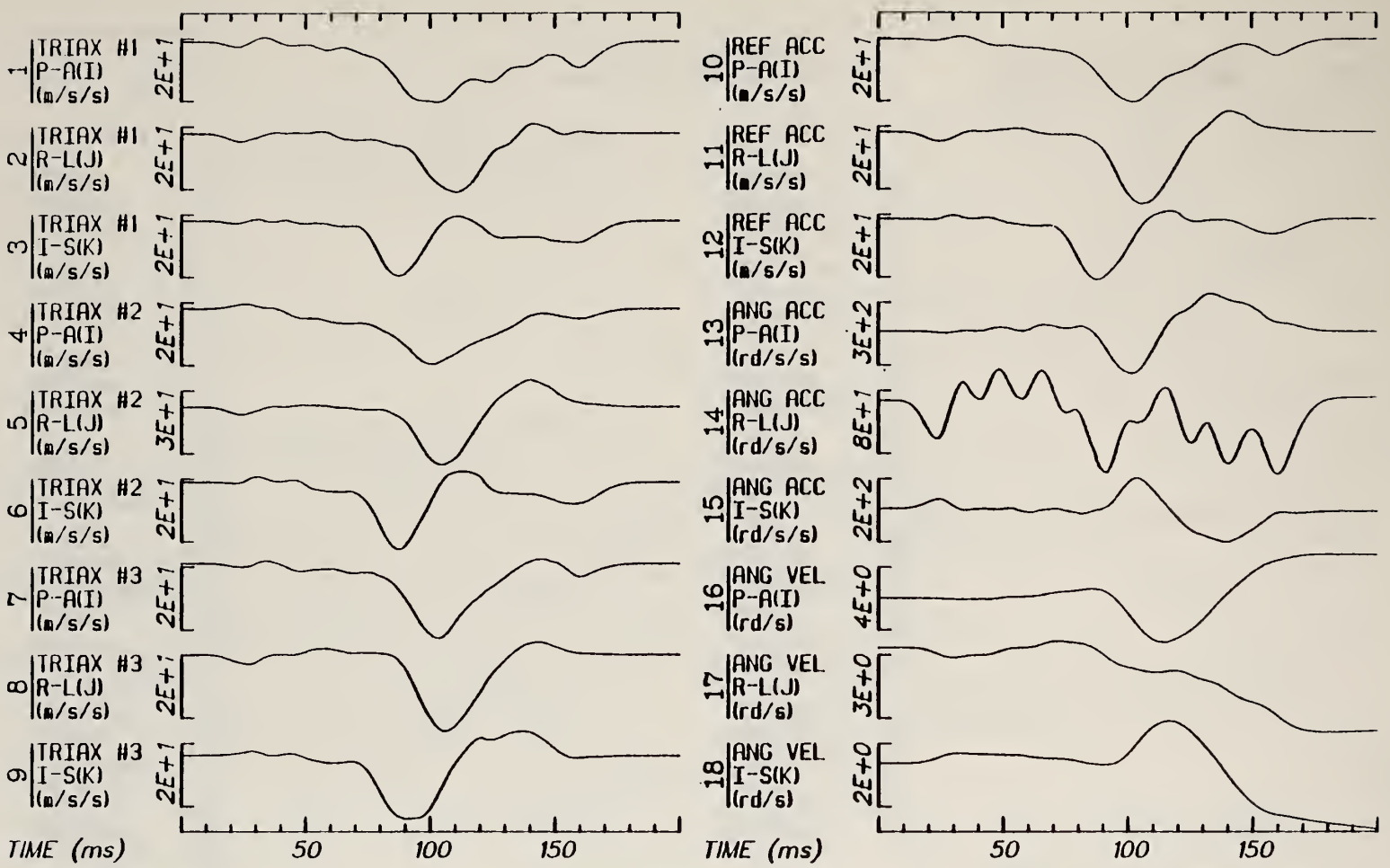

Run ID: 82E045 Disk: 82E045.3 File: 1 Date: MAY 23, 1985 Sheet: 1

*Filter:1600*4C*

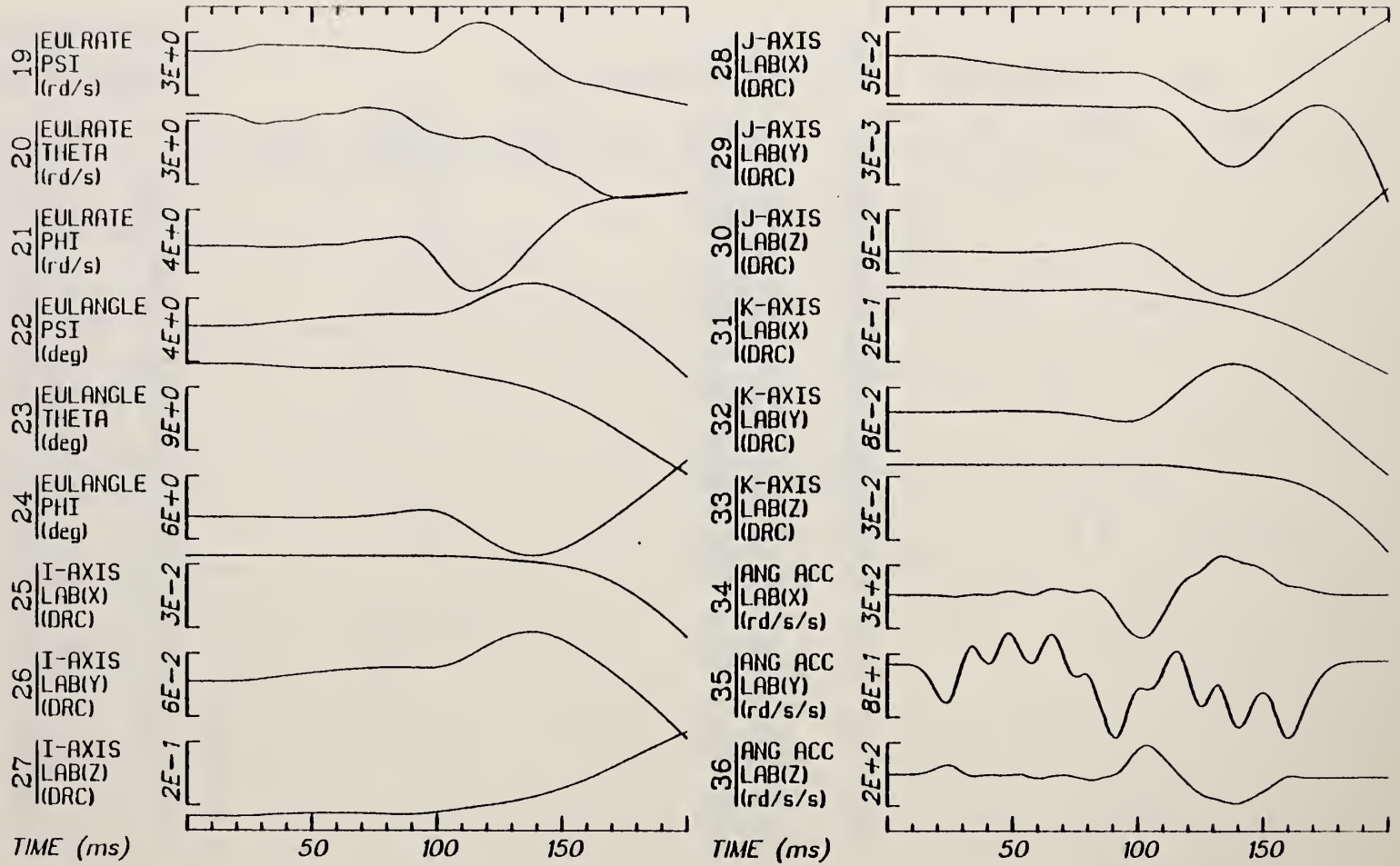

Run ID: 82E045 Disk: 82E045.3 File: 1 Date: MAY 23, 1985 Sheet: 2

*Filter:1600*4C*

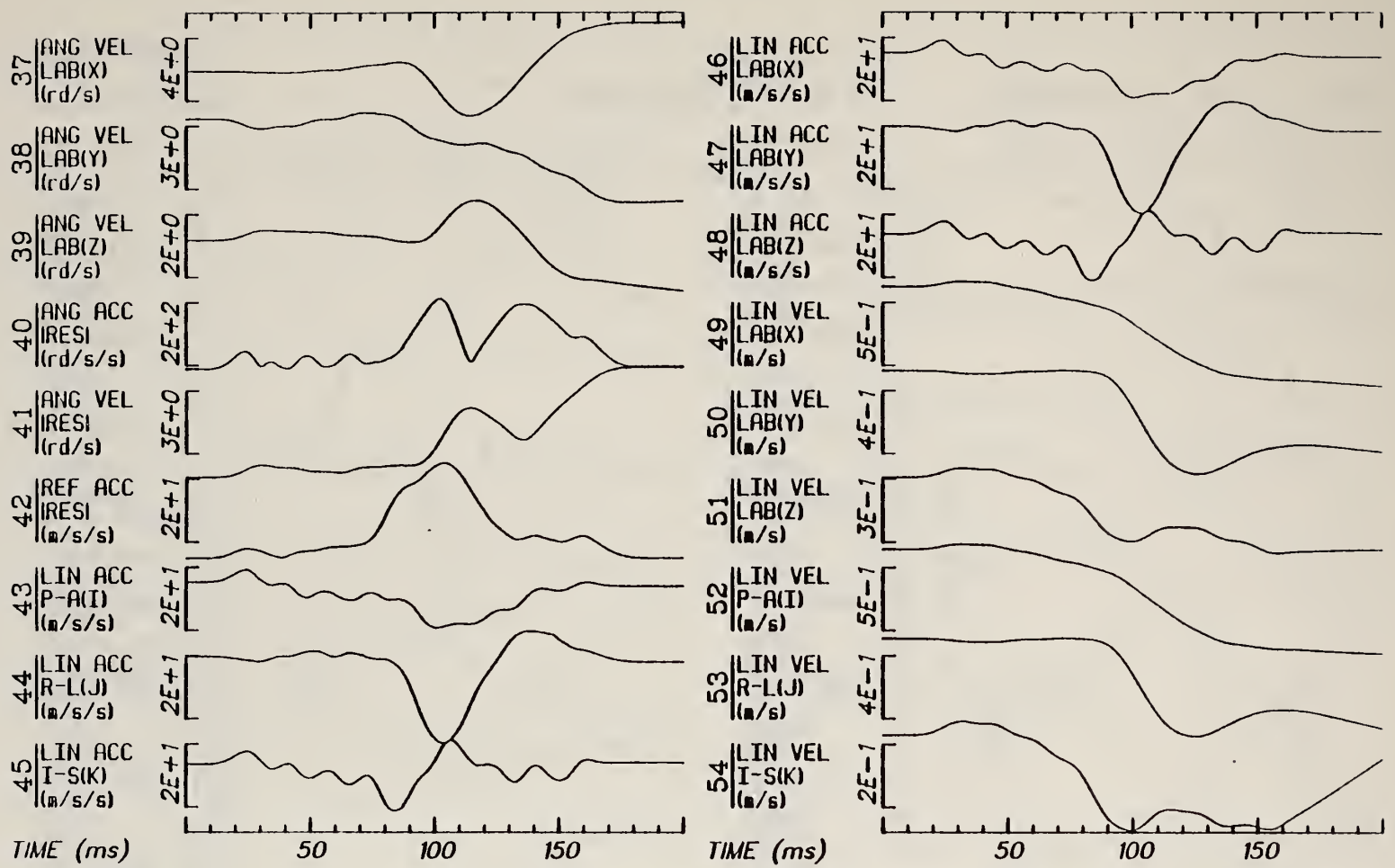

Run ID: 82E045 Disk: 82E045.3 File: 1 Date: MAY 23, 1985 Sheet: 3

*Filter:1600*4C*

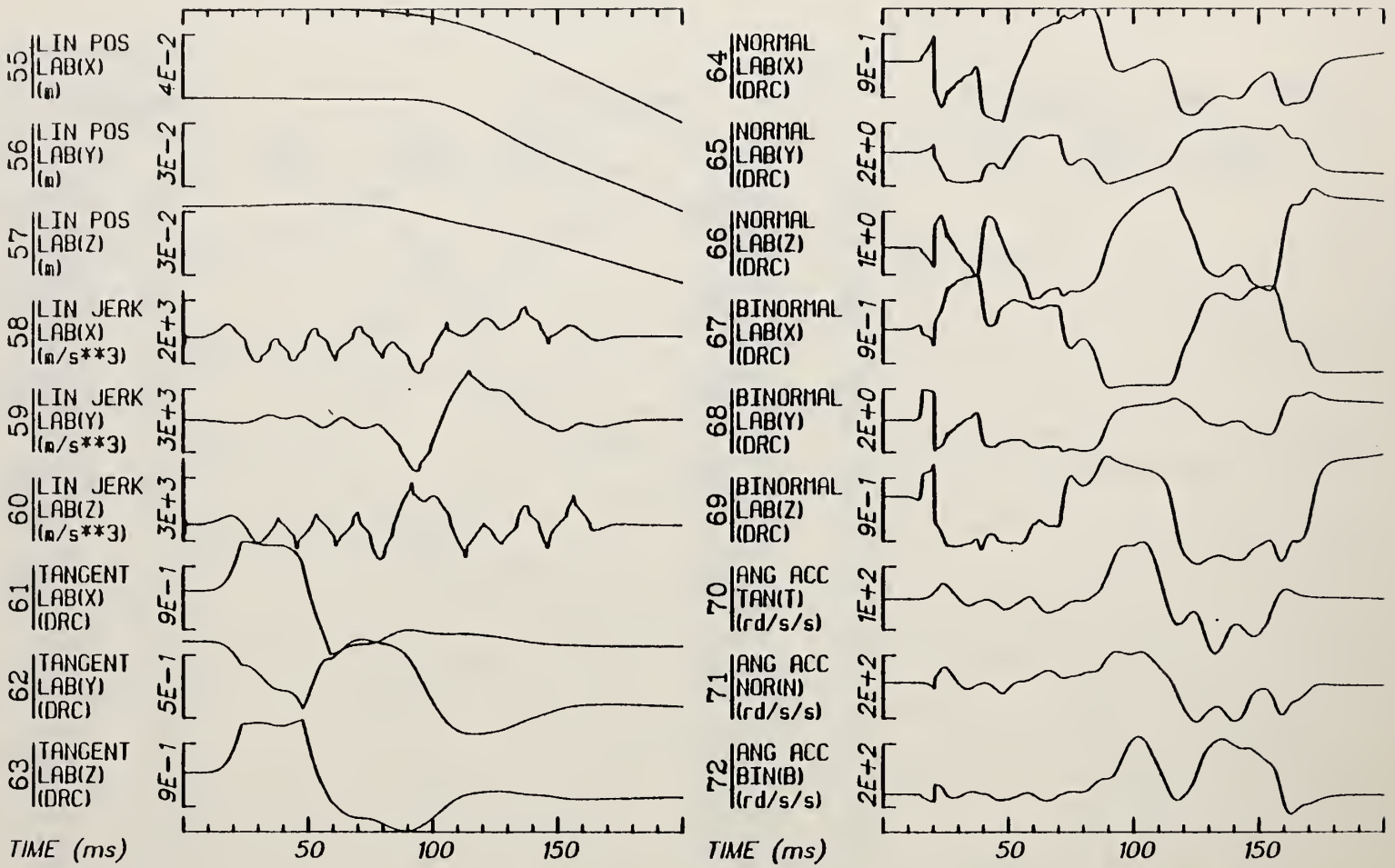

Run ID: 82E045 Disk: 82E045.3 File: 1 Date: MAY 23, 1985 Sheet: 4

*Filter:1600*4C*

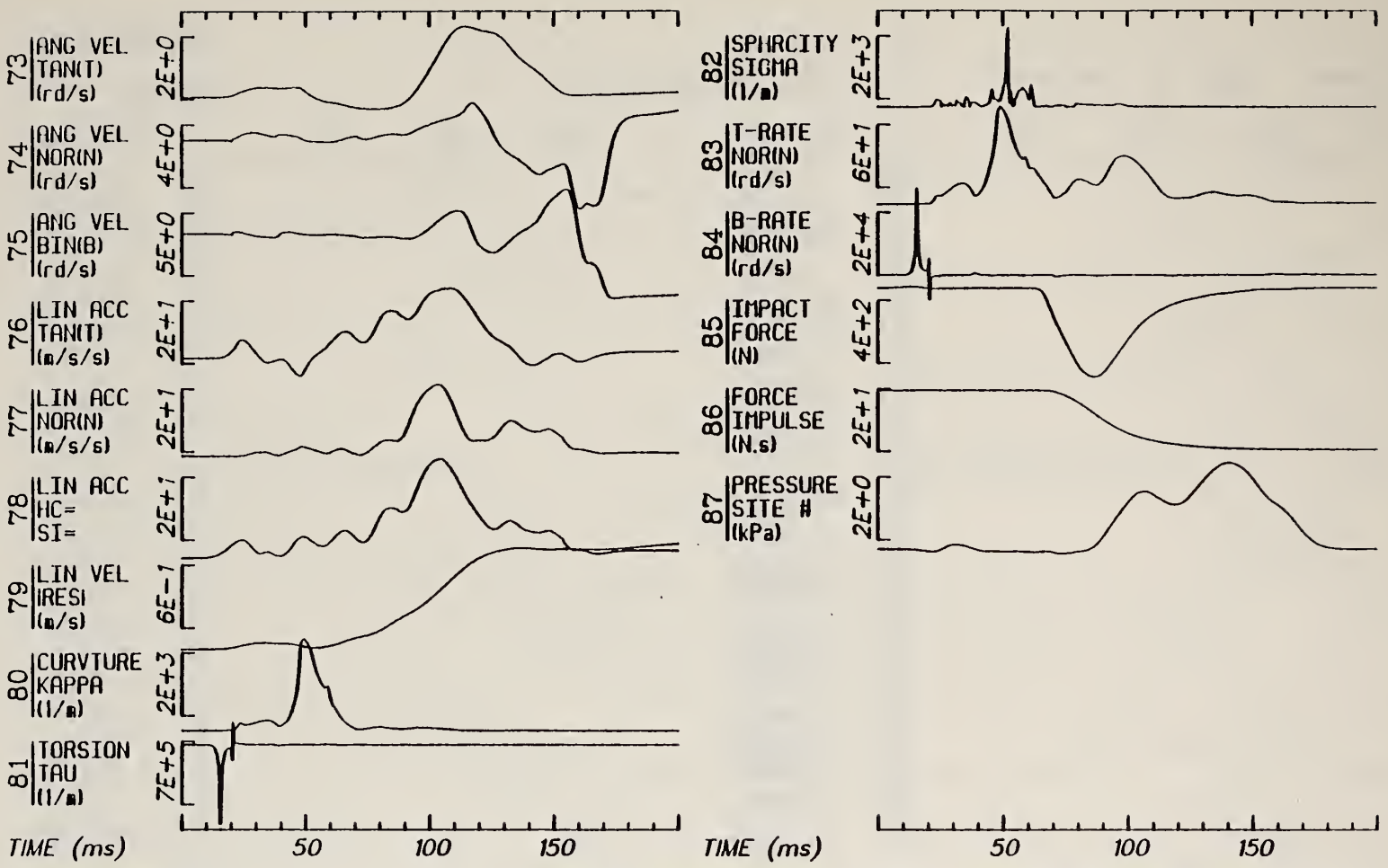

Run ID: 82E045 Disk: 82E045.3 File: 1 Date: MAY 23, 1985 Sheet: 5

Filter:1600*4C

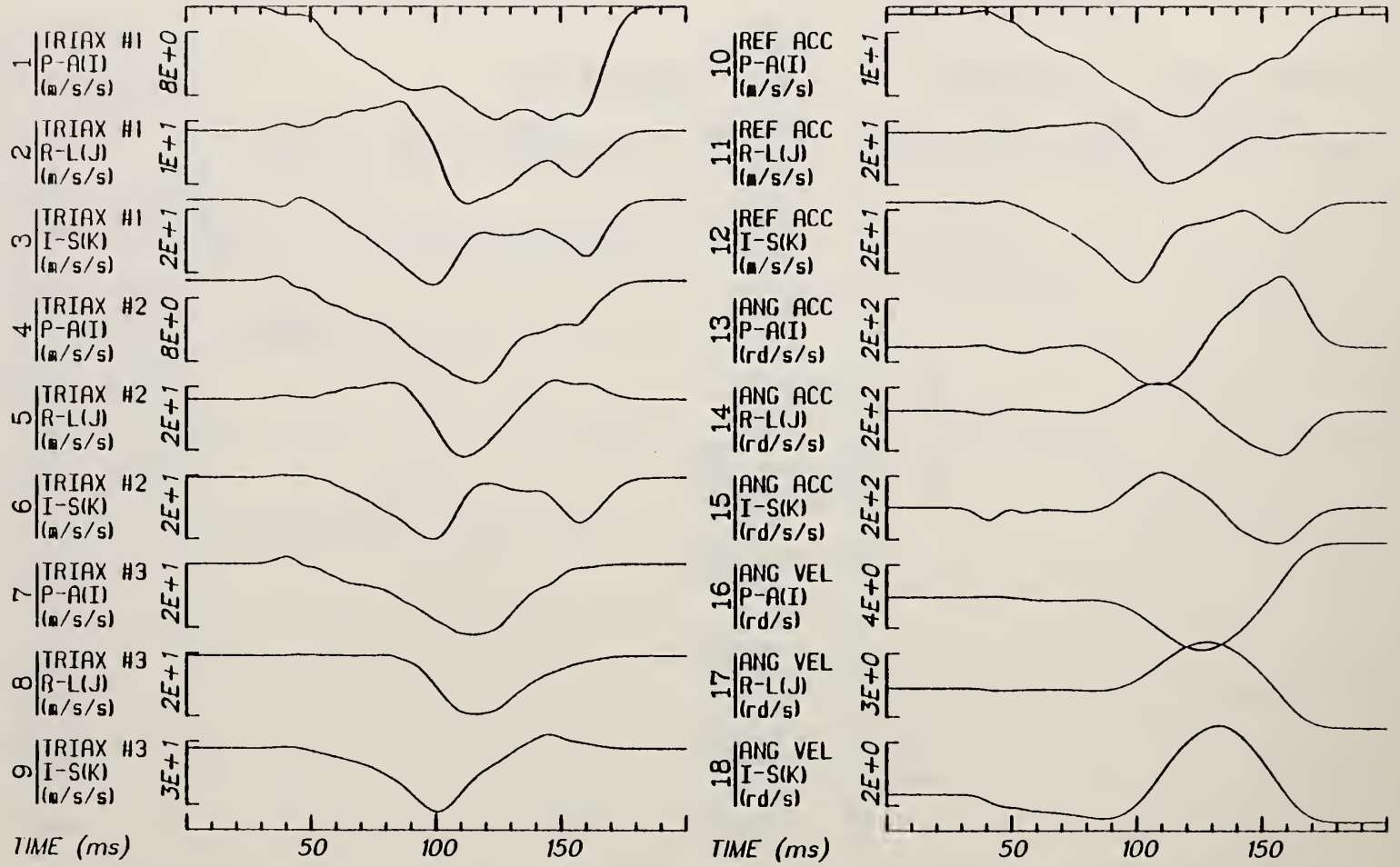

Run ID: 82E046 Disk: 82E045.3 File: 1 Date: MAY 12, 1985 Sheet: 1

*Filter:1600*4C*

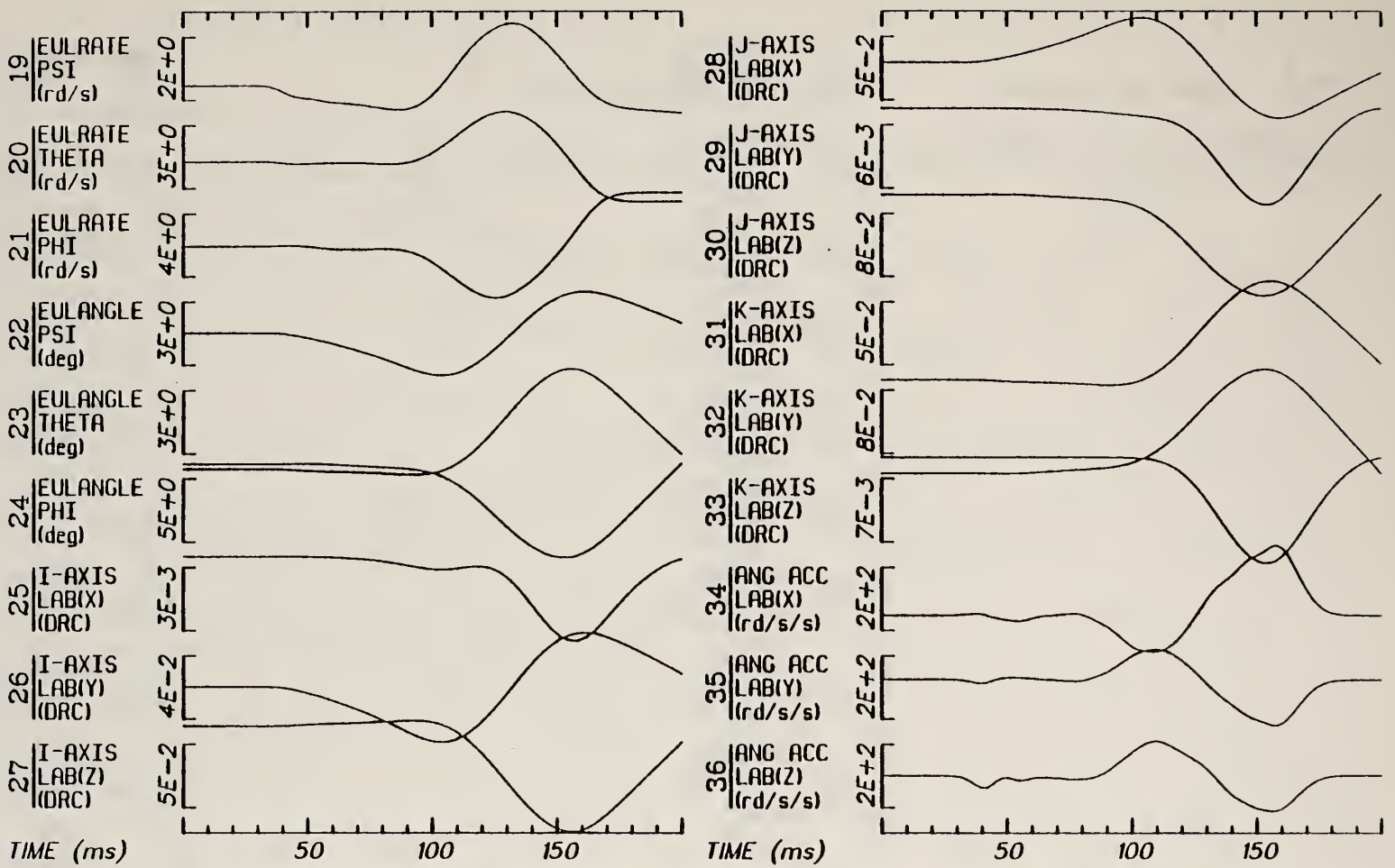

Run ID: 82E046 Disk: 82E045.3 File: 1 Date: MAY 12, 1985 Sheet: 2

*Filter:1600*4C*

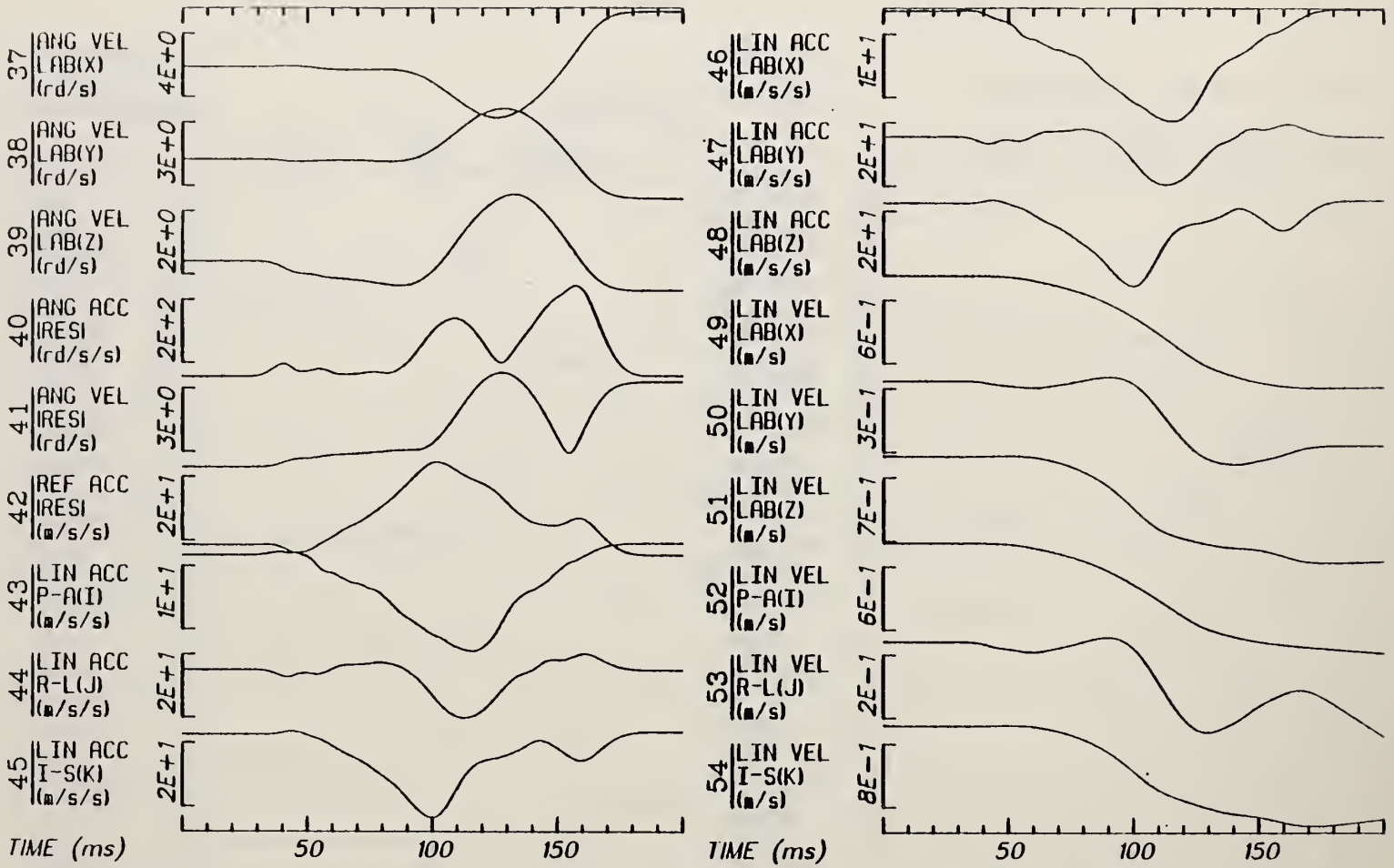

Run ID: 82E046 Disk: 82E045.3 File: 1 Date: MAY 12, 1985 Sheet: 3

*Filter:1600*4C*

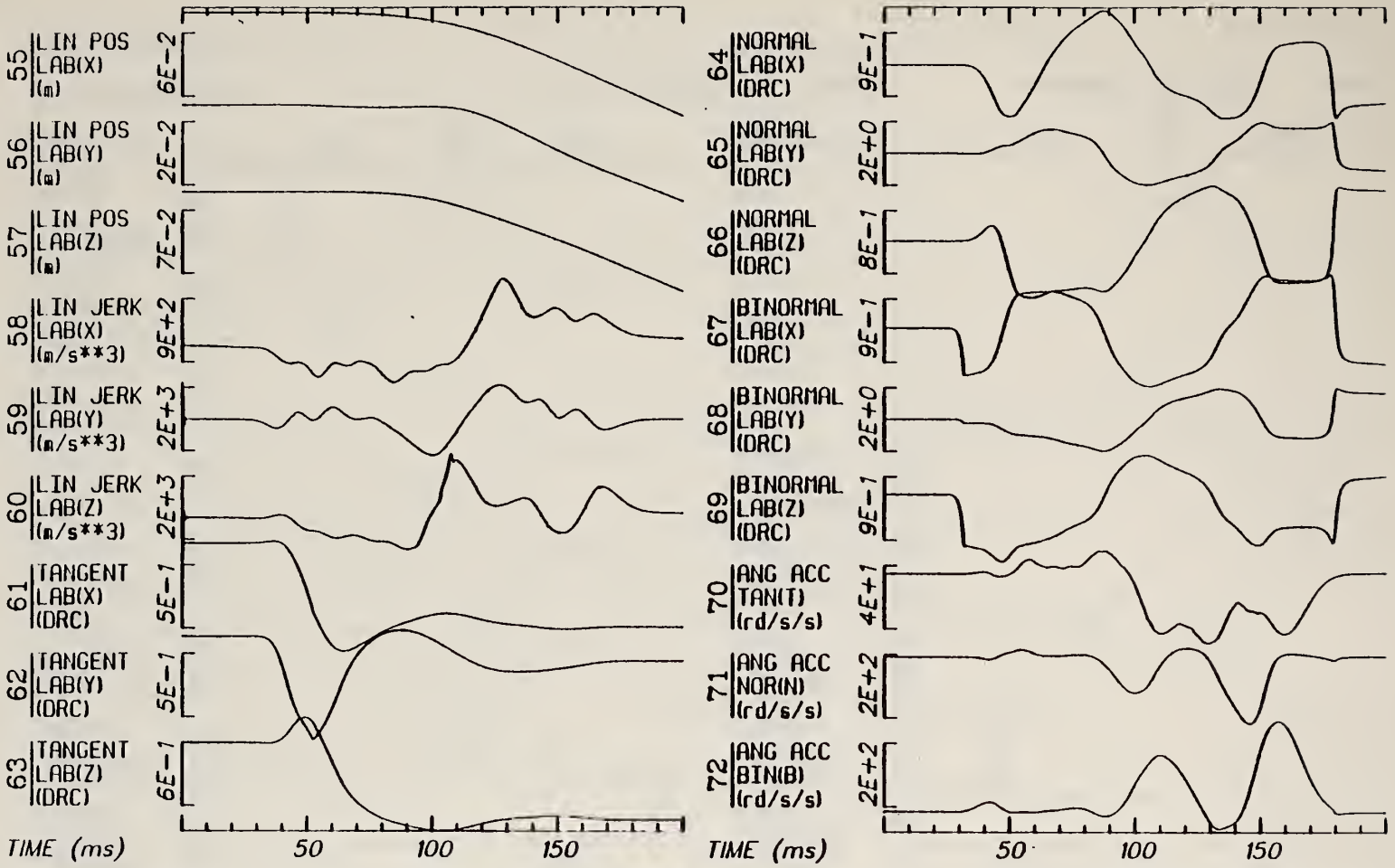

Run ID: 82E046 Disk: 82E045.3 File: 1 Date: MAY 12, 1985 Sheet: 4

*Filter:1600*4C*

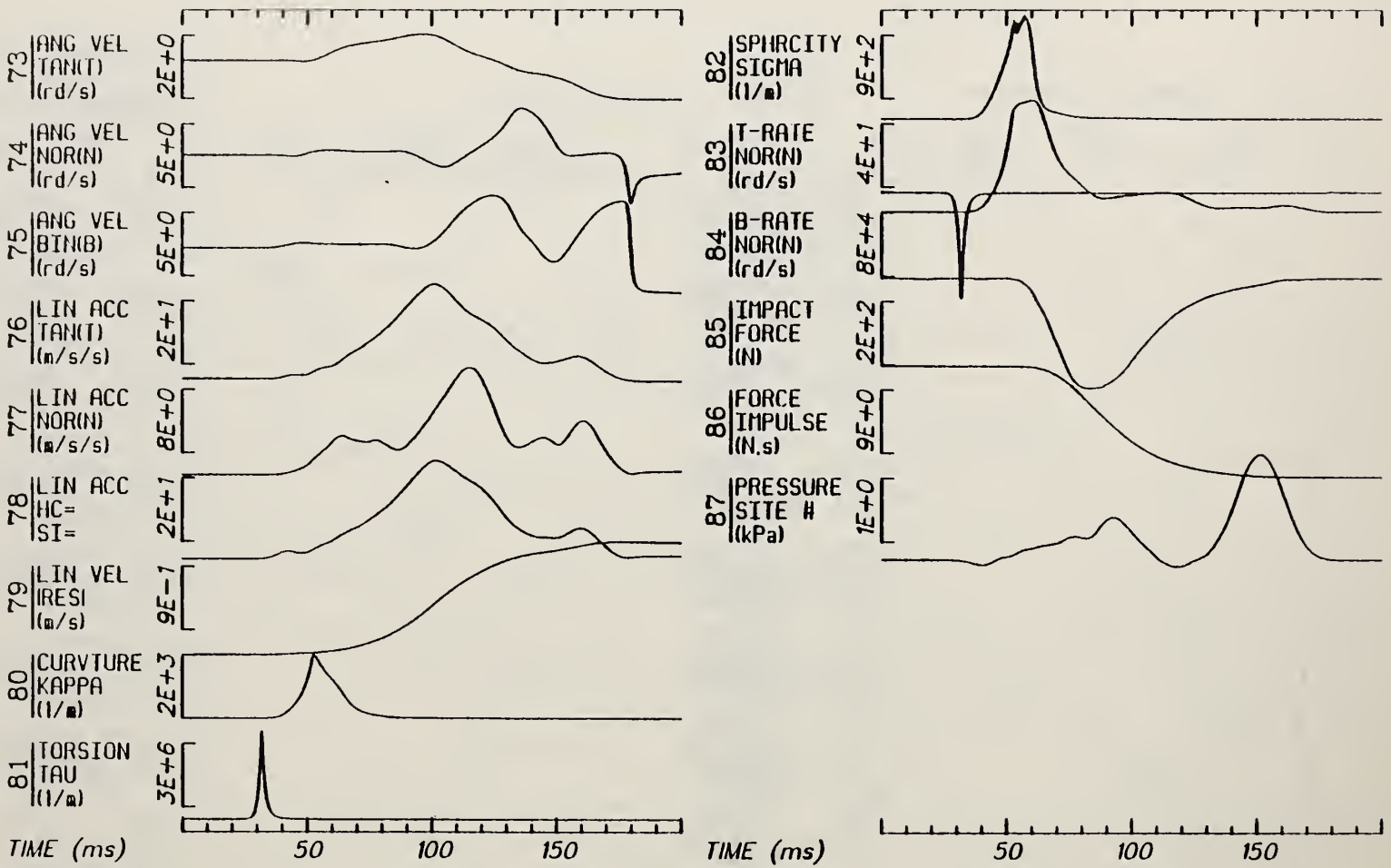

Run ID: 82E046 Disk: 82E045.3 File: 1 Date: MAY 12, 1985 Sheet: 5

*Filter:1600*4C*

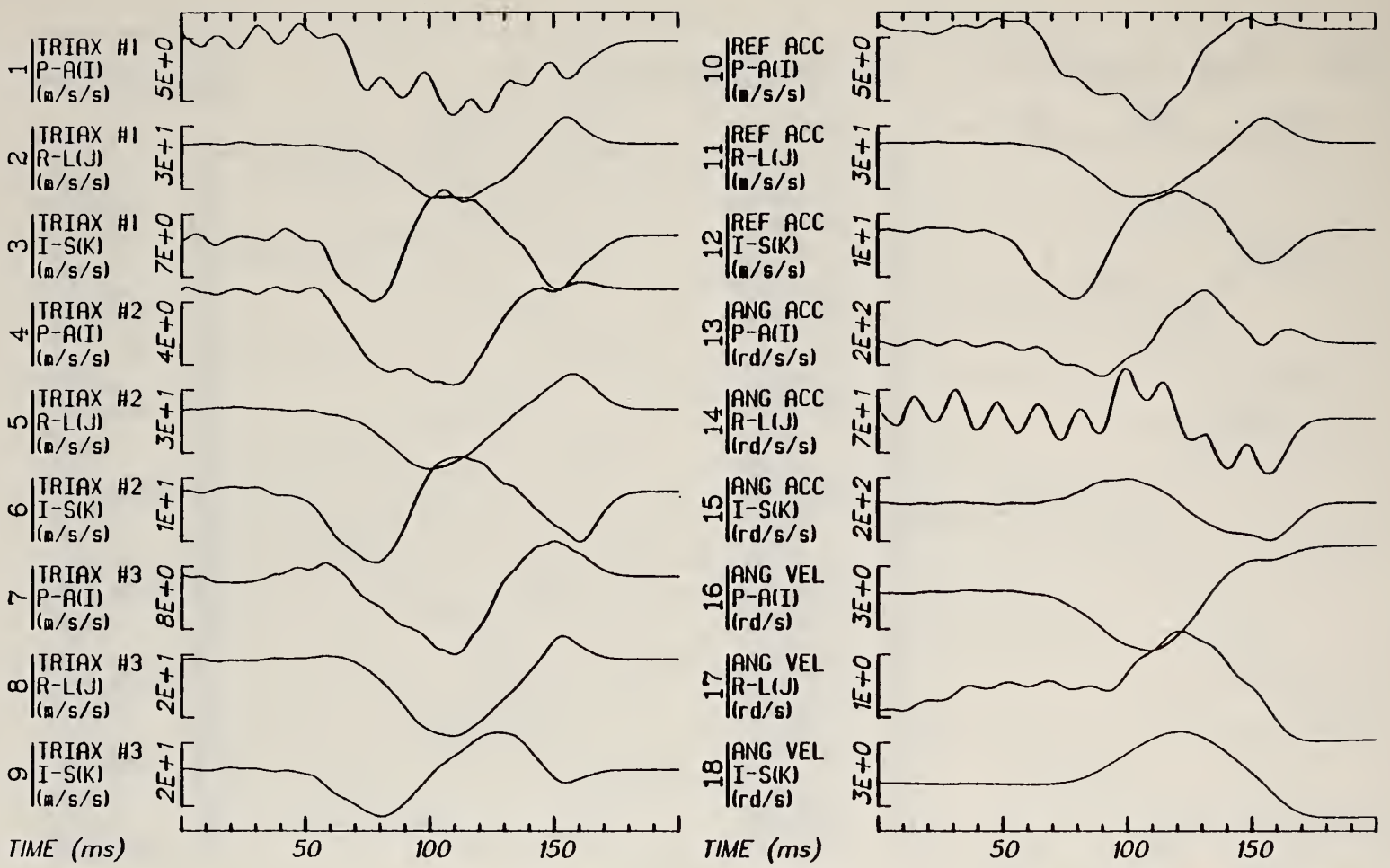

Run ID: 82E047 Disk: 82E046.3 File: 1 Date: MAY 12, 1985 Sheet: 1

*Filter:1600*4C*

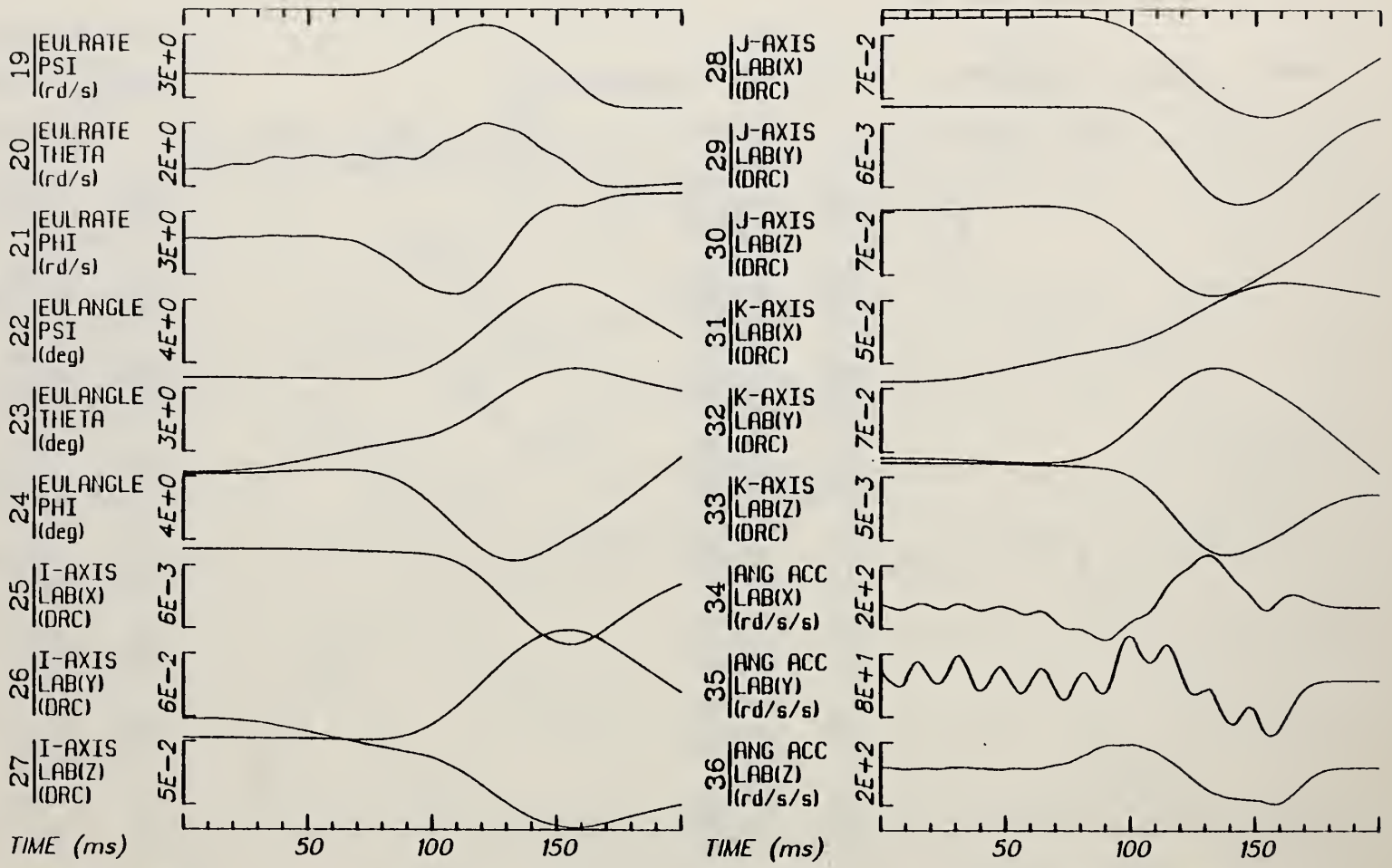

Run ID: 82E047 Disk: 82E046.3 File: 1 Date: MAY 12, 1985 Sheet: 2

*Filter:1600*4C*

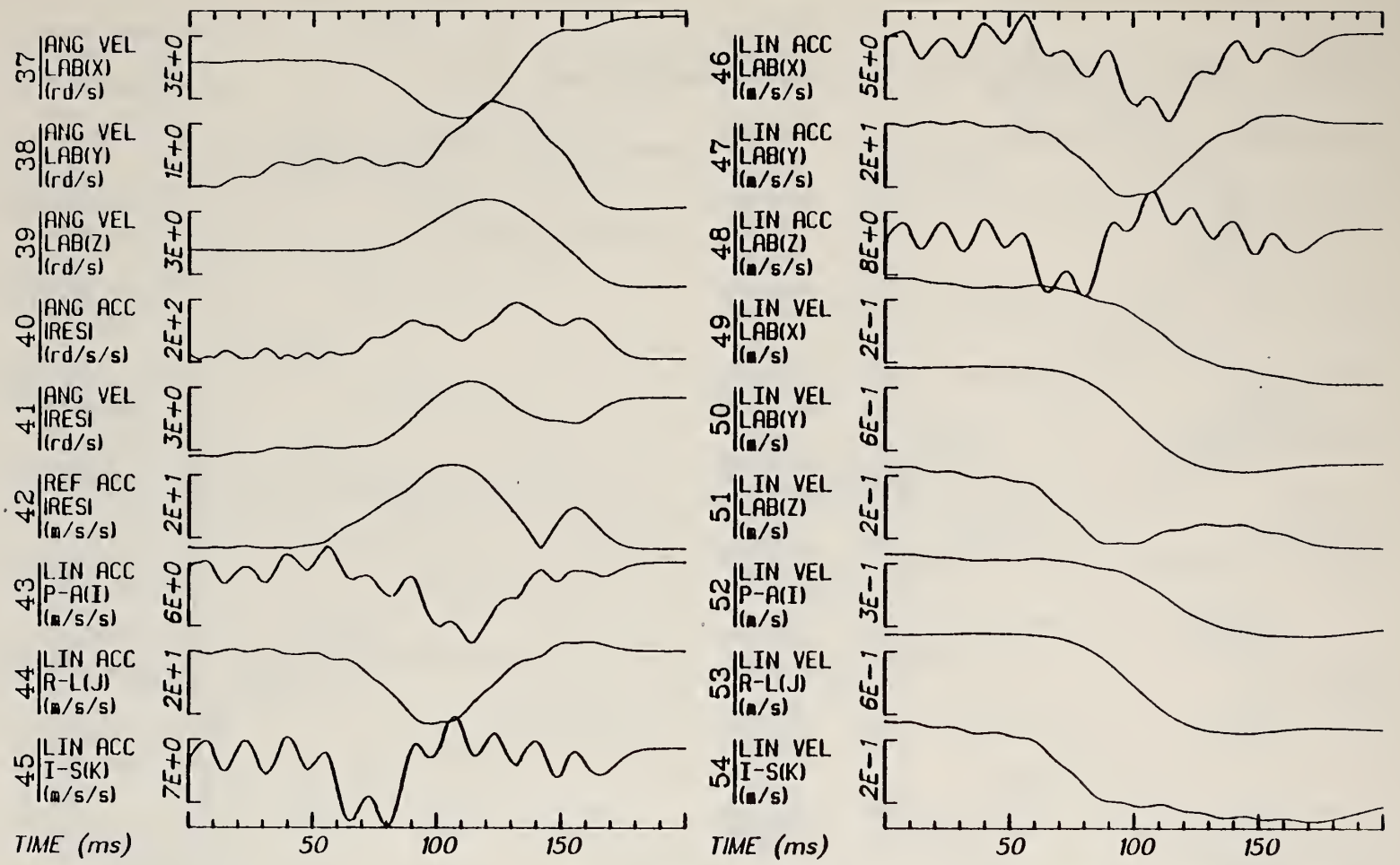

Run ID: 82E047 Disk: 82E046.3 File: 1 Date: MAY 12, 1985 Sheet: 3

*Filter: 1600*4C*

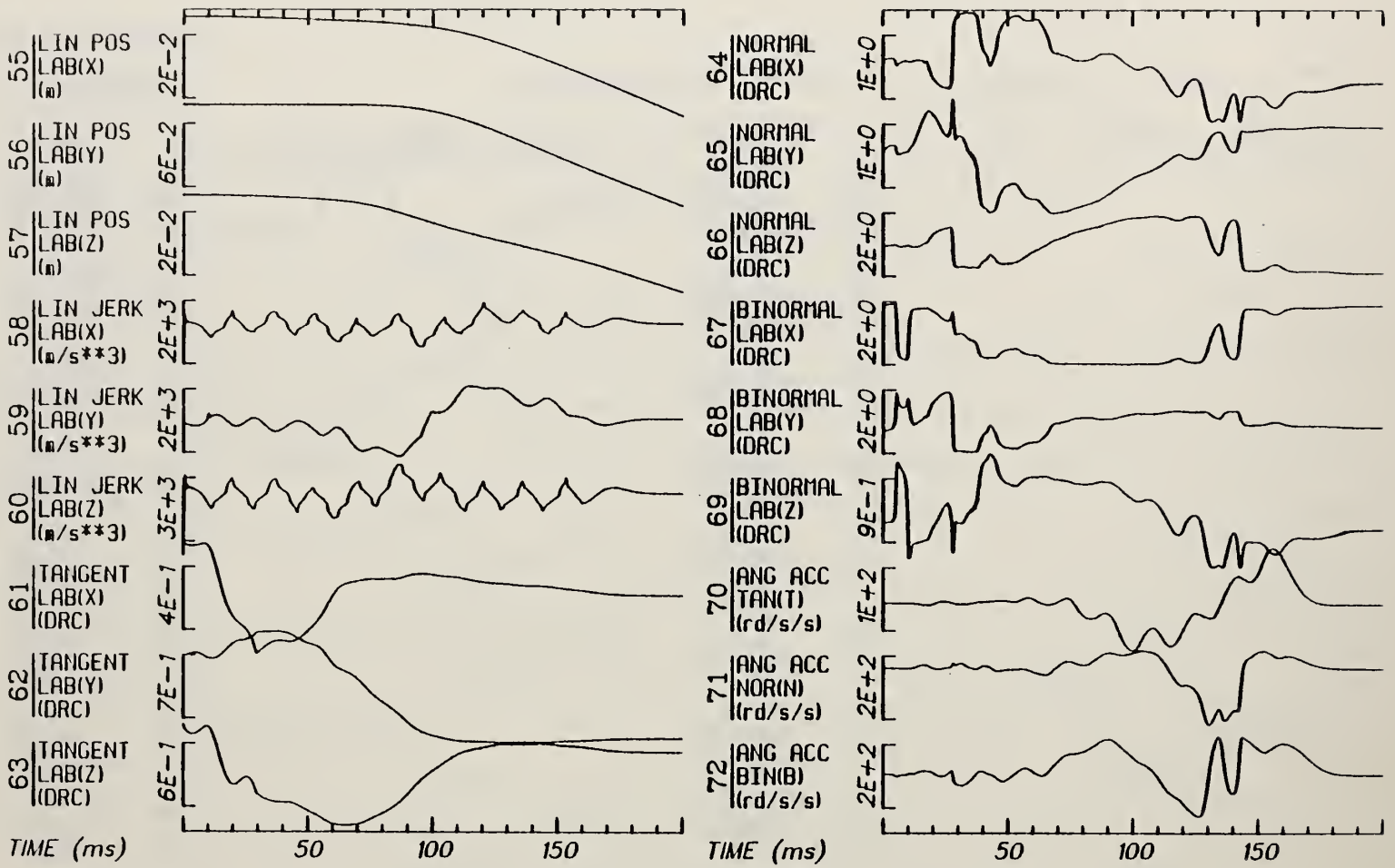

Run ID: 82E047 Disk: 82E046.3 File: 1 Date: MAY 12, 1985 Sheet: 4

*Filter:1600*4C*

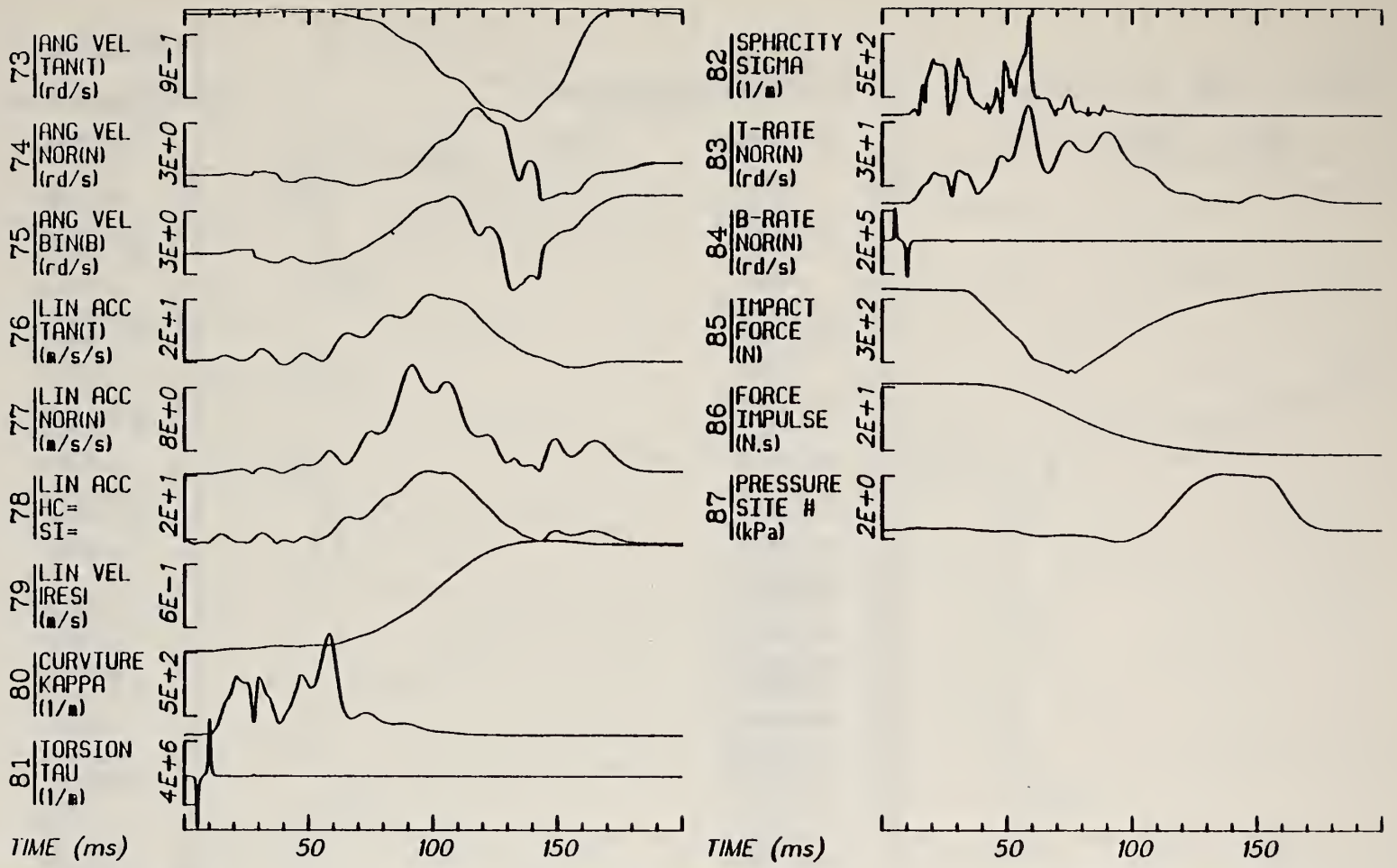

Run ID: 82E047 Disk: 82E046.3 File: 1 Date: MAY 12, 1985 Sheet: 5

*Filter:1600*4C*

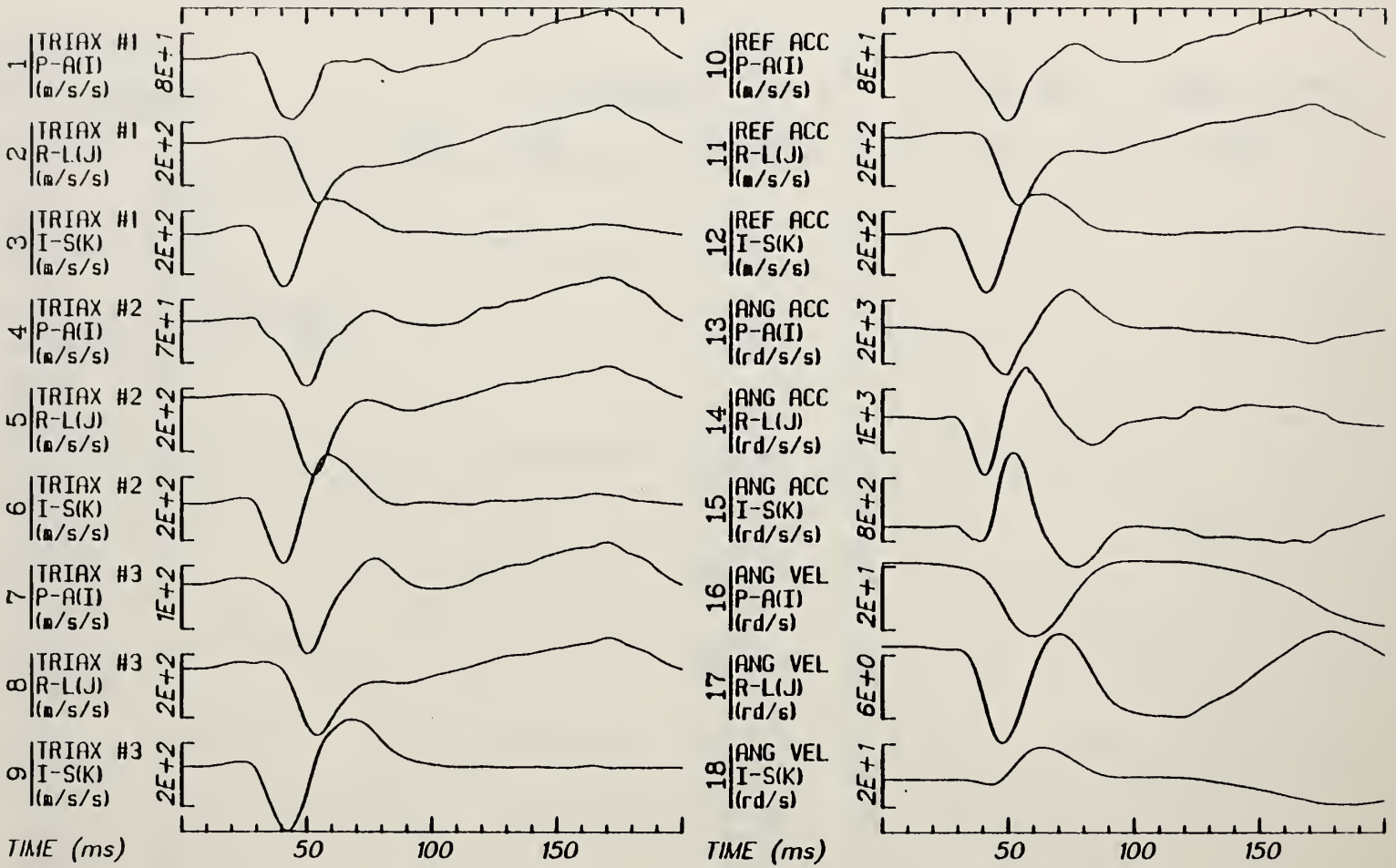

Run ID: 82E048 Disk: 82E048.3 File: 1 Date: MAY 23, 1985 Sheet: 1

*Filter:1600*4C*

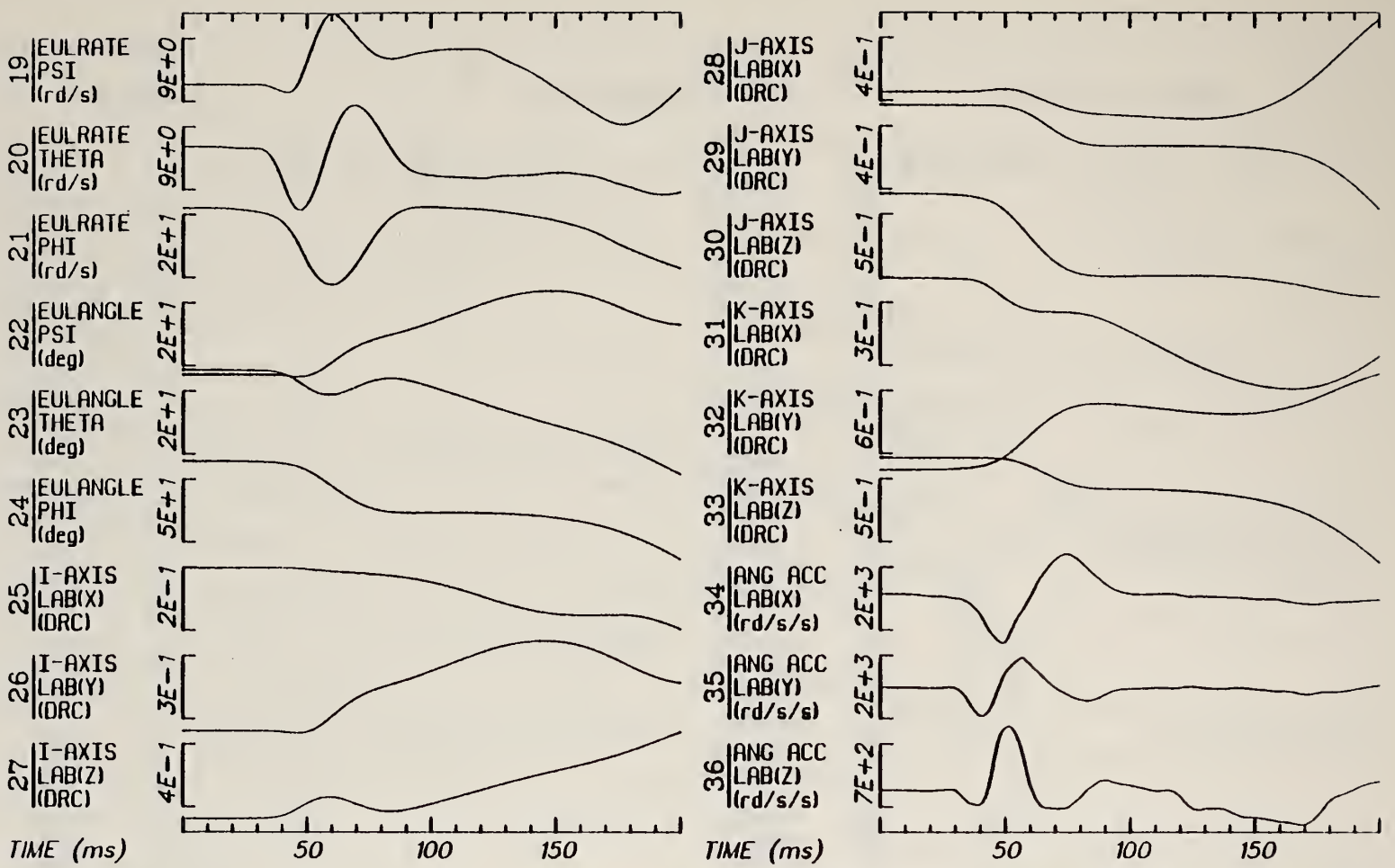

Run ID: 82E048 Disk: 82E048.3 File: 1 Date: MAY 23, 1985 Sheet: 2

*Filter:1600*4C*

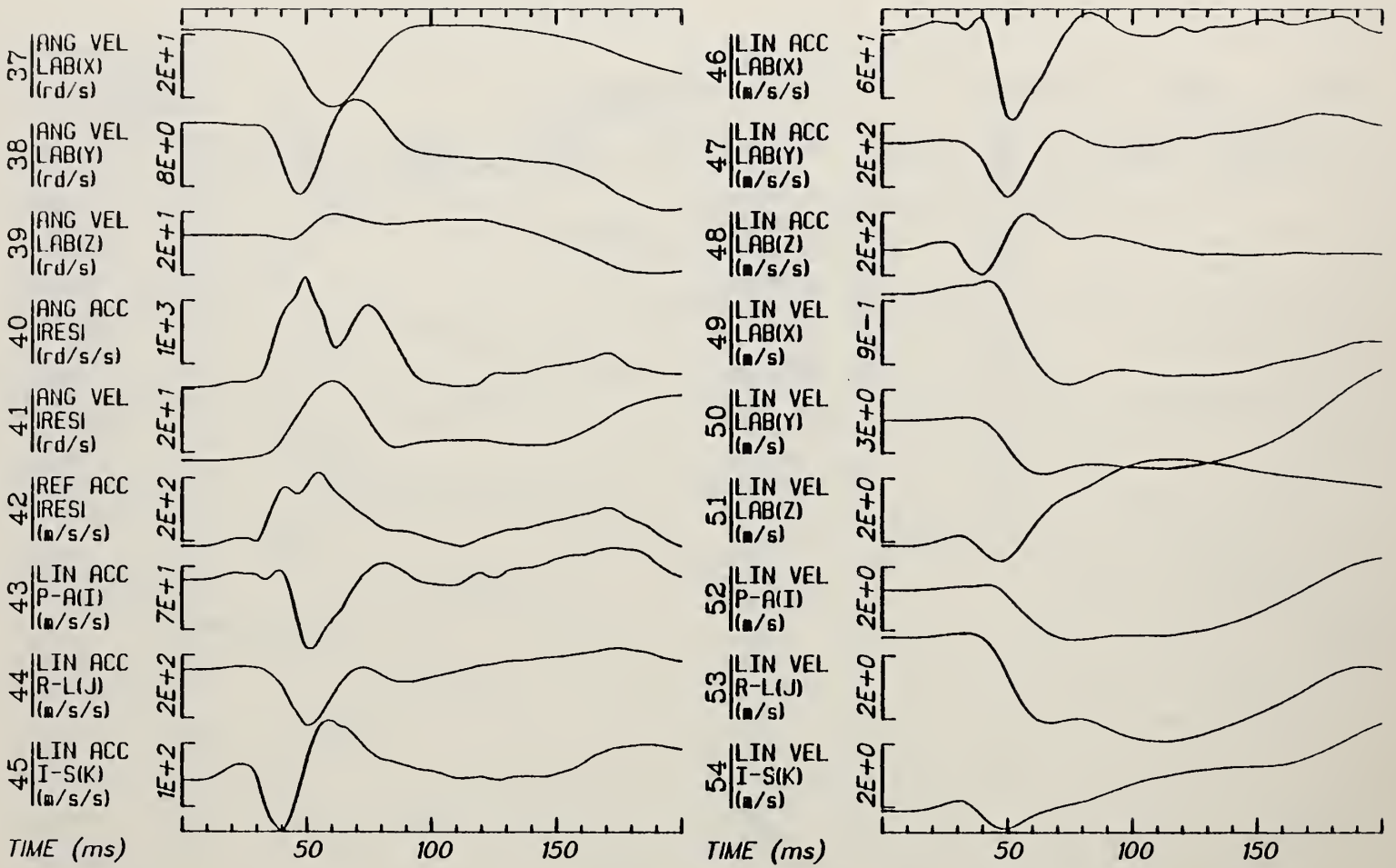

Run ID: 82E048 Disk: 82E048.3 File: 1 Date: MAY 23, 1985 Sheet: 3

*Filter:1600*4C*

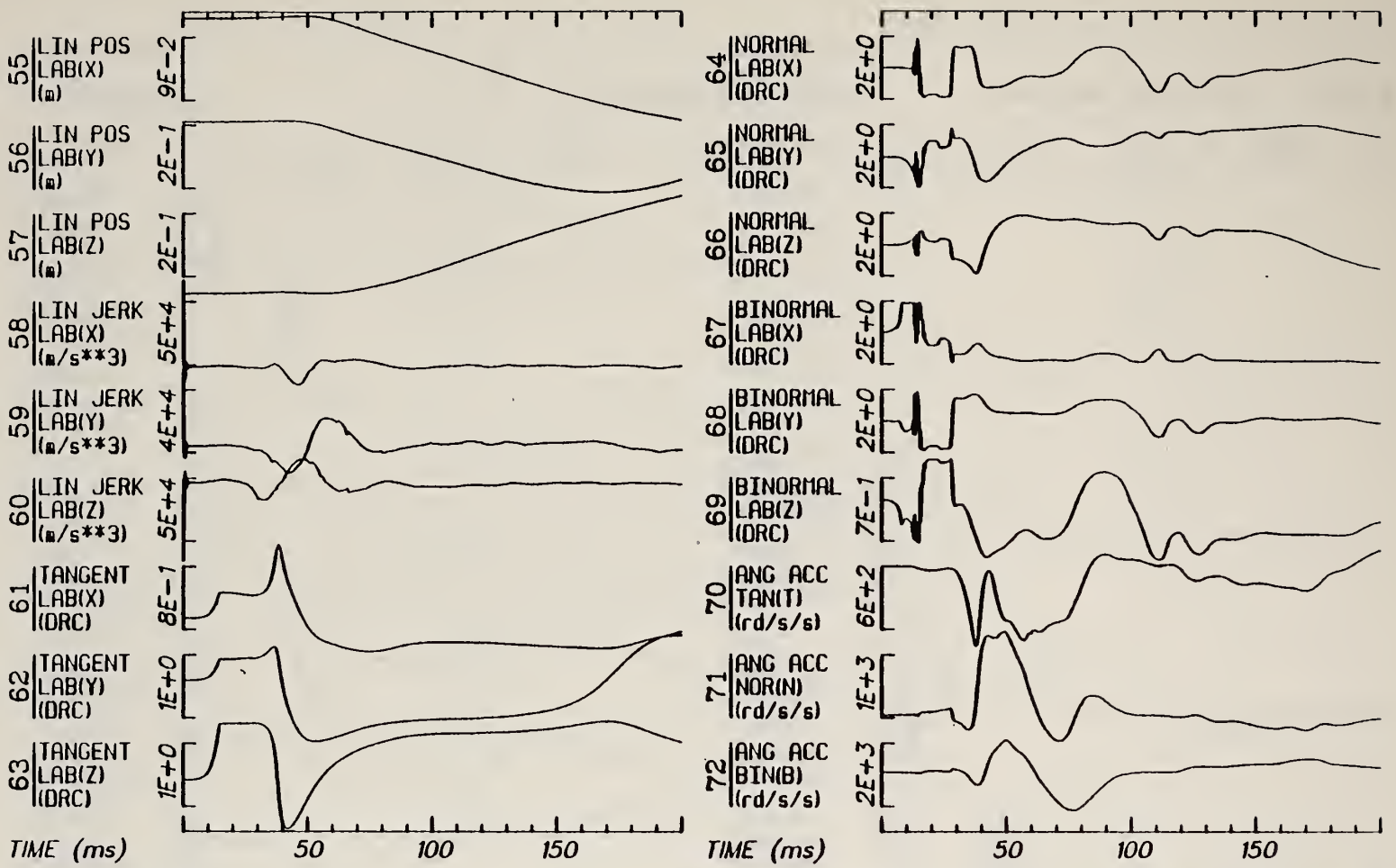

Run ID: 82E048 Disk: 82E048.3 File: 1 Date: MAY 23, 1985 Sheet: 4

*Filter:1600*4C*

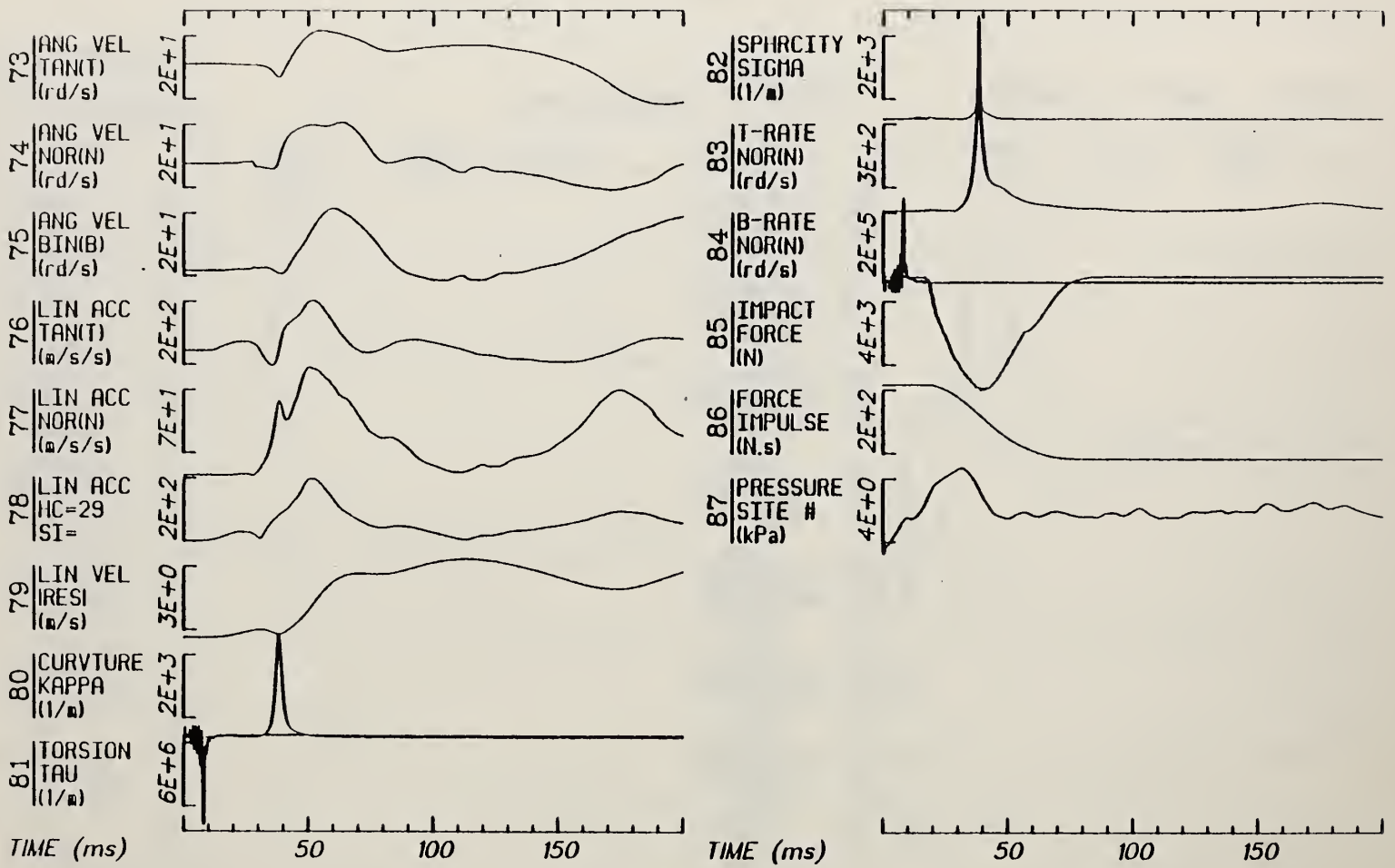

Run ID: 82E048 Disk: 82E048.3 File: 1 Date: MAY 23, 1985 Sheet: 5

*Filter:1600*4C*

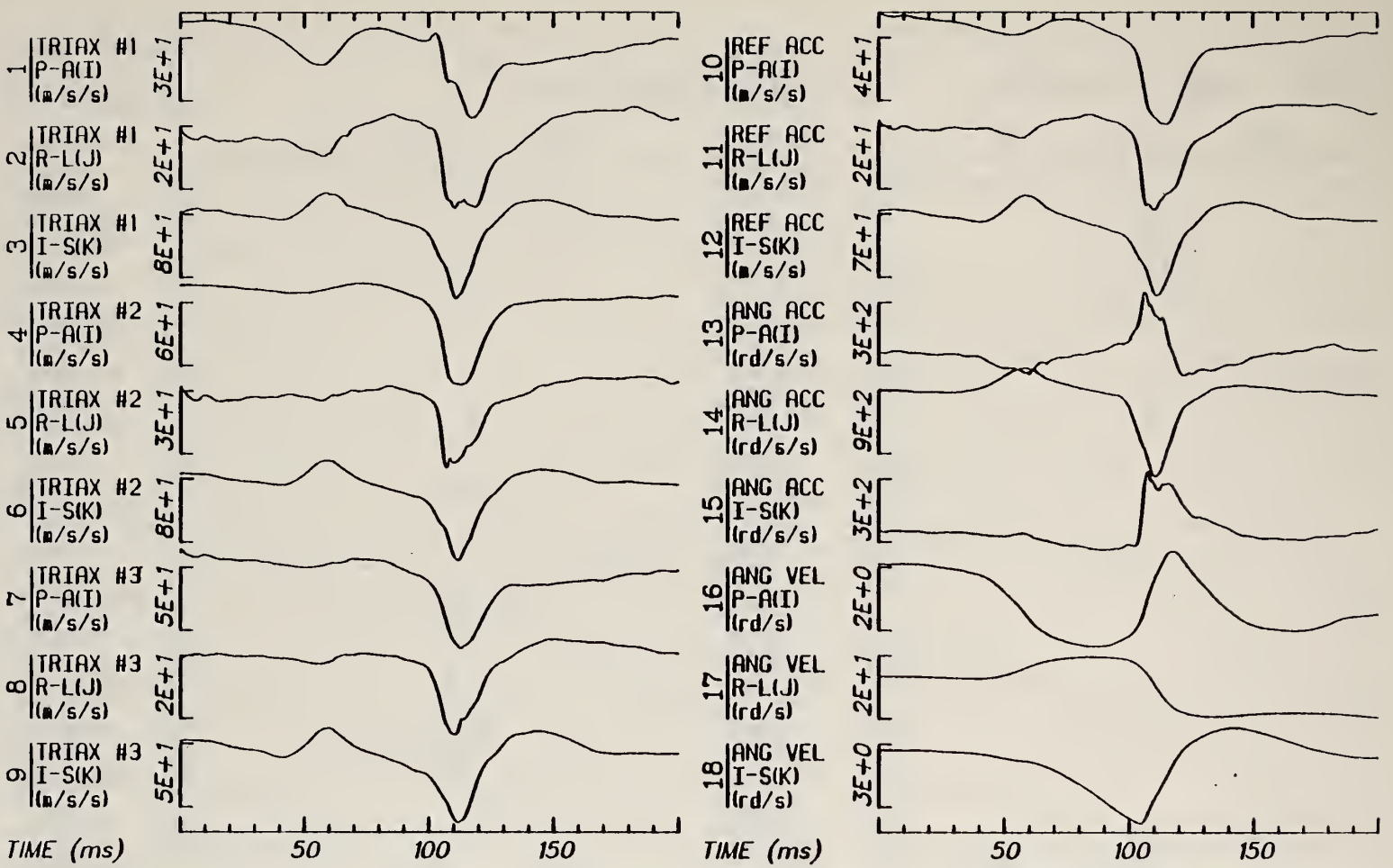

Run ID: 82E063 Disk: 82E063.3 File: 1 Date: MAY 23, 1985 Sheet: 1

*Filter:1600*4C*

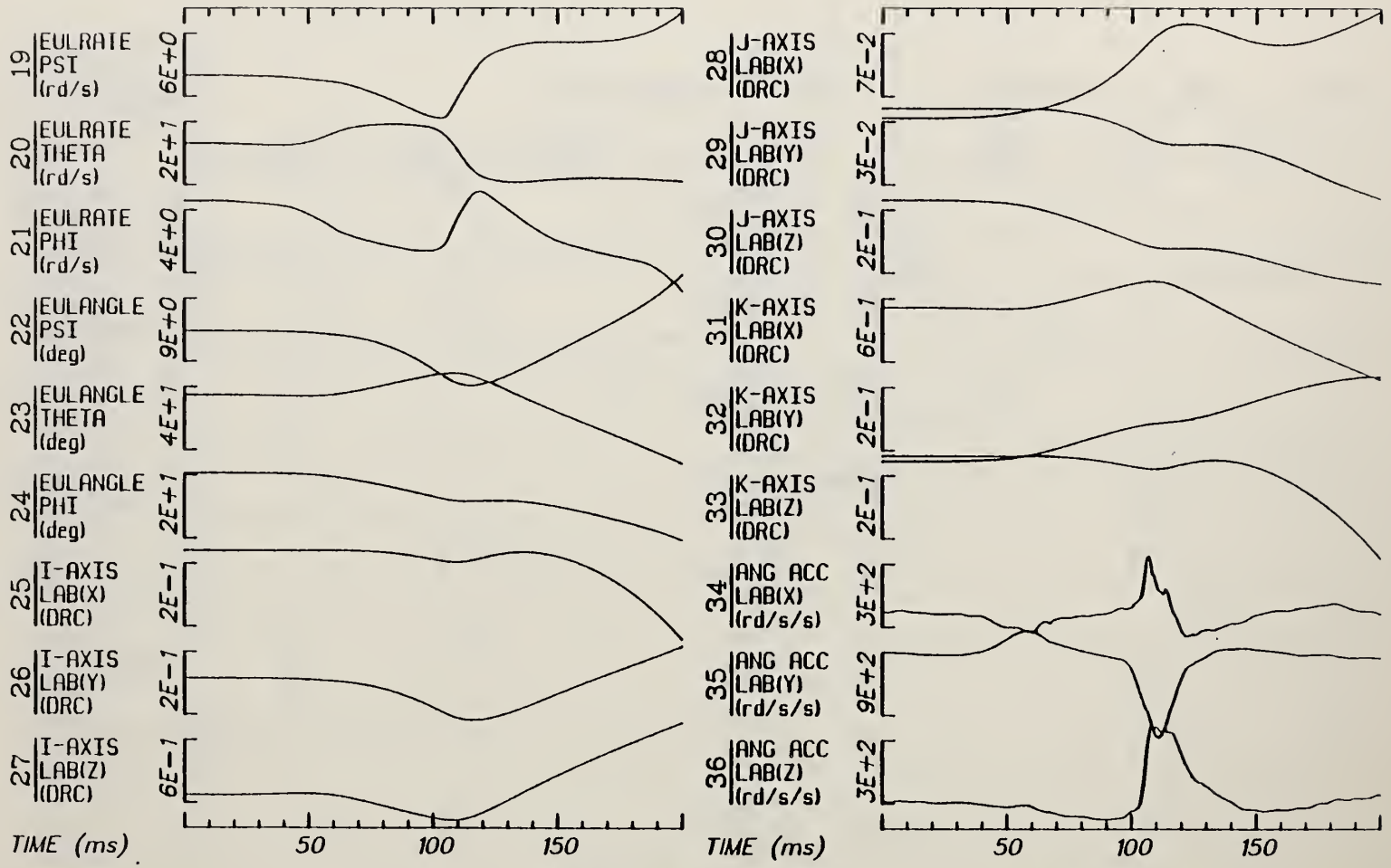

Run ID: 82E063 Disk: 82E063.3 File: 1 Date: MAY 23, 1985 Sheet: 2

*Filter:1600*4C*

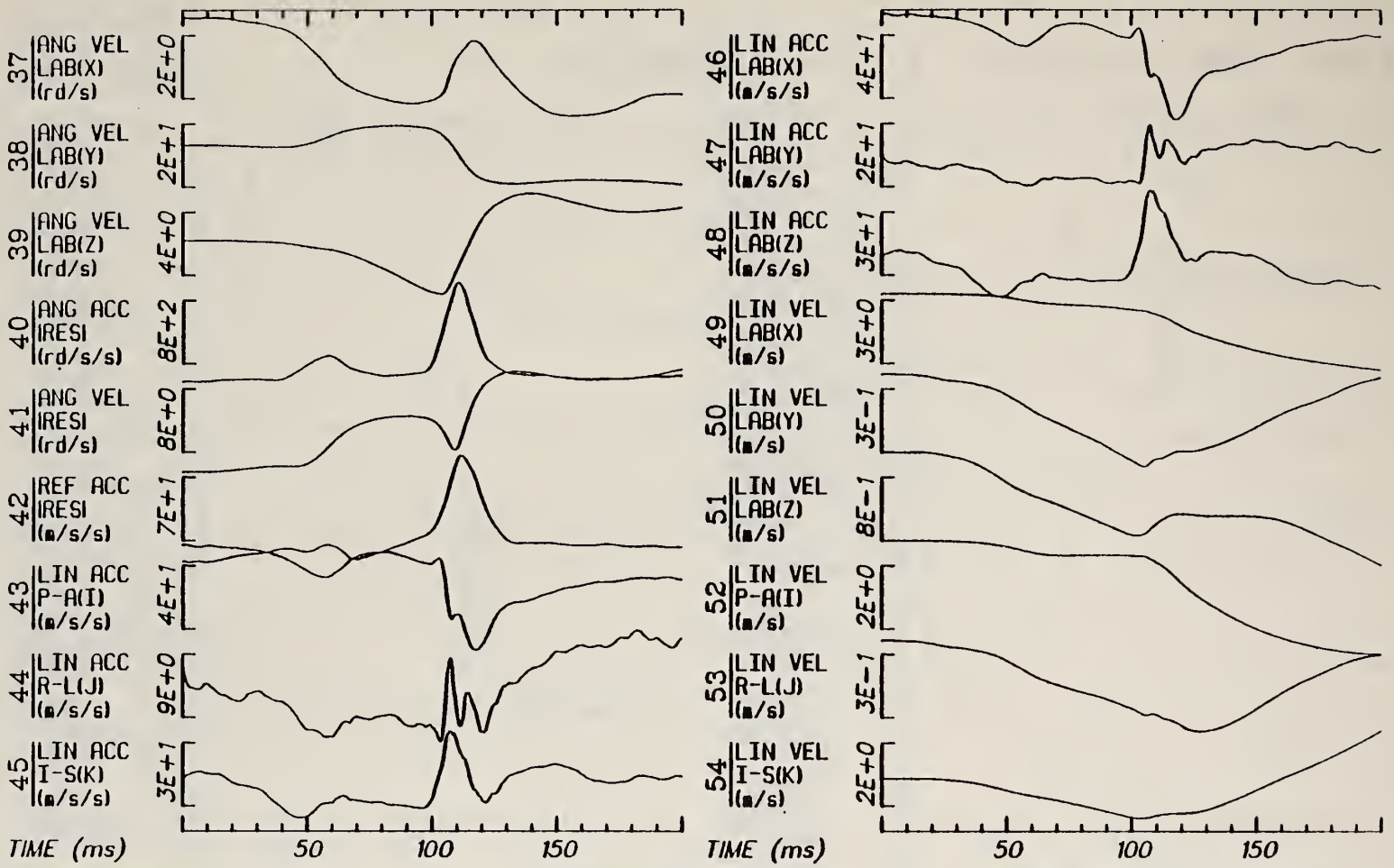

Run ID: 82E063 Disk: 82E063.3 File: 1 Date: MAY 23, 1985 Sheet: 3

*Filter:1600*4C*

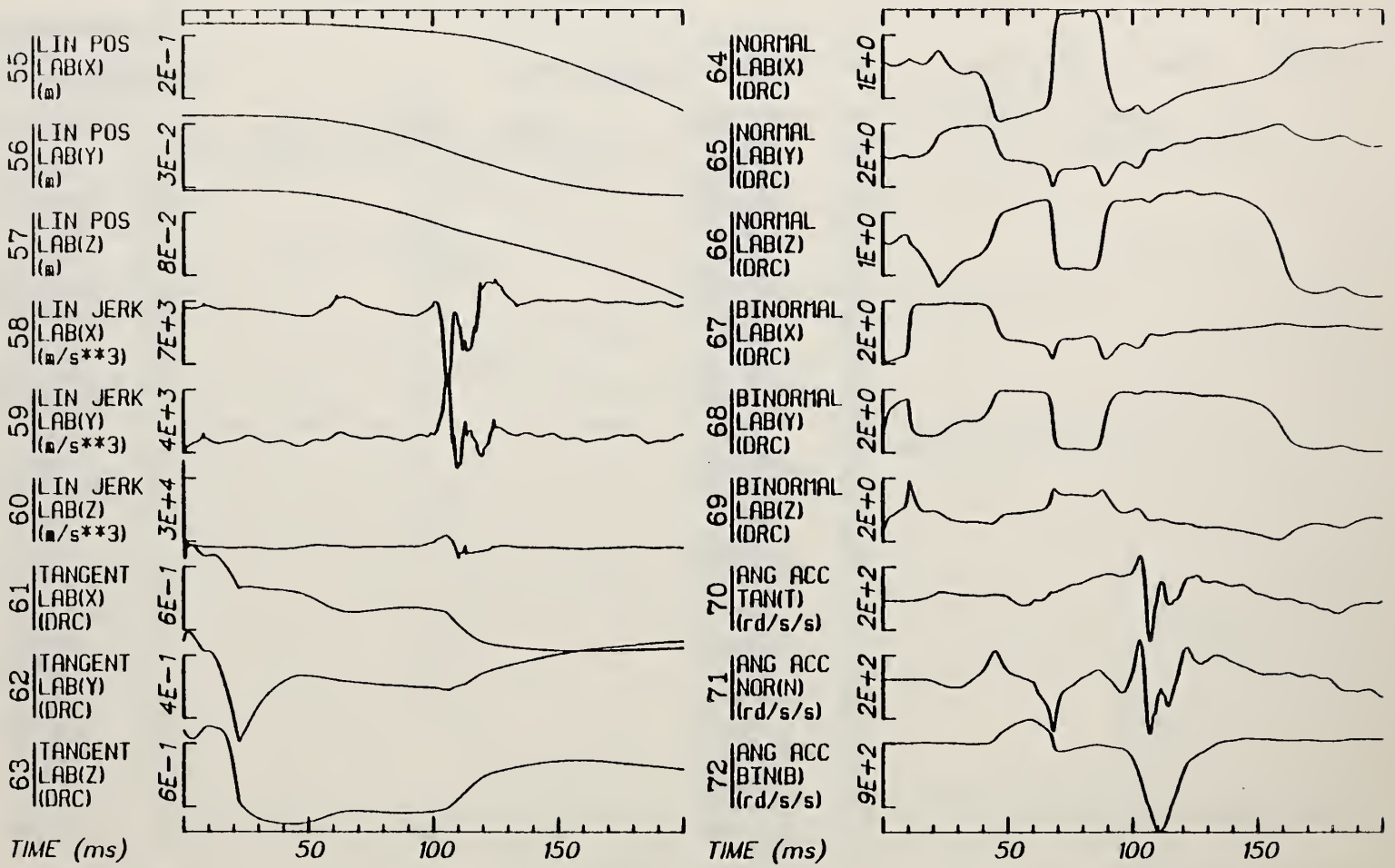

Run ID: 82E063 Disk: 82E063.3 File: 1 Date: MAY 23, 1985 Sheet: 4

Filter:1600*4C

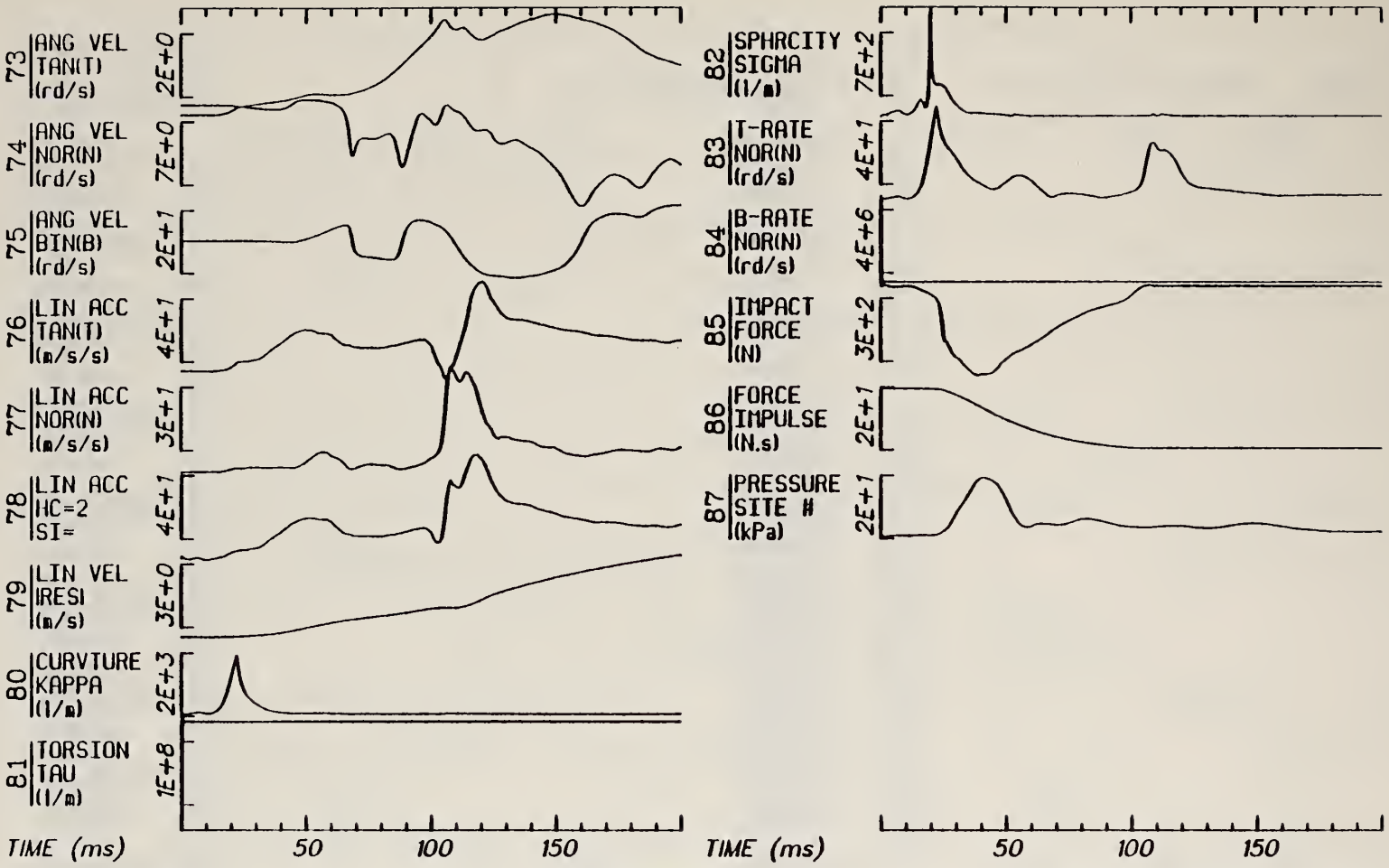

Run ID: 82E063 Disk: 82E063.3 File: 1 Date: MAY 23, 1985 Sheet: 5

*Filter:1600*4C*

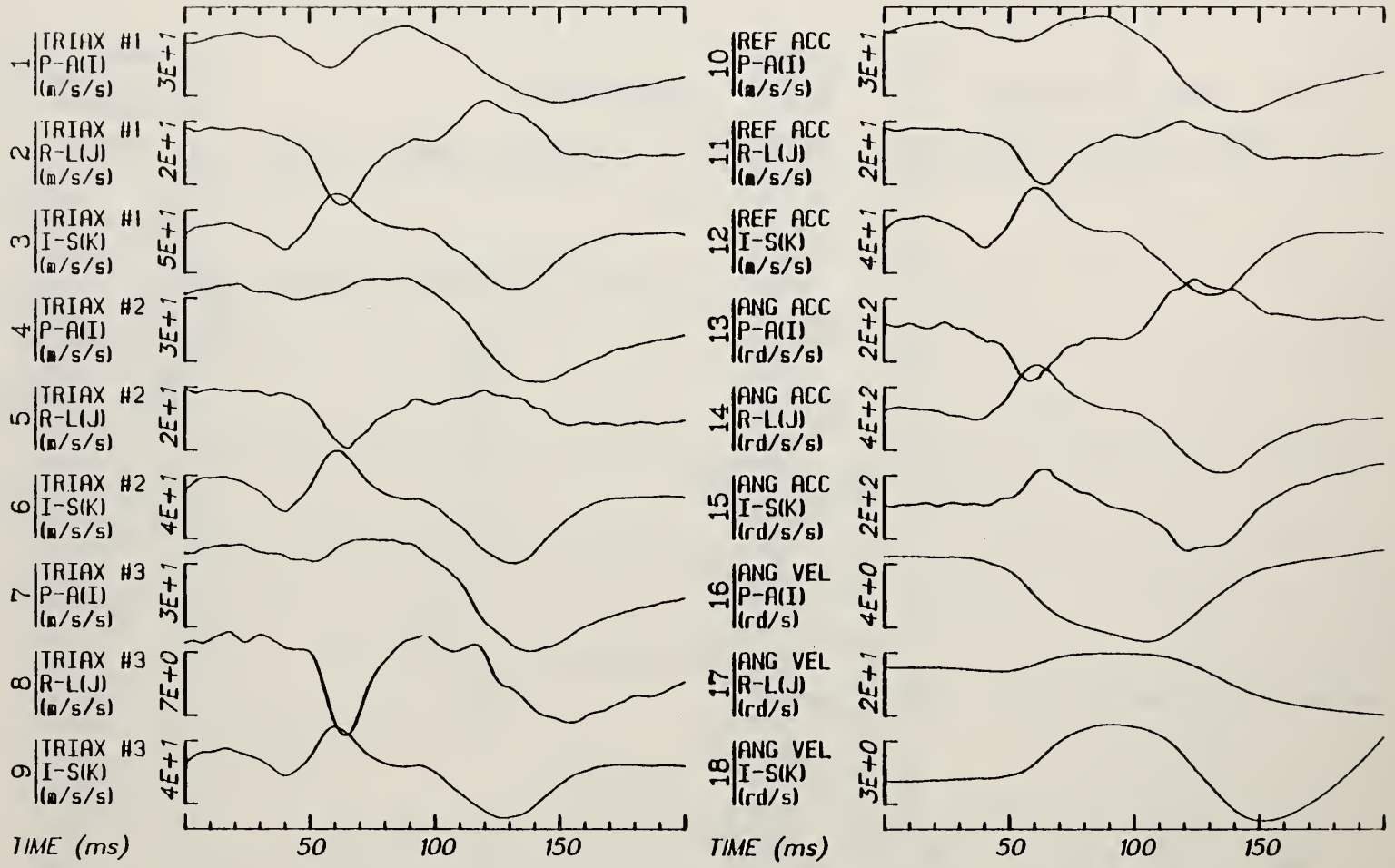

Run ID: 82E064 Disk: 82E064.3 File: 1 Date: MAY 23, 1985 Sheet: 1

*Filter:1600*4C*

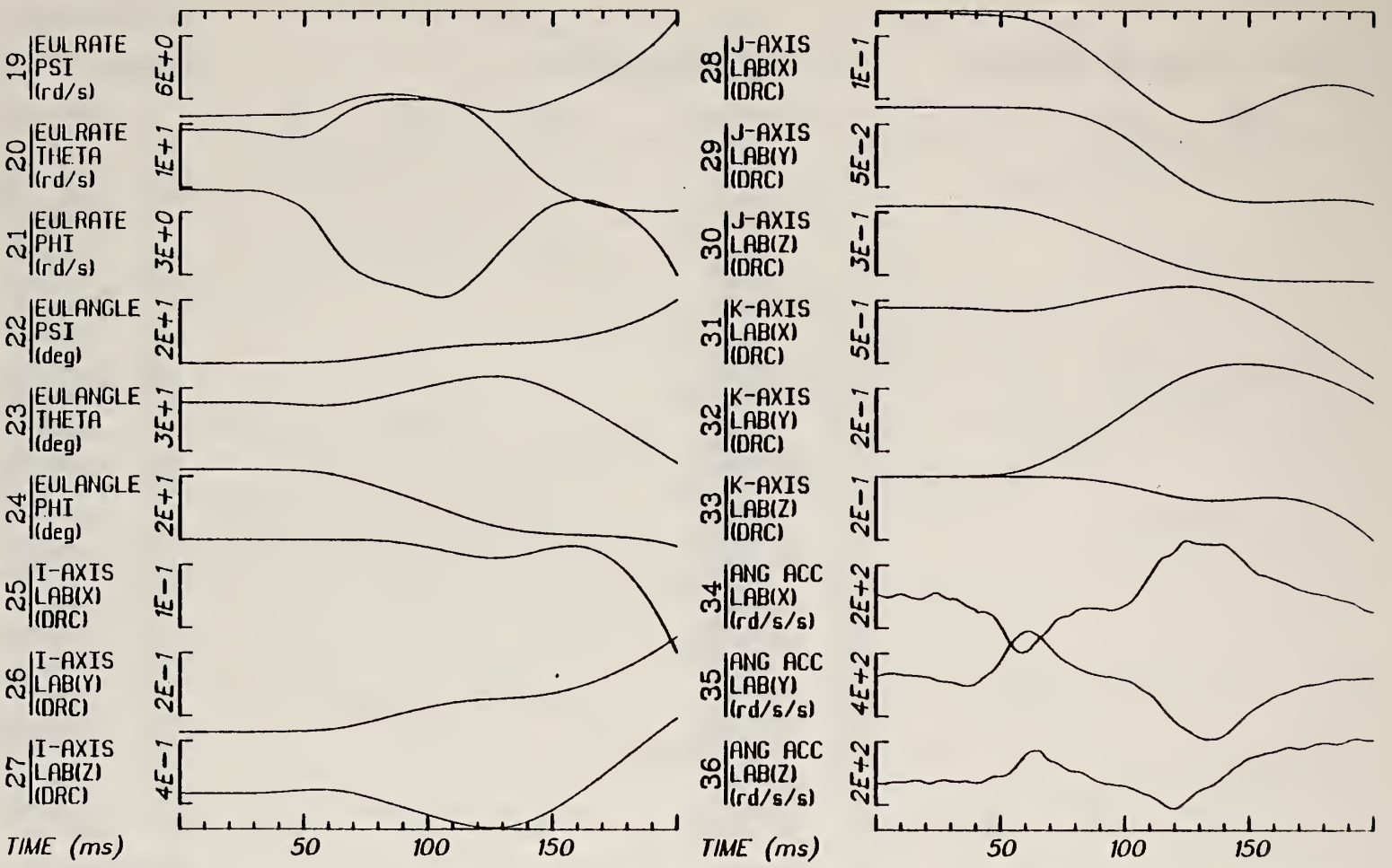

Run ID: 82E064 Disk: 82E064.3 File: 1 Date: MAY 23, 1985 Sheet: 2

*Filter:1600*4C*

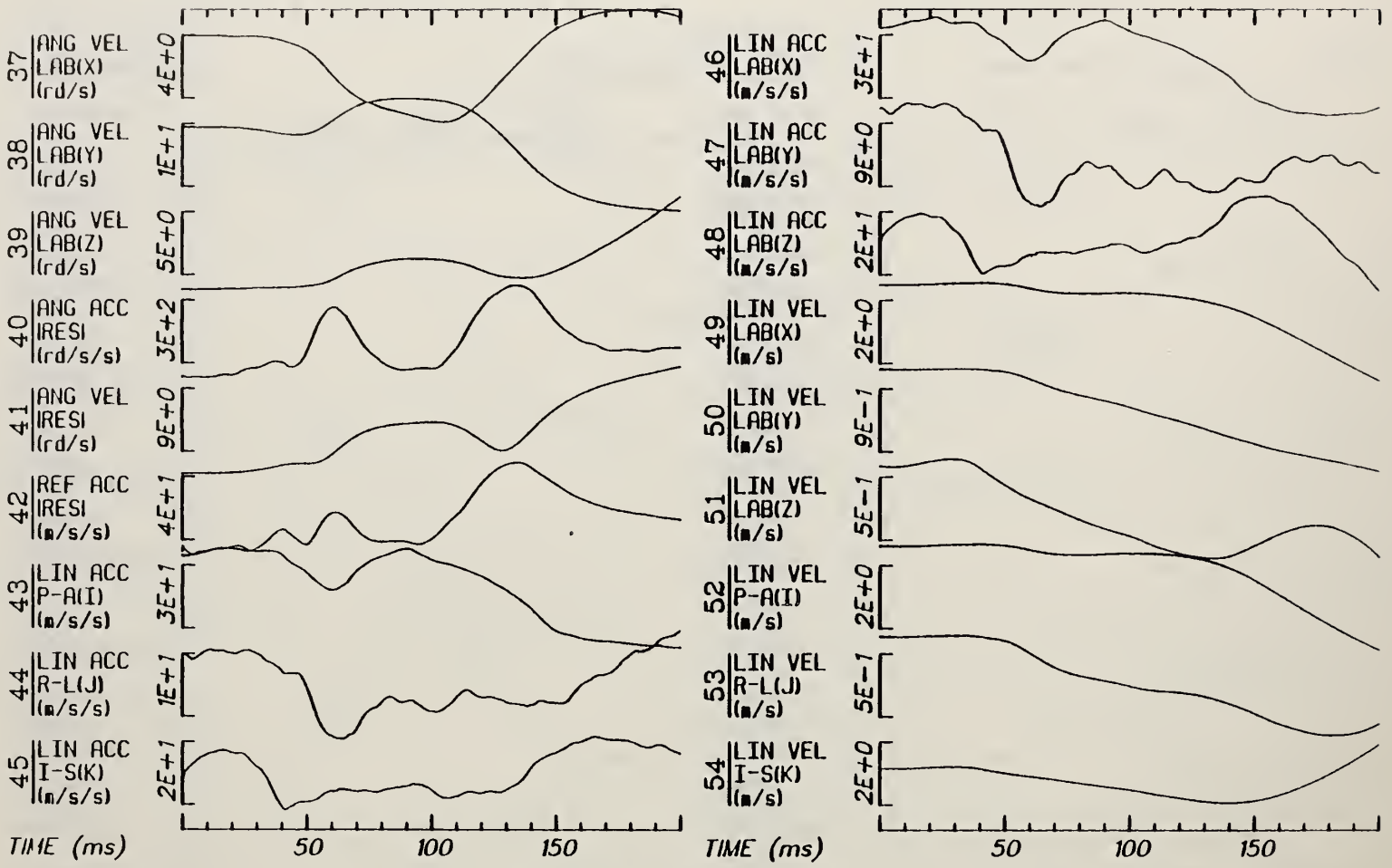

Run ID: 82E064 Disk: 82E064.3 File: 1 Date: MAY 23, 1985 Sheet: 3

*Filter:1600*4C*

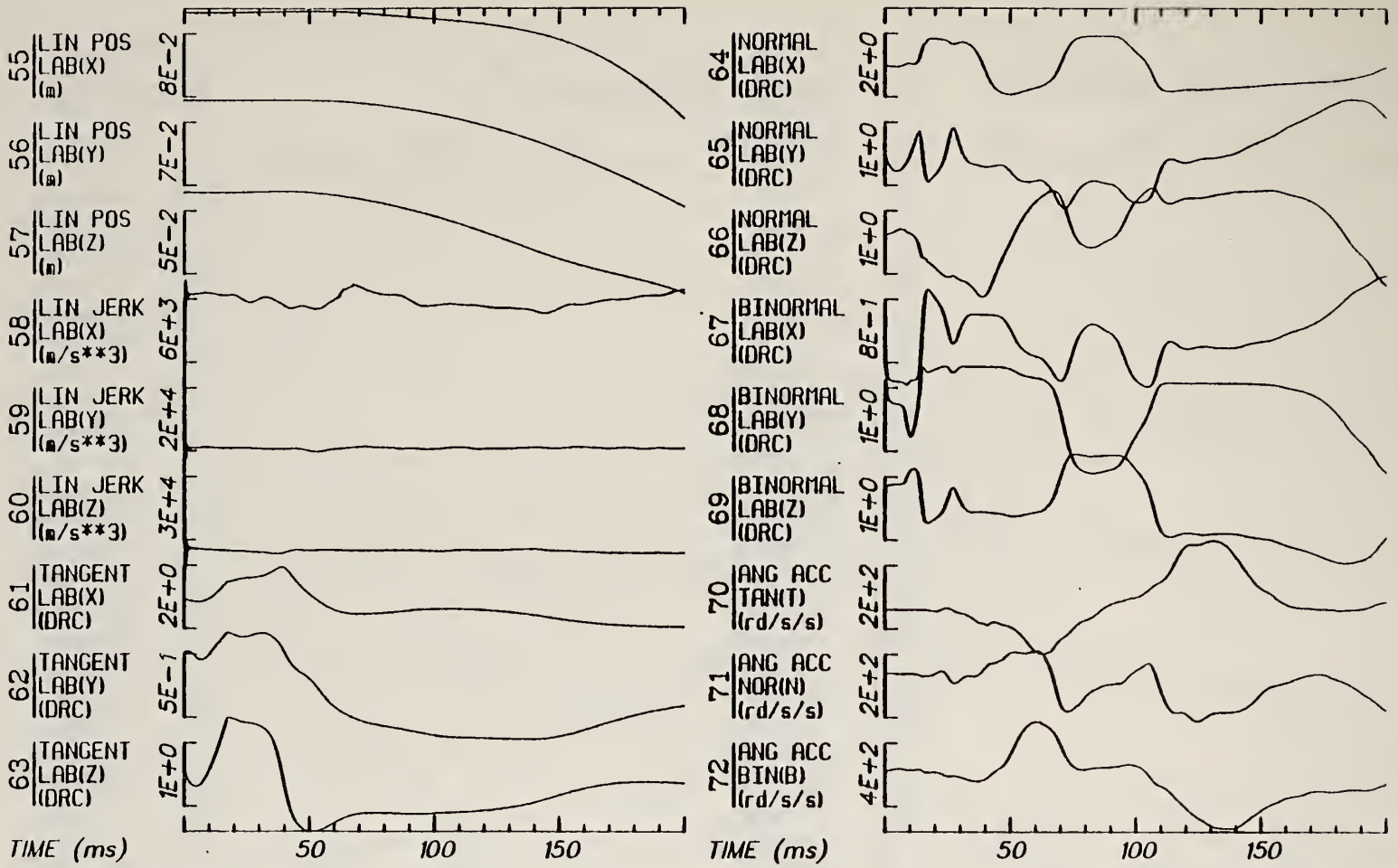

Run ID: 82E064 Disk: 82E064.3 File: 1 Date: MAY 23, 1985 Sheet: 4

*Filter:1600*4C*

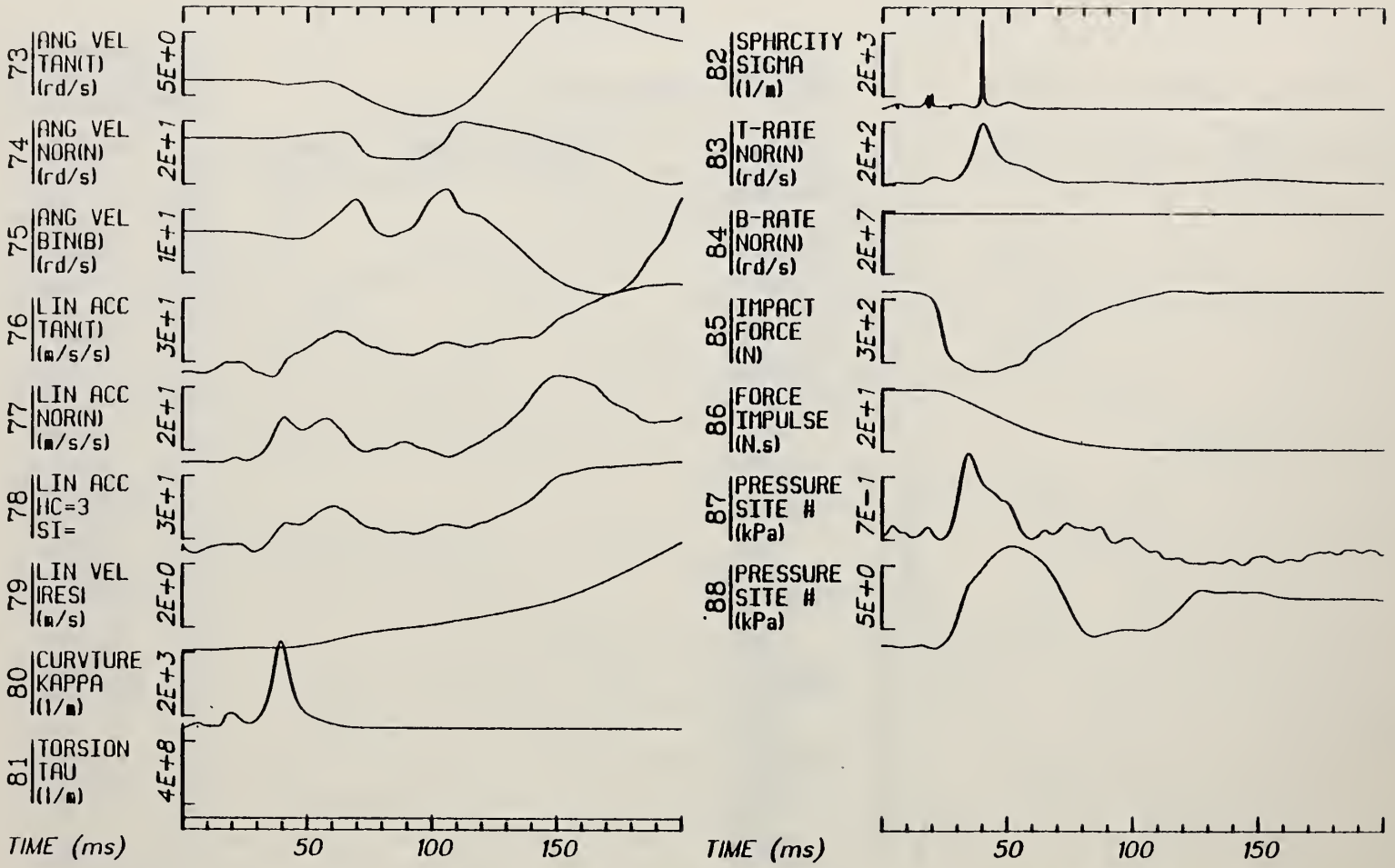

Run ID: 82E064 Disk: 82E064.3 File: 1 Date: MAY 23, 1985 Sheet: 5

*Filter:1600*4C*

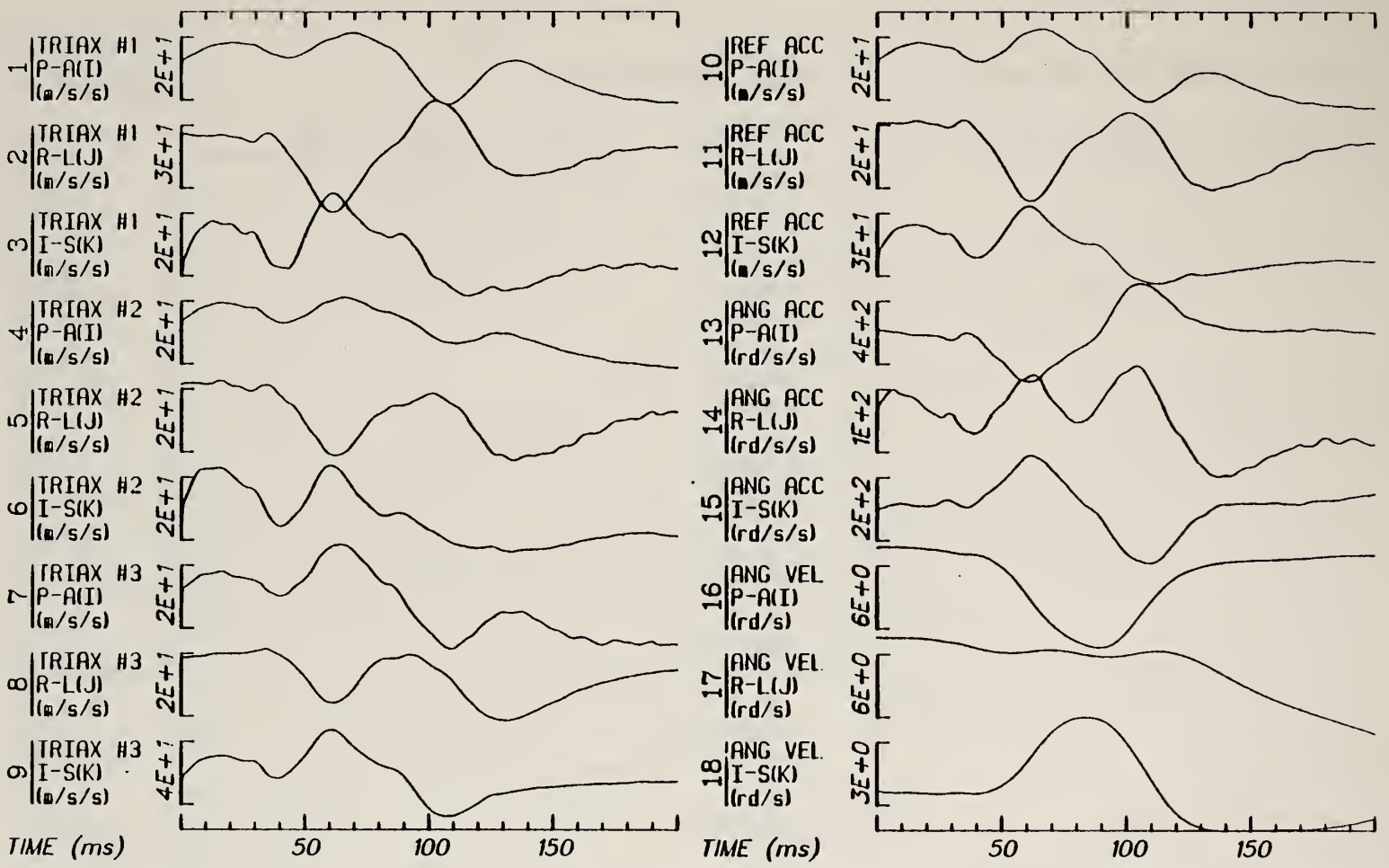

Run ID: 82E065 Disk: 82E065.3 File: 1 Date: MAY 23, 1985 Sheet: 1

*Filter:1600*4C*

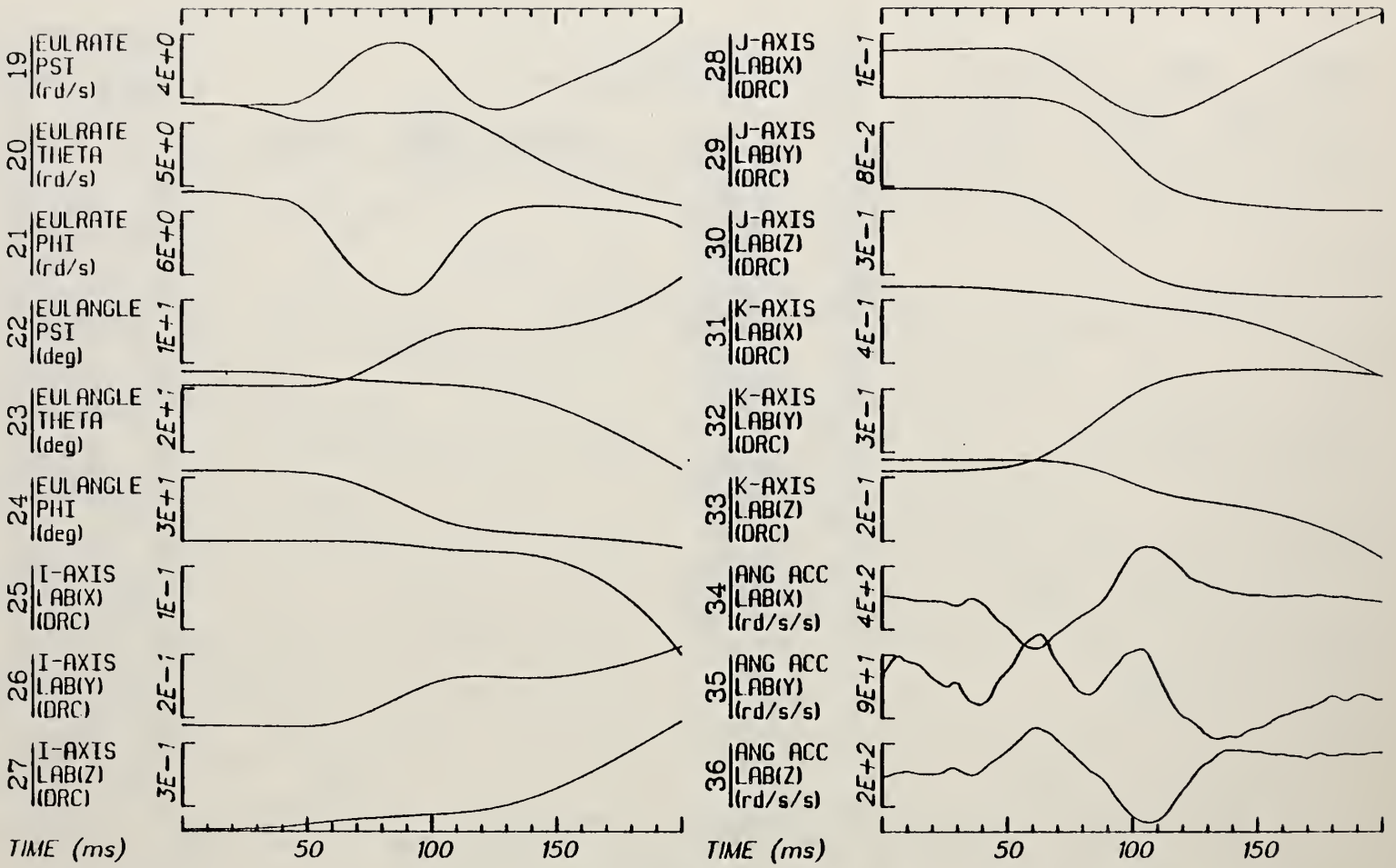

Run ID: 82E065 Disk: 82E065.3 File: 1 Date: MAY 23, 1985 Sheet: 2

*Filter:1600*4C*

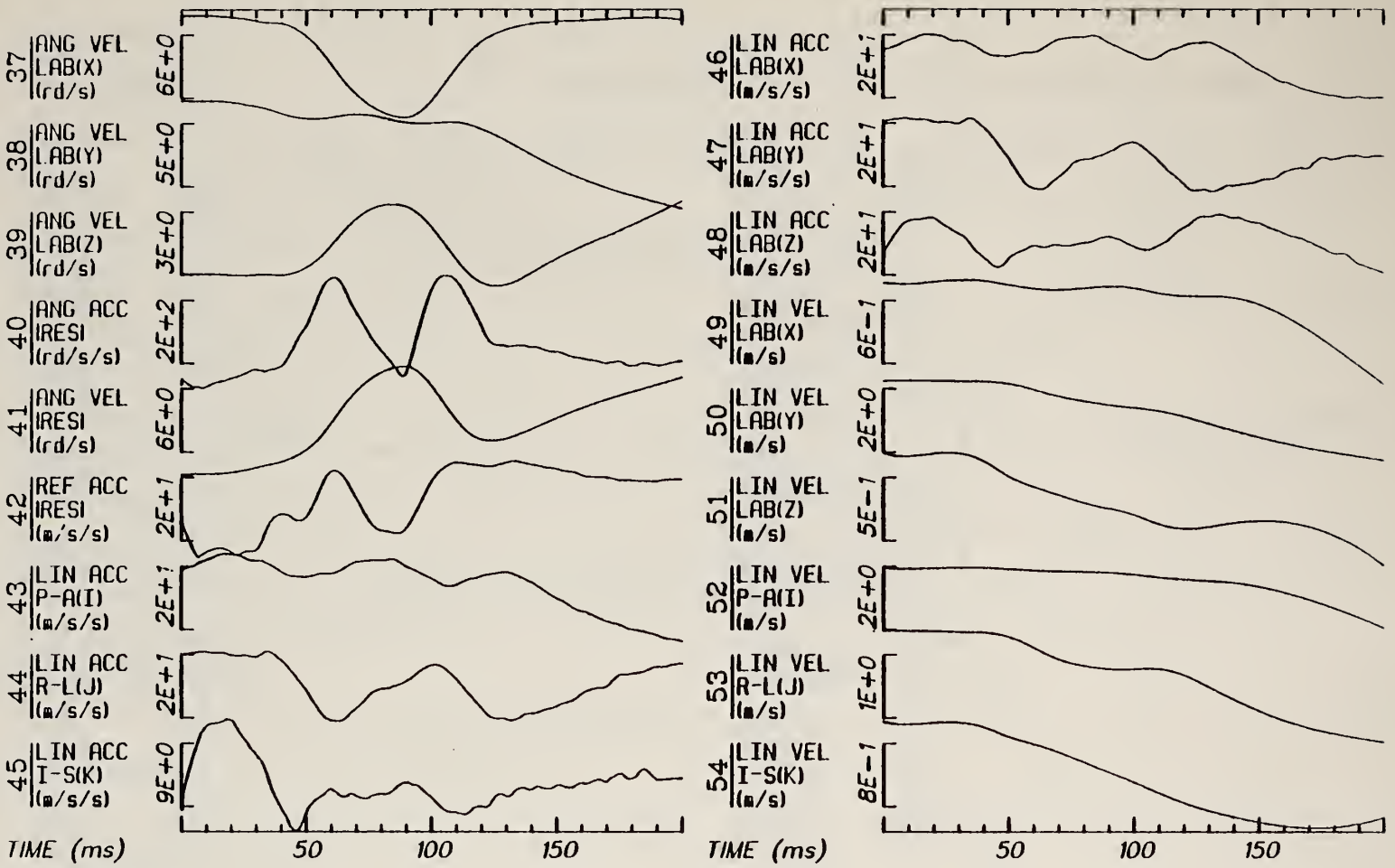

Run ID: 82E065 Disk: 82E065.3 File: 1 Date: MAY 23, 1985 Sheet: 3

*Filter:1600*4C*

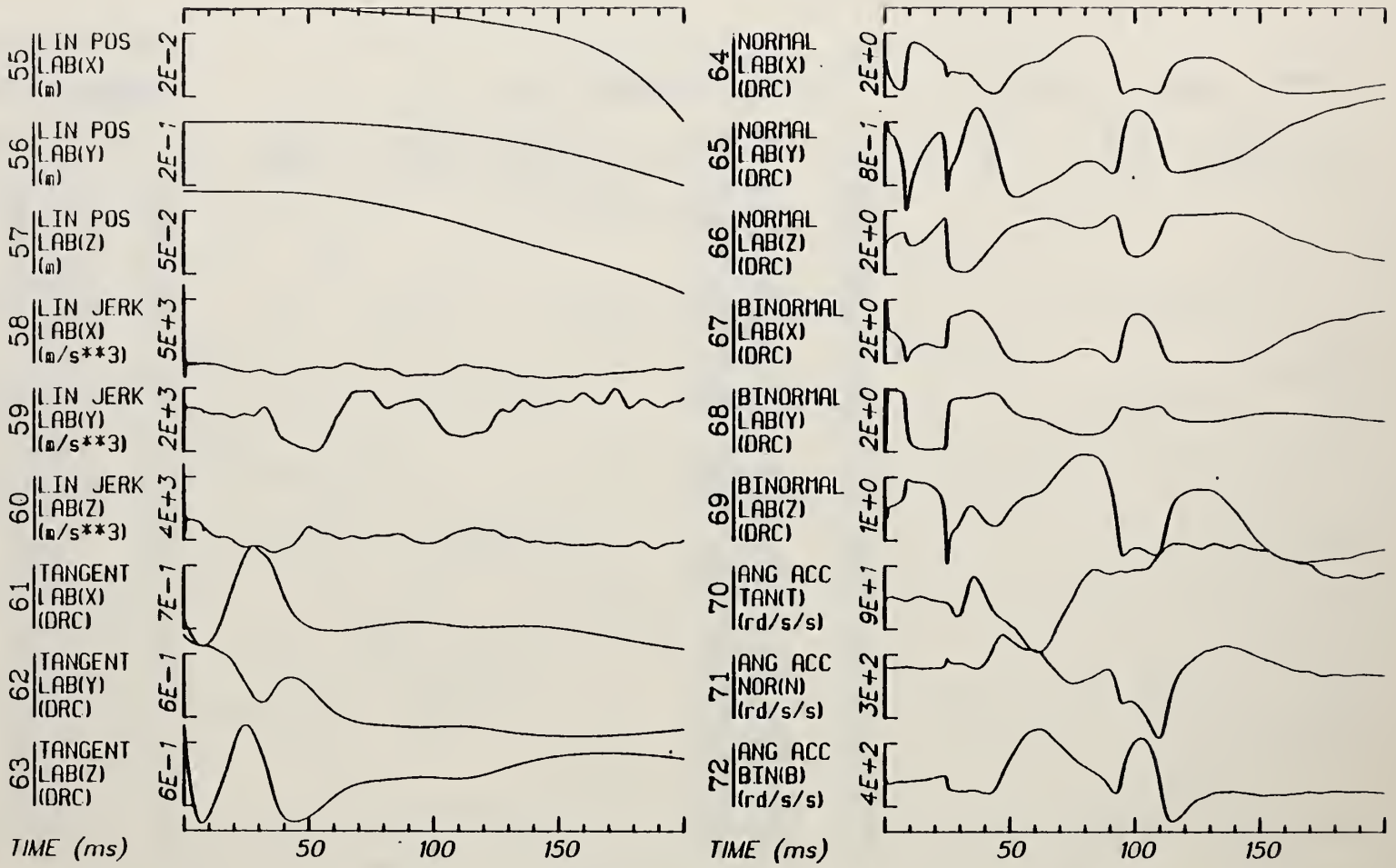

Run ID: 82E065 Disk: 82E065.3 File: 1 Date: MAY 23, 1985 Sheet: 4

*Filter:1600*4C*

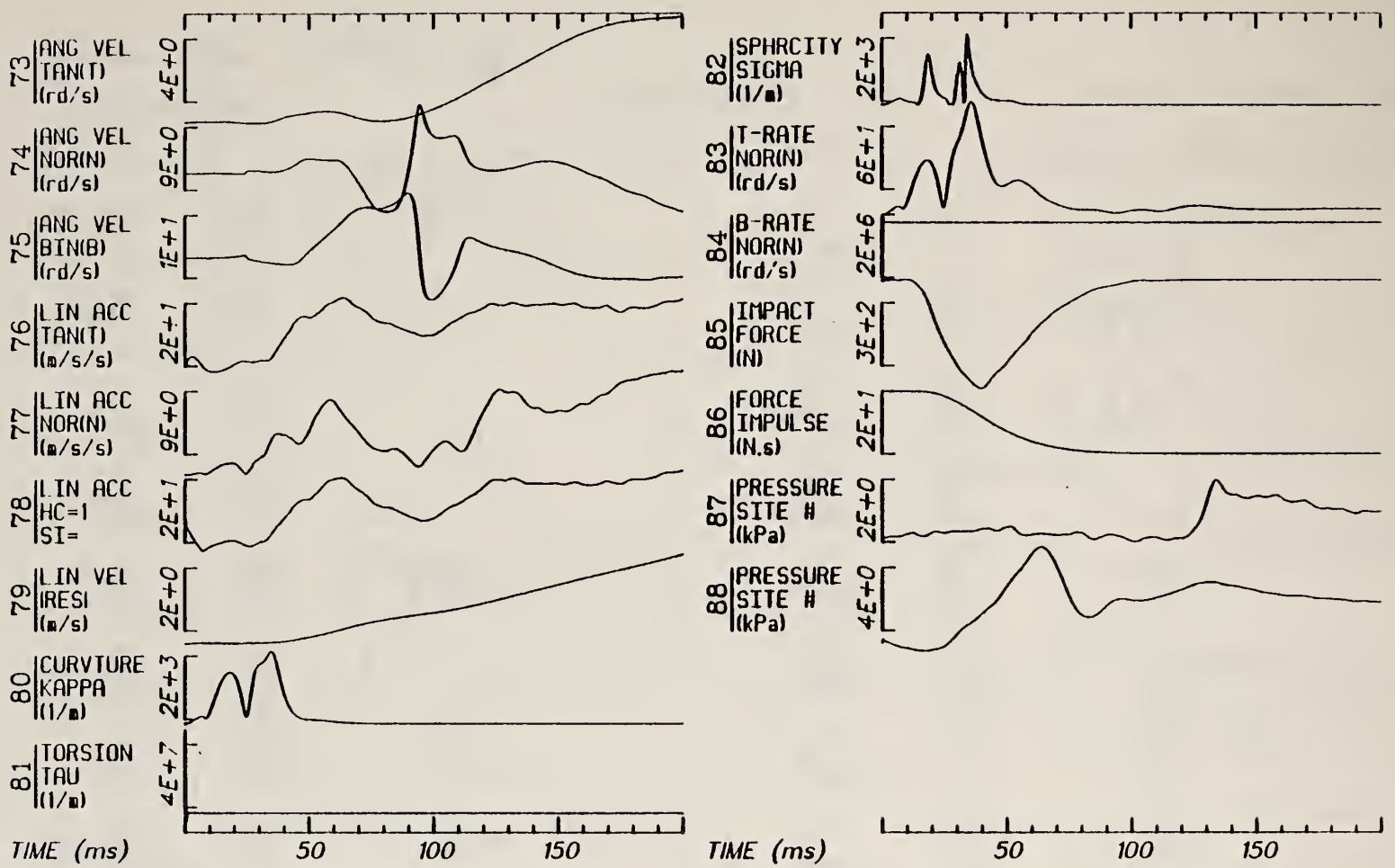

Run ID: 82E065 Disk: 82E065.3 File: 1 Date: MAY 23, 1985 Sheet: 5

*Filter:1600*4C*

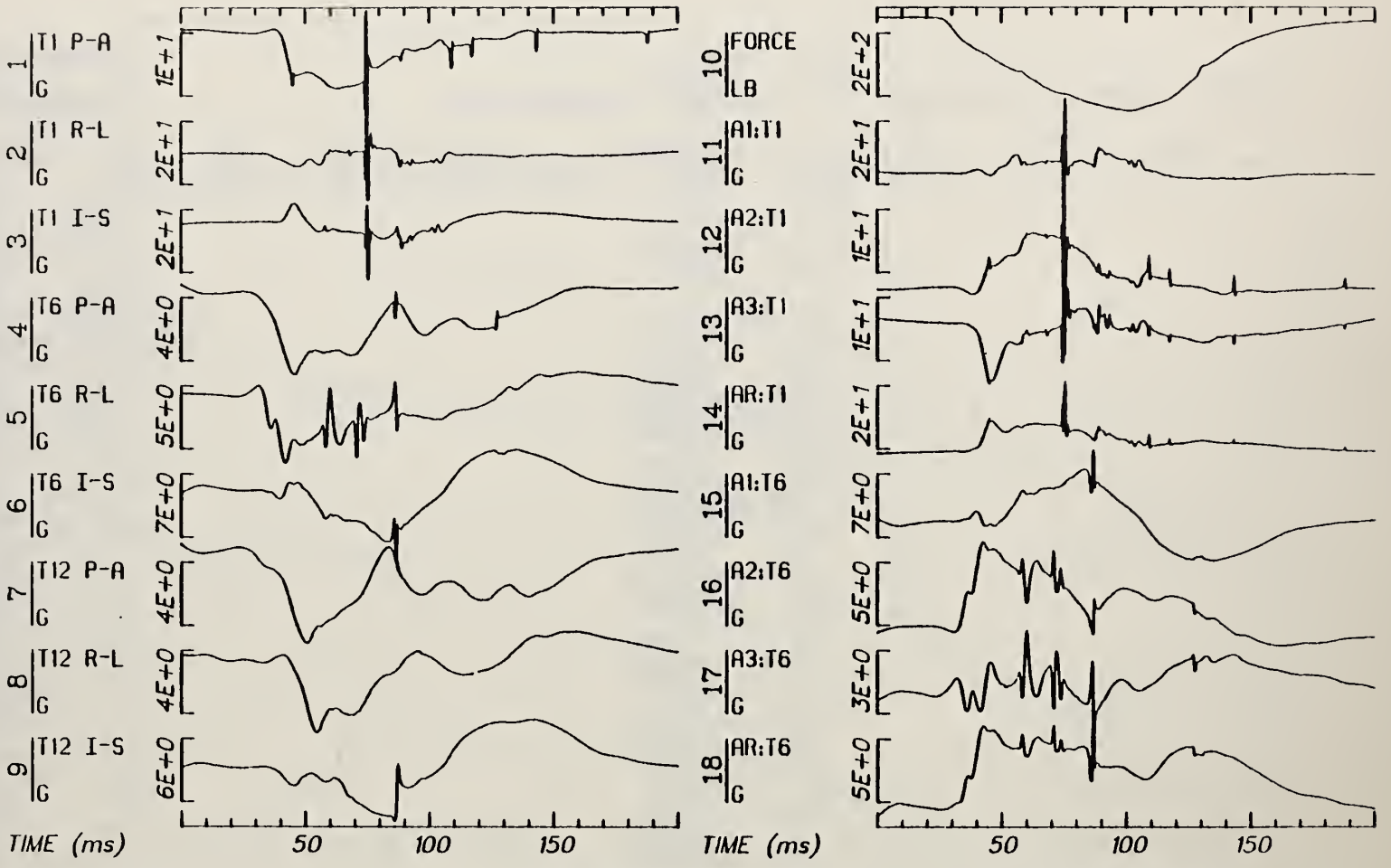

Run ID: 83E071 Disk: 83E071.S File: 1 Date: MAY 10, 1985 Sheet: 1

*Filter:1600*4C Smooth: 3SD*

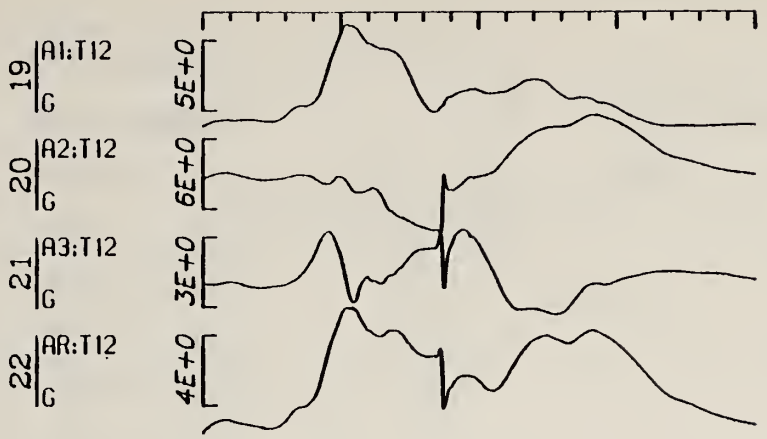

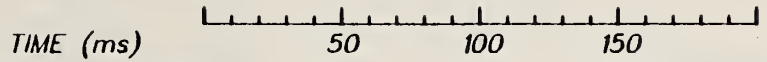

Run ID: 83E071 Disk: 83E071.S File: 1 Date: MAY 10, 1985 Sheet: 2

Filter:1600*4C Smooth: 3SD

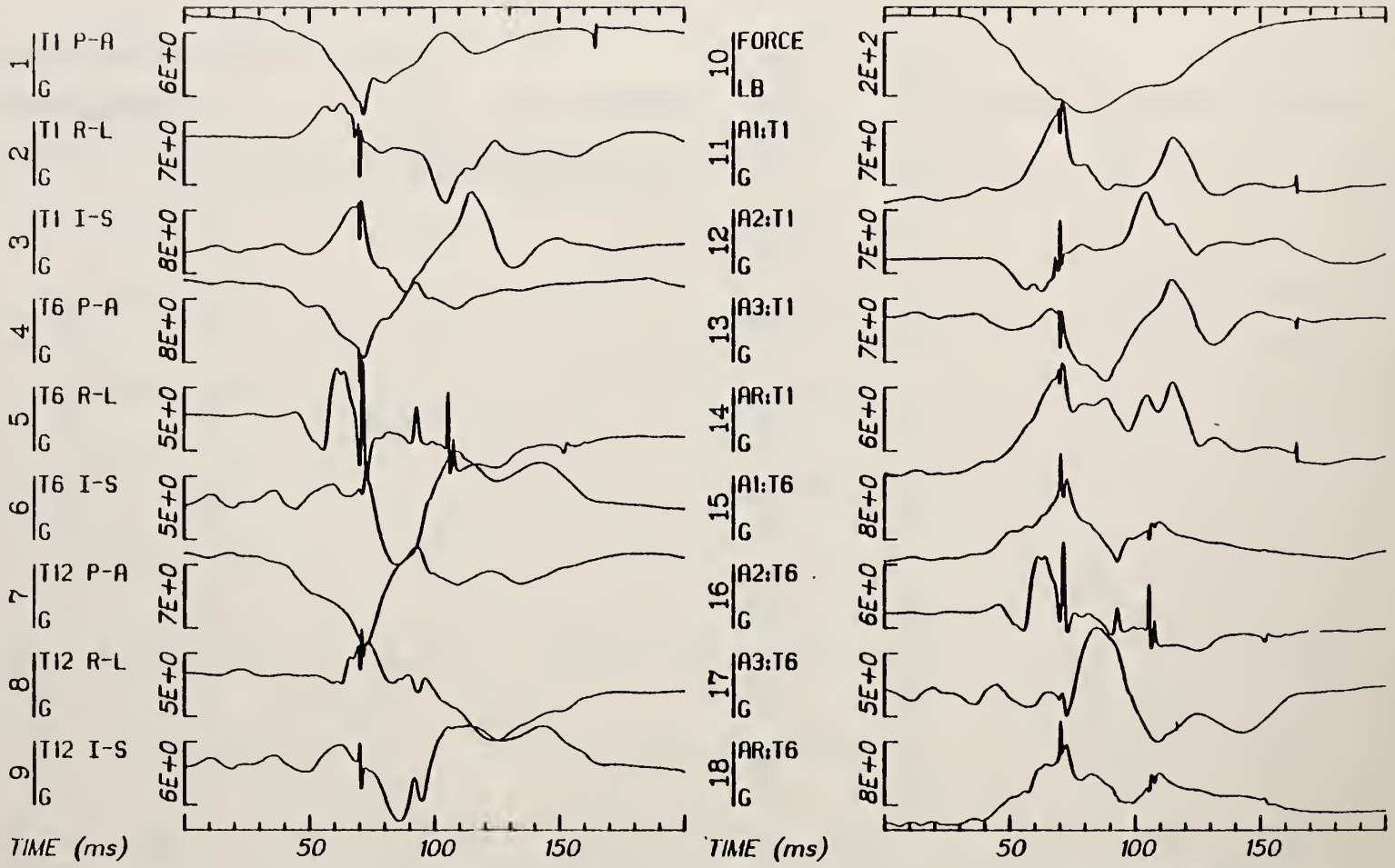

Run ID: 83E073 Disk: 83E073.S File: 1 Date: MAY 14, 1985 Sheet: 1

*Filter:1600*4C Smooth: 3SD*

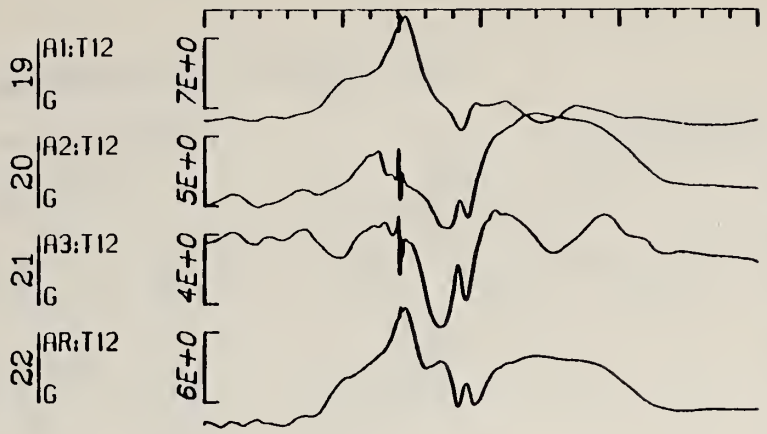

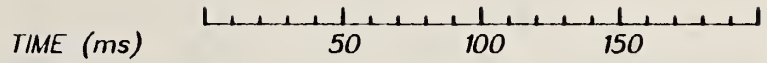

Run ID: 83E073 Disk: 83E073.S File: 1 Date: MAY 14, 1985 Sheet: 2

*Filter: 1600*4C Smooth: 3SD*

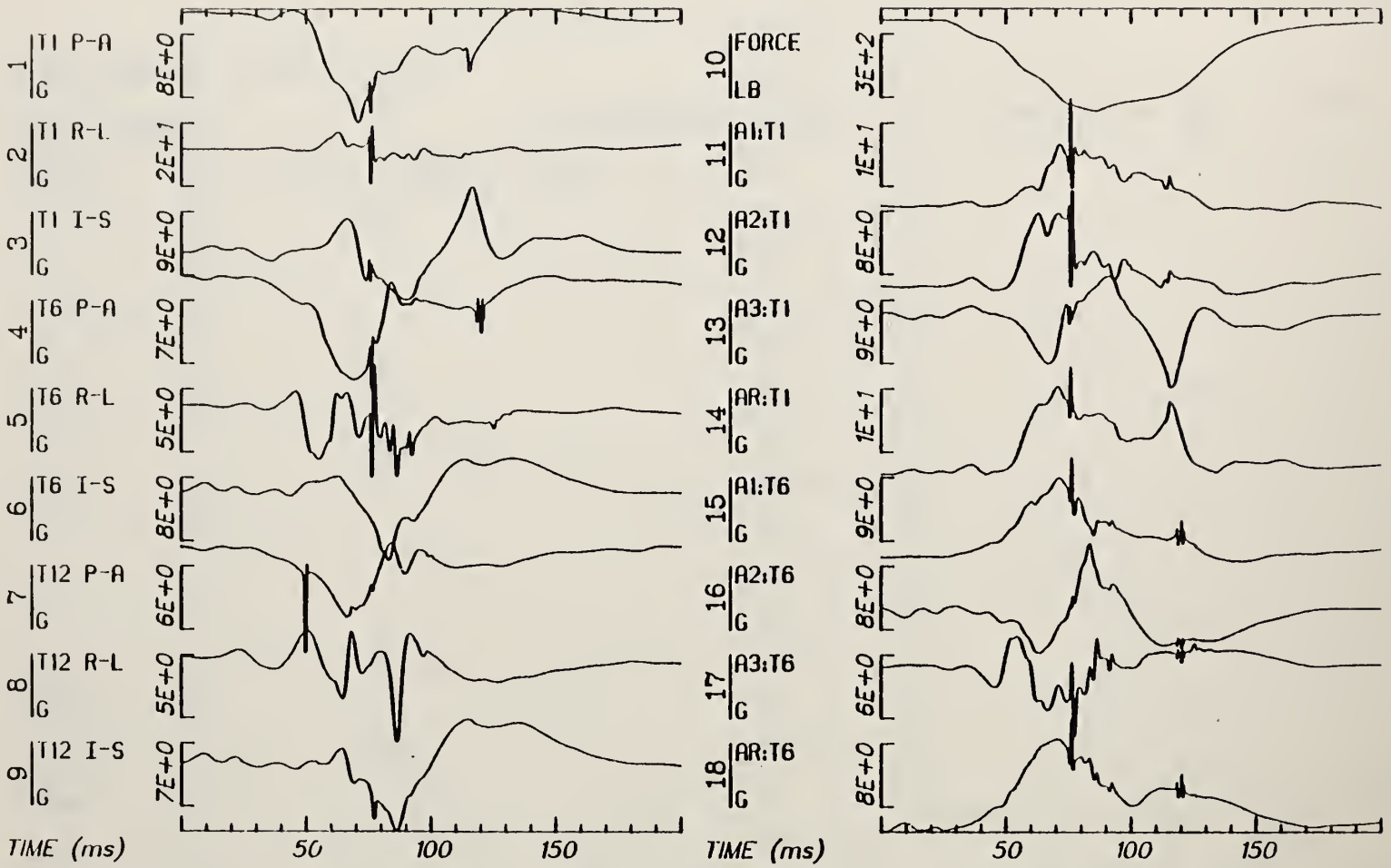

Run ID: 83E074 Disk: 83E074.S File: 1 Date: MAY 14, 1985 Sheet: 1

*Filter:1600*4C Smooth: 3SD*

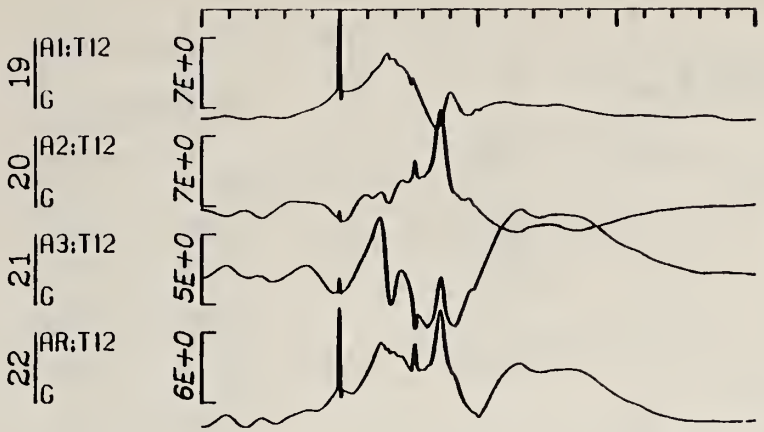

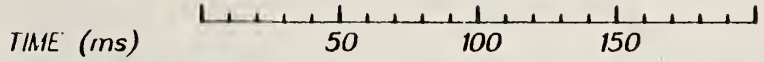

Run ID: 83E074 Disk: 83E074.S File: 1 Date: MAY 14, 1985 Sheet: 2

*Filter: 1600*4C Smooth: 3SD*

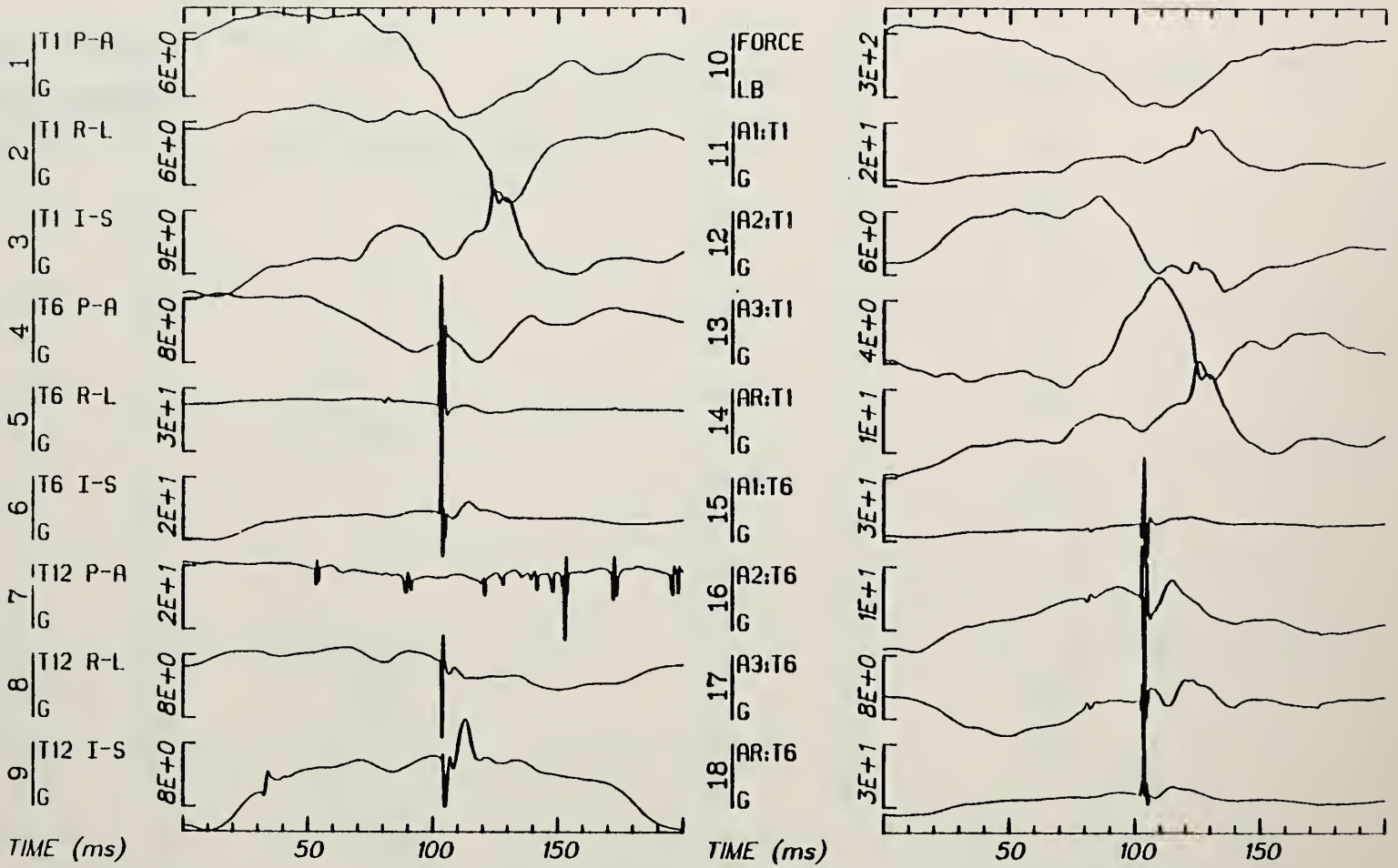

Run ID: 83E075 Disk: 83E075.S File: 1 Date: MAY 14, 1985 Sheet: 1

*Filter:1600*4C Smooth: 3SD*

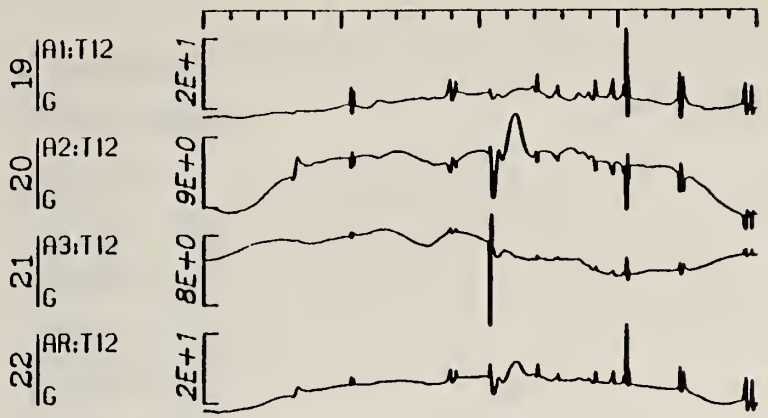

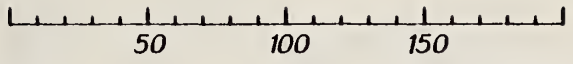

Run ID: 83E075 Disk: 83E075.S File: 1 Date: MAY 14, 1985 Sheet: 2

*Filter: 1600*4C Smooth: 3SD*

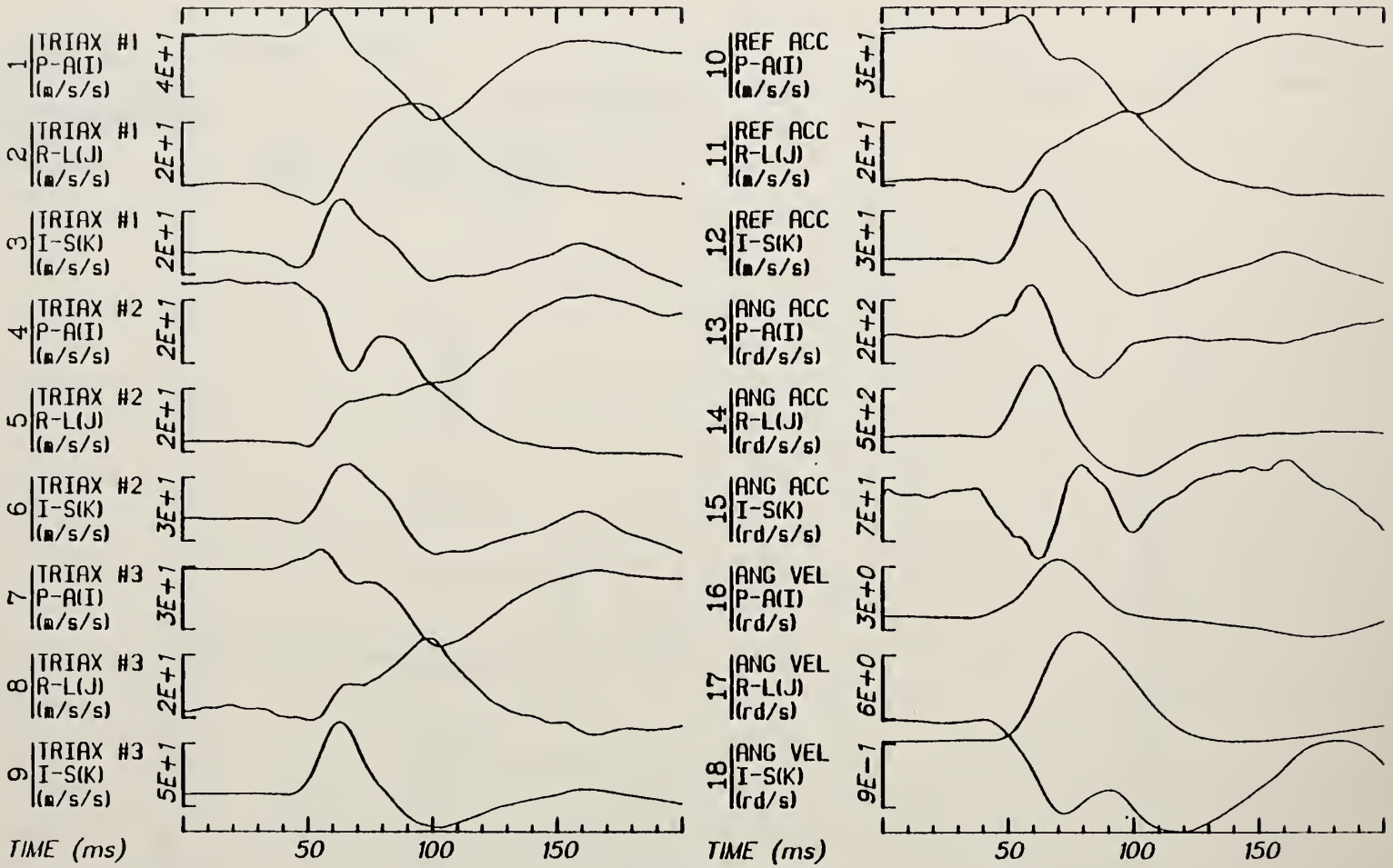

Run ID: 83E083 Disk: 83E083.3 File: 1 Date: MAY 23, 1985 Sheet: 1

*Filter:1600*4C*

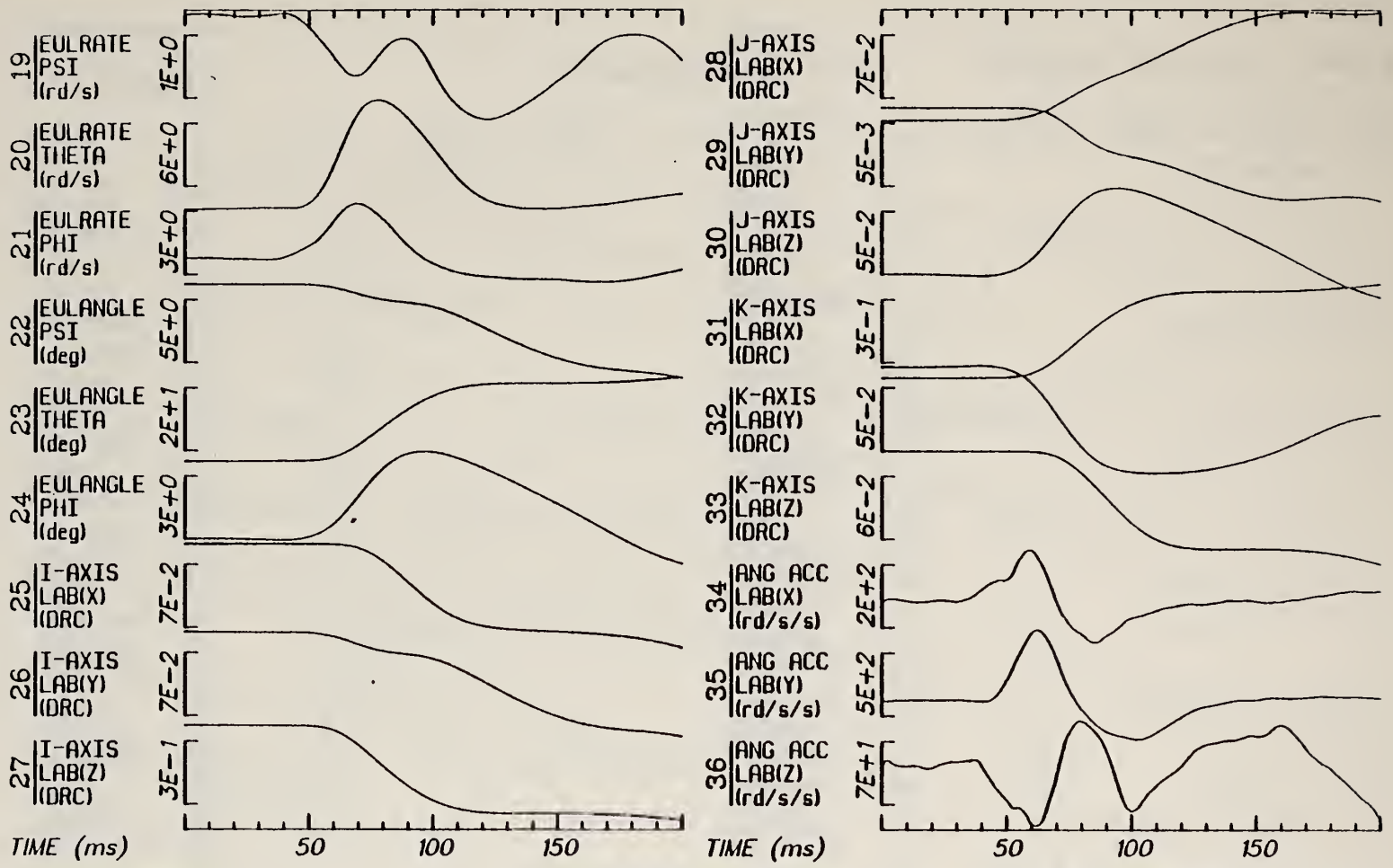

Run ID: 83E083 Disk: 83E083.3 File: 1 Date: MAY 23, 1985 Sheet: 2

*Filter:1600*4C*

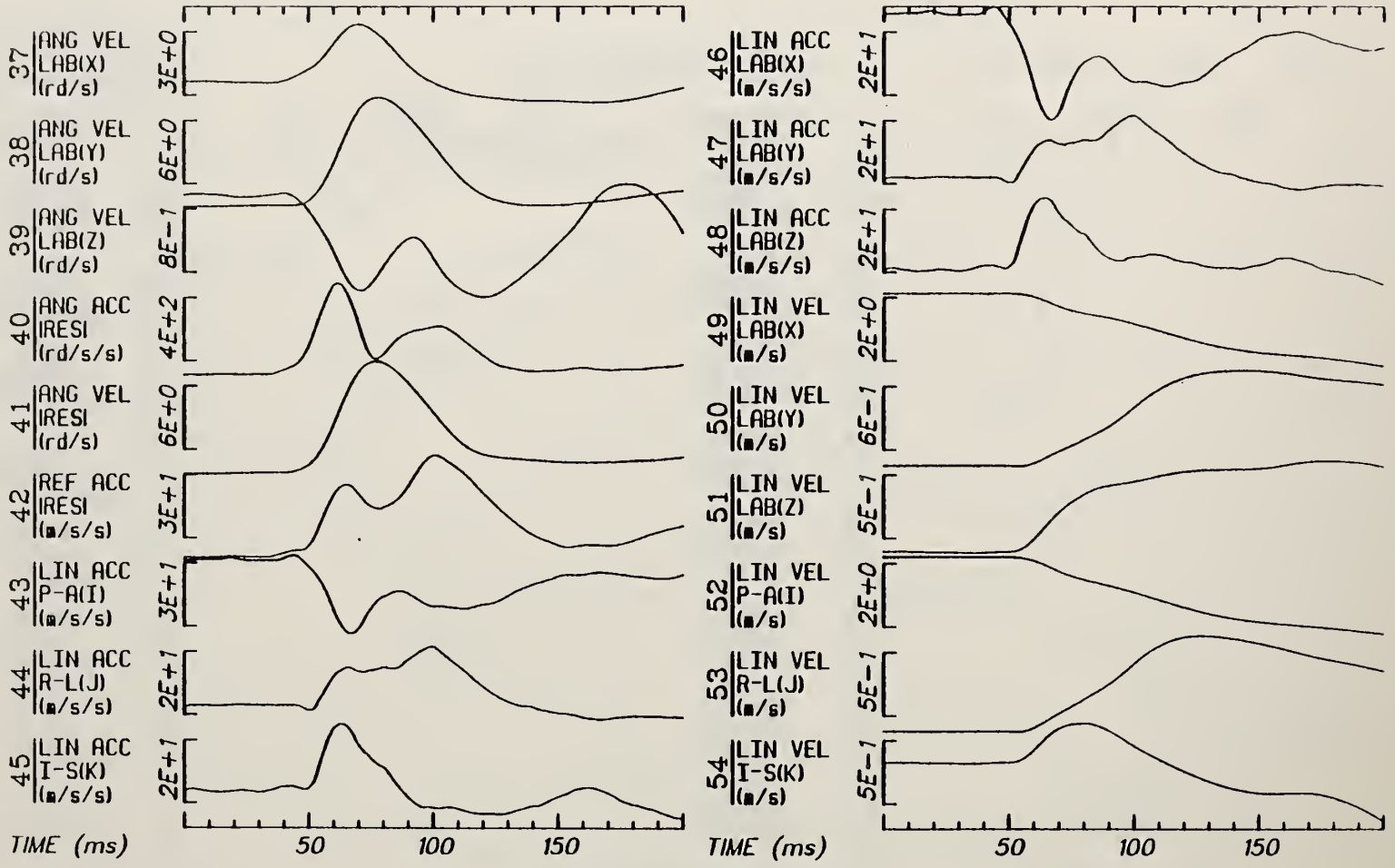

Run ID: 83E083 Disk: 83E083.3 File: 1 Date: MAY 23, 1985 Sheet: 3

*Filter:1600*4C*

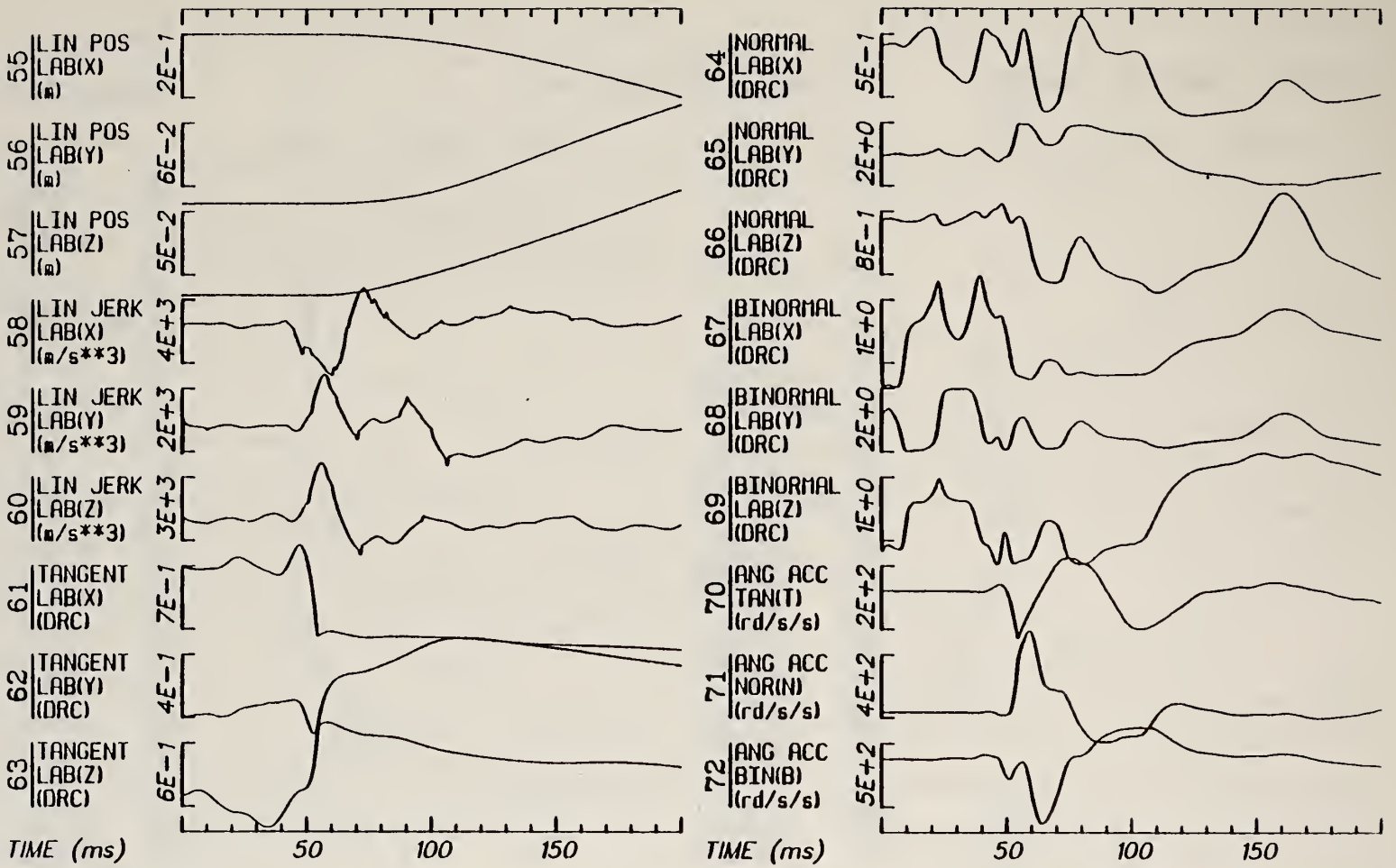

Run ID: 83E083 Disk: 83E083.3 File: 1 Date: MAY 23, 1985 Sheet: 4

*Filter:1600*4C*

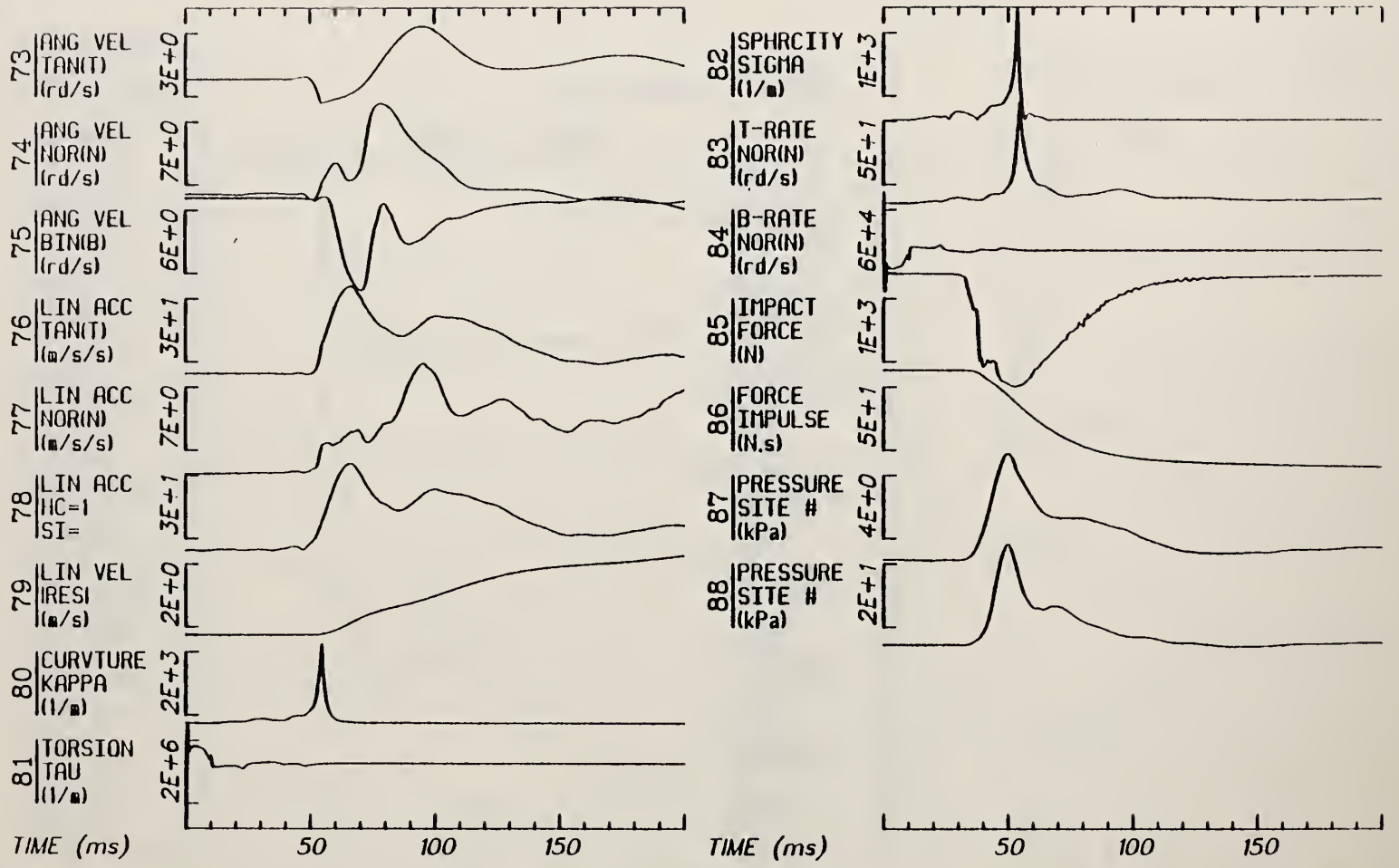

Run ID: 83E083 Disk: 83E083.3 File: 1 Date: MAY 23, 1985 Sheet: 5

*Filter:1600*4C*

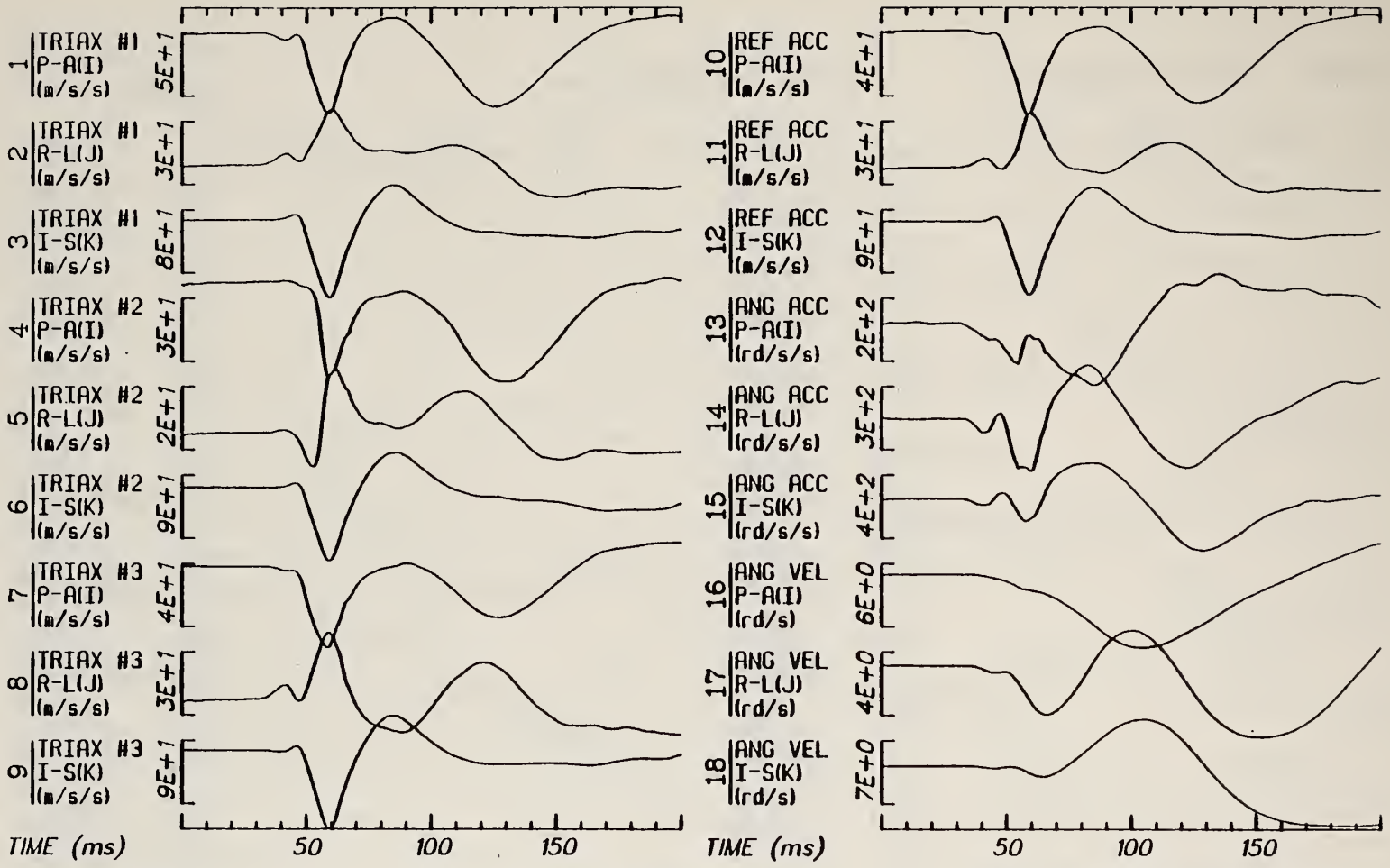

Run ID: 83E084 Disk: 83E084.3 File: 1 Date: MAY 23, 1985 Sheet: 1

*Filter:1600*4C*

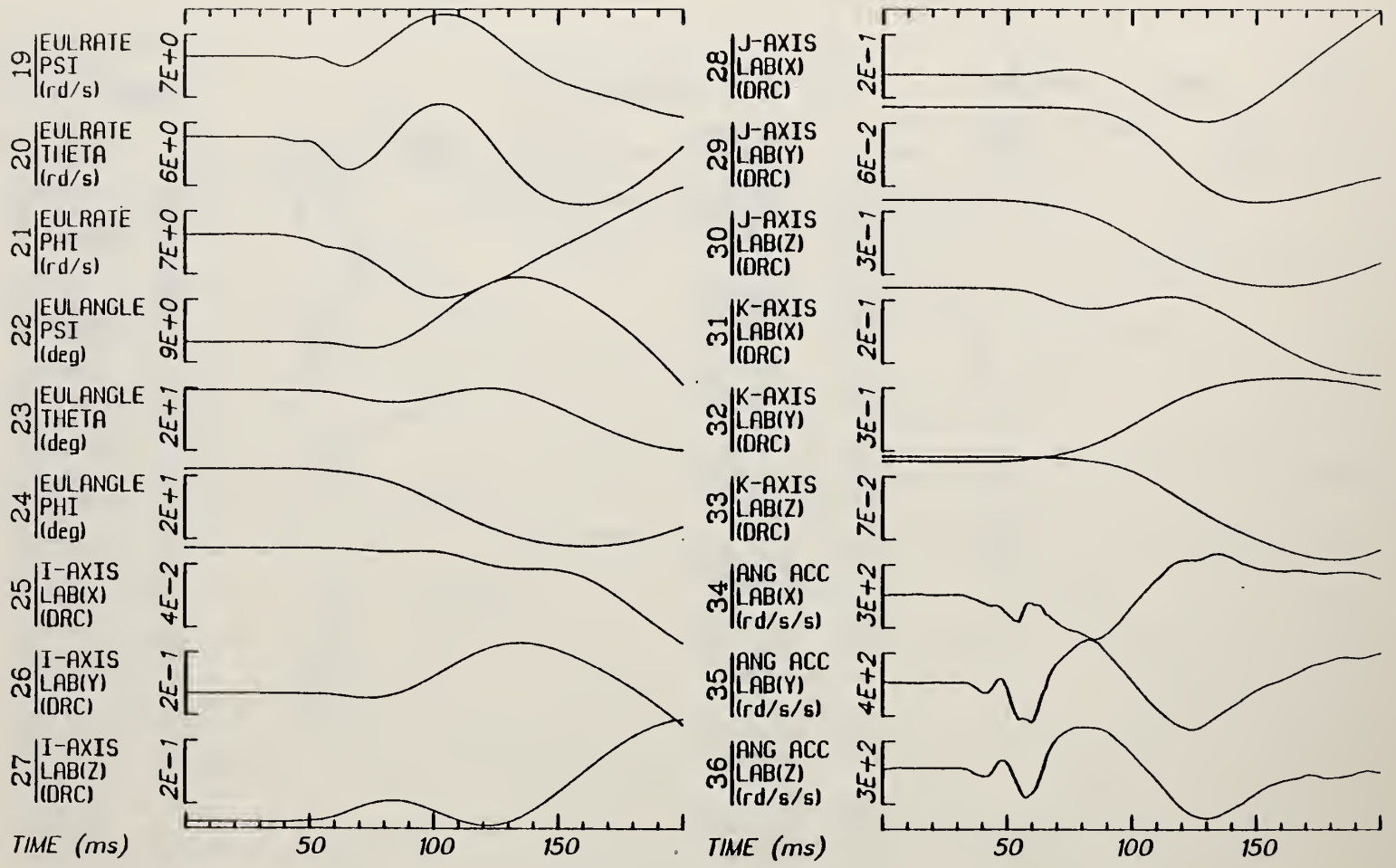

Run ID: 83E084 Disk: 83E084.3 File: 1 Date: MAY 23, 1985 Sheet: 2

*Filter:1600*4C*

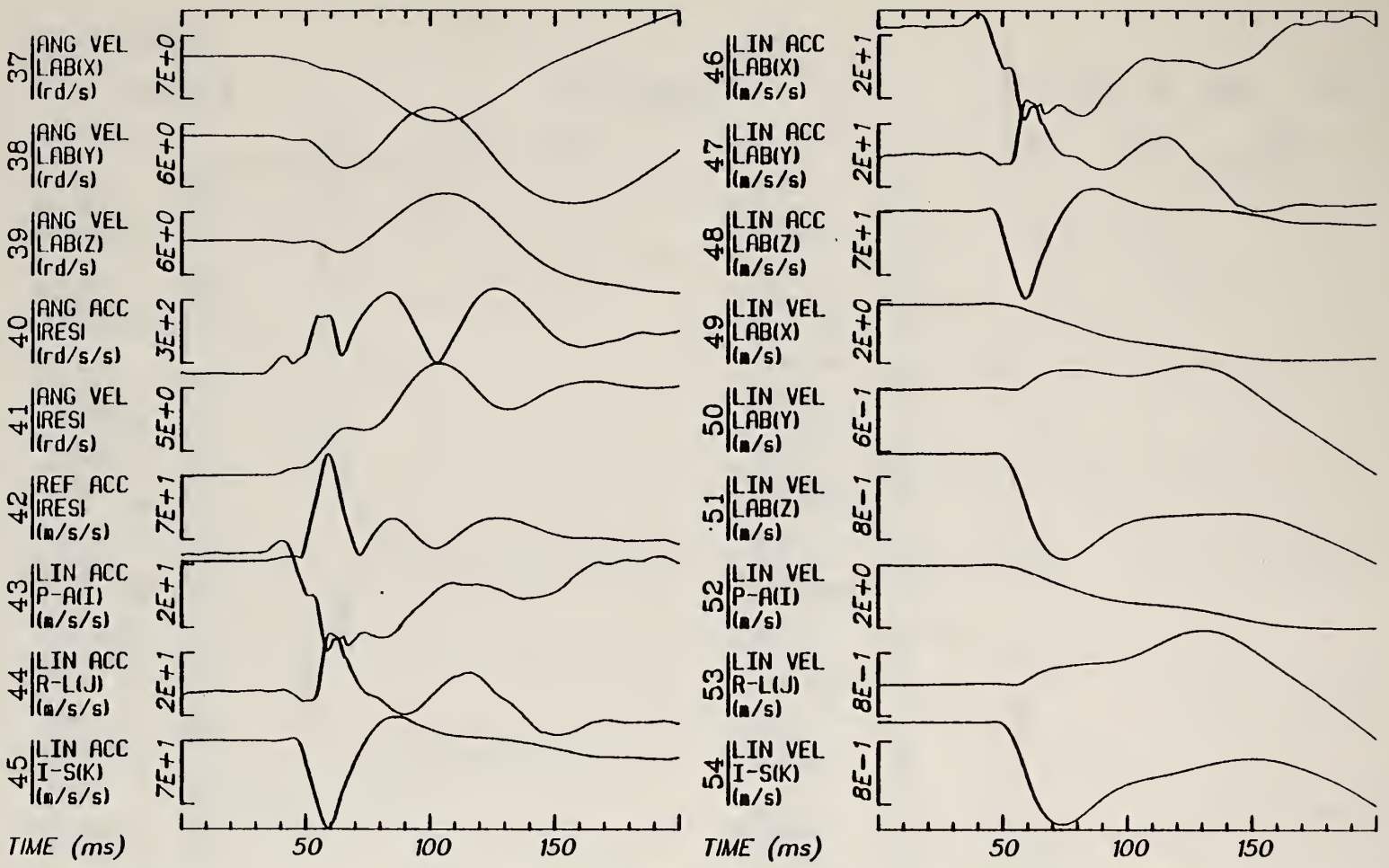

Run ID: 83E084 Disk: 83E084.3 File: 1 Date: MAY 23, 1985 Sheet: 3

*Filter:1600*4C*

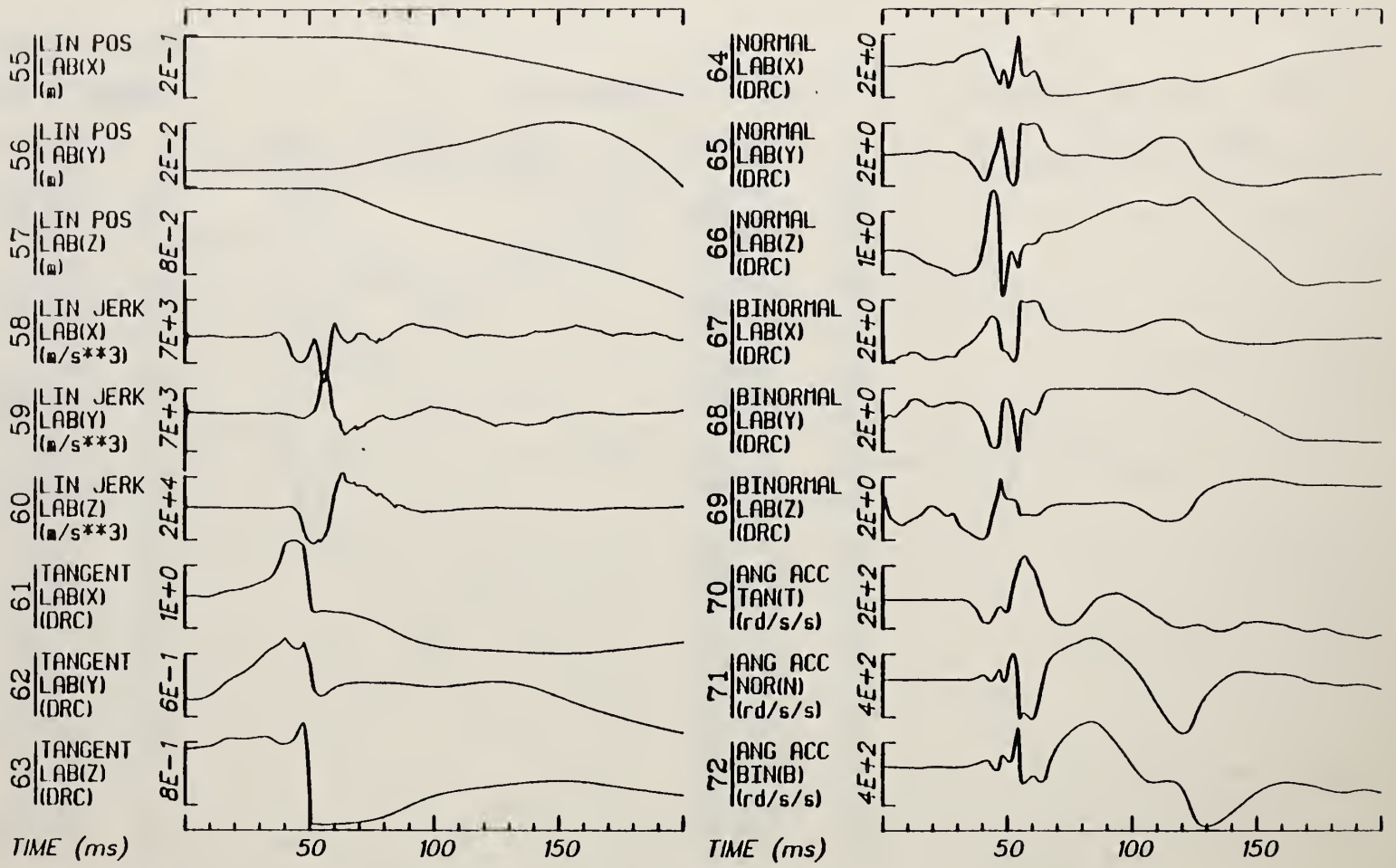

Run ID: 83E084 Disk: 83E084.3 File: 1 Date: MAY 23, 1985 Sheet: 4

*Filter:1600*4C*

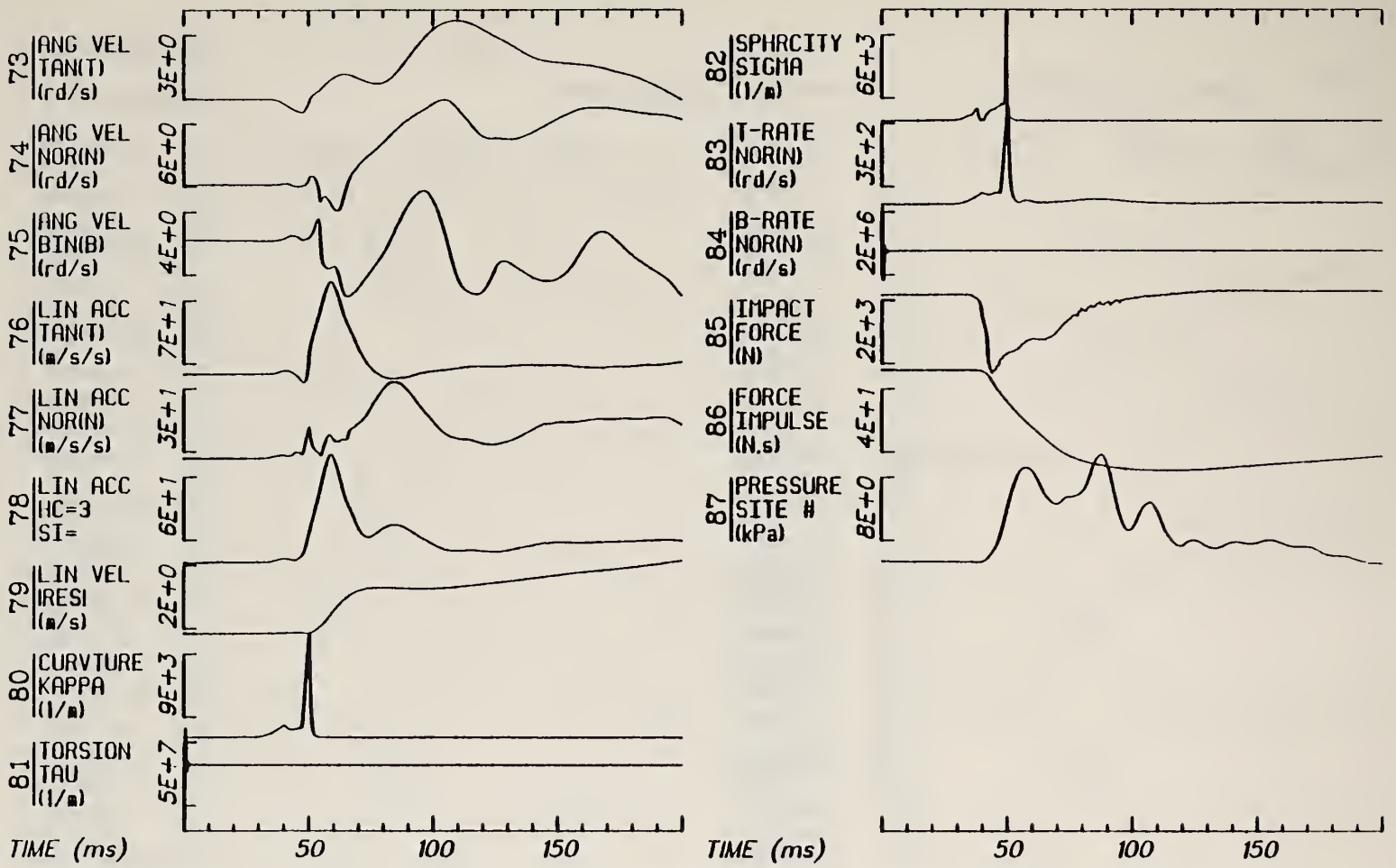

Run ID: 83E084 Disk: 83E084.3 File: 1 Date: MAY 23, 1985 Sheet: 5

*Filter:1600*4C*

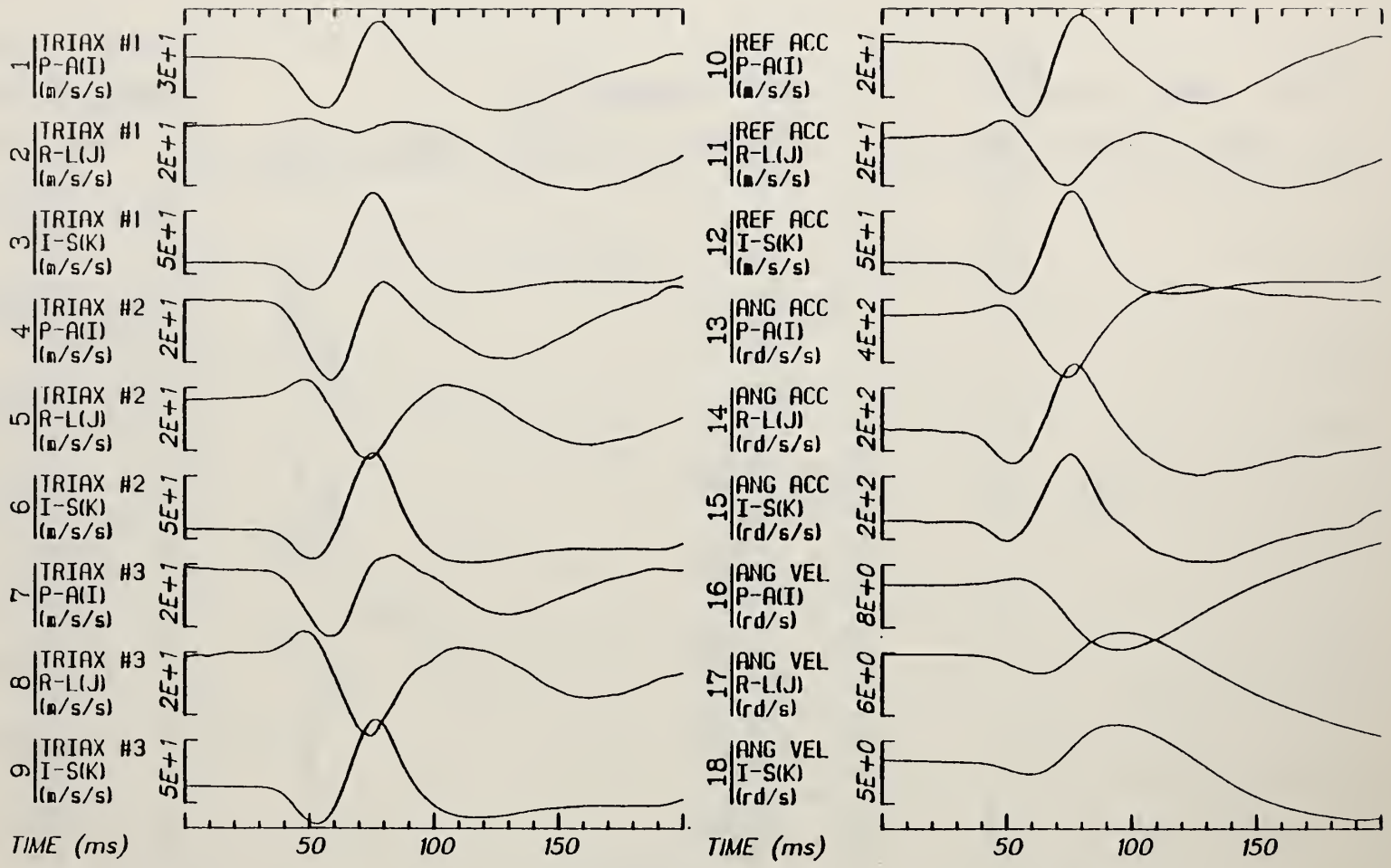

Run ID: 83E085 Disk: 83E085.3 File: 1 Date: MAY 23, 1985 Sheet: 1

*Filter: 1600*4C*

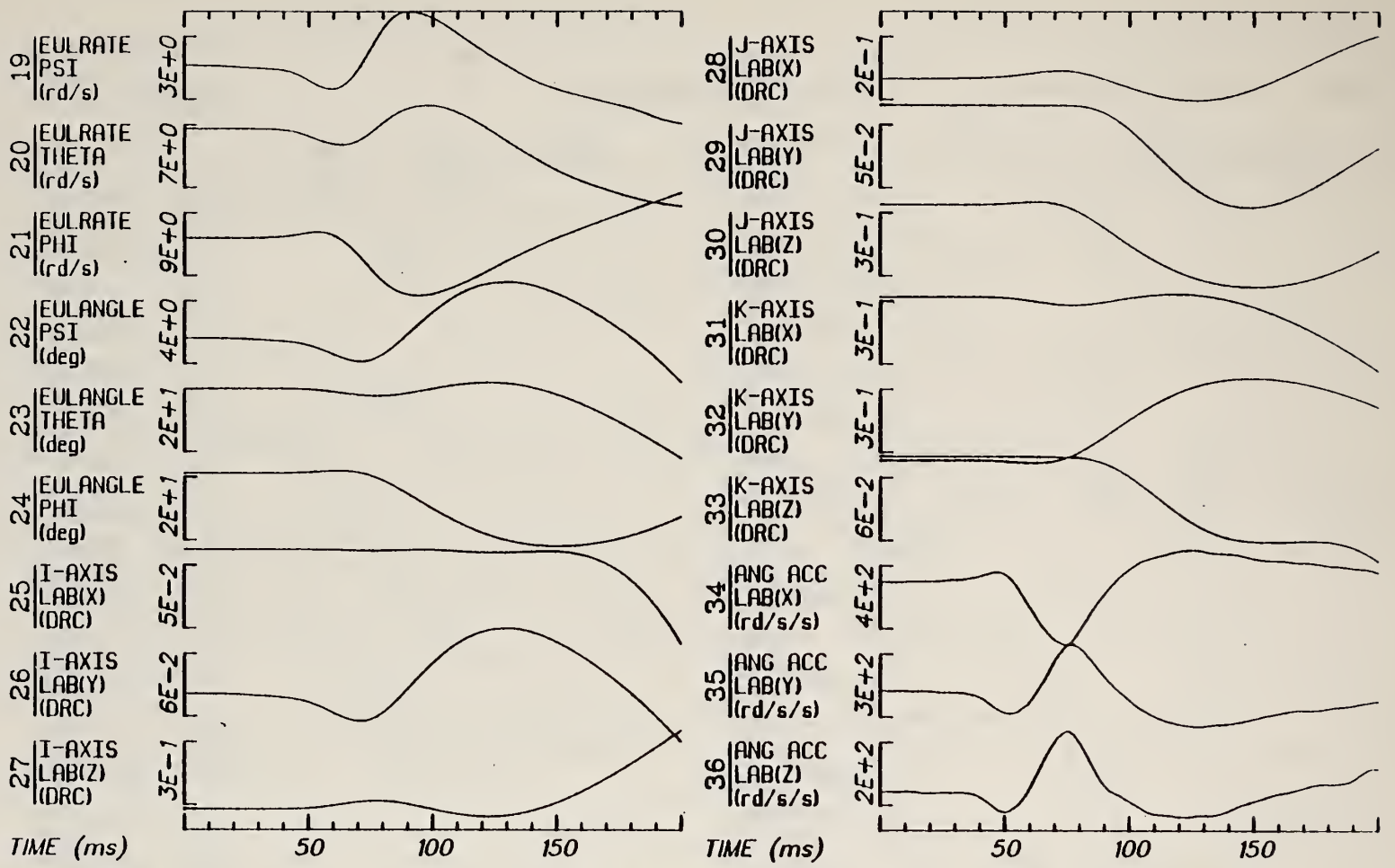

Run ID: 83E085 Disk: 83E085.3 File: 1 Date: MAY 23, 1985 Sheet: 2

*Filter:1600*4C*

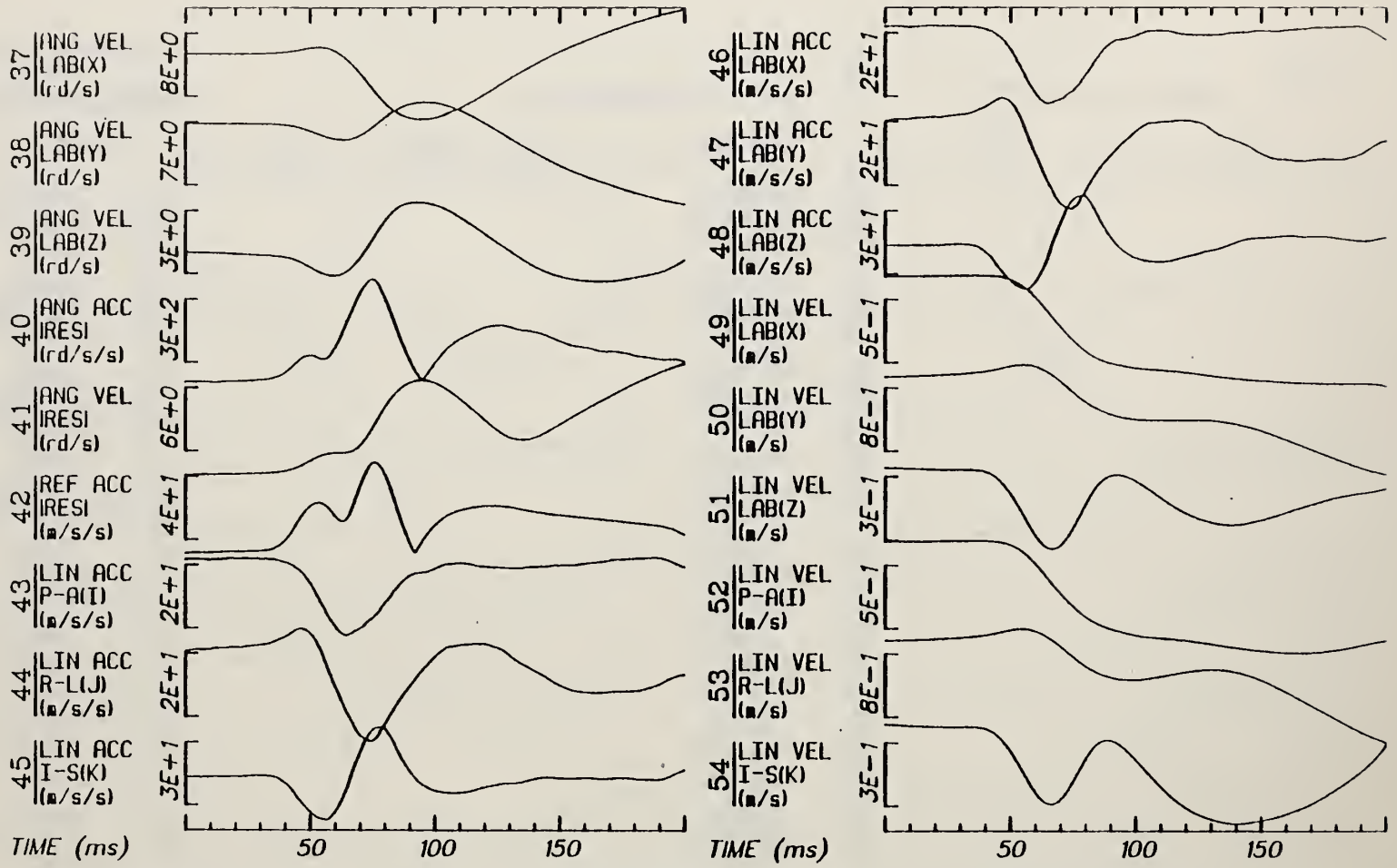

Run ID: 83E085 Disk: 83E085.3 File: 1 Date: MAY 23, 1985 Sheet: 3

Filter:1600*4C

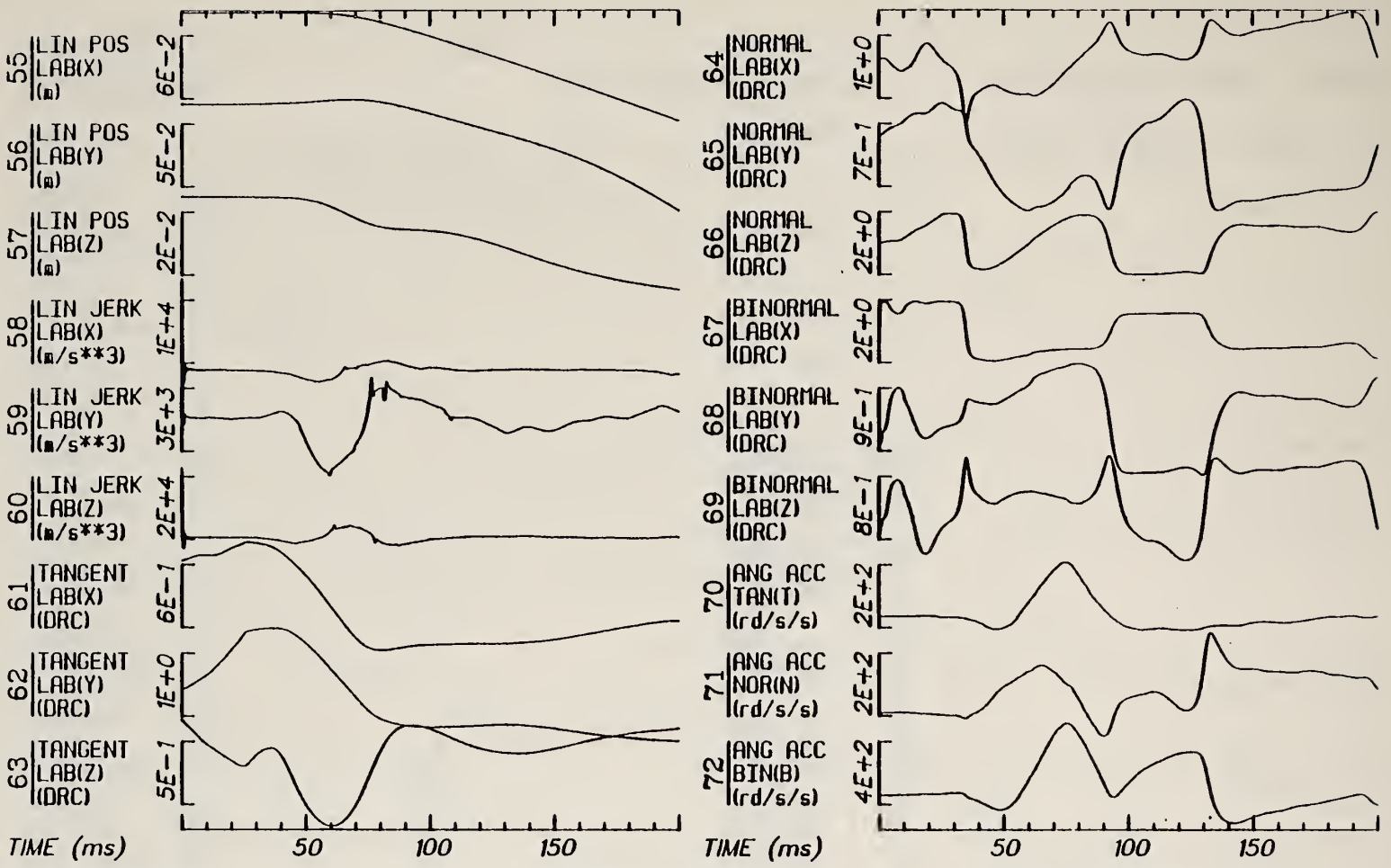

Run ID: 83E085 Disk: 83E085.3 File: 1 Date: MAY 23, 1985 Sheet: 4

*Filter:1600*4C*

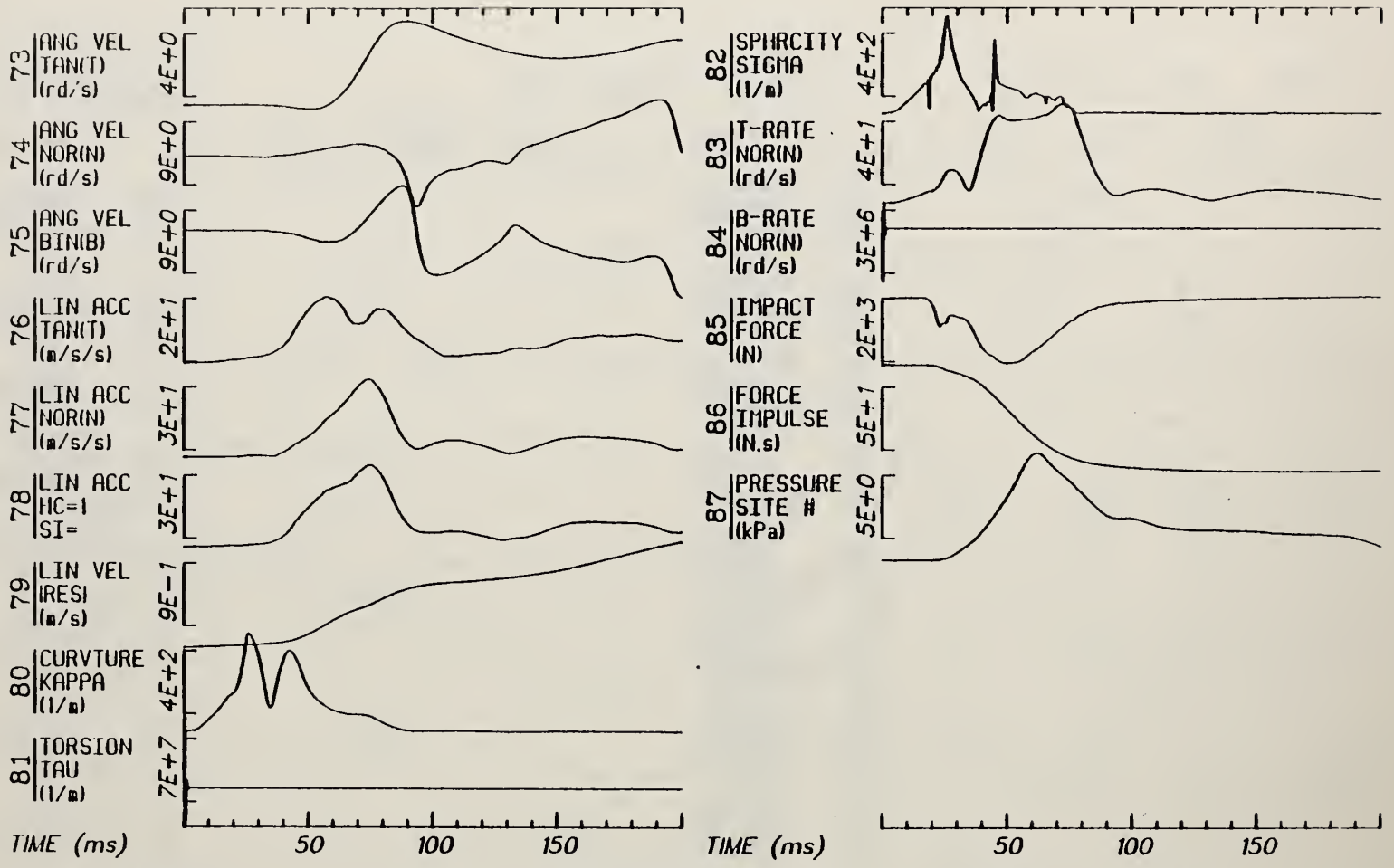

Run ID: 83E085 Disk: 83E085.3 File: 1 Date: MAY 23, 1985 Sheet: 5

*Filter:1600*4C*

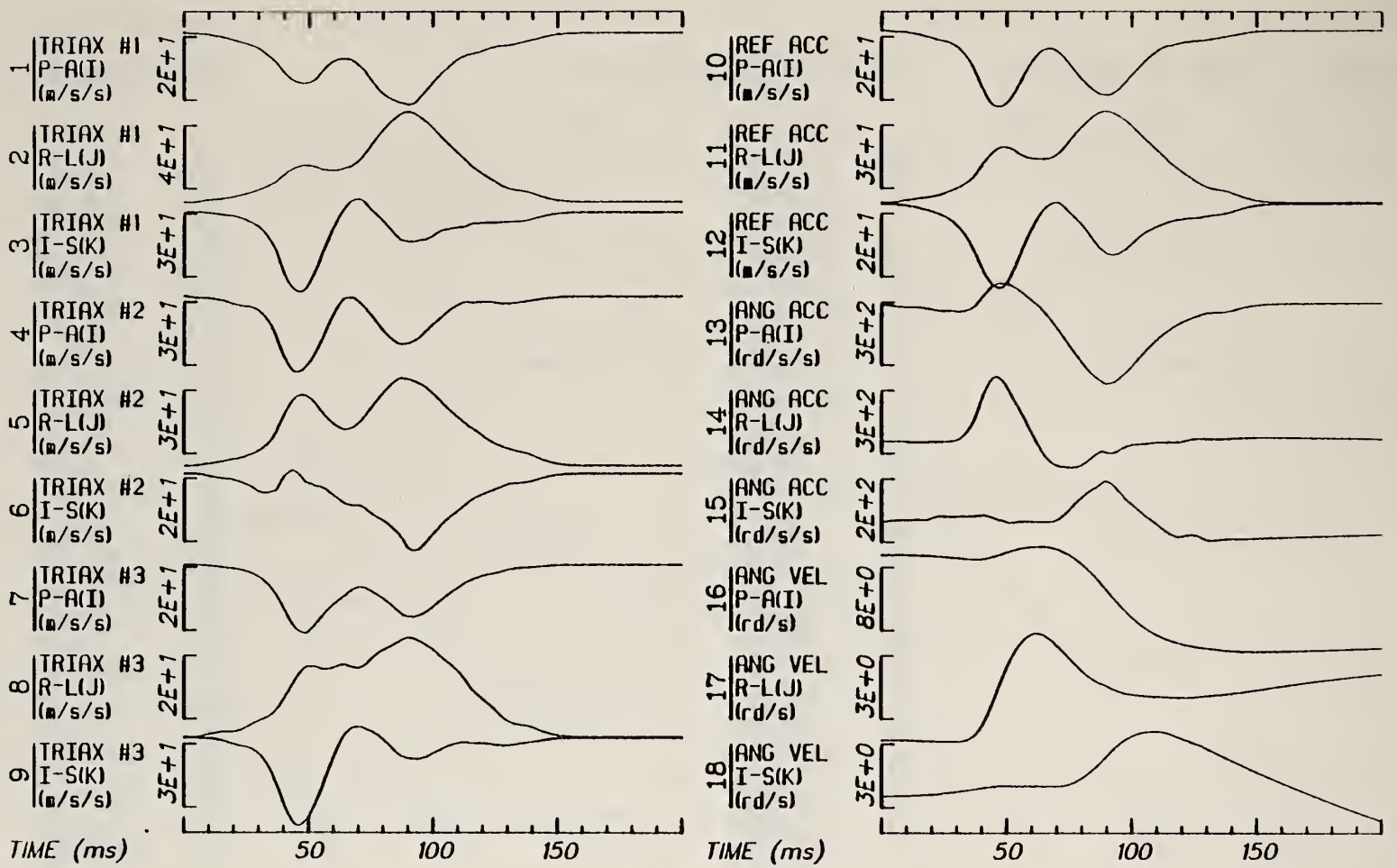

Run ID: 83E104 Disk: 83E104.3 File: 1 Date: MAY 23, 1985 Sheet: 1

*Filter:1600*4C*

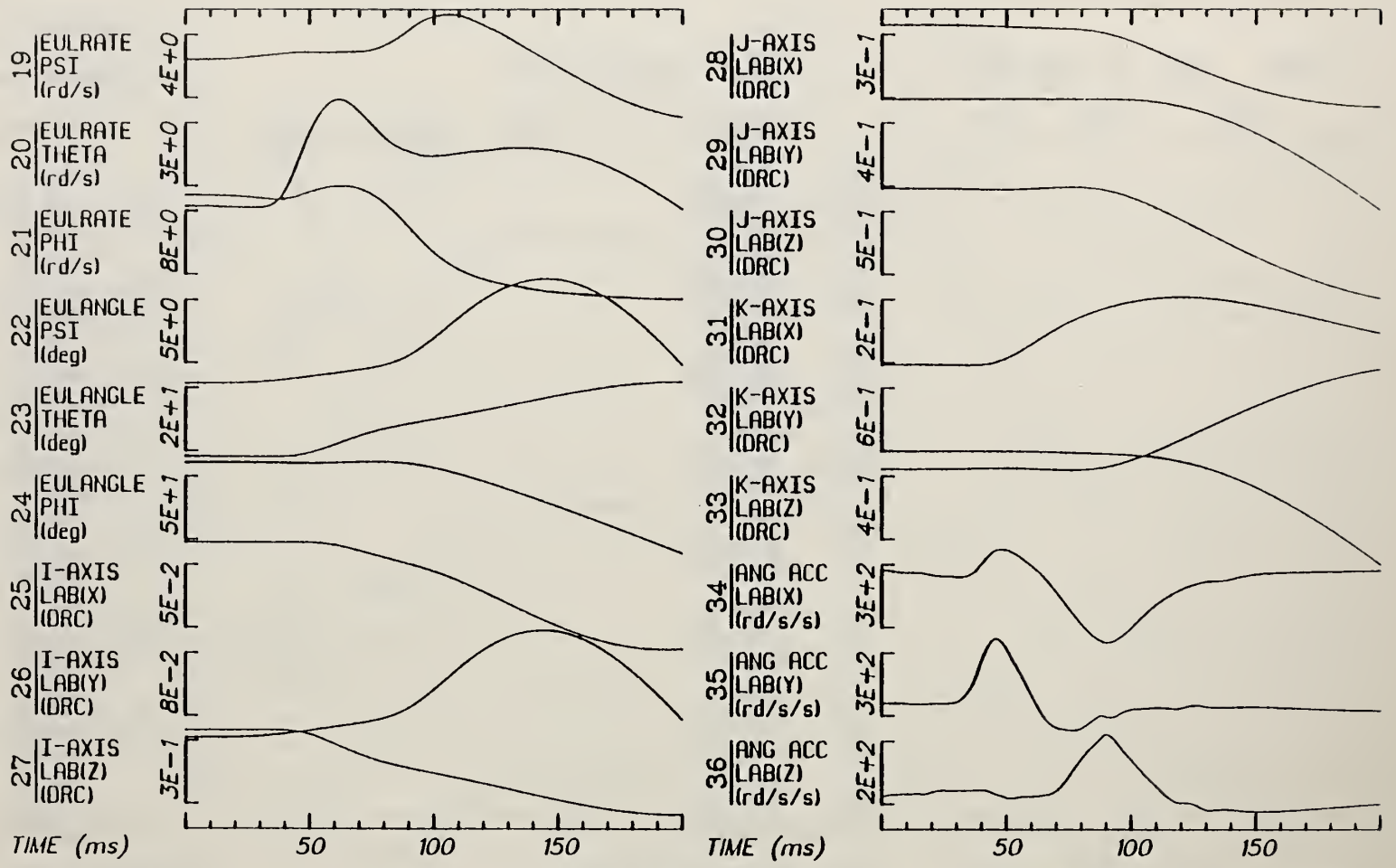

Run ID: 83E104 Disk: 83E104.3 File: 1 Date: MAY 23, 1985 Sheet: 2

*Filter:1600*4C*

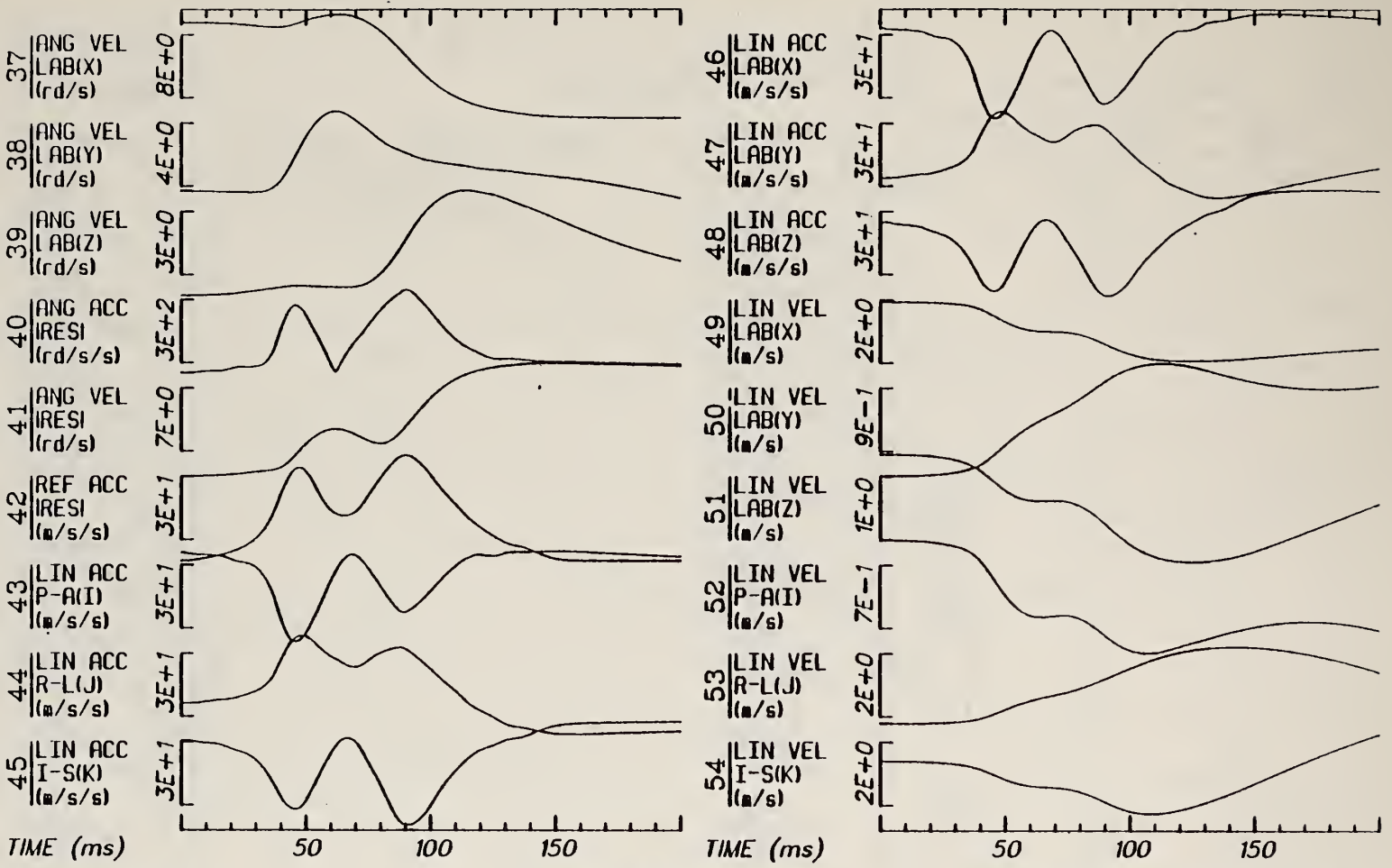

Run ID: 83E104 Disk: 83E104.3 File: 1 Date: MAY 23, 1985 Sheet: 3

*Filter:1600*4C*

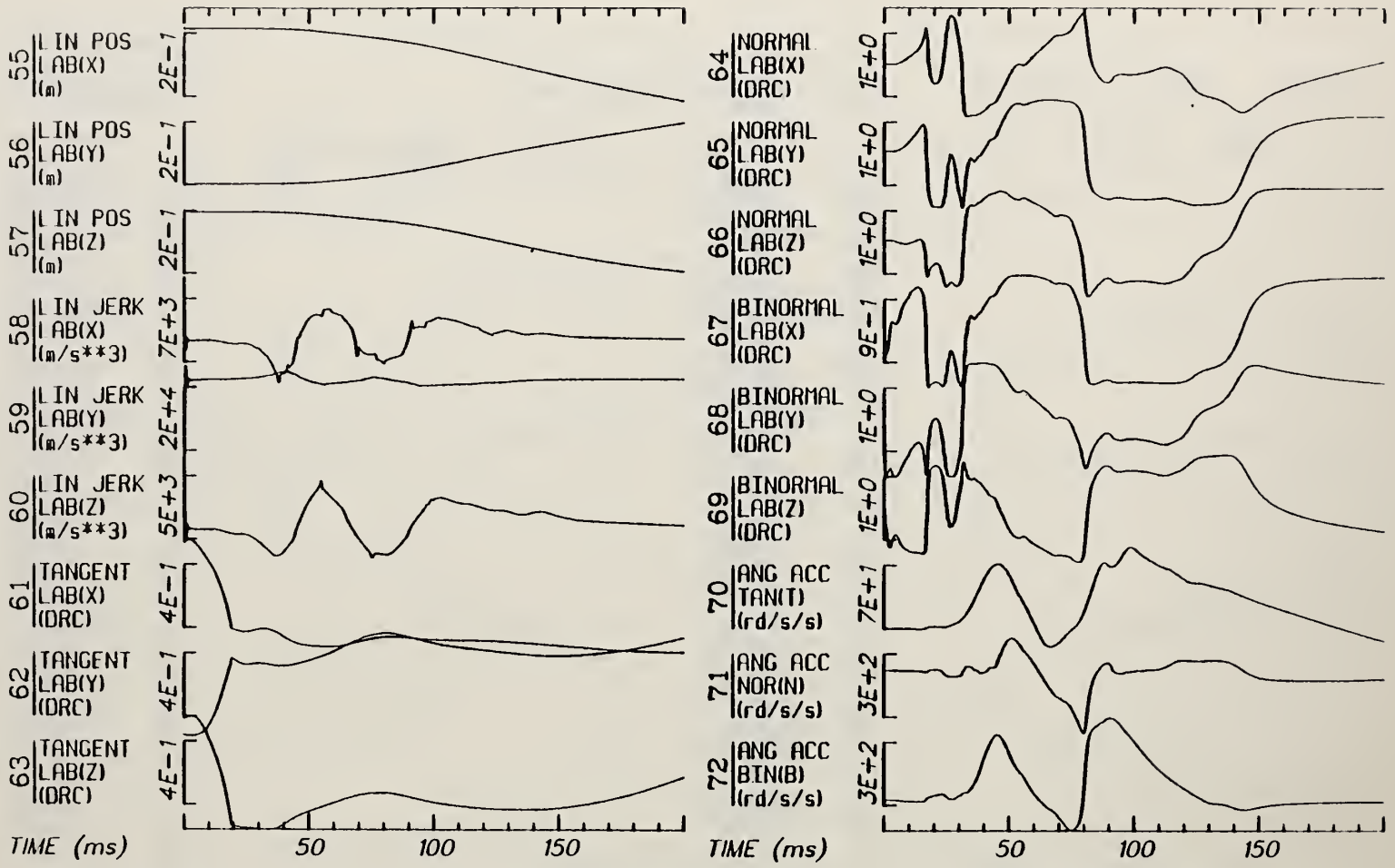

Run ID: 83E104 Disk: 83E104.3 File: 1 Date: MAY 23, 1985 Sheet: 4

*Filter:1600*4C*

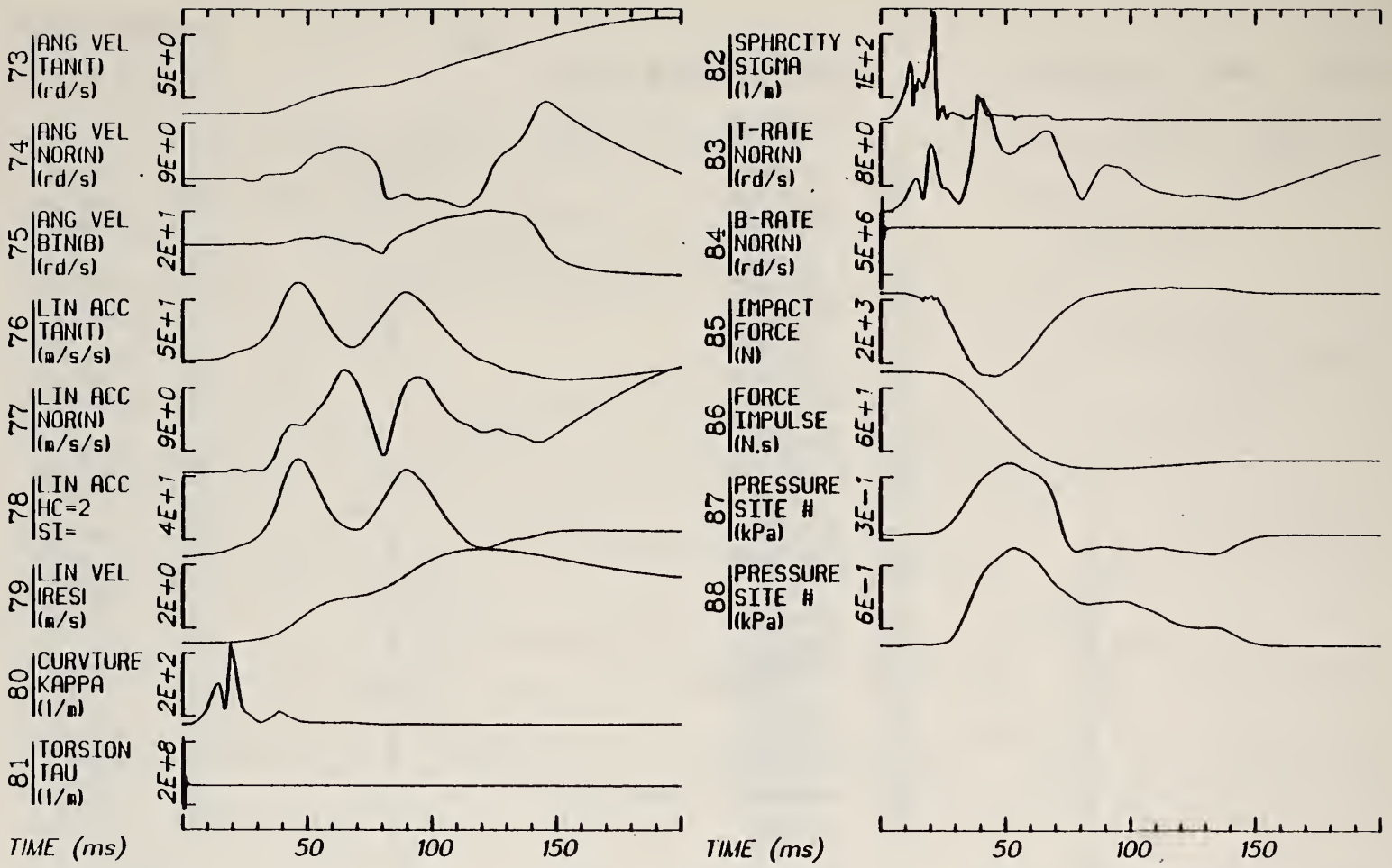

Run ID: 83E104 Disk: 83E104.3 File: 1 Date: MAY 23, 1985 Sheet: 5

*Filter:1600*4C*

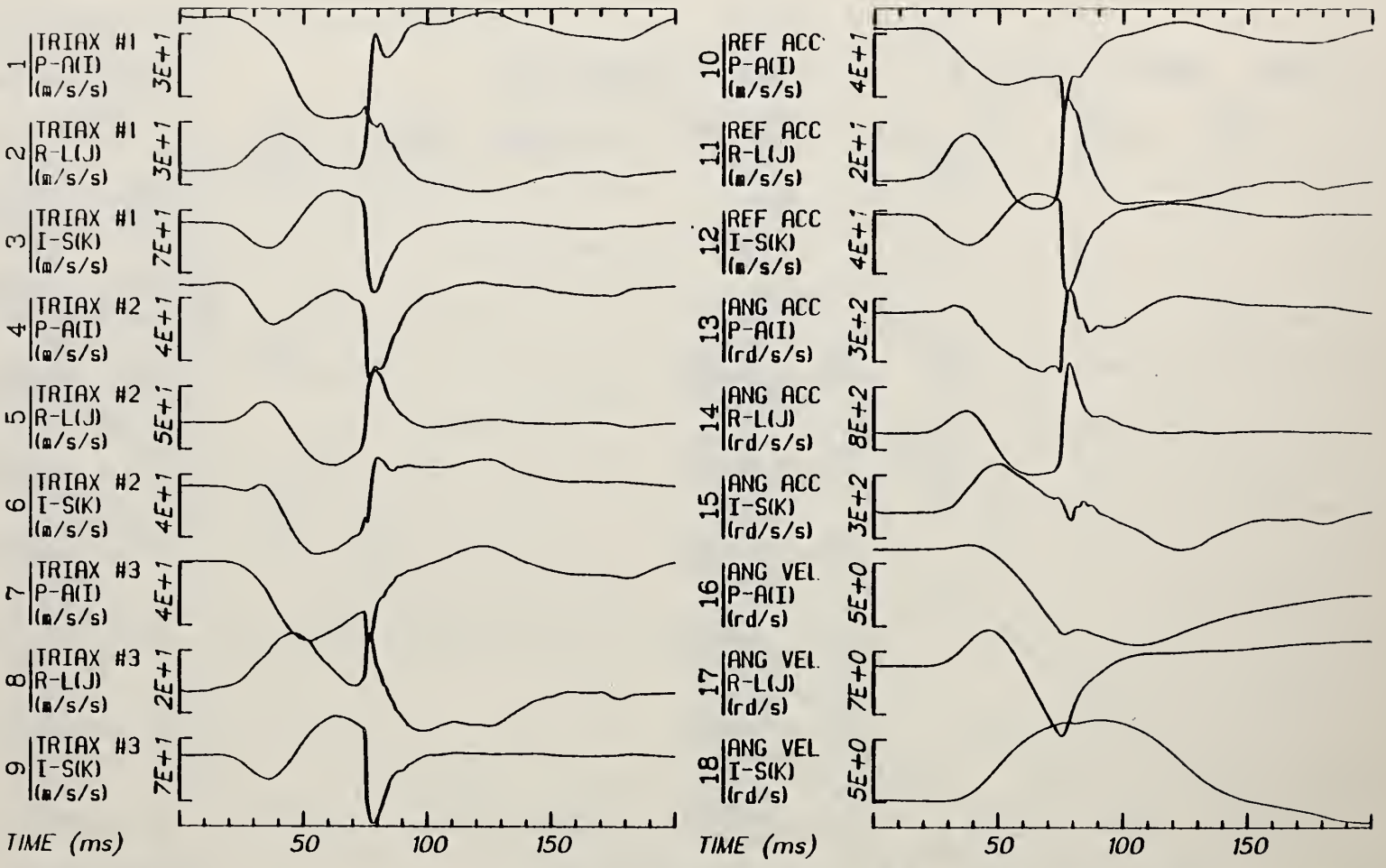

Run ID: 83E105 Disk: 83E105.3 File: 1 Date: MAY 23, 1985 Sheet: 1

*Filter:1600*4C*

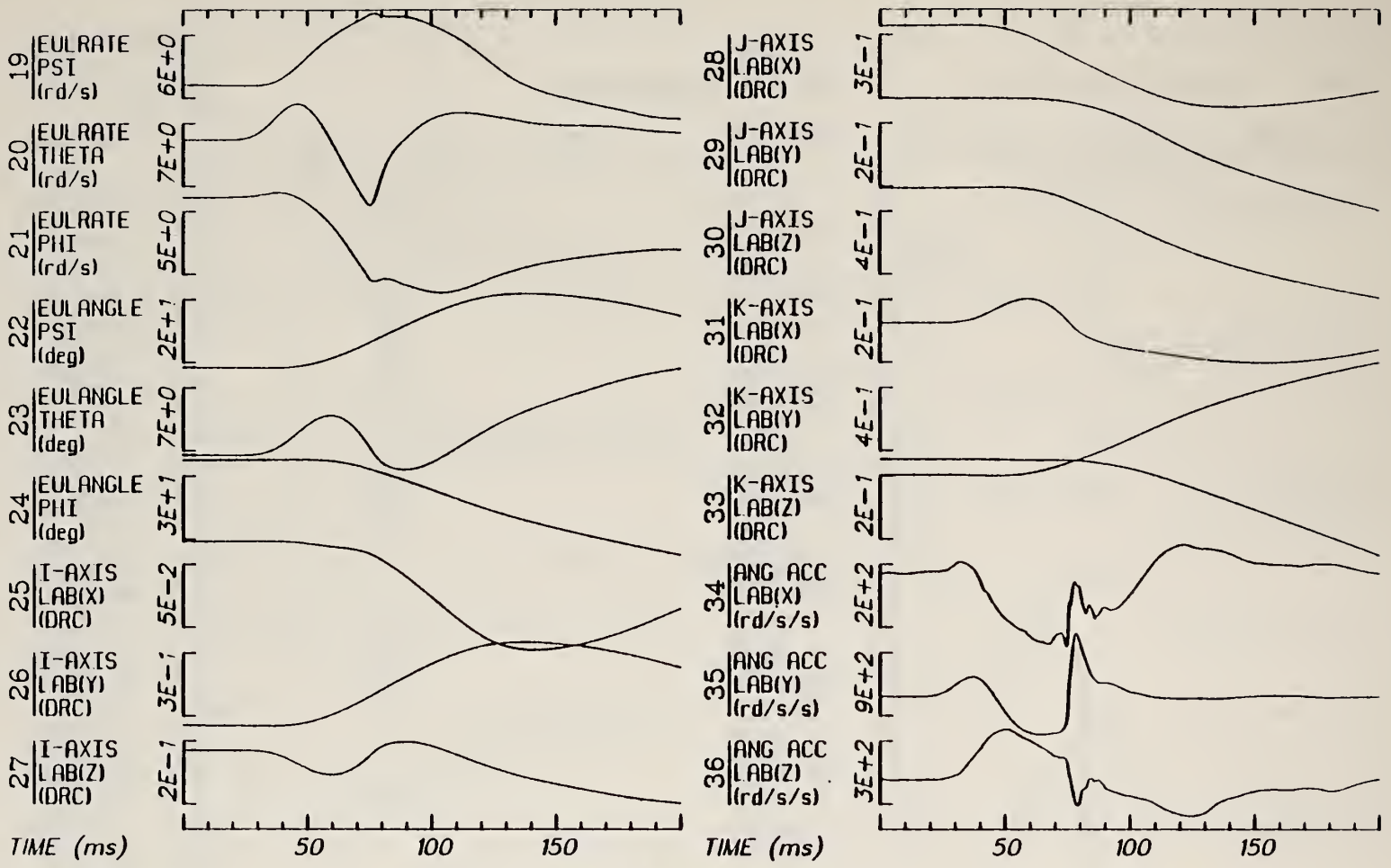

Run ID: 83E105 Disk: 83E105.3 File: 1 Date: MAY 23, 1985 Sheet: 2

*Filter:1600*4C*

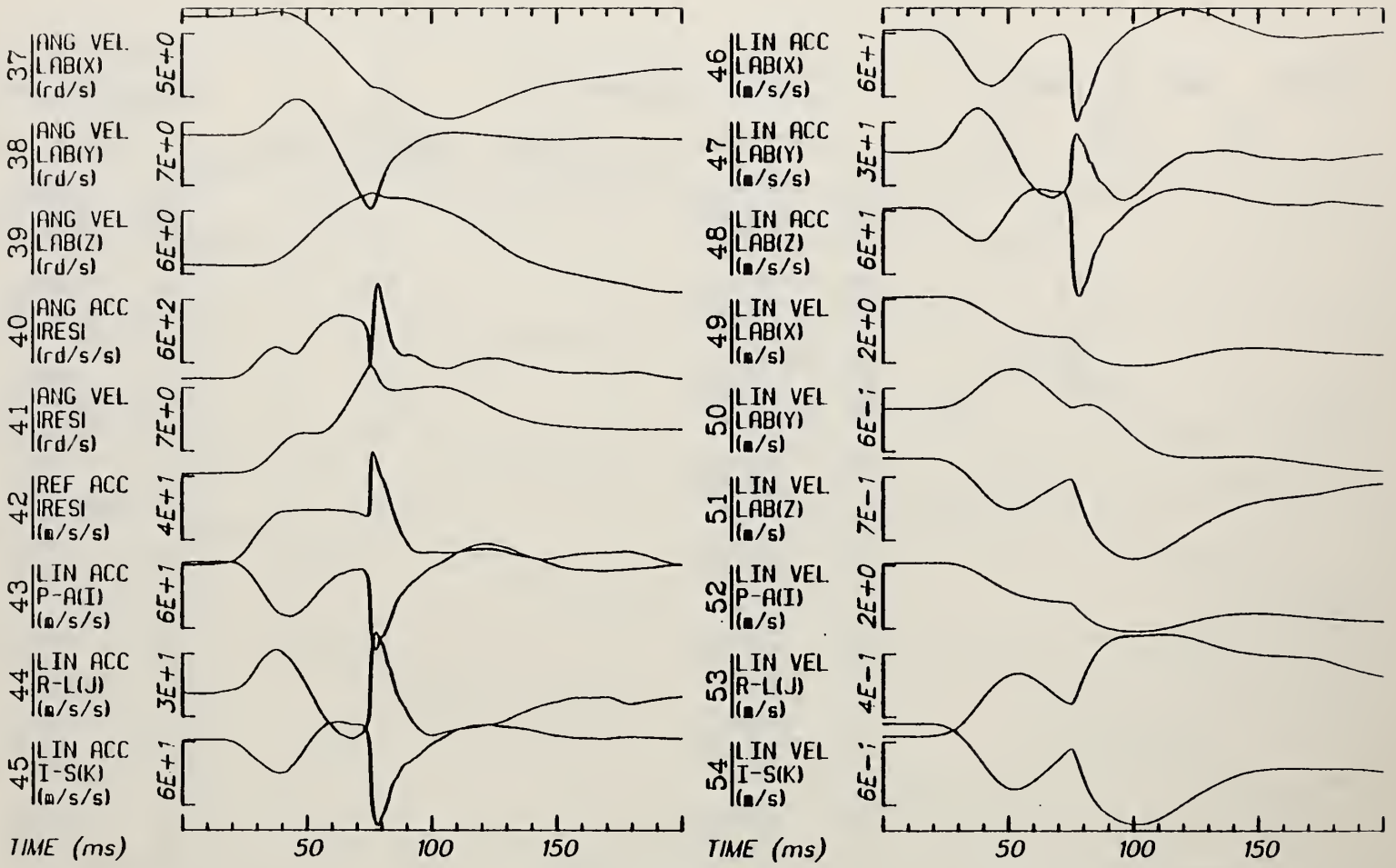

Run ID: 83E105 Disk: 83E105.3 File: 1 Date: MAY 23, 1985 Sheet: 3

*Filter:1600*4C*

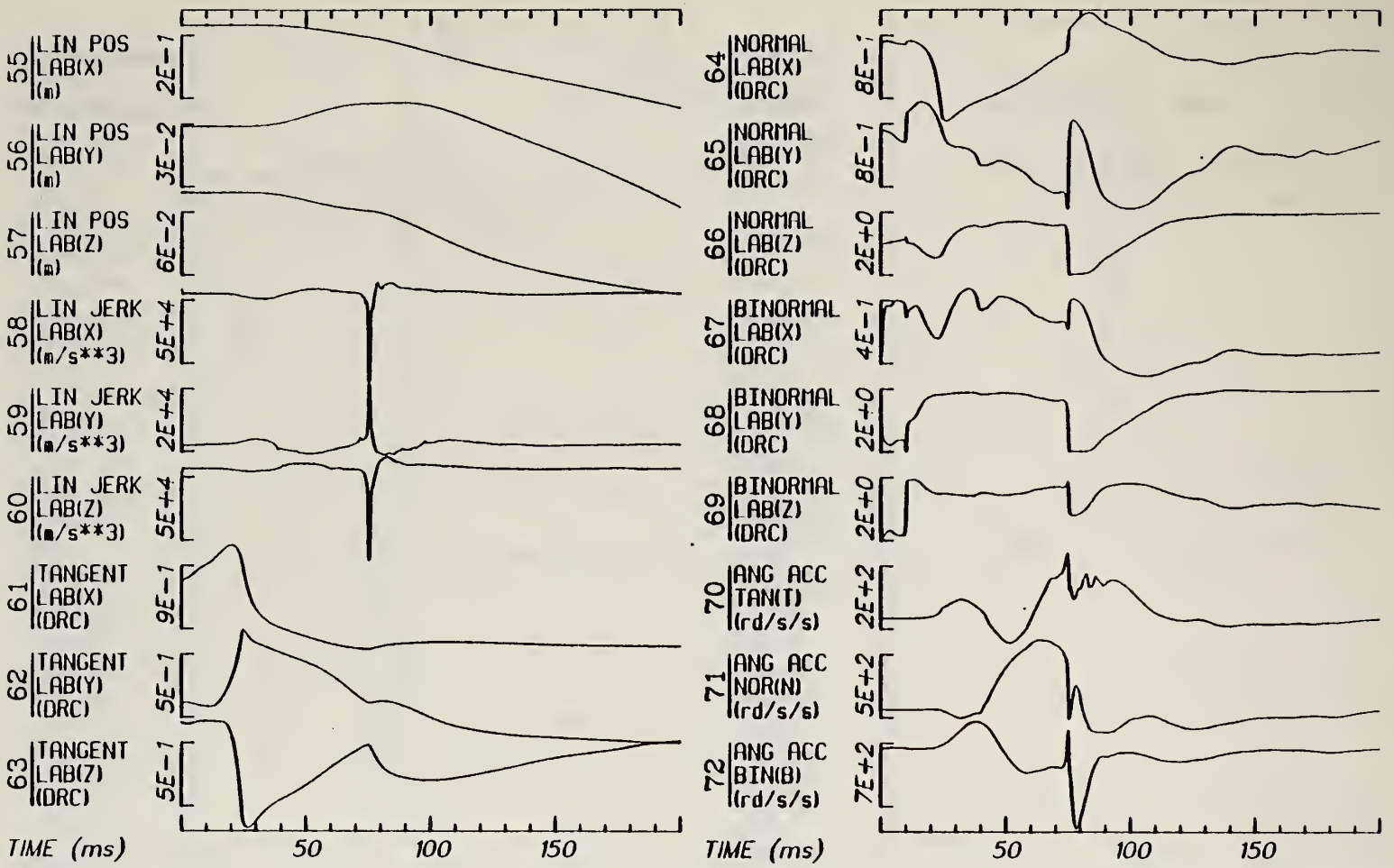

Run ID: 83E105 Disk: 83E105.3 File: 1 Date: MAY 23, 1985 Sheet: 4

*Filter:1600*4C*

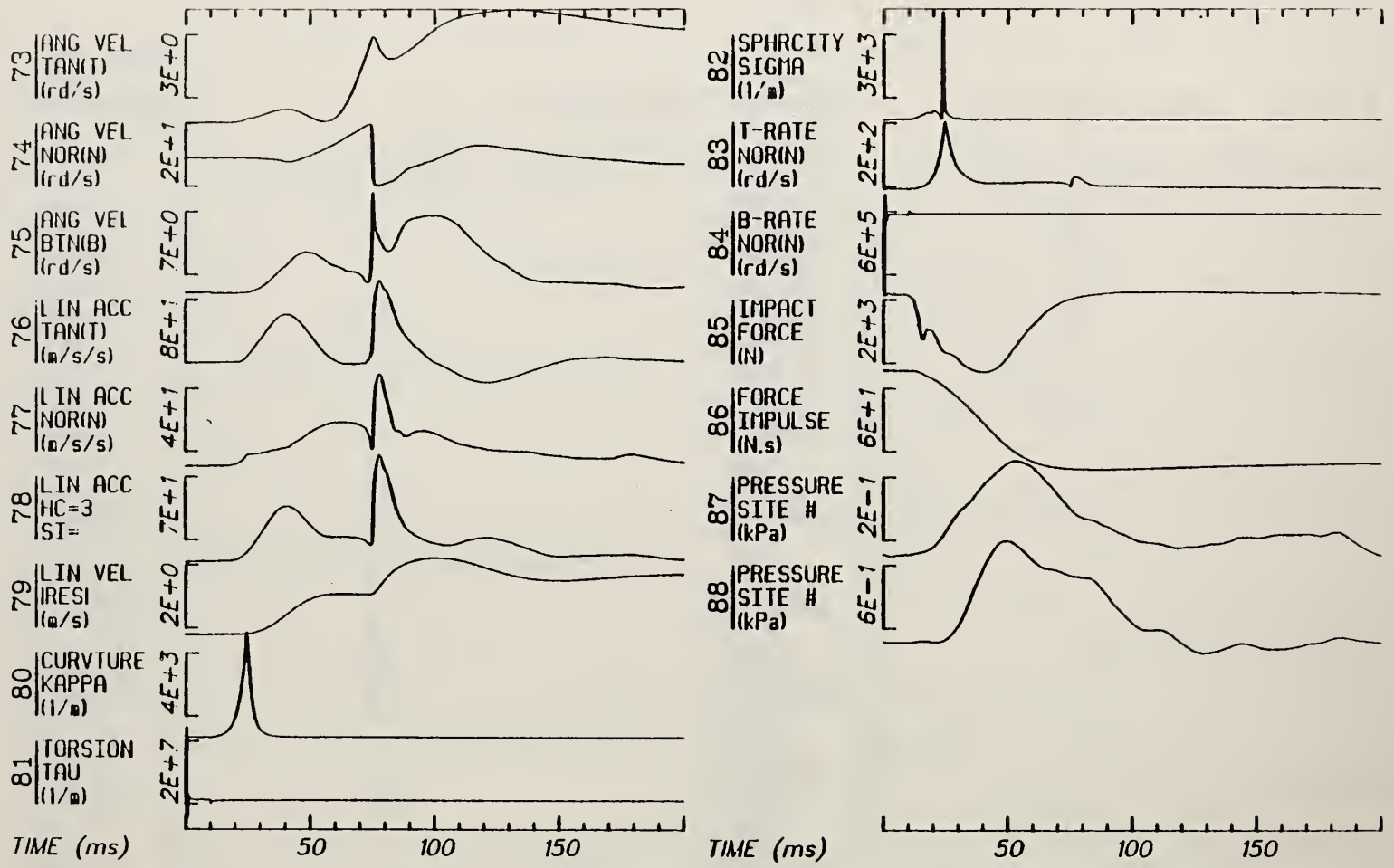

Run ID: 83E105 Disk: 83E105.3 File: 1 Date: MAY 23, 1985 Sheet: 5

*Filter:1600*4C*

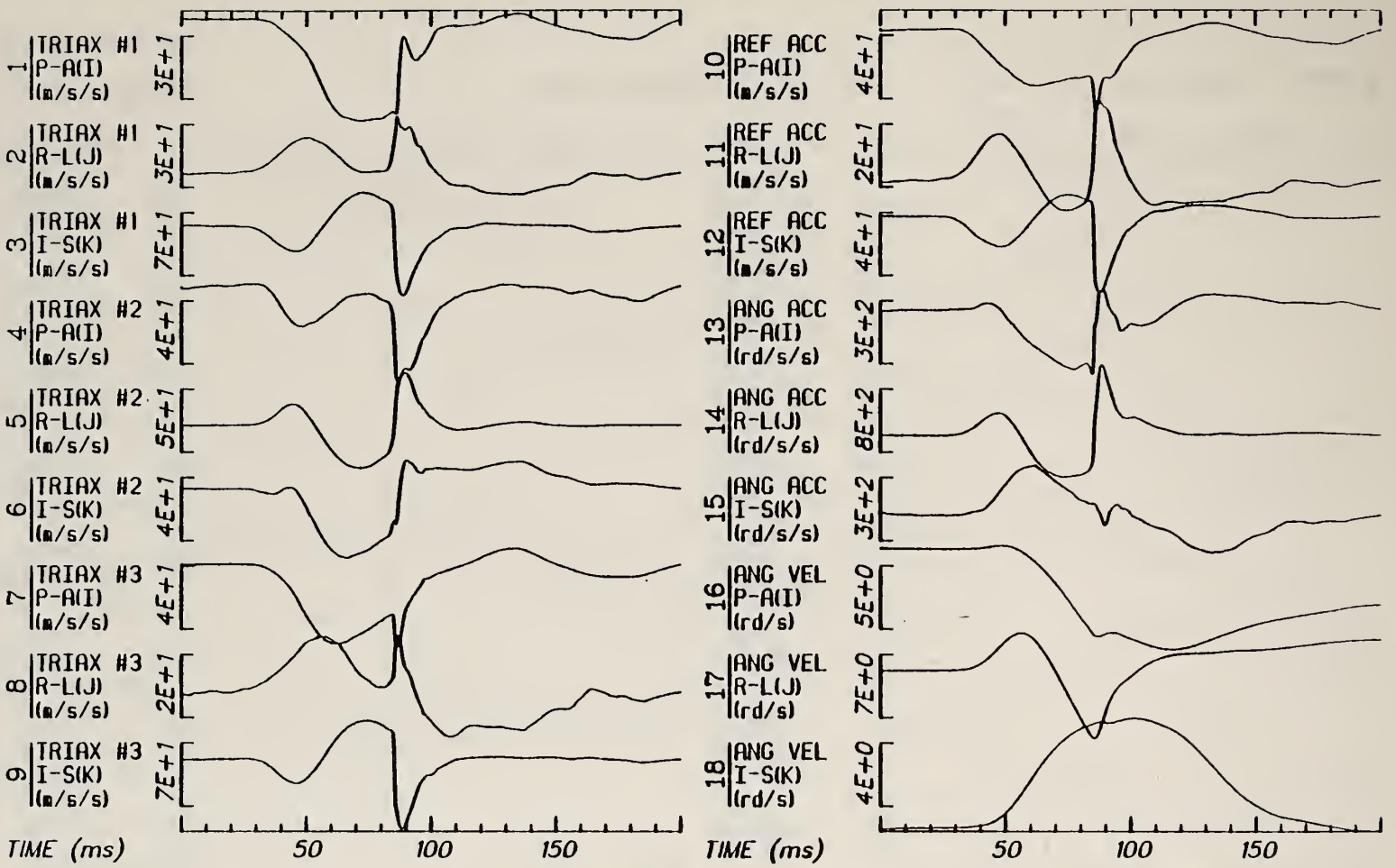

Run ID: 83E106 Disk: 83E106.3 File: 1 Date: MAY 30, 1985 Sheet: 1

*Filter:1600*4C*

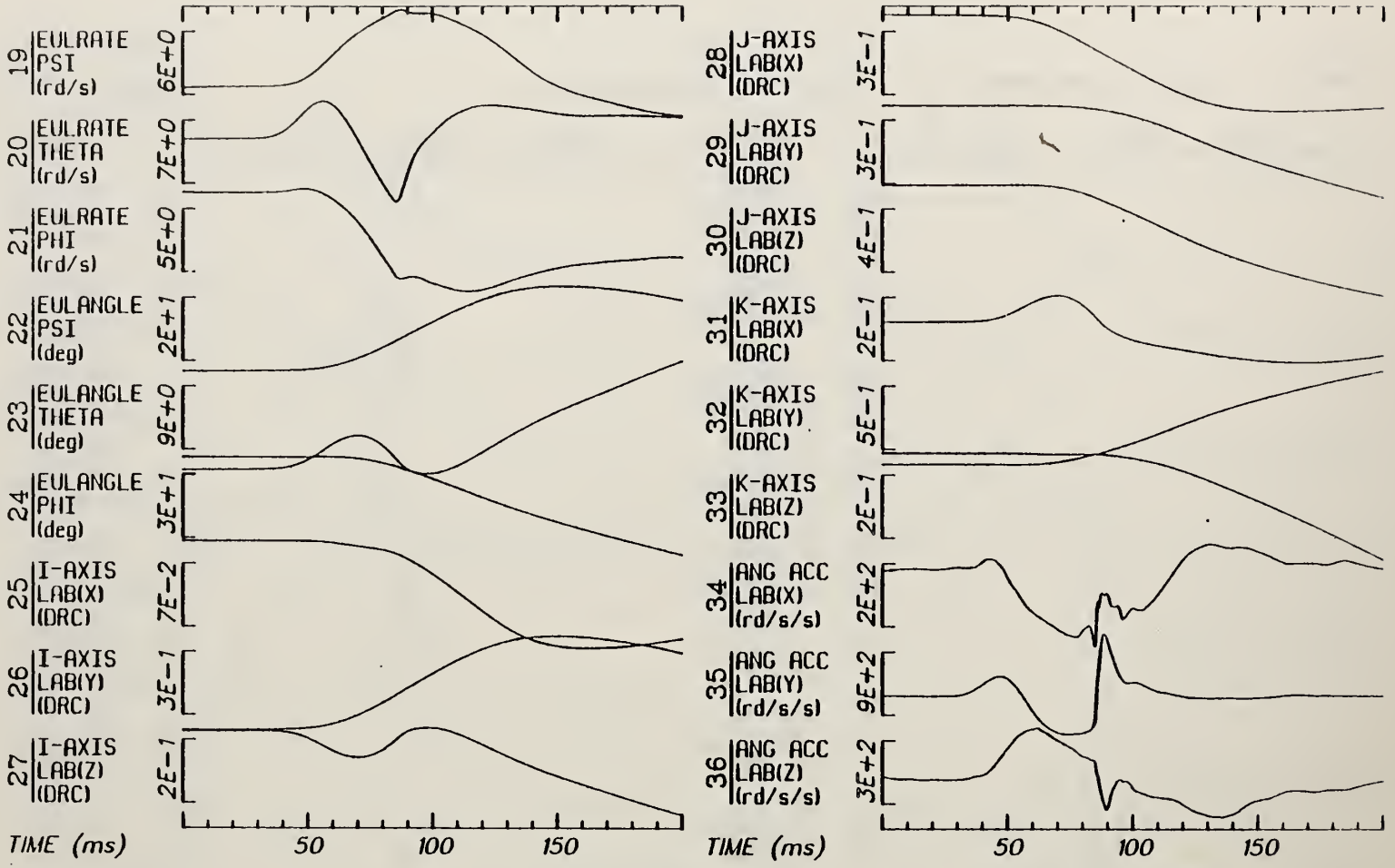

Run ID: 83E106 Disk: 83E106.3 File: 1 Date: MAY 30, 1985 Sheet: 2

*Filter:1600*4C*

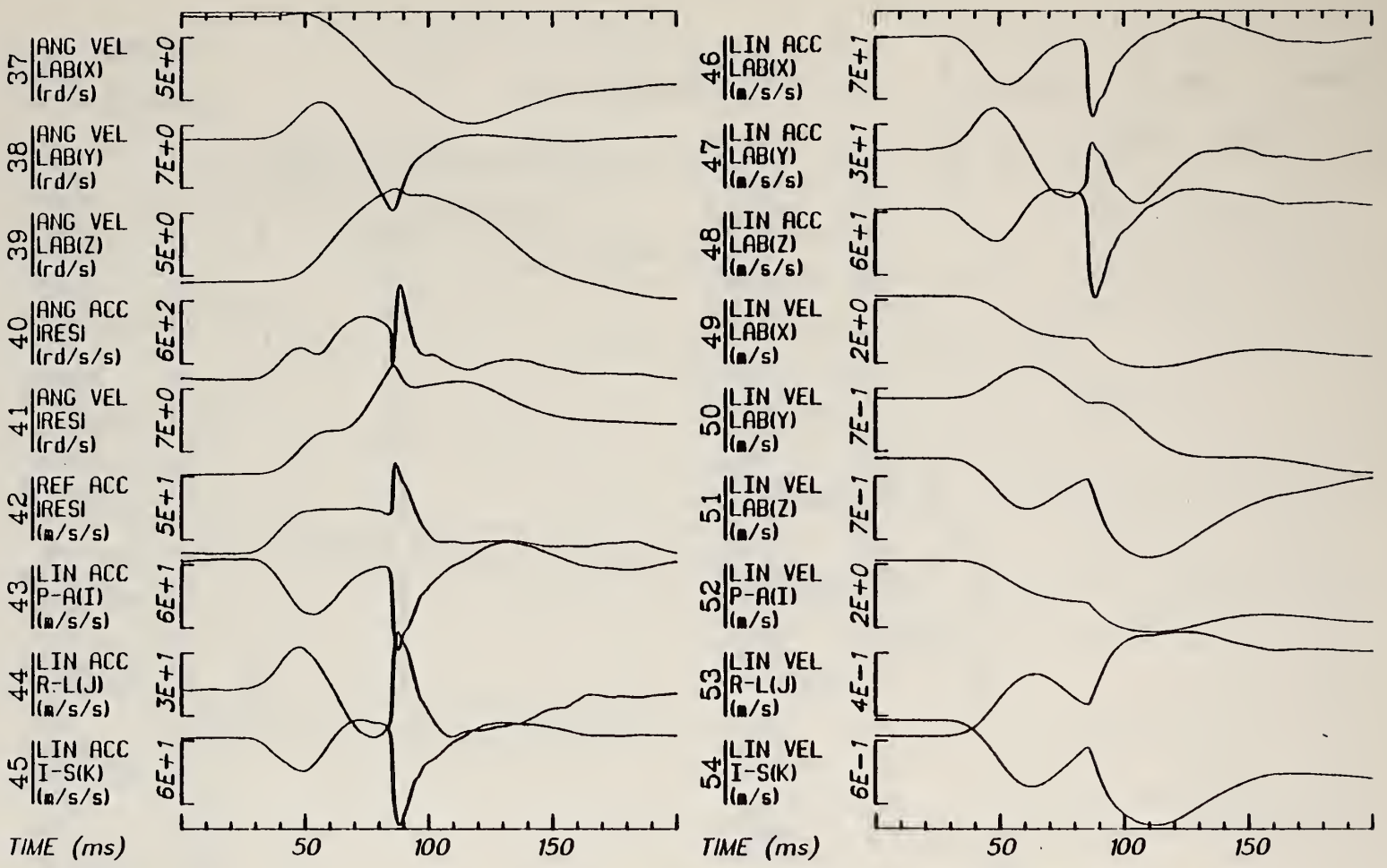

Run ID: 83E106 Disk: 83E106.3 File: 1 Date: MAY 30, 1985 Sheet: 3

*Filter:1600*4C*

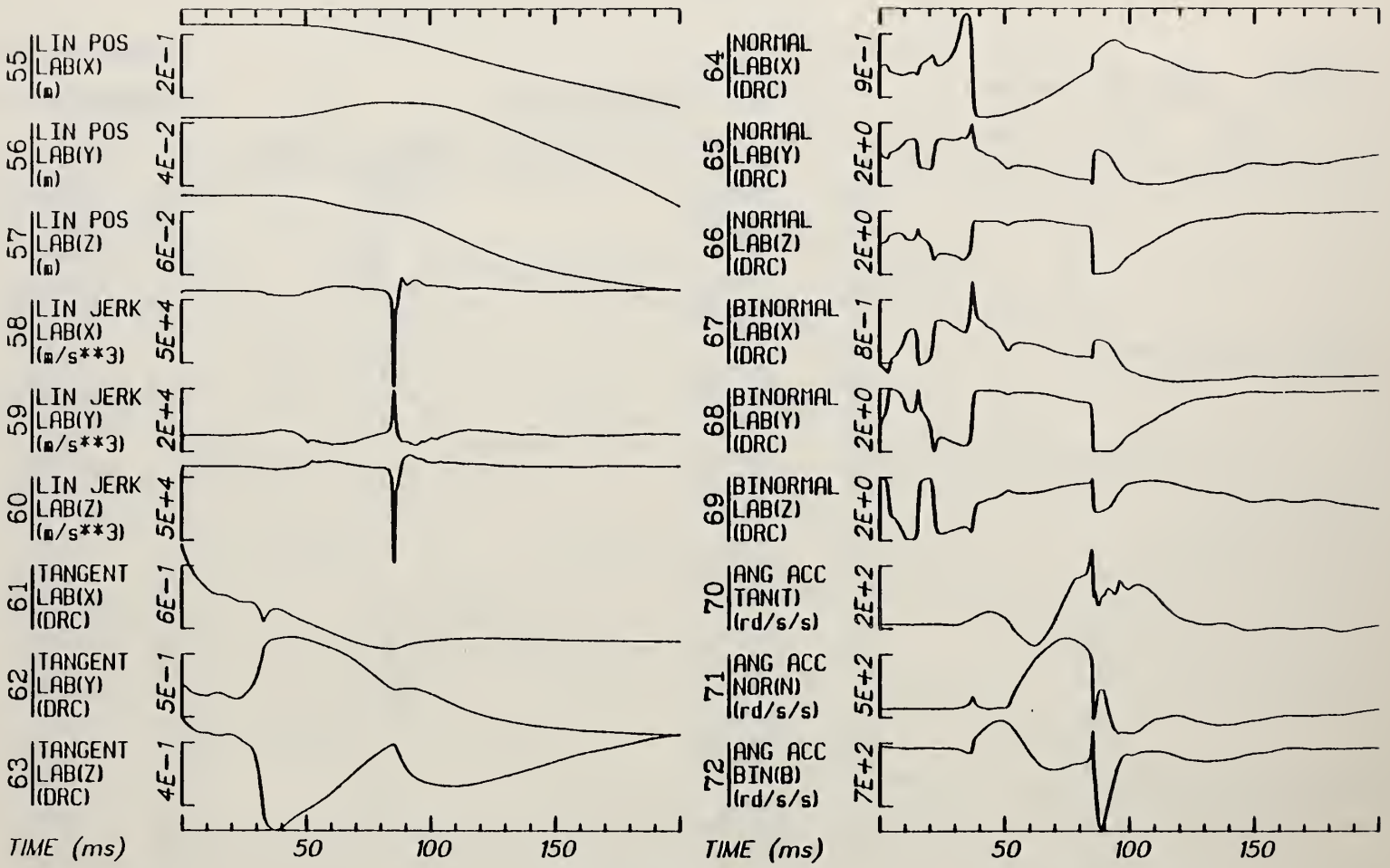

Run ID: 83E106 Disk: 83E106.3 File: 1 Date: MAY 30, 1985 Sheet: 4

*Filter:1600*4C*

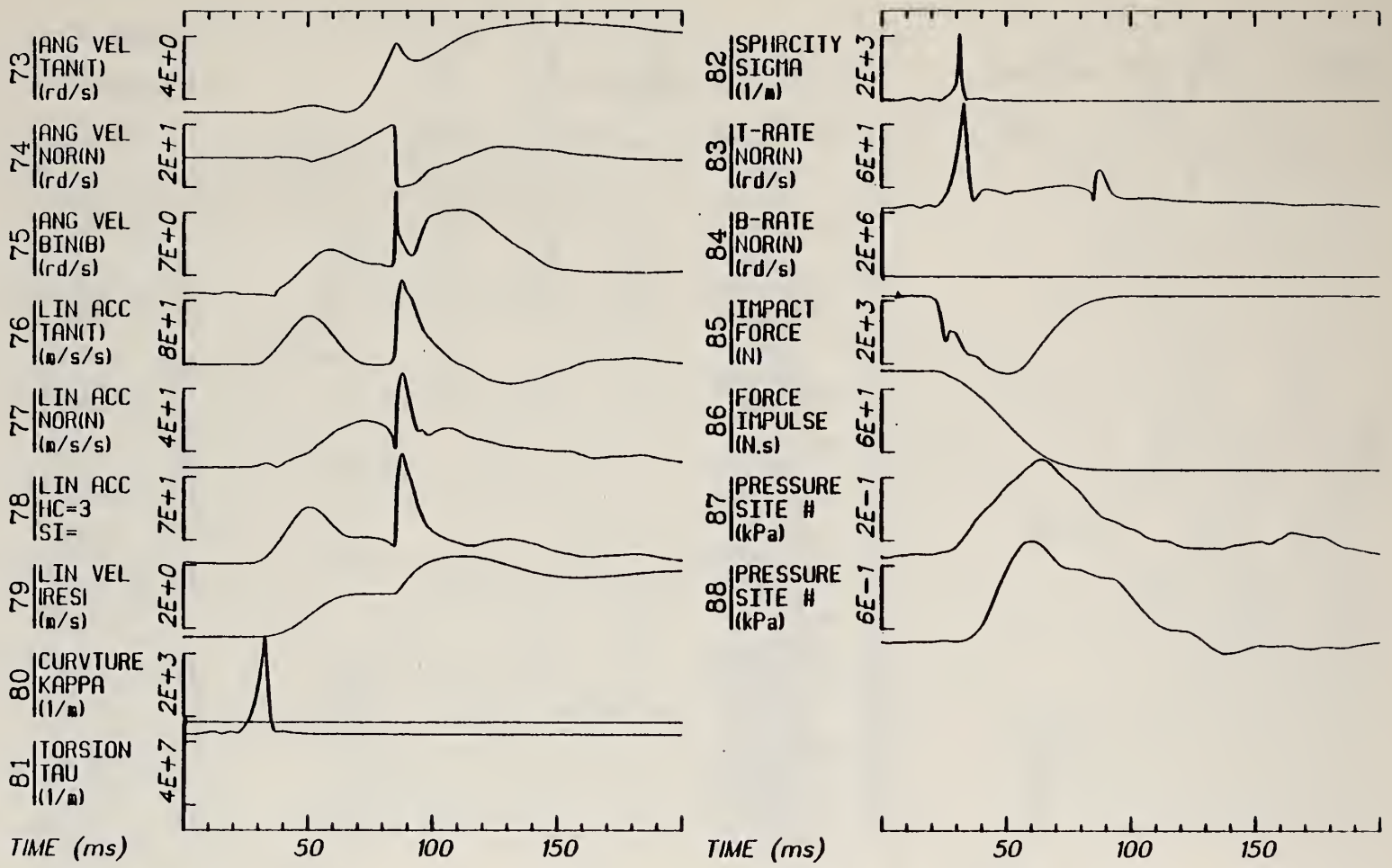

Run ID: 83E106 Disk: 83E106.3 File: 1 Date: MAY 30, 1985 Sheet: 5

*Filter:1600*4C*

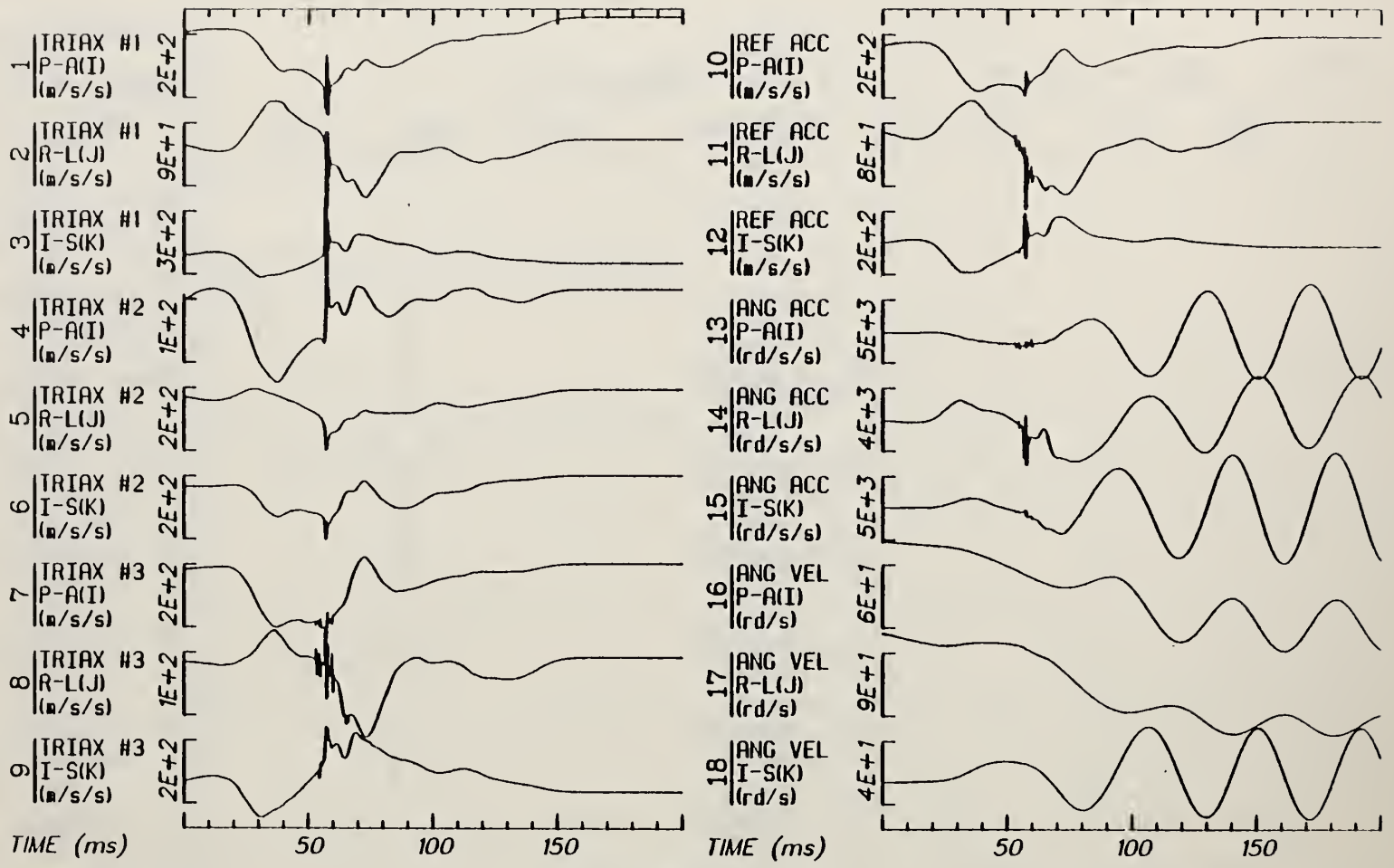

Run ID: 83E107 Disk: 83E107.3 File: 1 Date: MAY 30, 1985 Sheet: 1

*Filter: 1600*4C*

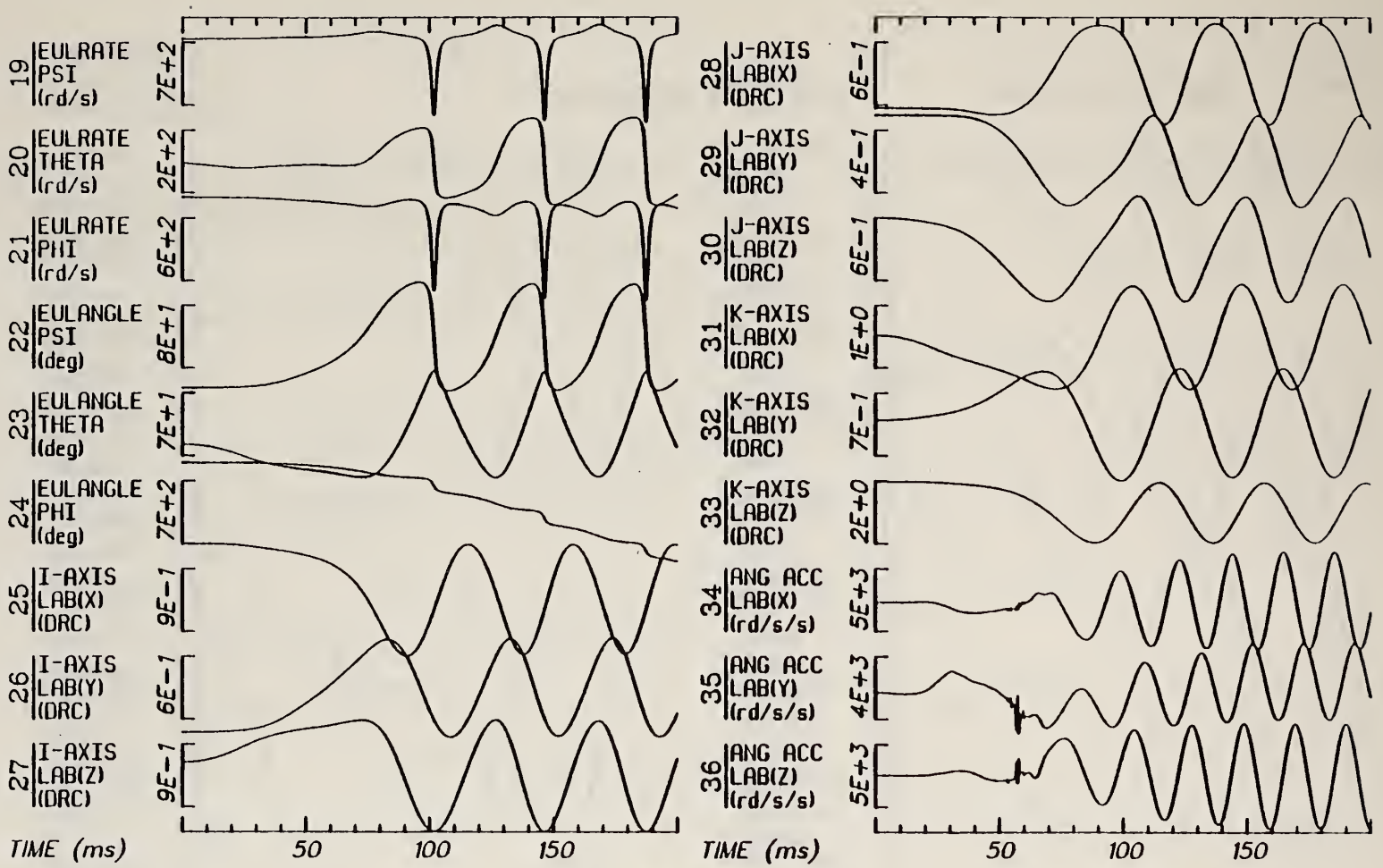

Run ID: 83E107 Disk: 83E107.3 File: 1 Date: MAY 30, 1985 Sheet: 2

*Filter:1600*4C*

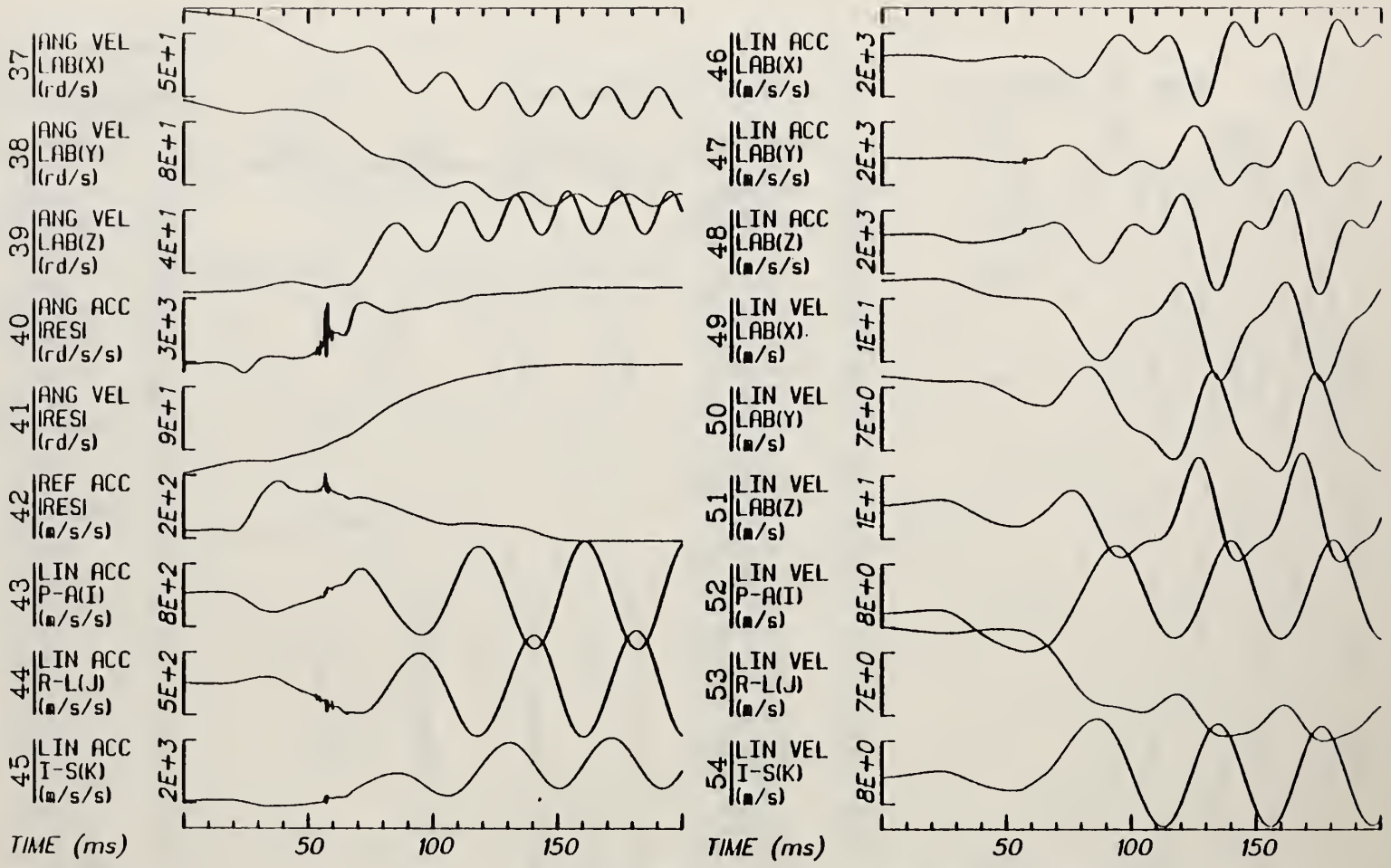

Run ID: 83E107 Disk: 83E107.3 File: 1 Date: MAY 30, 1985 Sheet: 3

*Filter:1600*4C*

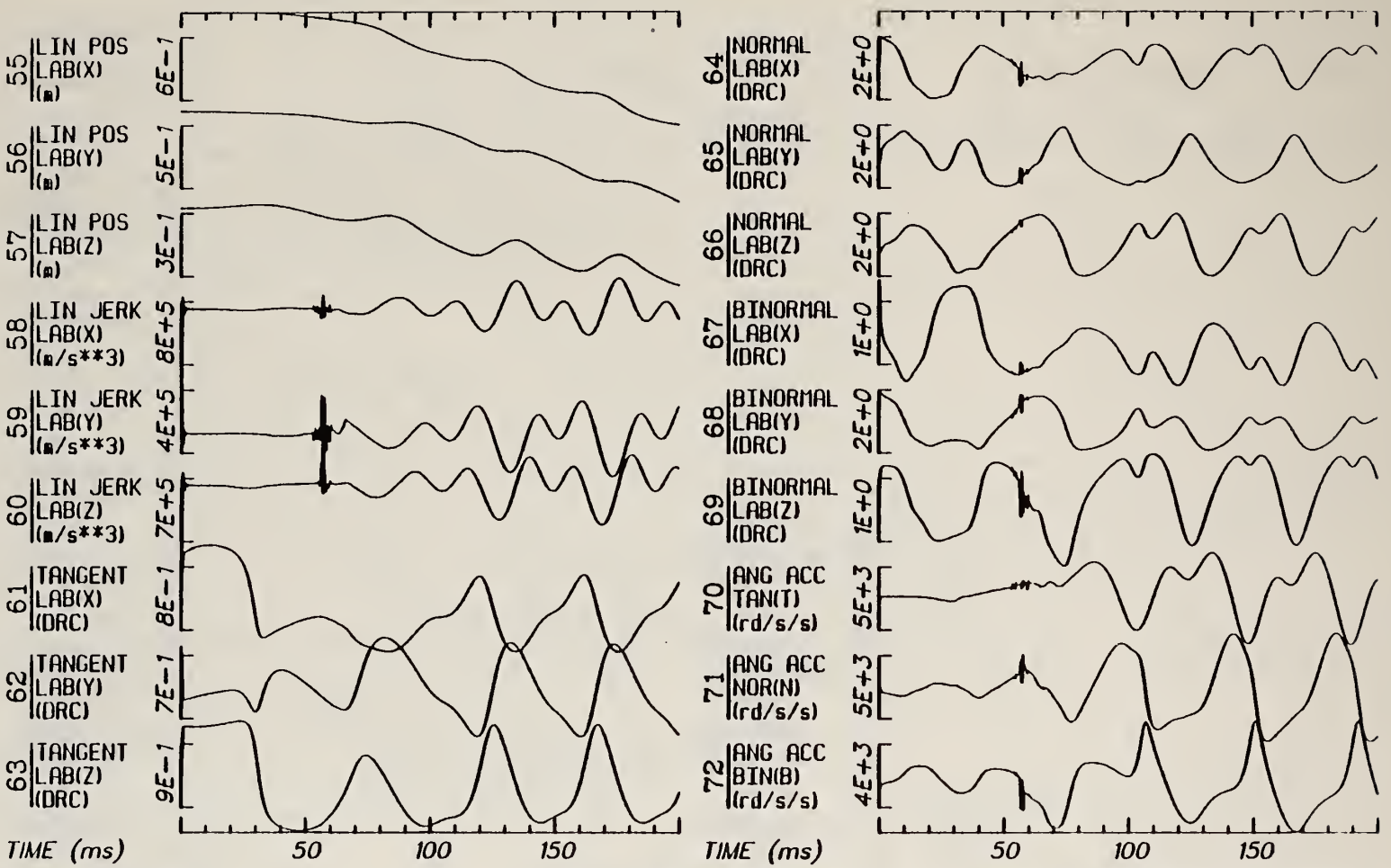

Run ID: 83E107 Disk: 83E107.3 File: 1 Date: MAY 30, 1985 Sheet: 4

*Filter:1600*4C*

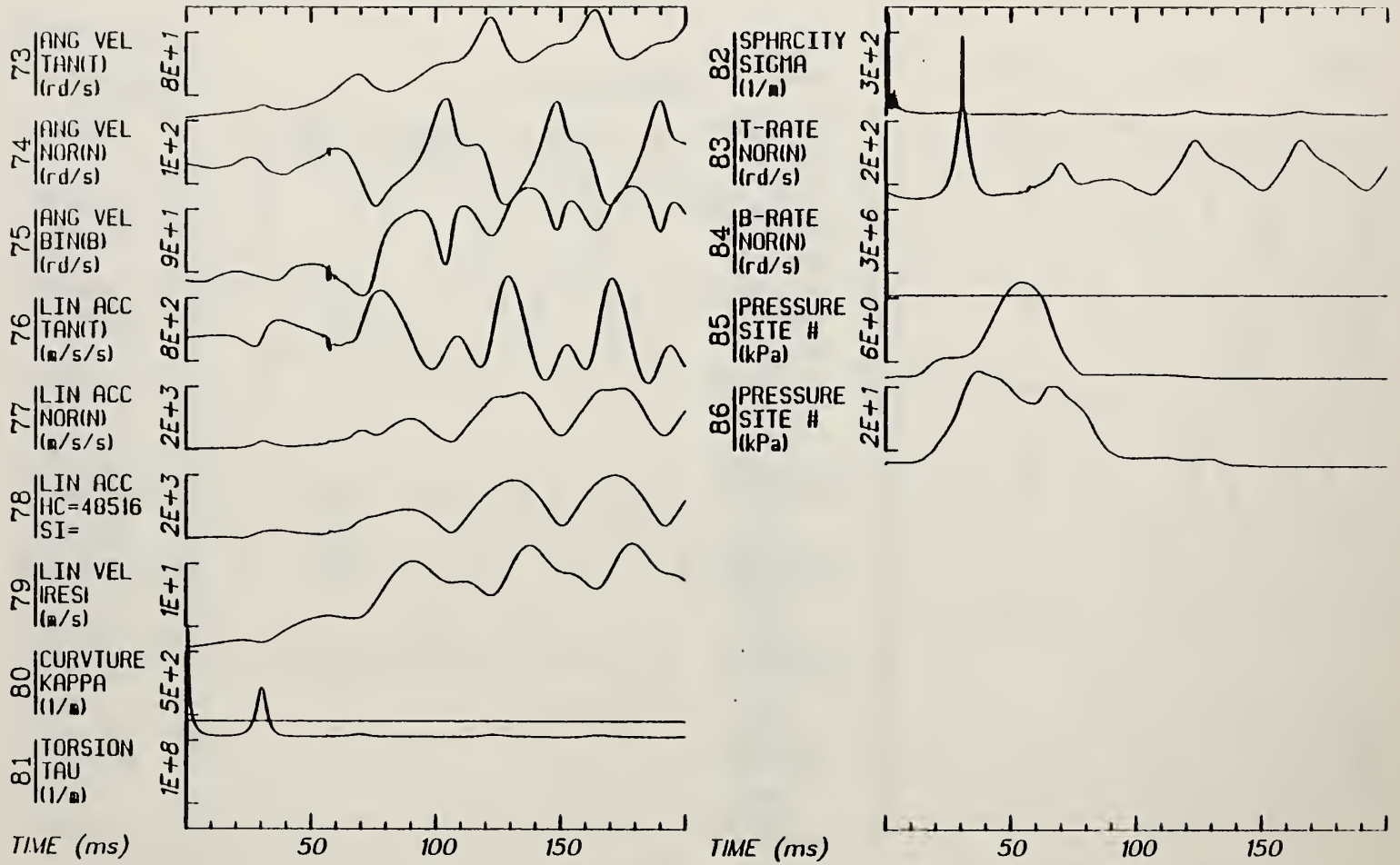

Run ID: 83E107 Disk: 83E107.3 File: 1 Date: MAY 30, 1985 Sheet: 5

*Filter:1600*4C*

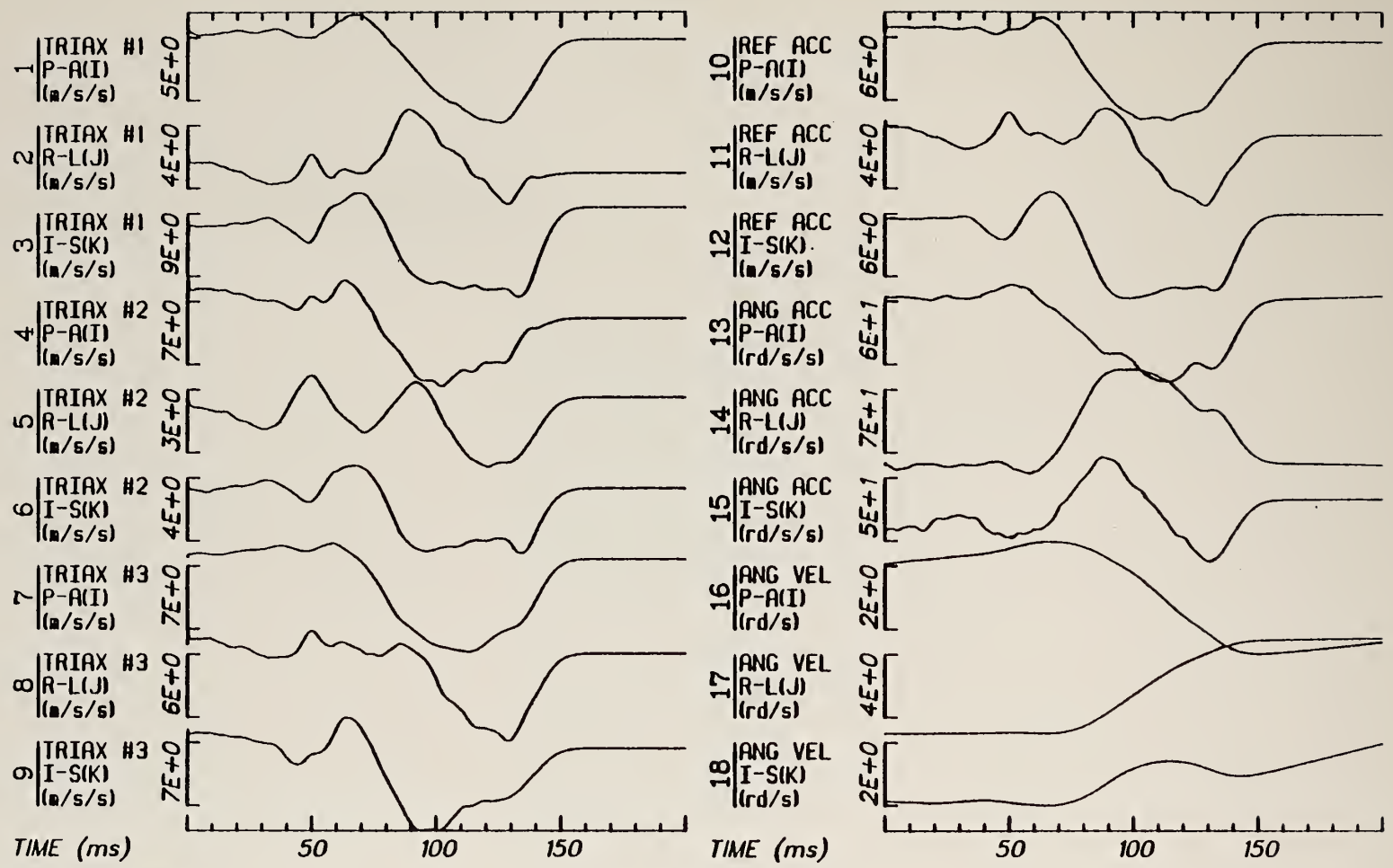

Run ID: 83E108 Disk: 83E108.3 File: 1 Date: MAY 30, 1985 Sheet: 1

*Filter:1600*4C*

*U.S. GOVERNMENT PRINTING OFFICE:1989-617-000:03694

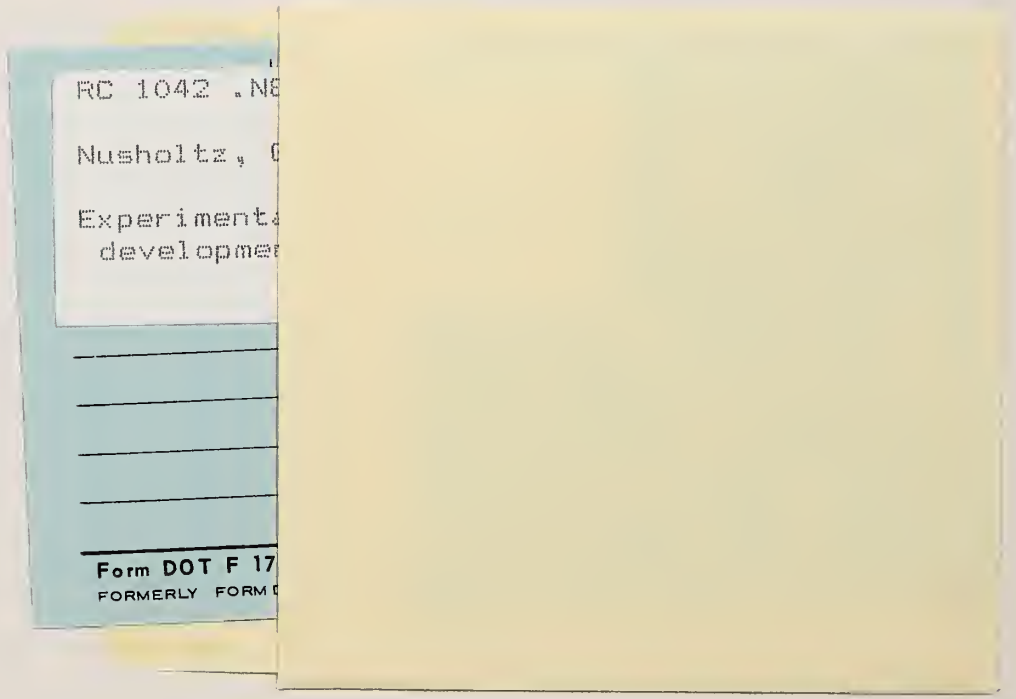
RC 1042 .N
Nusholtz,
Experimenta
develop
Form DOT F 17
FORMERLY FORM

DOT LIBRARY
00040591